

Paper No	Paper Title	Author Details	Company	Page
	Opening Address: Flow Measurement – The Last 10 Years	H Danielsen	Statoil	3
1.1	The Orifice Plate Discharge Coefficient Equation – Further Work	M J Reader-Harris, J A Sattary and E Spearman	NEL	11
1.2	Orifice Metering Research – A User’s Perspective	J E Gallagher R E Beaty	Shell Amoco	38
1.3	Optimal Flow Conditioner	W T Lake J Reid	Amoco NEL	70
2.1	Multiphase Flowmeter Measurement Uncertainties	B C Millington and T S Whitaker	NEL	114
2.2	A Multi-Capacitor Multiphase Flowmeter for Slugging Flow	D Brown, J J den Boer and G Washington	Shell Research	127
2.3	A Flow-Regime Independent Multiphase Flowrate Meter	E Dykesteen and Ø Midttveit	CMI	139
2.4	Framo Multiphase Flowmeter – Prototype Test	A B Olsen and B-H Torkildsen	Framo Engineering AS	155
2.5	Ultrasonic Flowmeter in a Gas Metering Station	R M Watt	NEL	187
3.1	Flow Conditions in a Gas Metering Station	D Thomassen and M Langsholt R Sakariassen	Institutt for Energiteknikk Statoil	189
3.2	CFD Analysis of Fluid Property Effects in Coriolis Mass Flowmeters	R M Watt	NEL	203

Paper No	Paper Title	Author Details	Company	Page
4.1	Results of Investigations Comparing Some of the Recommendations Given for Turbine Meters by ISO-9951 and AGA-7	J F Cabrol and A Erdal	Statoil K-Lab	205
4.2	The AGA Transmission Measurement Committee and the Revision of AGA Report No 8 Compressibility Factors of Natural Gas	J Stuart J Savidge S Beyerlain and E Lemmon	Pacific Gas and Electric Gas Research Institute University of Idaho	225
4.3	Density Metering Installation Methods	J Gray	Peak Measurement	242
5.1	A New Multi-Phase Ultrasonic Flowmeter for Gas	A Lygre R Sakariassen D Aldal	CMI Statoil Fluenta	283
5.2	Experience with Comparative Testing and Calibration of Coriolis and Turbine Meter Offshore and in the Laboratory	L Mandrup-Jesnen	Force Institute	305
5.3	Compact Large Bore Direct Mass Flowmeters	A J Mathews and C J Ayling	Schlumberger Industries	319
5.4	Pipe Elbow Effects on V-Cone Flowmeter	S A Ifft and E D Mikkelsen	Ketema Inc	335
	Closing Address: Flow Measurement – The Next Ten Years	J E Gallagher	Shell	351

FLOW MEASUREMENT - THE LAST TEN YEARS

by

H B Danielsen
Statoil

1.0

NORTH SEA FLOW MEASUREMENT WORKSHOP
26-29 October 1992

NEL, East Kilbride, Glasgow

FLOW MEASUREMENT-THE LAST 10 YEARS

H B Danielsen

Statoil, Stavanger, Norway.

Summary

A review of developments within North Sea flow metering is given. Most of the issues reviewed here are those which were brought up at the first Workshop ten years ago. In addition the development of Coriolis massmeters, ultrasonic gasmeters and multiphase meters are reviewed.

The first North Sea Flow Metering Workshop

This first Workshop took place in Stavanger in 1983 where the idea of a yearly metering seminar, alternating between Norway and UK, had been conceived at a more local seminar the year before.

A copy of the program is included on the last page of this paper.

Let's have a look at the main issues of this program and use them as a basis for reviewing what has happened from then and up till to-day.

Dr. Spencer

Among the names on the program you will probably notice Dr. Spencer.

No review of flow measurement for the last ten years can be said to be complete without commenting on the significant role played by this man.

Anybody working with flow measurement in the 1980s would inevitably become aware of Dr. Spencer: As an author of papers, as chairman of seminars and conferences, always having a prominent position in whatever he took part.

Also, he was one of the key persons in the process of establishing the North Sea flow Measurement Workshop

Dr. Spencer was pensioned from NEL some time late in the 1980s and then seemed to drop out of sight for most of us. From what I understand, however, he has kept himself busy by working for UN and for the EEC.

Hopefully, he is still in activity with the same energy and enthusiasm as he displayed at the past Workshops.

ISO 5167

The first lectures, given by Dr. Spencer, was about the development of ISO flow measurement standards, measurement uncertainty and comparisons between ISO 5167 and AGA Report No. 3 .

ISO 5167 was relatively "new" at that point of time. It had been issued in 1980 to replace ISO R-541 and had some significant improvements, such as the Stolz equation for calculation of flow coefficients. ISO 5167 had become the standard to which all new orifice metering stations for North Sea flow measurement now were designed. In the years to come it was "retro-fitted" on those metering systems which had been originally designed to ISO R-541.

In America, however, there seemed to be less enthusiasm for ISO 5167 and they still seemed to put their trust in AGA Report No. 3 with the "old" flow coefficient formulas.

In addition, a lot of the measurement engineers with a practical job were aware that ISO 5167 was not perfect. Its scope was so that it was not the complete document they would have liked to have available to use as a basis for design and operation of industrial orifice metering systems.

ISO was aware of this and had already, as early as 1977 initiated work with a separate document, "Code of practice for ISO 5167".

Also, right after the issue of ISO 5167 in 1980 a working group in ISO had already started its work to revise it.

On this background, a lot of metering engineers probably would have predicted the following development within the next ten years from 1983 onwards:

-The flow coefficients of ISO and AGA would not be different.

-ISO 5167 will be supplemented by a "Code of Practice Document" to cover the more practical sides of orifice metering.

To-day, however, there is still some way to go. The COP has not been issued and there is still a conspicuous difference between the 1992 revision of ISO 5167 using the Stolz-formula and the AGA 3 now using the new Reader-Harris-Gallagher formula.

Metering Regulations

Metering regulations was the second subject at that first measurement workshop. The lecture was given by Mr. Øglænd of NPD.

At the time of the workshop a draft of the NPD fiscal metering regulations had been completed and had been sent out for comments to the industry. The regulations were put into force in 1984.

Although everybody were not always happy with everything that these regulations implied,I think that they had a positive effect in terms of setting a standard to be met by the industry .In addition they implied that NPD had to give their specific approval of a metering system when all documentation had been provided and all the required tests had been sucessfully completed .

As the years went on the industry got used to live with the regulations.If the oil companies should initiate a revision,a relaxed regulation for metering of smaller streams with less fiscal importance would probably have been on the top of their wishing list.

It was, however,NPD who initiated a revision of their metering regulations in 1990.Their main objective were to make the fiscal metering regulations consistent with the other regulations they had issued for other areas,i.e. introducing more "functional" requirements and to a larger extent rely on the internal control of the oil companies.

The revised NPD fiscal metering regulations were put into force last year.

About the same time , work on other metering regulations started .As a new tax on gas burnt as fuel or flare on offshore platforms on the Norwegian continental shelf was imposed in 1989,regulations for measurement of this gas had to be made.The draft of these regulations has now been completed and it is expected that they will be put in force in a few months from the time of this workshop.

Gas Turbine Meters

Two lectures ,titled " Gas Metering at high Reynolds Number" and "New Standard for Gas Turbine Meters" respectively,were given by Joe Bonner .

Both of these lectures focused on gas turbine meters.

Although the first lecture also deals with orifice meters,one of the issues of the lecture is a discussion about plotting the calibration curves of turbine meters as error against Reynoldsnumber instead of flowrate.

The second lecture was about an ISO standard for gas turbine meters .At that time, a draft was being made by Working Group 15 of ISO TC 30, 90% of the draft was completed and only the difficult last 10% remained to be made.Although not stated directly,I think the audience got a feeling that Mr. Bonner was very worried about the progress in the last phase of drafting this standard.

Sometime between now and then things must have stopped up as I can find no standard for gas turbine meter in the 1992 ISO catalogue.

Liquid Densities

Already from the start,the North Sea Flow measurement Workshop managed to attract lecturers from overseas.

A lecture with the title "Calculation of Liquid Densities and their Mixtures" was given by Risdon W. Hankinson from Phillips Petroleum Company's headquarters in Bartlesville, Oklahoma.

Because there seemed to be an increasing number of fiscal metering systems for unstabilised oil, LPG and LNG in the North Sea area at that point of time, there was a great interest in methods to calculate densities and volume correction factors for other liquids than stabilised crude oils.

Hankinson's lecture was partly about the then new temperature correction factors of the ASTM/IP/API Petroleum Measurement Tables.

These tables had been issued in 1980, replacing the very old table 6 of API 2450. This was a very big step forward as the old tables had been issued in 1940 based on a limited number of crude oils produced before 1930.

After the workshop the Petroleum Measurement tables were further extended in 1984 and 1986 by new sections for compressibility factors.

The part of Hankinson's lecture that attracted most interest, however, was the part about the COSTALD compressed liquid density correlation. At that stage, in 1983, the Costald correlation was being used in fiscal measurement, but not by many and only for "offline" calculations.

At seminars later during the 80s, Phillips personnel promoted the use of COSTALD and outlined their plans to improve the correlation to be valid for temperatures near to the critical temperature and for higher pressures.

Up till to-day, COSTALD has gained increased acceptance and is being used as an "online" density calculation method in the flowcomputers in several North Sea metering systems.

Calculation of Gas density

This was the second lecture by R.W. Hankinson.

The paper is missing in my folder but I think the main topic of the lecture was about what was called at that time the "GRI method" for compressibility calculation.

Two years later, in 1985, this method was introduced as a standard, in AGA report no. 8. It is now the most commonly used calculation method for gas compressibility in the North Sea gas metering.

On Line Gas Densitymeters

Two lectures were given on this subject.

Jim Stansfeld gave a lecture on the basic details of the Solartron 7810/7811 gas densitometers.

The second lecture, by Paul Wilcox, was about practical experience with gas densitometers.

The lectures and the comments from the audience highlighted two problems:

The velocity of sound correction method for this kind of densitometer and

The effects of any temperature difference between the instrument's chamber and the gas in the meter-run.

The first of these problems became a hot subject at one of the later workshops. There was a lot of different opinions on which calibration and correction methods would give a correct density reading.

However, the discussions gave a positive result, the manufacturer started to offer nitrogen calibration for the instruments and the users started to use the complete VOS correction formula and went into the 90s with new confidence in their densitometers.

Piston-type Compact Provers

The last day of the first Flow Measurement Workshop was, in practice, entirely entitled to compact provers.

Bill Pursley gave the first lecture. Although this lecture was about conventional provers, its final remarks were about compact provers probably taking over a lot of the role of the conventional prover on the future offshore platforms.

Also, Bill Pursley's lecture on pulse interpolation techniques must be said to have a direct tie to compact provers.

Terry Noble gave a lecture on what was later named the Brooks Compact Prover.

This was followed up by Peter Jelffs who gave a lecture on compact provers in general and a short description of what MBR saw as desirable design features for this kind of prover.

To my knowledge there was only one compact prover in use in the North Sea activity in 1983. Phillips Petroleum Norway/Basic Resource Services were using their "Ballistic Flow Prover" as a transportable calibration unit for provers in the Ekofisk Area. This had been very successful and the prover is still in use for the same purpose at Ekofisk.

As time went by, most of the companies offering prover calibration services in the North Sea started to operate one or more transportable compact provers. But up till now the compact provers have not been used on a large scale as permanently installed units.

To my knowledge only 3 units have been installed for this purpose: One in each of the Danish, Dutch and Norwegian Sector. Reportedly, all these units operate satisfactorily.

However , most people present at the first Workshop would probably have guessed a higher number of compact provers in 1992.

Significant Developments 1983-1992

Although not brought up at the first Flow Measurement Workshop,I cannot finish this review of flow measurement for the last ten years without saying a few words about Coriolis mass meters,ultrasonic transit time gas flowmeters and multiphase metering .

Coriolis Mass Meters

The existence of the Coriolis mass meter was probably known to most of us in 1983 but not much attention was paid to it.One of the reasons for this may have been that ,at that stage, flowrates were big and mass meters were small.

As time went on, the streams to be metered have tended to get smaller while the massmeters have grown bigger.Also, an extensive evaluation activity were started to evaluate the massmeters' operational characteristics.

To-day, a number of manufacturers offer Coriolis massmeters,the largest have a capacity in excess of a 6-inch liquid turbinemeter .Standards are being drafted by ISO and other bodies and we have even got a Coriolis-based fiscal metering system for condensate at Total's shore terminal in St. Fergus.

Being aware of that there is a lecture titled "The next 10 Years" at the end of this Workshop, I should not try to make any predictions about the future of the massmeters in the North Sea.But I think that these meters will have a great potential for crude oil measurement if it turns out that their calibration is so stable that they may be installed without a permanent prover.

Ultrasonic Gas Meters

At the time of the first Workshop, a development to use ultrasonic transit time meters for gas measurement had already started.Among the challenges they had at that time was to make the ultrasonic transducers powerful enough to send their signal through gas and to develop methods to calculate flowrate from a number velocity readings along chords of a cross section of flow.

To-day,ten years later, the manufacturers offer both multipath ultrasonic gas meters for fiscal applications and flare gas meters with less accuracy but very wide flowranges.A number of ultrasonic flare meters have been installed in the North Sea .No fiscal meter is in operation yet but we will see them in the very near future.

Multiphase Flowmeters

Even before the 1983 Workshop the North Sea oil companies were aware that some of the fields found were too small to be developed with dedicated platforms,separation equipment and conventional fiscal metering.

New technology in terms of subsea wells, multiphase pumps and multiphase metering was needed. As a result of this a lot of the oil companies started or sponsored development projects to provide the technology to measure multiphase flow. The objective was to get a meter that could measure the flow of each of the components oil, water and gas.

Generally, not much of concrete information was given to outside world. At the Offshore Northern Seas Conference in Stavanger in August 1992, however, a number of multiphase measurement devices were on display. Some impressions of state of the art from the ONS were:

Very large amounts of money had been spent during a number of years on the development of each device.

Although one got the impression that the meters were for sale, most of them had not yet been out in the field.

The "readout" varied between the various meters, one could get one or more of actual cubic meters, standard cubic meters or mass of the full stream, each phase or each component of the liquid phase.

The main impression were, however, that the oil companies involved now definitely had moved from the stage when they limited themselves to pay for development and tests in a laboratory to a stage where they also would let the meters be installed in the field for testing.

THE ORIFICE PLATE DISCHARGE COEFFICIENT EQUATION - FURTHER WORK

by

M J Reader-Harris, J A Sattary and E P Spearman
NEL

Paper 1.1

NORTH SEA FLOW MEASUREMENT WORKSHOP
26-29 October 1992

NEL, East Kilbride, Glasgow

THE ORIFICE PLATE DISCHARGE COEFFICIENT EQUATION - FURTHER WORK

M J Reader-Harris, J A Sattary and E P Spearman

NEL, East Kilbride, Glasgow

S U M M A R Y

This paper describes the work undertaken to derive the revised orifice plate discharge coefficient equation based on the final EEC/API database including the data collected in 50 mm and 600 mm pipes. It consists of several terms, each based on an understanding of the physics. An earlier version of this equation, based on a smaller database, was accepted at a meeting of EEC and API flow measurement experts in New Orleans in 1988, and emphasis is placed on the two principal changes to the equation: improved tapping terms for low Reynolds number have been calculated; and an additional term for small orifice diameter has been obtained, and its physical basis in orifice edge roundness given.

N O T A T I O N

A	Function of orifice Reynolds number (see equations (6) and (7))
C	Orifice discharge coefficient
C_c	Orifice discharge coefficient using corner tapplings
C_s	Dependence of C_c on Reynolds number
C_∞	C_c for infinite Reynolds number
ΔC_{down}	Downstream tapping term
$\Delta C_{down,min}$	Value of ΔC_{down} at the downstream pressure minimum
ΔC_{up}	Upstream tapping term
ΔC_{round}	Change in discharge coefficient due to edge roundness
D	Pipe diameter
d	Orifice diameter
L_1	Quotient of the distance of the upstream tapping from the upstream face of the plate and the pipe diameter
L_2	Quotient of the distance of the downstream tapping from the upstream face of the plate and the pipe diameter
L_2'	Quotient of the distance of the downstream tapping from the downstream face of the plate and the pipe diameter
H_2	Quotient of the distance of the downstream tapping from the upstream face of the plate and the dam height (equation (2))

M_2'	Quotient of the distance of the downstream tapping from the downstream face of the plate and the dam height (as in equation (2))
Δp	Differential pressure across the orifice plate
Δp_c	Differential pressure across the orifice plate using corner tappings
r_e	Edge radius
Re_D	Pipe Reynolds number
Re_d	Orifice Reynolds number
r_{em}	Mean value of edge radius
r_{max}	Maximum value of edge radius
u	Uncertainty of the pressure measurement
β	Diameter ratio
λ	Friction factor
$\Delta\lambda$	Shift in friction factor due to pipe roughness

1 INTRODUCTION

Although the orifice plate is the recognized flowmeter for the measurement of natural gas and light hydrocarbon liquids, the orifice discharge coefficient equations in current use are based on data collected more than 50 years ago. Moreover, for 20 years the United States and Europe have used different equations, a discrepancy with serious consequences for the oil and gas industry since many companies are multinational. For more than ten years data on orifice plate discharge coefficients have been collected in Europe and the United States in order to provide a new database from which an improved discharge coefficient equation could be obtained which would receive international acceptance.

In November 1988 a joint meeting of API (American Petroleum Institute) and EEC flow measurement experts in New Orleans accepted the equation derived by NEL. At that time the database contained 11 346 points, collected in pipes whose diameters ranged from 50 to 250 mm (2 to 10 inch); 600 mm (24 inch) data were being collected but had not yet been included in the database. 600 mm data have now been collected in gas and in water and extend the database both in pipe diameter and in Reynolds number. The data which were least well fitted by the equation presented at New Orleans were the 50 mm data; so additional 50 mm data have been collected in water and oil which provide additional information about discharge coefficients both for small orifice diameters and for low Reynolds numbers. All the additional data have now been included in the database and the equation refitted. This paper gives that revised equation and its derivation.

2 THE DATABASE

The final database consists of 16376 points: the diameter ratios range from 0.1-0.75, orifice Reynolds numbers from 1700 to 7×10^7 , and pipe diameters

from 50-600 mm. The data were collected in nine laboratories in four fluids: water, air, natural gas and oil. The data points for which the orifice diameter was less than 12.5mm ($\frac{1}{2}$ inch) and those for which the differential pressure across the orifice plate is less than 600 Pa are very scattered and were excluded. The American data remain as in References 1 to 3; no additional American data have been collected. The complete EEC data are tabulated in References 4 to 10; the data sets which have been accepted for analysis are indicated in Reference 11. A very small number of points (0.5 per cent of all the EEC points) was removed from the EEC data as outliers; each of those removed was identified as an outlier within its own set of data by the Grubbs' extreme deviation outlier test; details will be found in Reference 12.

3 TAPPING TERMS

The tapping terms are equal to the difference between the discharge coefficient using flange or D and D/2 tappings and those using corner tappings. They are expressed as the sum of an upstream and a downstream tapping term. The upstream term is equal to the change in discharge coefficient when the downstream tapping is fixed in the downstream corner and the upstream tapping is moved from the upstream corner to another position. The downstream term is equal to the change in discharge coefficient when the upstream tapping is fixed in the upstream corner and the downstream tapping is moved from the downstream corner to another position. In theory the total tapping term is the sum not only of the upstream and the downstream term but also of a product term because the discharge coefficient depends on the reciprocal of the square root of the differential pressure (Reference 13). In practice the product term is not included in the formula and, to compensate, the upstream tapping term in the formula is very slightly smaller than the true upstream term.

In the database only the total tapping term, the sum of the upstream and the downstream terms, is available. To divide the tapping term into two parts so that each can be accurately fitted, measurements of the individual tapping terms collected outside the EEC and API projects were used to indicate the form and approximate value of the upstream and downstream terms; however the constants in the formulae were obtained to fit the EEC/API database. The EEC collected data with several tapping systems; so the total tapping term could be simply obtained (References 13 and 14). Although the American data were collected with flange tappings alone small adjustments were made to the final tapping terms in order to obtain the optimum fit to the database as a whole.

On examining the measured tapping terms it has been shown (References 13 and 14) that for high Reynolds number (orifice Reynolds number, Re_d , greater than about 10^5) the tapping terms may be considered not to vary with Re_d , but that for low Reynolds number the terms depend on Re_d . An important part of the work undertaken since the meeting in New Orleans has been to provide more accurate low Reynolds number tapping terms. Since the high Reynolds number tapping terms need to be determined first they are described here first.

3.1 High Reynolds number tapping terms

For each diameter ratio mean total tapping terms for the EEC data for D and D/2 tappings and for flange tappings in 50, 100, 250 and 600 mm pipe were calculated and used for determining best constants and exponents. Low

Reynolds number data were excluded. Details of the method by which the values of the total tapping terms were calculated are given in References 13 and 14.

3.1.1 Upstream term

To determine the correct form of the tapping terms, the upstream term, ΔC_{up} , was determined first. The dependence of the upstream term on $\beta^4/(1-\beta^4)$ is well established (References 13 - 16); so here it is only necessary to consider the dependence on L_1 , the quotient of the distance of the upstream tapping from the upstream face of the plate and the pipe diameter. Several forms of equation were tried, and their exponents and constants determined, and the optimum one found to be the following:

$$\Delta C_{up} = (0.043 + 0.090e^{-10L_1} - 0.133e^{-7L_1}) \frac{\beta^4}{1 - \beta^4} \quad (1)$$

This equation is physically realistic: it has the required dependence on $\beta^4/(1-\beta^4)$, is equal to 0 for $L_1=0$, does not become negative, tends rapidly to a constant once L_1 exceeds 0.5, and has a continuous derivative. Together with the downstream term it gives a very good fit to the total tapping term data. It is plotted in Fig. 1 against many sets of experimental measurements of the upstream tapping term and the quality of the fit is good. References to the work of the many experimenters who collected the data in Fig. 1 are given in References 13 and 14.

3.1.2 Downstream term

Many experimenters have measured the pressure profile downstream of the orifice plate, and, although the data are more scattered than those upstream of the plate, the pattern is clear: the pressure decreases downstream of the plate till it reaches a minimum and then quite a short distance downstream of the minimum it begins to increase rapidly. The orifice plate should not be used with the downstream tapping in the region of rapid pressure recovery.

An important step in the determination of the downstream formula was the work of Teyssandier and Husain (Reference 17) who non-dimensionalised downstream distances with the dam height rather than the pipe diameter. Instead of working in terms of L_2 , the quotient of the distance of the downstream tapping from the upstream face of the plate and the pipe diameter, it is better to use M_2 , the quotient of the distance of the downstream tapping from the upstream face of the plate and the dam height, which is given by

$$M_2 = \frac{2L_2}{1 - \beta} \quad (2)$$

L_2' and M_2' are defined identically except that in each case the distance from the downstream face of the orifice plate is used.

From consideration of data from many experimenters References 13 and 14 confirmed the advantage of non-dimensionalising with dam height by showing that the pressure minimum occurs for

$$M_2 = 3.3. \quad (3)$$

Although it is theoretically better to work in terms of M_2 , it is more convenient to work in terms of M_2' since it avoids the need to include the plate thickness in the discharge coefficient equation. Provided appropriate restrictions are placed on plate thickness, an equation for M_2' can be used without introducing significant errors (Reference 13). These plate thickness restrictions are satisfied by the EEC and API plates.

To determine the downstream tapping term, ΔC_{down} , it is desirable first to determine an appropriate dependence on β : this can be done by considering $\Delta C_{\text{down,min}}$, its value at the downstream pressure minimum. Fig. 2 gives values of measured downstream tapping terms from various experimenters (given in References 13 and 14). It is not necessary to determine the best fit, but the following, from equation (5), gives a good fit to the data:

$$\Delta C_{\text{down,min}} = -0.0101\beta^{1.3} \quad (4)$$

Several forms of equation for the complete downstream tapping term were tried, and their exponents and constants determined, and the optimum one found to be the following:

$$\Delta C_{\text{down}} = -0.031(M_2'^{1.1} - 0.8M_2'^{1.3})\beta \quad (5)$$

This equation is physically realistic: it has an appropriate dependence on β , is equal to 0 for $M_2'=0$, has a minimum, and has a continuous and finite derivative. Together with the upstream term it gives a very good fit to the total tapping term data. It is plotted in Fig. 3 against many sets of experimental measurements of the downstream tapping term.

3.2 Low Reynolds number tapping terms

When data were taken by NEL in oil in 50 mm pipe in 1990 for inclusion in the EEC database not only discharge coefficients but also direct measurements of pressure profile were made: the pressure rise to the upstream corner from tappings at distances D , $D/2$, $D/4$ and $D/8$ upstream was measured, where D is the pipe diameter, as well as the pressure drop from the downstream corner to tappings at distances $D/8$ and $D/4$ downstream of the downstream face of the orifice plate and to the downstream $D/2$ tapping. Whereas for high Re_d the tapping terms do not depend on Re_d , the tapping terms at the Reynolds numbers obtained in oil are significantly different. Previous work by Johansen (Reference 18) had shown that the upstream tapping term at the upstream pressure minimum decreases as Re_d decreases. Similarly the downstream tapping term at the downstream pressure minimum decreases in magnitude as Re_d decreases. Data from Witte and Schröder (quoted in References 19 and 20), who only measured the upstream tapping term, agree with Johansen. So the equation presented at New Orleans reflected these data on the reasonable assumption that the tapping terms, though decreasing in size as Re_d decreases, retain the same shape as a function of distance from the plate, since data were not available except at the pressure minima.

However, the data collected on tapping terms by NEL in 50 mm pipe (Reference 21) show that the reality is more complex than the previous

analysis, but also provide revised tapping terms which correspond much better to the tapping term collapse found in the database as a whole than the New Orleans tapping term did. Fig. 4 shows all the data for $\beta \approx 0.74$: it can be seen that all the data collapse on to one another as Re_d decreases. However, the amount of data makes it difficult to see that the flange data collected in 50 mm, 100 mm and 150 mm pipes collapse on to one another at a higher Reynolds number than that at which the corner tapping data collapse on to the other data. The collapse of the flange tapping data on to one another can be seen clearly in Fig. 5 which shows the US data for $\beta \approx 0.74$: the approximately constant values of the tapping terms for high Re_d can also be seen. Figures 4 and 5 confirm the need for tapping terms which are functions of Reynolds number, but also show that the simple dependence on Re_d used in the New Orleans equation is insufficient.

The main features of the tapping term data collected in 50 mm pipe (in Figs 83-100 of reference 21) are as follows: the upstream tapping term for D and for D/2 tapplings decreases with decreasing Re_d as expected from the work of Johansen and of Witte and Schröder, although the NEL data decrease slightly more slowly with Re_d ; the upstream tapping term for D/4 tapplings remains approximately constant; the upstream tapping term for D/8 tapplings increases with decreasing Re_d . The dependence of the downstream tapping terms on Re_d depends on β : for $\beta > 0.7$ they decrease in magnitude with decreasing Re_d ; otherwise they are constant. At the bottom of the Re_d range the uncertainties in the data become large, especially for the upstream D/2 tapping data.

It is interesting that downstream of the orifice plate the data in Reference 21 are apparently inconsistent from those of Johansen: one possibility is that it is only near the pressure minimum that the magnitude of the downstream tapping term decreases with decreasing Re_d , through the pressure minimum becoming closer to the orifice. For, where the values of the downstream tapping term deduced from the data in Reference 21 were taken at the pressure minimum, that is for $\beta > 0.7$, they decrease in magnitude like those of Johansen; elsewhere the two sets of data are not directly comparable: the data in Reference 21 were not taken at the pressure minimum, whereas Johansen's were.

It is important to see the pattern in the tapping term data: to do this it is necessary to do an analysis of the uncertainty of these data. It is then possible to analyse all the upstream tapping term data simultaneously, and, in particular, to verify that the dependence on $\beta^4/(1-\beta^4)$ which characterizes the data for high Re_d continues to apply for low Re_d . Fig. 6 shows the change in discharge coefficient due to moving the upstream pressure tapping from the upstream corner for the 4 values of L_1 for which measurements were made. Where the data are multiplied by $(1-\beta^4)/\beta^4$ they fall on to a single curve for each value of L_1 . Data are only plotted if $(1-\beta^4)u/(\beta^4\Delta p_c) < 0.05$, where u is the uncertainty of the pressure measurement at that point and Δp_c is the pressure differential across the orifice plate using corner tapplings.

Various possible forms of the upstream tapping term, ΔC_{up} , for low Re_d data were tried, and the best one found to be the following:

$$\Delta C_{up} = (0.043 + (0.090 - aA)e^{-10L_1} - (0.133 - aA)e^{-7L_1}) (1 - bA) \frac{\beta^4}{1 - \beta^4}, \quad (6)$$

where

$$A = \left(\frac{2100\beta}{Re_D} \right)^n$$

and a, b, and n are to be determined.

This equation has the same behaviour for $L_1 = 1$ as the equation accepted in New Orleans, and is equal to 0 for $L_1 = 0$, but is significantly different for intermediate values of L_1 . With this form of equation the best fit to the upstream tapping term data included in Fig. 6 was obtained. Since the product term is not included in the final formula for the tapping terms, the fitted upstream term is adjusted to make allowance for it: following the argument in Reference 13, $\Delta C_{up} (1 + 3\Delta C_{down}/C_c)$, where C_c is the discharge coefficient using corner tapings, is fitted instead of ΔC_{up} itself. Allowance was also made for the fact that especially for $L_1 \leq 0.125$ the measured tapping term (adjusted to allow for the absence of the product term) even for $Re_d \approx 100000$ is not equal to the high Re_d value of the equation; the fitted equation was therefore calculated based on data points shifted so that for each L_1 the mean value of the data for $Re_d > 80000$ (adjusted to allow for the absence of the product term) agrees with the high Re_d version of the equation.

The best fit value for n was 0.925, but for simplicity this was rounded to 0.9, and with n = 0.9 the other constants were

$$a = 0.833$$

$$\text{and } b = 1.307.$$

However, these values were adjusted to give a better fit to the database: the best fit of the complete database gave a larger value of a than the fit to the upstream tapping term data: a compromise value was obtained as follows: from the Figures in Reference 21 it appears that the data for $L_1 = 1$, those for $L_1 = 0.25$ and those for $L_1 = 0.125$ cross at $Re_d \approx 13000$. Since in equation (6) the three curves representing the three values of L_1 do not intersect at a single point, a further simplification is to consider the intersection of the curve for $L_1 = 0.167$ (corresponding to flange tapings in 6-inch pipe) with the curve for $L_1 = 1$: this occurs for a = 1.03. This constant is then rounded to 1. Equation (6) with a = 1, b = 1.307, and n = 0.9 is then plotted in Fig. 6 for comparison with the data. This equation describes a change in the pressure profile upstream of the orifice in which, as Re_d decreases, the upstream tapping term at D decreases but the gradient of the tapping term near the corner increases.

It is unnecessarily complicated to construct a downstream tapping term which decreases in magnitude with decreasing Re_d for very large β but is constant for smaller β ; since the upstream term is significant for large β , but very small for small β , this downstream Re_d effect is incorporated in the upstream term by reducing b from 1.307 to 1. The final upstream

tapping term (incorporating a small downstream effect) is therefore

$$\Delta C_{up} = (0.043 + (0.090 - A)e^{-10L_1} - (0.133 - A)e^{-7L_1})(1 - A)\frac{\beta^4}{1 - \beta^4}, \quad (7)$$

where

$$A = \left(\frac{2100\beta}{Re_D} \right)^{0.9}.$$

With this upstream formula no change in the downstream formula is required for $Re_D > 4000$. However, from examination of the data for $Re_D < 4000$ in Reference 10 it can be seen that in this region the discharge coefficient using corner tapplings becomes increasingly larger than that using flange or D and D/2 tapplings as Re_D decreases; since this applies even for small β this can best be represented by the downstream tapping term being modified, although both upstream and downstream tapping terms change with Re_D . The model used was as follows:

$$\Delta C_{down} = -0.031(M_2' - 0.8M_2'^{1.1})\{1 + c \max(\log_{10}(T/Re_D), 0.0)\}\beta^{1.3}, \quad (8)$$

where c is a constant and T is the pipe Reynolds number at which transition to fully turbulent flow occurs. T varies, as would be expected, from one set of data to another, but a reasonable estimate of the range of values encountered in the database is 3000 - 4500, and $T = 3700$ has been used for both the tapping term and the slope term. With this value for T c is determined by fitting the data in Reference 10: using the difference between flange and corner tapplings only, $c = 8.20$; using the difference between D and D/2 and corner tapplings only, $c = 7.88$; using all the data, $c = 8.04$. The agreement between the values of c obtained using flange and D and D/2 tapplings is very good, and the downstream tapping term used in the final equation is as follows:

$$\Delta C_{down} = -0.031(M_2' - 0.8M_2'^{1.1})\{1 + 8 \max(\log_{10}(3700/Re_D), 0.0)\}\beta^{1.3}. \quad (9)$$

4 SMALL ORIFICE DIAMETER TERM

An additional term for small orifice diameters has been added to the equation accepted at New Orleans as a result of collecting the NEL 50 mm data which include measurements of edge sharpness. The problem here is that it is extremely difficult to obtain a sufficiently sharp edge where the orifice diameter is small: Fig. 7, which includes averages of measured edge radii from the plates used in the EEC tests, in which D was in the range 50-600 mm, shows that for orifice diameter, d , less than 50 mm the plates rarely meet the requirements of ISO 5167-1 (Reference 22). It is clear that for $d \leq 25$ mm there will be large shifts in C . When the edge radii themselves are plotted as in Fig. 8, it appears that the edge radius, r_e , (in mm) increases as d decreases from 50 mm, whereas to meet the standard it needs to decrease fairly rapidly.

The change in discharge coefficient due to edge roundness, ΔC_{round} , has been measured by Hobbs (Reference 23) as a function of change in edge radius, Δr_e , and can be expressed approximately as

$$\Delta C_{round} = 3.33 \Delta r_e / d. \quad (10)$$

It seems reasonable to suppose that the mean value of r_e , r_{em} , for $d < 50$ mm is given by

$$r_{em} = 0.01 + B(50 - d), \quad (11)$$

where B is a constant. This is linear with d and gives r_{em}/d equal to 0.0002 where $d = 50$ mm. Given that the discharge coefficient equation for large d is based on r_{em}/d being equal to 0.0002, the additional term for $d < 50$ mm will be

$$\Delta C_{round} = 3.33(r_{em}/d - 0.0002), \quad (12)$$

which on substituting from equation (11) becomes

$$\Delta C_{round} = 3.33(B + 0.0002)(50/d - 1). \quad (13)$$

When this term is determined by fitting the database a good approximation to the term is

$$\Delta C = 0.0015 \max(50/d - 1, 0), \quad (14)$$

which corresponds to $B = 0.00025$ and to

$$r_{em} = \max(0.0225 - 0.00025d, 0.0002d). \quad (15)$$

The maximum value of r_e , r_{max} , is $2r_{em}$, which is equal to

$$r_{max} = \max(0.045 - 0.0005d, 0.0004d), \quad (16)$$

and from Fig. 8 it can be seen that all the plates lie within this limit. Clearly this term gives rise to an increase in uncertainty for $d < 50$ mm.

5 C_∞ AND SLOPE TERMS

Given the tapping and small orifice diameter terms it is possible to determine the C_∞ and slope terms. C_∞ is the discharge coefficient using corner tappings for infinite Reynolds number, and the slope term, C_s , gives the dependence of the discharge coefficient using corner tappings on Reynolds number, so that the discharge coefficient using corner tappings is given by $C_\infty + C_s$. These terms are of the same form as in previous work (References 14 and 24) and are described there, but, in brief, the basis of these terms is as follows: C_∞ increases with β to a maximum near $\beta = 0.55$ and then decreases increasingly rapidly. Thus an appropriate form for C_∞ is

$$C_\infty = a_1 + a_2\beta^{m_1} + a_3\beta^{m_2}. \quad (17)$$

The slope term consists of two terms, an orifice Reynolds number term and a velocity profile term. For low β C_s depends only on orifice Reynolds number, and a simple expression as a reciprocal power of Re_d is appropriate:

$$\begin{aligned} C_s &= b_1(10^6/Re_d)^{n_1} \\ &= b_1(10^6\beta/Re_D)^{n_1}. \end{aligned} \quad (18)$$

This term is inadequate to describe C_s for large β : for large β there is

also a velocity profile term which can be derived using the fact that, for a fixed Reynolds number, as the pipe roughness changes the change in the discharge coefficient is approximately proportional to $\beta^{-1}\Delta\lambda$, where $\Delta\lambda$ is the change in the pipe friction factor and $l \approx 4$ (Reference 24). A simple integral of this expression together with the orifice Reynolds number term gives

$$C_s = b_1(10^6\beta/Re_D)^{n_1} + b_2\beta^l\lambda. \quad (19)$$

This term is adequate for high Reynolds number but for practical use it requires three further enhancements. There is no data on the effect of rough pipework on the discharge coefficient for low Reynolds number, and a better fit to the database is obtained by including an additional term proportional to A , on the basis that, as the tapping terms begin to change, so may the dependence on friction factor:

$$C_s = b_1(10^6\beta/Re_D)^{n_1} + (b_2 + b_3A)\beta^l\lambda. \quad (20)$$

λ is an inconvenient variable with which to work, but for the pipes used in collecting the data in the EEC/API database a typical pipe roughness as a function of Re_D can be determined; so typical values of λ as a function of Re_D can be calculated, and λ can be approximated by a constant (which leads to a term to be absorbed into C_∞ and a small term which is neglected) together with a reciprocal power of Re_D :

$$C_s = b_1(10^6\beta/Re_D)^{n_1} + (b_2 + b_3A)\beta^l(10^6/Re_D)^{n_2}. \quad (21)$$

It is also necessary to make provision for transition from turbulent to laminar flow since, except for very low β , the gradient of the discharge coefficient as a function of a reciprocal power of Re_D is very different below a transition point in the range $Re_D = 3000 - 4500$ from that above it. This change of gradient occurs because the velocity profile changes very rapidly as the flow changes from turbulent to laminar, and when the velocity profile term is extended so that it can be used below the fully turbulent range the slope term becomes:

$$C_s = b_1(10^6\beta/Re_D)^{n_1} + (b_2 + b_3A)\beta^l \max\{(10^6/Re_D)^{n_2}, c_1 - c_2(Re_D/10^6)\}. \quad (22)$$

It remains to determine the constants and exponents in equations (17) and (22). m_2 is equal to 8 in both the Stolz equation (Reference 22) and that adopted in New Orleans (Reference 14) and using this high value gives a good representation of the rapid decrease in C_∞ for high β . Previously m_1 has been taken to be 2, but the optimum value of m_1 , in terms of the lowest standard deviation of the data about the equation, lies between 1.2 and 1.3: the same value as the exponent of β in the downstream tapping term (equation (5)) is used. $n_1 = 0.7$ and $n_2 = 0.3$ give the optimum fit to the complete database. l is taken to be 3.5 rather than 4 because it gives a better fit to the complete database: in terms of the dependence of the effect of rough pipework on β an exponent of 3.5 is as acceptable as 4 (Reference 12). As stated in section 3.2 the mean Re_D at which the flow becomes fully turbulent was taken to be 3700. This gives c_1 in terms of c_2 . c_2 is obtained by trying appropriate values in turn and obtaining the best overall fit: $c_2 = 4800$ gives an excellent overall fit. Given the tapping terms in equations (7) and (9) and the small orifice diameter term in equation (14) a least-squares fit of the complete database was performed: on rounding the constants, the C_∞ and slope terms become

$$C_{\infty} + C_s = 0.5934 + 0.0232\beta^{1.3} - 0.2010\beta^8 + 0.000515(10^6\beta/Re_D)^{0.7} + (0.0187 + 0.0400A)\beta^{3.5}\max\{(10^6/Re_D)^{0.3}, 23.1 - 4800(Re_D/10^6)\}. \quad (23)$$

6 THE FINAL EQUATION AND ITS QUALITY OF FIT

The complete equation can be brought together from equations (7), (9), (14) and (23) and is as follows:

$$C = 0.5934 + 0.0232\beta^{1.3} - 0.2010\beta^8 + 0.000515(10^6\beta/Re_D)^{0.7} + (0.0187 + 0.0400A)\beta^{3.5}\max\{(10^6/Re_D)^{0.3}, 23.1 - 4800(Re_D/10^6)\} + (0.043 + (0.090 - A)e^{-10L_1} - (0.133 - A)e^{-7L_1})(1 - A)\frac{\beta^4}{1 - \beta^4} - 0.031(M_2' - 0.8M_2'^{1.1})\{1 + 8\max(\log_{10}(3700/Re_D), 0.0)\}\beta^{1.3} + 0.0015\max\left(\frac{50}{\beta D} - 1, 0\right), \quad (D: \text{mm}) \quad (24)$$

where

$$M_2' = \frac{2L_2'}{1 - \beta},$$

and

$$A = \left(\frac{2100\beta}{Re_D}\right)^{0.9}.$$

L_1 is the quotient of the distance of the upstream tapping from the upstream face of the plate and the pipe diameter, and

L_2' is the quotient of the distance of the downstream tapping from the downstream face of the plate and the pipe diameter.

Its quality of fit is quantified in Tables 1 to 4. Table 1 gives a description of the meaning of the different lines in Tables 2 to 4. These tables give the deviations of the data about equation (24) as a function of β , D , Re_D and pair of tappings used and of certain combinations of these. The tappings described as Corner (GU) are tappings in the corners which were designed by Gasunie and are simpler to make than those in ISO 5167-1. They are described in Reference 7. The standard deviation of all the data (including those for $Re_D < 4000$) about the equation is 0.269 per cent and the deviations are well balanced as functions of β , D , Re_D and pair of tappings used. Tables giving deviations as a function of other combinations of independent variables and for each laboratory which collected the data are given in Reference 12. It can be seen that the standard deviation increases for small d , large β , and small Re_D . If the

8515 data points for $0.19 < \beta < 0.67$, $Re_d > 30000$ and $d > 50$ mm are analysed the standard deviation of the points about the equation is 0.208 per cent.

7 CONCLUSIONS

The orifice plate discharge coefficient equation has been revised in the light of the complete EEC/API database including the data collected in 50 mm and 600 mm pipes. There are two principal changes to the equation accepted at New Orleans: using the additional data collected in 50 mm pipes improved tapping terms for low Reynolds number have been calculated; and an additional term for small orifice diameter has been obtained, and its physical basis in orifice edge roundness given. The revised orifice plate discharge coefficient equation is given as equation (24): the deviations of the database from the equation have been tabulated and shown to be well balanced as functions of β , D , Re_D and pair of tappings used.

ACKNOWLEDGEMENT

This paper is published by permission of the Chief Executive, National Engineering Laboratory Executive Agency, and is Crown copyright. The work reported here was supported by DGXII of the Commission of the European Communities and by the National Measurement System Policy Unit of the Department of Trade and Industry.

REFERENCES

- 1 WHETSTONE, J. R., CLEVELAND, W. G., BAUMGARTEN, G. P. and WOO, S. Measurements of coefficients of discharge for concentric, flange-tapped, square-edged orifice meters in water over a Reynolds number range of 1000 - 2 700 000. NIST Technical Note TN-1264. American Petroleum Institute, Washington DC, 1988.
- 2 BRITTON, C. L., CALDWELL, S., and SEIDL, W. Measurements of coefficients of discharge for concentric, flange-tapped, square-edged orifice meters in white mineral oil over a low Reynolds number range. American Petroleum Institute, Washington DC, 1988.
- 3 Coefficients of discharge for concentric, square-edged, flange-tapped orifice meters: equation data set - supporting documentation for floppy diskettes. American Petroleum Institute, Washington DC, 1988.
- 4 HOBBS, J. M. Experimental data for the determination of basic 100 mm orifice meter discharge coefficients (European programme). Report EUR 10027, Commission of the European Communities, Brussels, Belgium, 1985.
- 5 HOBBS, J. M. and SATTARY, J. A. Experimental data for the determination of 100 mm orifice meter discharge coefficients under different installation conditions (European programme). Report EUR 10074, Commission of the European Communities, Brussels, Belgium, 1986.

- 6 HOBBS, J. M., SATTARY, J. A. and MAXWELL, A. D. Experimental data for the determination of basic 250 mm orifice meter discharge coefficients (European programme). Report EUR 10979, Commission of the European Communities, Brussels, Belgium, 1987.
- 7 HOBBS, J. M., SATTARY, J. A. and MAXWELL, A. D. Experimental data for the determination of 250 mm orifice meter discharge coefficients under different installation conditions (European programme). Report EUR 10980, Commission of the European Communities, Brussels, Belgium, 1987.
- 8 HOBBS, J. M. The EEC orifice plate project, part II: critical evaluation of data obtained. Progress Report No PR5: EUEC/17. East Kilbride, Glasgow: National Engineering Laboratory, 1987.
- 9 SATTARY, J. A. and SPEARMAN, E. P. Experimental data for the determination of basic 600 mm orifice meter discharge coefficients - European programme. Progress Report No PR11: EUEC/17 (EEC005). East Kilbride, Glasgow: National Engineering Laboratory Executive Agency, 1992.
- 10 SATTARY, J. A., SPEARMAN, E. P. and READER-HARRIS, M. J. Experimental data for the determination of basic 50 mm orifice meter discharge coefficients - European programme. Progress Report No PR12: EUEC/17 (EEC005). East Kilbride, Glasgow: National Engineering Laboratory Executive Agency, 1992.
- 11 SPEARMAN, E. P., SATTARY, J. A. and READER-HARRIS, M. J. The EEC orifice plate project: index to the data tables. Progress Report No PR13: EUEC/17 (EEC005). East Kilbride, Glasgow: National Engineering Laboratory Executive Agency, 1992.
- 12 READER-HARRIS, M. J., SATTARY, J. A. and SPEARMAN, E. P. The orifice plate discharge coefficient equation. Progress Report No PR14: EUEC/17 (EEC005). East Kilbride, Glasgow: National Engineering Laboratory Executive Agency, 1992.
- 13 READER-HARRIS, M. J. The tapping terms in the orifice plate discharge coefficient formula. Progress Report No PR8: EUEC/17. East Kilbride, Glasgow: National Engineering Laboratory, 1990.
- 14 READER-HARRIS, M. J. and SATTARY, J. A. The orifice plate discharge coefficient equation. Flow measurement and Instrumentation, 1, 67-76, 1990.
- 15 STOLZ, J. An approach towards a general correlation of discharge coefficients of orifice plate meters. In Proc. of Fluid flow measurement in the mid 1970s, National Engineering Laboratory, East Kilbride, Glasgow, Paper K-1, 1975.
- 16 STOLZ, J. A universal equation for the calculation of discharge coefficients of orifice plates. In Flow Measurement of Fluids, H. H. Dijkstra and E. A. Spencer (eds), pp 519-534. North Holland Publishing Company, 1978.
- 17 TEYSSANDIER, R. G. and HUSAIN, Z. D. Experimental investigation of an orifice meter pressure gradient. Transactions of the ASME. J. Fluids Engineering, 109, pp 144-148, 1987.

- 18 JOHANSEN, F. C. Flow through pipe orifices at low Reynolds numbers. Aeron. Res. Committee, Report and Memo No 1252. London: HM Stationery Office, 1930.
- 19 ENGEL, F. V. A. Durchflußmessung in Rohrleitungen. Bericht über ein Symposium in East Kilbride (Schottland). Brennstoff-Wärme-Kraft, 13, pp 125-133, 1961.
- 20 ENGEL, F. V. A. New interpretations of the discharge characteristics of measuring orifices - an approach to improved accuracy. ASME paper 62-WA-237. New York: American Society of Mechanical Engineers, 1962.
- 21 2-Inch orifice plate investigation for Commission of the European Communities Directorate General for Science Research and Development Community Bureau of Reference. Report EEC004. East Kilbride, Glasgow: National Engineering Laboratory Executive Agency, 1991.
- 22 INTERNATIONAL ORGANIZATION FOR STANDARDIZATION. Measurement of fluid flow by means of orifice plates, nozzles and Venturi tubes inserted in circular cross-section conduits running full. ISO 5167-1, Geneva: International Organization for Standardization, 1991.
- 23 HOBBS, J. M. Determination of the effects of orifice plate geometry upon discharge coefficients. Report No: ORIF/01. East Kilbride, Glasgow: National Engineering Laboratory, 1989.
- 24 READER-HARRIS, M. J. The effect of pipe roughness on orifice plate discharge coefficients. Progress Report No PR9: EUEC/17 (EEC005). East Kilbride, Glasgow: National Engineering Laboratory, 1990.

T A B L E 1

GENERAL INFORMATION ABOUT THE ANALYSIS OF RESIDUALS IN TABLES 2 TO 4

For each cell, line 1 - Mean per cent error
 line 2 - Per cent standard deviation
 line 4 - Number of observations
 line 5 - Per cent standard deviation to model.

For the i^{th} point in a cell Per cent error, $P_i = \frac{(C_{im} - C_{ie})}{C_{im}} \times 100$,

where C_{im} is the measured discharge coefficient of the i^{th} point and C_{ie} is the corresponding discharge coefficient from equation (24).

$$\text{Mean per cent error, } \mu = \frac{\sum_{i=1}^N P_i}{N}$$

where N is the number of points in the cell.

$$\text{Per cent standard deviation} = \left(\frac{\sum_{i=1}^N (P_i - \mu)^2}{N - 1} \right)^{\frac{1}{2}}$$

$$\text{Per cent standard deviation to model} = \left(\frac{\sum_{i=1}^N P_i^2}{N} \right)^{\frac{1}{2}}$$

Statistics for the entire population appear in the bottom right hand cell.

T A B L E 2

RESIDUALS FROM EQUATION (24) AS A FUNCTION OF β AND D

D (mm) β	50	75	100	150	250	600	Summary by β
0.100 (0.0991 to 0.1028)	0.000	0.000	0.000	-0.060	0.060	0.000	-0.001
	0.000	0.000	0.000	0.230	0.270	0.000	0.257
	-	-	-	-	-	-	-
	0	0	0	81	79	0	160
	0.000	0.000	0.000	0.237	0.274	0.000	0.256
0.200 (0.1982 to 0.2418)	0.055	-0.435	-0.125	0.094	-0.020	0.176	-0.005
	0.462	0.125	0.226	0.106	0.186	0.238	0.305
	-	-	-	-	-	-	-
	507	57	645	111	714	394	2428
	0.465	0.452	0.258	0.141	0.187	0.296	0.305
0.375 (0.3620 to 0.3748)	0.184	-0.197	-0.012	0.123	-0.119	0.022	0.015
	0.303	0.099	0.259	0.254	0.159	0.113	0.241
	-	-	-	-	-	-	-
	444	106	429	133	439	591	2142
	0.354	0.220	0.259	0.281	0.198	0.115	0.242
0.500 (0.4825 to 0.5003)	0.065	0.027	0.099	0.040	0.001	-0.101	0.004
	0.294	0.055	0.198	0.100	0.164	0.119	0.205
	-	-	-	-	-	-	-
	398	69	285	109	392	526	1779
	0.300	0.061	0.221	0.107	0.163	0.156	0.205
0.570 (0.5427 to 0.5770)	-0.024	0.050	0.010	-0.049	0.059	-0.110	0.001
	0.386	0.076	0.232	0.109	0.258	0.120	0.249
	-	-	-	-	-	-	-
	348	72	992	136	1123	567	3238
	0.386	0.091	0.233	0.120	0.264	0.162	0.249
0.660 (0.6481 to 0.6646)	-0.025	0.119	-0.007	-0.120	0.072	-0.123	-0.015
	0.287	0.102	0.236	0.128	0.190	0.151	0.224
	-	-	-	-	-	-	-
	498	64	627	92	823	643	2747
	0.287	0.156	0.236	0.175	0.203	0.195	0.225
0.750 (0.7239 to 0.7509)	-0.023	0.114	0.105	0.097	-0.005	-0.238	0.005
	0.322	0.105	0.312	0.203	0.315	0.359	0.326
	-	-	-	-	-	-	-
	866	101	971	130	1478	336	3882
	0.322	0.155	0.329	0.225	0.315	0.430	0.326
Summary by D	0.031	-0.045	0.013	0.027	0.011	-0.063	0.001
	0.353	0.210	0.266	0.192	0.250	0.217	0.269
	-	-	-	-	-	-	-
	3061	469	3949	792	5048	3057	16376
	0.354	0.215	0.266	0.194	0.251	0.226	0.269

T A B L E 3

RESIDUALS FROM EQUATION (24) AS A FUNCTION OF D AND PAIR OF TAPPINGS

Tappings D (mm)	Corner (ISO)	Flange	D&D/2	Corner (GU)	Summary by D
50	0.080	0.013	0.020	0.000	0.031
	0.403	0.310	0.383	0.000	0.353
	-	-	-	-	-
	728	1605	728	0	3061
	0.410	0.311	0.383	0.000	0.354
75	0.000	-0.045	0.000	0.000	-0.045
	0.000	0.210	0.000	0.000	0.210
	-	-	-	-	-
	0	469	0	0	469
	0.000	0.215	0.000	0.000	0.215
100	-0.003	-0.002	0.061	0.000	0.013
	0.224	0.254	0.323	0.000	0.266
	-	-	-	-	-
	1084	1932	933	0	3949
	0.224	0.254	0.328	0.000	0.266
150	0.000	0.027	0.000	0.000	0.027
	0.000	0.192	0.000	0.000	0.192
	-	-	-	-	-
	0	792	0	0	79
	0.000	0.194	0.000	0.000	0.19
250	0.042	-0.027	0.006	0.056	0.011
	0.237	0.210	0.266	0.305	0.250
	-	-	-	-	-
	1155	1841	1167	885	5048
	0.241	0.212	0.266	0.310	0.251
600	-0.153	0.025	-0.061	-0.084	-0.063
	0.213	0.171	0.217	0.256	0.217
	-	-	-	-	-
	828	876	1130	223	3057
	0.262	0.173	0.226	0.269	0.226
Summary by Tappings	-0.006	-0.001	-0.003	0.028	0.001
	0.281	0.242	0.296	0.301	0.269
	-	-	-	-	-
	3795	7515	3958	1108	16376
	0.281	0.242	0.296	0.302	0.269

T A B L E 4

RESIDUALS FROM EQUATION (24) AS A FUNCTION OF Re_D AND β

Re_D β	100 to 4000	4000 to 10^4	10^4 to 10^5	10^5 to 10^6	10^6 to 10^7	10^7 to 10^8	Summary by β
0.100 (0.0991 to 0.1028)	-0.111	0.069	0.038	0.000	0.000	0.000	-0.001
	0.183	0.243	0.293	0.000	0.000	0.000	0.257
	-	-	-	-	-	-	-
	52	49	59	0	0	0	160
	0.213	0.250	0.293	0.000	0.000	0.000	0.256
0.200 (0.1982 to 0.2418)	-0.003	-0.026	-0.082	0.030	0.249	0.000	-0.005
	0.552	0.370	0.246	0.167	0.169	0.000	0.305
	-	-	-	-	-	-	-
	237	238	1190	447	316	0	2428
	0.551	0.370	0.259	0.170	0.301	0.000	0.305
0.375 (0.3620 to 0.3748)	0.444	0.207	-0.012	-0.092	0.033	0.066	0.015
	0.493	0.286	0.199	0.147	0.085	0.083	0.241
	-	-	-	-	-	-	-
	125	133	748	671	325	140	2142
	0.662	0.352	0.199	0.174	0.091	0.106	0.242
0.500 (0.4825 to 0.5003)	0.027	-0.055	0.065	0.042	-0.128	-0.095	0.004
	0.769	0.247	0.182	0.167	0.136	0.086	0.205
	-	-	-	-	-	-	-
	33	83	436	773	205	249	1779
	0.758	0.252	0.193	0.173	0.186	0.128	0.205
0.570 (0.5427 to 0.5770)	-0.507	-0.320	-0.020	-0.009	0.064	0.008	0.001
	0.965	0.361	0.238	0.196	0.272	0.225	0.249
	-	-	-	-	-	-	-
	18	59	502	1420	776	463	3238
	1.066	0.480	0.238	0.196	0.279	0.225	0.249
0.660 (0.6481 to 0.6646)	-0.030	-0.296	-0.069	0.035	0.045	-0.087	-0.015
	0.116	0.391	0.283	0.203	0.187	0.180	0.224
	-	-	-	-	-	-	-
	5	35	466	1110	471	660	2747
	0.108	0.486	0.291	0.206	0.192	0.200	0.225
0.750 (0.7239 to 0.7509)	0.000	0.353	-0.067	0.042	-0.018	-0.038	0.005
	0.000	0.443	0.339	0.299	0.310	0.358	0.326
	-	-	-	-	-	-	-
	0	78	615	1668	1045	476	3882
	0.000	0.565	0.345	0.302	0.310	0.360	0.326
Summary by Re_D	0.086	0.027	-0.039	0.013	0.037	-0.043	0.001
	0.593	0.392	0.257	0.225	0.260	0.239	0.269
	-	-	-	-	-	-	-
	470	675	4016	6089	3138	1988	16376
	0.599	0.393	0.260	0.226	0.263	0.243	0.269

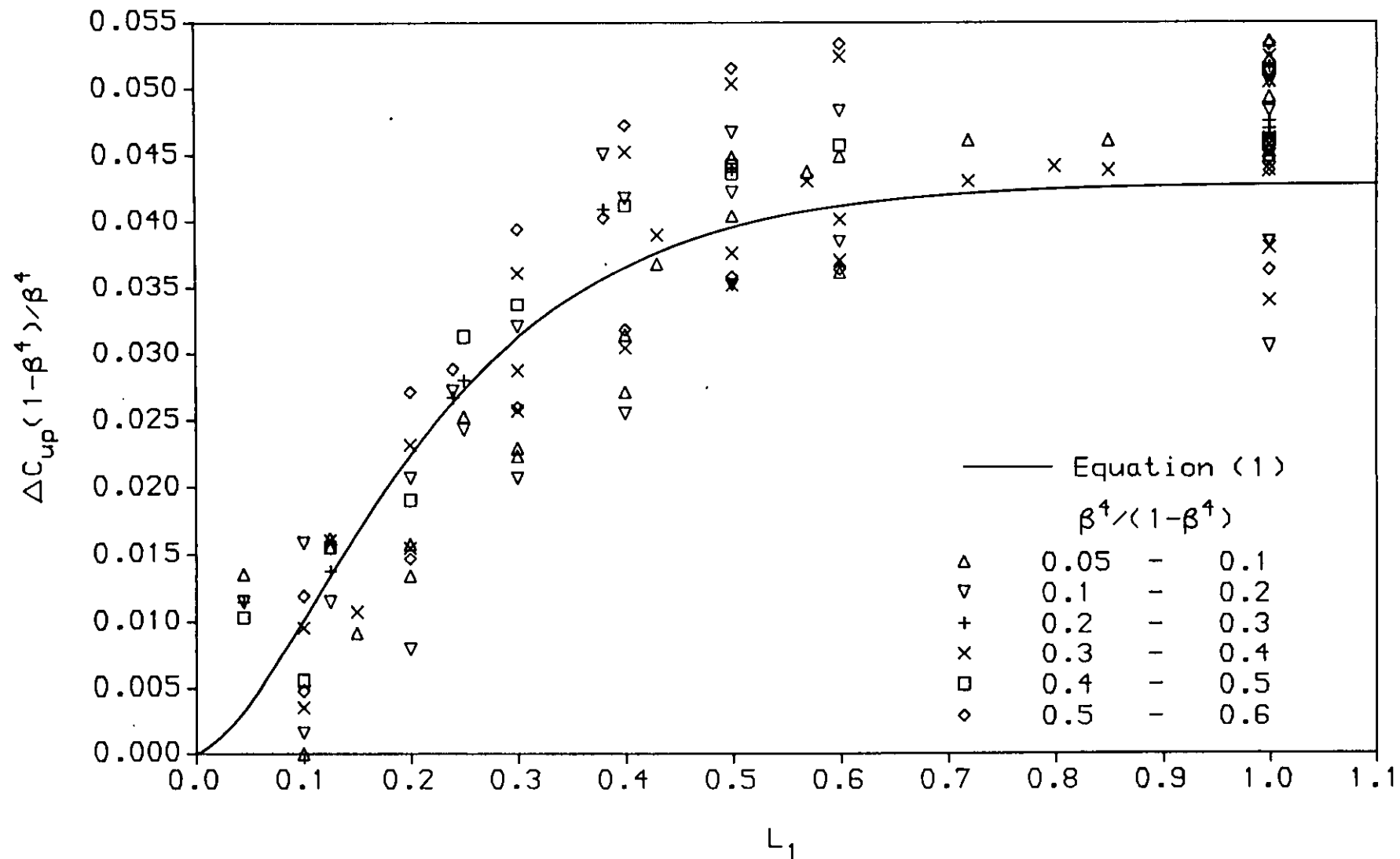


FIG 1 Upstream tapping term as a function of L_1

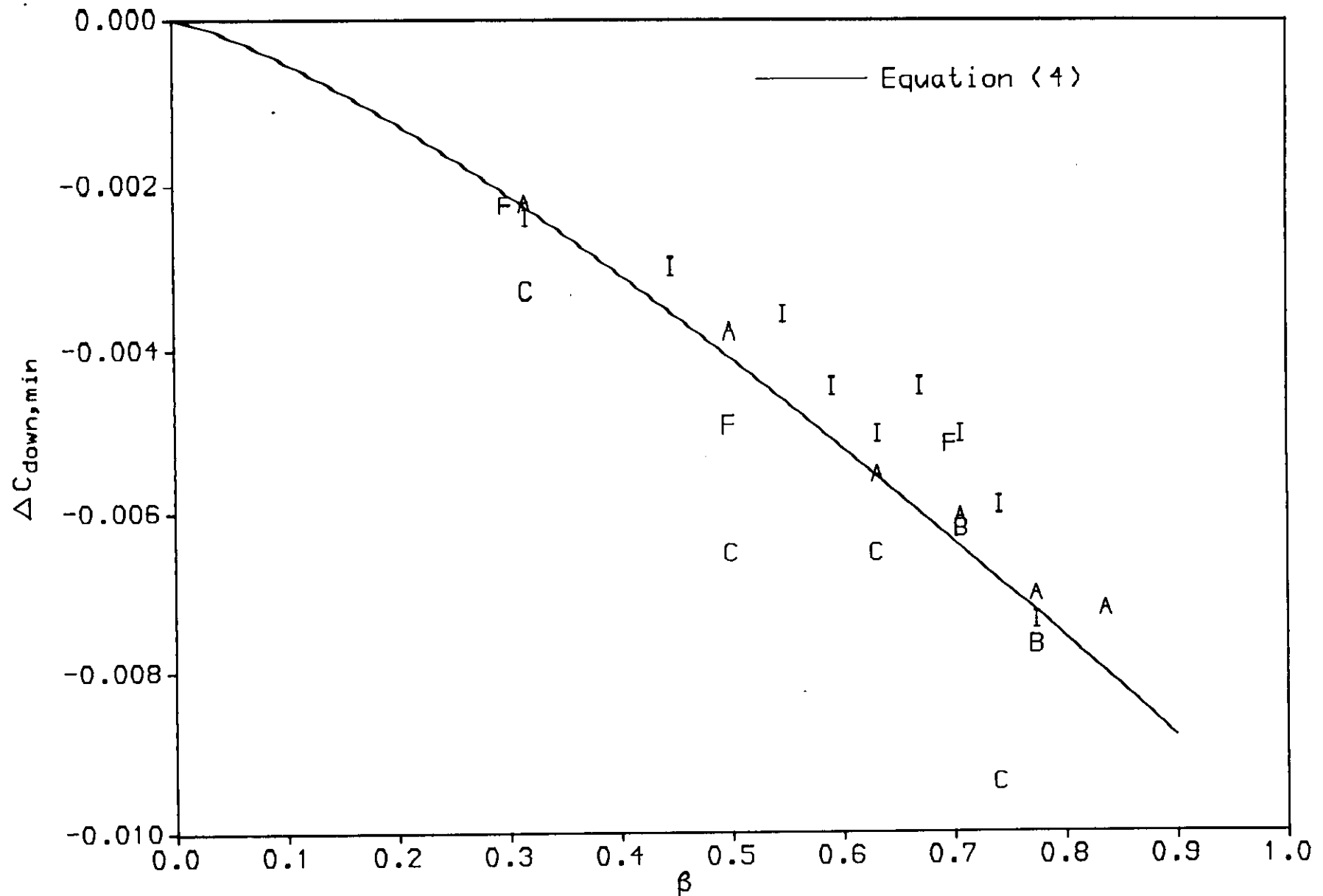


FIG 2 Downstream tapping term at the pressure minimum

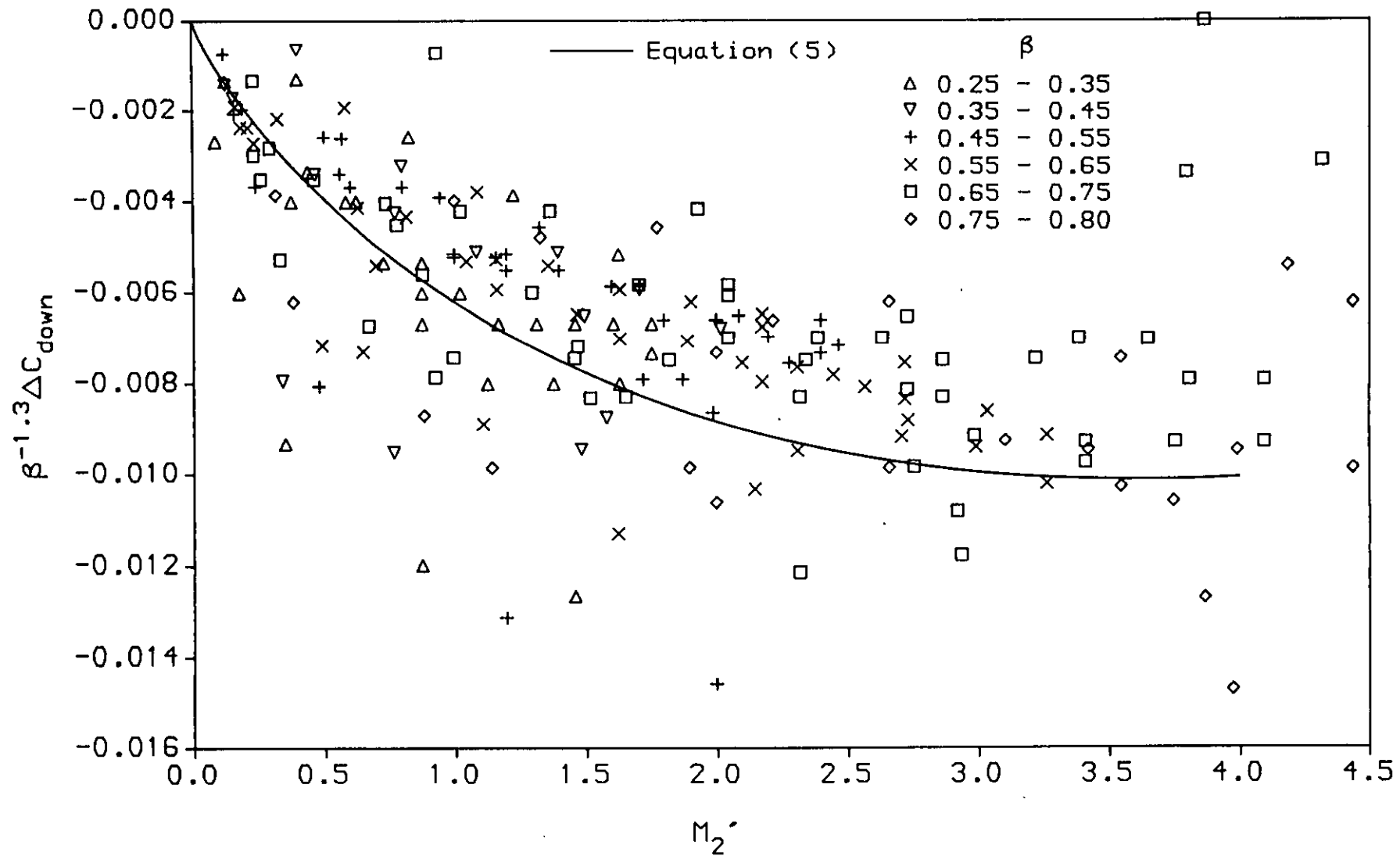


FIG 3 Downstream tapping term as a function of M_2'

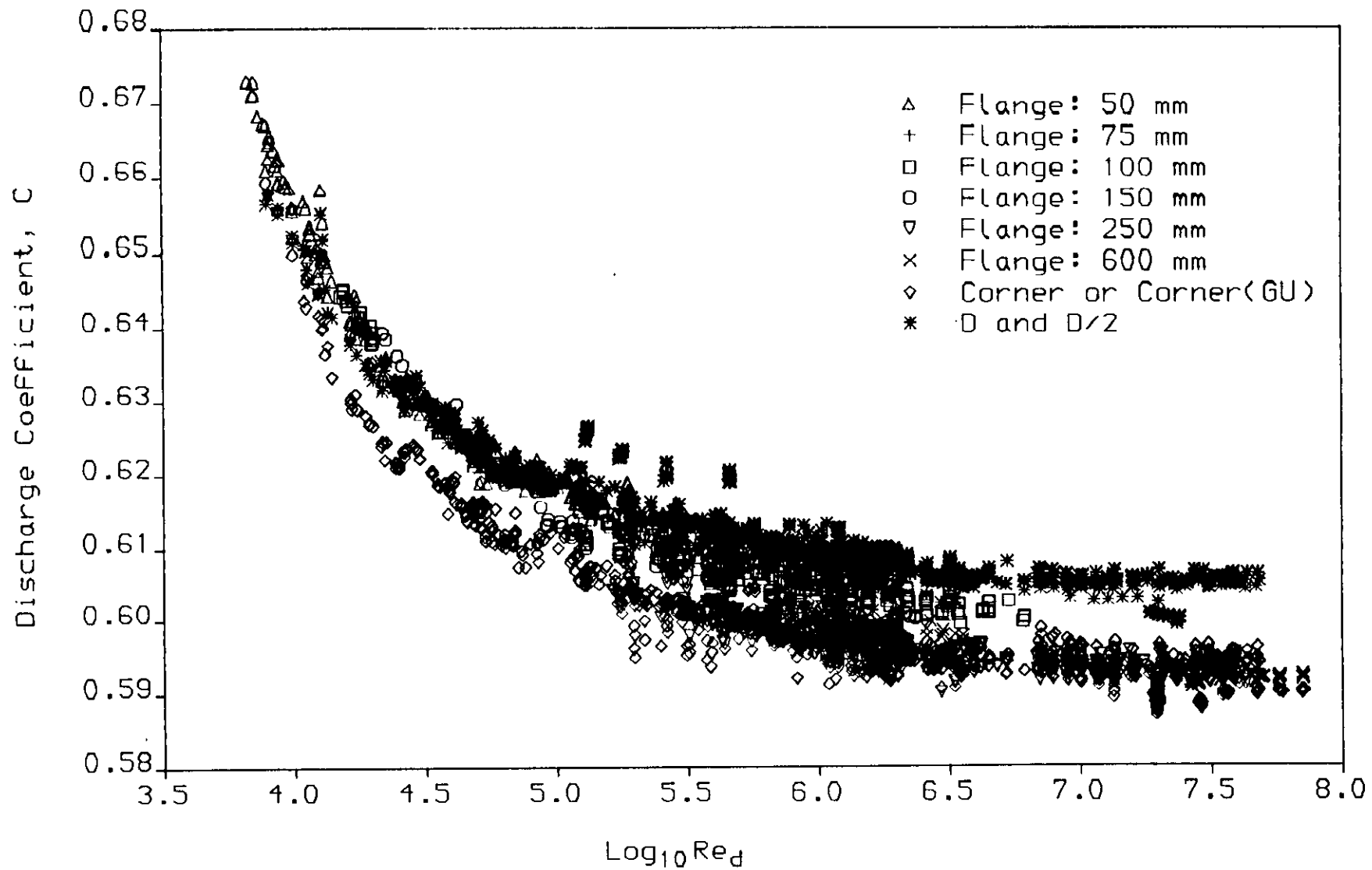


FIG 4 All data for $\beta = 0.74$

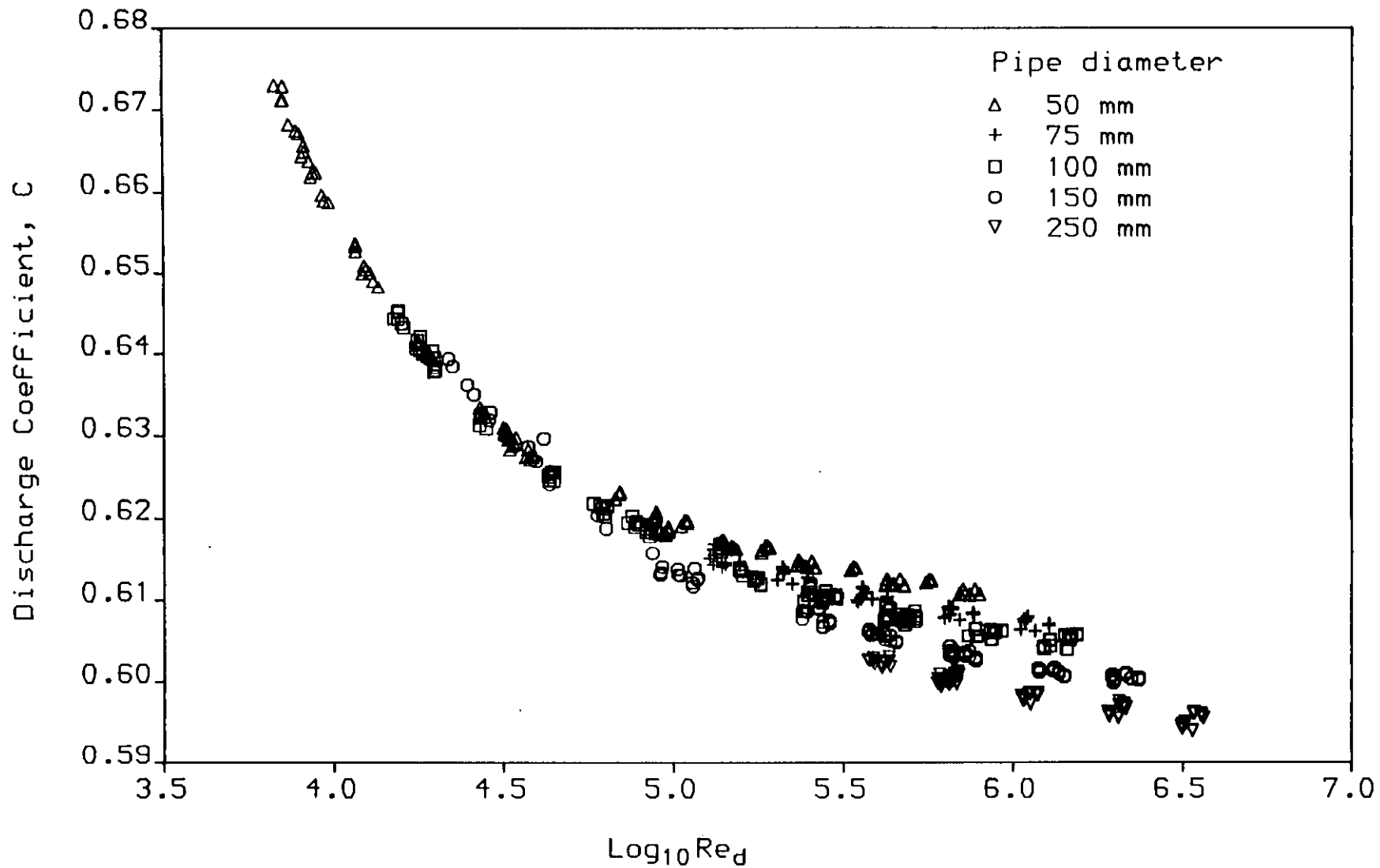


FIG 5 US data (Flange tappings) for $\beta = 0.74$

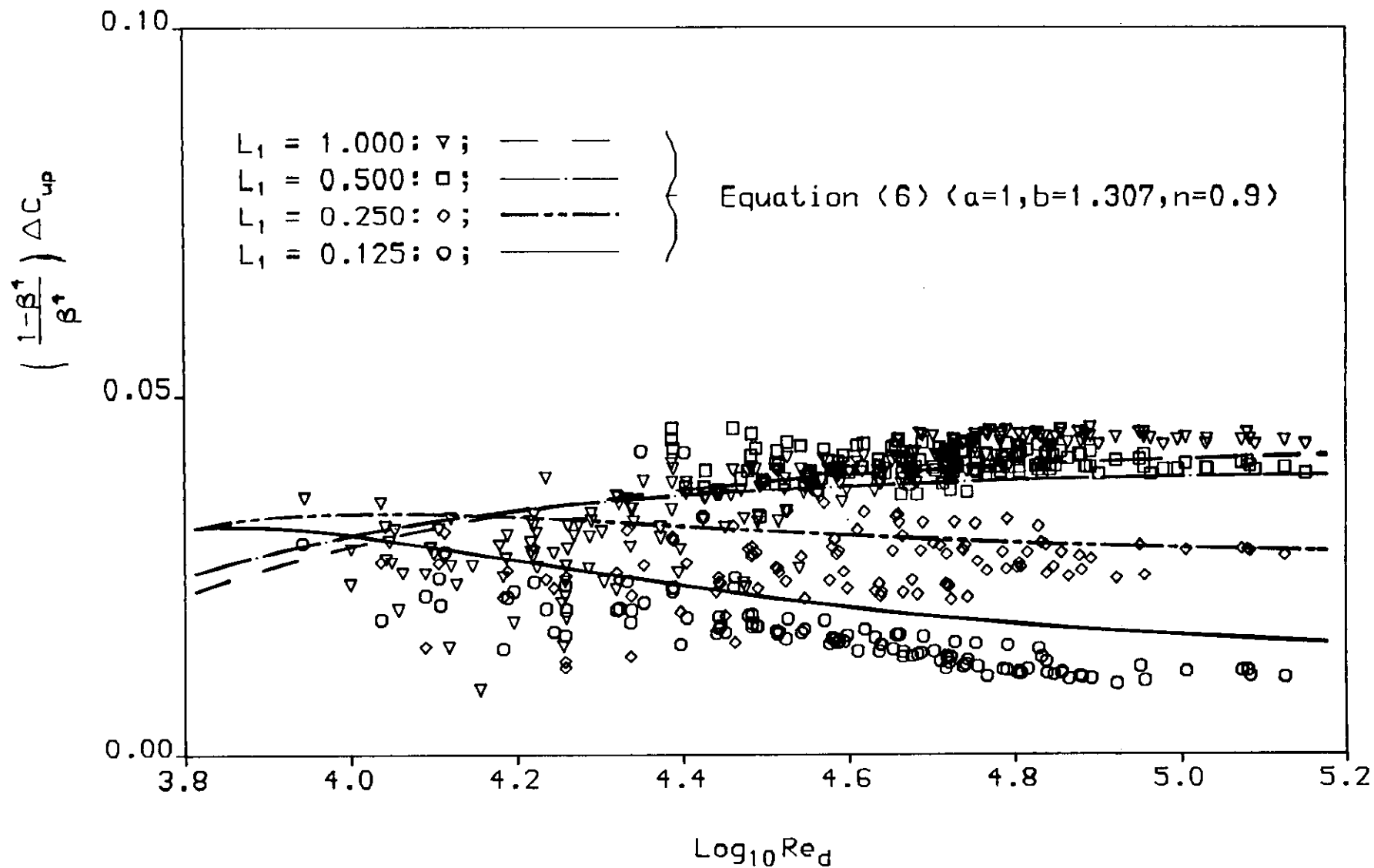


FIG 6 Upstream Tapping Term for low Re_d

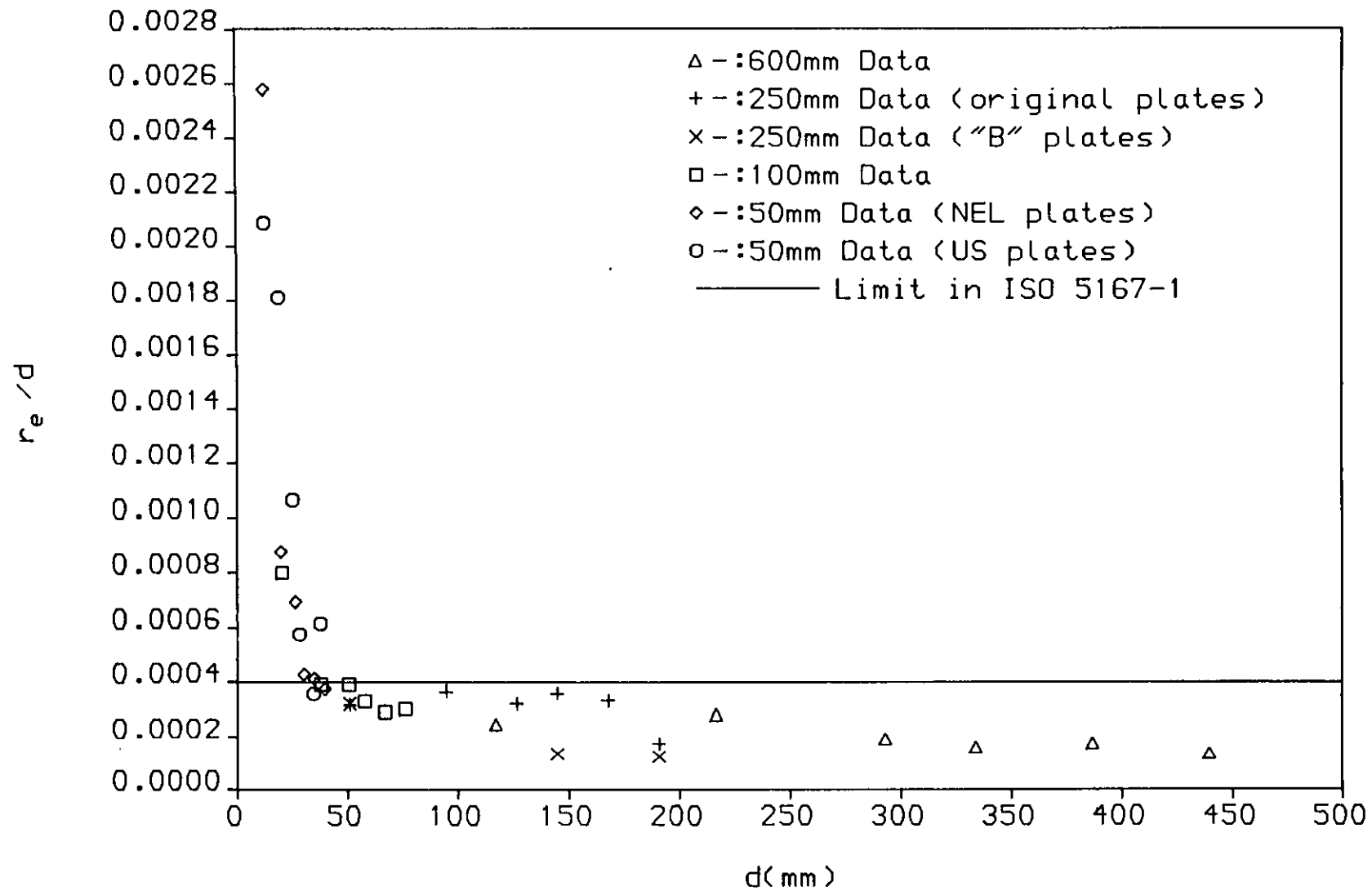


FIG 7 r_e/d as a function of d

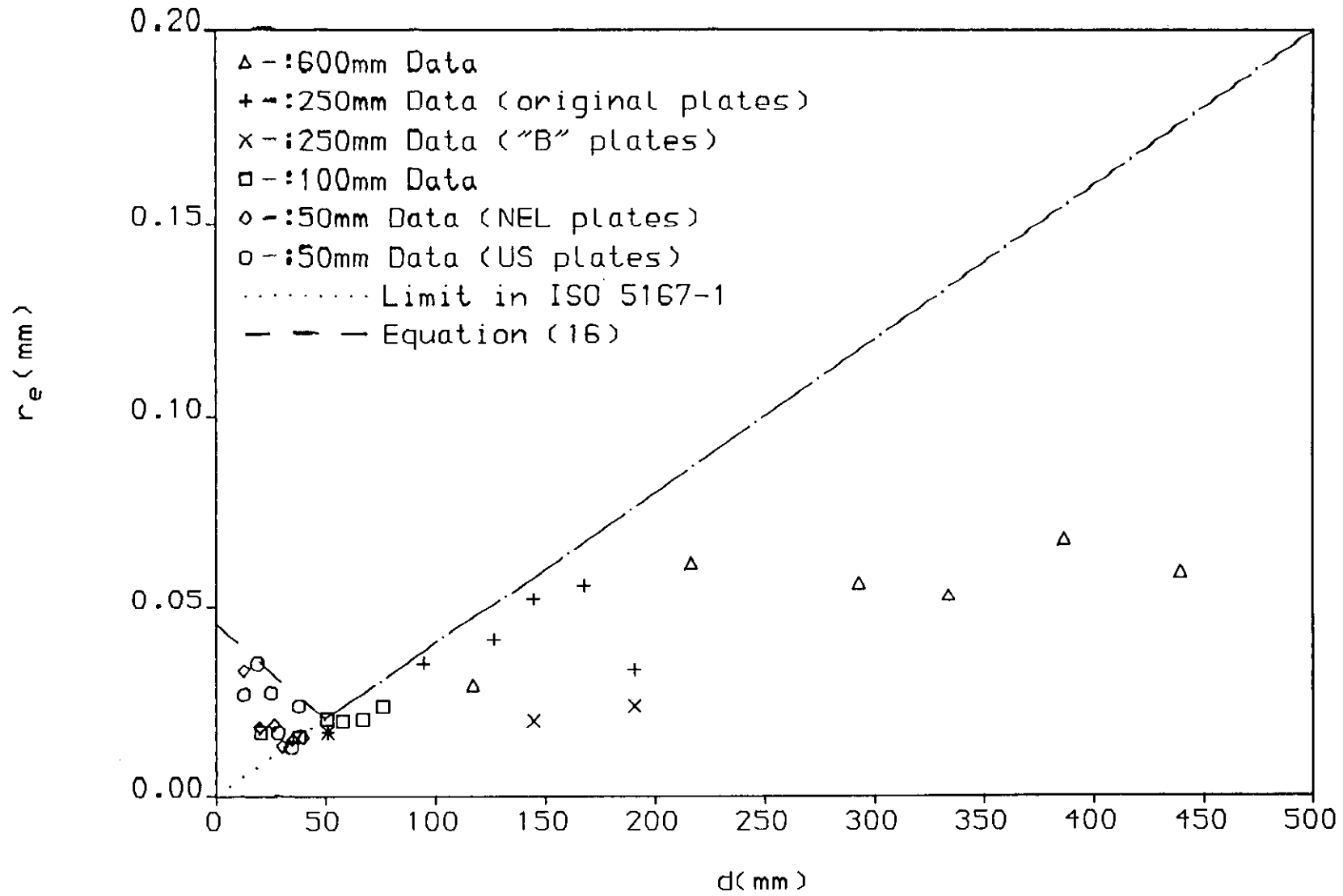


FIG 8 r_e as a Function of d

ORIFICE METERING RESEARCH - A USER'S PERSPECTIVE

by

J E Gallagher, Shell USA and R E Beaty, Amoco USA

Paper 1.2

NORTH SEA FLOW MEASUREMENT WORKSHOP
26-29 October 1992

NEL, East Kilbride, Glasgow

ORIFICE METERING RESEARCH - A USER'S PERSPECTIVE

J. E. Gallagher, P.E. - Shell, USA

R. E. Beaty - Amoco, USA

SUMMARY

International cooperation for concentric, square-edged orifice discharge coefficient research between North America and Western Europe is presented in light of A.G.A. Report No. 3's adoption of a new discharge coefficient equation.

Current North American research projects are headed towards various solutions on orifice metering installation effects. Interpretation of the results from the authors' viewpoints is discussed along with two recommended methods for determining the proper location of A.G.A. tube bundles.

The application of in situ calibration of flowmeters is discussed from a global perspective. Substantive issues concerning the application of sonic nozzles, gas piston prover development, utilization and performance are presented from an holistic viewpoint.

Several physical properties are required for fiscal calculations of natural gas - compressibility, absolute viscosity, isentropic exponent, CSTAR for sonic nozzles and calorific value. A summary of the current status is presented along with additional user needs.

The orifice meter has a long history of use and experimentation. Because of this, it sometimes may be perceived as outdated, inaccurate and unreliable. In reality the opposite is true. To illustrate this viewpoint, loss control performance is presented for several pipeline systems transporting compressible fluids.

Incentives are presented for additional research and standards development from an operator's perspective.

NOTATION

Beta	diameter ratio, (d_f/D_f)
CSTAR	critical flow factor for gas flowing through a sonic nozzle
d_f	orifice plate bore diameter at flow conditions
D_f	meter tube internal diameter at flowing conditions
D	nominal pipe diameter

EV	velocity of approach factor
k_p	perfect isentropic exponent
L1	distance from flow disturbance to flowmeter in nominal pipe diameters
L2	distance from piping disturbance to inlet of flow conditioner in nominal pipe diameters
L3	distance from outlet of flow conditioner to flowmeter in nominal pipe diameters
LC	length of flow conditioner in nominal pipe diameters
ρ_w	fluid density at flowing temperature and pressure
ρ_b	fluid density at base conditions

1 INTRODUCTION

The North American natural gas industry produces, transports, and distributes approximately 700 billion cubic meters of gas each year (25 trillion standard cubic feet). The Western European market transports and distributes 250 billion cubic meters of gas each year (9 trillion standard cubic feet). Because of the importance of gas measurement for industry operations and fiscal accountability, it is essential that metering be accurate, reliable, and cost efficient over a range of conditions.

All of this gas is measured at least once, and most of it several times, in meter sizes ranging from 25 - 900 mm (1 - 36 inches), at pressures from below atmospheric to 14 MPa (2,000 psi), at temperatures from 0 - 100 degC (32 - 212 degF), with several types of meters. For large volume flow applications utilize orifice and turbine meters. Rotary and diaphragm meters are generally used for lower flow applications. Ultrasonic, vortex, insertion turbine, integral orifice meter, and others are chosen for specialty applications.

The orifice meter remains the predominant meter for natural gas production, large volume natural gas flow applications and chemical metering applications (Figure 1). In fact, it is currently estimated that over 600,000 orifice meters in North America are being used for custody transfer and allocation measurement applications associated with the petroleum, chemical and gas industries.

As a result, the current focus of today's measurement community is lower uncertainty levels through an efficient and effective program. One goal is to minimize the uncertainty associated with "non-ideal" flow conditions. A second goal is improved predictive capabilities of the natural gas' physical and transport properties. A third goal is to provide pragmatic alternatives towards lower uncertainties through in-situ calibration of meters, centralized calibration of meters, and/or installation of dissimilar meters in

series.

2 WORLDWIDE DISCHARGE COEFFICIENT EQUATION

The greatest series of orifice coefficient of discharge data completed prior to 1980 was conducted at Ohio State University (OSU) under the direction of Professor S. T. Beitler. All of these experiments were conducted between 1932 and 1933 on water using seven pipe diameter ranging from 25 to 350 mm (1 to 14 inches). It is important to note that the experiments were conducted before the existence of any national or international orifice metering standard. The OSU data base was adopted by Dr. Edgar Buckingham and Mr. Howard Bean to derive mathematical equations to predict the flow coefficient for orifice meters. Pioneers like Buckingham and Bean developed excellent equations based on the data at that time.

A joint committee from the American Gas Association (A.G.A.) the American Petroleum Institute (API) and International Standards Organization (ISO) was formed in the early 1970's to investigate perceived problems with the OSU data base. Jean Stolz from France and Wayne Fling from the United States collaborated in the data base assessment. They discovered upon analysis of the OSU data that only 303 of the data points were technically defensible.

In 1978, Jean Stolz derived an empirical orifice discharge coefficient equation which physically linked near field pressure tappings. This innovative equation was based on the OSU 303 data set for flange and radius tappings. The corner tap data was obtained from Witte's corner tap experiments conducted in the 30s. In 1980, the Stolz equation was adopted by ISO 5167 replacing the Buckingham equation.

In 1981, recognizing the small amount of definitive data available, the Commission of European Communities (EC) and the United States simultaneously initiated a multimillion dollar program to develop an empirical discharge coefficient data base for concentric, square edged orifice meters. The original EC experimental pattern covered corner, radius and flange pressure tappings at nine laboratories on two sizes of meter tubes - 100 and 250mm. The EC added two additional meter sizes in the mid 80s - 50mm and 600mm. In the United States, a project undertaken by the API and the Gas Processors Association (GPA) investigated flange pressure tappings at two laboratories on five sizes of meter tubes - 50, 75, 100, 150 and 250mm.

The EC and API/GPA data were collected using oil, water, natural gas and air as the test media. The meter tubes used in the test were manufactured from commercial pipe. The criteria for the experiments was a uniform fully developed velocity profile. When the data base was combined into a regression data set, the US and EC experiments yielded highly compatible data.

Orifice Metering Research - A User's Perspective

In 1988, international cooperation between the North American and EC flow measurement experts resulted in unanimous acceptance of the equation form proposed by Reader-Harris of the United Kingdom's National Engineering Laboratory with two amendments by Gallagher. The combined EC and API/GPA experimental pattern was well balanced so that the data could be accurately evaluated for corner, flange and radius tappings. The Reader-Harris/Gallagher (RG) equation was regressed using this combined data set of 10,152 corner, flange and radius tap points. At the instruction of API's Board of Directors, this equation was balloted and subsequently adopted into the latest revision of A.G.A. Report No. 3 (ANSI 2530/API MPMS 14.3/GPA 8185) published in 1990.

Since the regression of the RG equation, additional EC discharge coefficient data on oil, water and natural gas has been accumulated on 50 and 600mm meter sizes. To date, none of the additional flange tapped data has fallen outside the predicted uncertainty of the RG equation. The RG equation could be updated to reflect the additional data. However, no equation is expected to significantly improve the prediction results for flange tappings.

3 FLOW CONDITIONS

All flowmeters are subject to the effects of velocity profile, swirl and turbulence structure approaching the meter. The meter calibration factors or empirical coefficients calculated from the discharge coefficient equations are valid only if similarity exists between the metering installation and the experimental data base. These parameters should not be significantly different from those at the time of meter calibration, or from those which existed in the empirical coefficients of discharge data base. Technically this is termed the Law of Similarity.

Many piping configurations and fittings generate disturbances with unknown characteristics. Even a simple elbow can generate very different flow conditions from "ideal" or "fully developed" flow. In reality, multiple piping configurations are assembled in series generating complex problems for standard writing organizations and flow metering engineers. The problem is to minimize the difference between "real" and "fully developed" flow conditions on the selected metering device to maintain a low uncertainty associated with the fiscal application. For clarity, we will refer to this as "pseudo-fully developed" flow.

A method to circumvent the influence of the fluid dynamics (swirl, profile and turbulence) on the meter's performance is to install a flow straightener in combination with straight lengths of pipe to "isolate" the meter from upstream piping disturbances. Of course, this isolation is never perfect. After all, the straightener's objective is to produce a "pseudo-fully developed" flow.

In general, upstream piping elements may be grouped into the following categories -

- * those that distort the mean velocity profile but produce little swirl
- * those that both distort and generate bulk swirl

With respect to installation effects and the near term flow field, the correlating parameters which impact similarity for orifice meters are summarized in Figure 2.

3.1 Fully Developed Flow

The classical definition for fully developed turbulent flow is stated by Hinze as follows -

"For the fully developed turbulent flow in the pipe the mean-flow conditions are independent of the axial coordinate, x and axisymmetric, assuming a uniform wall condition."

From a practical standpoint, we generally refer to fully developed flow in terms of axisymmetric velocity profile which is in accordance with the Power Law or Law of the Wall prediction. However, one must not forget that fully developed turbulent flow requires equilibrium of the forces to maintain the random "cyclic" motions of turbulent flow. This requires that the velocity profile, turbulence intensity, wall shear stress, Reynolds stresses, etc., are constant with respect to the axial position.

The dependence of the turbulence in the outer region (or pipe core) on upstream condition points toward a "long memory" of the flow in this region. In contrast, the inner region (or pipe wall) has a "shorter memory". Consequently, the recovery from any disturbance of the inner region will be much quicker than that for the outer region. Also, we cannot forget the interdependence of the two regions.

3.2 Types of Flow Conditioners

Flow conditioners may be grouped into three general classes based on their ability to correct the mean velocity profile, bulk swirl and turbulence structure (Figure 3).

The first class of straighteners is designed to primarily counteract swirl by splitting up the flow into a number of parallel conduits. This class of straighteners includes A.G.A. radial tube bundles, A.G.A. hexagonal tube bundles, ISO 5167 tube bundles, AMCA's honeycomb and the Etoile (Figure 4).

The second class of straighteners is designed to generate an axisymmetric velocity profile distribution by subjecting the flow to a single or a series of perforated grids or plates. The profile is redistributed by use of the blockage factor or porosity of the flow conditioner. This class of straighteners includes the Sprengle, Zanker and Mitsubishi designs.

The third class of straighteners are designed to generate a "pseudo-fully developed" velocity profile distribution through porosity of the straightener and the generation of a turbulence structure. The turbulence structure is generated by varying the radial porosity distribution. This class of straighteners includes the Sens and Teule, Bosch and Hebrard, K-Lab and Laws designs (Figure 5).

The optimal flow conditioner has the following design objectives:

- * elimination of swirl
- * production of axisymmetric, pseudo-fully developed mean velocity profile
- * production of pseudo-fully developed turbulence structure
- * low pressure drop across the flow conditioner
- * rigorous towards mechanical damage
- * low fabrication and construction costs

In achieving these objectives, the flow conditioner cannot and will not maintain fully developed turbulent flow with respect to the axial position. The reason is fundamentally simple - *the random cyclic forces are not controlled by the conditioner for self-maintenance of the velocity profile with respect to the axial position.*

All flow conditioners have the following shared geometrical limitations -

- * A minimum distance between the upstream piping elements and the inlet of the straightener to ensure that the straightener performance is optimized.
- * A minimum distance between the outlet of the straightener and the flow meter to ensure that the straightener does not act as a disturbance.

These shared geometrical limitations are based on Prandtl's Mixing Length Theory.

4 INSTALLATION RESEARCH

Historically, flow conditioners have defined an acceptable uncertainty of +/- 0.50 percent due to piping elements. The original research of A.G.A. on orifice meter effects could not discern effects below this level due to the limitation of the research equipment in the 30s, 40s, 50s and 60s.

With the birth of microchip technology, large steps towards lowering the uncertainty are possible due to the advent of smart transmitters, sophisticated flow computers, personal computers, Computational Fluid Dynamics (CFD), thermal anemometry (TA) probes (i.e., hot wire, hot film, x-wire), Laser Doppler Velocimetry or Anemometry (LDV/LDA), characterization of flow meters in real time, high pressure gas piston provers, ultrasonic flowmeters, coriolis flowmeters, videoimagescopes, etcetera. These "new" tools are providing significant advances in the refinement of existing metering equipment as well as the birth of new technology.

The advent of LDV/LDA technology has provided a tool to perform three dimensional flow field measurements. This technology is capable of measuring three non-orthogonal velocity components simultaneously, resolving from those three independent orthogonal velocity components, and then computing the mean velocity vector, the time averaged Reynolds stress tensor, and other items associated with those values. In this manner, variations in the flow field (upstream and downstream of flow conditioners, flow meters, fittings, etc.) can be documented. The next step involves comparing these measurements to Computational Fluid Dynamics (CFD) predictive models such as Creare's FLUENT code. Through these comparisons the optimum turbulence model can be identified. The final results should have a predictive model which approximates the decay of distorted flow fields through flow conditioners and flow meters.

A fundamental understanding of the effects of upstream flow conditioning on flowmetering is essential for significant improvements. Recent LDV/LDA and TA probe research is attempting to provide a thorough understanding of the complex flow field. The LDV/LDA, or TA probe are tools which provide us with the needed insight to the microscopic flow field. Studies at NIST Gaithersburg (Mattingly and Yeh), Texas A&M (Morrison et. al.), NIST Boulder (Brennan, et. al.), SwRI (Morrow, Park et. al.), NOVA Husky (Karnik, et. al.), CERT (Gajan et. al.), NEL (Reader-Harris, et. al.), Gasunie, K-Lab (Wilcox et. al.) and others have recently measured mean velocity profiles and turbulence structure associated with upstream flow conditioning effects.

The optimum turbulence model does not currently exist for CFD installation effects' applications. Hopefully, existing and planned turbulence structure measurements and installation effects

research will provide future scientists with the needed insight for this development. Irrespective of this limitation, CFD technology will still be utilized to maximum the experimental pattern efficiency and to provide sensitivity analyses.

5 ORIFICE METER INSTALLATION EFFECTS

The goal of current orifice research programs is to focus on the effects of various installation conditions for natural gas applications. Since significant deviations from the Law of Similarity cause measurement errors, the main goal is to identify and quantify the error associated with these flow disturbances.

Present industry standards provide installation specifications for pipe length requirements and flow conditioner location upstream of orifice meters (A.G.A. 3/ANSI 2530/API MPMS 14.3 and ISO 5167). Unfortunately, considerable disagreement over straight length requirements exist between these two highly respected standards. Current upstream effects research has focused on assembling experimental data for evaluation of straight length requirements stated in the respective standards.

In North America, the design practice is to minimize the upstream piping and utilize A.G.A. tube bundles to provide "pseudo-fully developed" flow. Typical North American installations consist of 90 degree elbows or headers upstream of the orifice meter. Tube bundles are commonly used to eliminate swirl and distorted velocity profiles. In Western Europe, the practice is to utilize long upstream lengths to generate "pseudo-fully developed" flow. Because of these design differences, the current research programs do not fully complement each other in their direction.

5.1 Flow Conditioner Location

Gas Research Institute's Meter Research Facility (MRF), located at Southwest Research Institute (SwRI) in Texas, was constructed to carry out definitive research in key flow metrology areas for the natural gas industry. In light of this charter, SwRI is conducting a series of experiments to address the user community concerns.

The sliding vane technique is essential to the efficient and effective research program at SwRI. This technique relocates the tube bundle without venting the meter run or disconnecting flanges, thereby saving considerable time and manpower without introducing additional laboratory uncertainties. Results for a 100mm tube clearly indicate the existence of a *cross-over zone* (Figure 6). Comparison of the results for an L1 of 100D and 45D indicate no perceptible difference in the *cross-over zone* between the two upstream lengths. These results are consistent with research data from several Western European flow laboratories. For example, the European Community (EC) program conducted at Gasunie and NEL

indicates the cross-over zone exists between 10 and 15D. However, when L1 is limited to 17D, a considerable shift in the cross-over zone is apparent (Figure 7).

Numerous research papers have attempted to specify the tube bundle location for zero additional uncertainty due to upstream installation effects. At times, the results between researchers have appeared to contradict each other. In an attempt to understand the physical cause for a cross-over, a number of researchers have measured the velocity profile and turbulence intensity at various positions in the upstream piping. Prior to these measurements, it was believed that swirl angle and velocity profile only were required to classify the approach flow as "pseudo-fully developed".

Velocity profile and turbulence measurements has provided key insights into understanding the flow field. Results have determined that the cross-over zone for a 90 degree elbow preceding the meter run's has a flatter profile than the allowance contained in ISO 5167. To date, it is evident that when the mean velocity profile downstream of the tube bundle was fully developed in accordance with ISO 5167 specifications, a significant orifice metering error existed. This implies that other factors contribute significantly to the orifice meter's flow field. The questions associated with this phenomena may be partly answered by the following postulates -

- * first order dependence on the type of upstream flow disturbance
- * first order dependence on the distance L3 (turbulence level, swirl angle, velocity profile, mixing length between the tube bundle and the flowmeter)
- * second order dependence on the distance L2 (turbulence level, swirl angle, velocity profile, mixing length between the disturbance and the flow conditioner)

In the authors' opinion, the turbulence structure generated by a flow disturbance has a significant impact on the cross-over zone associated with orifice meters. Apart from the measurements of Mattingly, Morrow, and Karnik, no turbulence measurements downstream of a tube bundle appears in the literature. Several researchers (Karnik, Morrison, etc.) have postulated a relationship exists between orifice metering error and the turbulent velocity field. Until further measurements are conducted on the physics of the flow downstream of conditioners (Reynolds stresses, mean and turbulent velocity field, integral length scales and the Taylor microscale), additional insight into this interaction is not

possible.

5.2 Pragmatic Solutions

The guiding principle of this section is to provide a systematic compilation of instructions and basic rules for the location of flow conditioners for new and existing orifice metering facilities.

To assist the user community, the authors propose two methods for determining the proper location of A.G.A. tube bundles - fixed location method and correlation method. The Beta should be limited to a range of 0.20 to 0.60 for both approaches.

For the first method, the authors recommend a fixed location for the tube bundle as follows:

- * a fixed L3 length of 11D
- * a minimum L2 length of 3D

For the second method, the authors propose a correlation which predicts the cross-over zone for A.G.A. tube bundle (19 tube radial design) flow conditioners. The correlation predicts the cross-over zone as a function of Beta, E_v , L1, and L3 for A.G.A. tube bundles (Figures 8 and 9). In the authors' opinion, a minimum L2 length of 3D is applicable for all flow conditioners. This requirement has been included in the correlation method.

Many factors affect the solutions to flow conditioning problems - economics, piping limitations, operating windows, etcetera. The options proposed by the authors provide pragmatic solutions to real problems for operators of orifice metering facilities (Figure 10 and 11). The user selection is based on economic justification to minimize the uncertainty associated with upstream conditions.

For example, in evaluating existing large volume installations (fixed L1 distance), the user could select any of the following options -

- * lower the Beta limit based on existing L3 length and the correlation method
- * relocate the existing flow conditioner using the correlation method
- or,
- relocate the flow conditioner to an L3 of 11D and a minimum L2 of 3D
- * install a new flow conditioner (Laws, etc.) with an L3 of 11D and a minimum L2 of 3D

Orifice Metering Research - A User's Perspective

- * calibrate the metering facility in situ with the current flow conditioner, orifice plate, and associated instrumentation
- * install a new flowmetering device

The options described above are listed in order of increasing capital expenditures. Please note that the authors consider it impractical to relocate existing manifolds and headers.

Using the methods described above, the authors have estimated the additional uncertainty due to flow disturbances. For Betas below 0.40, the uncertainty should not exceed +/- 0.10 percent and may be considered negligible. For Betas above 0.40 and below 0.60, the uncertainty should not exceed +/- 0.25 percent.

6 IN SITU CALIBRATION

6.1 Introduction

The first measurement standards were based on weight. Any commodity to be traded could be judged against a known weight to evaluate its true worth. With solids the procedure is relatively simple. However, liquids measured with this procedure require additional information if the data obtained is to be reported in traditional units. The additional information is the density of the fluid. To avoid measurement inequities, corrections are required for acceleration due to local gravity and air buoyancy. These correction converts observed weight to mass. It is obvious that this procedure is well suited for a laboratory environment.

Verifying the accuracy of flowmeters in specific applications has been one of the desires of the user community. Shop tests of orifice meters and turbine meters with various upstream configurations has been conducted for several years to aid in the design of high volume metering facilities. The question posed by the user community is - "Can the operator ensure the parties involved in the fiscal transfer that the measurement station is adequately described by the tested design?".

At this point, the scientific community followed three parallel branches for high pressure/volume applications -

- * high pressure bell provers (> 33 bars)
- * "bootstrapping" method
- * sonic or critical flow nozzles

In response to the North American community's request, the Gas Research Institute (GRI) has initiated funding for assessment of in

Orifice Metering Research - A User's Perspective

situ calibration devices - sonic nozzles, master meters and piston provers. These tests, planned for 1993, will be conducted at GRI's MRF facility.

One of the oldest laboratory volumetric gas measurement standards is the bell prover. The early systems employed a low pressure bell which was limited to extremely low pressures. As measurement technology progressed, the demand to measure gas at elevated pressures increased.

The "bootstrapping" method requires a bell prover to prove a number of highly accurate lower capacity meters. These parallel meters are, in turn, used to prove larger capacity meters. A group of these larger capacity meters are then used in parallel to prove an orifice meter or turbine meter. The process works well in the laboratory, but is less acceptable in a field environment. A master turbine meter proven at low pressure and operated at elevated pressures will exhibit K-factor shifts in the positive direction. When air is used as the proving media for meters normally used to measure natural gas, conversion errors occur. Another major problem is one of logistics. Moving a large group of master meters to a number of locations is difficult. Equally difficult is the ability to duplicate actual operating conditions in the laboratory. Since transporting master meters may result in damage, time consuming validation cross testing may be required at each test site. Contaminants in a gas stream can damage or reduce the accuracy of the master meters. As a result, field tests can be biased and costly repair and recertification of the master meter is required.

Sonic nozzle technology remained dormant until Matz, Smith and Stratford's design work in the early 60s. Real gas critical flow factors, CSTAR, were developed by Johnson of NASA in 1965 allowing the application of sonic nozzles for calibration purposes. Sonic nozzles have been successfully applied as laboratory standards on single component gas streams. Varying degrees of success has been achieved on multiple component gas streams in field and laboratory applications. A modification of the sonic nozzle, the Digicell, incorporates eleven parallel sonic nozzles sized in a binary progression and mounted in a single housing.

For sonic nozzles, clean, dry natural gas is a prerequisite. Solids and liquids swept along with the gas can damage the bore of the sonic nozzle. Some contaminants (i.e., sulfur) can deposit in the nozzle throat. Entrained or free water in the natural gas combine to form hydrates due to the drop in flowing pressure and temperature. Additionally, hydrocarbon dewpoint concerns are real for multiple component streams. Compositional analysis from a gas chromatograph in combination with an equation of state are normally used to predict the physical properties of the flowing gas. The sonic nozzle's mass flow equation requires an iterative solution to

determine the critical flow factor, CSTAR. The master meter's mass flow equation requires the calculation of density at both operating and base conditions. Analytical errors and uncertainties related to the physical properties' predictions increase the uncertainties associated with this technique. Continued research on the speed of sound prediction used in the CSTAR iteration is necessary to provide a long term viable method for multiple component streams. Estimates by Studzinski et al place the current uncertainty for CSTAR as high as 0.60 percent for a multiple component natural gas stream.

6.2 High Pressure Gas Piston Prover

In the last decade, high pressure gas piston provers were introduced to the natural gas community. The application of this device was inspired by the chemical industry's development for highly compressible polymer grade ethylene systems in Europe and North America. At this same time, the liquid small volume prover (SVP) demonstrated the acceptability of double chronometry interpolation techniques for turbine meters. Through the pioneering efforts of Gasunie, Shell, Amoco, DSM, Ruhrgas and Ogasco, a modified SVP approach was developed for chemical, CO₂ and natural gas applications.

The modified SVP technology launches a piston into the flowing stream and measures its progress through the prover using high precision detector switches. The area between the detector switches, known as the calibrated section, is traversed by the piston for calibration purposes. Most designs use free floating pistons, although, ram assisted pistons work equally well. The critical requirement is to assure that the pressure disturbance associated with launching the piston has subsided before the initial detector switch is activated. Steady state conditions during the calibration of the flowmetering device is mandatory for application of the results.

Two gas piston prover designs are currently available - single wall and double wall. Both design are available in unidirectional or bidirectional options.

In the single wall design, the pipe wall acts as both the measuring chamber and pressure containment vessel. As a result, correction for the change in the calibrated volume is required due to the flowing temperature and pressure.

The double wall design incorporates a smaller pipe inside a larger pipe. The double wall design uses the outer pipe as a pressure containment vessel resulting in the pressure across the inner pipe wall to be approximately zero. This negates the need for a correction due to pressure. A correction for the change in the calibrated volume is required due to the flowing temperature.

Orifice Metering Research - A User's Perspective

The piston prover has been used as a primary standard to prove a turbine meter or a master turbine meter installed in series with an orifice meter. This arrangement ensures calibration under normal operating conditions - velocity profile, instrumentation, etcetera. Additionally, wet gas will not alter the performance of the piston prover as long as the flowing conditions are not lower than the hydrocarbon dew point. Small amounts of fine solids will have no effect unless the bore of the calibrated section or the piston seals are damaged.

At this time, the high pressure gas piston prover is being successfully applied by Gasunie, Shell USA, Amoco USA and Ruhrgas for fiscal applications and/or laboratory flow standards. Gasunie has replaced their "bootstrapping" method with the piston prover. Shell USA has applied this technology to chemical and CO₂ systems since 1984 to identify out of tolerance metering facilities. Amoco USA has operated an Ogasco design for the calibration of small turbine meters in a coal degasification project since 1990.

Clearly the piston prover offers the best opportunity for successful field calibration of flowmeters on multiple component natural gas streams. However, the measurement community needs; additional research, an established gas piston prover design and certification standard. The additional research needs will be assessed with the GRI activities for 1993. In answer to the need for standards, the API Committee on Gas Measurement (COGM) has recently established a Working Group to address the global community input and concerns.

7 PHYSICAL PROPERTIES

Several physical properties are required for fiscal calculations of natural gas - compressibility, absolute viscosity, isentropic exponent, CSTAR for sonic nozzles and calorific value.

7.1 Density

Accurate values of flowing density, $\rho_{t,p}$, and base density, ρ_b , are required for accurate base volume calculation. The densities may be obtained using two methods - direct measurement using density meters or an acceptable equation of state.

Online density meters, for both flowing and base density, has exhibited problems when a fluid is measured near a phase boundary or passes through the hydrocarbon dew point. Small amounts of liquid dropping out of solution will cause density meters to perform erratically. Calibration of gas density meters, not conducive to field operations, should be performed in an ISO 9000 certified laboratory.

The use of equations of state to accurately predict the density of

Orifice Metering Research - A User's Perspective

gases and liquids has met with varying degrees of success. When the data used to derive the equation was representative of the flowing fluid, the results have been acceptable. The density uncertainty increases as the operating composition, pressure or temperature deviates from the data base used for the equation of state.

Attempts have been made since the turn of the century to develop an equation of state that accurately predicts the physical properties of a variety of natural gas streams. Developers were hindered in their endeavors by a lack of high quality data.

Research directed by Howard Bean of the United States National Bureau of Standards produced the first generally accepted supercompressibility data in 1928 and 1929. The data was limited to 4 Mpa (600 psia). The next significant body of work in the US was published by Professor Samuel Beitler of Ohio State University (OSU) in 1954. The Beitler work was extended and an equation of state was completed in 1962 by Mr. R. H. Zimmerman at OSU. The results of this work were published by the American Gas Association as the "Manual for Determination of Supercompressibility Factors for Natural Gas" (PAR Project NX-19).

In 1981, the Gas Research Institute (GRI) began to sponsor a program at the University of Oklahoma in close liaison with the American Gas Association. The work, directed by Dr. K. E. Starling, was aimed at expanding the temperature, pressure and compositional limits of Project NX-19. The results of this work provided the basis for the 1985 A.G.A. Report No. 8, "Compressibility Factors For Natural Gas And Other Related Hydrocarbon Gases".

The data used for the 1985 A.G.A. Report No. 8 used data up to approximately 6 Mpa (900 psia). The data was obtained from open literature as well as data supplied by the Groupe Europeen de Recherches Gazieres (GERG). GERG continued to expand their high quality data base through 1989. This work demonstrated that the equation of state used in Report No. 8 needed to be improved. It also showed the velocity of sound data obtained under GRI sponsorship between 1985 and 1989 lacked sufficient accuracy for sonic nozzle applications.

GERG developed an equation form for compressibility that produces accurate results within the defined pressure, temperature, density, heating value and compositional limits. The GRI team, which consisted of the Universities of Oklahoma and Idaho and GRI staff, also utilized the new data collected and revised the generalized equation of state for the 1992 Report No. 8. Both the GERG and the GRI equations are utilized in the revised report.

The data base continues to have areas of high uncertainty. Report

No. 8 is recommended for use within restricted compositional ranges. The report also states that an acceptable database for water, heavy hydrocarbons, and hydrogen sulfide is not available at this time. The accuracy of the report is likely to be equivalent to other existing generalized equations of state.

International cooperation towards development of a single standard for the prediction of compressibility of multiple component natural gas streams has been highly successful due to strong leadership from the Western European and North American communities. This effort has culminated in a draft standard currently being balloted at the ISO Technical Committee 193, A.G.A. Transmission Committee, A.G.A. Distribution Committee and API COPM levels.

Large errors usually occur in the gas sampling and compositional analysis arena. In the United States, most analytical work is performed using a gas chromatograph. Significant improvements have been made in gas chromatography in the past decade. The advent of the capillary column has increased the ability of the analyst to produce accurate extended analyses. The major problem remaining is the need for highly accurate multiple component chromatographic standards. Pure component calibration is not economically feasible on a routine basis. As this problem is solved, laboratory analytical uncertainty will be reduced. As the laboratory problems are resolved, the use of sophisticated online gas chromatographic systems will be followed by sophisticated portable systems. Systems now being marketed are capable of analysis through nonanes plus.

7.2 Absolute Viscosity

The absolute fluid viscosity is required to calculate the pipe Reynolds number for the new orifice coefficient of discharge equation. Viscosities may be measured or computed from appropriate equations of state. In some areas additional data could improve the accuracy of the predicted viscosity. For high Reynolds number applications the absolute accuracy of the viscosity is not as critical. The coefficient of discharge is not as effected by small inaccuracies in Reynolds number. In low Reynolds number application the accuracy of the viscosity prediction has a much greater impact on the accuracy of the volume calculation.

A NIST program known as TRAPP can calculate the viscosities for multiple component natural gas streams. It represents the state of the art in predictive codes for transport properties. Developed by Ely of NIST in Boulder, the program is based on a corresponding states model of fluid mixtures containing as many as sixty-one different constituents.

A.G.A. Report 8 should be revised to provide the user community with multiple component viscosity calculations.

7.3 CSTAR

Uncertainties in the critical flow factor, CSTAR, contribute to the uncertainty of mass flow rate through a single sonic nozzle. The flow through the nozzle is taken to be isentropic and one-dimensional, the plenum velocity is assumed to be zero, and the throat velocity is assumed to be that of the speed of sound of the gas at throat conditions.

Additional research is needed to assist the user community to determine the speed of sound for multiple component streams, guidelines for dewpoint concerns, guidelines for deposition concerns, and uncertainty estimates for CSTAR, throat density, throat temperature, entropy and enthalpy predictions.

7.5 Isentropic Exponent

From a practical standpoint, the perfect isentropic exponent or specific heat ratio (k_p) is required to calculate the expansion factor (Y) for the orifice mass flow equation. For certain gas compositions, the perfect isentropic exponent (k_p) should be calculated using an equation of state rather than the fixed value contained in A.G.A. Report 3.

A.G.A. Report 8 should be revised to provide the user community with perfect isentropic exponent (k_p) calculations for multiple component streams.

8 LOSS CONTROL PERFORMANCE

All measurements have errors - the difference between the indicated value and the true value. Uncertainty is an estimate of the error that in most cases is not expected to be exceeded. The method for estimating the uncertainty is contained in the metering standards previously referenced.

Many factors influence the overall measurement uncertainty associated with a metering application. Major contributors include construction tolerances in the meter components, tolerances of the empirical coefficient data bases or in situ calibrations, predictability and variations in the fluid properties, and uncertainties associated with the secondary devices.

For pipeline operators, accurate measurement is essential for both fiscal and line integrity purposes. One indication of the uncertainty of metering technology is the replication of measurements on a pipeline system. In practice, this is commonly referred to as the loss control performance. Since we have discussed the concern for proper flow conditioning, it is appropriate to also present the performance of properly applied and maintained orifice metering systems.

Orifice Metering Research - A User's Perspective

The first loss control example is one of four polymer grade ethylene grids operated by Shell USA. The annual commodity value for the grid presented is approximately 800 million USD (Figure 12). The results exhibited in the graph were achieved as a result of; in situ calibration, enforcing a Beta range of 0.2 to 0.6, maintaining an L3 of 10 to 12D and an L1 of at least 17D. The in situ calibration was accomplished using small volume prover (SVP) technology in combination with master turbine meter techniques for compressible fluids. The calibration factor was used for analytical purposes only, not for fiscal purposes. The results of the orifice meter calibrations were used to identify facilities which exhibited high bias errors. Upon investigation, the bias associated with the orifice meters was always a result of physical deviations from the standards, human errors or electronic errors.

The second example is one of two carbon dioxide systems operated by Shell USA (Figure 13). The annual throughput for the CO₂ system presented is approximately 6 billion cubic meter of gas (200 billion standard cubic feet). The same techniques applied to the ethylene grid were utilized on the carbon dioxide system. In addition, the majority of the physical problems were identified through the use of videoimagescope technology.

The orifice meter has a long history of use and experimentation. Because of this, it sometimes may be perceived as outdated, inaccurate and unreliable. In reality the opposite is true. The orifice meter is a well established device with known weaknesses and strengths. If applied with expertise, the long term performance is exceptional.

9 FUTURE RESEARCH DIRECTION

Additional research into the application of orifice meters and metering standards development is justified by the current capital investments. Maximization of current capital investments is an efficient and effective approach for the petroleum, chemical and natural gas industries.

Continuation of current installation effects research for orifice meters (and other flowmeters) will identify uncertainty limitations. Assessment of new flow conditioner designs would improve users' alternatives. Two new approaches (Laws, K-Lab) to flow conditioners has shown significant potential towards elimination of upstream disturbances with minimal permanent pressure drop. The benefits to the global community will be efficient and effective improvements of line integrity and loss performance with minimal capital investments.

In situ calibration techniques for multiple component gas streams should be assessed in light of achievable laboratory and/or field uncertainty estimates. In particular, two areas have particular

Orifice Metering Research - A User's Perspective

interests to the user community -

Improvements in the high pressure piston prover would yield tremendous benefits to the global community. Development research is needed to provide static/dynamic leak detection of the piston seal. Piston seal material research would also be a significant benefit by reducing the frictional forces and increasing the serviceability of the seal materials. The piston/seal design should be improved to minimize the pressure disturbance caused when launching the piston. This would reduce the required upstream barrel length, prover weight and initial cost of the device. Alternatively, the calibrated section could be lengthened increasing the device's resolution.

The concerns for sonic nozzles' velocity of sound, entropy and enthalpy predictions need additional empirical research and correlations.

Increasing the evaluation and development of the ultrasonic flowmeter for gas streams would provide the global community with economic alternatives to the current orifice and turbine meter selections. Several questions concerning ultrasonic meters need further addressing - installation effects, velocity of sound, long term and short term drift, and identification of influence quantities.

International round robin testing of laboratories and in situ calibration devices are envisioned to take place in this decade. Round robin testing will provide assessment of bias and precision for the laboratories and methods employed in the tests. The user community needs a realistic assurance of lower biases between flow laboratories as well as analytical laboratories. The end result will require ISO 9000 certifications of these testing services.

Operational enhancements are needed in extending the calibration intervals of the associated secondary equipment (flow computers, smart transmitters, chromatographs, etc.), required physical inspection intervals (i.e., videoimagescopes, etc.), required certification of field standards on specified intervals and statistical footprinting of field devices and standards.

Additional improvements in the prediction of physical and transport properties for multiple component gas streams are a prerequisite for the 90s. CSTAR for sonic nozzles, viscosity and perfect isentropic exponent calculations, extension of the compositional limits for density or compressibility predictions are the most apparent improvement areas.

Multiple component gas sampling is more "art" than science. Prediction of hydrocarbon dewpoint, free and entrained water

levels, high molecular weight components are needed to assess the ability to obtain a "true" composite gas sample for fiscal purposes. Having obtained this sample, the user must know how to maintain its representivity by ensuring that molecular separation, condensation, and deposition does not occur prior to analysis.

Improvements in the analytical arena should occur with the further improvement of portable high precision gas chromatographs. Extended analysis methods should be standardized with clear guidelines to the global community. In addition, the development of an international standard for multiple gas standards (i.e., reference standards) would provide consistency and accuracy in operations.

10 ACKNOWLEDGEMENTS

The authors wish to thank the management of Shell USA and Amoco USA for their valuable support and dedication towards publications of the results and opinions presented herein.

In addition, the authors wish to thank the Gas Research Institute (GRI), National Institute of Standards and Technology (NIST), API's Committee on Petroleum Measurement (COPM), American Gas Association (A.G.A.), Gas Processors Association (GPA), the European Community's Dr. D. Gould, and many individuals for their commitment to excellence.

We also want to express our sincere respect to past researchers such as Buckingham, Bean, Beitler, Witte and Marchetti.

REFERENCES

Worldwide Discharge Coefficient Equation

OSU Experimental Program

1. Beitler, S. R., "The Flow of Water Through Orifices"; The Ohio State University, The Engineering Experiment Station, Bulletin 89, 1935, Columbus, Ohio, USA.
2. Fling, W. A., "API Orifice Meter Program", American Gas Association, Operating Section Proceedings, Paper 83-T-23, p. 308-311, 1983.

API/GPA Experimental Program

3. "Coefficients of Discharge for Concentric, Square-Edged, Flange-Tapped Orifice Meters: Equation Data Set - Supporting Documentation for Floppy Diskettes"; American Petroleum Institute, 1988, Washington, D. C., USA.

Orifice Metering Research - A User's Perspective

4. Britton, C. L., Caldwell, S., and Seidl, W., "Measurements of Coefficients of Discharge for Concentric, Flange-Tapped, Square-Edged Orifice Meters in White Mineral Oil Over a Low Reynolds Number Range"; American Petroleum Institute, 1990, Washington, D.C., USA.
5. Whetstone, J. R., Cleveland, W. G., Baumgarten, G. P., Woo, S., and Croarkin, M. Carroll, "Measurements of Coefficients of Discharge for Concentric, Flange-Tapped, Square-Edged Orifice Meters in Water Over the Reynolds Number Range of 1,000 to 2,700,000"; NIST Technical Note 1264, June 1989, Gaithersburg, MD, USA.
6. Whetstone, J. R., Cleveland, W. G., Bateman, R. B., and Sindt, C. F., "Measurements of Coefficients of Discharge for Concentric, Flange-Tapped, Square-Edged Orifice Meters in Natural Gas Over the Reynolds Number Range of 25,000 to 16,000,000"; NIST Technical Note 1270, September 1989, Gaithersburg, MD, USA.

EC Experimental Program

7. Hobbs, J. M., "Experimental Data for the Determination of Basic 100mm Orifice Meter Discharge Coefficients"; Commission of the European Communities, Report EUR 10027, 1985, Brussels, Belgium.
8. Hobbs, J. M., Sattary, J. A., and Maxwell, A. D., "Experimental Data for the Determination of Basic 250mm Orifice Meter Discharge Coefficients"; Commission of the European Communities, Report EUR 10979, 1987, Brussels, Belgium.
9. Hobbs, J. M., "The EC Orifice Plate Project, Part I: Traceabilities of Facilities Used and Calculation Methods Employed"; Commission of the European Communities, Report PR5:EUEC/17, 1987, Brussels, Belgium.
10. Hobbs, J. M., "The EUEC Orifice Plate Project, Part II: Critical Evaluation of Data Obtained During EC Orifice Plate Tests"; Commission of the European Communities, Report EUEC/17, 1987, Brussels, Belgium.
11. Hobbs, J. M., "The EC Orifice Plate Project: Tables of Valid Data for EC Orifice Analysis"; Commission of the European Communities, Report EUEC/17, 1987, Brussels, Belgium.

Japanese Experimental Program

12. Watanabe, N., "Coefficients of Discharge for Corner-Tapped Orifice Meters"; National Research

Orifice Metering Research - A User's Perspective

Laboratory of Metrology, Private Communication, 1987, Japan.

Equation Development

13. Stolz, J., "A Universal Equation for the Calculation of Discharge Coefficient of Orifice Plates"; Proc. Flomeko 1978 - Flow Measurement of Fluids, H. H. Dijstelbergen and E. A. Spencer (Eds), North-Holland Publishing Co., Amsterdam (1978), pp 519-534.
14. Reader-Harris, M. J. and Sattary, J. A., "The Orifice Plate Discharge Coefficient Equation"; Flow Measurement & Instrumentation, vol 1, Jan. 1990, London, UK.
15. Gallagher, J. E. and Teyssandier, R. G., "Influence of Tap Hole Geometry on Concentric, Square-Edged Orifice Meters"; Report to the Joint Experts Committee, April, 1990.
16. Private Communication with J. Stolz, 1985-1990.
17. Private Communication with M. J. Reader-Harris, 1986-1990.
18. Gallagher, J. E., "The A.G.A. Report No. 3 Orifice Plate Discharge Coefficient Equation", 1990 North Sea Flow Measurement Workshop.

Measurement Standards

19. API MPMS Chapter 14 Section 3 (ANSI 2530, A.G.A. Report No. 3), "Concentric, Square-Edged Orifice Meters", American Petroleum Institute, Washington, D.C., USA, 1990.
20. International Standard ISO 5167-1, "Measurement of Fluid Flow by Means of Orifice Plates, Nozzles and Venturi Tubes Inserted in Circular Cross-Section Conduits Running Full", International Standards Organization, Geneva, Switzerland, 1992.

Flow Conditions

21. Schlichting, J., "Boundary Layer Theory", McGraw-Hill, New York, NY, 1979.
22. Hinze, J. O., "Turbulence", second edition, McGraw-Hill, New York, NY, 1975.

Installation Research

23. Mattingly, G.E., Yeh, T. T., "Summary Report of NIST's

Orifice Metering Research - A User's Perspective

Industry-Government Consortium Research Program on Flowmeter Installation Effects", NISTIR 4751, NISTIR 4753, NISTIR 4779, U.S. Department of Commerce, Technology Administration, National Institute of Standards and Technology, Gaithersburg, MD, 1992.

24. Morrison, G. L., DeOtte, R. E., "3-D Laser Anemometer Study of Compressible Flow Through Orifice Plates", GRI Report 91/0177, Gas Research Institute, Chicago, IL, December, 1991.

Orifice Meter Installation Effects Research

25. Bean, H. S., "The Effects of Orifice Meter Indications of Various pipe Fittings Near the Orifice Plate", Western Gas Measurement School, USA, March, 1929.
26. Sattary, J. A., "Progress Report No. 10 on The Effect of Installations and Straighteners on the Discharge Coefficient of Orifice Plate Flowmeters", Department of Trade and Industry, National Engineering Laboratory, East Kilbride, Scotland, March, 1991.
26. Scott, J. L. et al, "The Effects of Flow Conditioners and Tap Location on Orifice Flowmeter Performance", NIST Technical Note 1352, U.S. Department of Commerce, Washington, DC, 1991.
28. Morrow, T. B., "Orifice Meter Installation Effects: Sliding Vane Test With a 100D Meter Tube and a Tube Bundle Straightening Vane Downstream of a 90 Degree Elbow", GRI Technical Memorandum No. MRF-UE-04, Gas Research Institute, Chicago, IL, March, 1992.
29. Morrow, T. B., Park, J. T., "Orifice Meter Installation Effects: Sliding Vane Test With a 17D Meter Tube and a Tube Bundle Straightening Vane Located 13D Upstream of an Orifice Plate Downstream of a 90 Degree Elbow", GRI Technical Memorandum No. MRF-UE-02, Gas Research Institute, Chicago, IL, March, 1992.
30. Morrow, T. B., Park, J. T., "Baseline Calibrations for Orifice Meter Calibration", GRI Topical Report No. GRI-92/0097, Gas Research Institute, Chicago, IL, 1992.

In Situ Calibration

31. Bellinga, H., Hoecks, C.P., van Laak, F. A. L., Orbons, P.J., "Piston Prover Used to Calibrate Gas Meters", Oil & Gas Journal, August 19, 1985.

Orifice Metering Research - A User's Perspective

32. Gallagher, J. E., "Shell Tests Indicate Ethylene Meters Best Proved With Master Meter Method", Oil & Gas Journal, December 15, 1986.
33. Hoecks, C. P., "Overall Gas Measurement Accuracy", Proceedings of International School of Hydrocarbon Measurement, 1986, University of Oklahoma, OK.
34. Reid, J., and Pursley, W. C., "An Online Prover for the Calibration of Flowmeters in High Pressure Gas", Proceedings of International Conference on Flow Measurement, National Engineering Laboratory, East Kilbride, 1986.
35. Oliver, P. D., "The Development of a Primary Standard for Calibrating Flowmeters on Gaseous Media", Proceedings of International Flow Measurement Conference, American Gas Association, Washington, D.C., 1986.
36. Ting, V. C., Halpine, J. C., "Portable Piston Prover for Field Calibration of Flowmeters", 64 Technical Conference and Exhibition, Society of Petroleum Engineers, October, 1989.
37. Beeson, J., "Proving Gas Turbine Meters Onsite Using Sonic Nozzles", American Gas Association, Operating Section Proceedings, 1989.
38. Beaty, R. E., "Field Operation of a Portable Piston Prover for Testing Gas Meters", American Gas Association, Operating Section Proceedings, 1990.

Physical Properties

39. American Gas Association, "PAR Research Project NX-19; A.G.A. Manual for the Determination of Supercompressibility Factors for Natural Gas", Arlington, VA, 1969.
40. American Gas Association Report No. 8, "Compressibility and Supercompressibility for Natural Gas and Other Hydrocarbon Gases", American Gas Association, Washington, D.C., 1985.

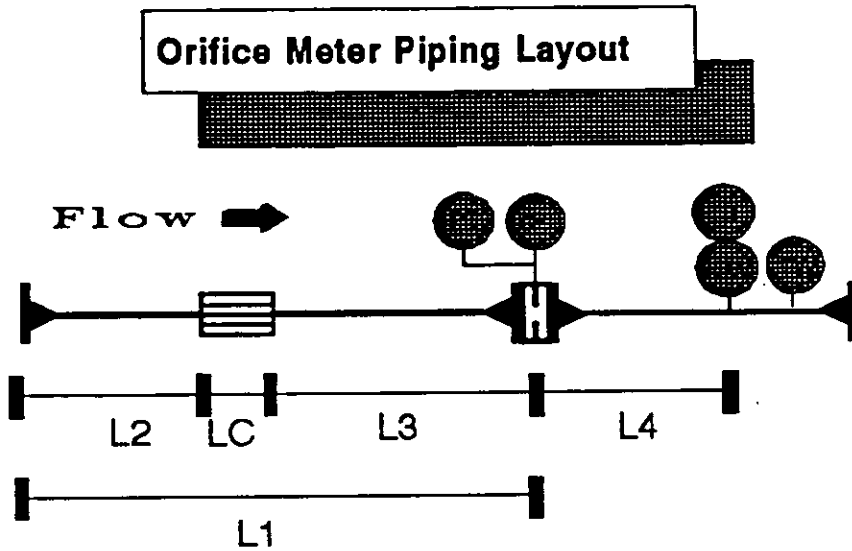


Figure 1

Correlating Parameters

- Beta or Diameter Ratio
- Piping Specifications
 - L1 specifications
 - L4 specifications ($\geq 5D$)
 - relative roughness
- dP Sensing Tap Location (12, 3, 6, 9 o'clock)
- Flow Conditioner Design
 - L2 specifications ($\geq 3D$)
 - L3 specifications
- Fluid Dynamics
 - type of disturbance
 - Reynolds Number
 - velocity profile
 - swirl angle
 - turbulence structure

Figure 2

Classification of Flow Conditioners

Type	Class	Head Ratio	Cost
Tube Bundles			
Radial	I	1	Lo
Hexagonal	I	1	Lo
Etolle	I	1	Med
AMCA Honeycomb	I	1	Med
Mitsubishi	II	2	Lo
Zanker	II	6	HI
Sprinkle	II	15	HI
Laws	III	2	Med
K-Lab	III	3	Med
Sens & Teule	III	5	VHI
Bosch & Hebrard	III	5	VHI

Figure 3

A.G.A. Tube Bundle

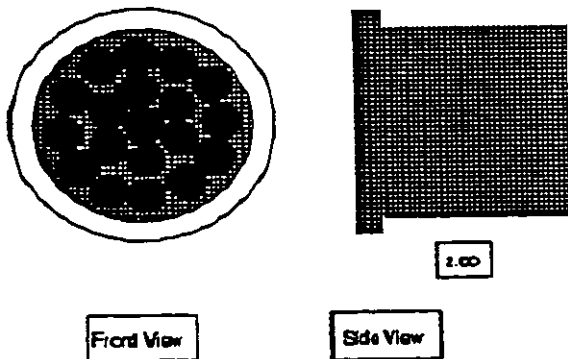


Figure 4

LAWS Conditioner

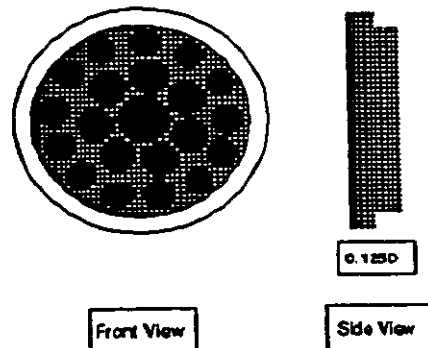
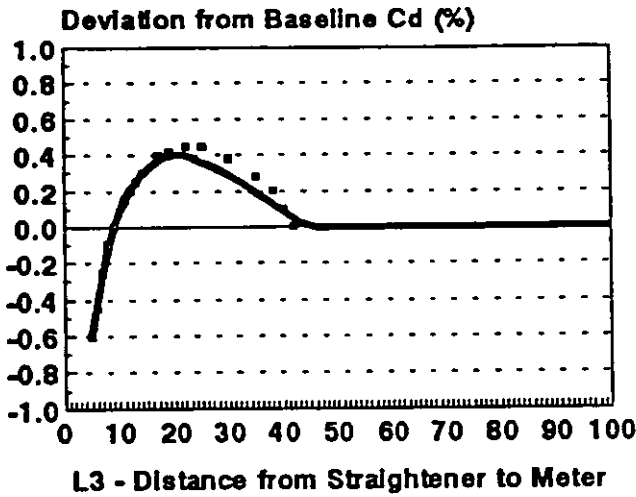


Figure 5



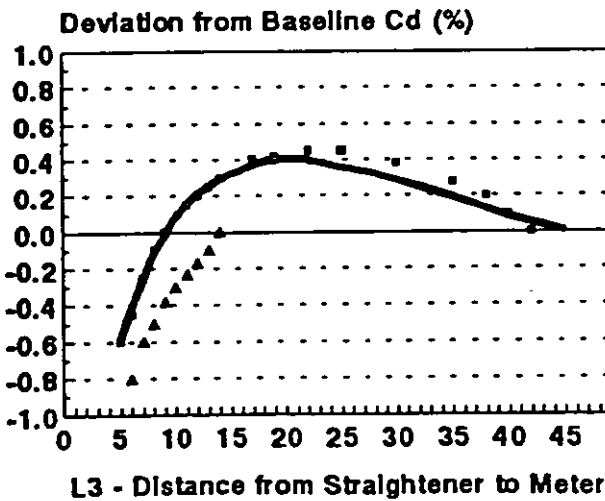
A.G.A. Tube Bundle
 Meter Tube Downstream of 90 Degree Elbow



Beta of 0.750
 — L1 of 100D
 ■ L1 of 45D

Figure 6

A.G.A. Tube Bundle
 Meter Tube Downstream of 90 Degree Elbow



Beta of 0.750
 — L1 of 100D
 ■ L1 of 45D
 ▲ L1 of 17D

Figure 7

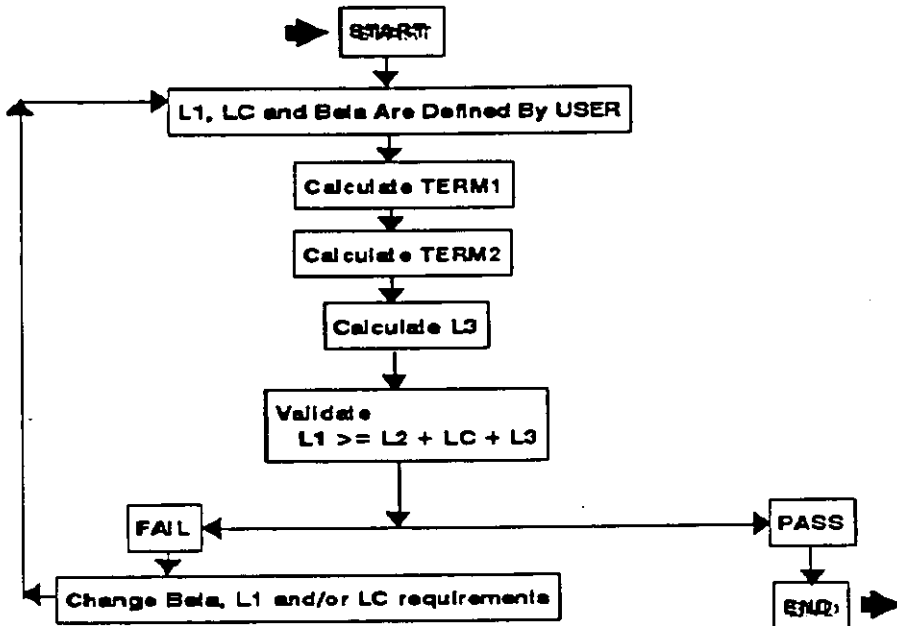


Figure 8

A.G.A. Short Tube Bundle Correlation L1 of 17D, 29D and 100D

Beta	17D L3	29D L3	100D L3
0.10	5.1	5.1	5.0
0.15	5.3	5.2	5.0
0.20	5.5	5.4	5.0
0.25	5.7	5.6	5.0
0.30	6.0	5.8	5.0
0.35	6.4	6.1	5.0
0.40	7.2	6.7	5.3
0.45	8.0	7.4	5.6
0.50	8.9	8.2	6.0
0.55	9.9	9.0	6.4
0.60	11.0	10.0	6.8
0.65	NA	11.1	7.4
0.70	NA	12.4	8.1
0.75	NA	13.9	9.0

$TERM1 = 3.5 \cdot EXP(Beta) \cdot Ev$
 $TERM2 = TERM1 + 2.2 \cdot Beta^2 \cdot MAX[0, (46 - L1)^{0.5}]$
 $L3 = MAX(5, TERM2)$

Figure 9

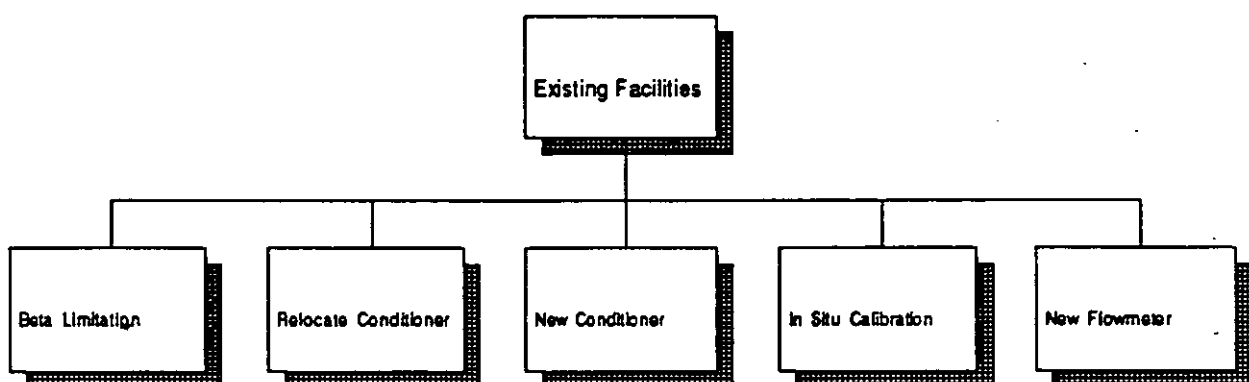


Figure 10

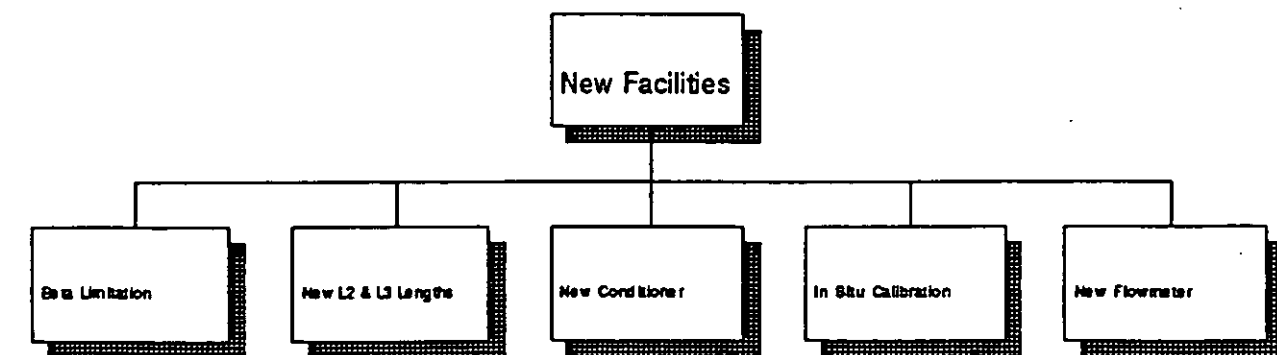


Figure 11



Ethylene Pipeline Annual Loss Control Performance

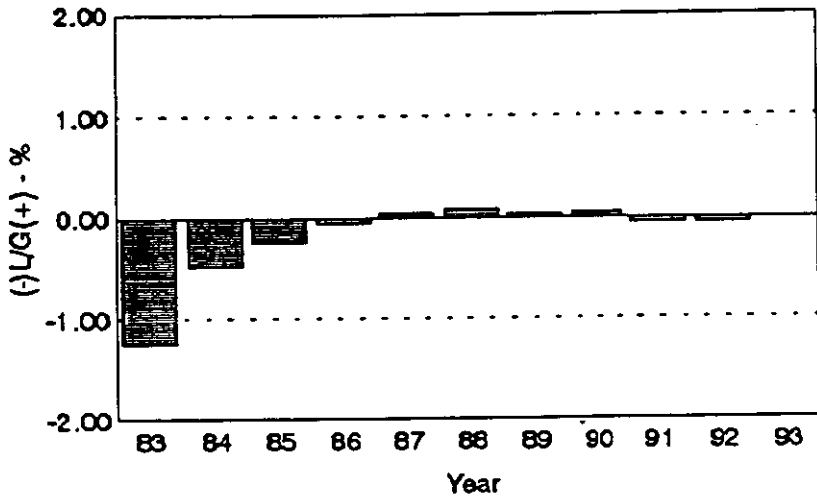
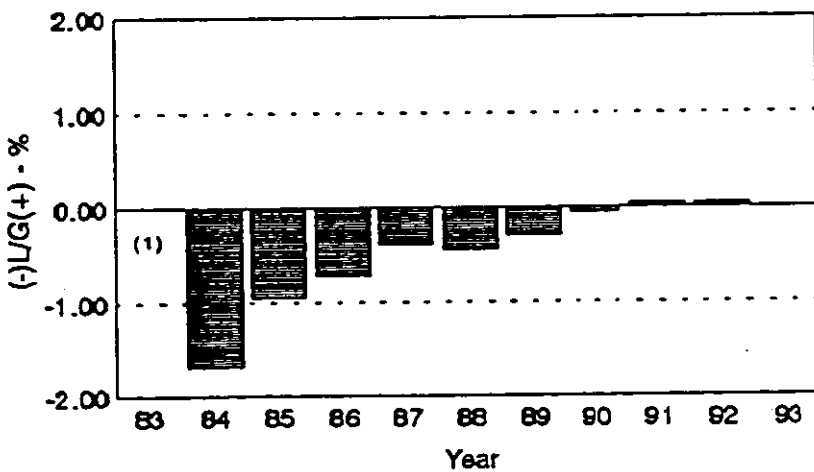


Figure 12

Carbon Dioxide Pipeline Annual Loss Control Performance



(1) Commenced Operations in 1984

Figure 13



FUTURE RESEARCH DIRECTION

- ▶ Installation Effects
- ▶ In Situ Calibration
- ▶ Ultrasonic Flowmeters
- ▶ Round Robin Testing
- ▶ Operational Enhancements
- ▶ Physical & Transport Properties
- ▶ Gas Sampling Technology
- ▶ Gas Analysis Technology

Figure 14

OPTIMAL FLOW CONDITIONER

by

W T Lake, Amoco Production Co
and J Reid, NEL

Paper No 1.3

NORTH SEA FLOW MEASUREMENT WORKSHOP
26-29 October 1992

NEL, East Kilbride, Glasgow

C O N T E N T S

- 1 INTRODUCTION**
- 2 CATS METERING DESIGN**
- 3 TEST ARRANGEMENT**
- 4 NEL TESTS**
- 5 NEL TEST RESULTS**
- 6 HIGH PRESSURE NATURAL GAS TESTS**
- 7 CONCLUSIONS**
- 8 REFERENCES**
- 9 LIST OF FIGURES**
- 10 APPENDIX**

1 INTRODUCTION

The Central Area Transmission System (CATS) is a North Sea pipeline development scheduled for operation in April 1993. The pipeline is 400 kilometers long and 36 inches in diameter capable of transporting up to 1.4 billion standard cubic feet of gas per day. The gas is delivered to Teesside, England to fuel a new combined cycle heat and power station being constructed by Teesside Power Limited. Amoco-operated gas fields (Everest and Lomond) will flow 300 million SCFD which is only 21 per cent of the total pipeline capacity.

This excess capacity along with the connectors that have been built into the pipeline will allow other gas fields to tie into the line and act as a common transportation system for any newly developed gas fields.

Amoco is committed to accurate natural gas measurement throughout the CATS system both onshore and offshore as it is essential for an equitable financial allocation. Accurate and consistent orifice metering relies on a fully developed velocity profile, free of swirl at the upstream plane of the orifice plate. In order to achieve this objective of accurate gas measurement, Amoco intends to install (and also intends to require all third party pipeline entrants to install) flow conditioner devices upstream of all meters critical to sales and allocation, both onshore and offshore.

2 CATS METERING DESIGN

In an effort to meet the appropriate metering standards and guidelines set forth for Licensees and Operators in the UK Continental Shelf and provide the safest possible equipment and operating procedures consistent with the Cullen Report, Amoco CATS project group has designed each offshore gas metering system with three (3), single chambered type orifice fittings sized so that any single meter may be serviced during any expected flowing conditions. This design philosophy incorporates an 18 inch header with 10 inch branch connections (1.7 to 1 reduction in diameter) for each meter run.

ISO 5167: 1980, Section 6 'Installation Requirements' requires that an orifice flow measuring device be installed in the pipe-line at a position such that the flow conditions immediately upstream approach those of a fully developed profile and are free from swirl as described in Section 6.4. These conditions are deemed to exist when straight pipe of a certain length separate the orifice plate from the nearest upstream and downstream flow disturbances. Section 6.2 provides the minimum straight lengths of pipe required between the orifice plate and various fittings such as single bends, combination of bends, reducers and expanders, fully open globe and gate valves and abrupt reductions from large vessels. Although it is extremely common to design meter stations with multi-tube header arrangements, due to operating conditions and economics of design, there is no mention of this

configuration in this section leaving the Licensee with the task of trying to 'interpret' the standard, subject to government bodies approval, when installing any header arrangement. Section 6.3 of the Standards recommends that particular types of flow straightening devices can be used to permit the installation of a flow measuring device downstream of fittings not listed above. However it also specifies a minimum overall length of 42 diameters shall be used for all straightening devices unless the conditions stated in Section 6.4 are met. This generally discourages the use of conditioners as it invariably requires longer (rather than shorter as expected) upstream run lengths or an expensive and time consuming test to demonstrate compliance with Section 6.4.

After considerable research into recent developments in the field of flow straighteners and conditioners for orifice meters, Amoco proposed an optimum installation design for the upstream meter tube length and straightener location as shown in the meter layout in Fig. 1 (29 diameters (D) overall upstream with the straightening device at 10D from the closest disturbance). The metering design has an upstream configuration consisting of a 12-inch vertical (down) inlet into a 18-inch horizontal header with three 10-inch meter tubes off branch type connections. Each meter tube is constructed with two matched bore valves (10D total), a flanged type flow straightening or conditioning device, a straight section of 17-19 pipe diameters (depending on the straightening device length) and a flange neck single chambered orifice fitting.

3 TEST PIPE ARRANGEMENT

A drawing of the test pipe is shown in Fig. 2 and a photograph of the pipe in Fig. 3. The test pipe was designed for maximum flexibility in testing by using several doweled flanges for precise alignment. The design allows the flow conditions to be measured at up to seven pitot locations (6D, 7D, 9D, 10D, 13D, 16D and 19D) downstream of the flanges holding the conditioner (from the upstream end of the respective conditioner to the centreline of the pitot/orifice plate). The 19D location corresponded to Amoco's proposed metering system design.

The traversing pitot companion flanges were modified orifice flange unions designed so that the pitot ring holder was centred in the pipe without any gap, step or offset from the pipe wall and the pitot was perpendicular to the flow. Each set of test flanges was designed for precise alignment with or without the pitot installed. The test pipe was designed to meet the pressure requirements (70 bar) at the Bishop Auckland facility and the 12-inch inlet and outlet flanges are in the same plane and elevation.

The test pipe was carefully selected so that it was as concentric as commercially available with consistent roughness to meet normal ISO 5167 requirements. The flanges and ring

were machined to best fit the pipe. The companion orifice flange unions were machined and dowelled for near perfect alignment regardless of the arrangement of the conditioners or pitot. Spacers (12 mm thick by 10.060 ID) with standard 'O-ring' seals were placed between all flanges not holding the pitot or conditioner so that there was a smooth transition, free of gaps or intrusions, throughout the entire pipe section.

For determination of the unrecovered pressure drop across the straightener or conditioner, taps were provided at 1D upstream and 7D downstream of the upstream face of the device. For the determination of density, a 1/2-inch BSP connection was provided 7D downstream of the 19D flange location (for temperature measurement) and a static pressure tapping was provided on each of the flanges.

Pipe Measurements. NEL Metrology Section inspected and measured⁽¹⁾ the test pipe and pitot carrier ring internal diameters and the relative roughness of the pipe bore. A total of 75 roughness and 132 diameter measurements were taken throughout the test pipe section. The pitot ring internal diameter was measured with the same instrument at four diameters with an average of 10.060-inch. The test pipe was found to be consistently round and adjacent flanges within 0.002-inch of the pitot diameter.

The pipe relative roughness was measured using a portable surface texture measuring instrument after a calibration check using the 'calibrated scratch pad' (239 microinch per inch). These measurements were taken at three radial positions in 25 different planes for a total of 75 readings along the pipe at one diameter (10-inch) increments from 2 1/2 diameters upstream of the conditioner to 2 1/2 diameters downstream of the last pitot device. The average of the relative roughness measurements was 150, and the mean, 123.5 microinch per inch with only four readings above 300 (two of which were in a hand-ground region).

The pipe internal diameter was measured over the same region of pipe with one additional radial reading (four per plane) plus additional planes, one inch into the flanges between pipe spools, for a total of 33 planes or 132 diameters. The mean of the diameter readings was 10.0626-inch with a single standard deviation of 0.0100-inch. When only measurements in the flanges were considered (adjacent to pitot ring), the average was 10.0572-inch. The pitot ring was machined for 10.060-inch pipe relating to an average step change at the pitot ring of 0.0014-inch or about 1/10000 of the pipe diameter.

In order to protect the pipe from corrosion during shipment, a rust inhibitor was applied to the internal surfaces. All internal measurements were taken prior to the application of rust inhibitor. The inhibitor was removed with white spirit prior to testing at NEL and the process again repeated before transit to and from the British Gas test site.

Flow Conditioners. The following four flow straighteners or conditioners (all designed to be held between 10-inch 600# ANSI Raised Face flanges) were tested.

- a Conventional 19 tube 2D long Short Tube Bundle (Fig. 4).
- b Zanker (1D long) constructed to ISO 5167 requirements (Fig. 5).
- c Laws Conditioning Plate (University of Salford) (Fig. 6).
A perforated plate flow conditioner with an open area or porosity of about 51.5 per cent.
- d K-Lab Mark 5 Conditioning Plate (Confidential).

Pitot Tube. The single traverse assembly unit (Fig. 7), designed by Gasunie for the EEC orifice discharge coefficient tests, incorporated a constant blockage swirl angle and impact pressure probe. Pitot side pressure sensors were located $\pm 40^\circ$ from the centre impact pressure sensor. The device was installed between modified orifice flange unions designed to enable it to be centred in the pipe, without any gap, step or offset from the pipe wall, and perpendicular to the flow. Before each new installation the pitot ring was centred on the outer diameter of the companion flanges using adjustable matched 'tee blocks', such that no internal offset could be detected visually or by touch.

4 NEL TESTS

The main objective of the tests was to determine the optimum location of various flow conditioning and straightening devices within the upstream orifice meter tube and to verify that the velocity profile and swirl components of the installation were within the specified limits set out in ISO 5167, Paragraph 6.4. In order to establish the amount of swirl generated by the header configuration and the effectiveness of the conditioners, flow profiles were measured at OD and 19D without any flow conditioner installed. After the profile tests were completed the discharge coefficient of a nominal 0.6 diameter ratio orifice plate was measured with the Laws and Tube bundle conditioners in the test line. Selection of the various test configurations, by Amoco, were based on data from the conditioner plates designers, published papers and Amoco's own research and design expertise.

The face of the flange located 10D from the header to branch connection was chosen as the datum from which the positions of the flow conditioners were measured. Since the overall length of the various flow conditioners varied from 0.12D to 2D the distance between the conditioner and pitot was measured from the face of the conditioner flange. The majority of the tests were conducted with a flow conditioner (with its flange upstream) installed at the datum pipe flange; exceptions to this were the K-Lab device at 6D and the tube bundle at 13D as

mentioned below. For each test, the pitot device was moved to a position representing a possible orifice plate location.

Pitot traverses were conducted in the vertical and horizontal planes; with negative radius ratios corresponding to the bottom or left-hand pipe wall (looking downstream) respectively. The swirl angle was measured by rotating the pitot tube until the differential pressure, across the side pressure sensors, was zero; the angular rotation of the tube representing the swirl angle. The impact pressure was then measured at that angle with the central pitot orifice since it represented the peak impact pressure. Any offset (bias) of indicated swirl angle at the centreline was subtracted from the other readings as the actual swirl angle was assumed to be zero at the centreline of the pipe.

For the profile tests the mass flow through the test rig was held constant during each traverse. The first flow conditioner to be tested was the tube bundle and the flowrate was set to give the maximum possible Reynolds number; the K-Lab and Zanker devices, having greater pressure losses, had to be tested at lower flowrates, the Laws device was tested at the same flowrate as the K-Lab. During the orifice plate tests the flow was varied between the minimum and maximum rate attainable.

The reference flowrate was measured by a venturi meter. Air temperature at the outlet of the flowmeter and test section were measured by platinum resistance thermometers together with a precision thermometer digital readout. The static and differential pressures at the flowmeter and pitot were measured by Rosemount pressure transmitters and the barometric pressure by a precision quartz pressure gauge. The calibration of the reference flowmeter and all recorded measurements are traceable to national standards.

Data from the pressure transmitters and resistance thermometers was collected by a data logging system controlled by a PC. Pressure readings were integrated over a ten second period, the average of five periods were used for each test point: single temperature readings were recorded within the same time period.

5 NEL TEST RESULTS

The results of the NEL profile tests are given in Figs 8 to 19. Each figure shows the traverse results compared with the theoretical flow profile (using $n = 9.9$, see Appendix), with ± 5 per cent error bands; the corrected swirl angle is also shown. The overall accuracy of the pitot determination of swirl angle is estimated to be less than ± 0.75 degree including dead band and mechanical hysteresis.

The velocity calculated from the pitot differential pressure was corrected for compressibility using:

$$V_c = V \left[\left(\frac{\gamma}{1 - \gamma} \right) \frac{P_1}{\delta p} \left(\left[\frac{\delta p}{P_1} + 1 \right]^{\frac{\gamma-1}{\gamma}} - 1 \right) \right]^{\frac{1}{2}}$$

where V is pitot velocity, δp and P_1 are the pitot differential and inlet pressures and γ is the isentropic component for air.

The velocity ratio, V_R , (point velocity, V_c , to centreline velocity, V_{CL}) was rationalised with respect to the volume flow associated with the centreline velocity, ie

$$V_R = \frac{Q_{cl}}{Q} \times \frac{V_c}{V_{CL}}$$

No Flow Conditioner. Figs 8 and 9 shows that the velocity profiles at both positions were significantly inverted. The maximum swirl angle at the 0D position was found to be 24 degrees with 20 degrees of swirl remaining at the 19D position. The initial test (0D) demonstrated flowing conditions at the flow conditioner inlet. The second test (19D) approximates flowing conditions for a common North Sea installation without a flow conditioner, that is, in general accord with ISO 5167 design criteria of 30 diameters downstream of a 2 to 1 header to branch connection.

Zanker Flow Conditioner. The velocity profile from the Zanker was examined only at the 19D position (Fig. 10). Although it produced a reasonable velocity profile it did not remove enough of the swirl, a total of approximately five degree remained in both the horizontal and vertical planes. The profile produced was a bit flat and somewhat asymmetric.

K-Lab Flow Conditioner. The K-Lab flow conditioner was tested with the pitot at 6D and 19D from the datum pipe flange (Figs 11 and 12). At 6D the device was installed in reverse with it's datum face downstream allowing a full 6D between the end of the device and the traverse plane. The measured profile was flat compared to the theoretical profile and slightly more than one degree of swirl remained. At 19D, the remaining swirl was similar but the flow profile was nearer the theoretical prediction but slightly asymmetric in the vertical plane such that the end points were outwith the five per cent limit.

E. Laws Flow Conditioner. The flow profile was examined at three positions: 6, 9, and 19 diameters downstream of the conditioner (Figs 13 to 15). Since the length of this device was so short it was not reversed as was the K-Lab conditioner. The profile at 6D was rather flat and slightly asymmetric with

a maximum swirl angle of about one degree. The asymmetry caused the profile to be greater than five per cent above the theoretical profile near the wall of the pipe. At 9D, the overall swirl angle was similar and the flow profile was slightly improved so that it was just on the five per cent limit. The swirl angle remained practically unchanged at 19D, and the flow profile was well within five per cent of the theoretical profile.

Tube Bundle. The flow profile was examined at four positions measured from the datum flange of the conditioner: 9D, 13D, 13D-Reversed (13DR) and 19D (Figs 16 to 19). In the 13D-Reversed position the tube bundle was installed in reverse in a 3D pipespool so that the inlet of the conditioner was ID downstream of the datum pipe flange and the pitot 13D downstream of the datum face of the conditioner. Thus for these four configurations the pitot was 7D, 11D, 13 D and 17D respectively, from the downstream end of the bundle. At all of the locations the maximum swirl angle was less than one degree.

At 9D the flow profile deviated significantly from the theoretical profile and the outer annular portion exceeded the mid 25 per cent to produce an inverted or collapsed profile.

The 13D velocity profile exhibited slight inversion and moderate asymmetry, but exceeded the profile limits. This configuration had the least swirl of any of the flow conditioners evaluated. At 13DR (26D overall), the asymmetry was significantly less than at 13D but the profile still departed from the theoretical, but to a lesser degree. In this configuration the swirl angle increased only slightly.

At 19D the profile was nearer the theoretical than at the other locations but still exceeded the five per cent criteria at radius ratios between 0.5-0.8. The swirl angle near the edge of the pipe began to increase but did not exceed two degrees.

Pressure Drop. The pressure drop for each device, recorded during the test, is shown in Fig. 20. The tube bundle displayed the lowest loss of less than one velocity head and the Laws was next with less than two.

Coefficient of Discharge (C_d) Tests. Orifice discharge coefficient tests, using a 0.597 beta ratio orifice plate in two positions, were conducted with the Laws and tube bundle conditioners. The plate was manufactured to ISO 5167 specifications, and the edge sharpness and internal diameter measurements were checked by the Metrology Section of NEL. Each test consisted of a C_d at five flow rates; the results, compared with the NEL standard C_d equation⁽²⁾, are shown in Figs 21 to 24.

The Laws conditioner was tested with the orifice plate 9 and 19 diameters downstream (19D and 29D overall length). As expected, the test C_d results, Figs 21 and 22, are nearer the

standard at the higher flow rates and larger Reynolds numbers. The results at 9D are slightly better than those at 19D.

The tube bundle was tested with the plate in the 13D and 13D-Reversed positions downstream (23D and 24D overall). The 13D position, Fig. 23, produced the Cd results most near the NEL standard (within 0.25 per cent). Overall, the 13D tube bundle Cd was closer to the NEL prediction than the Laws at 19D. The Laws at 9D and tube bundle at 13D produced similar results at the larger Reynolds numbers.

6 HIGH PRESSURE NATURAL GAS TEST

Based on the NEL low pressure air results, a short list of optimum conditioners were chosen for the high pressure (850 psi) natural gas test at British Gas' Bishop Auckland facility. The flow conditioners and their respective locations chosen for the second phase of testing at Bishop Auckland were: E. Laws at 9D and 19D and the tube bundle at 13D and 19D.

Note: For these tests, the pitot device was fixed at the 29D flange location so that the length upstream of the conditioner device changed (increased) instead of the overall length.

At NEL, the different test locations were achieved by moving the pitot closer to the conditioner with the conditioner fixed at the 10D location except for the tube bundle at the 13D Reversed position).

Profile Tests Tests were conducted at three flow rates with approximate pipe Reynolds Numbers of 5,000,000, 10,000,000 and 12,500,000 (CATS Everest and Lomond normal maximum is about 10,000,000. Gas samples were taken after each test for an average composition.

In general, the velocity profile data obtained from the HP natural gas tests did not vary significantly from the NEL LP air tests. The tube bundle profile data remained relatively flat while removing swirl to about 1 degree or less. The E Laws device at 19D (Figure 26) yielded the velocity profile closest to the theoretical.

Discharge Coefficient Tests. Using the same plate tested at NEL ($\beta = 0.597$), discharge coefficient tests were conducted with the E. Laws device at 9D and 19D and the tube bundle at 13D and comparisons made to the ISO or Stoltz equation. Each coefficient test consisted of three points at four flow rates between 5,000,000 and 10,000,000 Reynolds Number.

Although the precision of the individual coefficient tests is estimated to be no better than 0.3 per cent due to variations in natural gas composition found in the grid system, the data have been included in order to validate the profile tests. In order to minimise the effects of natural gas composition

resulting in a density variation, three points are averaged at each flow rate for a single comparison point.

The Laws at 19D was within 0.2 per cent of the ISO equation at all four test points and within 0.1 per cent (Figure 27) in the Reynolds Number range of expected flowing conditions of CATS offshore meter systems. The discharge coefficient test with the E. Laws conditioner at the 9D location also yielded data within 0.1 per cent of the ISO equation (Figure 28).

7 CONCLUSIONS

- The header arrangement with vertical inlet and branch connections which is commonly used in North Sea gas metering stations is a significant swirl generator.
- The length of 10 inch commercially smooth, straight pipe installed downstream of the conventional header that would be required to reduce swirl to 2 degrees or less (per the intent of the standard) would far exceed the 30 diameters required in the standard.
- The tube bundle eliminates swirl almost completely but produces a much flatter velocity profile than that predicted by the theoretical power law equation.
- There is no appreciable Reynolds Number affect on the velocity profile or swirl angle as shown by the close correlation between the NEL Low Pressure air and British Gas High Pressure natural gas data.
- All of the conditioners tested eliminated the swirl to within the 2 degree criteria except for the Zanker.
- In general, the velocity profiles produced by all of the conditioners were more flat than the fully developed theoretical flow profile.
- The relationship between actual velocity profile and coefficient of discharge is not fully understood as shown by the tube bundle results which give a very flat profile (with deviation up to 10 per cent from the theoretical) at 13 diameters but produce orifice coefficients very close to predicted values in tests at NEL for a beta ratio of 0.6.
- The orifice coefficient tests at British Gas, although informative, have limitations due to the natural gas composition variations and other uncontrollable factors such as ambient conditions. It would seem appropriate to ascribe an uncertainty of 0.3 percent (for an individual test point) to the coefficient results. Averaging the points before comparison may reduce the effects significantly. This uncertainty does not apply to the velocity profile and swirl data as the results of these measurements are presented in relative terms.

- When installing orifice meters downstream of headers, the predicted orifice coefficients may be used with greater confidence if a flow conditioner is installed at the proper location.
- The installation requirements for flow conditioners set forth in ISO 5167 Section 6.3.1 exceed the actual requirements for custody transfer meters with a diameter ratio maximum of 0.6 when such orifice meters are downstream of common headers with branch connections.
- The minimal upstream installation piping required for conditioners downstream of headers for the tube bundle or perforated plate may be much shorter than tested herein as the inlet section (upstream of conditioner) could probably be reduced to three diameters (perforated plate) or five diameters (tube bundle) without affecting results.

When additional data on the relationship between fully developed flow profiles and orifice discharge coefficients become available, the minimum length between the conditioner and the orifice plate may be further reduced such that the overall upstream meter tube section is no greater than 12 to 16 diameters when using conditioner plates or tube bundles.

- The Laws type flow conditioner performed best overall as it met the profile and swirl criteria set forth in ISO 5167 Section 6.4 and exhibited the lowest pressure drop of the perforated plates.

The results of the discharge coefficient tests in high pressure natural gas with a 0.6 beta ratio installed 19D downstream of the Laws conditioner show good agreement with the ISO equation (within 0.1% at operating Reynolds number values) and provide significant additional evidence that the requirements of ISO 5167 can be met fully, using this conditioner configuration.

APPENDIX

Velocity Profile in Fully Developed Pipe Flow

In order to meet the requirements of Clause 6.4 of ISO 5167 it is necessary to determine what velocity profile would be obtained in swirl-free flow after a long straight length of pipe similar to that used in the tests. Schlichting⁽³⁾ describes work of Nikuradse⁽⁴⁾ who collected extensive data on velocity profiles in smooth pipes. His data can be represented by the empirical equation

$$\frac{u}{U} = \left(1 - \frac{r}{R}\right)^{\frac{1}{n}} \quad (1)$$

where U is the pipe maximum axial velocity, R the pipe radius and u is the axial velocity at a point where the radial distance is r . This gives a good fit to experimental data, but there is no accurate theoretical way of determining n . In Nikuradse's data n ranged from 6.0 where the pipe Reynolds number, Re_D , was 4000, to 10.0 where Re_D was 2.0×10^6 or 3.2×10^6 .

The best method of determining n is to calculate it by fitting data whose Reynolds number is similar to that in the installation being tested for acceptability. Data collected in air at NEL⁽⁵⁾ with $Re_D = 9 \times 10^5$, pipe diameter = 102 mm and 140D of straight pipe upstream were available: fitting these data using a least-squares fit gave n a 9.9.

One problem with the velocity profile in equation (1) is that it does not have a zero derivative on the pipe axis. To solve this problem the following was tried:

$$\frac{u}{U} = \begin{cases} a \left(1 - \frac{r}{R}\right)^{\frac{1}{n}}, & \frac{r}{R} > c \\ 1 - b \left(\frac{r}{R}\right)^2, & \frac{r}{R} \leq c \end{cases} \quad (2)$$

where a and b are chosen so that the equation both is continuous and has a continuous derivative at $r/R = c$. This equation has a zero derivative on the pipe axis and has a very similar behaviour to equation (1) in the neighbourhood of the wall. However, when the NEL air data in Ref. 5 were fitted there was almost no improvement in quality of fit from that obtained with equation (1); moreover n was almost unchanged.

Data, collected by British Gas, with a least 100D of upstream pipe in 250 mm pipe at $Re_D = 1.4 \times 10^7$ and in 600 mm pipe at $Re_D = 2.2 \times 10^7$, were included in reports to the EEC^(6,7), but only in graphical form. The data, in tabular form, for the 600 mm pipe were obtained from British Gas.

Three sets of data were available, on two planes at $Re_D = 2.2 \times 10^7$, and on one plane at $Re_D = 8 \times 10^6$. Only the data at the higher Reynolds number have been analysed, since those at the lower have a maximum velocity two per cent higher than the centre-line velocity. The exponent n in equation (1) was obtained by using a least-squares fit to the data on each plane: on the 45 degree plane $n = 9.7$; on the 30 degree plane $n = 10.1$. This supports the use of the power law profile in equation (1) with $n = 9.9$ as a good representation of what the velocity profile would be after a long length of pipe at the Reynolds numbers encountered in both the air and gas tests. The 600 mm data have been plotted in Fig. 25 for comparison with equation (1) with $n = 9.9$ and it can be seen that there is good agreement.

Gasunie have also collected data downstream of 80D of 600 mm pipe⁽⁸⁾ (including a full-bore ball valve 50D upstream of the measuring point) for Re_D from 2.5×10^6 to 5×10^7 and found that the profile can be described quite well with a power law and that n appeared to be around 10. The value of n is a little larger for higher Re_D than for lower.

From the data analysed the power law profile in equation (1) with $n = 9.9$ gives a good representation of what the velocity profile would be after a very long straight length of pipe at the Reynolds numbers encountered in both the air and the gas tests.

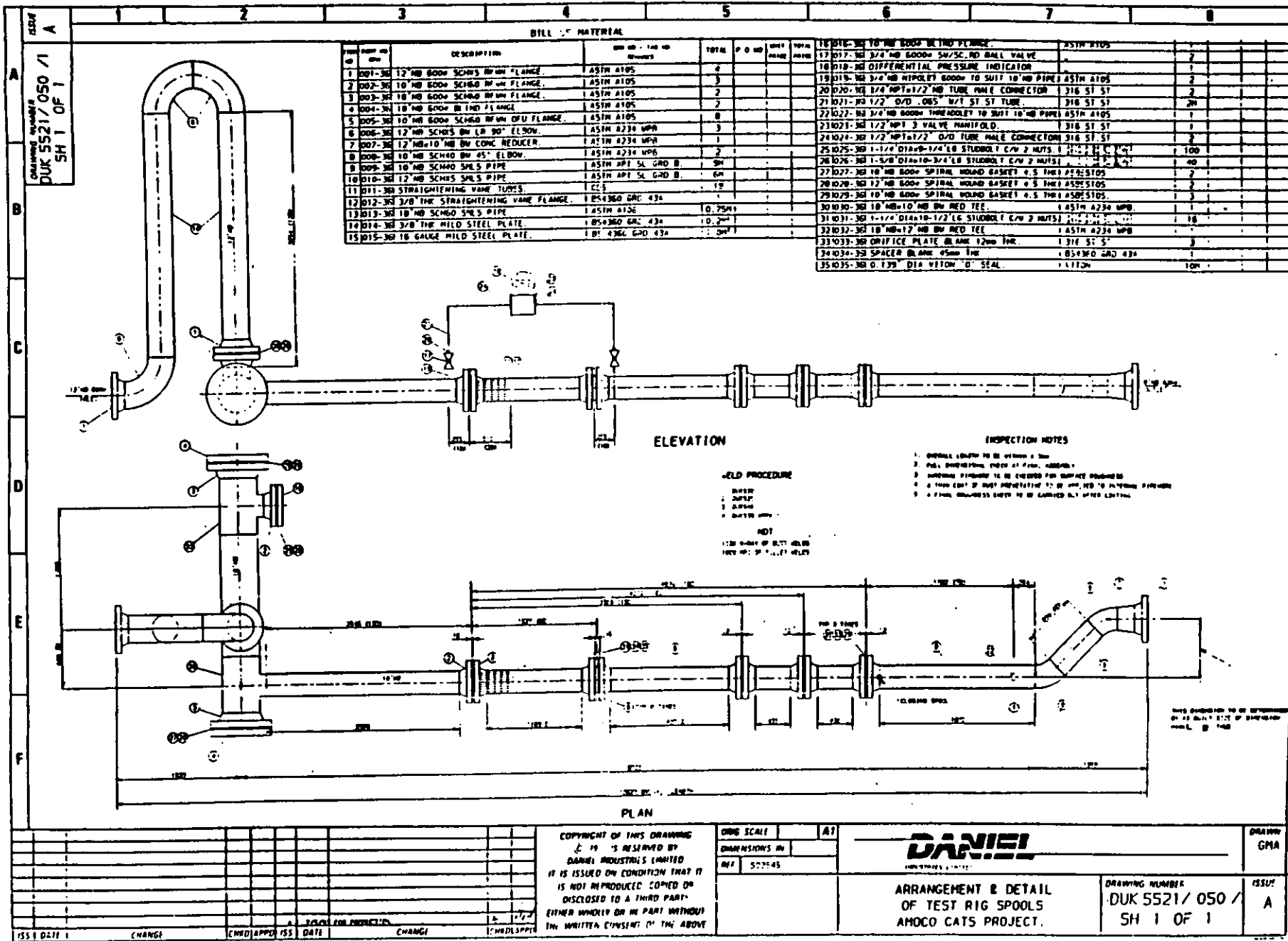
REFERENCES

- 1 Certificate of Calibration of a Selection of Pipe Spools for Daniel Industries. Certificate Serial No 01039, Ref 478/1. Scottish Calibration Centre, National Engineering Laboratory East Kilbride, Glasgow. June 1991.
- 2 READER-HARRIS, M. J. and SATTARY, J. A. The Orifice Plate Discharge Coefficient Equation. Flow Measurement and Instrumentation, Volume I. January 1990.
- 3 SCHLICHTING, J. Boundary Layer Theory. McGraw Hill, New York, 1960.
- 4 NIKURADSE, J. Gesetzmäßigkeit der Turbulenten Stromung in Glatten Rohren. Forschungsheft 356, 1932.
- 5 BRAIN, T. J. S. and REID, J. Progress Report No 3 on EEC Orifice Plates Coefficients Project. Progress Report No PR 3: EUEC/O3. National Engineering Laboratory, East Kilbride, Glasgow, 1980.
- 6 NORMAN, R. and DREW, W. A. The EEC 250 mm Orifice Meter Project, Part III, Basic Calibration Tests, ERS R.3I28. Killingworth, Newcastle-upon-Tyne: British Gas Engineering research Station, 1985.
- 7 STEWART, I. A. and DREW, W. A. The EEC 600 mm Orifice Meter Project, Part III, Discharge Coefficient. ERS R.4256. Killingworth, Newcastle-upon-Tyne: British Gas Engineering Research Station, 1989.
- 8 600 mm Orifice Plate Project, Part RI. Flow Profile Measurements. TP/T 88.R.2051, Groningen: Gasuine, 1988.

LIST OF FIGURES

- 1 Proposed Metering Station
- 2 Drawing of Test Pipe Arrangement
- 3 Test Pipe
- 4 Tube Bundle
- 5 Zanker Flow Straightener
- 6 Laws Conditioner
- 7 Pitot Traverse Unit
- 8 Profile at OD - No Flow Straightener
- 9 Profile at 19D - No Flow Straightener
- 10 Zanker - Profile at 19D
- 11 K-Lab - Profile at 6D
- 12 K-Lab - Profile at 19D
- 13 Laws - Profile at 6D
- 14 Laws - Profile at 9D
- 15 Laws - Profile at 19D
- 16 Tube Bundle - Profile at 9D
- 17 Tube Bundle - Profile at 13D
- 18 Tube Bundle - Profile at 13DR
- 19 Tube Bundle - Profile at 19D
- 20 Flow Conditioner Head Loss
- 21 Discharge Coefficient - Laws at 9D
- 22 Discharge Coefficient - Laws at 19D
- 23 Discharge Coefficient - Tube Bundle at 13D
- 24 Discharge Coefficient - Tube Bundle at 13DR
- 25 Velocity Profile - British Gas 600 mm Pipe.
- 26 HP Gas Velocity Profile - Laws at 19D
- 27 HP Gas Discharge Coefficient - Laws at 19D
- 28 HP Gas Discharge Coefficient - Laws at 9D

Fig. 2 Drawing of Test Pipe Arrangement



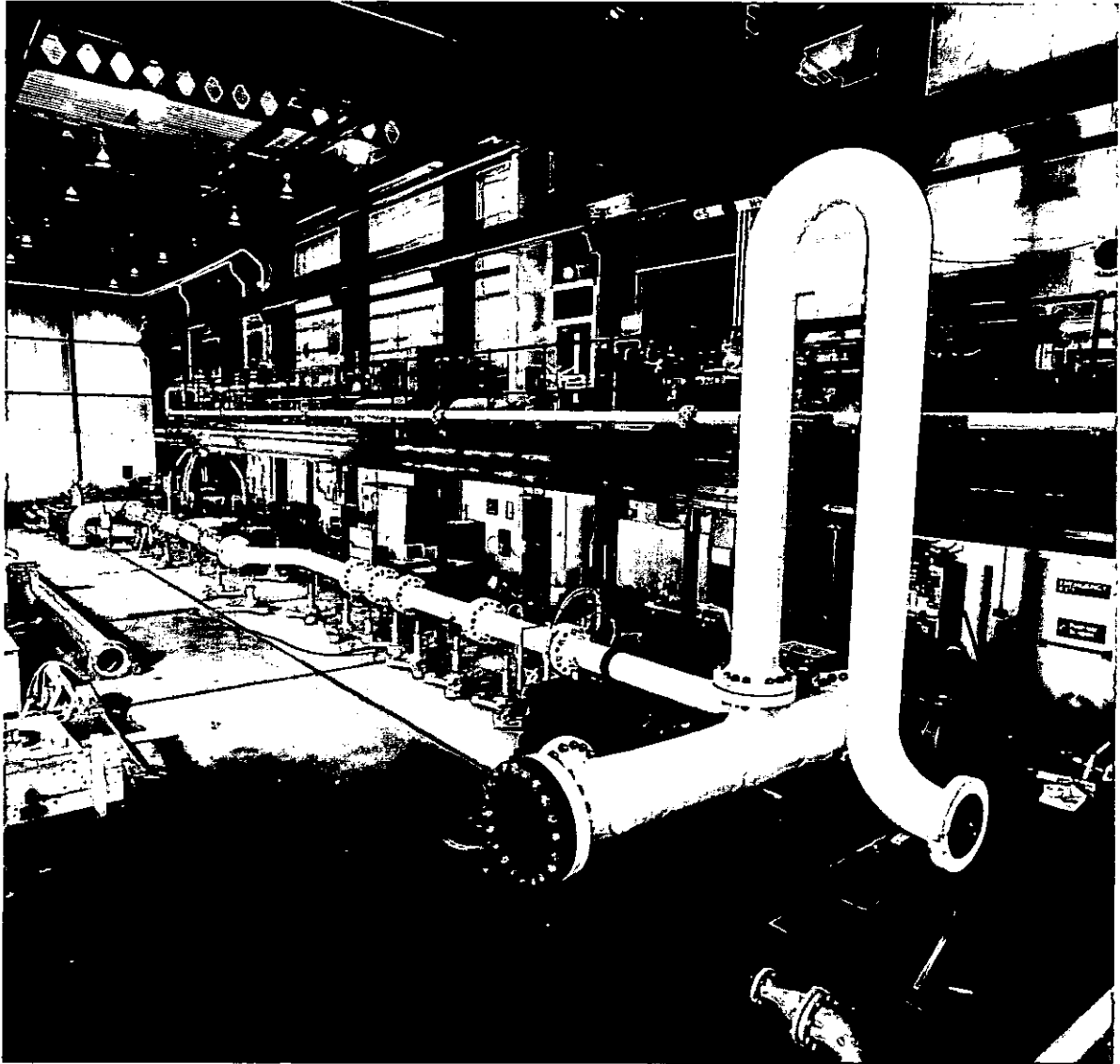


Fig. 3 Test Pipe

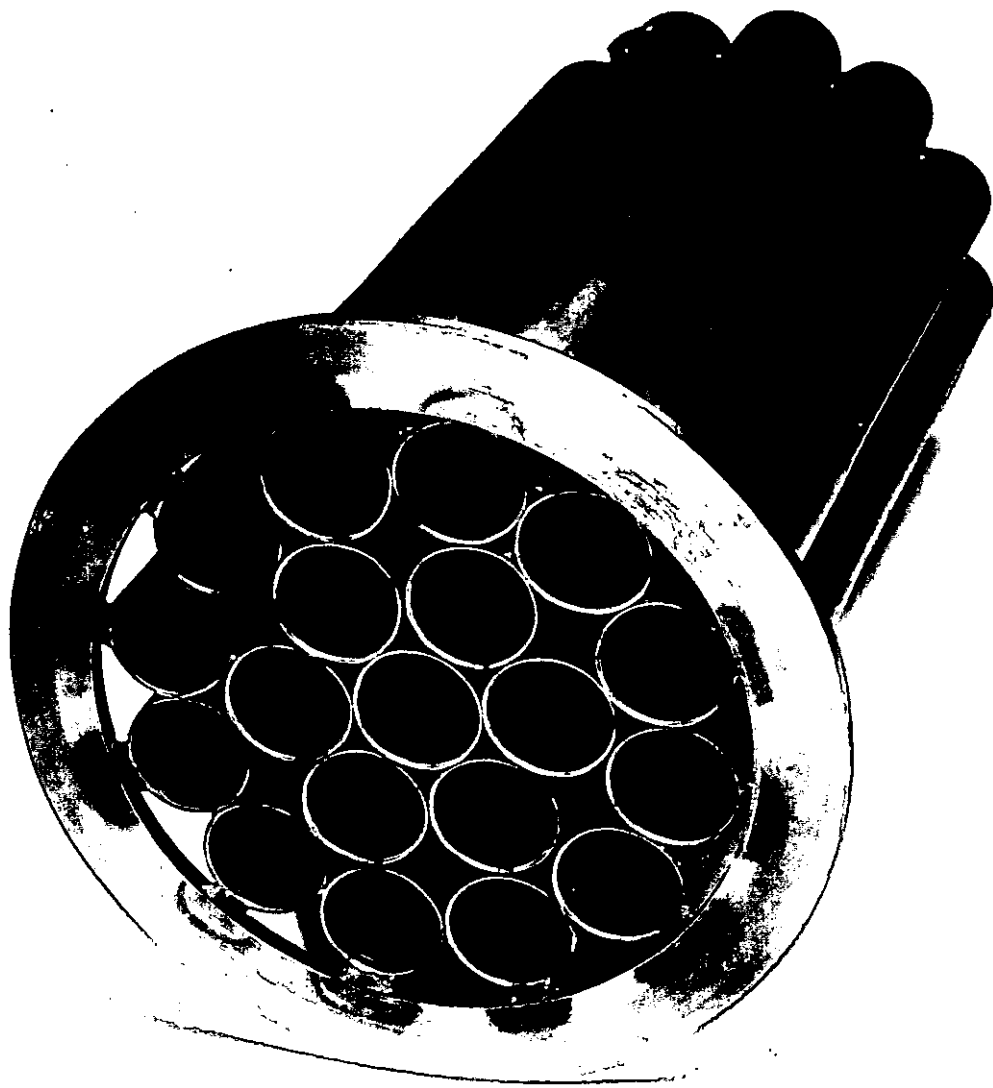


Fig. 4 Tube Bundle

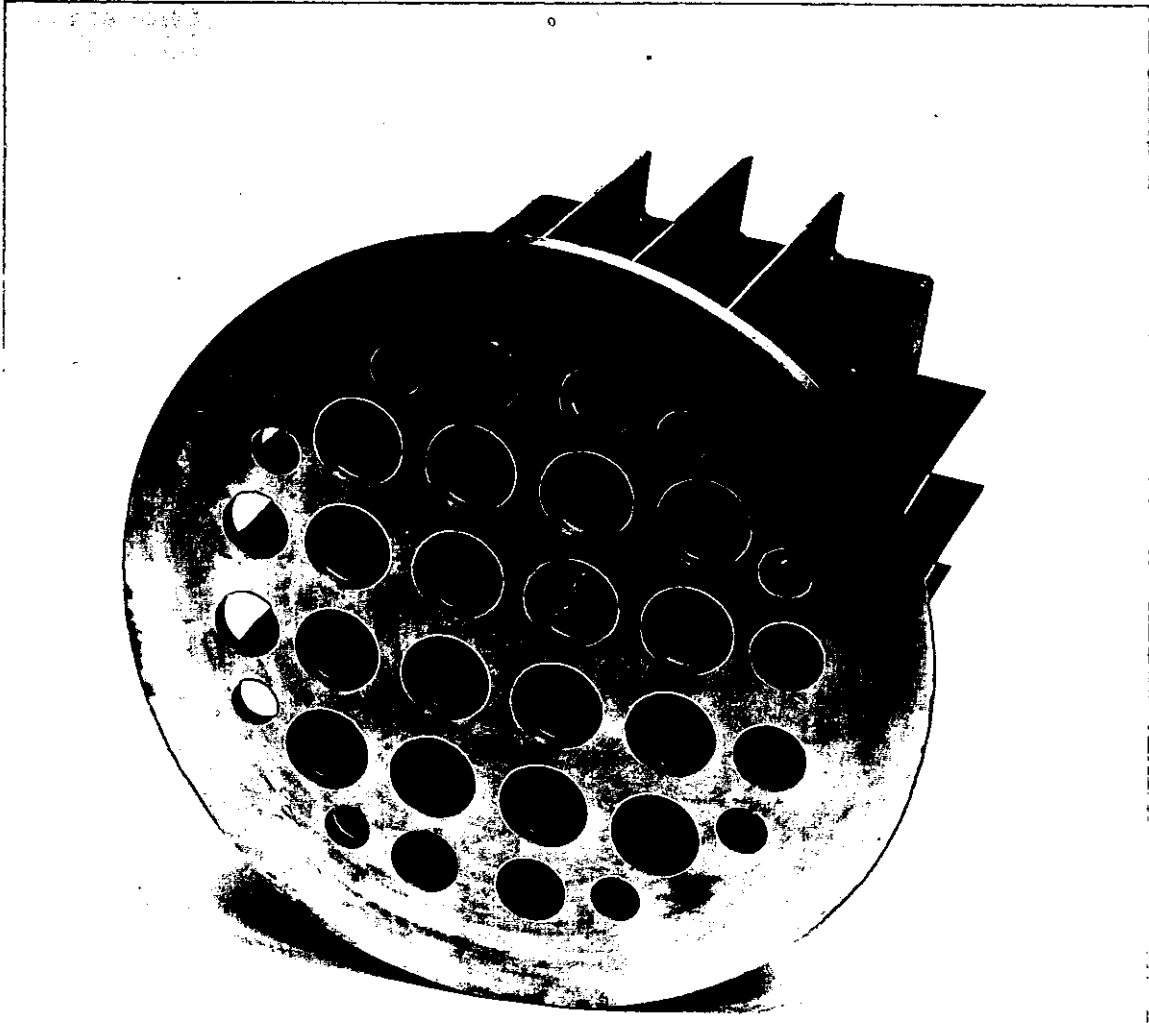


Fig. 5 Zanker Flow Straightener

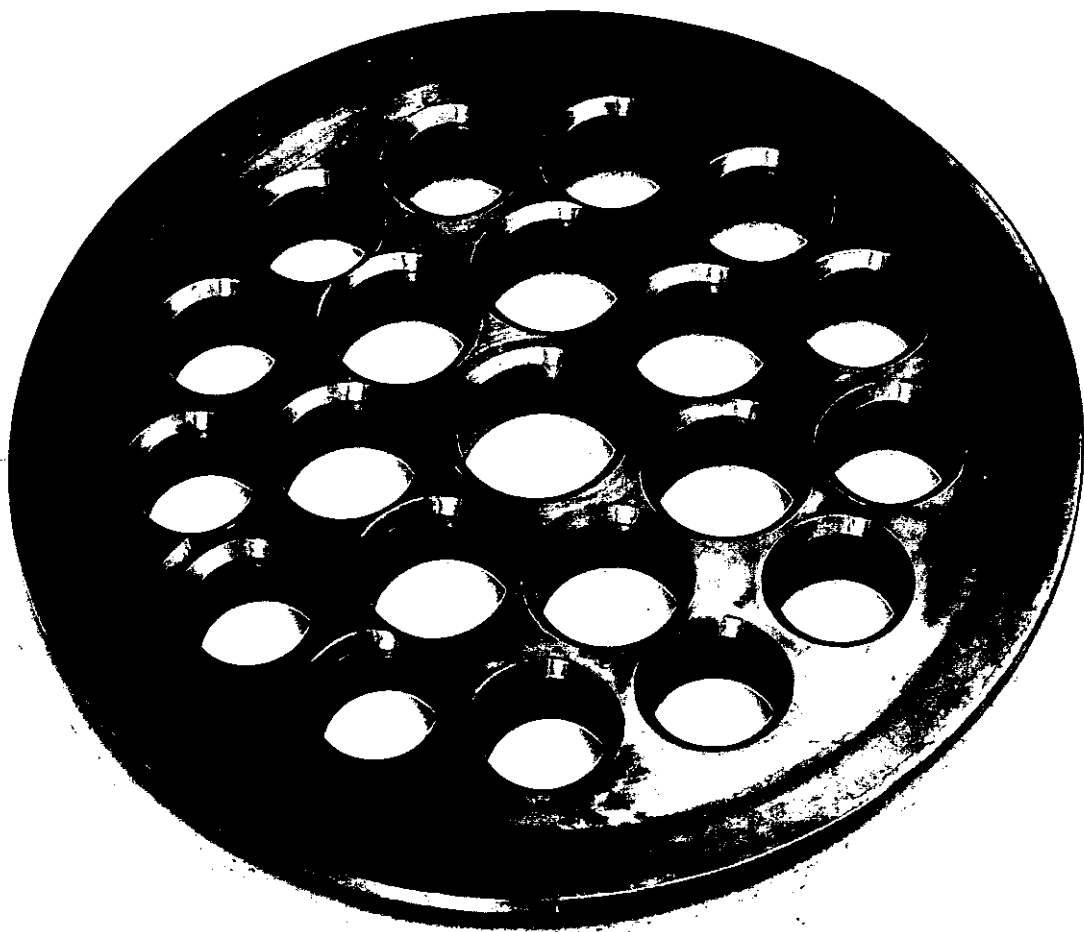


Fig. 6 Law Conditioner

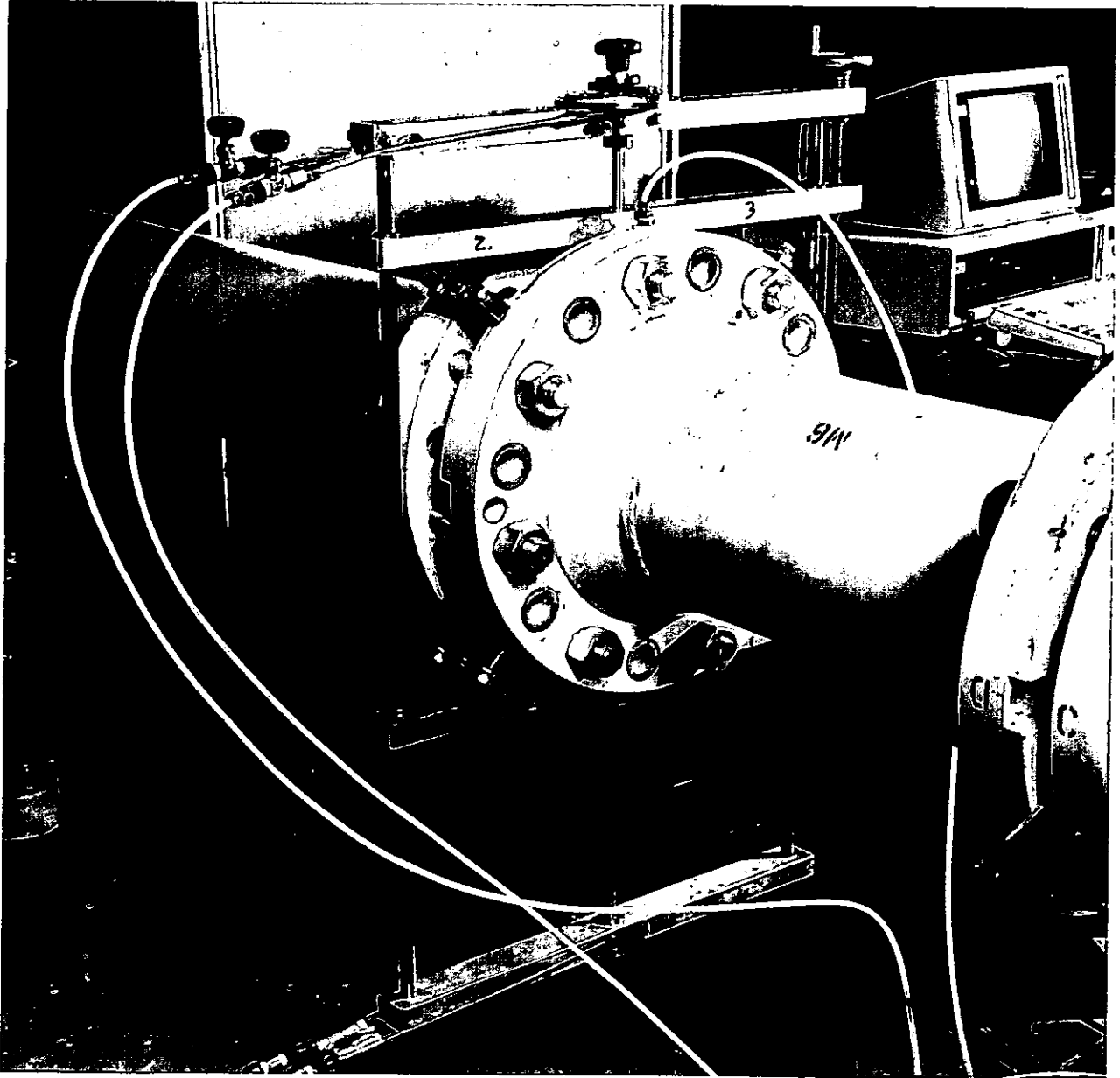


Fig. 7 Pitot Traverse Unit

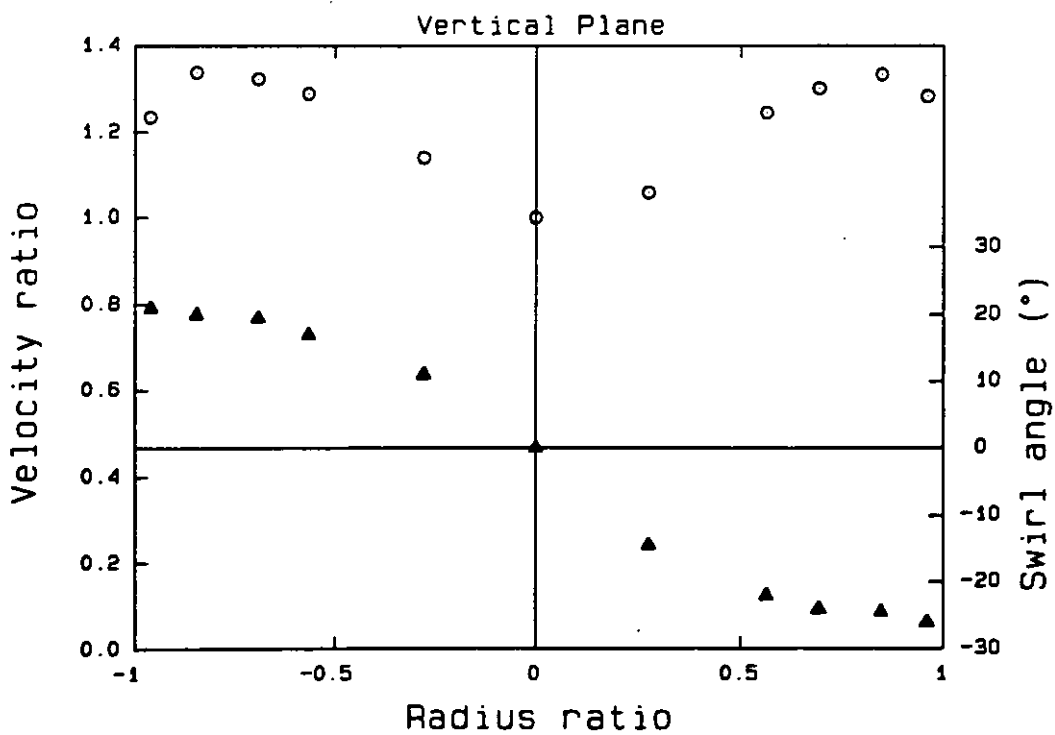
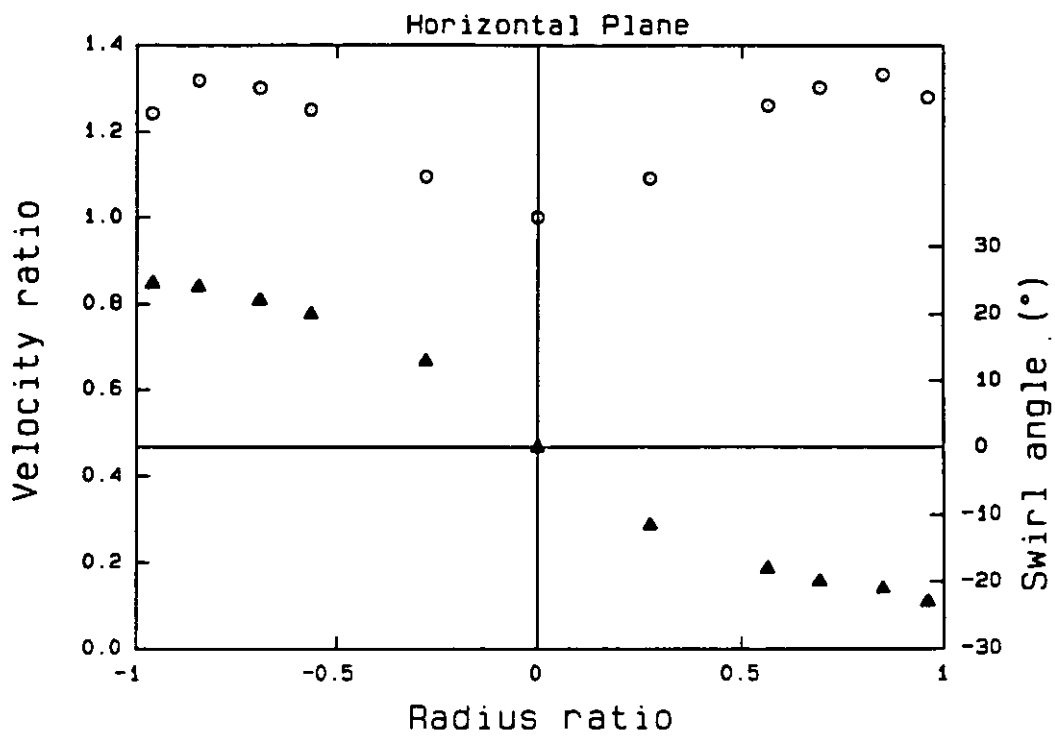


Fig 8 Profile at OD - No flow straightener

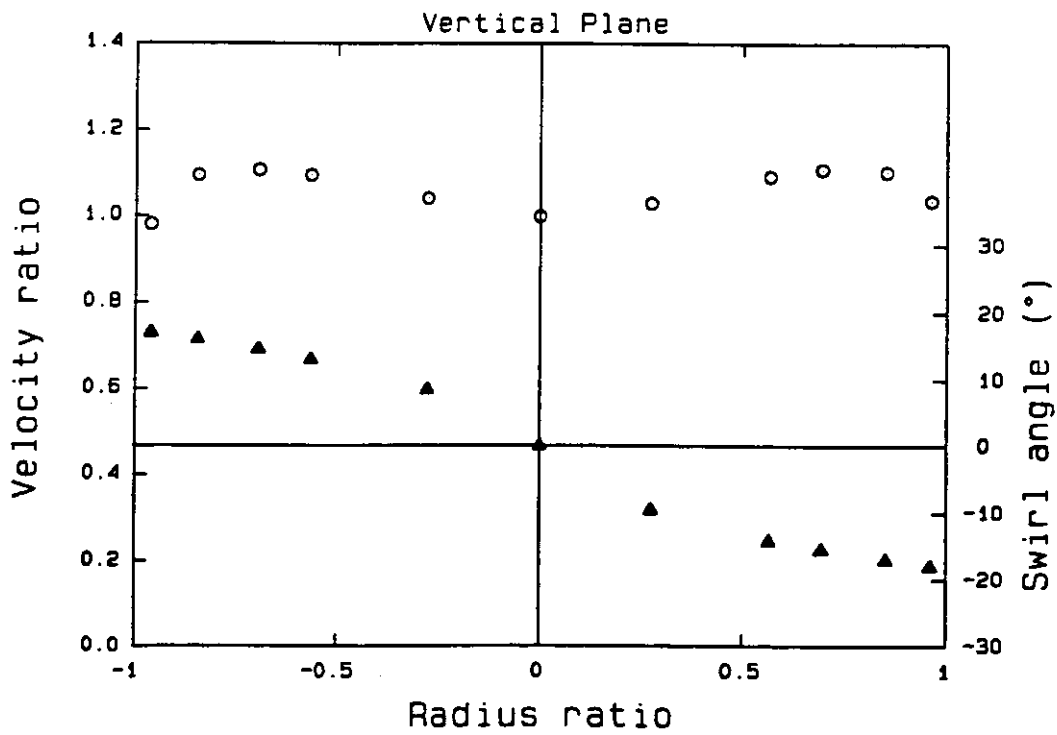
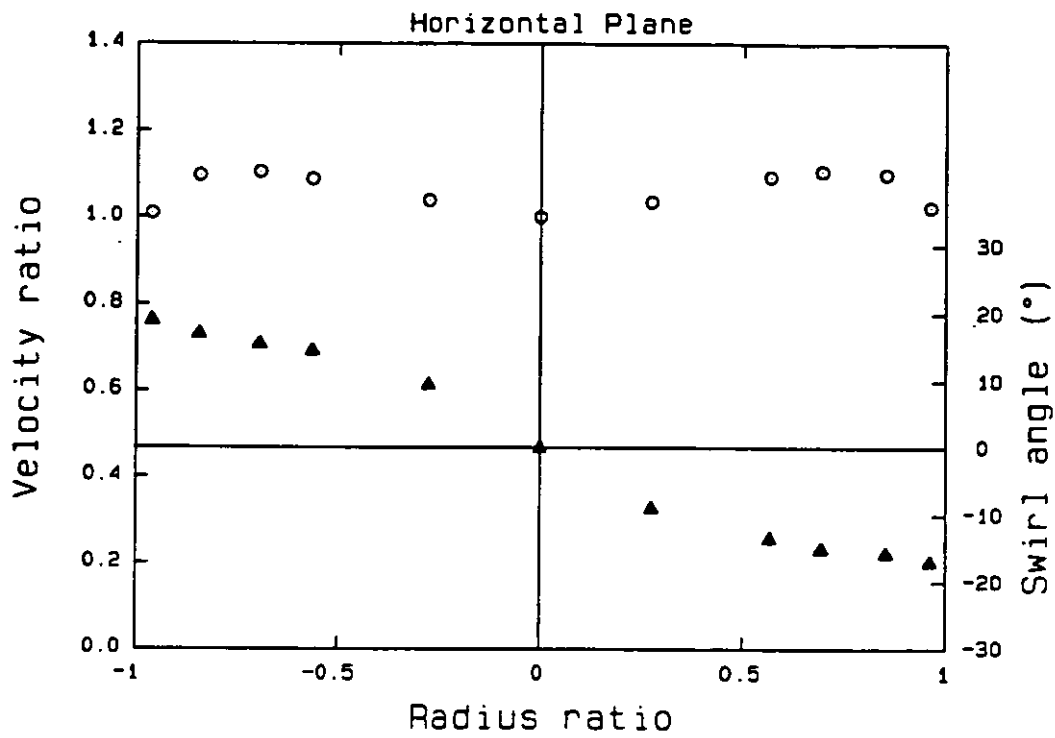


Fig 9 Profile at 19D - No flow straightener

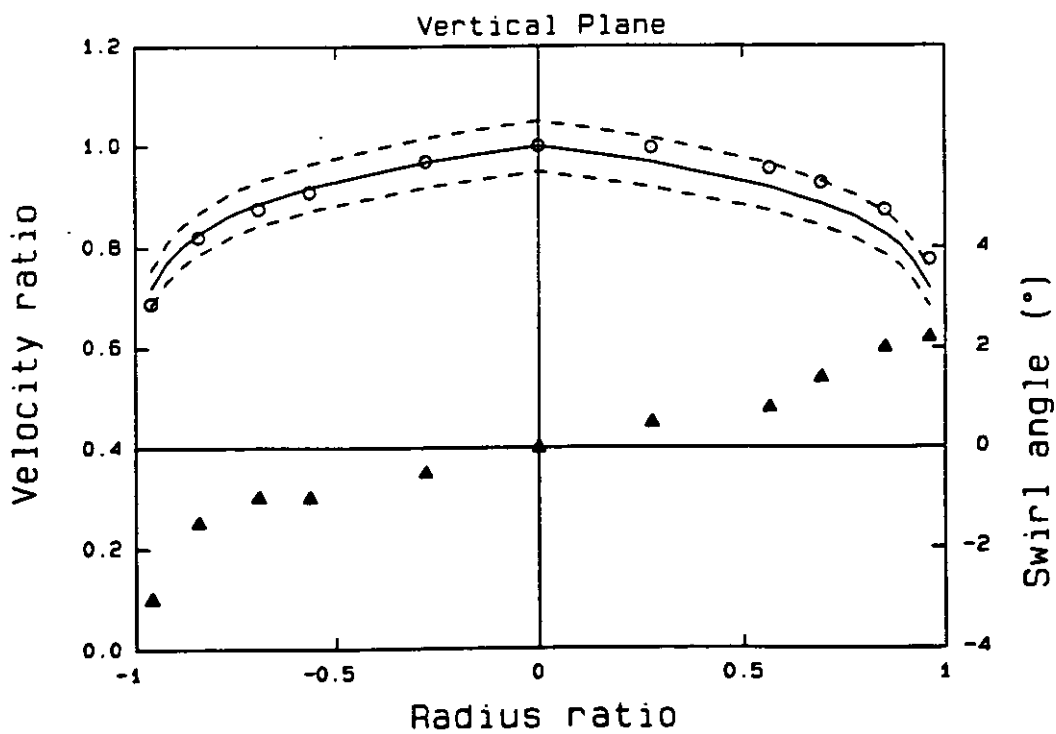
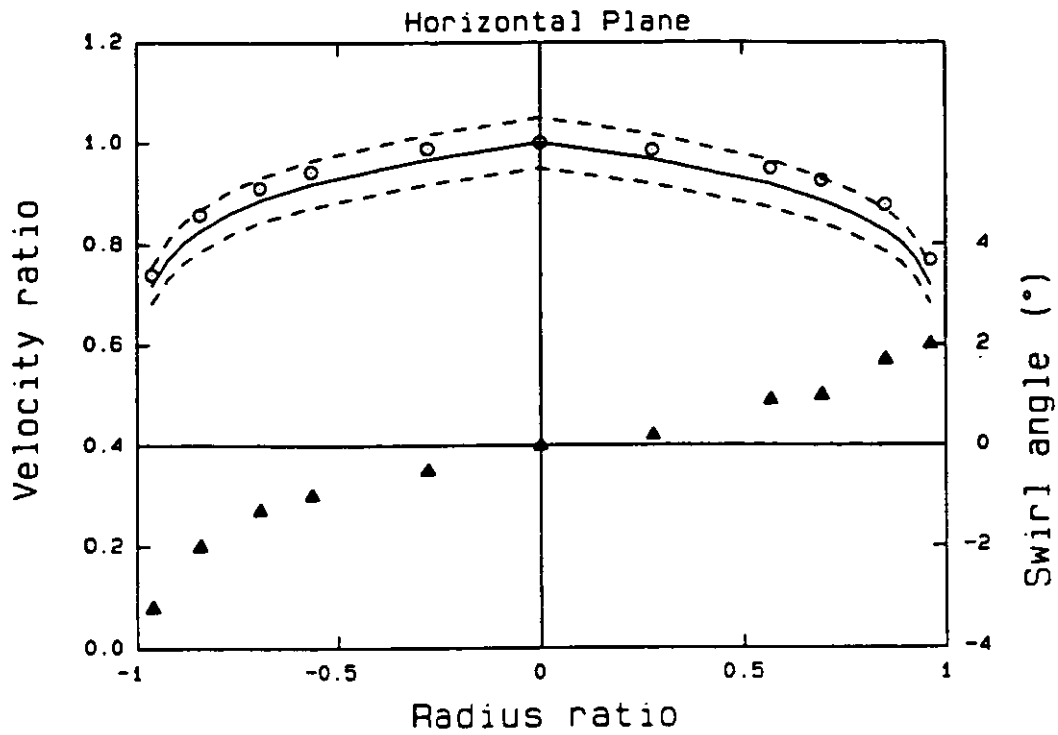


Fig 10 Zanker - Profile at 19D

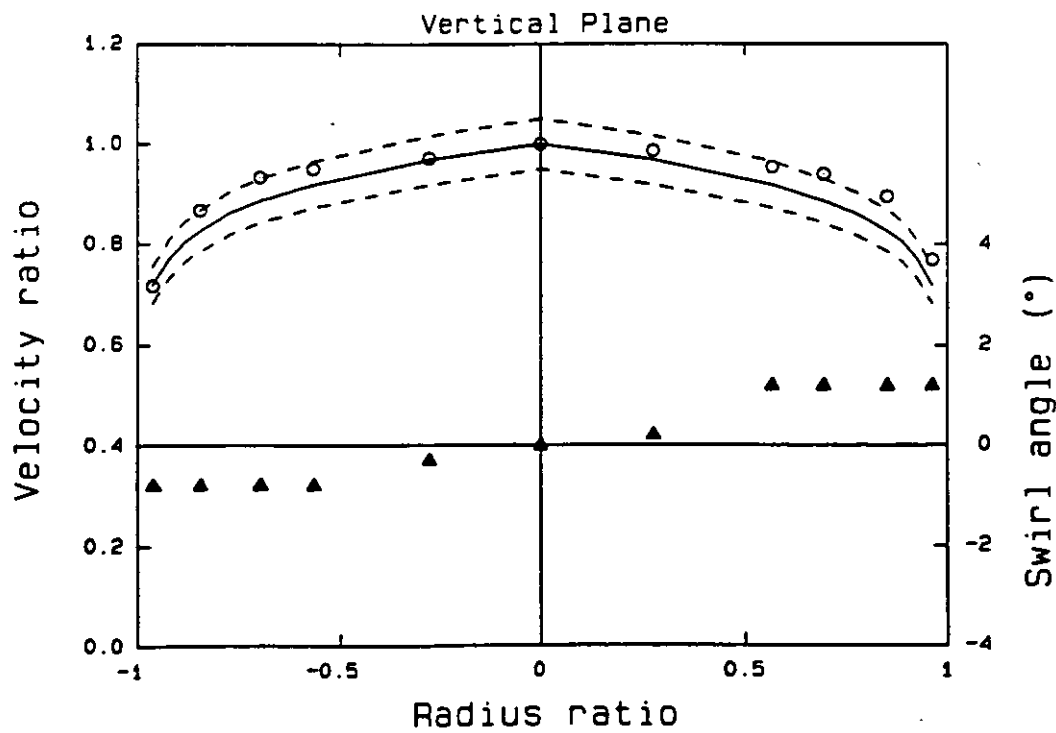
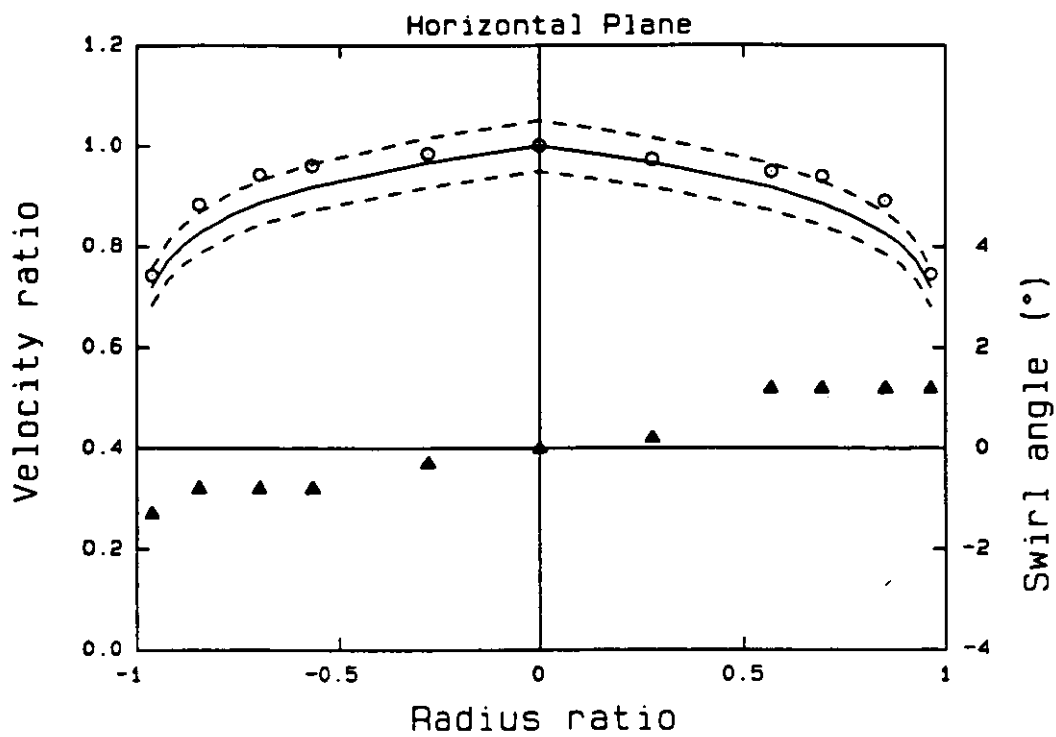


Fig 11 K-Lab - Profile at 6D

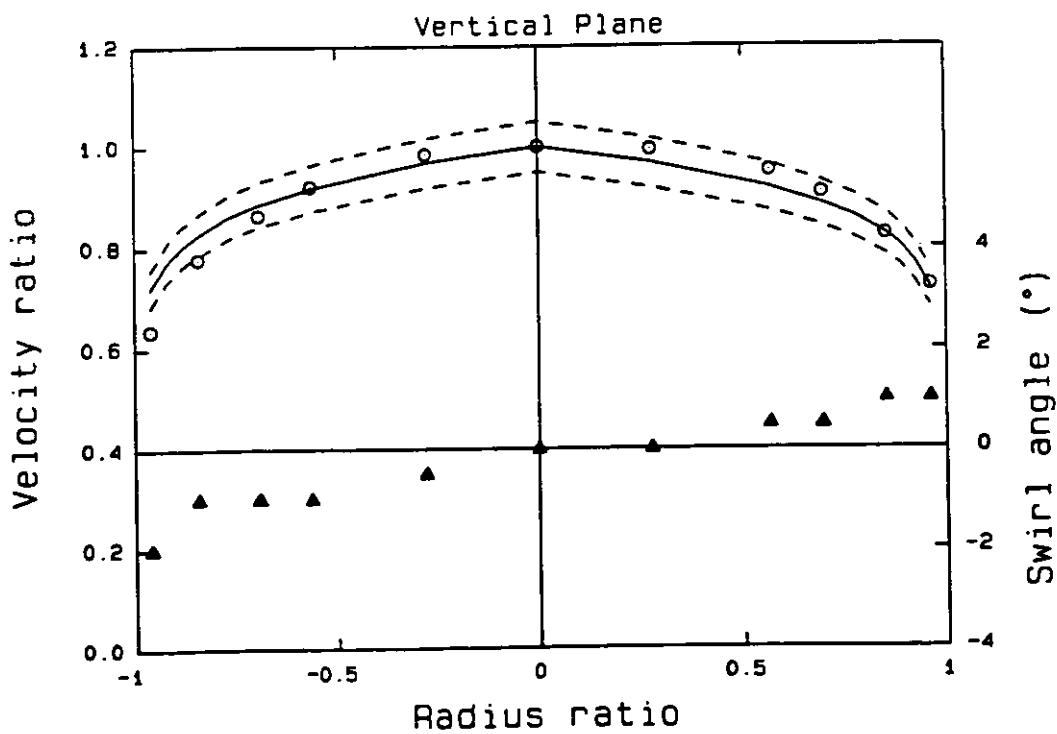
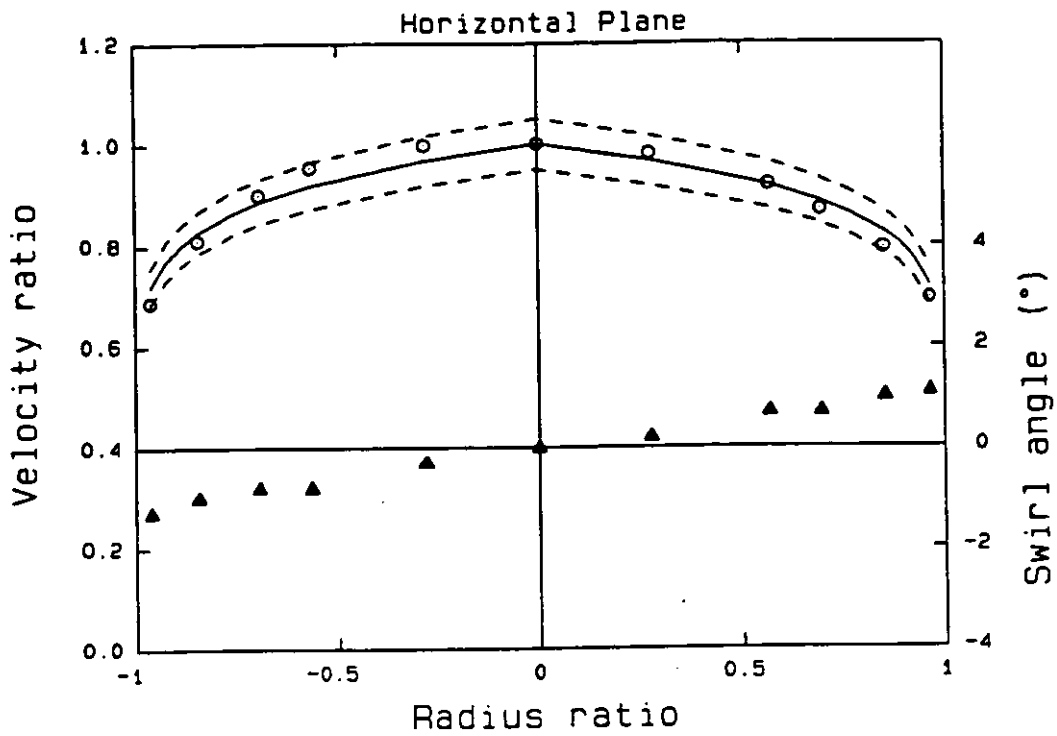


Fig 12 K-Lab - Profile at 19D

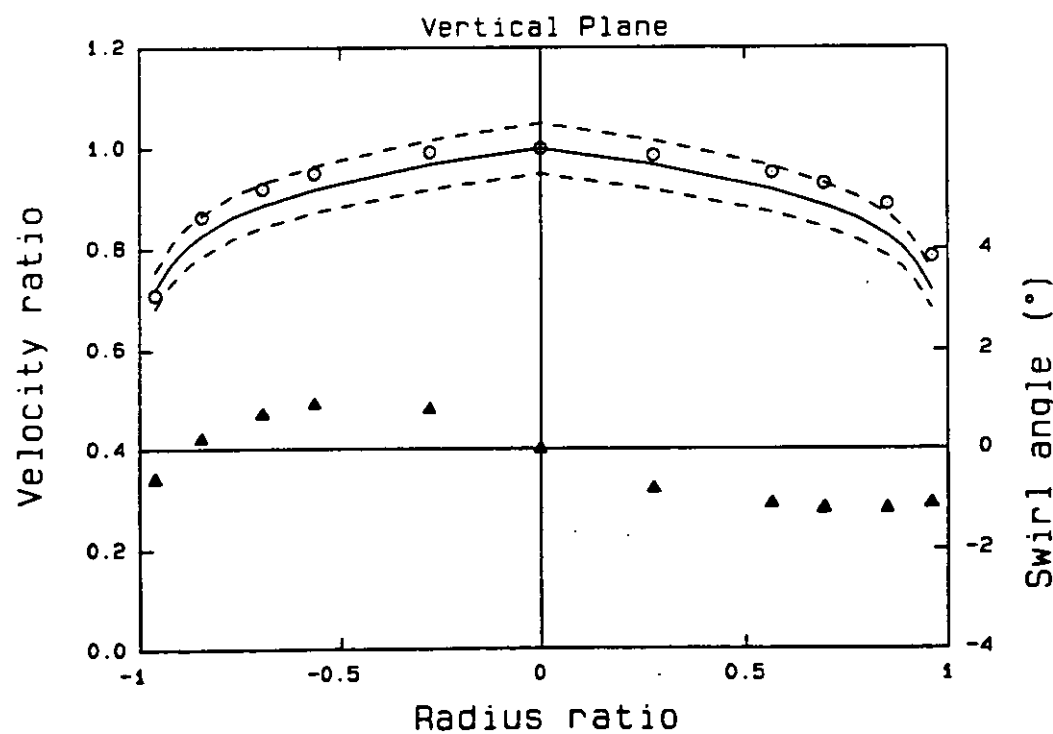
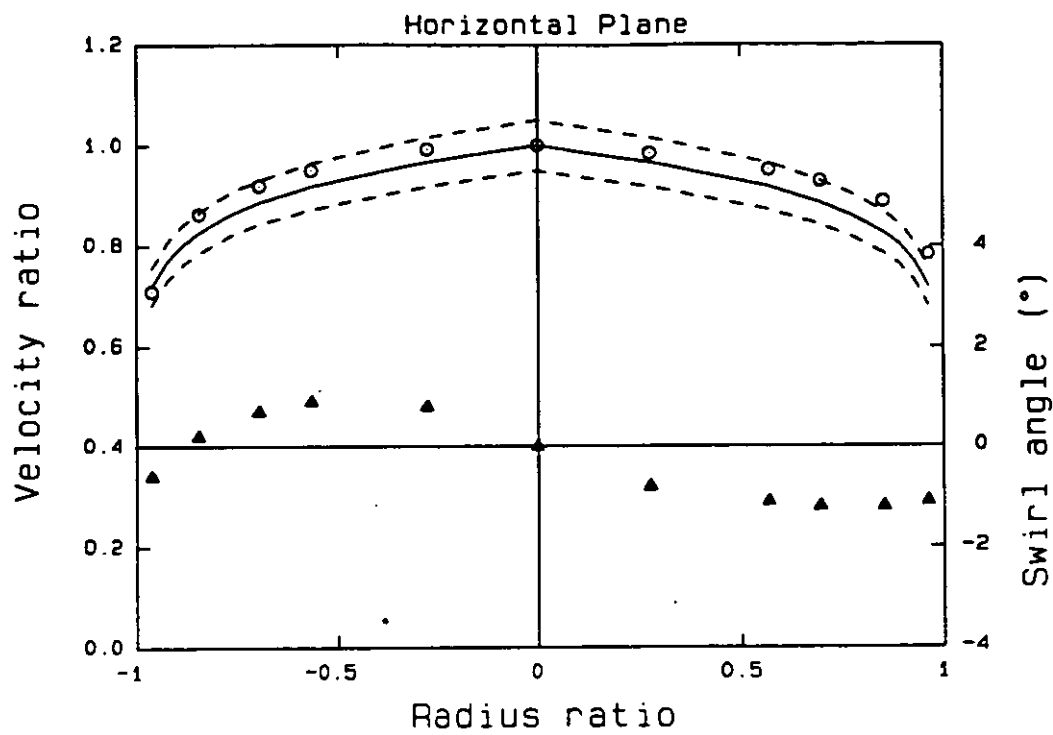


Fig 13 Laws - Profile at 6D

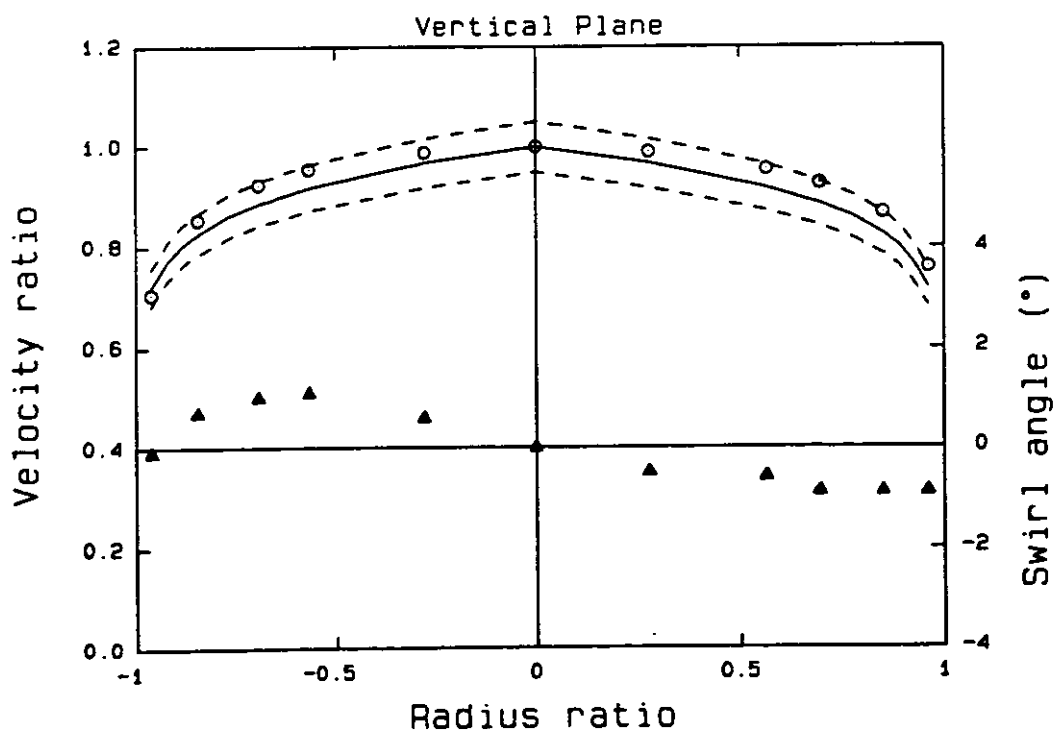
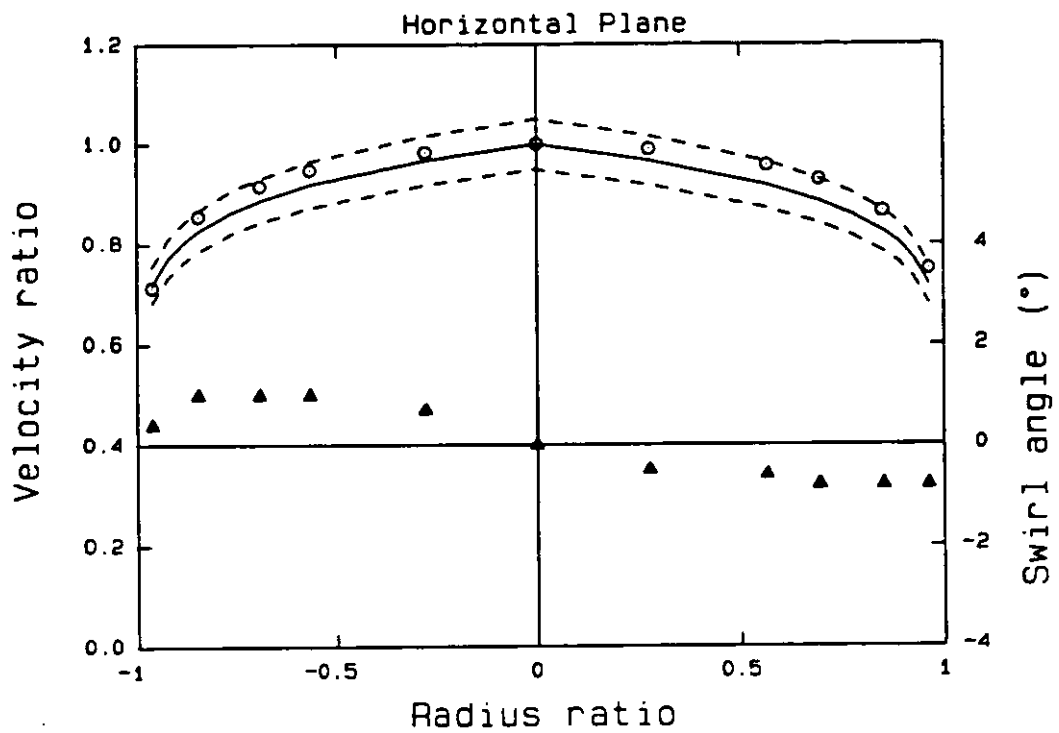


Fig 14 Laws - Profile at 9D

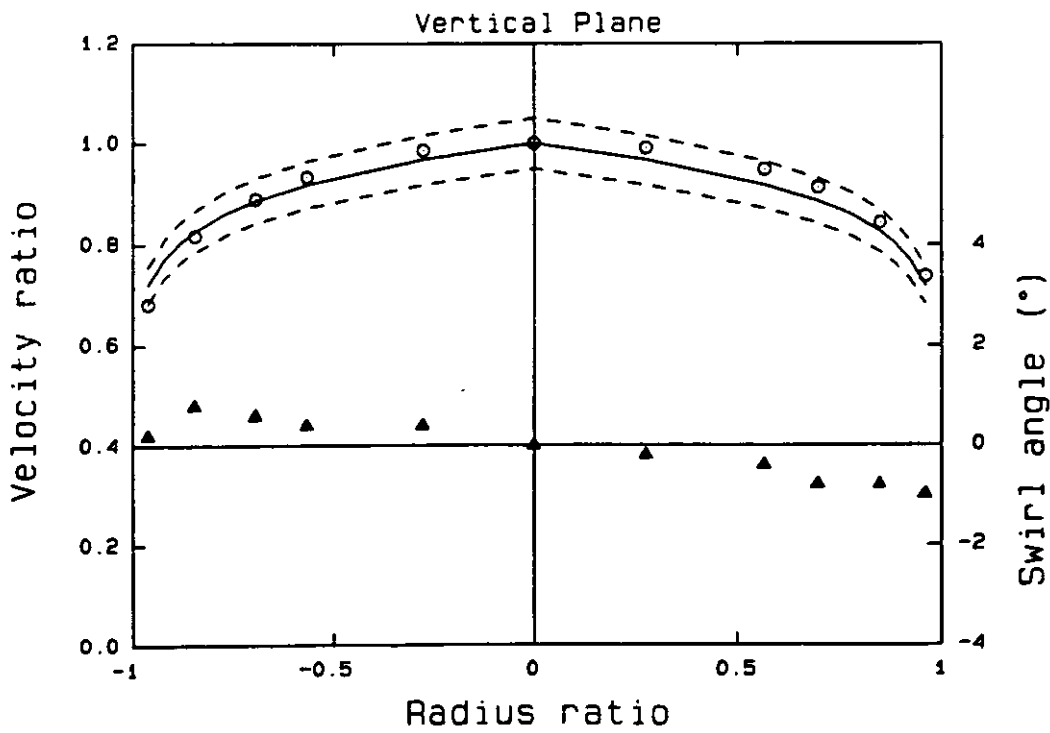
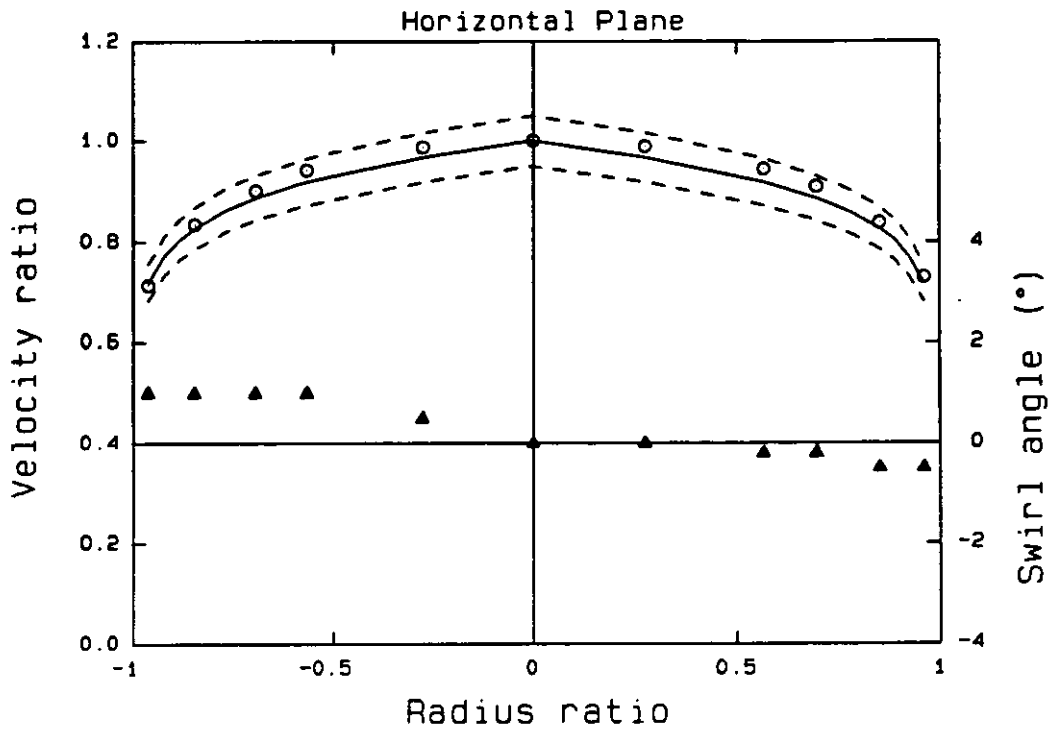


Fig 15 Laws - Profile at 19D

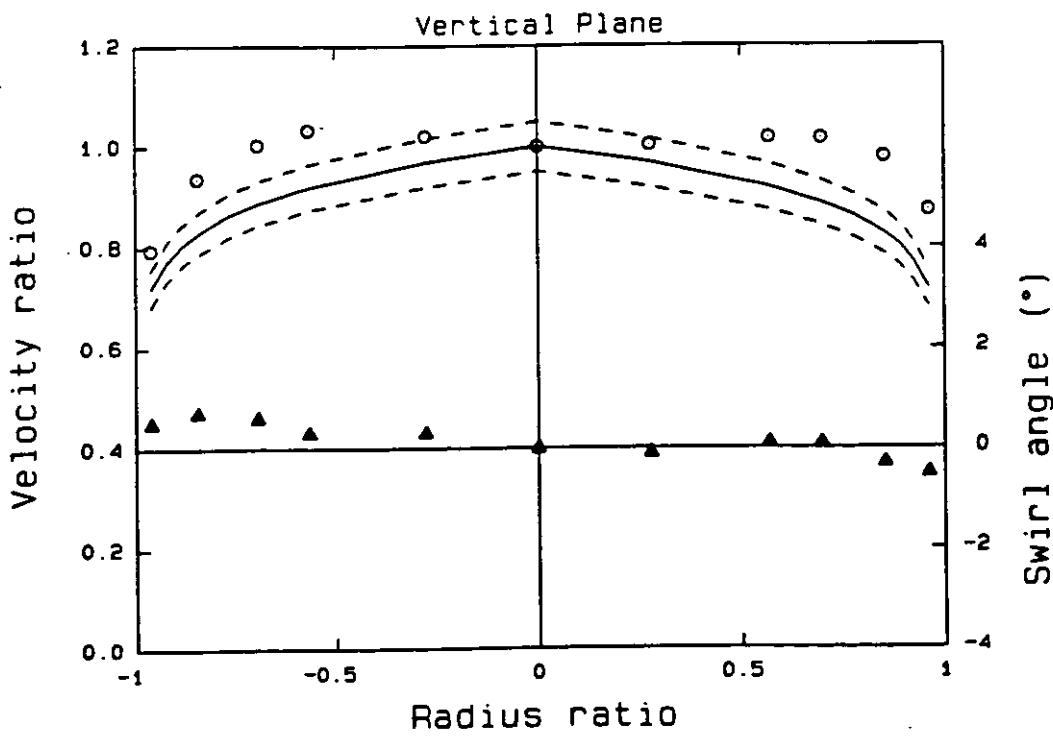
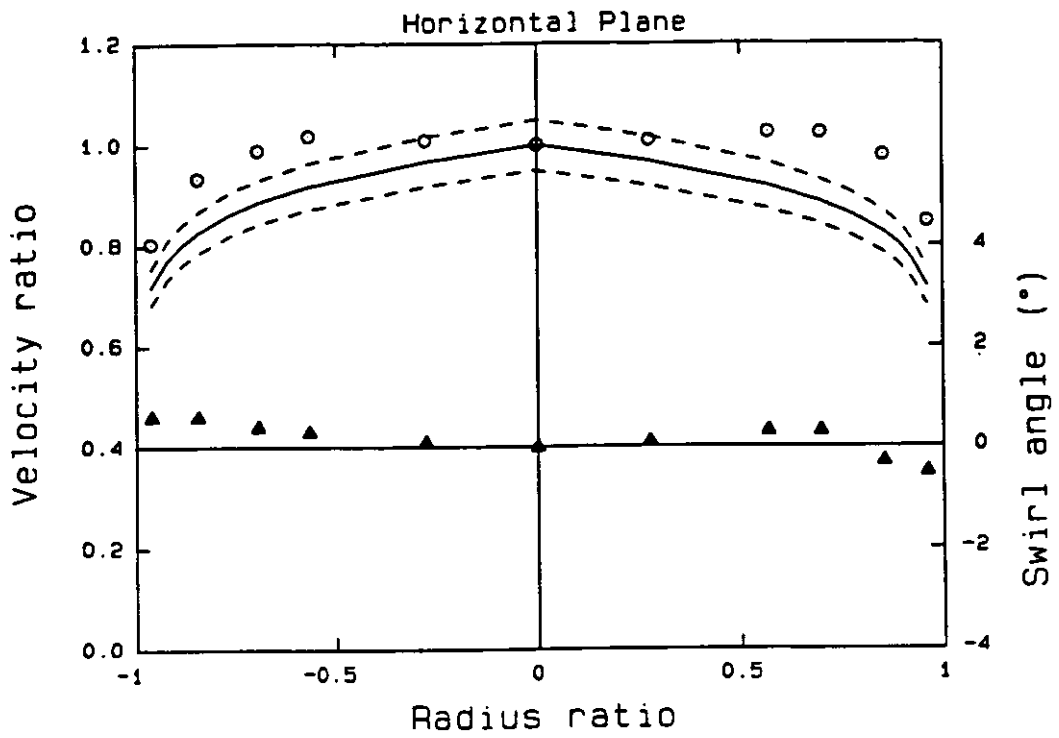


Fig 16 Tube bundle - Profile at 9D

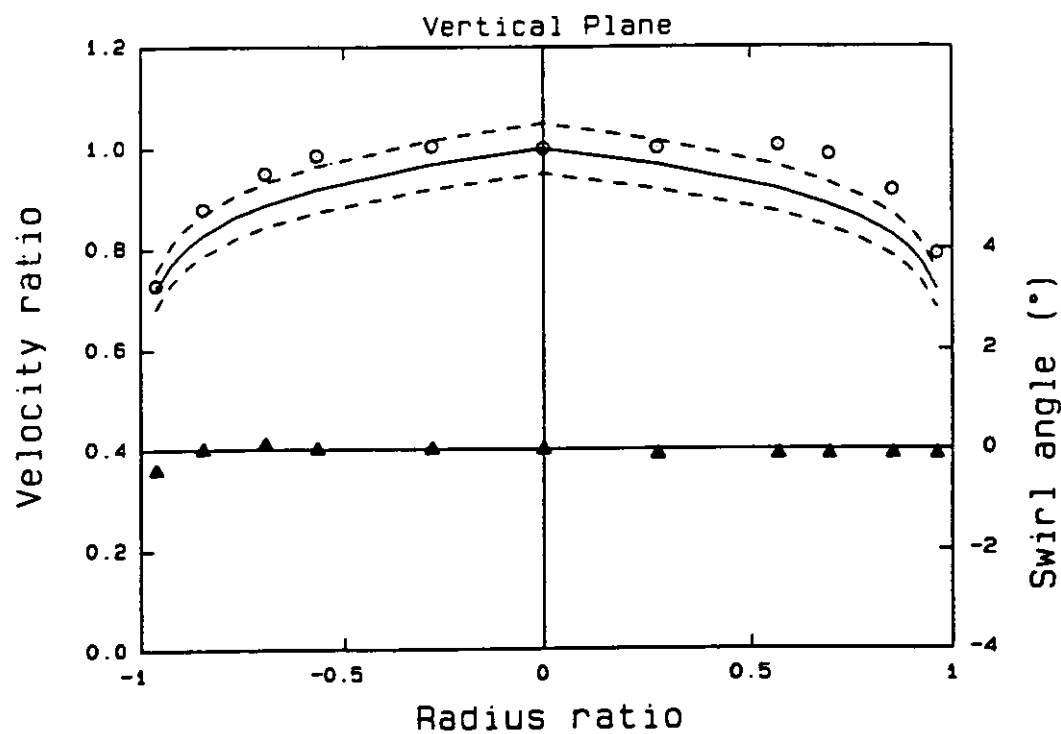
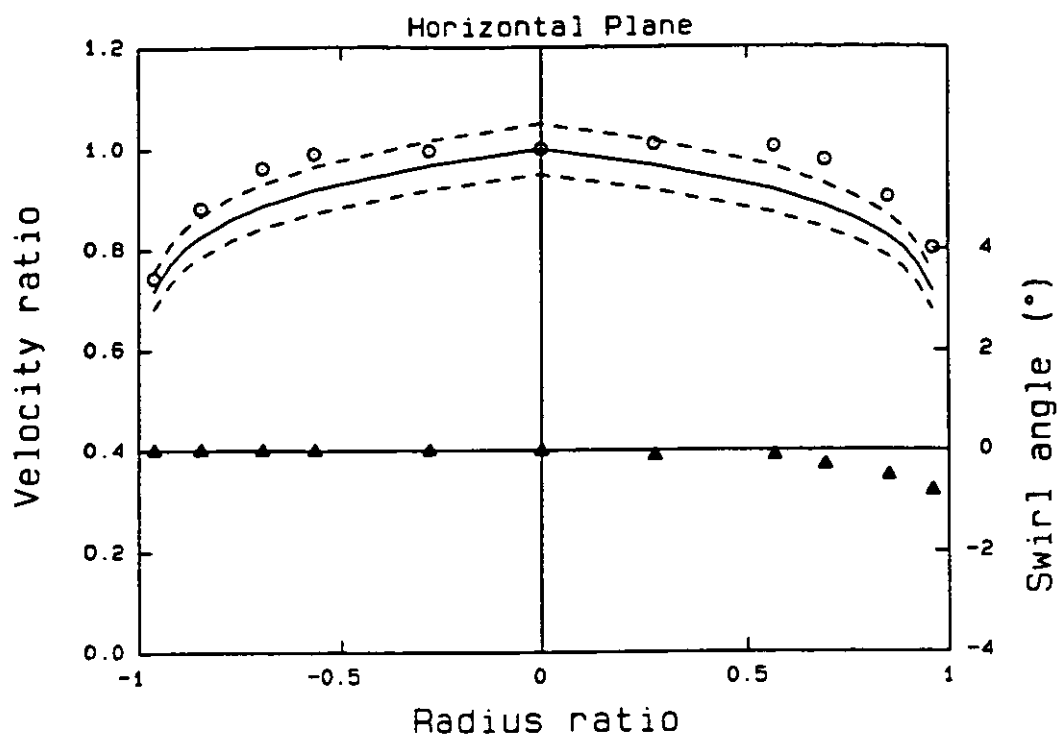


Fig 17 Tube bundle - Profile at 13D

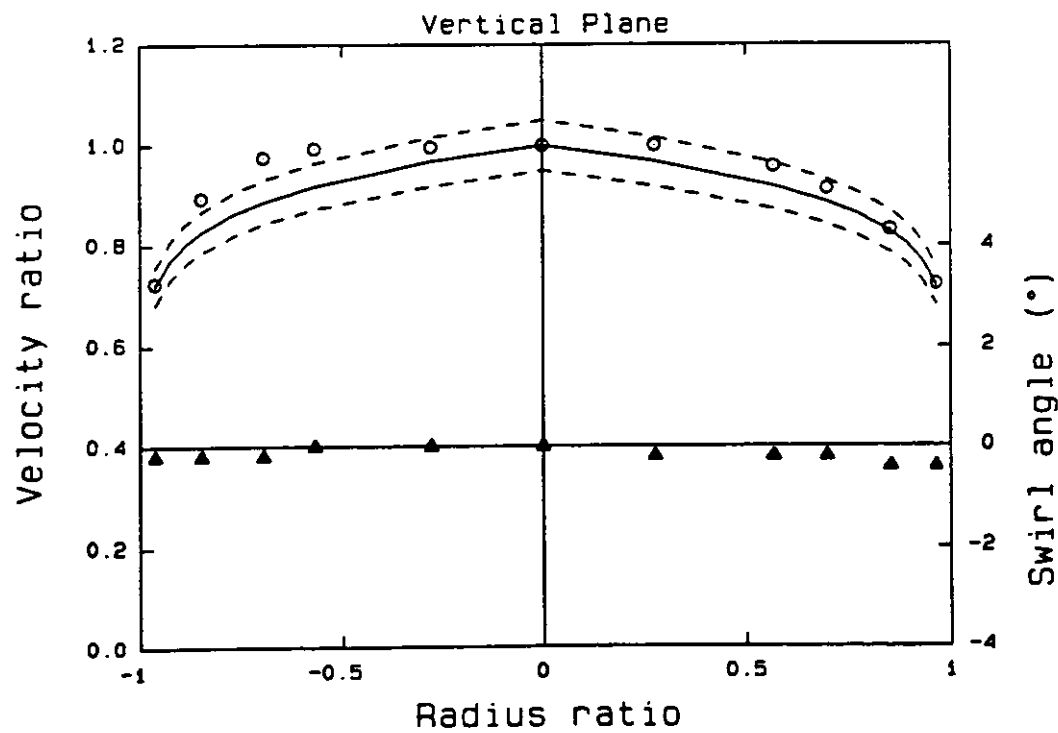
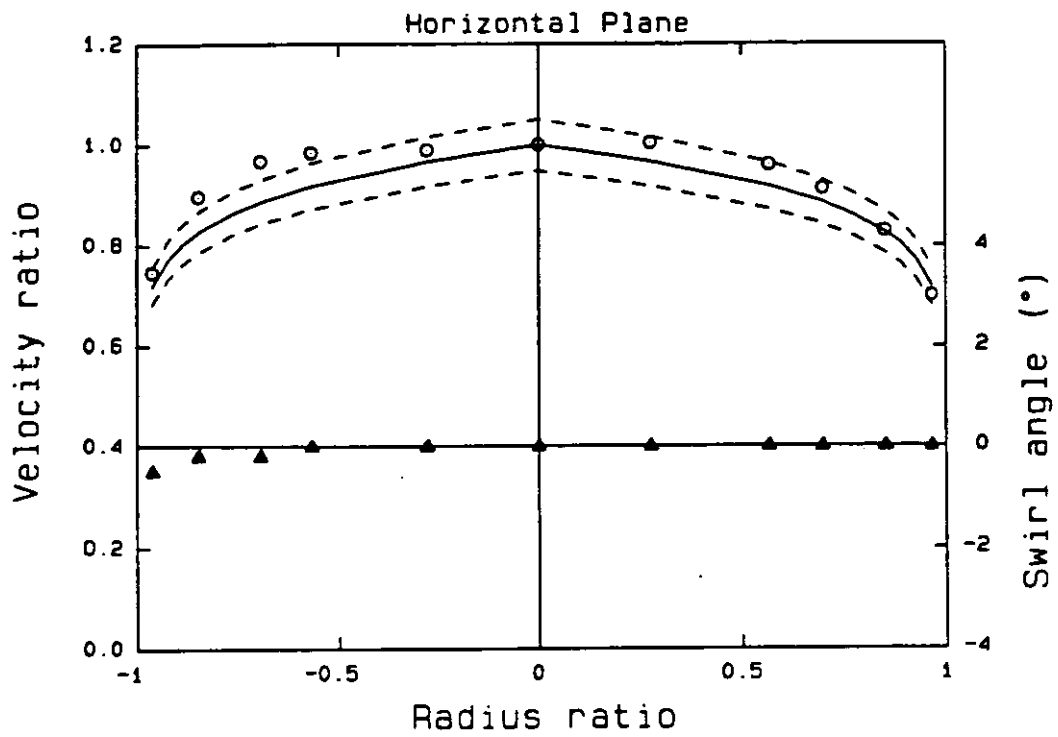


Fig 18 Tube bundle - Profile at 13DR

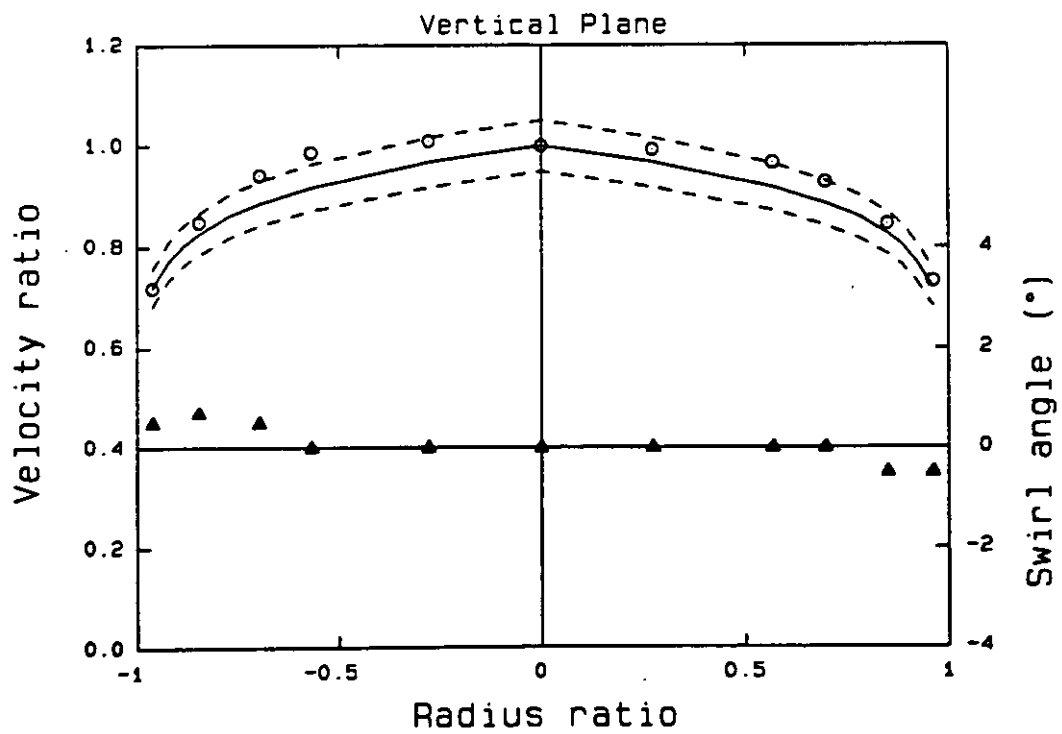
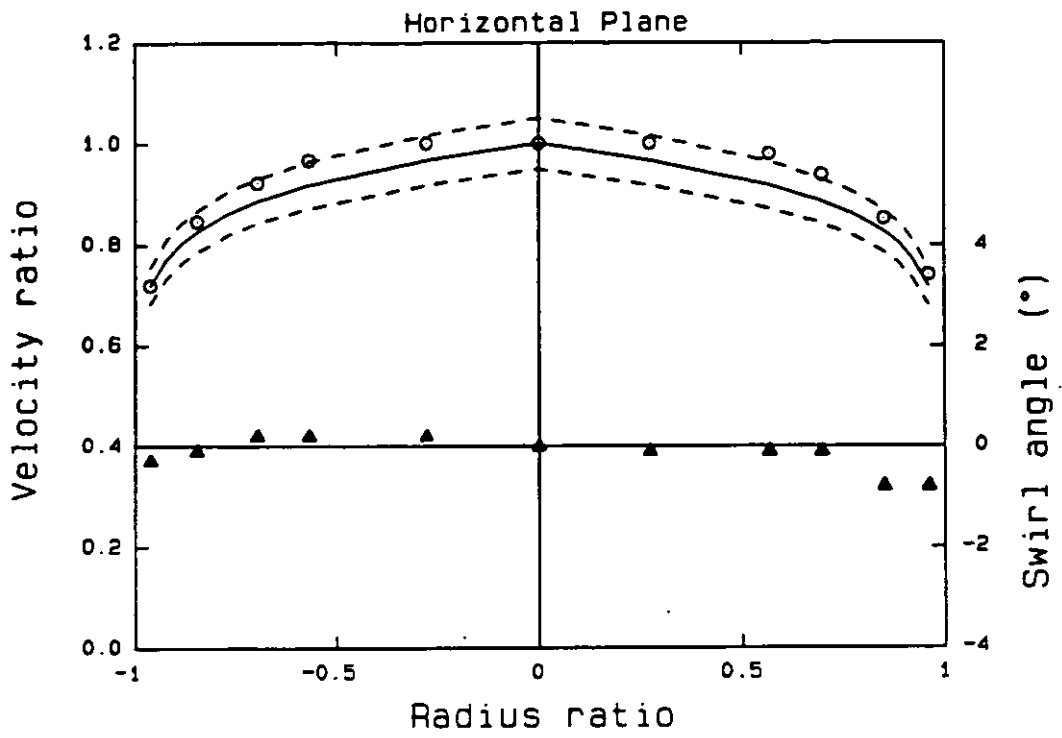


Fig 19 Tube bundle - Profile at 19D

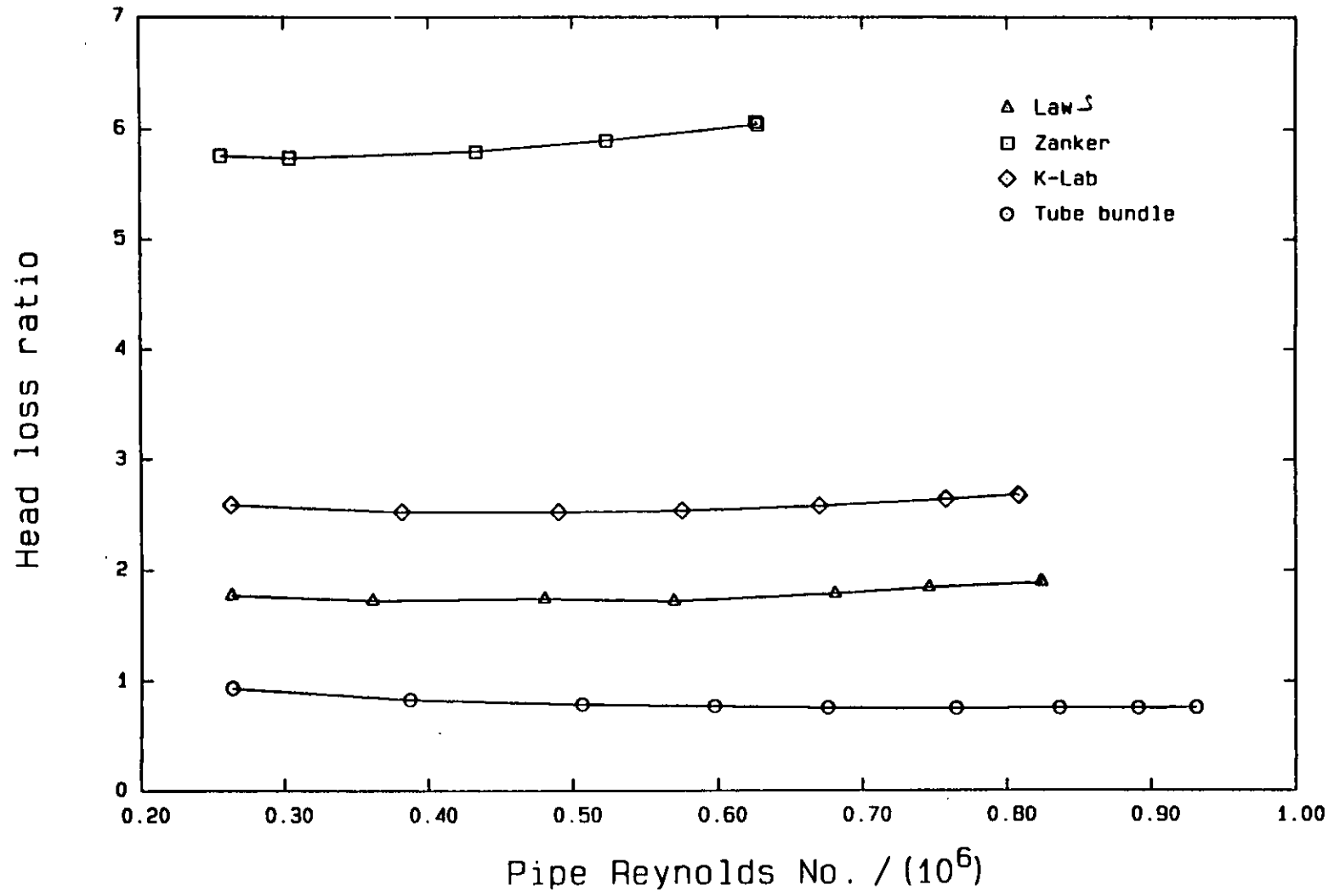


Fig 20 Flow conditioner head loss

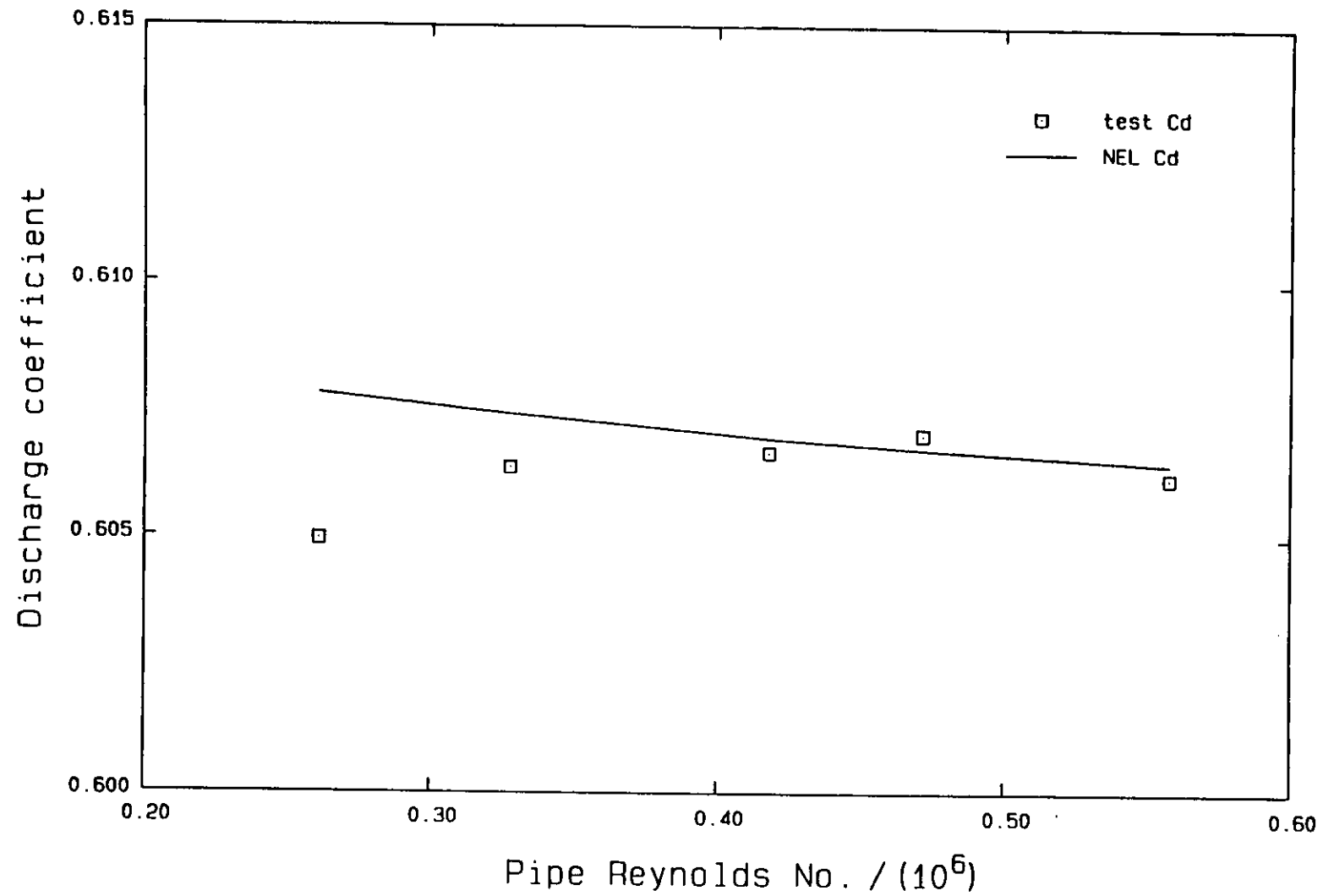


Fig 21 Discharge coefficient - Laws at 9D

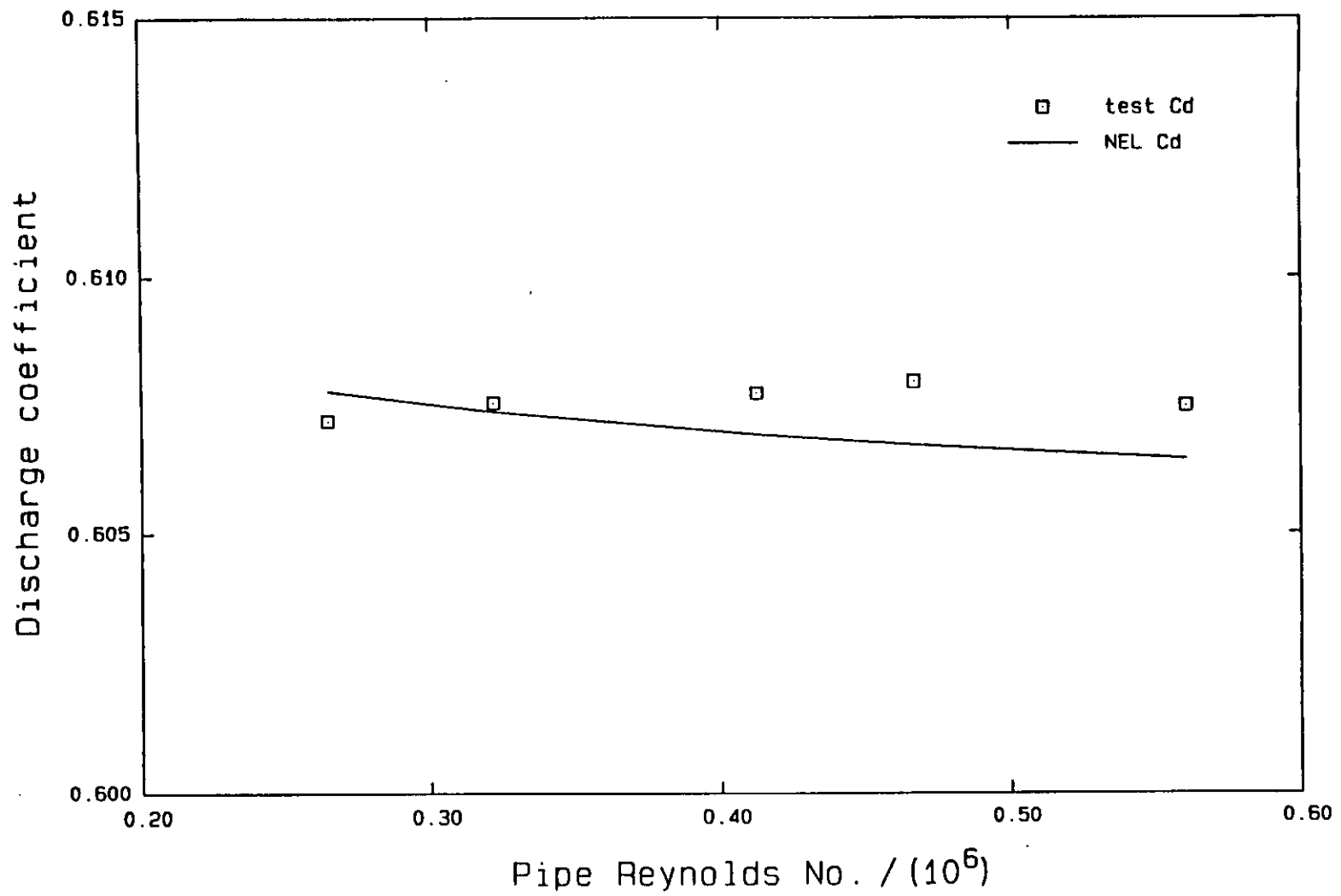


Fig 22 Discharge coefficient - Laws at 19D

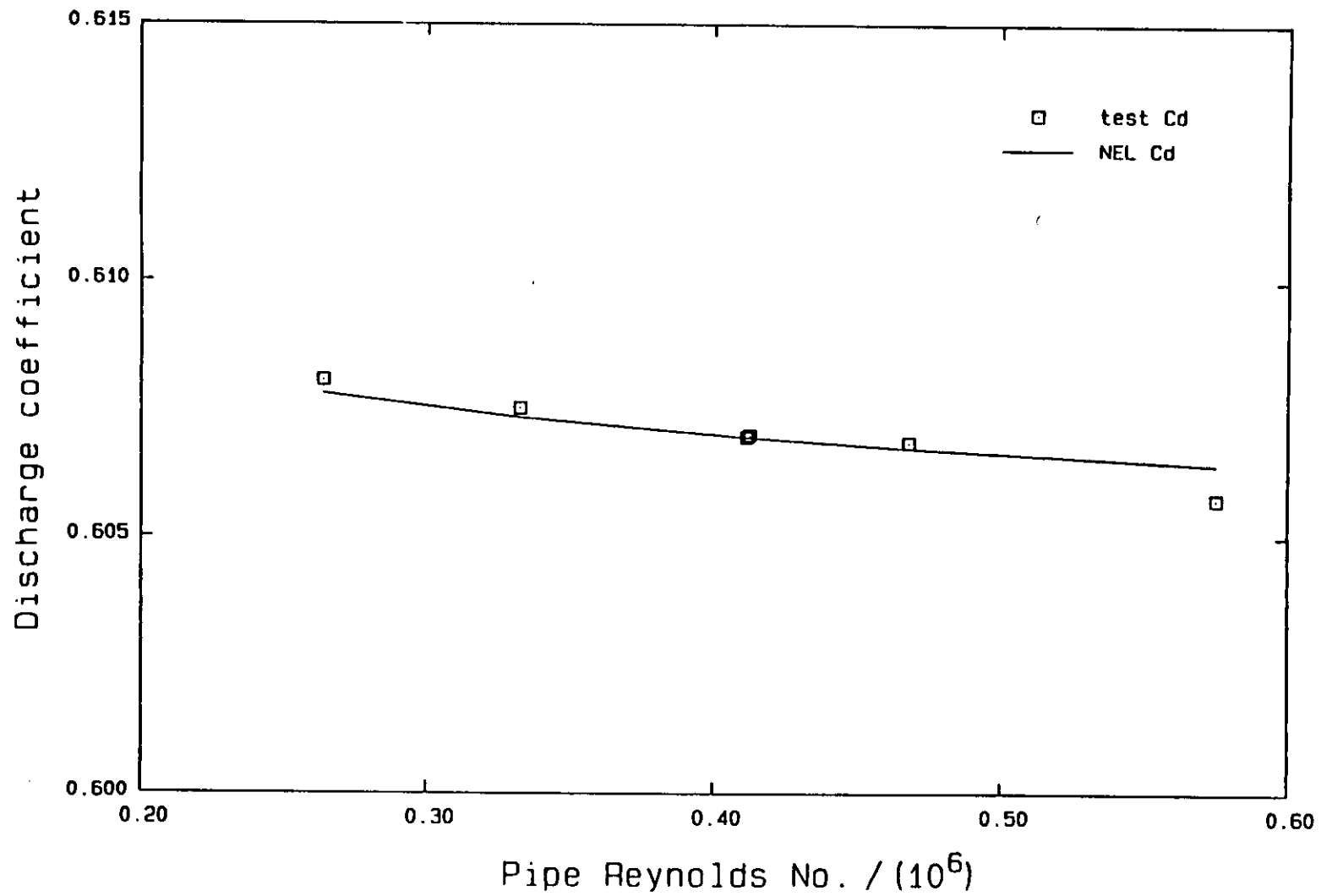


Fig 23 Discharge coefficient - Tube bundle at 13D

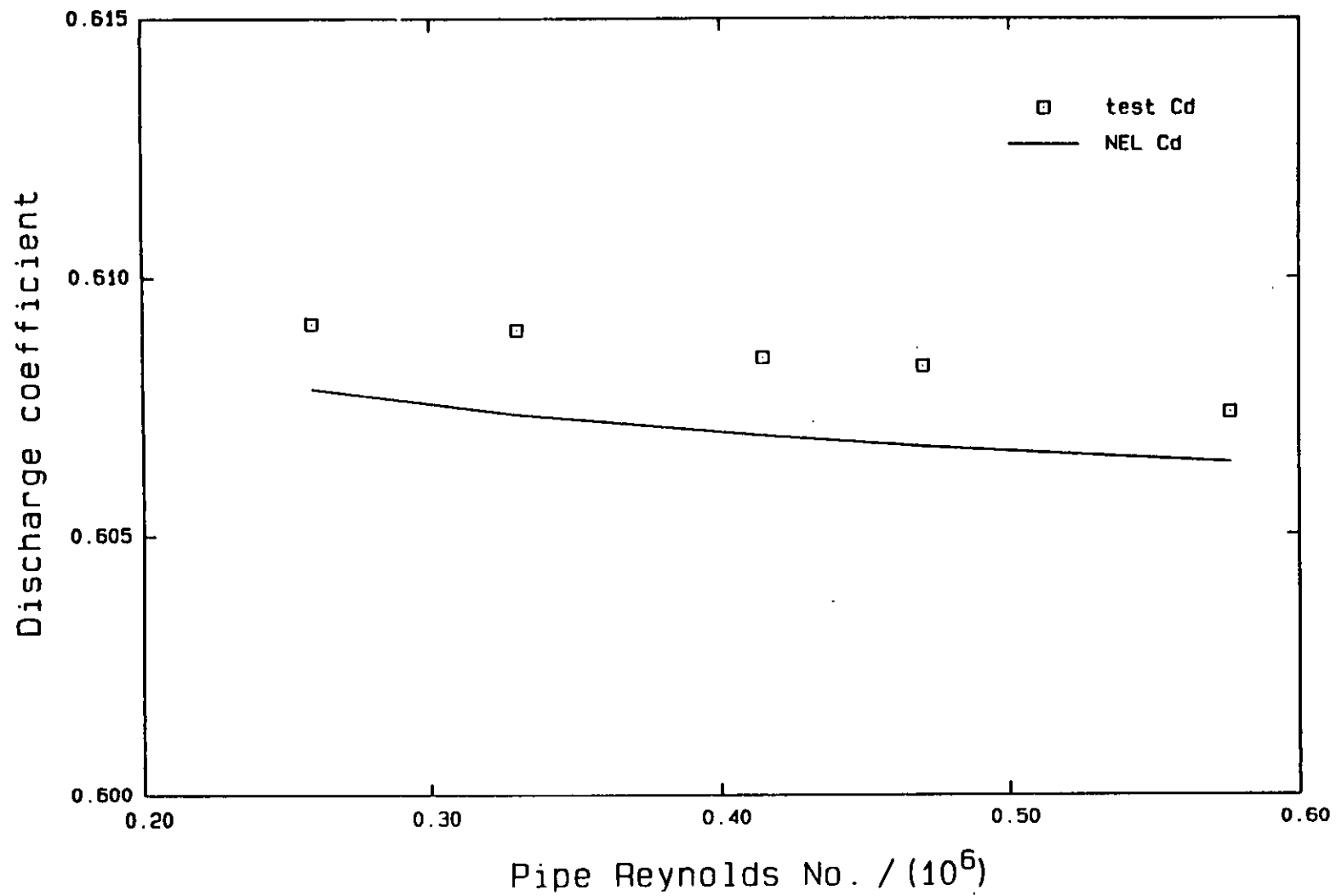


Fig 24 Discharge coefficient - Tube bundle at 13DR

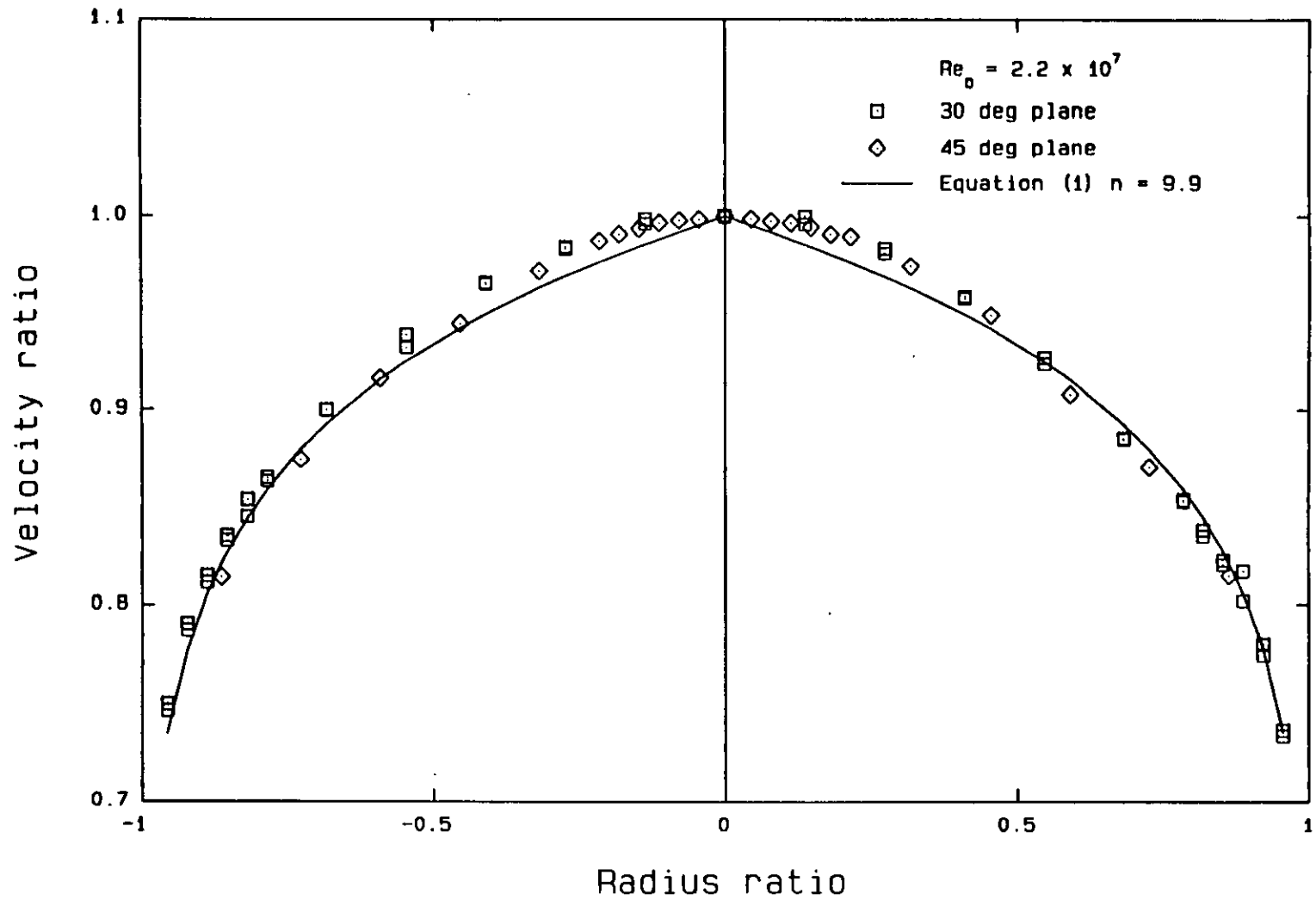
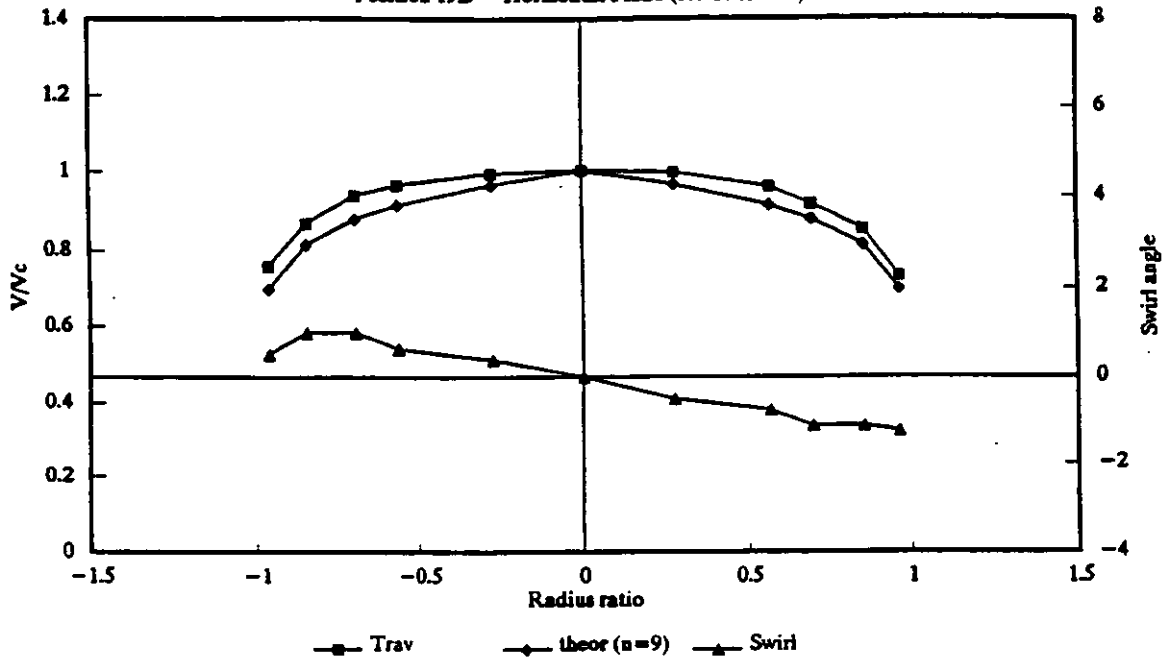


Fig 25 Velocity profile - British Gas 600mm pipe

Velocity Traverse (British Gas) - Laws

Position 19D - Horizontal Plane ($Re\ 10 \times 10^6$)



Velocity Traverse (British Gas) - Laws

Position 19D - Vertical Plane ($Re\ 10 \times 10^6$)

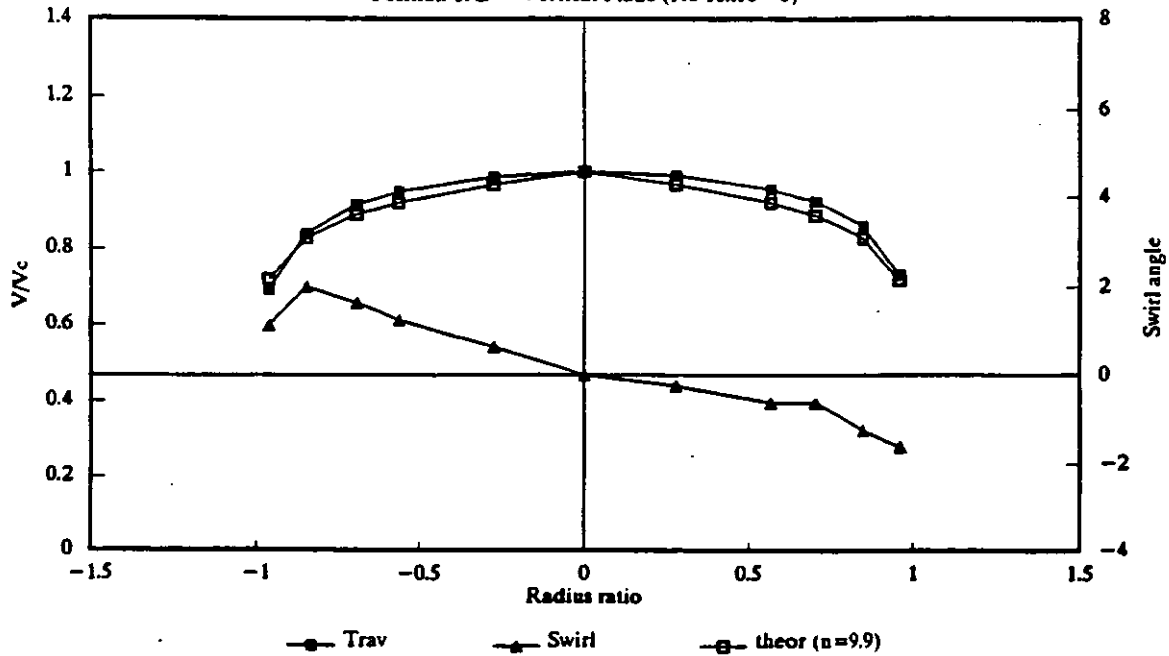


Figure 26

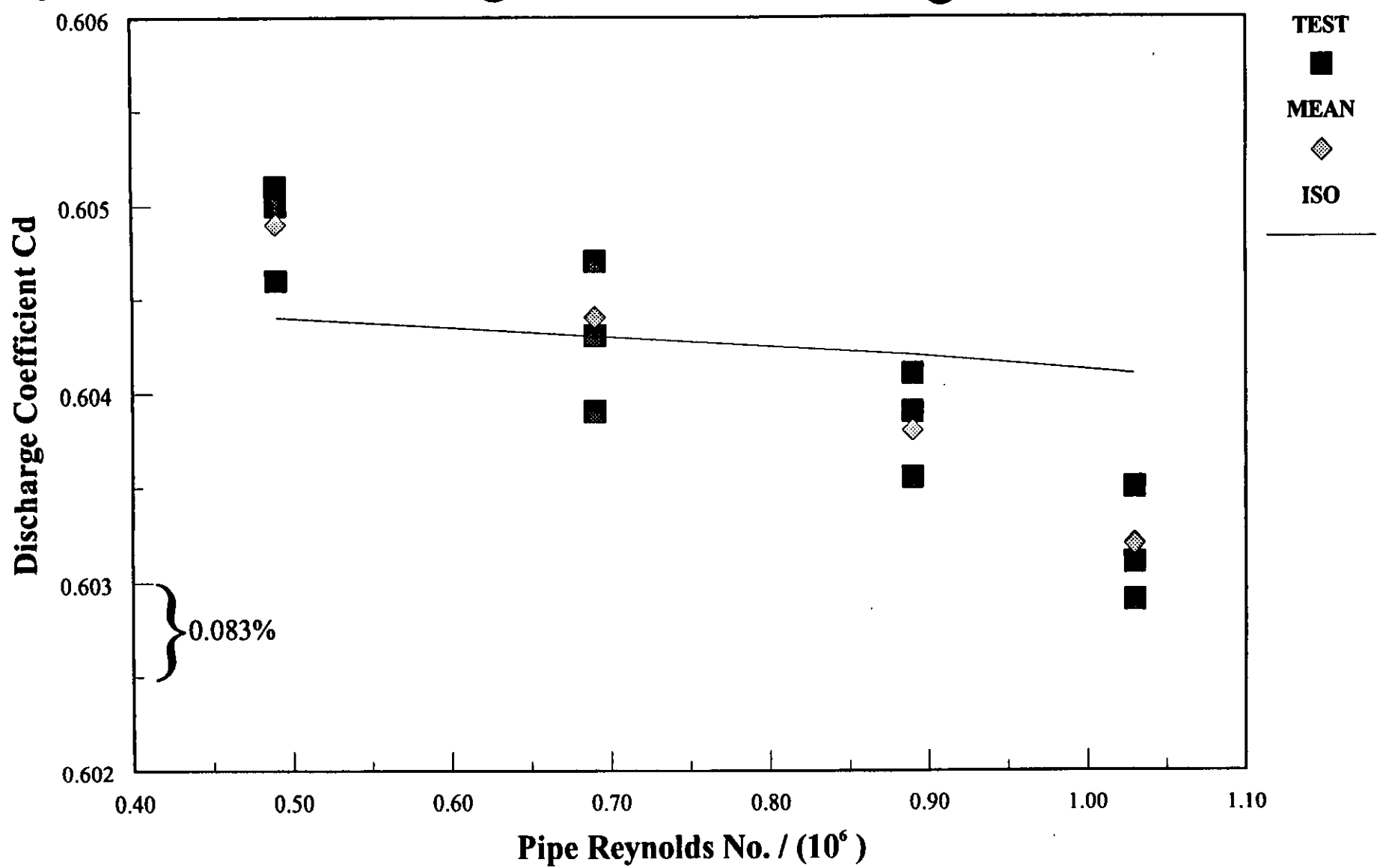


Fig 27 British Gas - Cd v Pipe Reynolds No.

Beta = 0.597 at 19D (Laws : 2nd test)

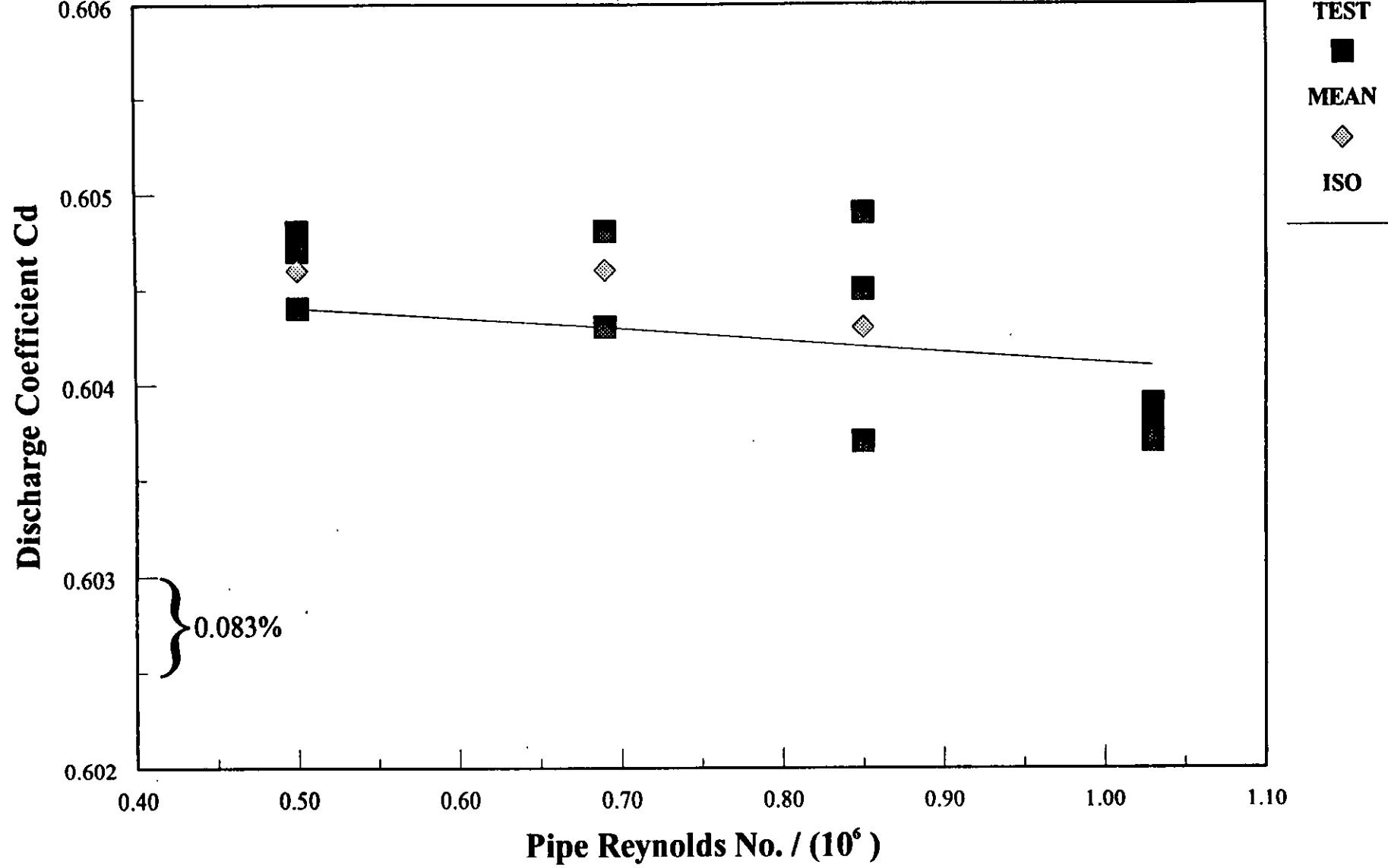


Fig 28 British Gas - Cd v Pipe Reynolds No.
 Beta = 0.597 at 9D (Laws)

MULTIPHASE FLOWMETER MEASUREMENT UNCERTAINTIES

by

B C Millington and T S Whitaker
NEL

Paper 2.1

NORTH SEA FLOW MEASUREMENT WORKSHOP
26-29 October 1992

NEL, East Kilbride, Glasgow

MULTIPHASE FLOWMETER MEASUREMENT UNCERTAINTIES

B C Millington and T S Whitaker

Flow Centre, NEL

SUMMARY

The paper describes the state of the art in multiphase flow metering from a theoretical point of view, giving brief details of how the individual mass flowrates of each phase are derived. The limitations imposed by using such calculation procedures are then fully explained in terms of metering uncertainties.

By referring to previous theoretical work, the level of uncertainty in the individual mass flowrate measurements for a typical multiphase flowmeter are shown to be in excess of 10 per cent for virtually all possible combinations of oil, water and gas phase fractions. Most importantly though, it is shown that the individual mass flowrate uncertainties are very dependent upon the flow composition. It is therefore concluded that for any multiphase flowmeter, uncertainty data must be qualified with a statement of the flow composition to which it applies.

NOTATION

m_g	<i>mass flowrate of gas</i>
m_o	<i>mass flowrate of oil</i>
m_w	<i>mass flowrate of water</i>
Q_t	<i>total volumetric flowrate at the metering conditions</i>
α_g	<i>gas phase fraction at the metering conditions</i>
α_o	<i>oil phase fraction at the metering conditions</i>
α_w	<i>water phase fraction at the metering conditions</i>
β	<i>liquid water content</i>
μ	<i>liquid fraction of the multiphase mixture</i>

- ρ_g *gas density at the metering conditions*
- ρ_o *oil density at the metering conditions*
- ρ_w *water density at the metering conditions*
- ρ_t *total multiphase density at the metering conditions*
- ρ_L *liquid density at the metering conditions*

1 BACKGROUND

Throughout the late 1980's and early 1990's the transportation and measurement of multiphase flows, especially oil/water/gas flows, has come under increasing scrutiny because of the economic advantages to be gained by using the technology to avoid platform based separation processes. One of the key short term objectives that has been identified is to replace test separators with multiphase flowmeters, saving both weight and space on platforms. In the medium term subsea multiphase flowmeters located on each well will give near instantaneous flow data for reservoir control and allocation purposes, and in the longer term multiphase meters will be used for fiscal purposes. The economic gains to be made are considerable and will greatly improve the viability of some of the more marginal fields, and will certainly aid the exploitation of fields in deeper water.

Most oil companies are therefore vigorously pursuing the development of multiphase flowmeters which would be capable of replacing the test separators, and which can also be located subsea. At the present time the authors are aware of 18 separate multiphase flowmeter development projects worldwide.

In the haste to achieve an operational prototype multiphase meter, some of the fundamental measurement difficulties have often been overlooked. It is the purpose of this paper to rectify this situation, giving a balanced assessment of the likely measurement uncertainties involved in this type of metering, and identifying the major problems.

This information will be of interest to both the developer and user alike, and it is hoped it will provide a basis for realistic performance aims for first generation multiphase flowmeters.

2 MULTIPHASE FLOWMETER DESIGNS

Ideally a multiphase flowmeter would make 3 separate, but simultaneous measurements: one of the oil flowrate, one of the water flowrate, and one of the gas flowrate. Each of the separate measurements not being influenced by the fact that the other two phases are present. This type of meter is not yet technically possible, and it is unlikely that such a meter will be available within the next 10 years.

However, instrumentation is available which is capable of discriminating between two flow components; water-in-oil monitors are a good example. By combining a number of indirect measurements it is possible to determine the flow composition of 3-phase flows, and coupling this information with a measurement of the total volumetric flowrate it is then possible to determine the individual mass flowrates of each phase. All of the present multiphase meters under development use this same basic technique, although the measurements made vary from meter-to-meter.

An example of a typical system configuration is shown in fig.1. In this design the three key measurements are the water content in the liquid after sampling and removing any entrained gas; the total oil/water/gas density; and the total flowrate. The procedure used to calculate the oil, water and gas phase fractions and flowrates is given below. (For simplicity it is assumed that pressure and temperature variations are accounted for)

Consider the flow to be gas-liquid with a liquid fraction of μ , then the total density can be written:

$$\rho_t = (1 - \mu)\rho_g + \mu\rho_L \quad (1)$$

Similarly, if the water content in the liquid is denoted by β then the expression for the liquid density is

$$\rho_L = (1 - \beta)\rho_o + \beta\rho_w \quad (2)$$

Substituting the expression for the liquid density into equation (1) gives an alternative expression for the total density

$$\rho_t = (1 - \mu)\rho_g + \mu(1 - \beta)\rho_o + \mu\beta\rho_w \quad (3)$$

where the coefficients of the oil, water and gas densities are the volumetric phase fractions, therefore

$$\alpha_g = 1 - \mu$$

$$\alpha_o = \mu(1 - \beta)$$

$$\alpha_w = \mu\beta$$

So if μ and β can be measured or calculated then the flow composition can be derived.

In the system shown in fig.1 assume that the water content in the liquid is found by measuring the liquid density, then from equation (2)

$$\beta = \frac{\rho_L - \rho_o}{\rho_w - \rho_o} \quad (4)$$

where the oil and water densities are known from the well characteristics.

Likewise from equation (1) the liquid fraction μ can be found by re-arranging to give

$$\mu = \frac{\rho_t - \rho_g}{\rho_L - \rho_g} \quad (5)$$

where the liquid density and the total density are measured, and the gas density is known from the well characteristics.

Having calculated the phase fractions using the values of μ and β , the individual mass flowrates of each phase can be found by obtaining a measurement of the total volumetric flowrate

$$m_g = \alpha_g \rho_g Q_t$$

$$m_o = \alpha_o \rho_o Q_t$$

$$m_w = \alpha_w \rho_w Q_t$$

There are many technical difficulties in achieving a working system of this type, but from a theoretical point of view the above analysis is the basis common to all of the multiphase flowmeters under present development.

3 MULTIPHASE FLOWMETER MEASUREMENT UNCERTAINTIES

3.1 The key problems

The technique outlined above is a perfectly acceptable method of calculating the individual flowrates of oil, water and gas, but there are fundamental limitations on the measurement uncertainties achievable.

Unlike a single phase flow in which any measurements made relate directly to the liquid or gas present, the measurements taken to define the flow composition of a two-phase or multiphase flow are indirect, and relate to 2 or more phases. If the phase fraction of the required flow component is low, then in relative terms the measurement uncertainties in the instruments used can have a major effect on the uncertainty in the mass flowrate calculation.

To demonstrate this effect a simple analogy using distances to represent phase fractions can be used. Consider two points A and C with a third point B lying on the line between A and C, but located quite close to C. The distances AB and BC can therefore be thought of as the phase fractions of two flow components in a two-phase mixture: one with a high phase fraction, the other with a relatively low phase fraction. The short distance BC can be measured by two ways, either a single direct measurement, or by measuring AC and AB and subtracting AB from AC.

To estimate the uncertainty in the values obtained let $AB = a$, $BC = b$, and $AC = c$, and take the percentage uncertainty in any measurement of distance to be 1 per cent. Then for the direct measurement of BC the absolute uncertainty in the reading would be

$$e(b) = \left[\frac{1}{100} \right] b \quad (6)$$

By the indirect technique the uncertainty in BC would be

$$e(b) = \sqrt{e^2(a) + e^2(c)} \quad (7)$$

Substituting for the absolute uncertainties in AC and AB, this equation reduces to

$$e(b) = \left[\frac{1}{100} \right] \sqrt{a^2 + c^2} \quad (8)$$

To give an indication of the potential difference in measurement uncertainty between the two methods, set $c = 100 \text{ mm}$ with $a = 95 \text{ mm}$ and $b = 5 \text{ mm}$. Then the absolute uncertainty in BC using both methods would be

$$\text{Direct measurement} \quad e(b) = 0.05 \text{ mm}$$

$$\text{Indirect measurement} \quad e(b) = 0.9513 \text{ mm}$$

so the uncertainty in the deduced value of BC would be 19 times greater than if a single direct measurement were made. In percentage terms the indirect method of measuring BC would have a random uncertainty approaching 20 per cent, compared to the 1 per cent associated with the direct measurement.

The above analogy highlights quite clearly the limitations of taking multiple indirect measurements to determine flow composition. The only way of overcoming these difficulties is to have extremely low uncertainties on all such measurements, but because of the multiphase flow environment this is very difficult to achieve.

There are two principal difficulties: the natural structure of the flow can vary considerably, and measurements involving two of the flow components can be hampered by contamination

by the third phase. Liquid water content monitors are an excellent example of this because the measurement technologies presently used tend to give erroneous readings if there is gas in the flow.

However, it is the spatial and temporal variations in the flow structure which are technically most challenging. For example, a common technique used in multiphase flowmeters is gamma densitometry, in which the absorption of gamma rays gives a measure of the total flow density. If the flow is well mixed then a reasonable average density measurement will be obtained quite quickly, but if the flow is slugging it becomes much more difficult to define an average density let alone measure it. In such circumstances the longer the averaging period the better, but there is obviously a practical limitation if real time readings are required. A balance has to be struck, which is inevitably to the detriment of the uncertainty in the total density measurement.

Finally, and perhaps most importantly, any instrument within a metering system that requires an input from another instrument in order to interpret its own measurement is clearly at risk of having an increased uncertainty. An example of this is described in the next section.

3.2 An assessment of the uncertainties involved

Consider the multiphase metering system shown in fig.1, with the three key measurements being the water content in the liquid, the total flow density, and the total volumetric flowrate. These measurements being made by a vibrating tube densitometer, a gamma densitometer and a venturi, respectively.

To calculate the liquid water content, phase fractions and individual mass flowrates the following must be known:

Liquid water content

- the representivity of the liquid sample stream
- the liquid density
- the oil density
- the water density

Phase fractions

- the liquid water content
- the gamma densitometer path length (internal pipe diameter)
- the gamma densitometer count rate with dry pipe
- the gamma densitometer count rate under flowing conditions
- the mass absorption coefficient of the oil
- the mass absorption coefficient of the water
- the mass absorption coefficient of the gas
- the gas, oil and water densities

Individual mass fractions

- the individual phase fractions
- the multiphase density
- the venturi differential pressure
- the oil, water and gas densities

The first thing to be noted is that the interpretation of the gamma densitometer measurements requires knowledge of the liquid composition in order to assign the mass absorption coefficients correctly. Likewise the venturi requires the total flow density measurement from the gamma densitometer to correctly convert the differential pressure measurement into a measurement of volumetric flow. So if the water content measurement has a high random uncertainty associated with it, then this will add additional uncertainty to the total density measurement and this in turn will be transferred through to the volumetric flowrate measurement.

This interdependence makes a rigorous derivation of the uncertainties in the oil, water and gas mass flowrates lengthy, and consequently unsuitable for inclusion in this paper. The full derivation can however be found in reference 1.

Using the equations derived in reference 1 a computer program was written to perform the calculation of the uncertainties in the individual mass flowrates over a wide range of oil, water and gas phase fractions. Table 1 gives an example of the data produced, and from this it is evident that the percentage uncertainty in the individual mass flowrates of oil varies considerably according to flow composition, and can be extremely high. (Note that this data was produced using best estimates of the measurement uncertainties in each parameter listed above, and these values are shown in Table 2)

Tables showing the uncertainties for the water and gas mass flowrates are available in reference 1, and they show similar trends to that of Table 1. Summarising all the uncertainty data produced gave the following ranges:

oil	13.8 - 181.2 per cent
water	10.9 - 169.8 per cent
gas	7.1 - 76.2 per cent

There is a lot of information available from the full uncertainty analysis, particularly regarding the sensitivities of each measurement uncertainty. However, there are two points of major importance:

a A multiphase flowmeter using a series of indirect measurements to find the individual mass flowrates can only be expected to attain an uncertainty of approximately 10 per cent of the actual mass flowrate over a very limited range of flow compositions. To cover a wider operating range a target uncertainty of 15 - 20 per cent of the actual mass flowrate would be a more realistic goal.

b All things being equal, the flow composition has the greatest affect on the percentage uncertainty in the individual mass flowrates. For credibility the uncertainty figures for any multiphase flowmeter must be quoted at a specific flow composition. Ideally an upper and lower limit (as above) should be given.

4 CONCLUDING COMMENTS

The main points arising from the study of multiphase flowmeter uncertainties are:

4.1 Present designs are far from ideal, because they do not measure the individual mass flowrates directly. Inferring the mass flowrates from a collection of less direct measurements gives scope for large uncertainties to develop.

4.2 In such systems the interpretation of signals from some instruments often requires precise measurements from other instruments. An uncertainty in one measurement can therefore have considerable knock-on effects.

4.3 A full uncertainty analysis of a typical multiphase metering system has shown the minimum uncertainty that can reasonably be expected is 10 per cent, and this occurs when the phase fraction approaches unity (ie nearly single phase).

4.4 As the phase fraction reduces, the percentage uncertainty in the individual mass flows increases and can be over 100 per cent as the phase fraction approaches zero.

4.5 In the light of 4.3 and 4.4 it is essential that multiphase flowmeter uncertainty data is quoted along with the phase fraction at which it applies.

4.6 The complexity of specifying multiphase flowmeter uncertainties will inevitably lead to confusion, and it is therefore of paramount importance that a standardised method of quoting the uncertainties is developed in the near future which is easy for manufacturers to understand and comply with, yet conveys the maximum amount of information to the user. NEL are actively pursuing suitable techniques at present.

ACKNOWLEDGEMENT

This paper is published by permission of the Chief Executive, NEL Executive Agency, and is crown copyright.

REFERENCE

MILLINGTON, B. C. An uncertainty analysis for the proposed design of the NEL/SGS multiphase flowmeter. NEL Flow Measurement Memo 418. East Kilbride, Glasgow: National Engineering Laboratory, September 1991.

LIST OF TABLES

- 1 The percentage uncertainty in the oil mass flowrate measurements as a function of flow composition
- 2 The percentage uncertainty in each of the parameters used to calculate the oil, water and gas mass flowrate uncertainties

LIST OF FIGURES

- 1 Schematic diagram of a multiphase metering system

TABLE 1

THE PERCENTAGE UNCERTAINTY IN THE OIL MASS FLOWRATE MEASUREMENTS AS A FUNCTION OF FLOW COMPOSITION

(The water cut is the percentage water in the liquid)

		Gas fraction in the multiphase flow, (%)								
		10	20	30	40	50	60	70	80	90
Water Cut (%)	5	13.77	14.03	14.40	14.96	15.85	17.37	20.29	26.98	49.43
	10	13.91	14.17	14.53	15.07	15.93	17.41	20.26	26.80	48.91
	15	14.15	14.39	14.73	15.25	16.08	17.52	20.29	26.69	48.42
	20	14.47	14.70	15.03	15.53	16.33	17.71	20.39	26.63	47.98
	25	14.90	15.12	15.43	15.91	16.67	17.99	20.58	26.64	47.59
	30	15.46	15.66	15.96	16.41	17.13	18.39	20.87	26.74	47.26
	35	16.16	16.35	16.63	17.05	17.73	18.92	21.29	26.95	47.01
	40	17.04	17.21	17.47	17.86	18.50	19.62	21.86	27.29	46.84
	45	18.13	18.30	18.53	18.90	19.48	20.53	22.63	27.80	46.79
	50	19.51	19.66	19.87	20.20	20.74	21.71	23.66	28.55	46.90
	55	21.25	21.38	21.58	21.88	22.36	23.24	25.04	29.60	47.22
	60	23.49	23.61	23.78	24.05	24.48	25.27	26.89	31.10	47.86
	65	26.44	26.54	26.69	26.92	27.30	27.99	29.44	33.24	48.99
	70	30.44	30.53	30.65	30.85	31.18	31.77	33.02	36.39	50.91
	75	36.13	36.20	36.31	36.47	36.74	37.23	38.29	41.16	54.17
	80	44.77	44.83	44.91	45.04	45.25	45.65	46.49	48.84	60.00
	85	59.32	59.36	59.42	59.52	59.68	59.97	60.60	62.38	71.28
	90	88.63	88.66	88.70	88.76	88.87	89.06	89.48	90.67	96.88
95	177.04	177.05	177.07	177.11	177.16	177.25	177.46	178.05	181.22	

TABLE 2

THE PERCENTAGE UNCERTAINTY IN EACH OF THE PARAMETERS USED
TO CALCULATE THE OIL, WATER AND GAS MASS FLOWRATES

Path length of gamma ray across the pipe	2.0
Gamma densitometer calibration count rate	0.5
Gamma densitometer count rate	1.0
Oil mass absorption coefficient	5.0
Water mass absorption coefficient	5.0
Gas mass absorption coefficient	5.0
Liquid sample representivity	1.0
Water monitor (vibrating tube densitometer)	0.5
Oil density	1.0
Water density	0.5
Gas density	4.0
Total volumetric flowrate	3.0

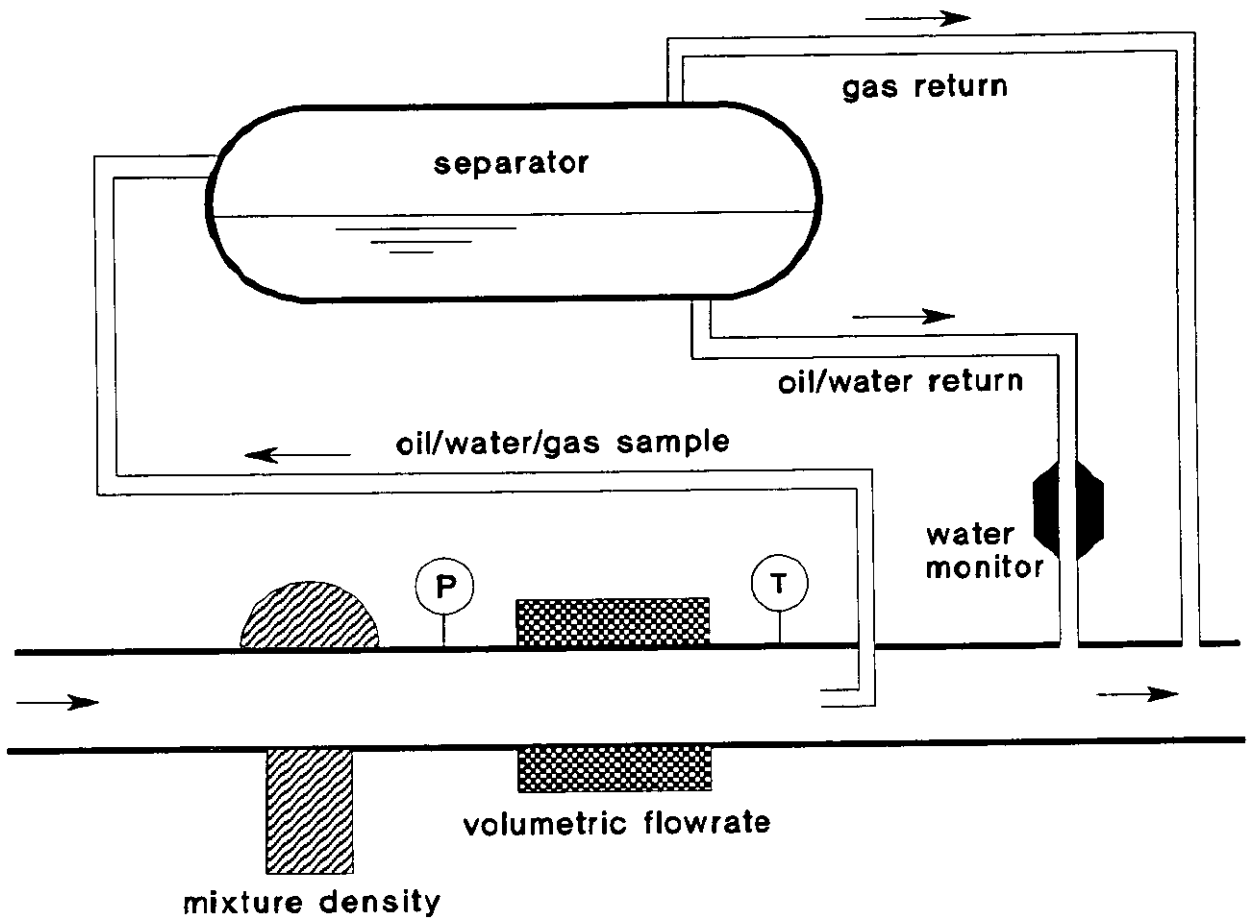


Fig.1 Schematic Diagram of a Multiphase Metering System

A MULTI-CAPACITOR MULTIPHASE FLOWMETER FOR SLUGGING FLOW

by

D Brown, J J den Boer and G Washington
Shell Research, The Netherlands

Paper 2.2

NORTH SEA FLOW MEASUREMENT WORKSHOP
26-29 October 1992

NEL, East Kilbride, Glasgow

A MULTI-CAPACITOR MULTIPHASE FLOWMETER FOR SLUGGING FLOW

D. Brown, J.J. den Boer and G. Washington
Shell Research, b.v., Rijswijk, The Netherlands

SUMMARY

A multiphase flowmeter suitable for use in individual flowlines has been developed and tested in a full-scale multiphase flow loop. The instrument, which operates in the slug flow regime, uses an array of capacitive sensors in the flowline to measure directly holdups and characteristic velocities. It is called, therefore, the multi-capacitor multiphase flowmeter or MCF. The measured parameters are used to derive the flowrates of the individual phases with an accuracy over a wide range of flow conditions of better than $\pm 10\%$ of reading. The present instrument is suitable for oil-external emulsions, with watercuts up to around 40%. The MCF system comprises a simple spool piece with certified local electronics, a remote signal conditioning unit and a control unit to calculate and display the results. It is unique both in its simplicity and the use of the slug flow characteristics. It will provide the operator with reliable flowrate data at a relatively low cost.

After a brief introduction to the operating principle, the results of laboratory tests with this new instrument are presented. The flowmeter is being commercialised by Kongsberg Offshore, a.s., Norway. The further development programme and planning resulting from this cooperation will also be briefly described. This is aimed at producing by 1994 an instrument with the functionality of a test separator at a fraction of the cost, making its application to individual well flowlines a real and attractive option.

1 INTRODUCTION

1.1 Flowmeter requirements

The need for a compact, reliable multiphase flowmeter is well established. Such a meter will enable the cost effective development of both offshore and onshore satellite fields and the possibility of optimising the operation of existing fields. Moreover, the availability of such a meter is essential to accompany the multiphase pressure-boosting systems currently appearing on the market.

Test separators, the conventional way of metering multiphase, can suffer from a range of operational problems and can also be unrepresentative because they sample the flow rate for only a small part of the production time of a well. They are bulky and expensive, particularly for use offshore where size and weight are at a premium, and for satellite developments they require the use of expensive manifolds and test lines. It is attractive to replace test separators with compact, low cost multiphase flowmeters. The requirement was defined for a multiphase meter with similar accuracy to existing test separators, i.e. around $\pm 10\%$ per phase, and sufficiently low cost to be applied economically to individual well flowlines

1.2 Alternative measurement approaches

Many approaches to multiphase flow measurement are being investigated by the oil industry. These can be grouped into three categories:

Separation: separate the phases and measure them individually before recombination.

Homogenisation: create a homogeneous mixture and measure total flow and the fractions of oil, water and gas to give the flowrates for the individual phases.

Leave as it is: change nothing to the flow and use intrinsic flow properties to derive flowrates.

The MCF belongs to the last category. Separation operates best at high gas volume fractions where the phases are already naturally separated in stratified or annular flow. Mixing is easiest at low gas volume fractions where the natural flow regime is close to bubble or plug. The MCF covers a large area between these two, operating in the intermittent flow regimes most often found or easily created in real well flowlines. No flow conditioning other than sufficient horizontal upstream pipe length is required.

Fig.1 shows a multiphase flow map for horizontal flow with the various flow regimes superimposed, and also lines of constant gas volume fraction at 50, 90 and 99%. The superficial velocity is the actual volumetric flowrate of one phase divided by the total cross-sectional area of the pipe. The gas volume fraction (GVF) is the ratio of actual gas flowrate to total flowrate.

2 OPERATING PRINCIPLE

2.1 Liquid and gas transport in slug flow

To understand how gas and liquid flow rates can be measured with the MCF, an understanding is needed of the way in which gas and liquid are transported in slug flow. A good description is still the simple, well accepted model first introduced by Duckler and Hubbard [1]. They describe slug flow in two parts, the slower-moving liquid film which partly fills the pipe, and the faster-moving liquid slugs which totally fill the pipe but only for a fraction of the time. As the slug moves down the pipe it picks up liquid at its front and sheds it again at its rear. The slug itself is made up of both liquid and gas because gas is trapped in the liquid at the front of the slug as it overtakes the slower-moving film. The model states that the actual gas velocity is almost constant and equal to the slug front velocity. Fig. 2 shows shows measured holdup as a function of time for various flow conditions, clearly demonstrating the dependence of both holdup and slug frequency on the gas and liquid flowrates.

The MCF gauges the liquid and gas flowrates in intermittent flow by measuring the cross-sectional areas occupied by each phase and multiplying each area by the velocity of that phase. To do this, it continuously measures the cross-section of the pipe occupied by liquid, the velocity of the liquid and the velocity of the slugs. Assuming that the slugs travel at the same velocity as the gas, the flowrates are calculated from the product of the cross-sectional areas occupied by the liquid and gas and their respective velocities.

2.2 Measurement technique

The measurements are all made with a pair of plates inserted into the pipe in line with the

flow. Etched onto these plates are a number of electrodes forming capacitors and it is the impedance variations in these capacitors that are used to produce the basic signals from which the flowrates are calculated. The plates have a width of just 4 cm along the pipe and typically contain one complete column of electrodes plus two further electrodes (Fig. 3).

One signal is obtained from each capacitor and this is scaled such that the zero voltage level represents the case when there is only gas between the capacitor electrodes and one volt represents the case when there is only dry oil between the electrodes. Each capacitor is actually connected to an electronic circuit that produces two output signals representing the real and imaginary parts of the admittance, one proportional to the conductance one proportional to the susceptance. Of these two signals, only the susceptance signal is used and this is scaled to give the zero and one voltage levels for gas and oil. The actual signal range is far higher than 0-1 volt as mixtures of oil and water have far higher susceptances than oil alone.

The way in which the signals are processed is described in subsequent sections.

2.2.1 Liquid holdup

The liquid holdup is defined as the actual fraction of the pipe's cross-section occupied by liquid. This is different to the level in the pipe because the liquid below the main liquid/gas interface also contains gas. It is calculated from the sum of the actual signals on each electrode weighted for the area that they represent divided by the signal that represents an electrode completely covered in liquid.

In this way, the proportion of each electrode covered with liquid is interpolated between the signal for gas only and that for liquid only. However, the signal representing liquid only is a priori unknown because it depends on the actual ratio of oil and water in the liquid. Finding the correct value to represent liquid only is crucial to the operation of the MCF and is, often, the factor most limiting its accuracy.

The simplest way of determining the signal representing liquid only, known as the span factor (SP), is to take the signal measured by a electrode when it is immersed in a homogeneous and gas free mixture of the oil and water. In the simple slug model presented previously, this situation occurs in the liquid film sometime between slugs. The slug, when it passes, creates a homogeneous mixture of the liquid but it also mixes in some gas. Sometime before the next slug this gas has time to separate out of the film, leaving only the homogeneous liquid mixture. The point at which the gas has disappeared is easy to recognise because this is the point at which the measured susceptance is a maximum. In its simplest form SP is, therefore, taken as the maximum signal over a defined measuring period of a few slugs.

2.2.2 Slug velocity

The slug velocity is calculated from the time difference between the signals from the two electrodes some distance apart at the same height near the top of the pipe. These signals are non-zero only during the passage of a slug. The signals are fed to an electronic circuit that produces a number of measurements per slug from the variations seen during the slug passage. These measurements are then averaged. It takes between 10 and 50 slugs to make a good measurement of the slug velocity depending on the flow conditions.

2.2.3 Liquid velocity

The liquid velocity is measured continuously from the signals from the two electrodes at the same height near the bottom of the pipe. These signals are fed to a cross-correlator to produce a continuous measurement of the time delay between the two analogue signals and hence, since the distance between the electrodes is known, the velocity of the liquid.

2.2.4 Flowrates

The flowrates are calculated from the average liquid holdup and the average liquid and gas velocities. The liquid flowrate is simply the product of the holdup and liquid velocity, the gas flowrate is the product of the pipe cross-section filled with gas, i.e. (1 - liquid holdup), and the slug velocity.

2.2.5 Watercut

The watercut is calculated from the span factor, SP, which is a measure of the dielectric constant of the liquid. The dielectric constant of an oil/water mixture is a unique function of the watercut while the oil remains the external phase, up to around 40% watercut.

3 METER DEVELOPMENT

3.1 Laboratory prototype

After an initial short feasibility study had clearly demonstrated that gas and liquid flow rates could be derived from slug parameters, a 4" prototype meter was constructed in 1989 and installed in the multiphase test loop at Shell Research, Rijswijk. This was used to further develop the sensor geometry and the signal processing to a stage where the target accuracy of +/- 10% per phase could be achieved over a wide range of flow conditions. This performance is discussed in more detail in the following section. The next step clearly had to be a field trial, but this required a commercial prototype certified for use in hazardous areas.

3.2 Commercial prototype

A joint development project was agreed between Kongsberg Offshore, a.s. (KOS) of Norway and Shell Research, co-sponsored by Norske Shell, leading to a number of 3" and 4" commercial prototype meters by the middle of 1992. These meters became available on schedule and have also been tested in the multiphase flow test loop. The MCF system comprises a simple spool piece, with certified local electronics, a remote signal conditioning unit and a control unit to calculate and display the results (Figs. 4 and 5). It is unique in its simplicity and will provide the operator with reliable flowrate data at a potentially relatively low cost. A field test is arranged for the period September-October at a suitable location in Oman. Results of this trial, if available, will be presented, but at the time of writing the equipment is still being installed.

4 PERFORMANCE

4.1 Test conditions

Testing was performed in the laboratory multiphase test facility, which can simulate flow behaviour in both 3" and 4" flowlines over a wide range of multiphase conditions using gasoil, water and air as the component fluids. The flowrates used covered as large a range of

liquid and gas superficial velocities as could be achieved with the nominally 100 mm diameter laboratory prototype and the 3" commercial prototype selected for the most extensive testing. Gas superficial velocities ranged from 1 to 12 m/s and liquid superficial velocities from 0.1 m/s to 3 m/s. These values reproduce the flow conditions in the majority of actual flowlines, and also give the approximate boundaries to the slug flow regime.

The meters were mounted in horizontal flowlines, with an upstream straight length of approximately 15 m for the 4" meter and of approximately 6 m for the 3" meter. This was sufficient to develop intermittent flow, thereby enabling the meters to operate, but no attempt has been made to determine the minimum straight length requirements. The technique does not depend on the slug flow being fully developed.

The sensor plates are constructed using the same production techniques and material as multilayer printed circuit boards. In parallel with the performance tests a separate sand resistance test was performed on a sensor plate. Using high levels of sand to accelerate testing, the plate was subjected to the equivalent of more than three years of operation at sand levels of 5 g/l (50 ppm). The conclusion was that sand erosion is not a problem for the MCF probe. The MCF probe material will have a service lifetime of at least 5 years at sand concentration levels of around 50 ppm, which is typical for those wells producing from unconsolidated sand formations which are especially prone to generate higher levels of sand.

4.2 Laboratory prototype

Figs. 6 and 7 show the areas on a flow map where the liquid and gas measurement errors respectively are below 10%. The liquid flow errors are shown for a 10% watercut emulsion, the gas flow errors for air and dry oil (0% watercut). Liquid velocity measurement becomes difficult at flows less than around 0.2 m/s since the slug frequency is low, and between slugs the film is almost standing still. Gas measurements are limited in the upper part of the flow map by the transition to bubble flow, and in the low liquid/high gas corner by the lack of slugs, essential for obtaining gas velocity. Nevertheless, for both liquid and gas a large range of conditions are contained within the +/- 10% flow error borders.

4.3 Commercial prototype

The questions to be answered with the commercial prototypes were twofold: the reproducibility of the technique with the changes made to the system necessary to ensure electrical safety, and the generality of the approach in going from a 4" to a 3" meter.

4.3.1 Flow accuracy

Figs. 8 and 9 show, similarly to the previous figures but now for a 3" meter, the areas on the flow map where the liquid and gas flow errors are below 10%, both at 0% watercut. It can be seen that very similar results are obtained as with the 4" laboratory prototype. Note that although the superficial velocity ranges remain the same, the actual flow rates differ by almost a factor two between the two meters.

Repeatability of the measurement depends on the time constant used since, by its very nature, multiphase flow contains a degree of randomness which must be averaged out. With a time constant of 100 seconds, short by multiphase standards, the measurements were repeatable to better than +/- 5%.

4.3.2 Watercut accuracy

Watercut, as previously explained, is obtained from a reference value, SP, measured in gas-free emulsion between slugs. Problems can be encountered at low flow rates, where the emulsion at the bottom of the flowline can become water-rich between the infrequent slugs, and at high flow rates where gas remains entrained in the film between slugs. However, because slug flow is generally efficient at maintaining a well mixed emulsion, watercut can be measured to an accuracy of +/- 4% absolute over a wide range of conditions. Table 1 shows results obtained around 10% , 20% and 30% watercuts.

Table 1 Watercut accuracy for a range of gas and liquid flows

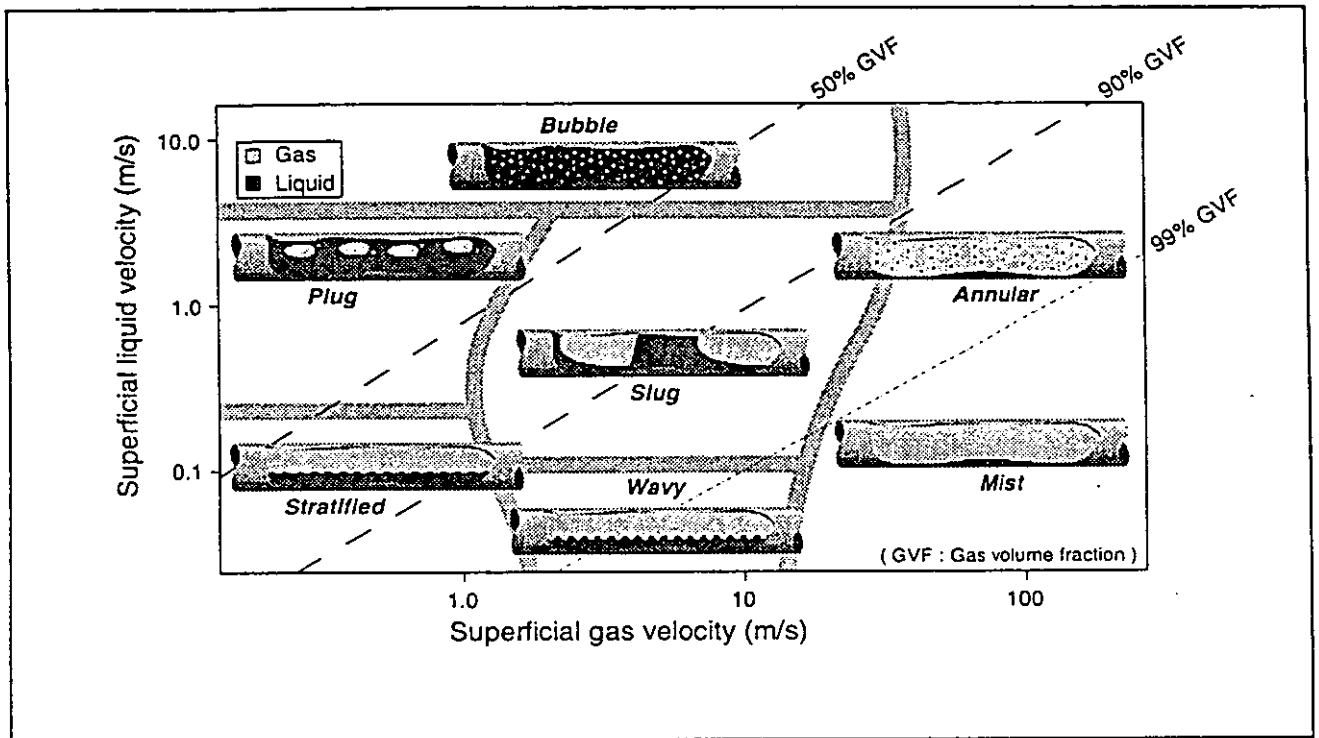
Liquid Flow m/s	True Watercut %	Measured Watercut % at Gas Flow of :	
		3.6 m/s	7.1 m/s
.8	28	28	
.3	19	18	22
1.0	20	21	16
1.7	20	20	16
2.2	20	19	17
1.0	9	9	8
1.7	9	8	8
2.2	9	8	8

5 PLANS

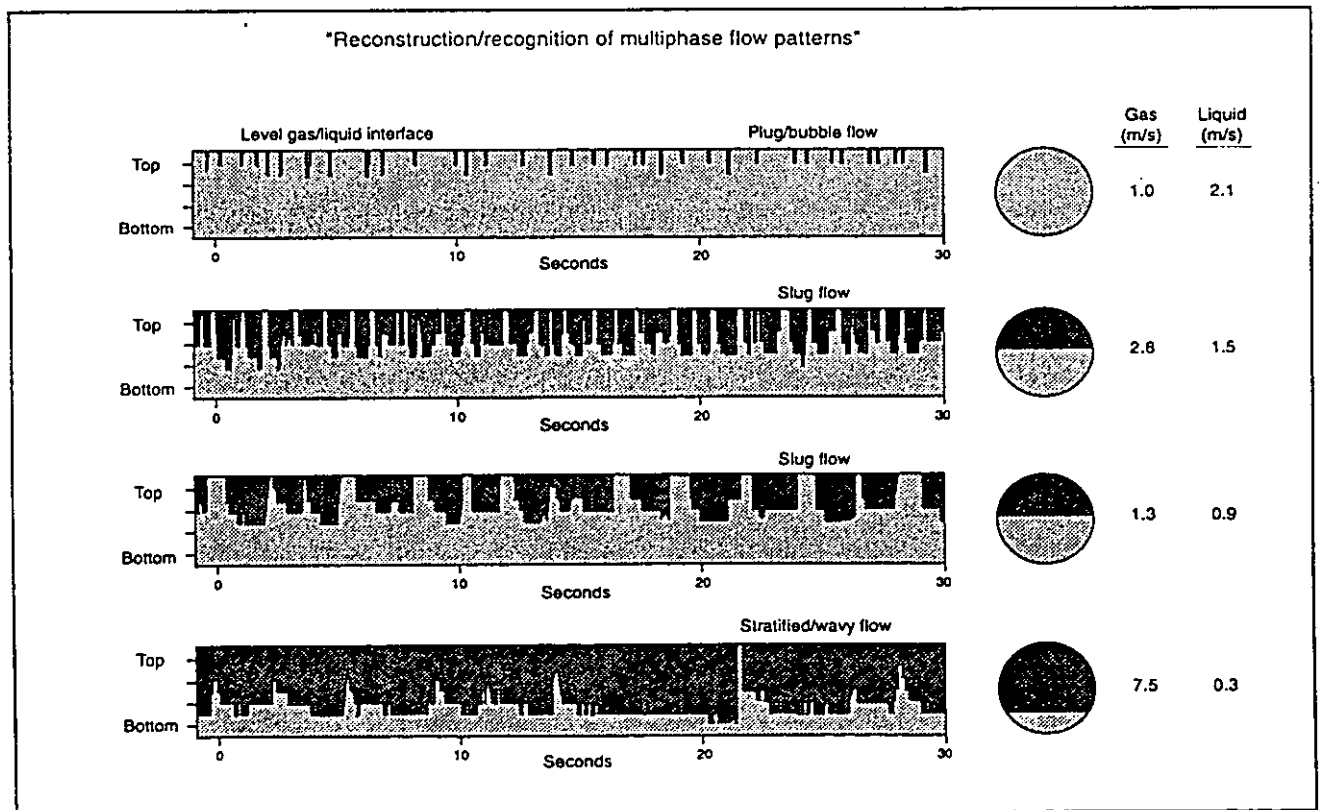
The present MCF multiphase flow meter is suitable only for oil-external emulsions. A second phase of the development, now underway, will lead in 1993 to flowmeters capable of metering across the full range of watercuts. These will use a similar measuring technique modified to cope with the different electrical properties found in water-external emulsions where water conductivity plays the dominant role. Results obtained in the laboratory show that these techniques are capable of measuring gas and liquid flow rates in water-external emulsions, but that an accurate measure of watercut could be problematic. An alternative technique might have to be incorporated for this measurement. Following a successful trial of a full range meter in 1993, it is planned, in cooperation with Kongsberg Offshore, a.s., to continue the development to improve the watercut measurement in water external emulsions, to extend the range to other flow regimes, and also to develop a version of the MCF suitable for application subsea.

REFERENCE

- [1] Duckler, A.E. and Hubbard, M.G.: "A model for gas-liquid slug flow in horizontal and near horizontal tubes," *Ind. Eng. Chem. Fund.* (1975) 14(4), 337-347.



Mandhane flowpattern map for horizontal multiphase flow



Examples of MCF level measurements

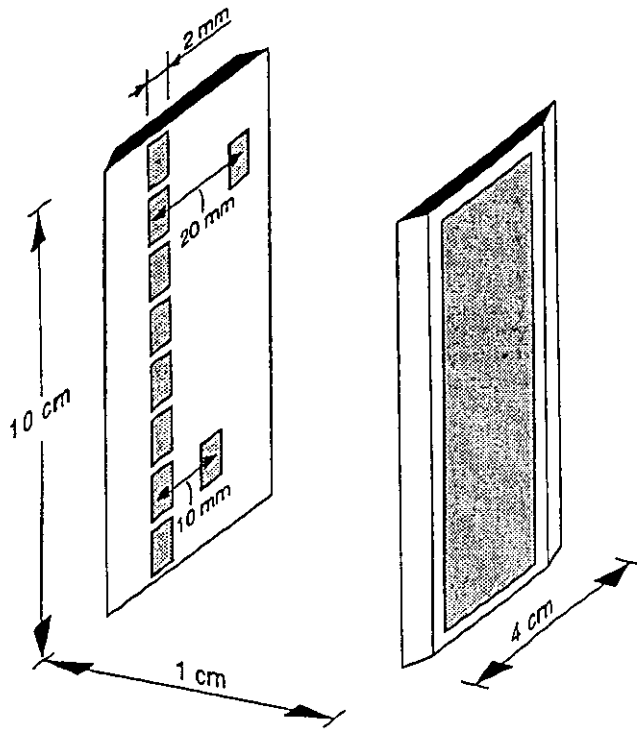


Fig. 3 MCF sensor plates

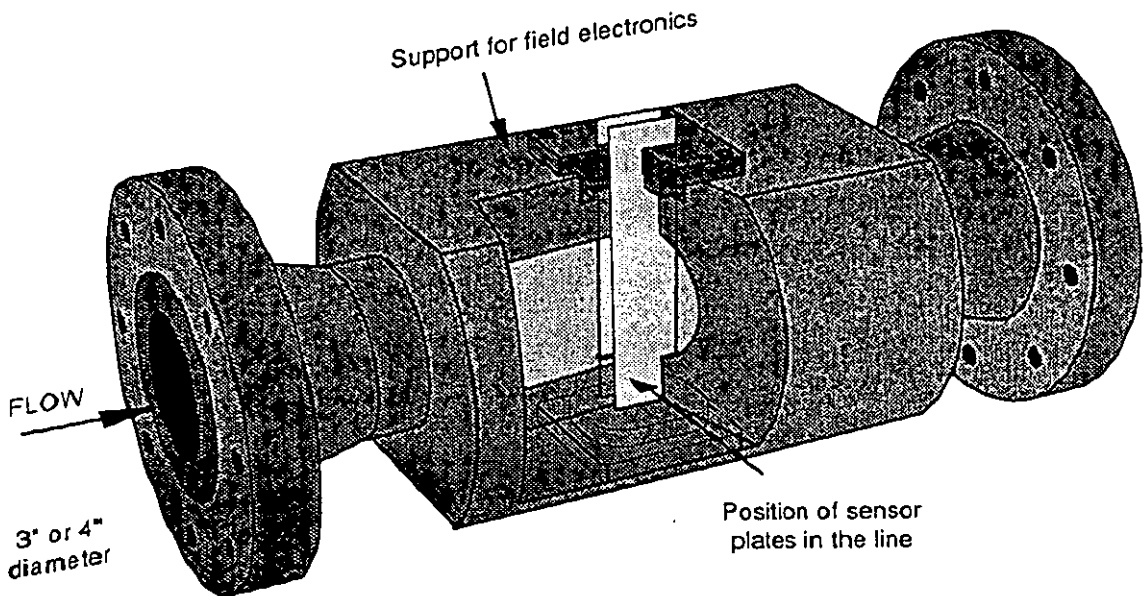
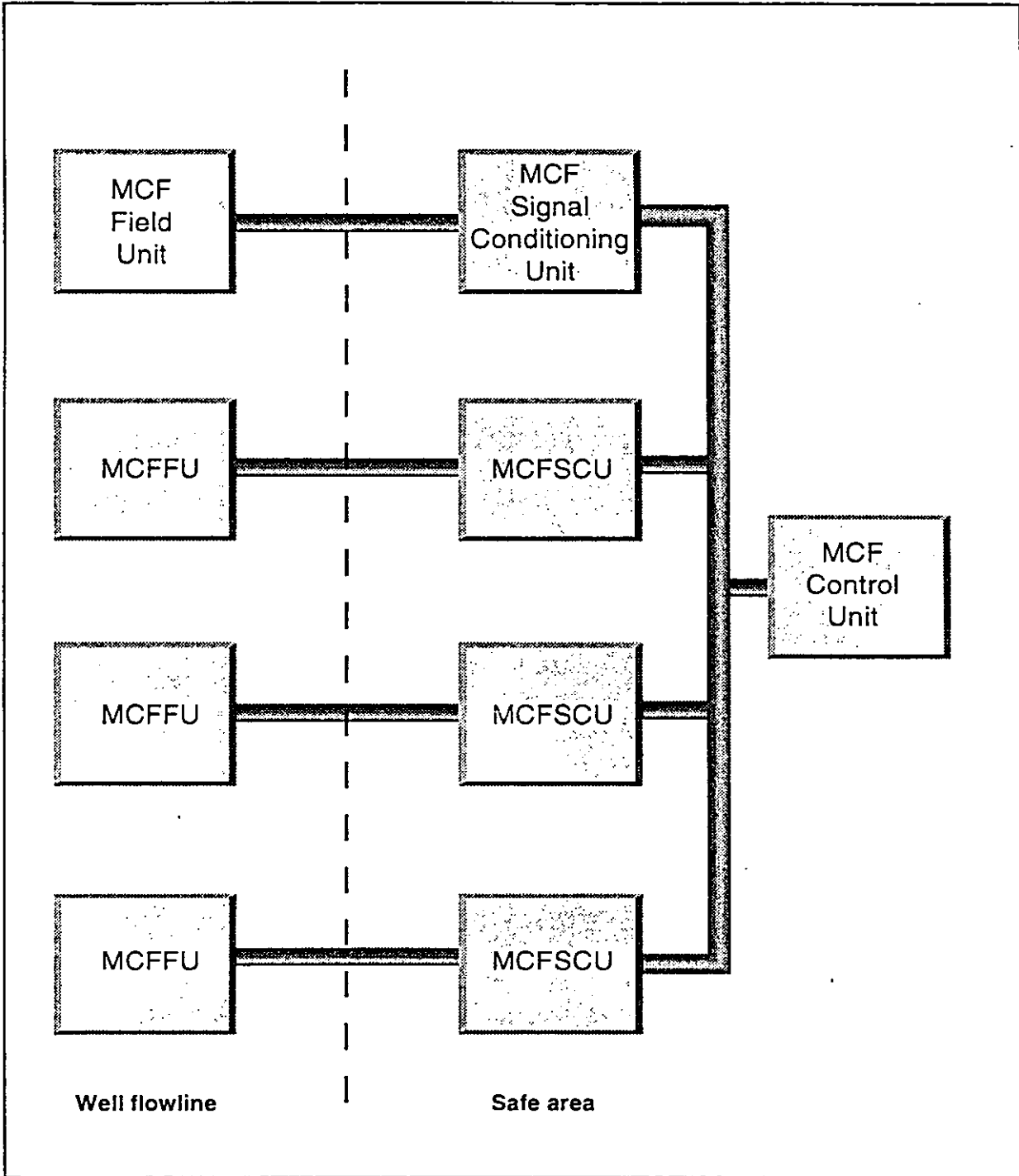


Fig. 4 MCF mechanical design



Complete four-well metering system

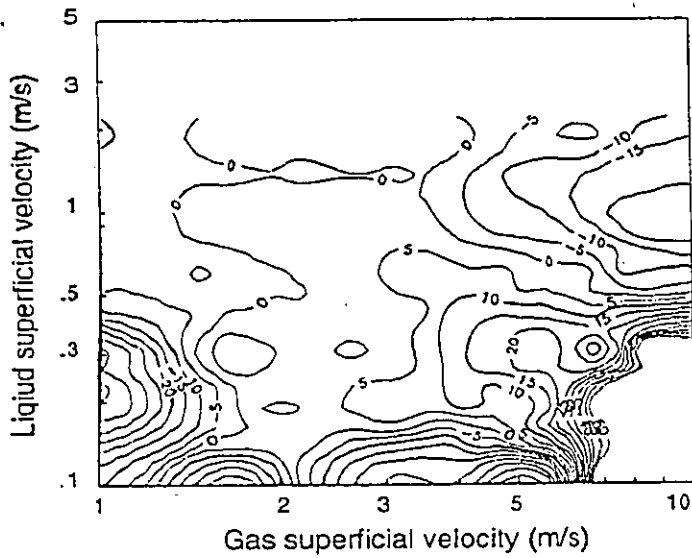
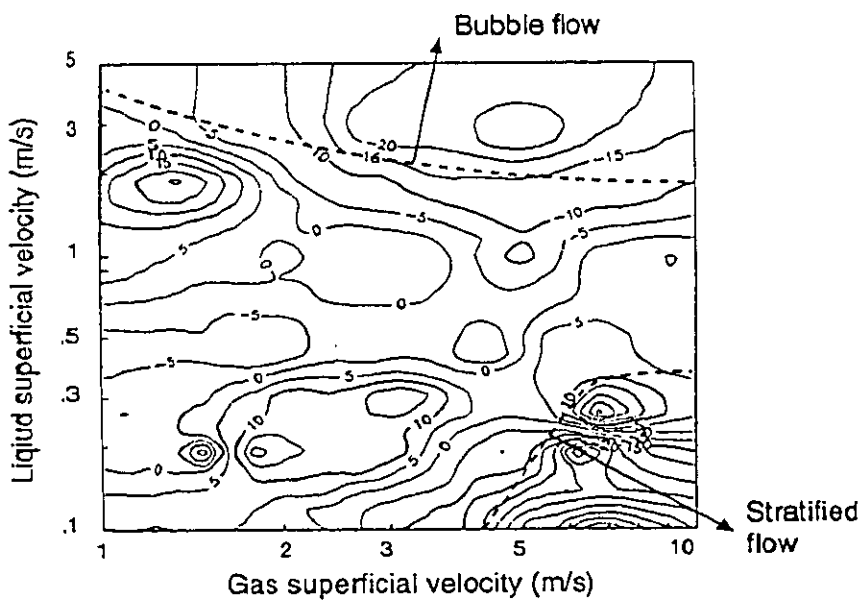


Fig. 6 Liquid Flowrate errors for KSEPL 4" prototype



Gas error, 0% watercut

Fig. 7 Gas Flowrate errors for KSEPL 4" prototype

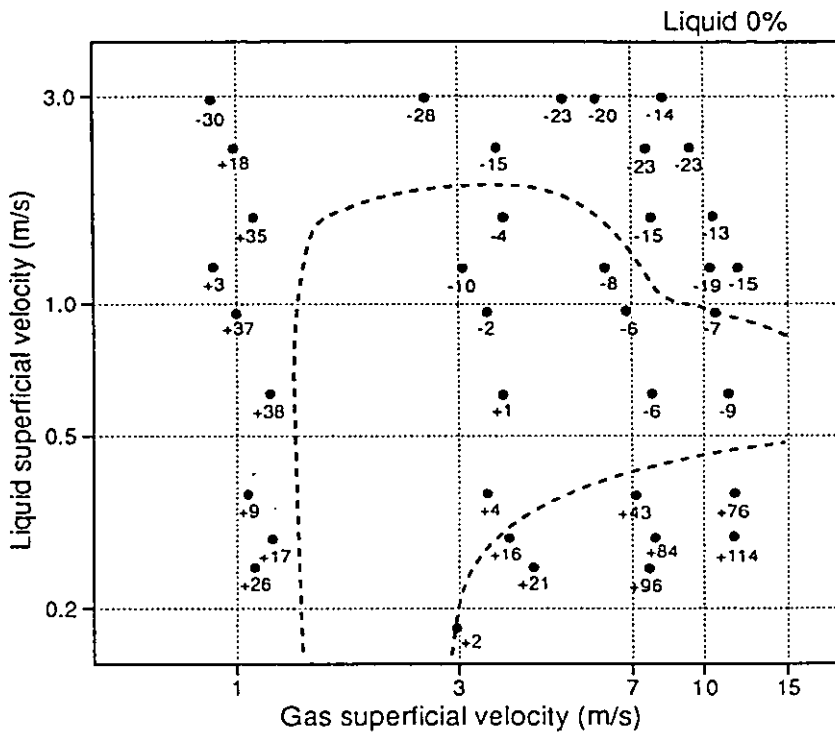


Fig. 8 Liquid flowrate errors for KOS 3" meter

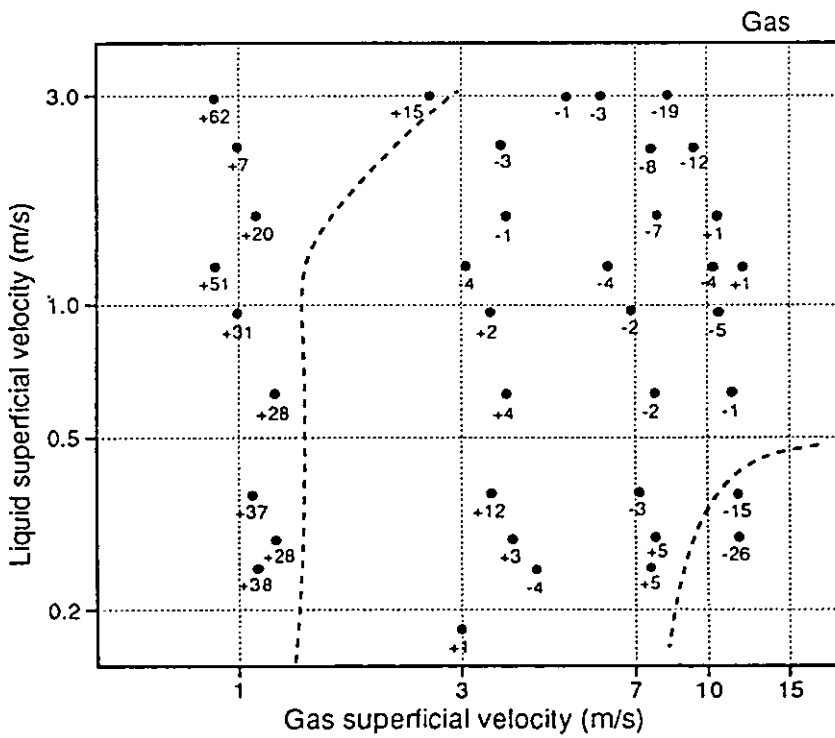


Fig. 9 Gas flowrate errors for KOS 3" meter

A FLOW-REGIME INDEPENDENT MULTIPHASE FLOWRATE METER

by

E Dykesteen and O Midttveit
Christian Michelsen Research

Paper 2.3

NORTH SEA FLOW MEASUREMENT WORKSHOP
26-29 October 1992

NEL, East Kilbride, Glasgow

A FLOW-REGIME INDEPENDENT MULTIPHASE FLOWRATE METER

E. Dykesteen and Ø. Midttveit

Christian Michelsen Research, Bergen, Norway.

SUMMARY:

In a paper presented at the North Sea Flow Measurement Workshop in 1990, Christian Michelsen Research (CMR) presented test results for a new concept for measuring the phase fractions of a multiphase flow. In the follow-up of this work, a new project to develop a multiphase flowrate meter was initiated in June 1990. This has now resulted in a commercially available multiphase meter, the Fluenta MPFM 1900.

The new flowrate meter is of a non-intrusive design, and mounted in a vertical upwards flow, it will accept a wide range of flowrates and compositions without any preconditioning of the flow. This has been achieved by advanced signal processing, and by building knowledge of multiphase flow behaviour into the model based measurement system. The distribution of velocities present in the flow are measured by correlation techniques, and thus interphasial slip is directly measured and compensated for.

The paper discusses why installation of mixers for preconditioning of the multiphase flow should be avoided, and it presents test results from extensive laboratory testing of the new multiphase flowrate meter. The first field test installation is already in progress.

THE FLUENTA MPFM 1900; A NEW MULTIPHASE FLOWRATE METER DEVELOPED BY CHRISTIAN MICHELSEN RESEARCH

In a paper presented at the North Sea Flow Measurement Workshop in 1990 [1], Christian Michelsen Research (CMR) presented test results for a new concept for measuring the phase fractions of a well mixed multiphase flow. The measurement principle is shown in Figure 1: Based on the density of a well mixed multiphase flow as measured by a clamp-on gamma densitometer, and the permittivity of the same flow as measured by a non-intrusive in-line capacitance sensor, the fractions of oil, gas and water at the sensor location are determined. This principle of measurement has been realised in the Fluenta MPFM 900 Multiphase Fraction meter.

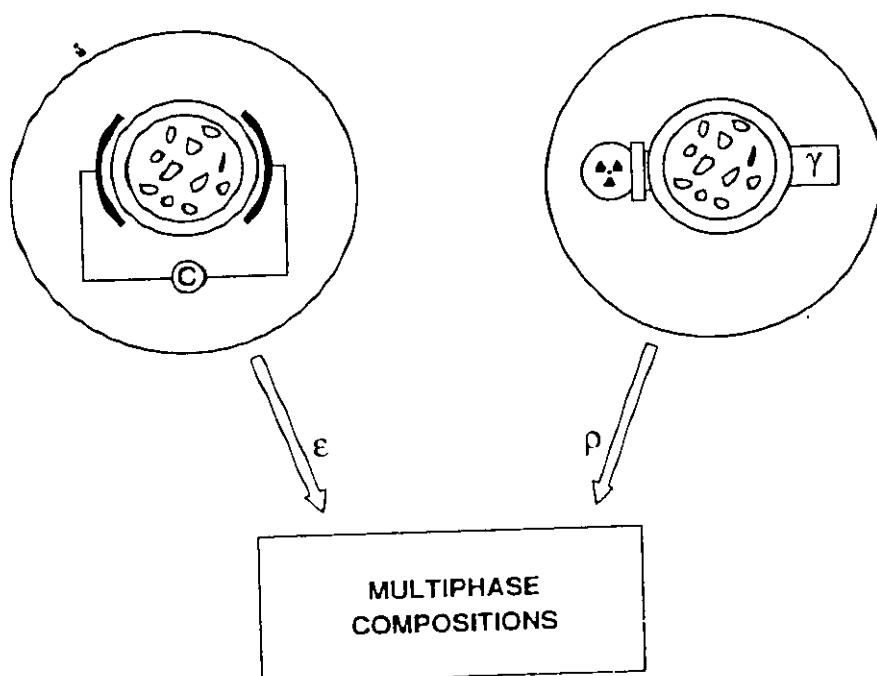


Figure 1 Measurement principle of the MPFM 900.

With support from BP Norway, Saga Petroleum, Elf Petroleum Norge and the Norwegian Petroleum Directorate, we have now also developed a velocity measurement technique based on cross correlation of signals from a multi-electrode capacitance sensor. Assuming that there is no inter-phasic velocity slip between oil, water and gas, this velocity measurement can be combined with the MPFM 900 in order to provide a multiphase flowrate meter suitable for no-slip conditions.

However, tests early in this project indicated that interphasial slip between liquid and gas is significant in a vertical multiphase flow, and is re-established rapidly after a mixing point. At best, no-slip will be established only over a limited range of flow rates and compositions, thereby limiting the range of any no-slip measurement system.

Therefore, the electrode layout and detector system of the capacitance sensor was optimised in order to be able to discriminate between the velocity of small bubbles dispersed in the liquid, and the velocity of fast moving larger bubbles/slugs. By using this additional information, in combination with knowledge of multiphase flow behaviour, the model based measurement system directly determines, and accounts for, interphasial slip. The new flowrate measurement system does therefore not require any upstream mixer to be installed.

The performance of the complete measurement system was put to a thorough test in the CMR multiphase flow-loop during March '92. The results from these performance tests are very satisfactory. Over most of the tested range, measured flowrates of liquid and gas are found to be well within $\pm 5\%$ from the reference flowrate.

As part of the test programme, two "production profiles" during approximately 3 hours were produced through the multiphase flowrate meter, and accumulated volumes of oil, gas and water were measured. During such a test all random errors due to natural fluctuations in the flow are filtered out and become insignificant, and the effects of any systematic errors are clearly shown. In Figure 2 it is shown how the liquid flow rate during one such test period has been varied between 35 and 45 m³/h, while gas flow rate has been varied between 10 and 35 m³/h. The water cut has been varied in the range 15-22 %. The results of this "production test", which could be compared to a test-separator run, are shown in Figure 3 and Figure 4.

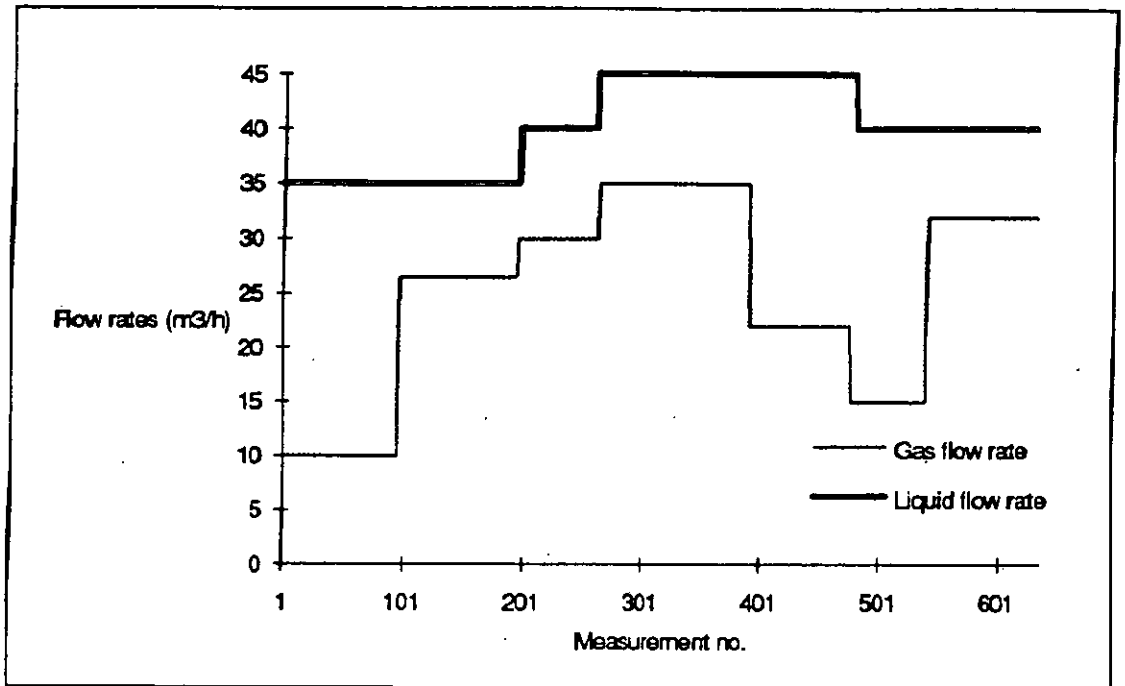


Figure 2 Production test. Production profiles of liquid and gas.

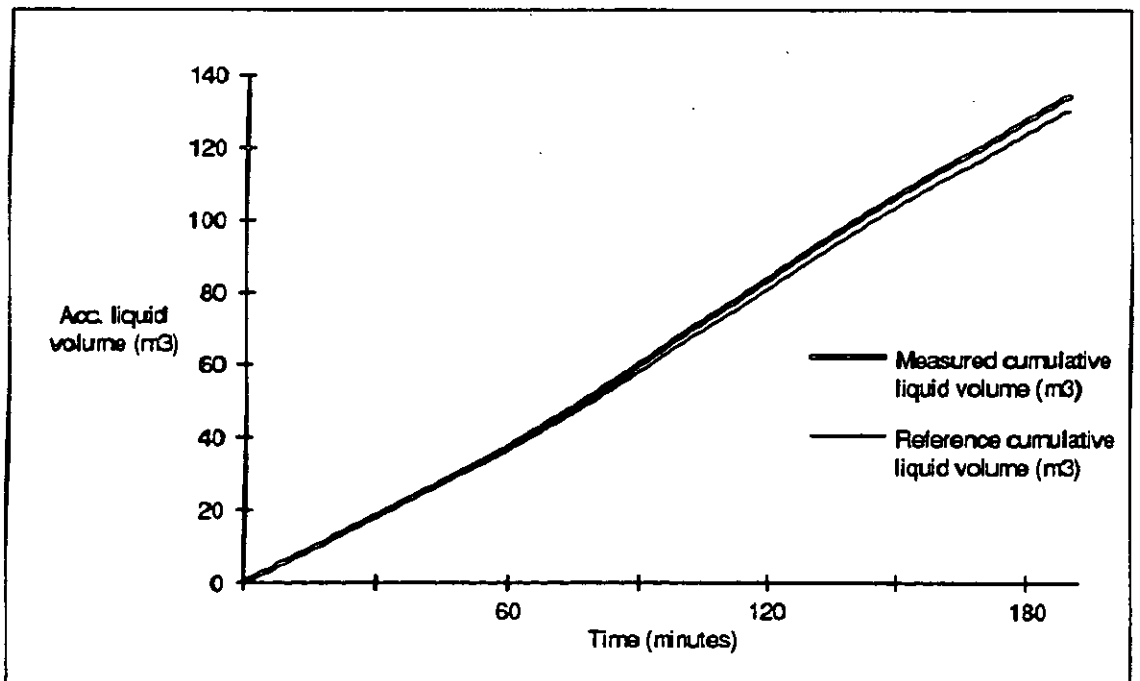


Figure 3 Measured accumulated liquid volume during a production test.

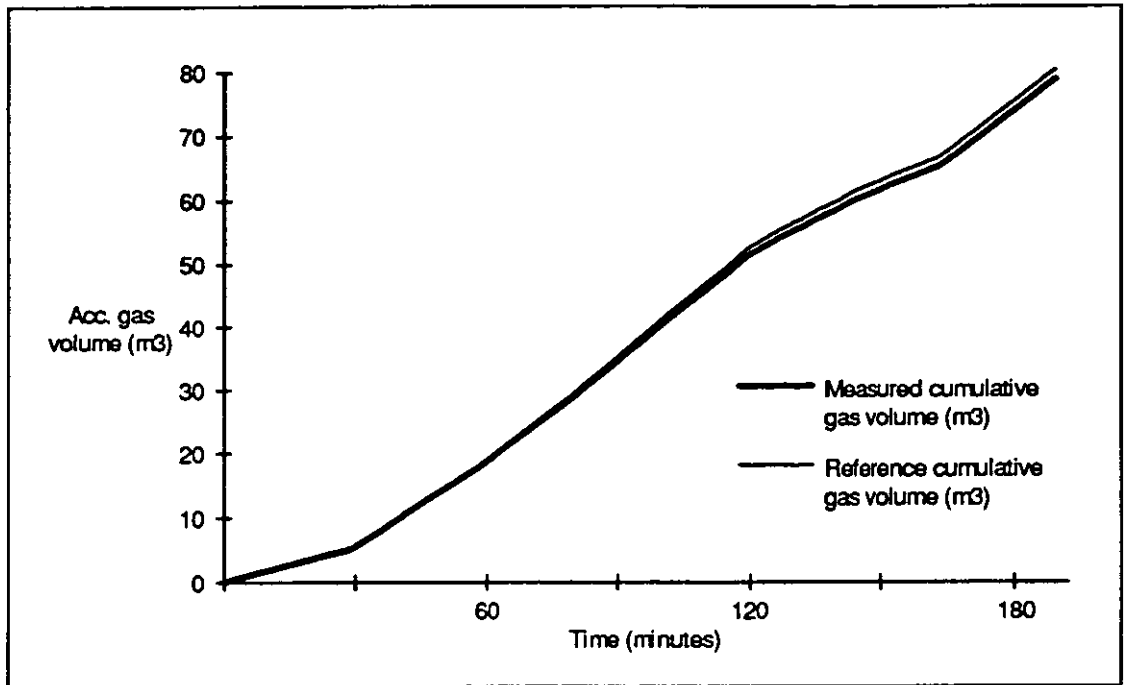


Figure 4 Measured accumulated gas volume during a production test.

The discrepancies between measured and reference volumes of liquid and gas in the two production tests were found to be between 2% and 5.5%. During the period of these tests the corresponding water-cuts were measured to be 14.7% and 19.7%, as compared to reference values of 13.0% and 19.4%, respectively.

Based on these very encouraging test results, Fluenta has already made an industrial version of the meter available to the market. This has been made possible through the co-operation with Conoco and the Norwegian Research council (NTNF) within the KAPOF - programme.

In the new instrument, analogue signals are converted to digital at the sensor head, and all signal transmission between the sensor and the control room unit is in digital form on a fibre-optic link. Thereby a low power, but high speed signal transmission has been achieved. The sensor head has also been fitted with a pressure compensation system. With this design the maximum pressure is no longer limited to the ceramic liner specifications. The measurement system has been approved by Baseefa for use in hazardous areas. Also the user interface has been improved from the MPFM 900 version.

The new meter, The MPFM 1900 Multiphase Flowrate meter, replaces the MPFM 900 fraction meter on the market. Saga Petroleum has purchased the very first unit, and following a

successful factory acceptance test in the CMR laboratory in August '92, Saga is now (September '92) in the process of installing the meter at Gullfaks B for offshore field testing.

The results of the performance testing of this new flowrate meter, prior to the delivery to Saga, are presented later in this paper.

NON-INTRUSIVE MEASUREMENT OF THE FLOWRATES OF OIL, WATER AND GAS IN A NON-CONDITIONED MULTIPHASE FLOW IS A COMPLEX MEASUREMENT PROBLEM

A variety of different flow patterns must be expected to occur in a non-conditioned multiphase flow. By restricting installation of the multiphase meter to vertical upwards flow, the possible flow patterns are fewer, usually classified into four flow regimes exhibiting significantly different features (see Figure 5):

In *bubble flow* the gas is uniformly distributed as small gas bubbles dispersed in a continuous liquid phase. It generally occurs when the gas flowrate is low compared to the liquid flowrate.

The *slug flow* regime develops from a bubbly pattern when the gas flow rate increases to such an extent that it forces the dispersed bubbles to become closely packed and coalesce into larger gas volumes. Stable slug flow is generated at high gas rates in pipes of long free vertical stretches.

Churn flow is observed as a transition regime from bubble to slug flow, and may also be experienced at very high gas flowrates in the transition region from slug to annular flow.

In *annular flow* the liquid phase moves upwards partly as a wavy liquid film along the pipe wall, and partly in the form of small droplets entrained in the gas core. Annular flow occurs when the flowrate of gas is significantly higher than that of the liquid.

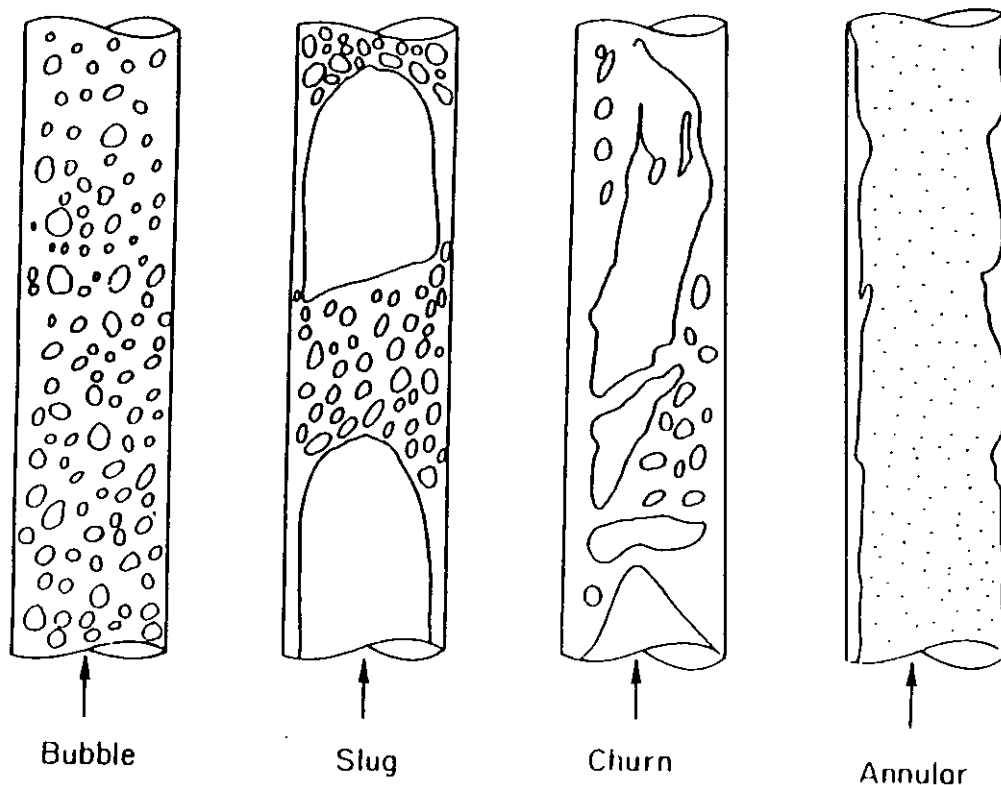


Figure 5 Flow patterns in vertical flow.

The natural grouping of gas and liquid into specific flow regimes at different flow conditions, clearly means that one cannot assume the gas to be uniformly distributed in the liquid across the cross-sectional area of the pipe. The degree of in-homogeneity will increase at high gas flow rates. The gas is only uniformly distributed in the liquid in bubble flow. For all other regimes the gas tends to collect itself in the middle of the pipe as large bubbles in slug and churn flow, and even more dominant in the form of a gas core in annular flow.

In a gas-liquid flow, the larger bubbles will rise in the fast moving liquid in the centre of the tube, other small bubbles will be near the wall and will consequently move more slowly. This velocity slip is further enhanced by buoyancy due to the difference in density of gas and liquid so that the gas phase will be transported with a larger average velocity than the liquid phase.

To measure multiphase flowrates in a non-conditioned multiphase flow, it is therefore necessary both to measure the total velocity distribution of the flow, as well as to measure and account for any in homogeneous phase distribution at the sensor location.

WHY NOT REDUCE THE COMPLEXITY OF THE MEASUREMENT PROBLEM BY PRECONDITIONING OF THE MULTIPHASE FLOW?

Within a certain range of multiphase compositions and flowrates, an inline mixer may be employed in order to reduce the interphasial slip to a minimum, and in order to create a radially homogeneous phase distribution, at the location of the multiphase meter. The efficiency of a mixer to achieve this, as well as the range over which sufficient mixing is achieved, and to which cost in terms of pressure drop, will to a large extent depend on the different mixer designs.

There are a range of different mixers available, both inline static devices which draw the mixing energy from the flow itself, as well as dynamic mixers which require energy input. One advantage of using some type of dynamic mixer is that little or no pressure drop is created across the mixer. However, in most cases a static mixer will be preferred, because no energy input is required, and because they generally are rugged devices with no moving parts. Pressure drop across a static mixer will typically be in the order of 0.5 to 3 bar, depending on flowrate and composition.

A multiphase flowrate meter which depend on a mixer to provide suitable measurement conditions will lend itself to the efficiency of available mixers. The range of such a flowmeter will be limited by the range where sufficient degree of mixing can be guaranteed. The uncertainty with respect to remaining slip at the flowmeter location, and/or in homogeneity of the radial phase distribution, will add a significant contribution to the overall measurement uncertainty.

To our knowledge a thorough analysis of the performance of mixers for use with multiphase meters has never been performed. It is however evident that even the most efficient mixer will not be able to create no-slip conditions and homogeneous phase distribution over an un-limited range of flowrates and compositions. Since the overall performance of many multiphase meters will directly depend on the performance of available mixers, a comprehensive test program for evaluation of available mixers over a wide range of flowrates and compositions should therefore be initiated. Some parameters important for evaluation of the mixer performance in such a test programme will be bubble size distribution, velocity profile, interphasial slip, axial and radial phase distribution, and pressure drop.

Awaiting the results of such a test programme, and, until now, not having identified a mixer with suitable performance parameters, we at CMR have chosen to accept the existence of slip, and to develop methods to measure the degree of interphasial slip, rather than try to avoid it by mixing.

In addition, we believe that the industry will see some advantages with a completely non-intrusive system with no pressure drop. In particular, some multiphase pipelines even require pressure boosting in order to transport the flow from a remote satellite to a processing platform. Since increasing the line pressure just a few bar using a multiphase pump will be quite expensive, it does not appear very cost efficient to consume pressure head just for the sake of creating suitable measurement conditions for a multiphase meter.

The major drawbacks by having to rely on a multiphase mixer can therefore be summarised as follows:

- it is not evident that there exist a multiphase mixer which will be able to create no-slip conditions and homogeneous phase distribution over a sufficiently large range of flowrates and compositions
- the range of the multiphase meter will be limited to the range where a mixer is able to provide acceptable flow conditions
- any remaining slip, or in-homogeneous phase distribution, will directly contribute to the overall measurement uncertainty
- the pressure drop can be significant

MEASUREMENT OF MULTIPHASE FLOWRATES UNDER PHASE SLIP CONDITIONS

As previously described, the gas in an un-conditioned vertical multiphase flow will be transported with different velocities relative to the bulk average velocity, depending on flow regime and bubble sizes. While small bubbles dispersed in the liquid phase will be transported with close to no slip, larger bubbles or gas slugs will take on a slip velocity in the range from 0.5 to 2 m/s relative to the liquid velocity. Therefore, in principle, the total velocity range must be measured, and correct volume fractions of liquid and gas must be allocated to each part of the velocity range. In order to do this correctly, we have found it necessary to try to understand the behaviour of multiphase flow, and to build such knowledge into signal interpretation models in the model-based measurement system.

Schematically the new multiphase flowrate meter is illustrated in Figure 6. Its operation will be described in the following.

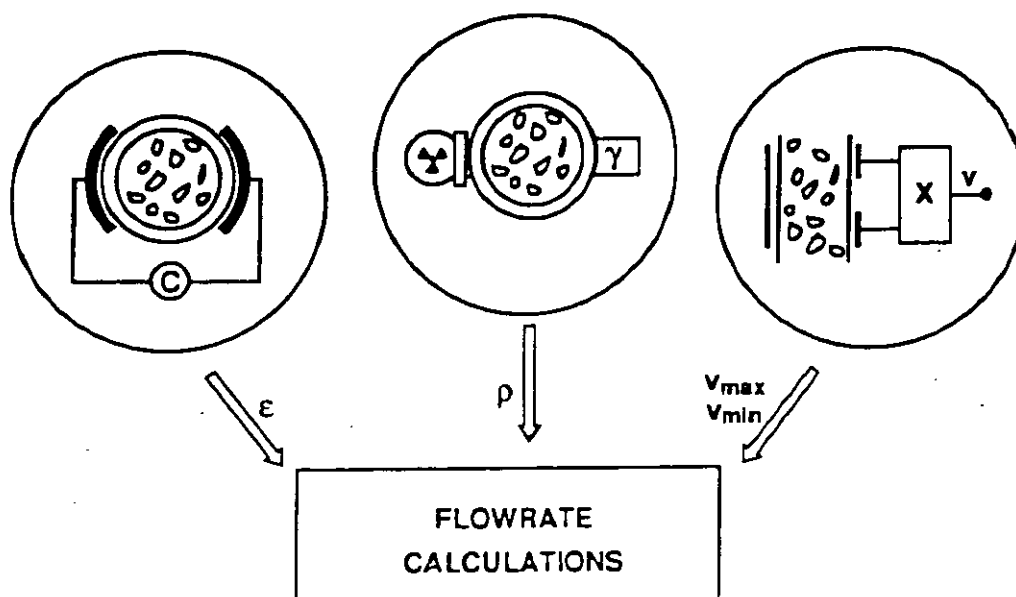


Figure 6 Measurement principle of the CMR multiphase flowrate meter.

Measurement of phase fractions

As in the MPFM 900, the multiphase fraction routine is based on a non-intrusive capacitance measurement to determine the mean permittivity (dielectric constant) of the mixture and a gamma meter measurement to determine the mean density. From these two independent measurements, and knowing that the sum of all the fractions will always be equal to one, the individual fractions of oil, gas and water at the sensor location are determined. Laboratory tests have shown that this measurement system is capable of determining the composition of a multiphase flow to an uncertainty of better than $\pm 3\%$ for each of the components [1]. The tests have been carried out in a vertical upwards bubble/churn flow in a gas fraction range from zero up to about 60%. A larger uncertainty is experienced at higher gas fractions where the impact from the in-homogeneous phase distribution becomes more significant as previously explained.

Measurement of phase velocities

The phase velocities are determined using cross-correlation of signals provided by different sequentially located surface plate capacitance electrodes. The gas phase in a multiphase flow generally comprises several velocity components.

Different sensor geometries or electrode lay-outs have shown to be sensitive to different bubble sizes of the flow due to different spatial averaging of the variations detected. It is also possible to use different types of detectors being sensitive to different physical properties of the mixture. In addition, further pre-conditioning of the signals may be carried out as they are recorded as discrete time series. This further tuning of each specific technique includes determination of optimal values of parameters connected to the correlation computation such as logging frequency, number of samples in time series, filtering schemes and averaging methods.

During the project correlation methods have been developed which determine two significant flow velocities of the flow. These are the velocity of the fast moving larger gas bubbles/slugs, and the velocity of the small bubbles dispersed in the liquid (with velocity very close to the liquid velocity). Slip between water and oil is generally assumed very low for crude oils in a vertical upward section, and is therefore neglected in the models.

Interpretation based process model for determination of the individual flowrates of oil, gas and water

To achieve the overall objective of obtaining the individual component flowrates of oil, gas and water, the velocities must be correctly combined with measured cross-sectional area proportions of the three phases. Since the gas phase moves with different velocities, the fraction routine has been further developed so that in addition to the average gas fraction, the fraction of large gas bubbles, as well as the fraction of small gas bubbles dispersed in the liquid, are measured on-line [2].

The signal interpretation models use these fractions, and the two significant flow velocities, to calculate the volumetric flow rates under phase-slip conditions. The interpretation based model thus determines the total gas flowrate as the sum of gas transported as large bubbles/slugs (Q_{GB}), and gas transported as small bubbles uniformly distributed in the liquid phase (Q_{GD}):

$$Q_{GAS} = Q_{GD} + Q_{GB}$$

The mutual order of magnitude of Q_{GD} and Q_{GB} will vary depending on the actual flow regime appearing in the flow.

In bubble flow the gas is mainly transported as small dispersed gas bubbles. In such a condition the main contribution to the gas flowrate is from Q_{GD} .

In churn flow there are larger bubbles moving faster than the surrounding highly aerated liquid mixture. In such flow conditions there is also a volumetric contribution, Q_{GB} , from the faster

moving churn bubbles along with the flowrate provided by small dispersed gas bubbles in the liquid, Q_{GD} .

In slug flow, an even larger portion of the gas will be carried by the large bubbles compared to the condition of churn flow.

RESULTS FROM LABORATORY TESTS OF THE MPFM 1900

During August 1992, prior to delivery to Saga Petroleum, the performance of the new MPFM 1900 Multiphase Flowrate Meter was put to a thorough test in the CMR multiphase flow-loop using diesel oil. The test programme included a wide range of flowrates and compositions.

Some volumetric flowrate results of the performance tests are shown in Figure 7 and Figure 8. Each point in the plots is the average of 10 independent measurements. The flow condition in the vertical test section of the CMR loop was bubble and churn flow.

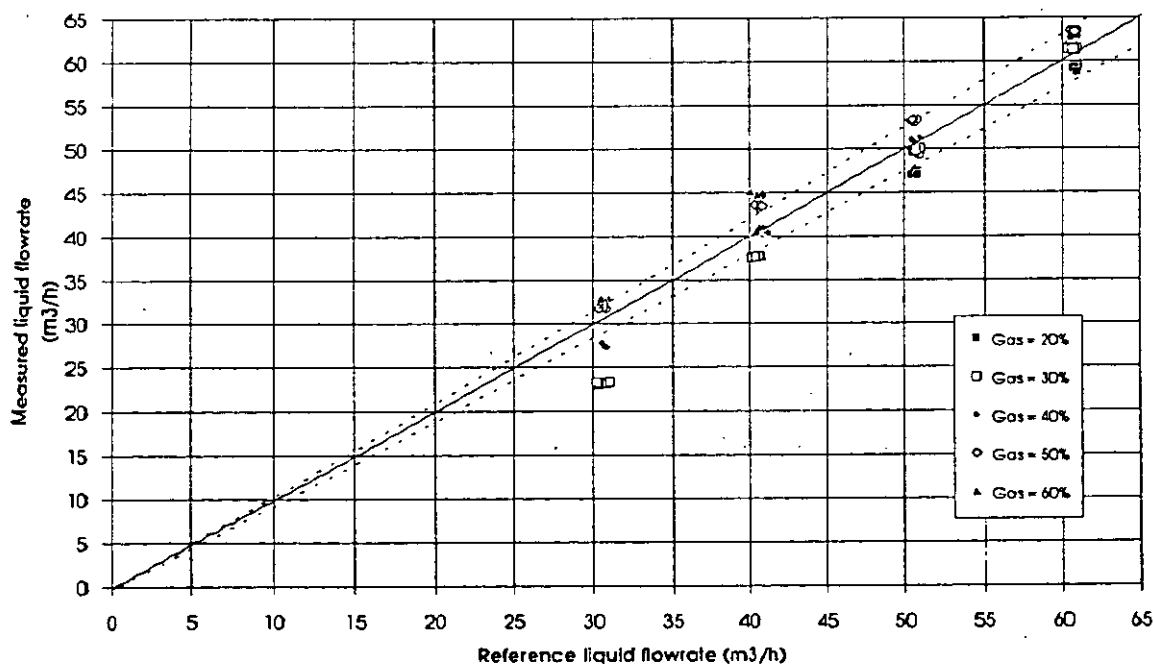


Figure 7 Liquid flowrate test results (m^3/h). Nominal gas fractions: 20-60%. Water cut: 20%. The dotted lines represent the $\pm 5\%$ relative error.

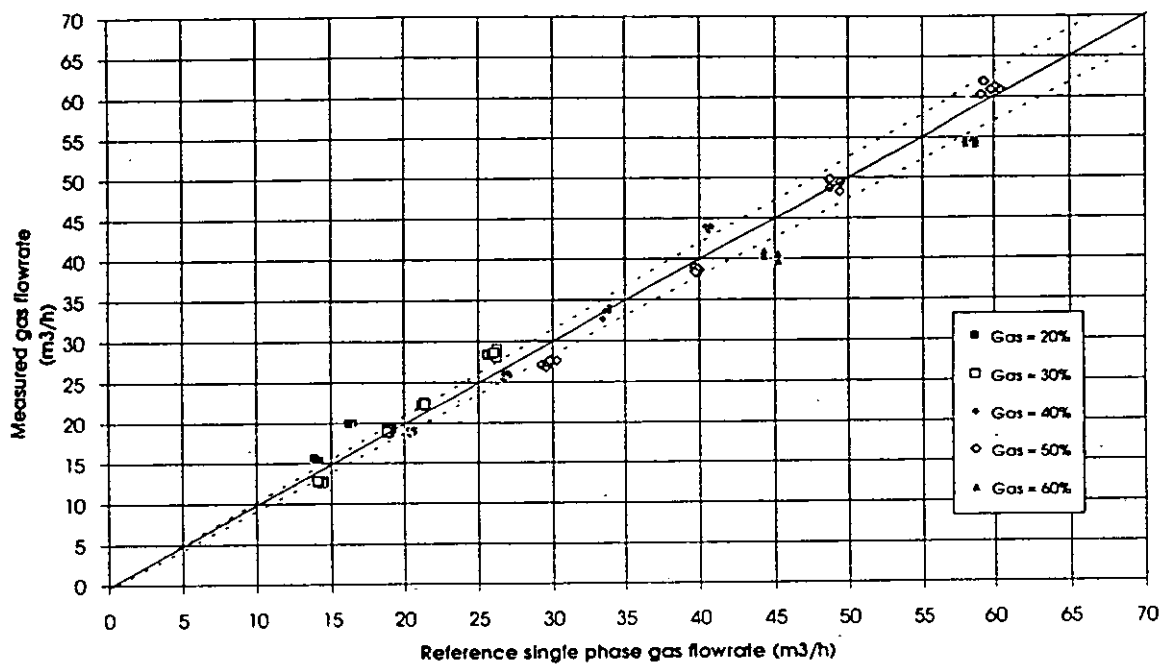


Figure 8 Gas flowrate test results (m³/h). Nominal gas fractions: 20-60%. Water cut 20%. The dotted lines represent the ±5% relative error.

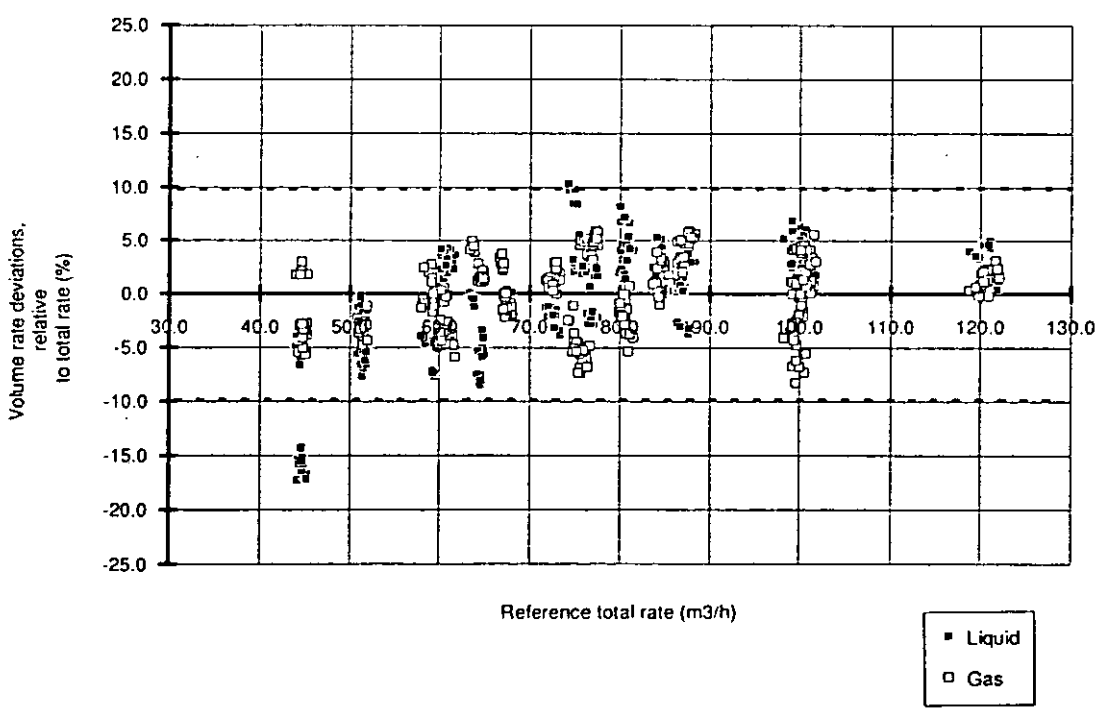


Figure 9 Deviations between measured and reference gas and liquid flowrates, relative to actual total flowrate. Nominal gas fractions: 20-60%. Water cut 5 - 40%.

The results from these performance tests are very satisfactory. Generally, over most of the tested range, measured flowrates of liquid and gas are found to be well within $\pm 10\%$ from reference single phase flowrates at the rig. Over a somewhat reduced range, the agreement between measured flowrates and reference flowrates is within $\pm 5\%$. As we can see from the flowrate deviation plot in Figure 9, the measurement uncertainty increases at low total flowrates. Measured watercut is also within $\pm 5\%$ over most of the tested range.

The deviations in measured flowrates at low total flowrates are explained by the fact that the fraction measurement, which is used as input to the flowrate routine, still assumes a homogenous mixture. Work is in progress to model in-homogenous phase distributions into the fraction measurement module. This way, simply an updated version of the system software, is expected to improve the system performance.

A RANGE OF NEW MULTIPHASE METERS ARE NOW BECOMING AVAILABLE TO THE MARKET. A TEST AND QUALIFICATION PROGRAMME IS NEEDED.

At the North Sea Flow Measurement Workshop in 1991 a discussion group compiled a list of 18 different organisations currently working to develop a multiphase flowrate meter. At the Offshore Northern Seas in August 1992, five out of these eighteen (including CMR/Fluenta) announced meters available for the market.

The application of such multiphase meters can drastically change a satellite development concept. Separate testlines and manifold systems at the satellite may be omitted. The same may be the case for test separators, inlet separators and complex single phase measurement systems at the processing platform. Such drastic changes to proven technology can of course not be accepted unless the reliability of the new technology has been thoroughly qualified. In order to progress the maturity of such technology towards proven and accepted technology, it is therefore now important that the oil companies involve in test and pilot installations of multiphase meters.

The step from testing in a friendly laboratory environment on a model oil, to tough field applications on live crude is huge. In order to qualify this new technology for a wide application in future field developments, it is therefore now of the utmost importance to gain field experience on non-critical installations. It may be a costly process both to install the meters and to maintain a qualification test programme, however, the potential future cost savings should make such an investment profitable.

Field scenario studies suggest that subsea satellites is one of the most interesting applications for multiphase meters in the future. The subsea challenge is addressed in several multiphase meter development projects, and the first subsea versions are likely to be available for field testing at least by 1994. Provided that sufficient reliability of topsides meters has been verified, there will then exist a need for places where meters can be installed subsea for qualification.

Several of the multiphase meters available or in development require an upstream mixer to provide suitable measurement conditions. In our opinion, it is however not evident that there exist a multiphase mixer which will be able to create no-slip conditions and homogeneous phase distribution over a sufficiently large range of flowrates and composition. Since the overall performance of many multiphase meters will directly depend on the performance of available mixers, a test programme for evaluation of available mixers should be initiated.

REFERENCES

- [1] NSMW 1990, Field Experience with the CMI multi-phase fraction meter, by K.H. Frantzen and E. Dykesteen
- [2] Model-based measurement of multiphase flow, Multiphase Transportation III, Present Application & Future Trends, 20.-22. September, Røros, Norway.

FRAMO MULTIPHASE FLOWMETER - PROTOTYPE TEST

by

A B Olsen and B-H Torkildsen
Framo Engineering AS

Paper No 2.4

NORTH SEA FLOW MEASUREMENT WORKSHOP
26-29 October 1992

NEL, East Kilbride, Glasgow

FRAMO MULTIPHASE FLOW METER PROTOTYPE TEST

Torkildsen, Bernt Helge and Olsen, Arne Birger

Framo Engineering AS, Bergen

SUMMARY

A prototype test of the FRAMO Multiphase Flow Meter has been performed under flow conditions typical for North Sea oil and gas production systems.

The prototype includes a combination of the FRAMO flow mixer, a multi-energy gamma meter and a venturi meter built together with a barrier fluid arrangement and electronic processing equipment in a vertical stack.

The results show that the multiphase flow meter can be used to measure volume fractions and flow rates of oil, water and gas over the entire range of gas volume fractions 0 - 100% and water cuts 0 - 100%.

Most of the test points measure liquid volumetric and total mass flow rates well within +/- 10% relative error.

CONTENTS

- 1.0 INTRODUCTION
- 2.0 MULTIPHASE METERING
- 3.0 MULTIPHASE FLOW METER - PROTOTYPE
 - 3.1 Flow Mixer
 - 3.2 Multi-energy Gamma Meter
 - 3.3 Venturi Meter
 - 3.4 Cartridge Seal System
 - 3.5 Barrier Fluid Arrangement
 - 3.6 Electric/Signal Connector
 - 3.7 Monitoring/Control System
- 4.0 PROTOTYPE TEST
 - 4.1 Test rig arrangement
 - 4.2 Test rig instrumentation
 - 4.3 Test conditions
- 5.0 RESULTS
 - 5.1 Two-phase Oil and Gas
 - 5.2 Two-phase Water and Gas
 - 5.3 Two-phase Oil and Water
 - 5.4 Three-phase Oil, Water and Gas
- 6.0 DISCUSSION
- 7.0 CONCLUSIONS
- ACKNOWLEDGEMENTS
- REFERENCES

1.0 INTRODUCTION

Multiphase metering has recently been subject to increasing interest due to its potential to enhance reservoir management and reduce capital expenditure and operating costs by eliminating the need for test separators and dedicated test lines. These advantages are particularly important for marginal fields and subsea satellite developments.

Several different methods can be used to distinguish between oil, water and gas in a production stream. One technique based on the attenuation of gamma rays at two energy levels was developed by Mitsubishi Electric Corporation (MELCO) in 1984/85. A prototype gamma ray compositional meter was built and extensively tested by MELCO, Petro-Canada Inc. (PCI) and Alberta Research Council (ARC), including a field test in 1987 and a subsequent flow loop test of a modified version in 1988, ref. /1/.

The meters capability of measuring volume fractions of oil, water and gas was demonstrated, and the results were excellent for homogeneous flow. However, due to flow effects such as phase slip and slugging, practical applications of the meter were limited to conditions with very low gas contents.

A static flow mixer was developed and tested by Framo Engineering AS in 1988, as part of the Subsea Multiphase Booster Station (SMUBS) programme for boosting of unprocessed well stream. It was demonstrated that the flow mixer significantly improves booster performance at multiphase conditions, and particularly at slugging conditions, use of the flow mixer is mandatory.

During the last five years this mixer has been extensively tested, and its performance has been demonstrated in flow loops and during several field tests. Today, the mixer is an integrated part of several multiphase booster concepts, including a version of the SMUBS which will be installed for subsea duty at the Draugen field in 1993, and the POSEIDON pump which will be installed on the Gullfaks B platform the same year.

In 1990 a joint industry project was established to qualify the combination of the FRAMO mixer, the MELCO compositional meter and a standard venturi meter for measuring oil, water and gas flow rates under flow conditions typical for North Sea oil and gas productions systems.

A successful test was performed in a high-rate oil, water and gas test facility. Tests with and without the mixer showed that the mixer was able to eliminate upstream flow effects well enough to obtain accurate and repeatable estimates of oil, water and gas flow rates. The test results was presented in ref. /2/.

Encouraged by the results we started the development of a subsea version of the tested metering system. A functional prototype for dry testing was designed and manufactured with some of the subsea parameters and equipment configuration aspects included. The subsea elements are based on the available SMUBS technology. The subsea flow meter was presented in ref. /3/.

This paper presents the test results from the prototype test of the FRAMO multiphase flow meter performed at the FRAMO test facility at Fusa, Bergen this year.

2.0 MULTIPHASE METERING

Multiphase flow metering without first applying phase separation is difficult due to the different flow effects resulting from the interminable variety of phase distribution which can occur in such flow.

The most important flow effects which can affect meter performance are:

- Uneven phase distribution
- Locally unsteady flow
- Phase slip

These effects are closely connected to various flow regimes. However, since flow regime description to some degree is arbitrary and the transitions between different flow regimes is a gradual process, the impact on flow meter performance can not be sufficiently predicted.

The implications of this are twofolds. Primary sensor response will obviously be sensitive to the flow effects, which not necessarily correlates with the quantities to be measured. Sensor integration and interpretation are therefore difficult and critical.

However, more seriously is the lack of reproducibility, and the need for in-line calibration at various flow conditions. Since flow conditions will not only change from field to field, but also during time for a given field, such calibration will neither be practical nor will it normally be possible.

The flow conditions will also depend on the actual physical location in the process relative to risers, manifolds, bends, etc. Conveying the performance of a multiphase flow meter from one system to another will therefore always be questionable.

Generally two approaches exist to these problems. One method is to measure the individual phase fractions and related phase velocities. To establish the mass flow rates of the three phases, oil, water and gas, five measurements are required; three velocities and two phase fractions (the third being reduced since the sum of the three phase fractions equals unity).

The other method, which is applied in the FRAMO multiphase flow meter, makes use of a flow mixer and measures the individual phase fractions and the velocity of the mixture. In this case the required number of measurements are reduced from five to three.

The application of an effective flow mixer to eliminate or reduce the influence of flow effects, is in this case essential in order to obtain accurate, repeatable and reproducible estimates of the individual oil, water and gas flow rates.

Multiphase flow metering in general is further complicated by the fact that it is utmost difficult to measure small components of a large system with high relative accuracy. This can be illustrated by the production composed by 90% gas volume fraction and 90% water cut. In this case the oil volume fraction is only 1% to the total production. A typical uncertainty in the fraction measurement for such conditions might be in the range 1-5%, resulting in 100-500% relative error in the measured oil fraction, 11-56% relative error in the measured water fraction and 1.1-5.6% relative error in the measured gas fraction. This fundamental problem will probably impede the use of multiphase metering for fiscal applications yet for a long time.

3.0 MULTIPHASE FLOW METER - PROTOTYPE

The multiphase flow meter prototype was originally designed to meet some of the requirements to a subsea retrievable installation, refer to figures 3.0.1-3.0.2.

The technology forming the basis for a subsea flow meter is to a large extent developed for other Framo products. All vital elements are maintained in a vertical stack-up configuration forming a retrievable cartridge. The cartridge is when installed, located inside a receiver barrel which totally protects it from the environments. The cartridge requires no orientation, and hence the crude inlet and outlet enter and leave the barrel through ring volumes sealed axially by pressure energized resilient seals.

Key elements such as:

- running tool
- lock-down mechanism
- receiver barrel
- cartridge seal system
- barrier fluid arrangement

have all reached a commercial level through the SMUBS project. In addition, an integrated wet mateable electric/signal connector has been developed and tested by Framo.

The multiphase flow meter prototype includes some of these elements such as the receiver barrel, cartridge seal system and the barrier fluid arrangement. The retrievable flow meter cartridge consists of these elements:

- Flow Mixer
- Multi-energy Gamma-Meter
- Venturi Meter
- Cartridge Seal System
- Barrier Fluid Arrangement
- Electric/Signal Connector
- Monitoring/Control System

3.1 Flow Mixer

The functional schematic of the flow mixer is shown in figure 3.1.1. The purpose of the mixing unit is to provide always identical homogeneous flow conditions in the measuring section, independent on upstream conditions.

Turbulent mixing is efficiently utilized in a turbulent shear layer, resulting in minimum pressure loss. The feature of axial mixing incorporated in the unit makes it possible for efficient operation also during intermittent and slug flow conditions.

The flow mixer is a purely static device comprising a tank into which the multiphase flow is fed. The most dense part of the fluid is drained from the bottom of the tank through an ejector, while the least dense part is drained from the top and directed via a pipe back to the ejector, where it is mixed with the dense part of the fluid, according to the ejection ratio.

Operation of the flow mixer can be described by grouping the various multiphase flow regimes into Dispersed, Separated and Intermittent flows.

DISPERSED or distributed flow regimes such as bubbles in the liquid or droplets in the gas:

This flow is by its nature already well mixed. The same mixture will therefore be drained from the top and the bottom of the tank, and mixed together in the ejector. Due to the very short residence time, there is no phase separation occurring in the tank.

SEPARATED flow regimes, such as stratified or annular flow with low entrainment rates:

In this case each phase is continuously distributed in the axial direction, resulting in a steady feed of both liquid and gas into the tank. Since the phases are already separated, the gravity force will result in the formation of a liquid pool in the lower part of the tank with a body of gas above it. The liquid flow from the pool creates a suction in the ejector. This draws gas from the top of the tank via a pipe into the liquid flow. The resulting gas volume fraction is in accordance to the ejection ratio. In the ejector where the gas and liquid meet, a strong shear layer is created. Consequently an effective turbulent phase mixing takes place in the downstream section.

INTERMITTENT flow regimes, such as slug flow and elongated bubble flow:

In this case the performance of the mixer is similar to the separated flow case, except that the gas and liquid are not continuously fed into the tank. Instead, gas bubbles and liquid slugs are entering the tank in a successive manner, causing the liquid level in the tank to vary. However, the perforations in the interior pipe acts as an integral regulator, ensuring that there is always both liquid and gas present in the tank. As the liquid level in the tank decrease and more gas flows through the perforations, the gas volume fraction drawn from the mixer will increase and consequently the liquid level will stabilize. If on the other hand, the liquid level increases, more liquid will flow through the perforations. This liquid will also partly choke the gas flow. As a result, the gas volume fraction drawn from the mixer will decrease, and consequently the increase in liquid level will be reduced. This system is stable and the liquid level will always find its equilibrium position.

3.2 Multi-Energy Gamma Meter

The multi-energy gamma meter provides the fractions of oil, water and gas in the flow, which can be considered as volume fractions since the gamma meter is located immediately downstream the flow mixer.

Calculation of the oil, water and gas fractions is based on the attenuation of different gamma energy levels. The prototype meter consists of two gamma isotopes, Americium 241 and Barium 133 with collimators and two independent NaI (TI) scintillation detectors of ruggedized design, which can accept rapid temperature changes and sustain shocks and vibrations.

The energy levels which can be used for determining the fractions are 18 keV and 60 keV from the Am 241 source and 30 keV, 80 keV and 350 keV for the Ba133 source. The combination of two different energy levels is sufficient to determine three fractions, since the third fraction can be deducted from continuity.

The use of a low energy level 18 keV or 30 keV is essential in order to distinguish between oil and water. It is, however, important that the pipe wall is transparent to the low energy gamma rays, since these absorb very quickly. A Boron Carbide cylinder is used as a gamma ray window material. Independent tests have shown that this material is very transparent for low energy gamma rays, and yet strong and hard enough to sustain the design pressure of 345 bara and any practical erosional load.

3.3 Venturi Meter

A venturi meter arrangement is used in combination with the gamma fraction meter to obtain the flow rates of oil, water and gas. This is possible since the venturi meter is located immediately downstream the flow mixer. Here the multiphase mixture can be treated as a single-phase fluid with an equivalent mixture density, and the single-phase venturi relation can be applied. Defining the equivalent mixture density as:

$$\rho_m = \text{OVF} \cdot \rho_{\text{OIL}} + \text{WVF} \cdot \rho_{\text{WATER}} + \text{GVF} \cdot \rho_{\text{GAS}} \quad (3.3.1)$$

the relation between venturi differential pressure (DP) and total mass flow rate (m_T), can be written as:

$$m_T = C_F \cdot C_G \cdot Y_{sm} \cdot \sqrt{\rho_m \cdot DP} \quad (3.3.2)$$

where;

$$Y_{sm} = \text{GVF} \cdot Y_a + (1 - \text{GVF}) \quad (3.3.3)$$

Y_a is the gas expansion factor, C_G is a geometry constant and C_F is the venturi flow coefficient. The venturi differential pressure is the measured differential pressure corrected for the static height between the pressure ports. Similar to the practice in single-phase measurements, the venturi flow coefficient must be found by calibration. This is possible since the total mass flow rate and the mixture density are known from the reference measurements.

It is an increase in dynamic pressure rather than the fluid velocity which is measured with a venturi meter. The fluid velocity as calculated from the venturi meter is therefore dependent on the mixture density obtained from the gamma meter. This is of great advantage when the flow rates of the liquid components are sought, because an error in the liquid fraction will be partly compensated by a resulting opposite error in the calculated fluid velocity.

The prototype venturi meter has a β ratio of 0.71, and is configured with high precision quartz crystal absolute pressure sensors, (Digiquartz 46K). These sensors are temperature compensated. By using absolute pressure sensors, the measured venturi differential pressure is not influenced by the density of the fluid in the wet legs. Included in the venturi meter is an arrangement which allow a continuous or intermittent flushing of the wet legs. This way any contamination in the wet legs is prevented, which otherwise could lead to a blockage of the pressure ports. Flushing becomes particularly important for subsea and long term applications.

3.4 Cartridge Seal System

The seal system provides the sealing of the inlet and outlet ring volumes. Double pressure energized lip seals above and below the ring volumes ensure proper sealing against the environment.

In a subsea installation, the seals are set and pressure tested via the running tool during installation and a pressure higher than wellhead pressure is maintained during operation of the flow meter. This pressure is fed through the barrier fluid arrangement.

3.5 Barrier Fluid Arrangement

The barrier fluid arrangement provides for cleaning and protection of vital elements in the flow meter cartridge. Important features are:

- Flushing of venturi wet legs to prevent contamination
- Flushing of electric/signal connector (for subsea applications)
- Cartridge seal setting pressure

3.6 Electric/Signal Connector

The electric/signal connector used for subsea installations provides for transmission of low voltage power and signals to and from the cartridge and consist of two assemblies:

- A female part integrated in the flow meter receiver barrel lower end
- A male connector mounted at the lower end of the flow meter cartridge

The connector requires no orientation and is made up simultaneously with the installation of the flow meter cartridge. The connector allows supply of hydraulic fluid to the barrier fluid arrangement.

3.7 Monitoring/Controls System

Communication with the prototype flow meter is performed via the control system which is located in and forms an integrated part of the flow meter cartridge.

The control system which applies transputer technology, conditions the signals from gamma-meter detector and the sensors and transmits them to the topside control unit (host computer) for further processing. The topside control unit will typically provide data communication, power transmission to subsea flow meter and remote calibration of the multiphase flow meter.

4.0 PROTOTYPE TEST

4.1 Test rig arrangement

The multiphase flow meter has been tested in a closed loop, where individual measurements of single-phase oil, water and gas streams were compared with the multiphase flow meter measurements on the combined oil-water-gas stream. The fluids used are Exsol D80, fresh water and nitrogen gas. Schematic of the test rig arrangement is shown in figure 4.1.1.

Oil is taken from the oil outlets of four identical vertically installed three-phase separators and routed to a horizontally installed two-phase oil-water separator for removal of any remaining water. The oil from this two-phase separator is then routed through pumps, a single-phase oil reference metering section and a remotely operated control valve before it is combined with the water and gas streams. Oil saturation pressure and temperature is measured at the oil exit from the three-phase separators.

Water is taken from the water outlets both from the four three-phase separators and the two-phase oil-water separator and routed to a large low pressure water tank for removal of any remaining oil. The water from this water tank is then routed through pumps, a single-phase water reference metering section and a remotely operated control valve before it is combined with the oil and gas streams. Any oil from the water tank is routed through a pump back to the three-phase separators.

Gas is drawn from the top of the four three-phase separators and routed through a gas compressor, a single-phase gas reference metering section and a remotely operated control valve before it is combined with the oil and water streams. Strainers and scrubbers are located both at the suction and the discharge side of the compressor.

The combined oil-water-gas stream is routed through a 26 m long 3" flow loop to ensure that any three-phase flow regimes are fully developed. Part of the flow loop has been made of transparent material, allowing flow regime visualization and registration. The stream is then routed through the multiphase flow meter and back to the four three-phase separators. Pressure is measured upstream and downstream the multiphase flow meter, so that the total pressure loss through the multiphase flow meter can be calculated.

To enhance test rig operation, the oil and water pumps are adjustable by means of two independently and remotely operated frequency converters, while the gas compressor is equipped with a remotely operated flow control valve.

The oil and water streams can each be individually routed to an open tank with an accurate known volume. This way the respective flow rates instruments can be checked, or when necessary recalibrated. Samples of the single phase oil, water and gas streams are taken regularly during testing and analysed in order to monitor separator efficiency.

4.2 Test rig instrumentation

As a reference to the multiphase flow meter the flow rates of oil, water and gas through it are calculated based on measurements of the single-phase oil, water and gas streams and known PVT correlations for the different phases. Minimum, maximum and standard deviations of the single-phase measurements during the sampling time are obtained as well.

The single-phase measurements are corrected for any water in the oil caused by an incomplete oil-water separation, and for the difference in the amount of gas dissolved in the oil and the water between the multiphase flow meter station and the single-phase metering stations.

Dual instrumentations are used for critical measurements. The arrangement and specification of the test rig instruments are shown in figures 4.2.1-4.2.5. For each instrument an operating range has been defined to ensure an optimum overall accuracy.

All instruments has been factory calibrated with the actual fluids used in the test rig. PVT-data of the fluids has been obtained from specific laboratorium analysis.

4.3 Test conditions

It was aimed to simulate flow conditions typical for North Sea oil and gas production systems, and emphasis was given on creating realistic flow regimes. Most of the tests were run in the slug flow regime, which is believed to represent the most demanding conditions.

Initially several two-phase conditions was tested in order to verify the mixer performance and the ability of the gamma fraction meter to distinguish between the different phases. The gamma meter was calibrated on single-phase oil, water and gas.

The following four test series have been performed, and are described in this paper:

TWO-PHASE OIL and GAS

Total flow rate:	20-230 m ³ /h
Gas volume fraction:	30-95%
Pressure:	9-14 bara
No. of test points:	155

TWO-PHASE WATER and GAS

Total flow rate:	20-185 m ³ /h
Gas volume fraction:	5-90%
Pressure:	9-12 bara
No. of test points:	68

TWO-PHASE OIL and WATER

Total flow rate:	20-135 m ³ /h
Water cut:	5-85%
Pressure:	3-11 bara
No. of test points:	44

THREE-PHASE OIL, WATER and GAS

Total flow rate:	60-220 m ³ /h
Gas volume fraction:	30-85%
Water cut:	5-70%
Pressure:	6-10 bara
No. of test points:	140

5.0 RESULTS

Performance of the Multiphase Flow meter is evaluated by comparing measured and reference quantities. "Measured" refers to the measurements obtained with the Multiphase Flow meter. When the term "error" is used, it is assumed that the reference quantity is correct, and the error is then relative to this quantity.

Some of the results obtained by using 18 keV from the Americum 241 were hampered by drift in the gamma meter, so this option could not be fully explored. All the results presented were obtained by use of the Barium 133 source. The two-phase results were obtained from the 30 keV energy level, while the three-phase results from the combination of the 30 and 350 keV energy levels. The sampling time was always 1 minute.

The isolated performance of the venturi meter is expressed through the venturi flow coefficient as defined in section 3.3, equations 3.3.1-3.3.3. It should be noted that any error in the measured venturi differential pressure or in the reference flow rates will also affect the venturi flow coefficient the way it is defined here.

The flow rate measurement results, as presented in this paper, are obtained by using a venturi flow coefficient equal to unity.

5.1 Two-phase Oil and Gas

Measured and reference gas volume fractions are compared in figure 5.1.1, and the corresponding relative errors in the measured gas and oil volume fractions are shown in figures 5.1.2 and 5.1.3 respectively.

The venturi flow coefficient is shown in figure 5.1.4.

Figures 5.1.5-5.1.7 compare measured and reference oil volumetric flow rates, gas volumetric flow rates and total mass flow rates respectively, while figure 5.1.8 shows the corresponding relative errors in the measured total mass flow rates.

5.2 Two-phase Water and Gas

Measured and reference gas volume fractions and total mass flow rates are compared in figures 5.2.1 and 5.2.2.

5.3 Two-phase Oil and Water

Measured and reference water cuts and total mass flow rates are compared in figures 5.3.1 and 5.3.2.

5.4 Three-phase Oil, Water and Gas

Measured and reference gas volume fractions, oil volume fractions and water cuts are compared in figures 5.4.1-5.4.3 respectively.

The venturi flow coefficient is shown in figure 5.4.4.

Figures 5.4.5-5.4.8 compares measured and reference liquid, oil, water and gas volumetric flow rates respectively, while measured and reference total mass flow rates are compared in figure 5.4.9. The relative error in the total mass flow rates is shown in figure 5.4.10.

6.0 DISCUSSION

Results from the two-phase oil and gas tests show that the gas volume fraction is predicted with good accuracy and repeatability over the whole range tested.

This has been possible since flow regime effects have been eliminated by the flow mixer. Nevertheless, large relative errors are associated with small volume fractions.

Also the venturi meter shows good performance over the whole range tested, with an average flow coefficient of 0.96. This shows that a simple equivalent single-phase venturi equation is valid for a venturi meter located immediately downstream the flow mixer. All flow rate measurements have been obtained by using a venturi flow coefficient equal to unity.

The oil volumetric and total mass flow rates correlate well with the reference values, while some more scatter is observed in the gas volumetric flow rates. By replacing the applied venturi flow coefficient of unity with the calibrated flow coefficient of 0.96, all measured flow rates would have been reduced by 4%, resulting in additional improvement of the accuracy.

Observe that the relative errors in the total mass flow rates, as obtained by combining the volume fraction measurements with the venturi measurements are significantly less than the relative error in the volume fractions. This is a favourable feature of applying a venturi meter.

The two-phase water gas tests (100% WC) and the two-phase oil water tests (5 - 85% WC) show similar performance to the two-phase oil gas tests.

Results from the three-phase oil water gas tests show that the gas volume fraction is predicted with good accuracy over the whole range tested. The predictions of water cuts are more scattered, however, some of the scattering can be explained by a slight drift in the gamma meter, and the fact that the gamma meter needed a longer warm-up period to stabilise than initially anticipated.

It is possible that these results could have been improved by an increased sampling time beyond one minute.

The venturi meter shows acceptable performance with an average flow coefficient equal to 0.96 for the range up to 60% gas volume fraction.

The venturi flow coefficient appears to increase slightly for higher gas volume fractions. However, it should be kept in mind that the flow coefficient as defined here, is affected by the accuracy and repeatability in the pressure sensors which, despite their high quality specifications, were no better than 0.02 bar. This influence can be particularly significant at high gas volume fraction.

The average value of the venturi flow coefficient for all the three-phase test points is equal to 1.0.

All flow rate measurements have been obtained by using a venturi flow coefficient equal to unity over the entire range. The liquid volumetric and total mass flow rates correlates well with the reference values while more scatters are observed in the individual components' flow rates. 90% of all the three-phase test points are measured within +/- 10% relative error in the total mass flow rates.

7.0 CONCLUSIONS

The results presented show that the FRAMO Multiphase Flow Meter can be used for measuring oil, water and gas volume fractions and flow rates over the entire range of gas volume fractions from 0 - 100% and water cuts from 0 - 100%, and under flow conditions typical for the North Sea oil and gas production systems.

The use of 30 keV and 350 keV energy levels from the Barium 133 source enabled accurate estimates of gas volume fractions and reasonable estimates of water cuts.

The venturi meter shows good performance over the entire range tested, with an average flow coefficient close to unity. This demonstrates that a simple equivalent single-phase venturi equation holds for a venturi meter located immediately downstream the flow mixer.

For most of the test points, liquid volumetric and total mass flow rates are measured well within +/- 10% relative error.

ACKNOWLEDGEMENTS

The authors express their gratitude to the partners in the flow meter development project; Shell, Norsk Hydro, BP, Conoco, Elf Aquitaine and Saga Petroleum for permission to publish this paper, and to Frank Mohn Fusa AS for co-operation during testing.

REFERENCES

- /1/ Rafa K., Tomoda T. and Ridley R. Flow Loop and Field Testing of a Gamma Ray Compositional Meter, Paper 89-Pet-7 presented at the Energy-Sources Technology Conference and Exhibition, Houston, Texas, Jan. 22-25, 1989.
- /2/ Martin W., Woiceshyn G. E. and Torkildsen B. H. A Proven Oil-Water-Gas Flow meter for Subsea. The 23rd Annual OTC in Houston, Texas, May 6-9, 1991.
- /3/ Olsen, A. B. and Torkildsen, B. H. Subsea Multiphase Flow Meter System. UTC'92 30 March - 1 April 1992 in Bergen, Norway.

PATENT PENDING

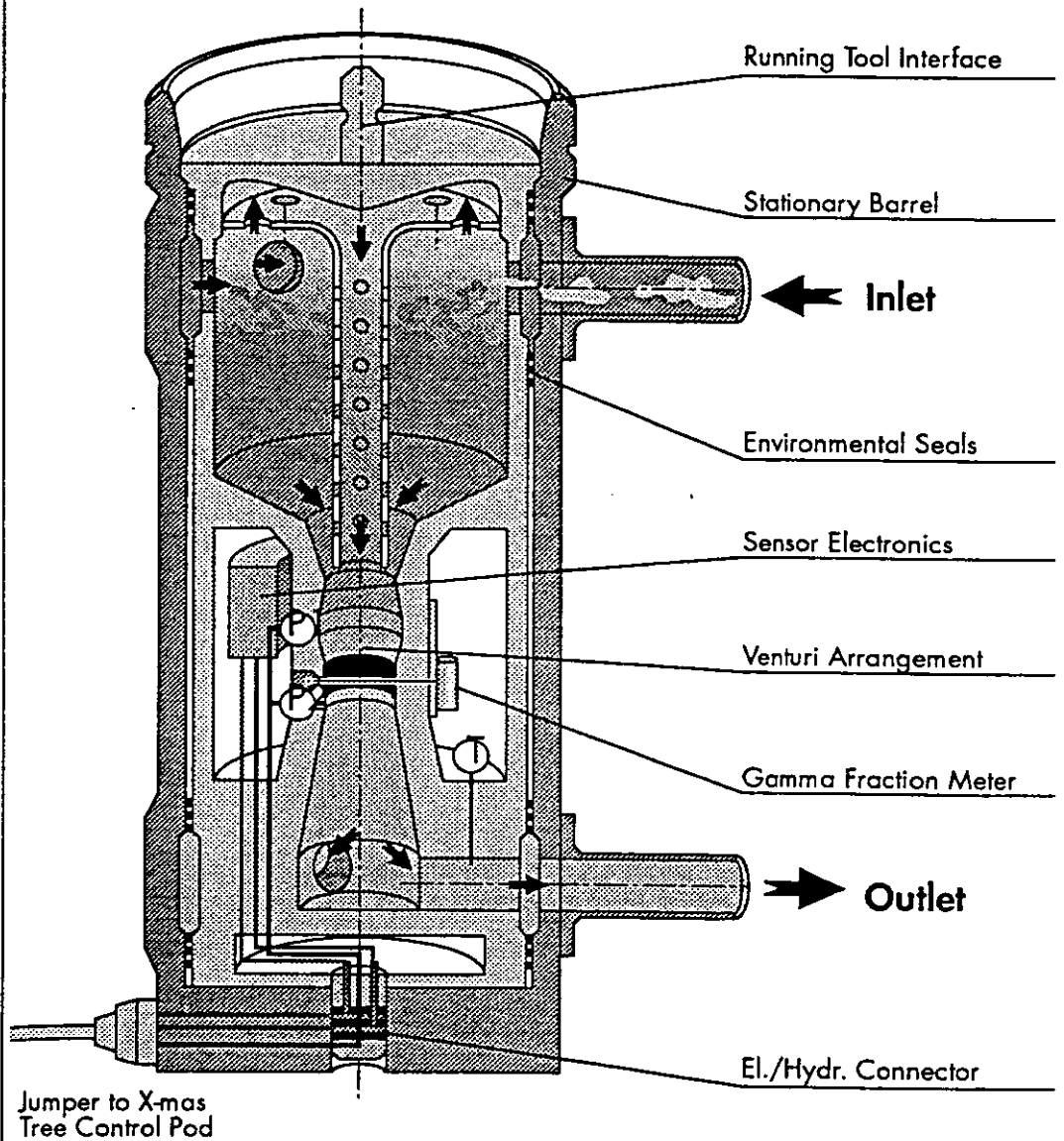
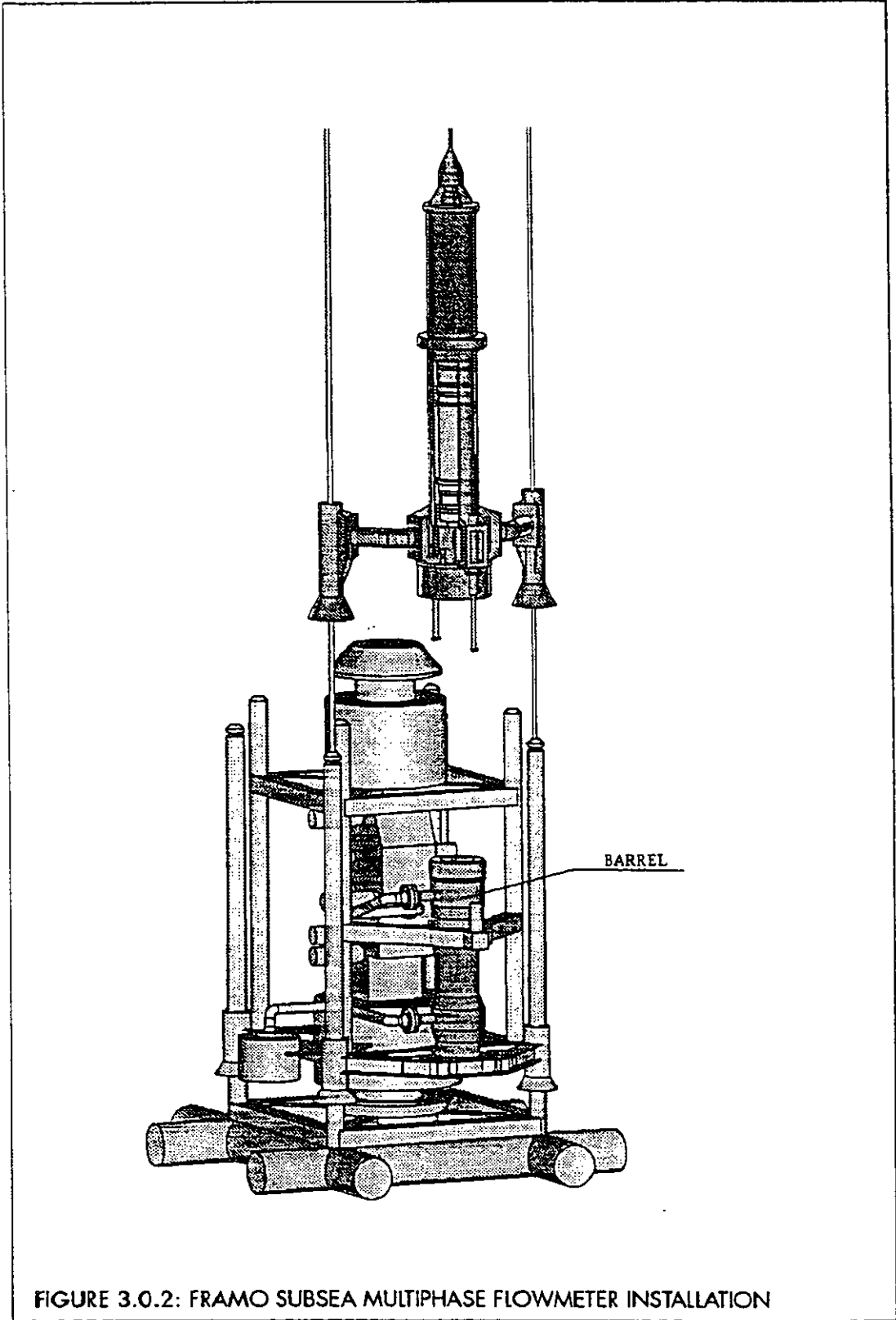


FIGURE 3.0.1: FRAMO SUBSEA MULTIPHASE FLOWMETER



PATENT PENDING

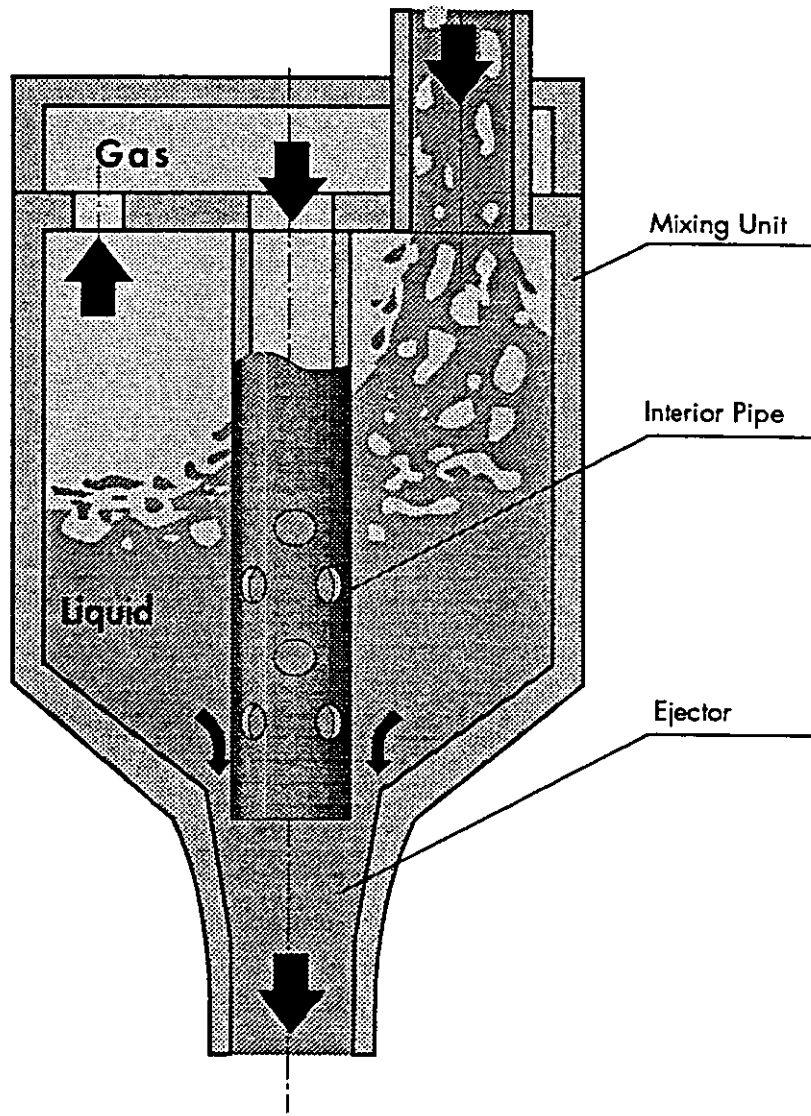


FIGURE 3.1.1: FLOW MIXER SCHEMATIC

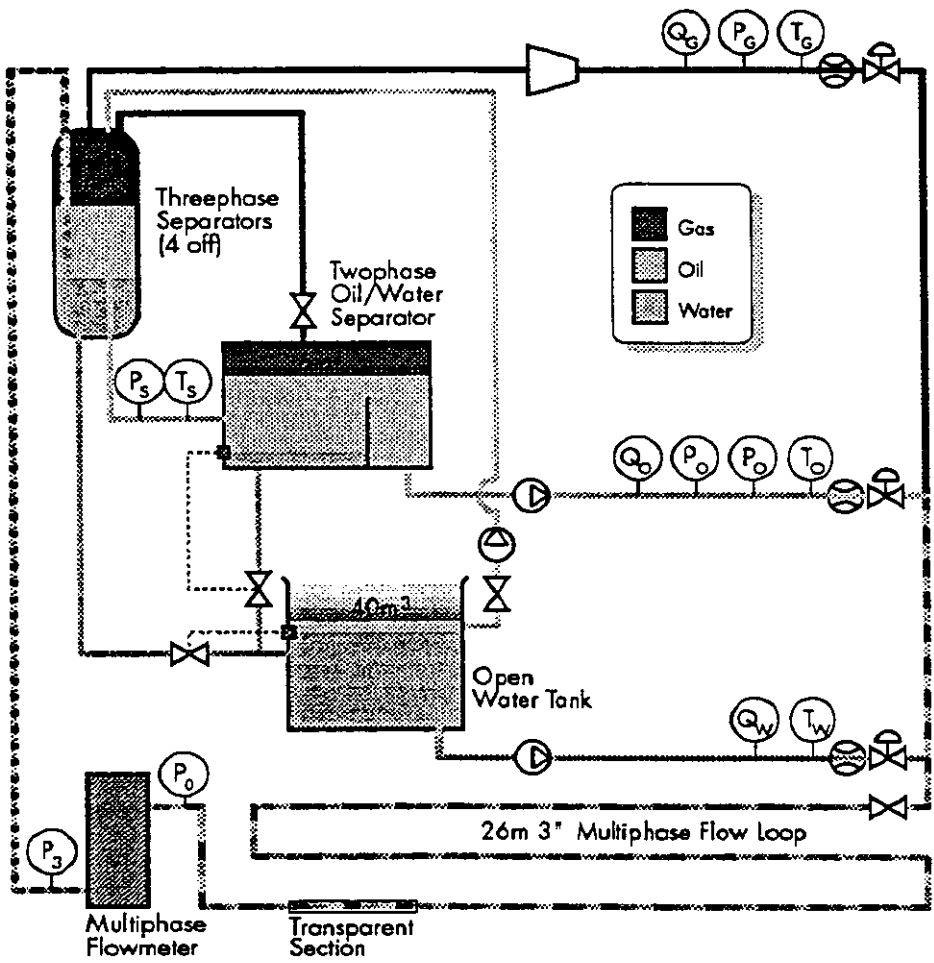


FIGURE 4.1.1: TEST RIG ARRANGEMENT

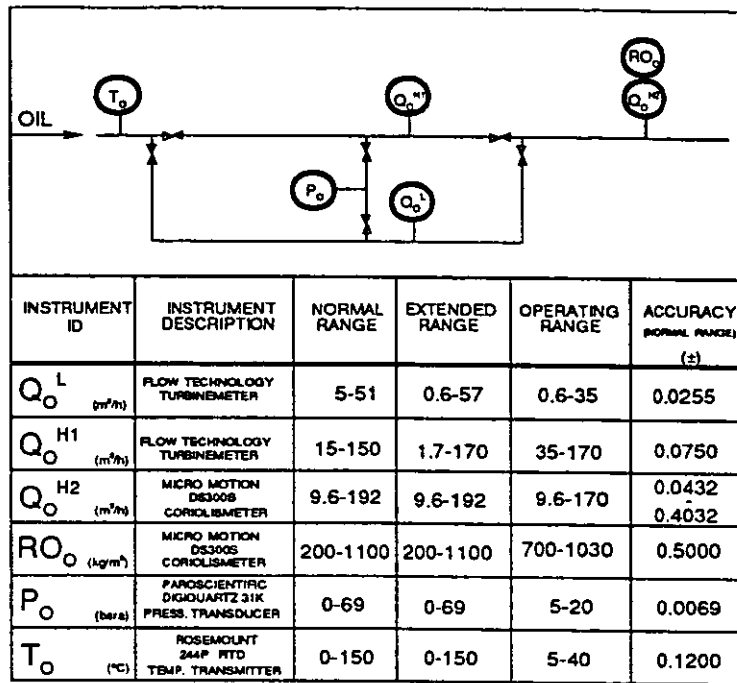


FIGURE 4.2.1: SINGLE-PHASE OIL METERING SECTION.

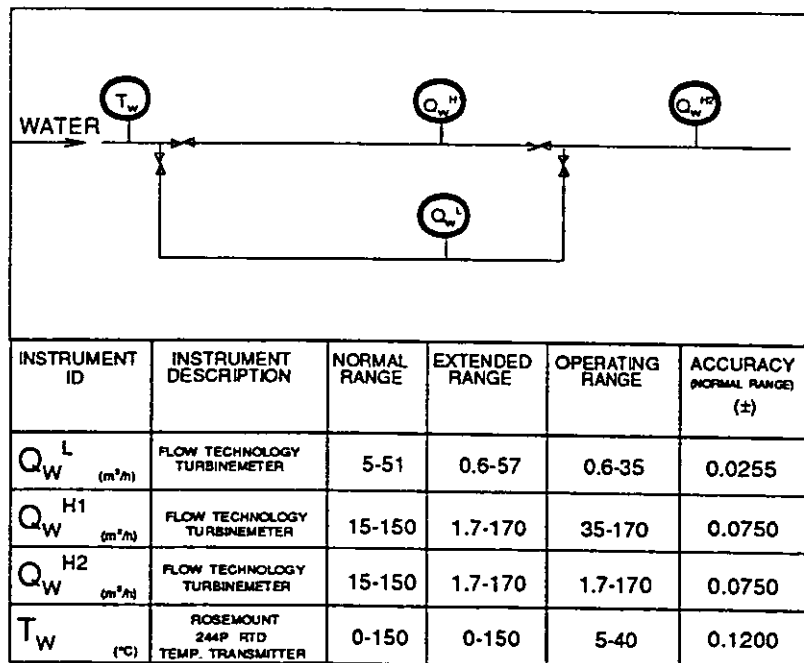


FIGURE 4.2.2: SINGLE-PHASE WATER METERING SECTION.

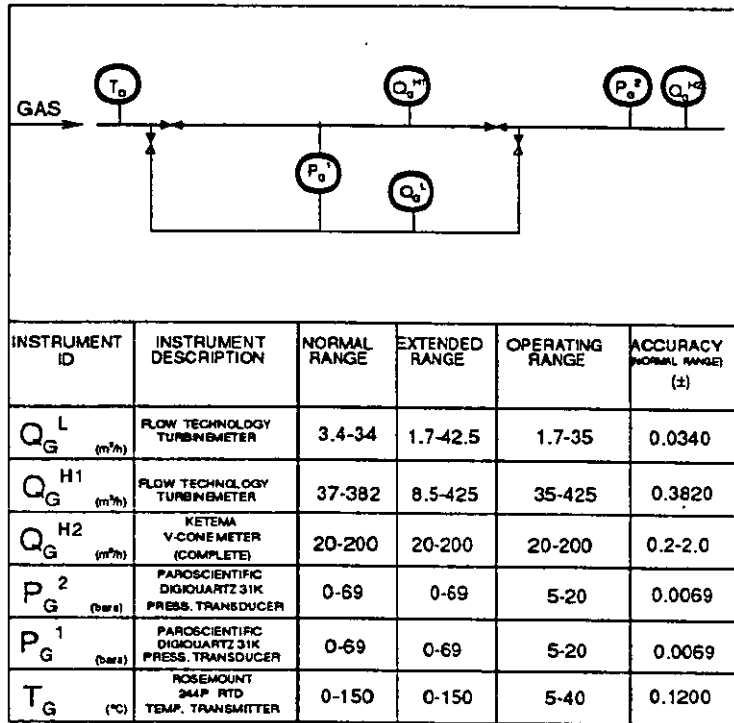


FIGURE 4.2.3: SINGLE-PHASE GAS METERING SECTION.

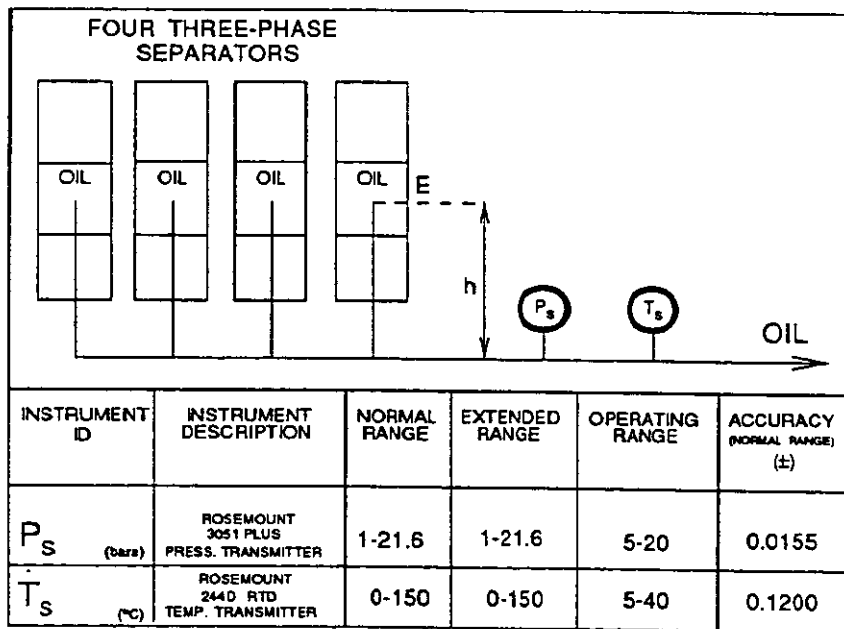


FIGURE 4.2.4: INSTRUMENTS LOCATED ON THE OIL STREAM DOWNSTREAM THE FOUR THREE-PHASE SEPARATORS.

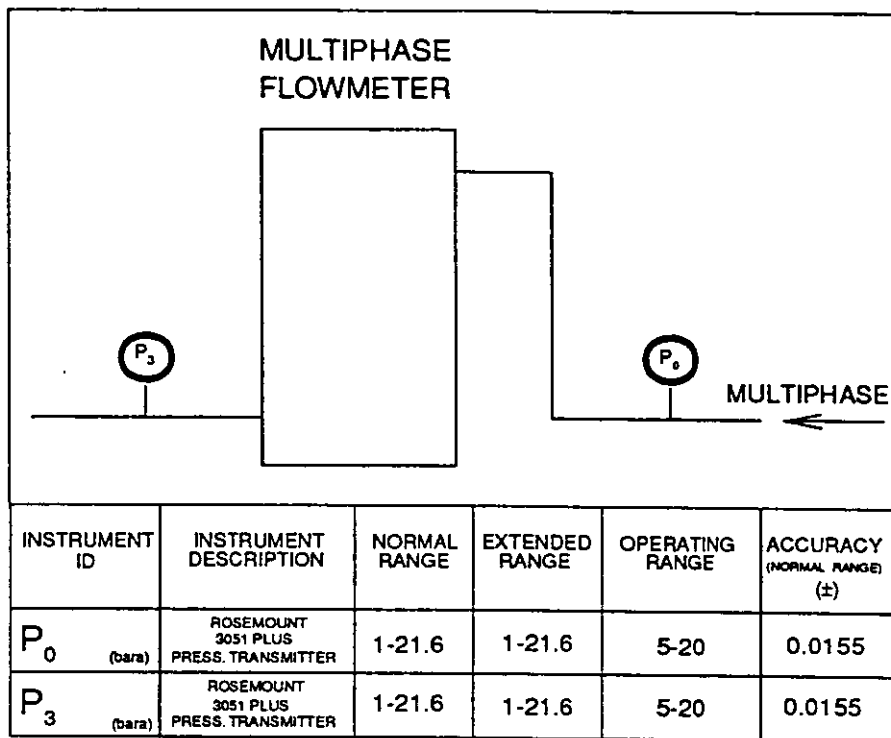
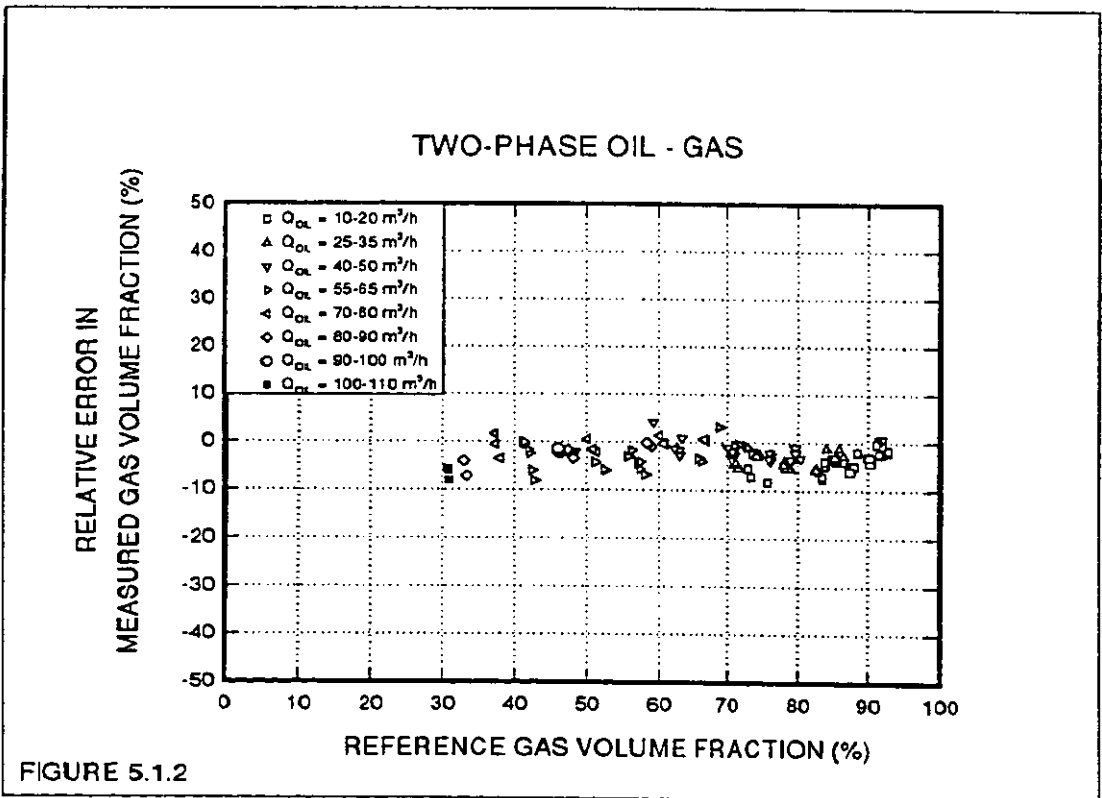
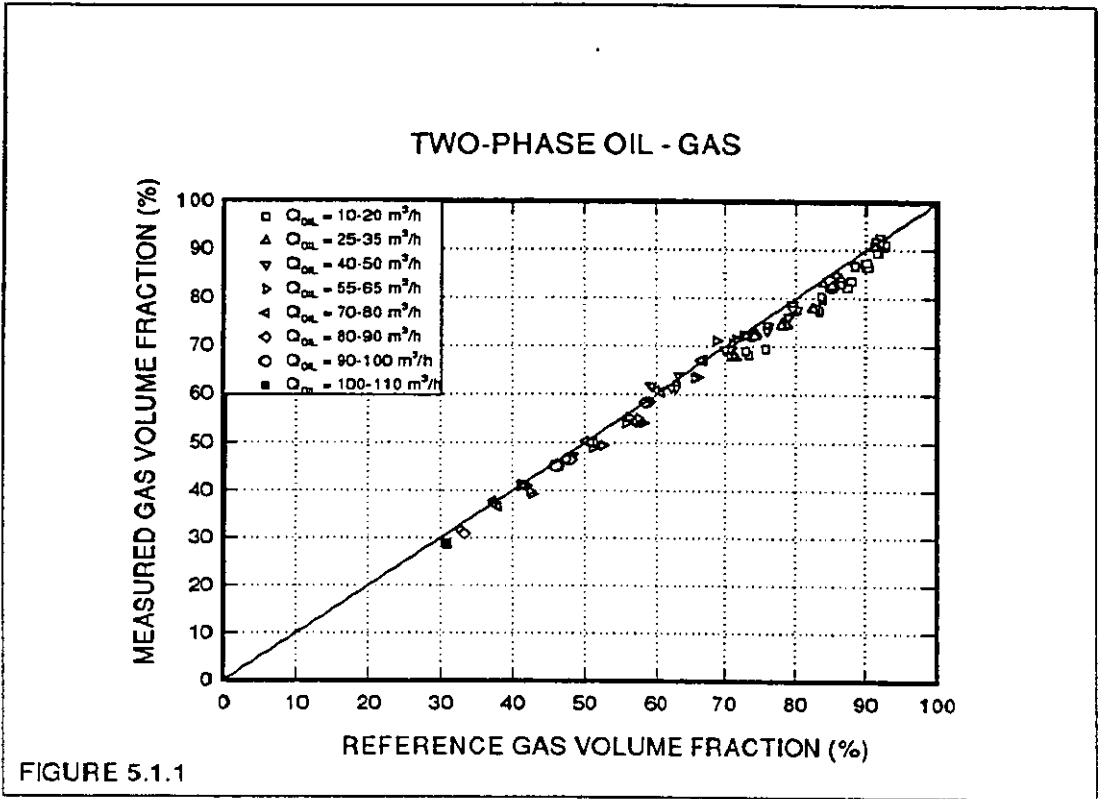
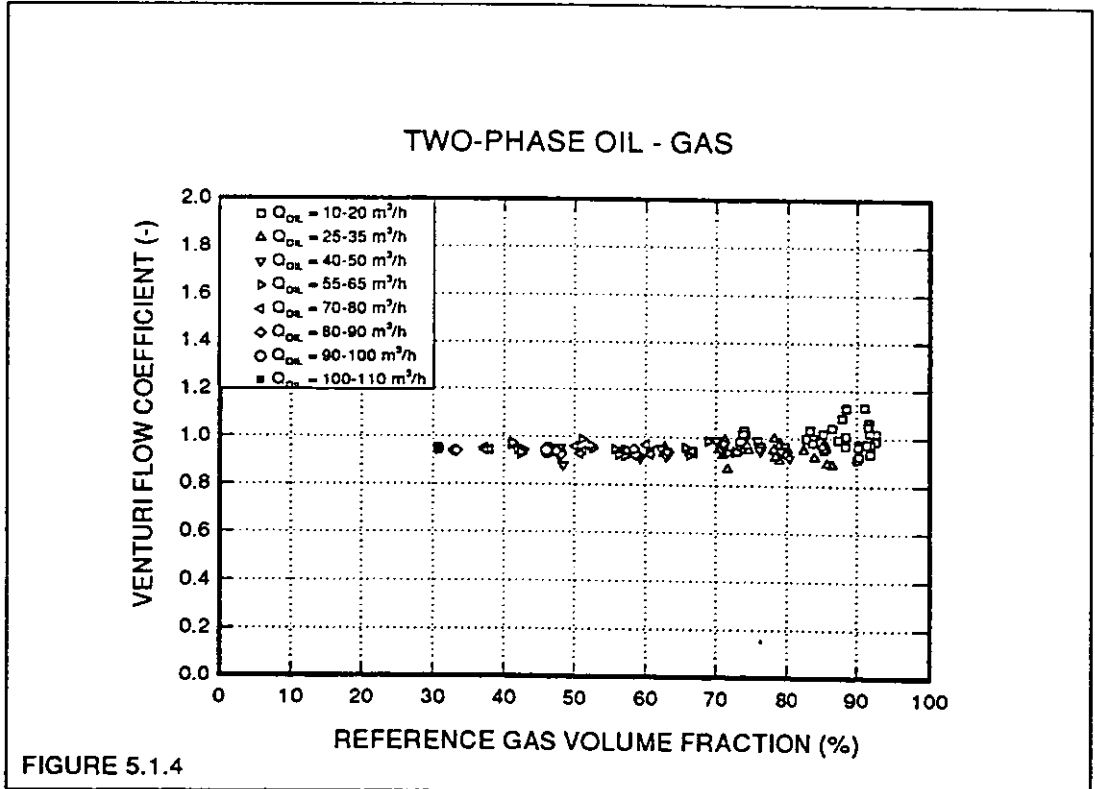
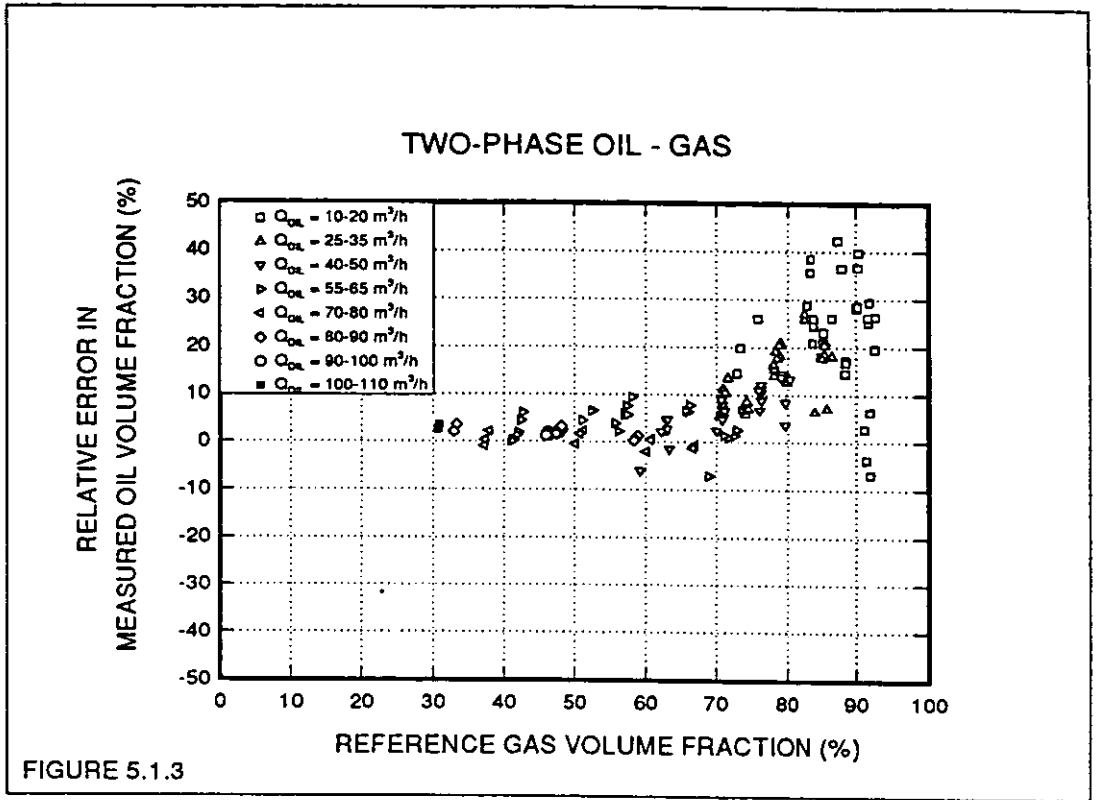


FIGURE 4.2.5: INSTRUMENTS LOCATED UPSTREAM AND DOWNSTREAM THE MULTIPHASE FLOWMETER.





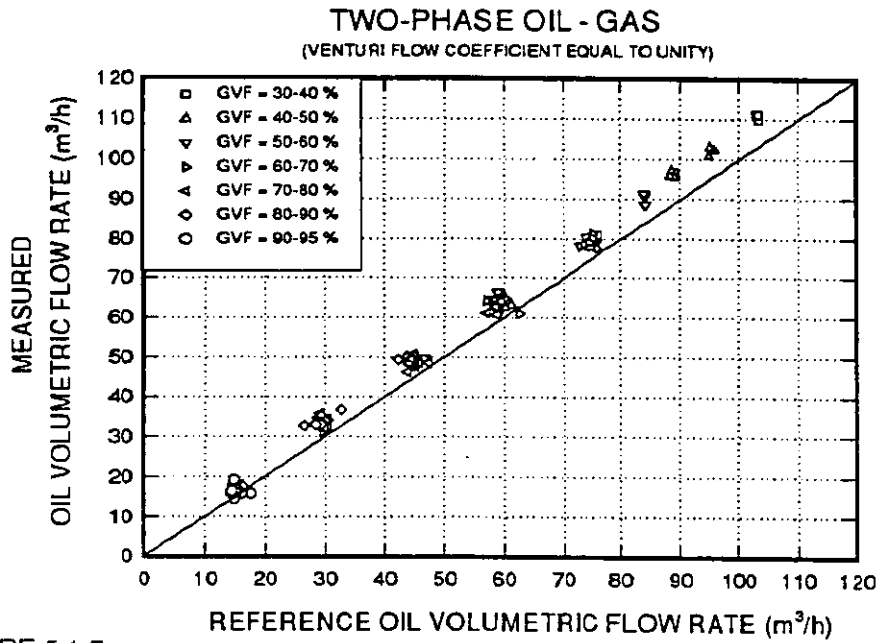


FIGURE 5.1.5

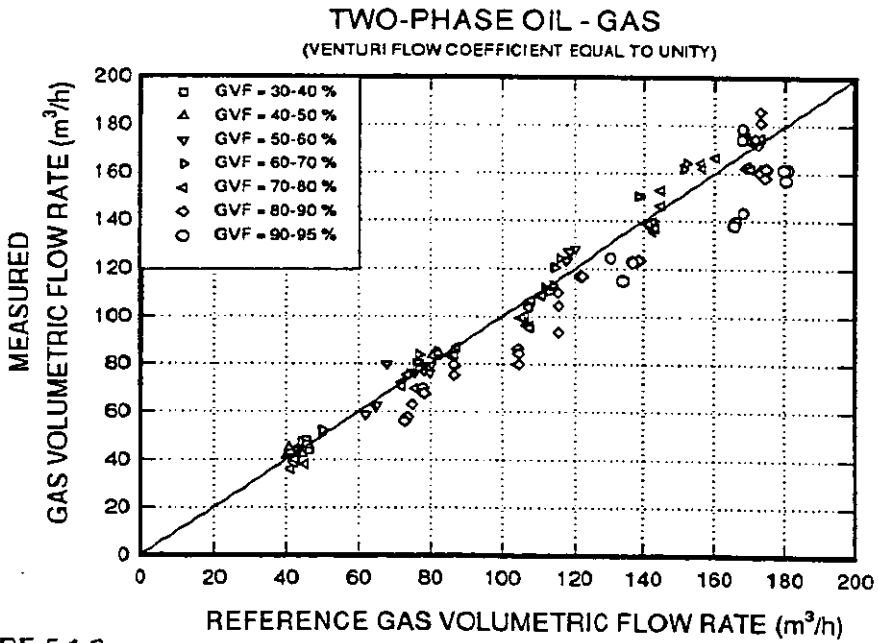
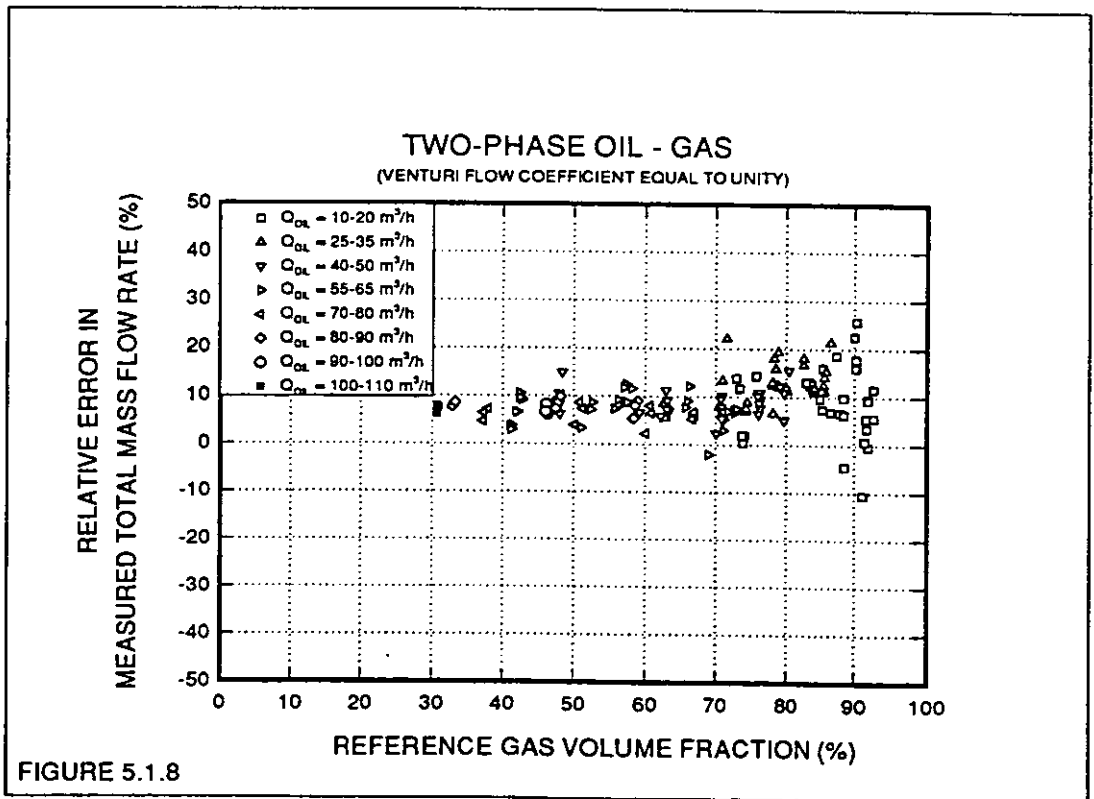
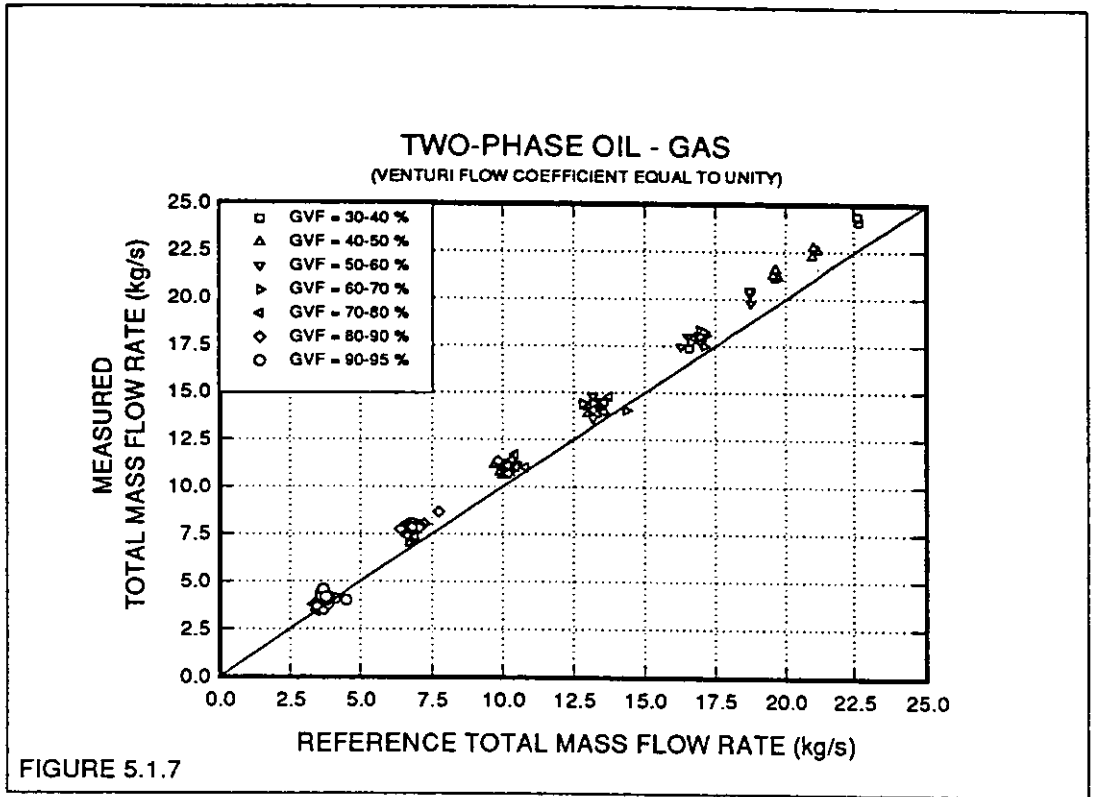
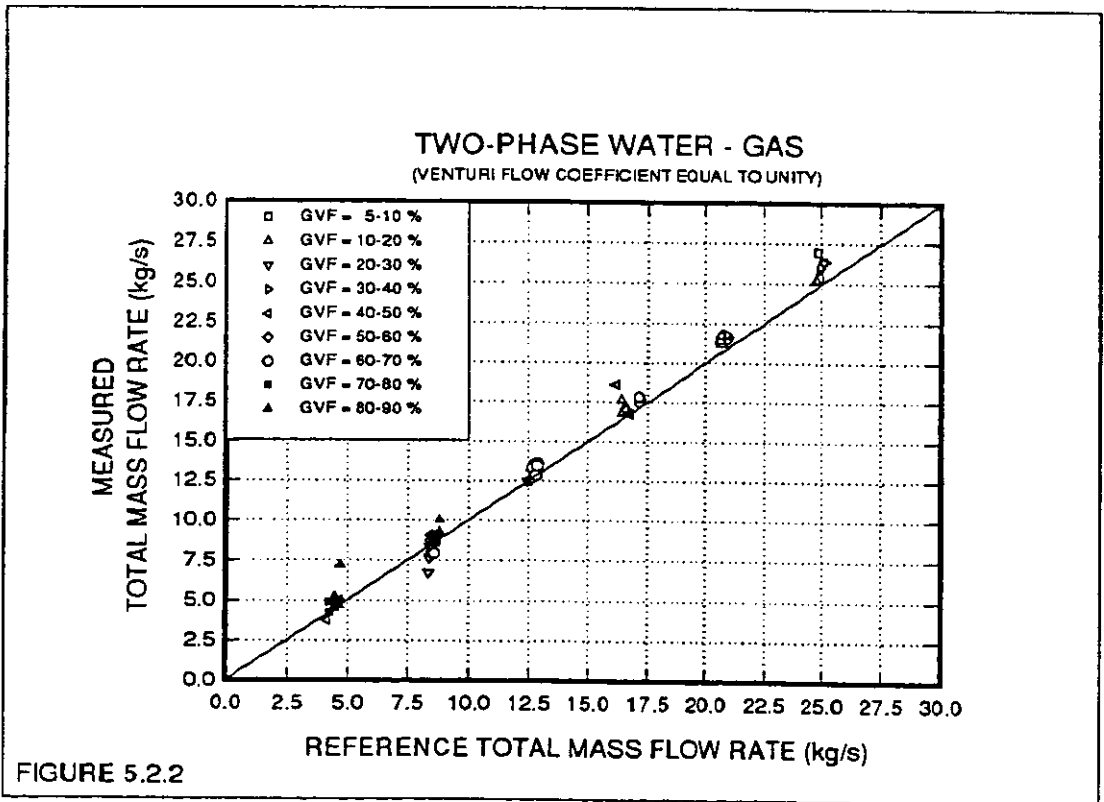
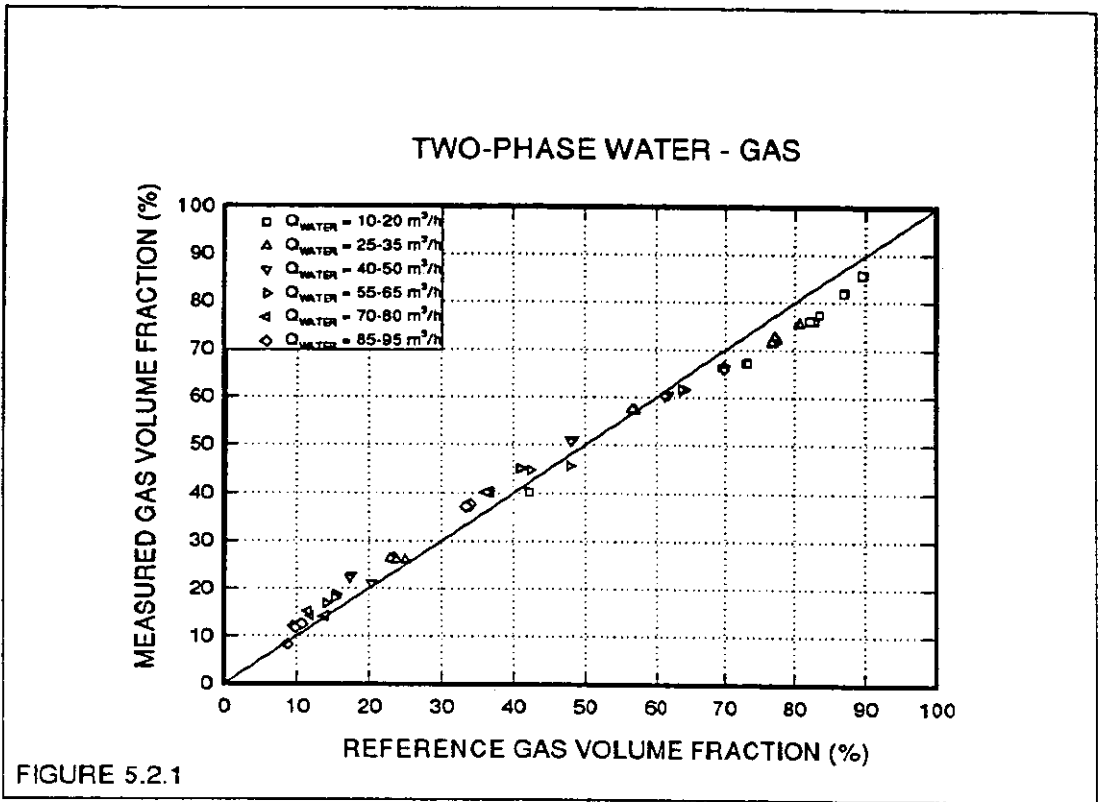
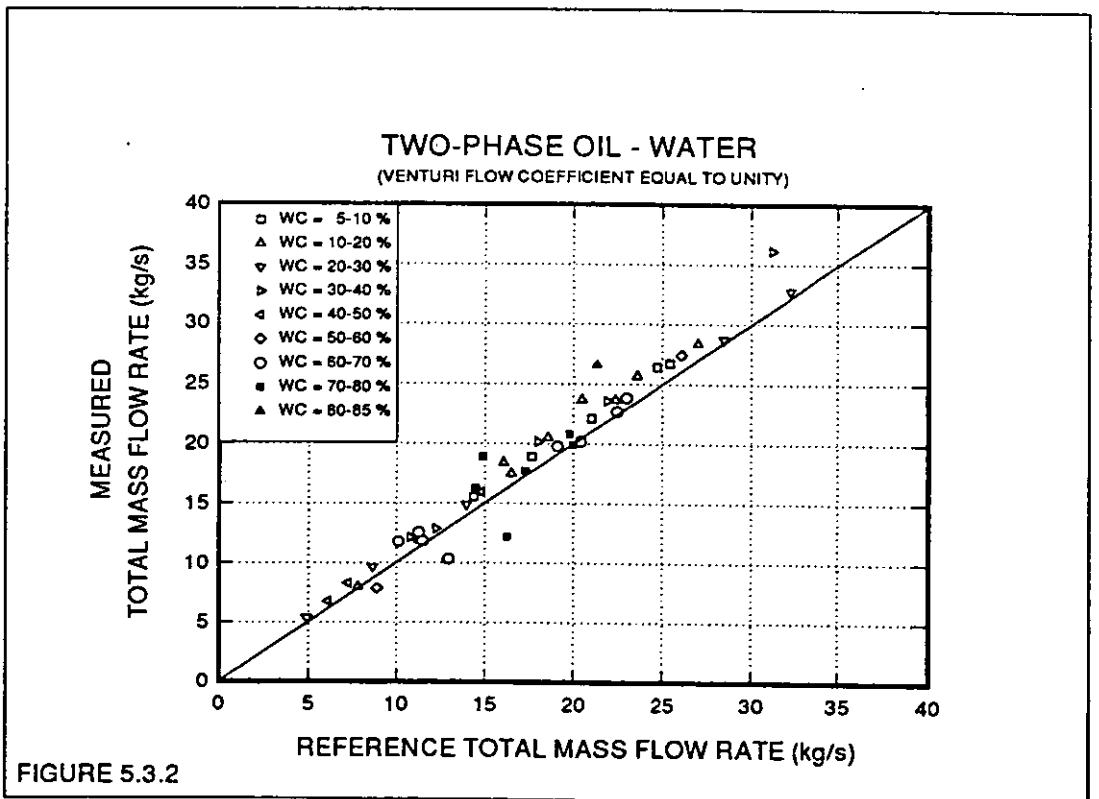
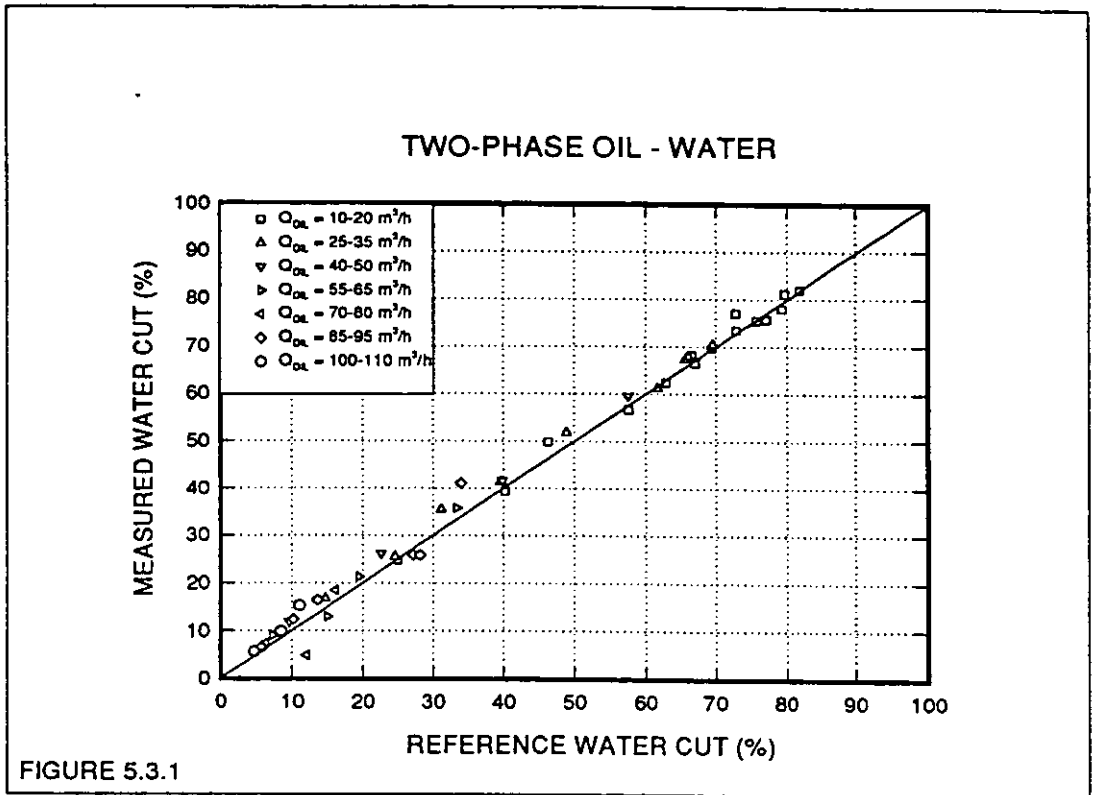
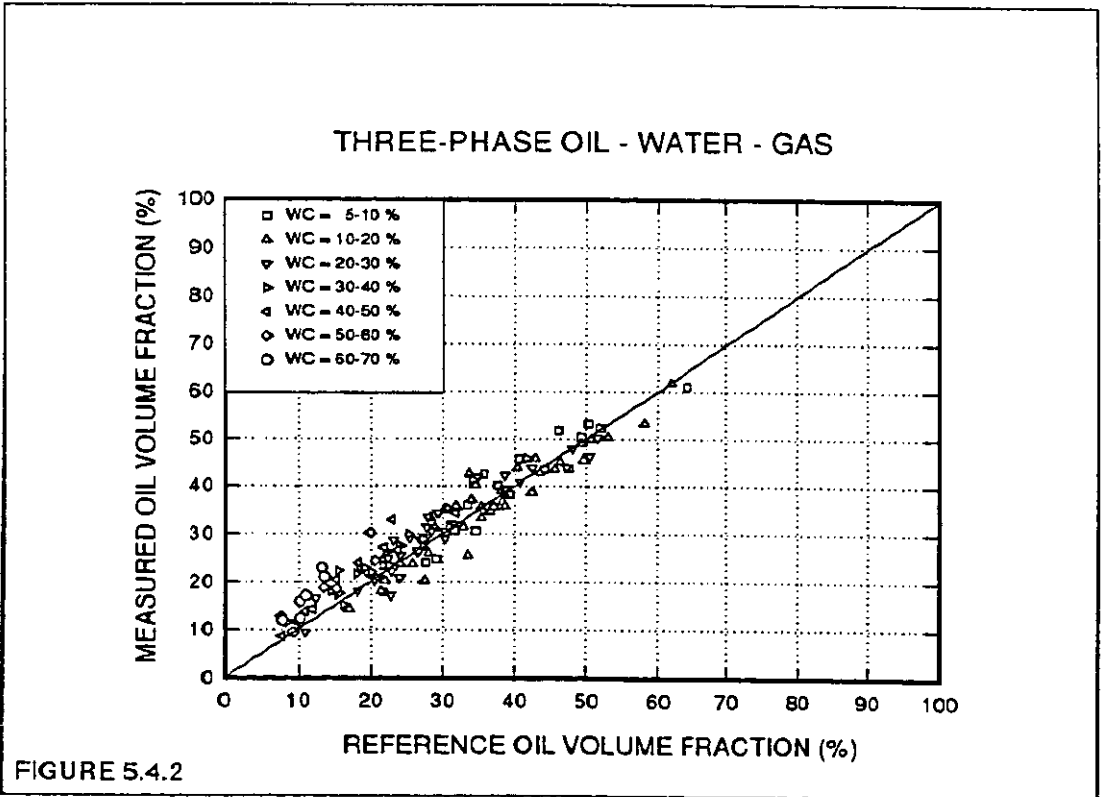
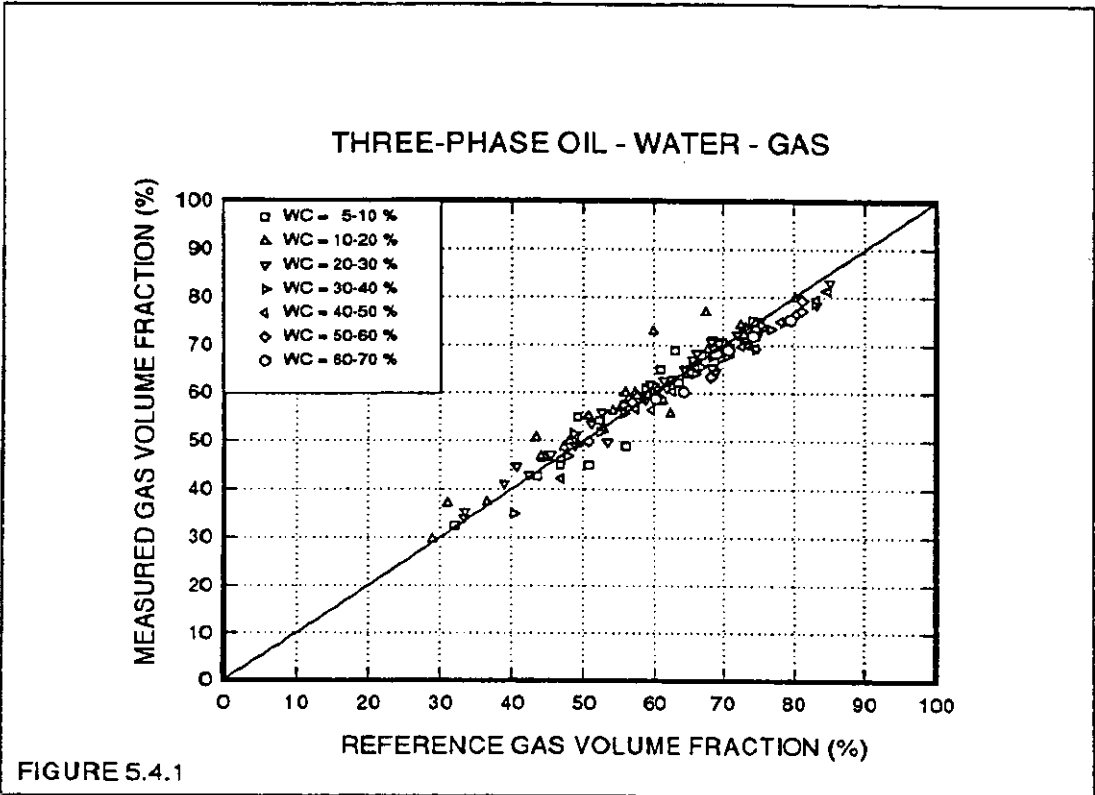


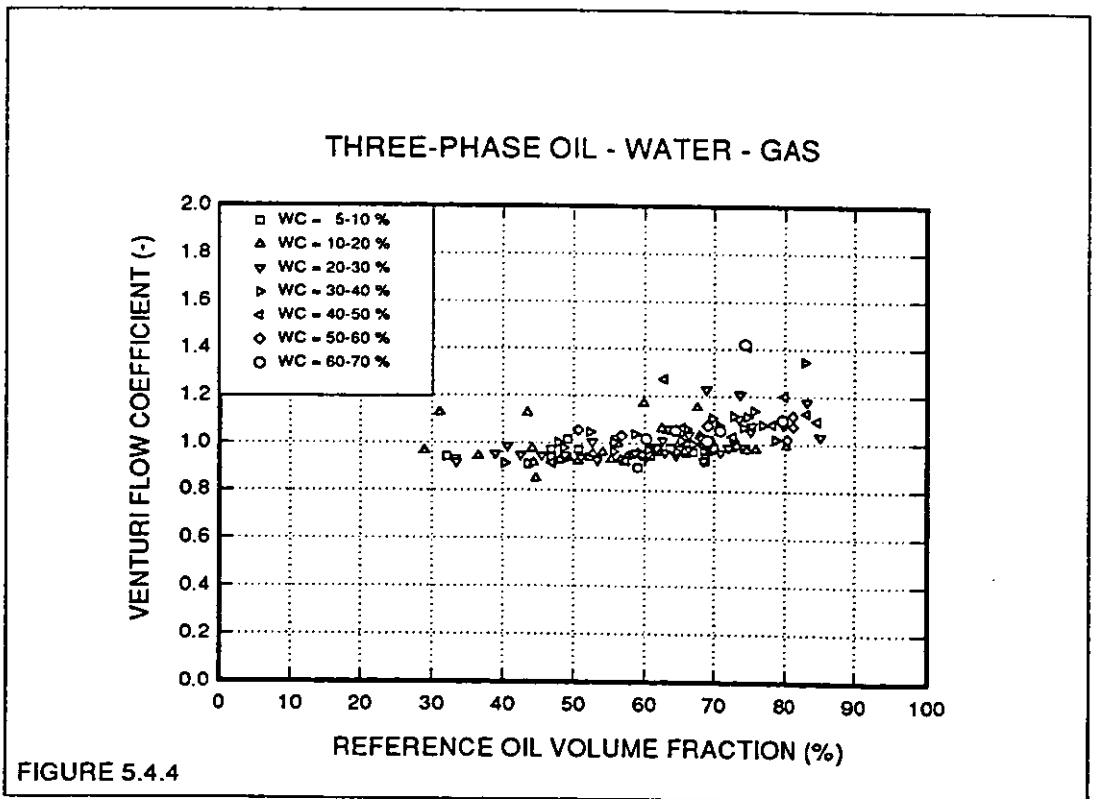
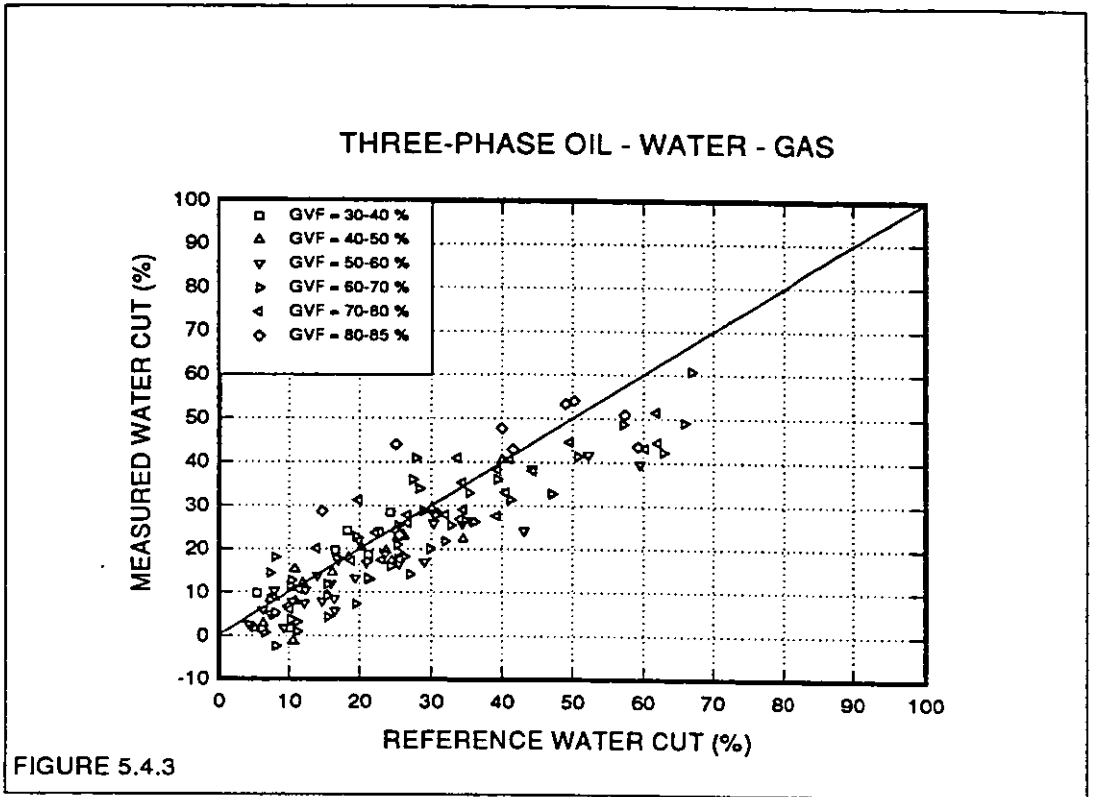
FIGURE 5.1.6

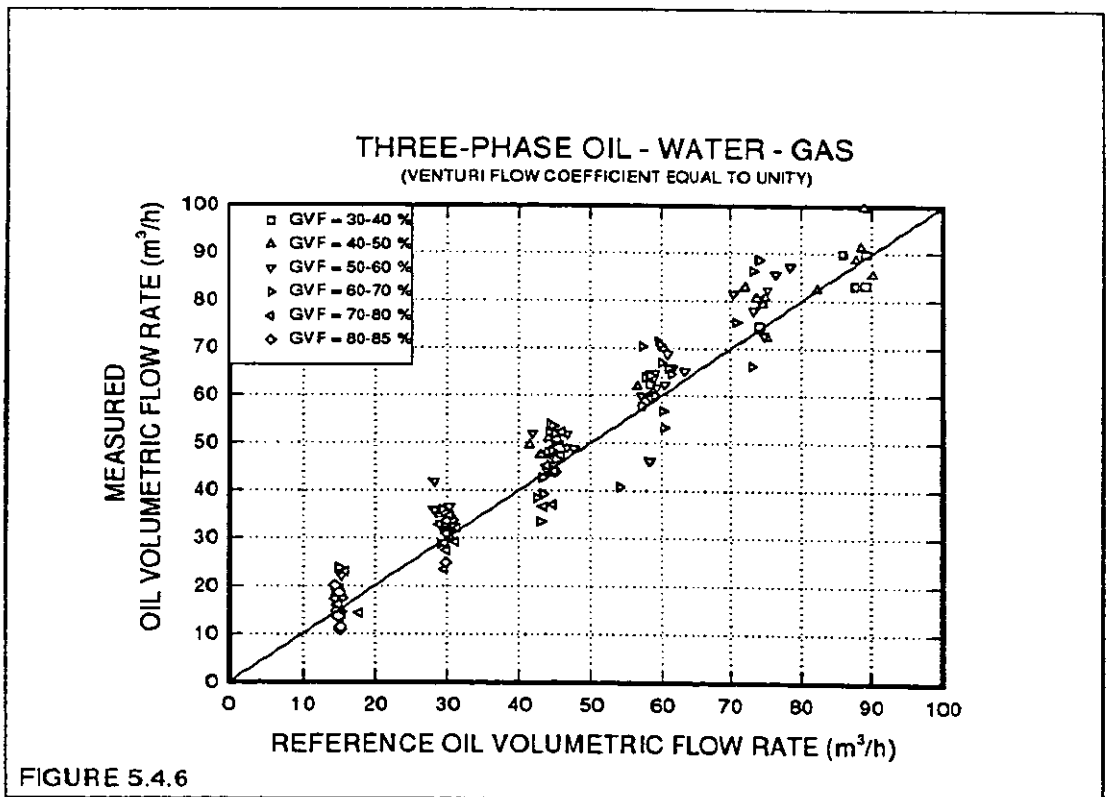
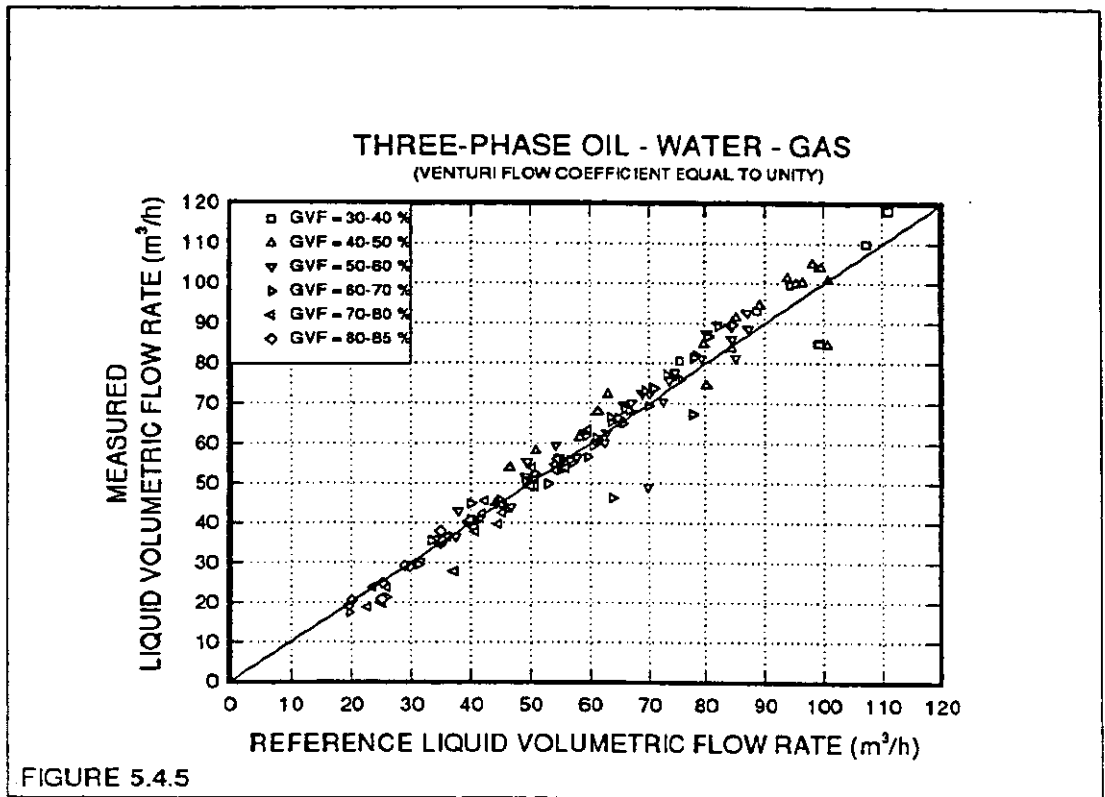


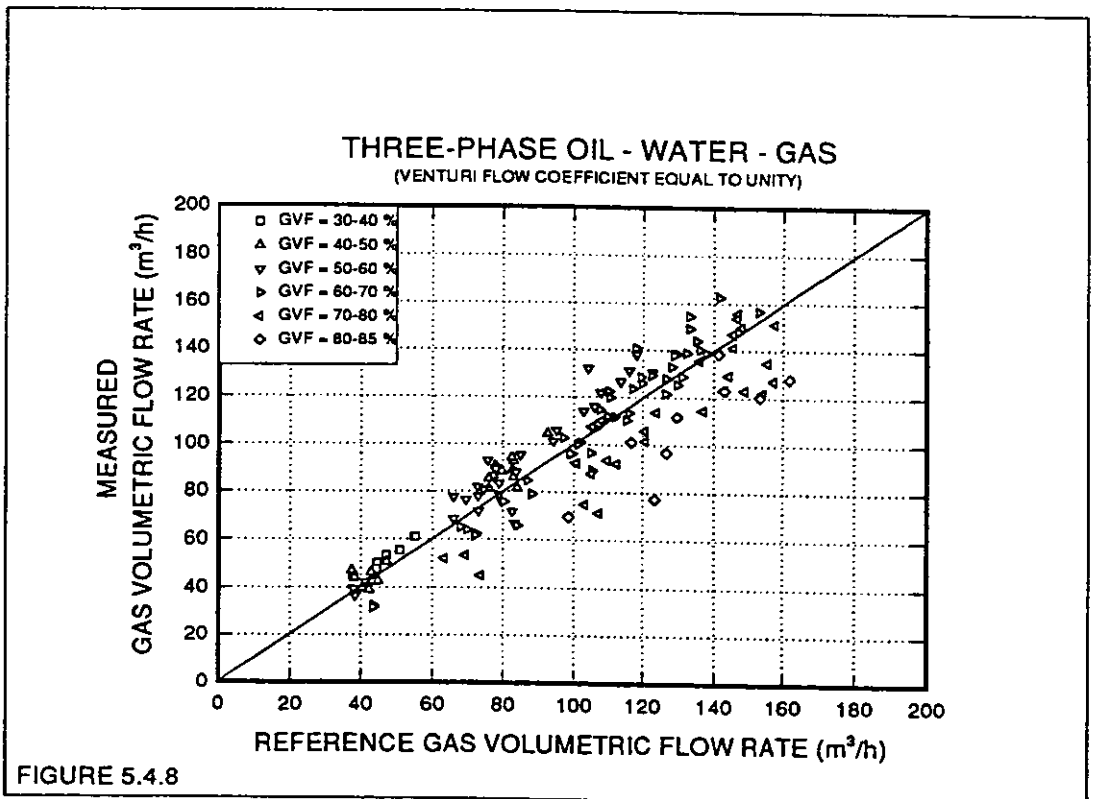
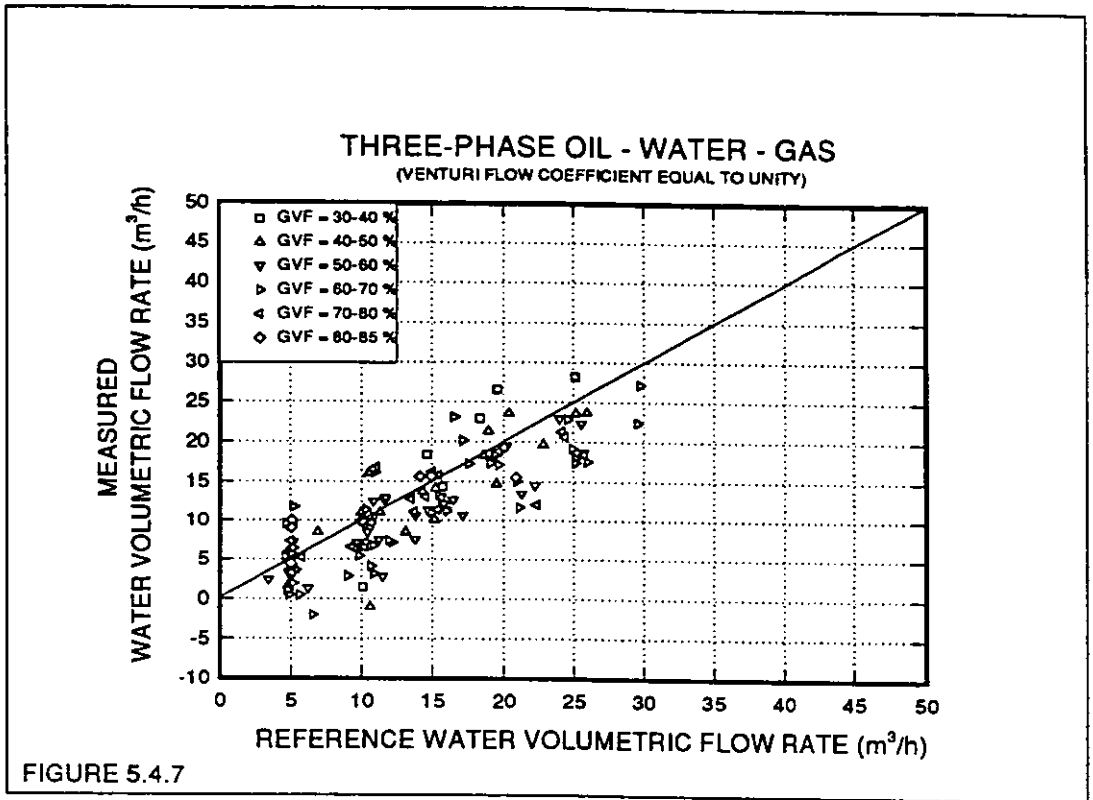












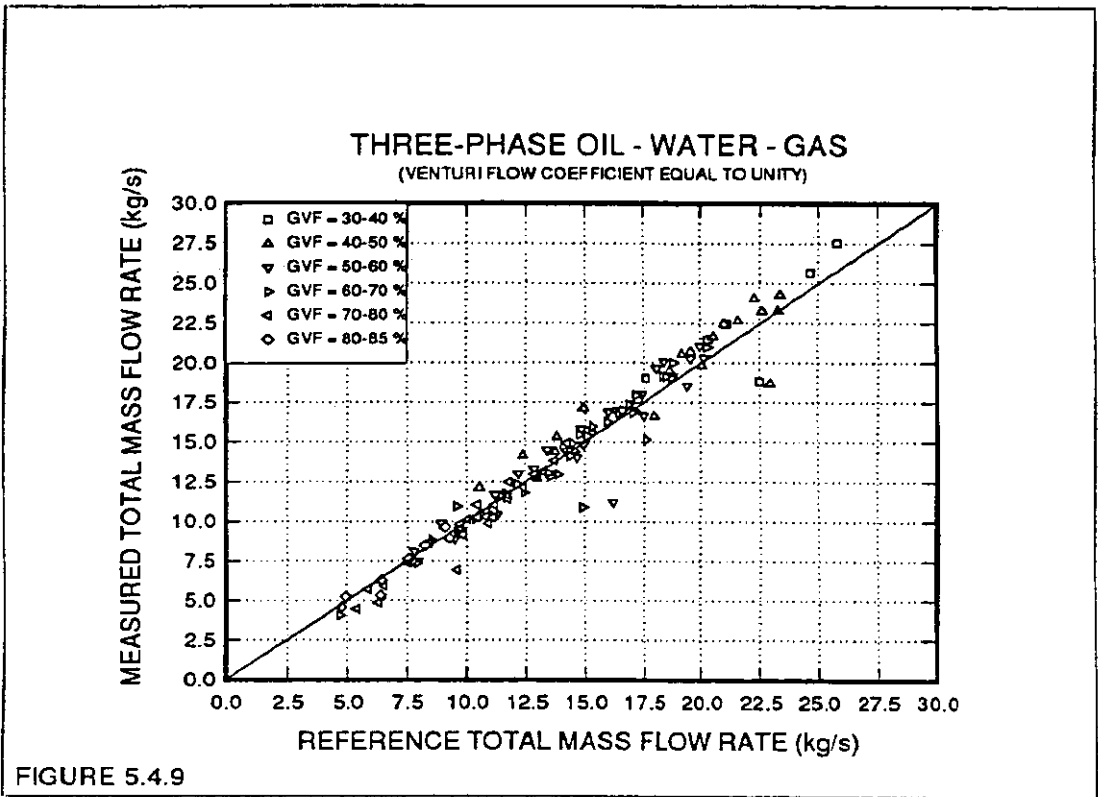


FIGURE 5.4.9

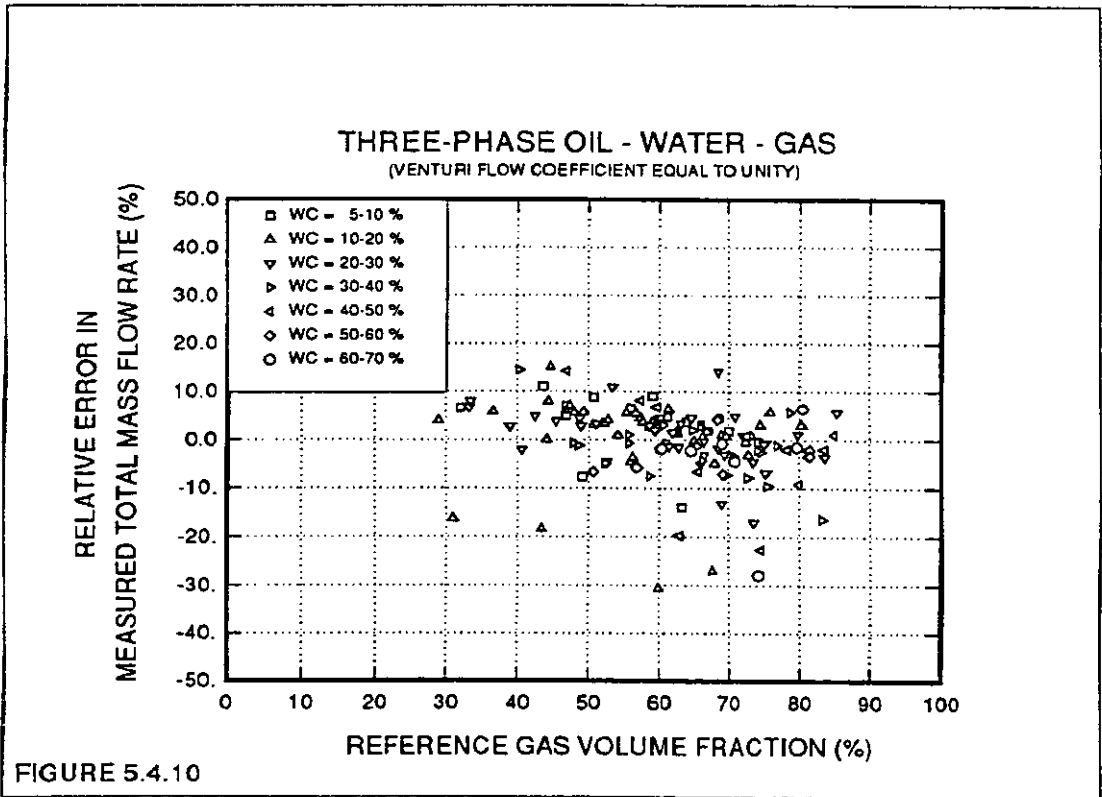


FIGURE 5.4.10

ULTRASONIC FLOWMETER 'WET' GAS TESTS AT NEL

by

R M Watt
NEL

Paper 2.5

NORTH SEA FLOW MEASUREMENT WORKSHOP
26-29 October 1992

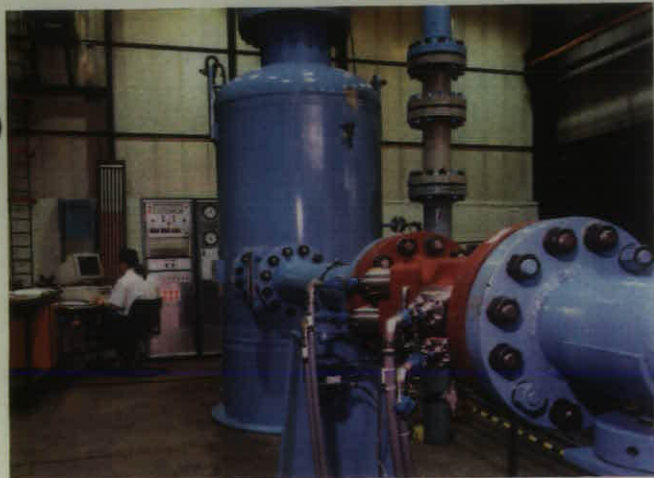
NEL, East Kilbride, Glasgow

ULTRASONIC FLOWMETER "WET" GAS TESTS AT NEL

R M Watt, Flow Centre, NEL

Introduction

As part of the "Ultraflow" Joint Industry Project to develop a "wet" gas flowmeter⁽¹⁾, the British Gas/Daniel multipath ultrasonic flowmeter is currently being tested at NEL. The High-Pressure Gas Recirculating Loop⁽²⁾, capable of the required gas flowrates and pressures, has been specially converted for the purpose. This brief note details the technical changes to the facility to accommodate liquid addition, separation and handling, as well as elements of the current test programme.



Close-up view of test meter with gas/liquid separator in background

drop). Inside the separator vessel is a meshpad demister (Knit-mesh Ltd) of a type developed specially for similar applications offshore.

From the separator, the liquid drains down to a storage reservoir while the dried gas continues around the loop. The liquid is fed back to the injection point by a positive-displacement pump (Wheatley T365M triple plunger type with variable-speed drive) capable of coping with the high suction pressure of up to 70 bar and of boosting this by the pressure differential required across the nozzles (25 bar).



General view of facility showing injection head and controls trolley

Modifications to the NEL flow loop

The NEL High-Pressure Gas Recirculating Loop is a continuous-running facility with a nominal bore of 150mm (6"), a pressure range of 1-7 MPa (10-70 bar) and a maximum gas velocity of approx. 20 m/s. Although other gases can theoretically be accommodated, the working fluid presently is air.

New technical features resulting from the conversion to wet gas include a liquid injection section, a gas/liquid separator, and various ancillary liquid-side items such as a heavy duty pump and reservoir.

The liquid injection head is installed between the reference turbine meter and the test meter (its axial position is actually variable from between 10 and 50 pipe diameters upstream of the test meter). It is fitted with 200 spray nozzles (Bete impingement type, PJ series) which inject the liquid in fine-mist form (droplets of 100 microns or less) over a wide flow range (0.2 l/m to 200 l/m). The flowrate is controlled by switching nozzles on or off incrementally as opposed to varying the pressure difference across them. This maintains a constant droplet size over the flow range.

At the end of the test-section, in order to protect the compressor and to avoid any deleterious effect on the performance of the reference meter, the liquid is removed in a gas/liquid separator. This has been custom built to match the particular flow conditions (ie to optimise catch efficiency and minimise pressure

Current tests

In consultation with the regulatory authorities, the Ultraflow consortium has drawn up a representative test programme intended to yield sufficient information to allow official assessment of the ultrasonic meter for fiscal and allocation duties. The programme is summarised as follows;

- Pressures: 10 barg and 70 barg
- Gas velocities: 5 levels up to 20 m/s
- Liquid concentrations: 5 levels up to 1% by volume
- Liquid types: Water, Glycol, Water/Glycol
- Injection types: "Fine-mist" spray, Free liquid along bottom of pipe
- Injection locations: 10d and 50d upstream of test meter

The tests are currently underway and are expected to run until early next year.

Refs.

- 1 Wilson, M, Ultraflow Project information sheet, October 1992.
- 2 Watt, R M, & Reid, J, "The NEL High-Pressure Gas Recirculating Loop", Int. Conf. on Flow Measurement in Industry & Science, London, May 1991.

FLOW CONDITIONS IN A GAS METERING STATION

by

D Thomassen and M Langsholt, Insitutt for Energiteknikk
and R Sakariassen, Statoil

Paper 3.1

NORTH SEA FLOW MEASUREMENT WORKSHOP
26-29 October 1992

NEL, East Kilbride, Glasgow

FLOW CONDITIONS IN A GAS METERING STATION

Dag Thomassen and Morten Langsholt

Institutt for energiteknikk, P.O.Box 40, 2007 Kjeller, Norway

Reidar Sakariassen

Statoil a.s, Transportdivisjonen, P.O.Box 308, 5501 Haugesund, Norway

SUMMARY

This paper focuses on the ability for computational models to predict the decay of asymmetries in axial velocity profiles in long straight pipes. In the design of gas metering stations this is an important parameter since it influences the required upstream straight lengths. Asymmetries are typically generated by bends or by sharp-edged tees. In this presentation we consider asymmetries with the latter origin, exemplified by the geometry of a gas metering station. Experimental data were retrieved from a scale model of the geometry. Numerical simulations have been performed using both the k - ϵ model of turbulence and the more advanced non-isotropic Reynolds stress turbulence model (RSTM). The results show clearly that the k - ϵ model is the RSTM superior in engineering applications of the kind presented in this paper at the present state of development. This is not to say that the k - ϵ model attains the desired accuracy - it gives too low decay rate for asymmetries generated by a sharp-edged tee.

1. INTRODUCTION

To predict geometry-related installation effects on orifice meters, three-dimensional simulation models of the flow field in typical piping components as bends, combinations of bends, headers, straight pipes and orifice meters have been developed and tested. The commercial fluid dynamics computer program Phoenics is used to solve the Navier-Stokes equations. The solved equations have been presented by Rosten and Spalding⁽⁴⁾ and will not be detailed here. A system, which we call Tandem, has been developed to enable the description of a complex piping arrangement using these standard components. This system automatically transfers the interface flow conditions between the individual components in a sequence. The Tandem system was described and its use was exemplified at the 1990 Installation effects on flow metering seminar at NEL through the presentation of Thomassen and Langsholt (1), (2).

The main objective in developing Tandem was to be able to predict the actual discharge coefficient for orifice meters in metering stations of different geometrical design. Provided a high degree of accuracy can be achieved in this kind of simulations, we have established a useful tool

for detailed flow studies of the effect of piping layout in new gas metering stations as well as for modification of old metering stations.

2. THE GAS METERING STATION

2.1. Geometry

The metering station is displayed in Figures 1 and 2. It has four meter runs, all with an internal diameter of 325mm. The header to meter run diameter ratio is 1.32. Upstream of the manifold is a twisted S-bend. 30 D of straight pipe separates the S-bend and the first branch-off from the manifold. Upstream of the S-bend is more than 200 D of straight pipe.

A question that is often raised is: Does the metering station comply with requirements given in ISO5167? One way of answering this question is to check the geometry against the required straight lengths given in the standard. This standard does not mention the manifold T disturbance explicitly, so one is left to interpret the standard at this point. In our mind, the layout does satisfy the standard.

Another method is to study whether the flow conditions satisfy the requirements given in ISO 5167 (1991) section 7.4. This section requires a swirl less than 2° and a deviation from fully developed velocity profile of less than 5%. Since no instrument has been available to measure the flow conditions on-site, mathematical simulations and scale model tests have been carried out.

2.2. Tandem simulation of the gas metering station

Figure 2 illustrates the geometry as it is defined for the Tandem simulator. A twisted S-bend of the kind preceding the manifold of the gas metering station is known to set up swirl in the flow. The distance between the two bends determines the strength of the generated swirl. The closer the bends, the stronger will the resulting swirl become.

Examination of the Tandem simulation results did show that with 3.5 D of straight pipe between the two bends in the S-bend combination the resulting swirl was weak. For all practical purposes it could be considered as dissipated after the next 30 D (branch off for the first meter run). Also the asymmetry in the axial velocity profile downstream of the S-bend, proved to 'die out' over these 30 D of straight pipe. The profile appeared near symmetric, although not being fully developed.

Altogether this means that the upstream geometry to the manifold of the gas metering station, i.e., primarily the S-bend, is of little influence to the conditions in the meter-runs. Further, since the manifold and the meter-runs all lie in one plane, the horizontal plane, one will not experience swirl of solid body type in the meter-runs. This was observed in the simulation work, but will not be presented here.

Since the flow situation is very similar in all the meter-runs we will limit the detailed results to be presented for meter-run B only. In these high pressure simulations we monitored the solution in cross-sections 6.8 D, 32.3 D and 50 D into the meter-runs. Figure 3 shows the non-dimensional axial velocity profiles along the horizontal diameter in these 3 cross-sections. Figure 3 also includes the simulated fully

developed turbulent profile, using the k- ϵ model of turbulence. The profiles are made dimensionless using the maximum axial velocity appearing along the same respective horizontal diameter.

As can be seen from Figure 3 the distinct asymmetry at 6.8 D is still significant at 32.3 D, and even after 50 D of straight pipe. The deviation from the fully developed profile was quantified using the definition given in ISO-5167⁽³⁾, section 7.4. Due to the applied definition and the strong asymmetry simulated at 6.8 D, the maximum deviation in this position is as high as 25 %. According to the simulation result it is still in excess of 10 % at 32.3 D, but has come just below the 5 % limit set in ISO-5167 in the position 50 D from the header.

2.3. Consequences

The results showed that the velocity profiles did not fulfill the requirements of ISO-5167. The Tandem/Phoenix tool was, during the verification phase, tested against experimental data for a geometry similar to the metering station manifold. This test showed reasonable agreement between measurements and simulations, but it must be added that the measurements suffered from lack of accuracy. Therefore, when we faced the simulation results, we did not have complete confidence in them. Therefore, it was decided to build a Plexiglas scale model of the metering station and measure the profiles.

3. THE SCALE MODEL - EXPERIMENTAL WORK

The Plexiglas model was built in IFE's atmospheric air rig in the scale 1:2.85. Figure 4 shows a photography of the header and the meter-runs of the scale model. Atmospheric air was sucked through the meter station from a 30 D long pipe entering the scale model header. At the inlet to this pipe we mounted a perforated plate to avoid external disturbances. The flow entering the header exhibited a close to fully developed velocity profile. When running the tests, three out of the four meter-runs were in operation while one was closed. The Reynolds-number in the meter-runs was approximately $9 \cdot 10^4$, corresponding to an average velocity of 11.5 m/s.

3.1. Measuring devices and procedure

A pitot static probe was used to measure the velocity profiles while a cylinder pitot probe served as the measuring device for the swirl angles. At meter-run position 32.2 D downstream of the header (referred to the header center line) a special arrangement made it possible to measure velocity and swirl angle profiles along both the horizontal and vertical diameter. The position 32.3 D downstream of the header corresponds to the location of the orifice meters in the gas metering station. In addition, velocity and swirl angle measurements were made at 3.8 D and 6.8 D from the header, although for meter-run B only.

All traverses were made at least twice and high repeatability in the measurements was experienced.

3.2. Experimental results

Again we will pay attention to meter-run B in the configuration where meter-run C is closed and the other three are all open. The flow

behavior in pipe B represents the typical situation for all the meter-runs, so there is really no need to bother with the others. What regards the swirl angle profiles these are relatively uninteresting since there were hardly measured any swirl angles at all. With reference to the previously made discussion of the probability for solid body rotation to occur in the meter-runs, this was as expected. Swirl angle profiles for meter-run B are therefore omitted.

The development of the axial velocity profiles in meter-run B of the scale model is shown in Figure 5. The positions 3.8D, 6.8D and 32.3D from the header were monitored along the horizontal diameter. We observed a strong asymmetry at 3.8D, which already at 6.8D was significantly reduced. At 32.3D the velocity profile was only slightly asymmetric, but still being flatter than the fully developed profile. The deviations from the fully developed profile, using the definition from ISO-5167, are plotted in Figure 6. The fully developed profile was taken in the same flow-rig, using tubes with the same wall-roughness as in the scale model. As can be seen from Figure 6 the deviation is higher than 50 % in the worst part of the 3.8 D traverse. After another 3.0 D, the maximum deviation along the examined horizontal traverse is reduced to approximately 25%. At the location of the orifice plate carrier, 32.3D from the header, the deviation over most of the traverse is below 4%.

3.3. Consequences

Through these scale model experiments we have experienced that in the position of the orifice plate the velocity profile has a maximum deviation from the fully developed profile of approximately 4%. This is below the upper limit allowed for according to the requirements in ISO-5167 regarding velocity profile conditions.

Compared to the simulation results for the high pressure gas metering station, there is a distinct difference between measurements and simulations at the position 6.8 D from the header as well as in the 32.3 D position. In the simulations the asymmetry in the axial profile tends to have a slower decay rate than found in the experiments. It must, however, be added that while the experiments were performed at a Reynolds number of $9 \cdot 10^4$, the high pressure natural gas simulations represented a Reynolds number of $9 \cdot 10^6$. The effect of increasing the Reynolds number is to reduce the decay rate for anomalies like swirl and asymmetries.

Therefore to achieve a proper evaluation of the Tandem simulator also the scale model experiments should be simulated. The results from this action are the topic of the next chapter.

4. THE SCALE MODEL - MEASUREMENTS VS. SIMULATIONS

The Tandem simulator was set up to simulate the flow in the Plexiglas scale model. Main geometrical data and operational properties for the simulations were in agreement with the specifications for the scale model experiments given in the previous chapter. The entire geometry was divided into 5 sub-geometries. The only modification relative to the gas metering station of Figure 2 is that the straight pipe and the S-bend were exchanged with a straight pipe, see also Figure 4. The manifold was operated with meter-runs A, B and D open for flow, while outlet C was closed.

4.1. Tandem simulation of the scale model.

The presented results are restricted to the flow conditions in meter-run B. Cross-sections 3.8D, 6.8D and 32.3D from the header were covered by axial velocity measurements along horizontal traverses. These velocity profiles are plotted together with the corresponding simulated profiles in Figure 7. Deviation between the fully developed simulated profile (k- ϵ turbulence model) and the various meter-run B profiles are plotted in Figure 8. The results show that:

- Close to the header, in the position 3.8D, the agreement between measurements and simulations is good. The measurements indicate a slightly stronger asymmetry than the simulations in this position.
- 6.8D from the header we observe that both the simulated and the measured profiles are asymmetric, but this characteristic is far more pronounced for the former. This demonstrates that the simulations were not able to reproduce the measured decay rate for the asymmetry between 3.8D and 6.8D.
- In the position 32.3D from the header the simulation predicts a velocity profile still containing a high degree of asymmetry. The measured axial velocities on the other hand, exhibit a profile that is nearly symmetric - but not fully developed. The maximum deviation from the fully developed profile (k- ϵ turbulence model) was found to be 6.5% according to the simulations (Figure 8) versus typically 4% for the measurements (Figure 6).

4.2. Discussion of the scale model results

Unexpectedly skew axial velocity profiles were found in the position of the orifice plates when simulating the gas metering station using the Tandem/Phoenix simulator.

This fact and the question it raised to the validity of the simulation results put forward the idea of building a Plexiglas scale model of the gas metering station. Measurements on this scale model showed that there were discrepancies between the high Reynolds number natural gas simulation results and the low Reynolds-number scale model measurements.

To examine the Reynolds-number effects, Tandem simulation of the scale model experiments was performed. As the results presented in this chapter illustrates, Tandem/Phoenix does not predict the development of the asymmetry in meter-run B in the metering station with desired accuracy. This is also the case for the scale model. Particularly between the positions 3.8D and 6.8D this is evident.

Reynolds-number effects. It is known that an increase in the Reynolds number tends to decrease the decay rate for swirl and asymmetry in long straight pipes. Through the two sets of geometrically similar simulations we have ascertained that in the position 32.3D into meter-run B the low Reynolds number case deviates from the fully developed profile by a maximum of 6.5% while the corresponding figure for the high Reynolds number case was 10%. The only conclusion we shall draw from this observation is that Reynolds number effects are present and must be considered when the scale model measurements are evaluated.

Wall roughness. All simulations are performed with hydraulically smooth walls. Due to prior experience this is a reasonable choice both for the Plexiglas tubes and for the process pipes in the gas metering station. However, the value used for the wall roughness parameter is itself a model assumption that influences the decay rate. A sensitivity test was therefore made. The main conclusion with respect to the decay rate in the meter-runs remained unchanged even with relatively rough walls. This excludes inappropriate setting of the roughness parameter to be the source of error for the deviation between measurements and simulations.

The turbulence model. Comparison of simulated and measured axial velocity profiles 3.8D from the header showed good agreement. This means that the entrance conditions for the velocity profile in meter-run B is essentially correct. In other words, the manifold geometry seems not to be the source for the disagreement between simulations and measurements. We know from earlier verification tests⁽¹⁾⁽²⁾ that the Tandem/Phoenix system is able to predict the development of an asymmetric velocity profile, when this is generated by a curved bend. One major difference in the flow conditions downstream of a curved bend relative to that downstream of a sharp-edged tee (which is the equivalence of the gas metering station manifold) is the much higher turbulence intensity associated with the latter.

The performance of the turbulence model is demanding for correct simulation of the decay of swirl and asymmetry in straight pipes. For the simulation of flow in bends, manifolds, tees, etc., the turbulence model is of minor importance for accurate prediction of the mean velocity field since the dominant forces in these geometries are inertia forces (e.g. pressure and centrifugal forces).

On the basis of the above observations and considerations our explanation to why the simulations fail to predict the developing process of the asymmetry downstream of a sharp-edged tee is lack of generality in the applied $k-\epsilon$ turbulence model. One major deficiency with the $k-\epsilon$ model is that it is isotropic. Particularly in 3-D problems of the kind examined here this might prove to be a deteriorating limitation.

5. SIMULATION OF THE SCALE MODEL USING REYNOLDS STRESS TURBULENCE MODEL

5.1. General

The most advanced turbulence model presently available to Phoenix, using curvilinear coordinates, is the $k-\epsilon$ turbulence model, which is the one we have used throughout the reported results.

We knew that the companies behind computer codes as Phoenix, Fluent and Flow-3D were working hard to support their codes with more advanced turbulence models than the $k-\epsilon$ model. Contact was taken with CHAM (Phoenix) and Fluent Europe and they were both requested to perform a simulation of the flow in a T-junction using their most advanced turbulence model. The boundary conditions for the T-junction was made so that the case became similar to the flow in the combined header and meter-run B of the scale model. At the time of completing this paper only Fluent Europe have accomplished the work.

5.2. Results

Simulations with the Fluent code⁽⁵⁾ have been performed using both the k- ϵ turbulence model and the full Reynolds-stress turbulence model. Both models are optional in the latest version of the program. The geometry is described in curvilinear coordinates and the grid density is approximately as in the Tandem set-up.

K- ϵ turbulence model. Figure 9 shows the axial velocity profiles resulting from the Fluent simulations plotted together with the measured velocity profiles. The Tandem/Phoenics counterpart to these results are found in Figure 7. We can see that the two sets of plots (Fluent versus Phoenics) compare relatively well (notice the difference in y-scale). The most striking difference between the two sets occurs for position 3.8D where the Fluent results deviates considerably more from the measurements in the 'lower end' of the curve than do the Phoenics results. This tendency lasts also for 6.8D. At 32.3D both sets of results have a maximum deviation from the measurements in the radial position 0.8D. Due to the Fluent results the deviation from the fully developed profile reached a maximum of 9% in this area.

The Reynolds stress turbulence model (RSTM). The results from the application of the RSTM of Fluent are plotted together with the measured velocity profiles in Figure 10. We observe that the solution has changed considerably due to the switch-over from the k- ϵ to the RSTM. Unfortunately the RSTM did not improve the performance of the simulations. On the contrary, both in the positions 3.8D and 32.3D from the header the RSTM results show a significant increase in the deviation from the measurements compared to the k- ϵ model. In the mid-position, 6.8D from the header, the results compare to the measurements approximately as the k- ϵ model does. Because of the poor comparison with the experimental data we have found no reason to include profiles showing the deviation from the fully developed profile for the RSTM.

6. CONCLUSIONS

In this paper we have focused on the ability for computational models to predict the decay of asymmetries in axial velocity profiles in long straight pipes. For the design of gas metering stations this is an important parameter since it influences the required upstream straight lengths. Here we have concentrated on the asymmetry in the meter-runs of the gas metering station. From scale model experiments and from computer simulations using two different turbulence models we draw the following conclusions:

- The velocity fields in the meter-runs of the gas metering station is entirely a consequence of the design of the manifold. The twisted S-bend upstream of the manifold has no influence to the flow in the meter-runs. Therefore the metering station can be considered as if laying entirely in the horizontal plane. This eliminates the occurrence of solid body rotation in the meter-runs.
- The sharp edged tees connecting the meter-runs to the header in the gas metering station generate a strongly asymmetric velocity profile in the entrance part of the meter-runs. The asymmetry decays and according to the measurements the profile deviates from the fully developed profile by less than 5% in the position of the orifice

plate, 32.3 D from the header. In this position the profile is nearly symmetric, but flatter than the fully developed profile.

- The simulation results based on the k-ε turbulence model was in good agreement with the measurements in position 3.8D. Over the next few diameters, however, relatively large discrepancies occurred. After 32.3D the maximum deviation from the fully developed profile was 6.5 % for the simulations versus approximately 4% for the measurements. The simulations using the k-ε model obviously underestimate the decay rate for asymmetries generated by a sharp-edged tee. It is likely to believe that the cause is lack of generality in the turbulence model.
- Adoption of the advanced Reynolds stress turbulence model (RSTM) to the test geometry proved to give velocity profiles that deviated even more from the measurements than the k-ε results. Effort should be made to try to determine why the RSTM failed to improve the k-ε results.

REFERENCES

- 1 Thomassen, D. and Langsholt, M. *Prediction of installation effects on orifice meters*. Proceedings from seminar Installation Effects on Flow Metering, NEL, East Kilbride, October 1990.
- 2 Thomassen, D. and Langsholt, M. *The computation of turbulent flow through pipe fittings and the decay of the disturbed flow in a downstream straight pipe*. Flow Measurement and Instrumentation Vol. 2 January 1991
- 3 ISO 5167 (1991). *Measurement of fluid flow by means of orifice plates, nozzles and venturi tubes inserted in circular cross-section conduits running full*. International Standardisation Organisation.
- 4 Rosten H I and Spalding D B. *The Phoenix equations*. CHAM TR/99 November 1987, program version 1.4. CHAM Ltd, Bakery House, 40 High Street, Wimbledon SW19 5AU, England.
- 5 *Fluent User's Guide - Version 4.0*. Fluent Inc., Canterra Resource Park, 10 Cavendish CT., Lebanon, NH 03766, USA

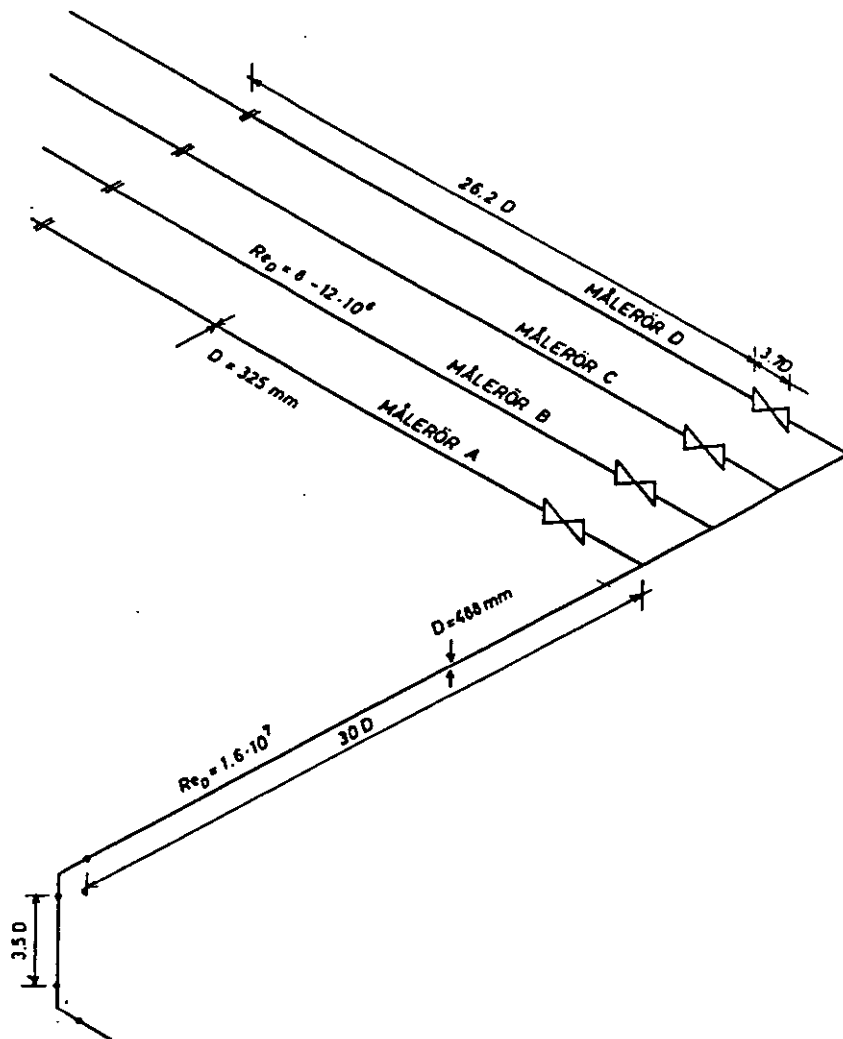


Figure 1. Outline of the Gas Metering Station

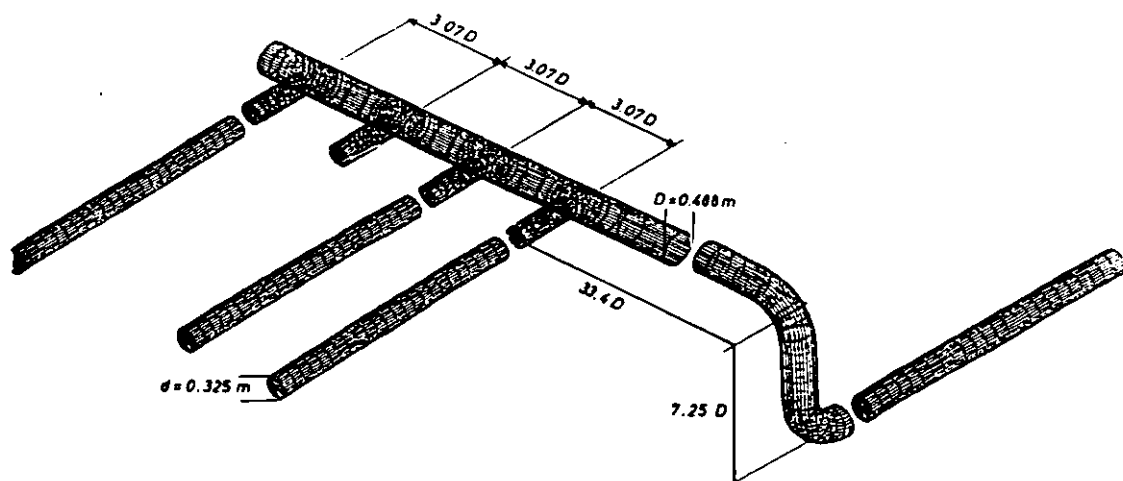


Figure 2. The gas metering station interpreted for Tandem

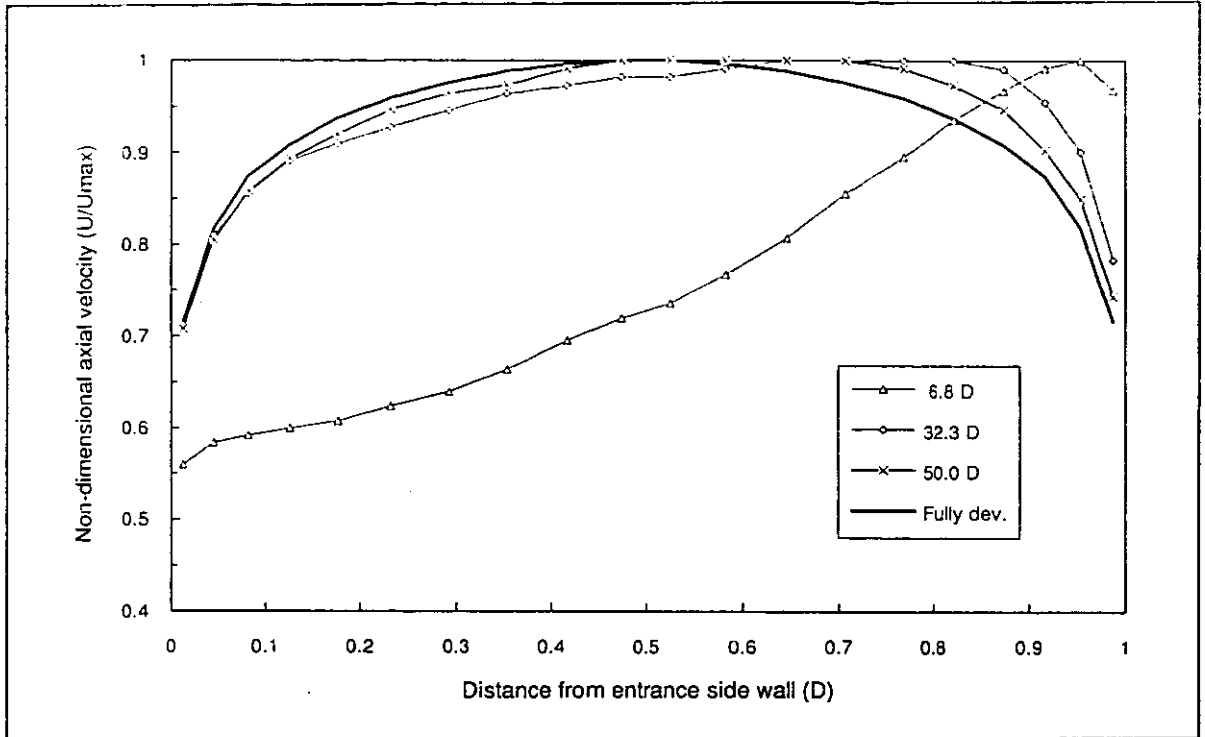


Figure 3. Simulated dimensionless axial velocity profiles along the horizontal diameter in three positions in meter-run B of the gas metering station.

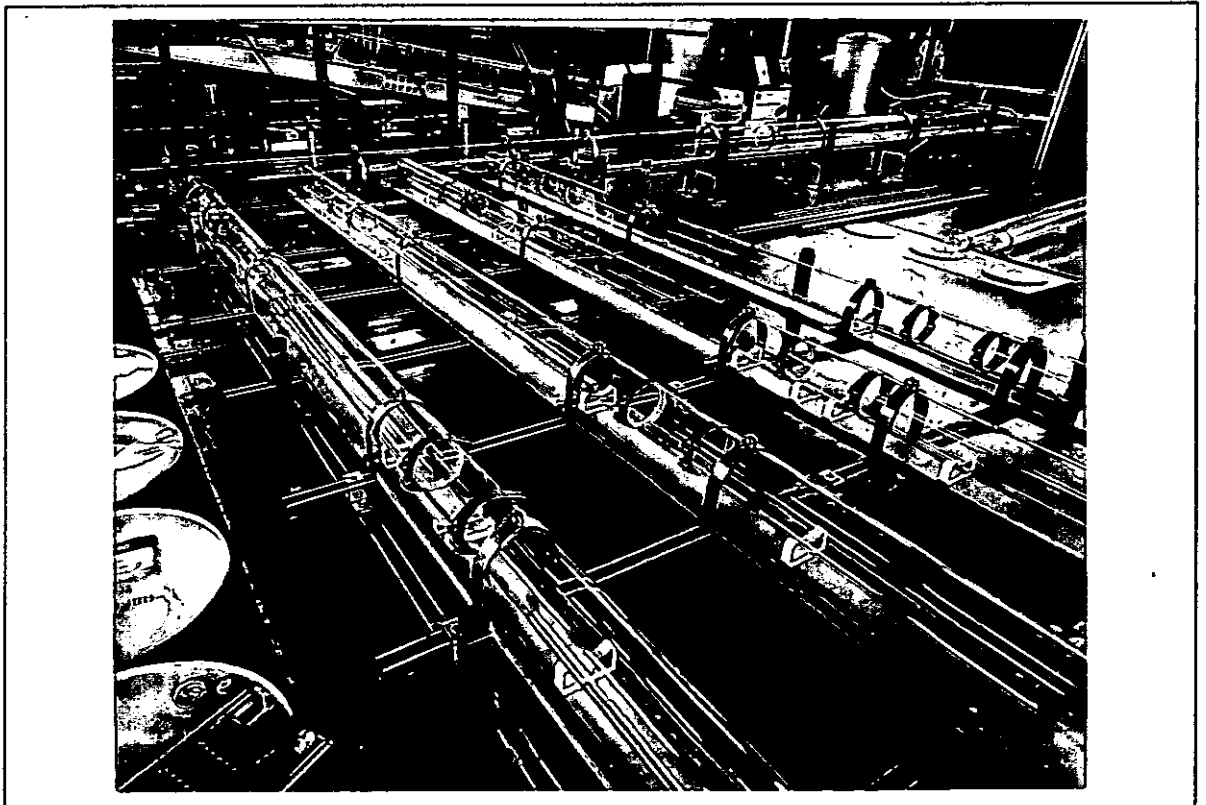


Figure 4. Photography showing the header and the meter-runs of the scale model

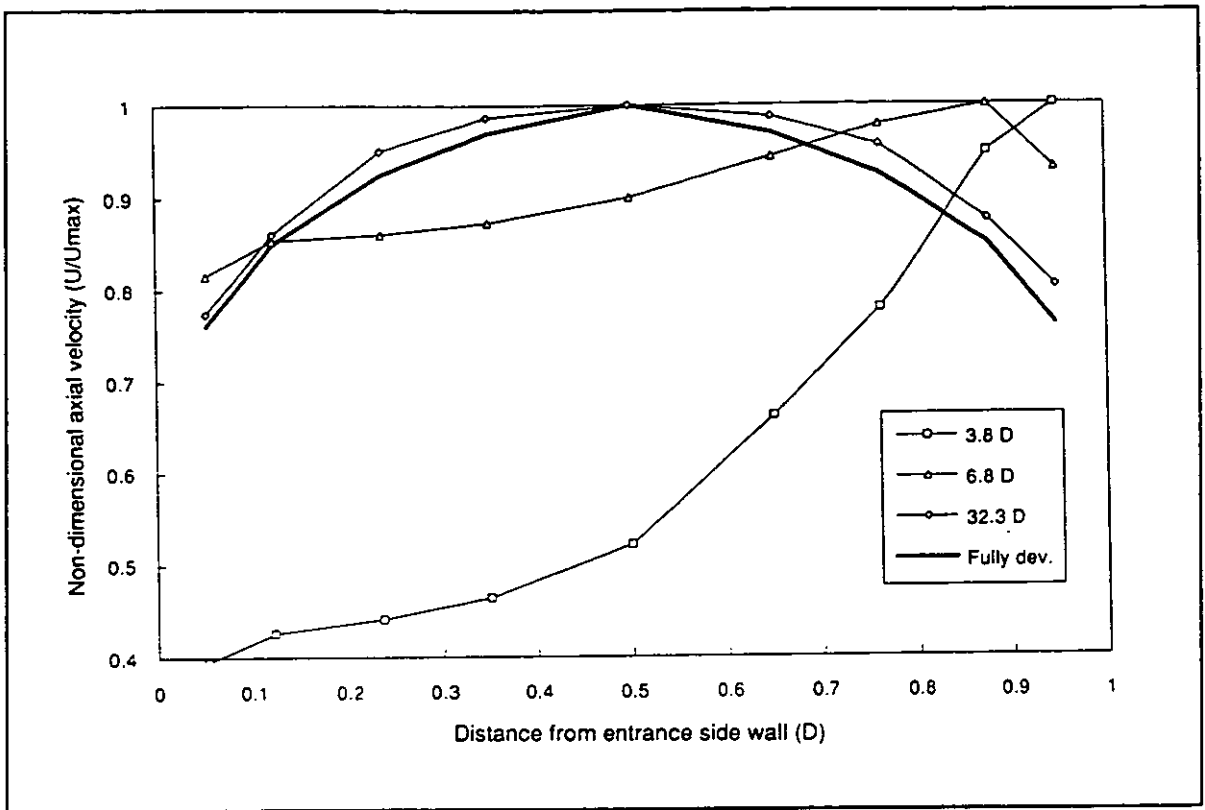


Figure 5. Velocity profiles horizontally traversed measured 3.8D, 6.8D and 32.3D downstream of the header in meter-run B of the scale model.

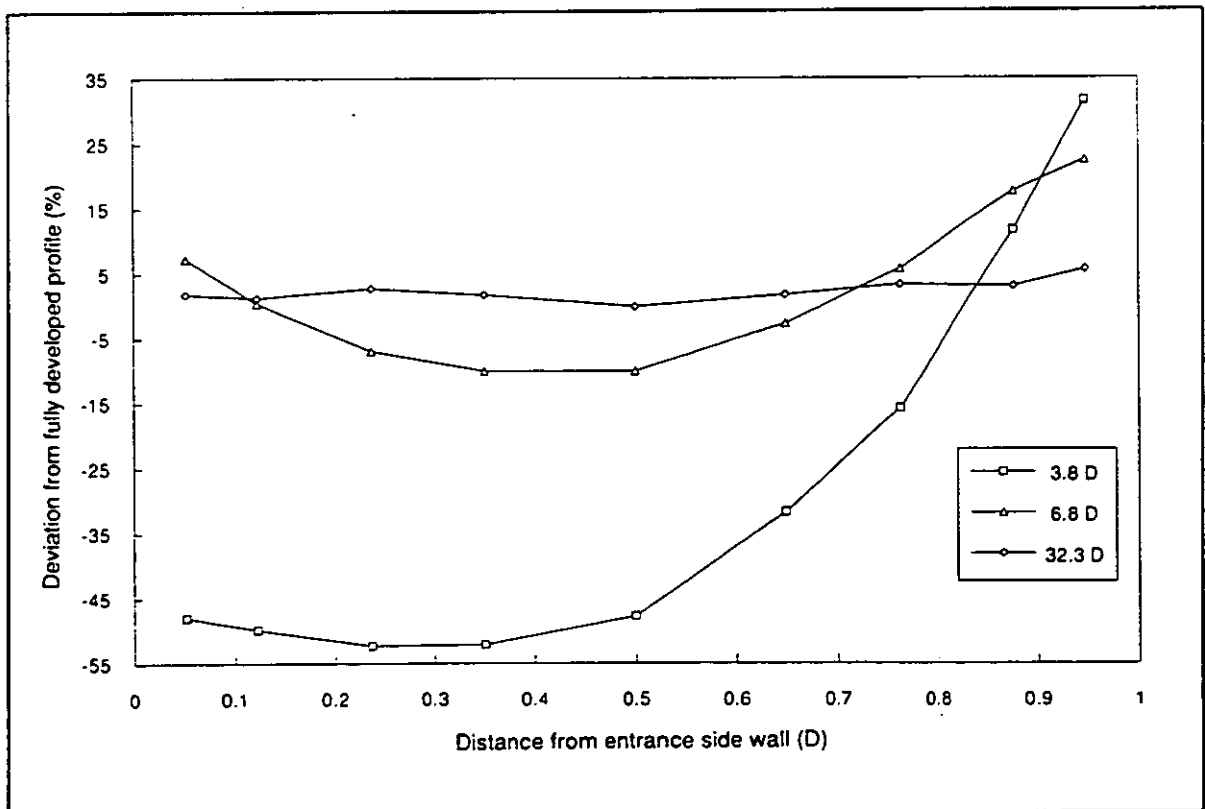


Figure 6. Deviations from the fully developed velocity profile for the profiles measured in the three highlighted cross-sections of meter-run B in the scale model.

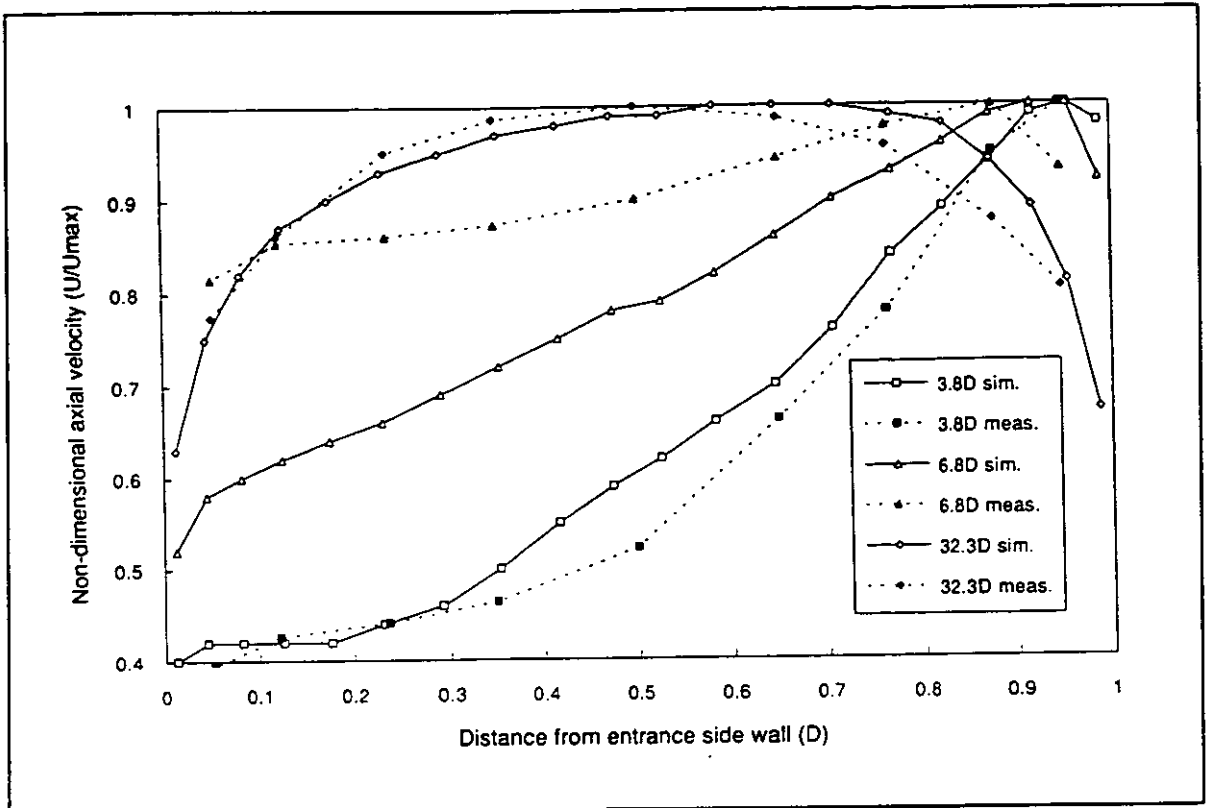


Figure 7. Comparison of simulated and measured axial velocity profiles in the positions 3.8D, 6.8D and 32.3D into meter-run B of the scale model.

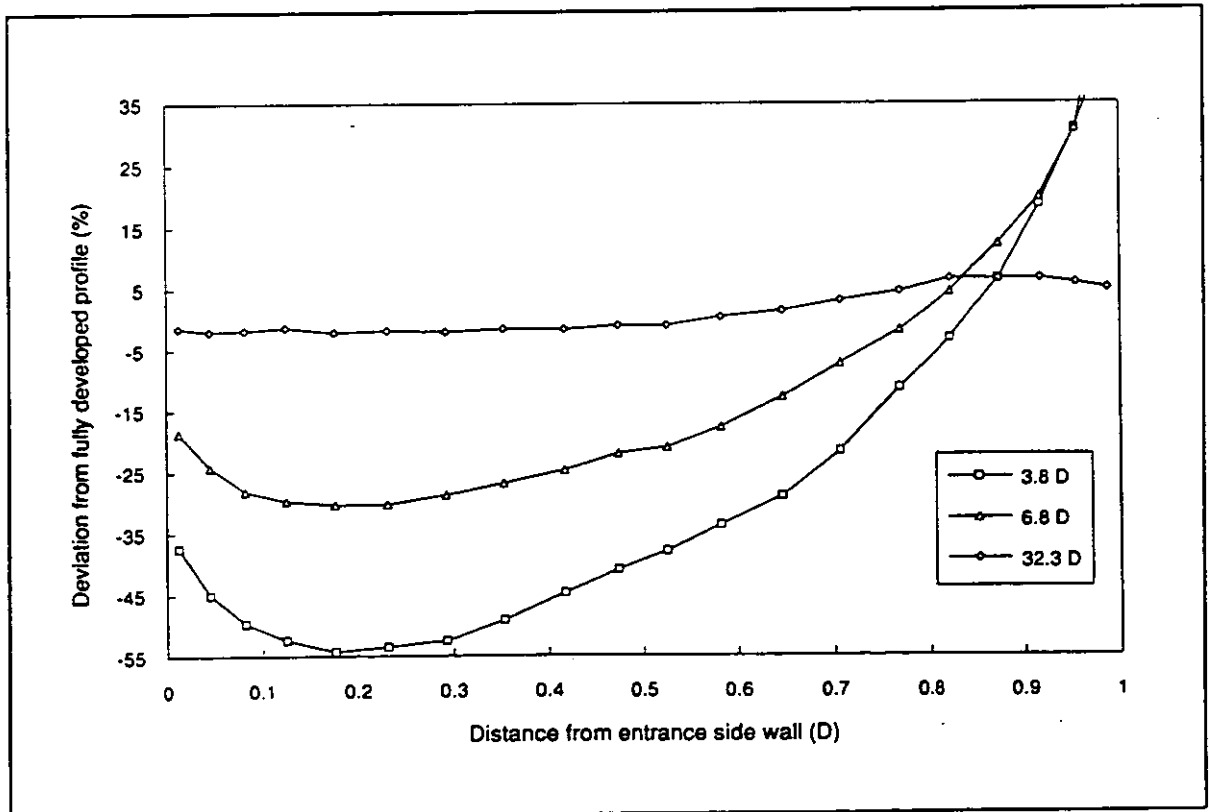


Figure 8. Simulated deviation from fully developed profile for the three highlighted cross-sections of meter-run B in the scale model.

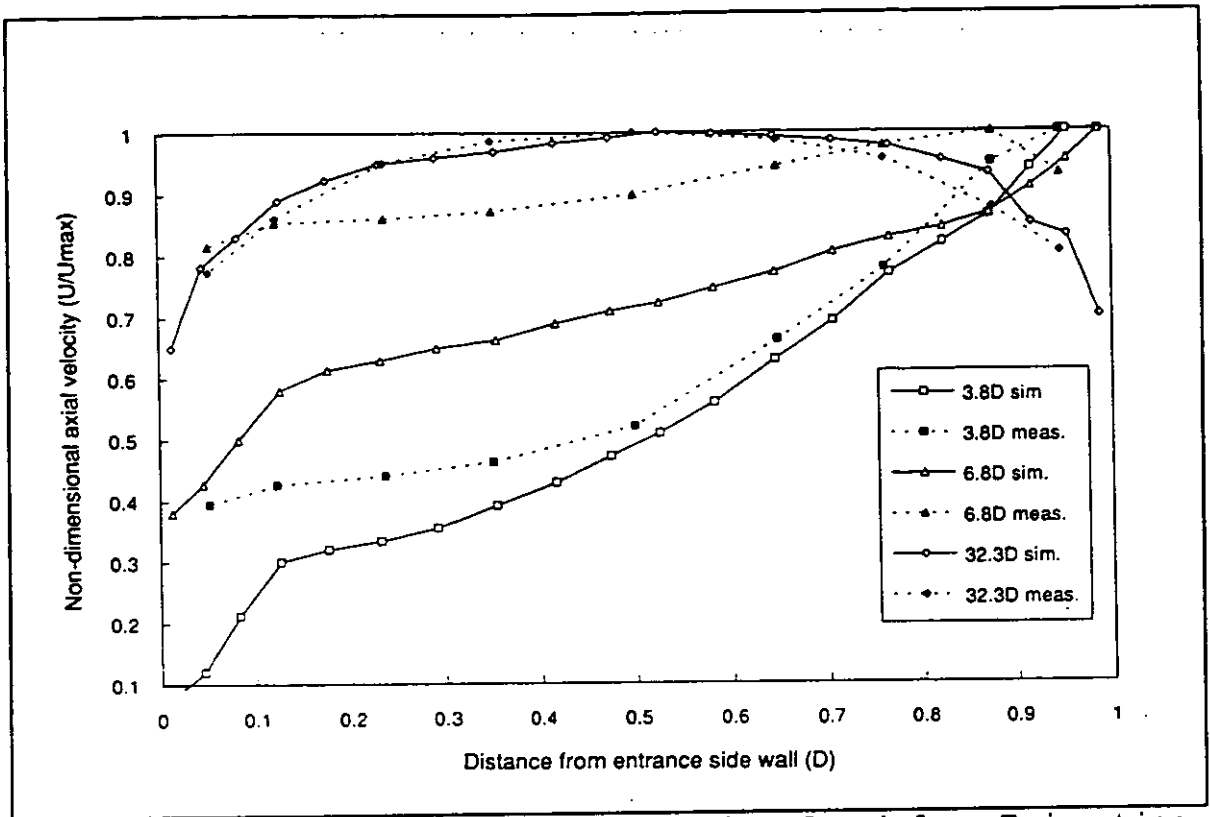


Figure 9. Comparison of velocity profiles found from T-junction simulation using Fluent with k-e model and from measurements in the scale model.

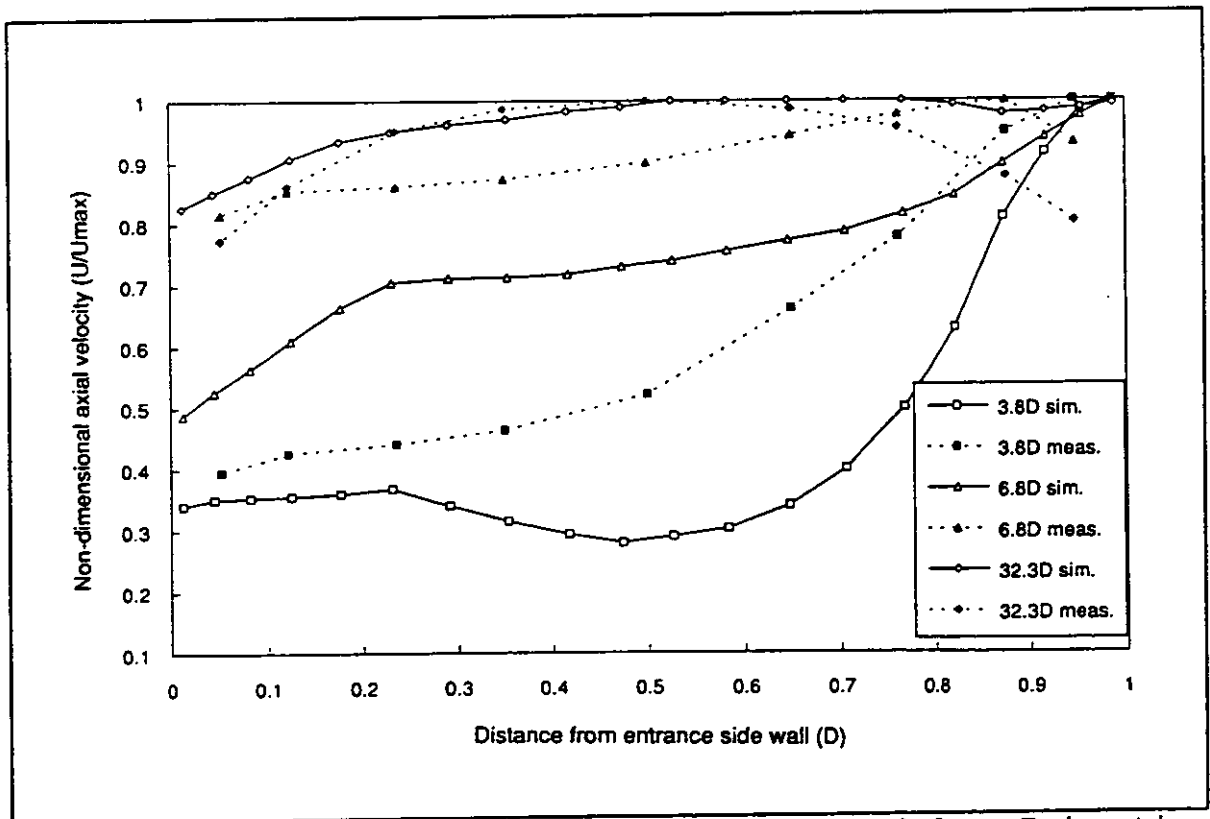


Figure 10. Comparison of velocity profiles found from T-junction simulation using Fluent with RSTM and from measurements in the scale model.

CFD ANALYSIS OF FLUID PROPERTY EFFECTS
IN CORIOLIS MASS FLOWMETERS

by

R M Watt
NEL

Paper No 3.2

NORTH SEA FLOW MEASUREMENT WORKSHOP
26-29 October 1992

NEL, East Kilbride, Glasgow

TO BE DISTRIBUTED AT THE WORKSHOP

RESULTS OF INVESTIGATIONS COMPARING SOME OF THE RECOMMENDATIONS
GIVEN FOR TURBINE METERS BY ISO-9951 AND AGA-7

by

J F Cabrol and A Erdal
Statoil K-Lab

Paper 4.1

NORTH SEA FLOW MEASUREMENT WORKSHOP
26-29 October 1992

NEL, East Kilbride, Glasgow

**RESULTS OF INVESTIGATIONS COMPARING SOME OF THE RECOMMENDATIONS
GIVEN FOR TURBINE METERS BY ISO-9951 AND AGA-7**

(Presented at the 10th N.S.F.M.W, Peebles, October 26/28, 1992)

Jean F. Cabrol and Asbjørn Erdal
K-Lab, Postboks 308, N-5501 Haugesund, Norway

SUMMARY

The paper investigates the recommendations given in the new draft international standard (ISO/DIS-9951) for gas turbine meter on density measurement, metering pressure tapplings, calibration and installation conditions, where they differ significantly from the AGA-7 report.

The volumetric flowrates measured by several 6" gas turbine meter have been compared to the mass flowrates from K-Lab's reference flowmeters of sonic nozzles. The density value, necessary to convert the reference flow from mass to volume, is either calculated at the rotor location (as per ISO/DIS-9951) or measured downstream of the meter (as per AGA-7). This investigation focuses on the importance of the density evaluation and its influence on the accuracy of the computed mass flowrate.

It reviews as well the location of pressure tapping points, the calibration conditions and the installation conditions during calibration.

Kårstø Metering and Technology Laboratory [K-Lab] is operated by STATOIL and jointly owned by STATOIL (2/3) and TOTAL (1/3).

KEY WORDS

Laboratory investigations, Turbine Metering, Standard Requirements

RESULTATER AV UNDERSØKELSER SOM SAMMENLIGNER NOEN AV ANBEFALINGENE I TURBINMÅLER STANDARDENE ISO-9951 OG AGA-7.

SAMMENDRAG

Artikkelen undersøker noen av de anbefalingene fra det nye internasjonale standardutkastet, ISO/DIS-9951, for gassturbinmålere mht. tetthetsmåling, tappepunkt for trykkmåling, kalibrerings- og installasjonsbetingelser, hvor de avviker betydelig fra AGA-7 rapporten.

Volumstrømmen målet fra flere 6" turbinmålerne har blitt sammenlignet mot K-Labs referansemålere som er soniske dyser. Tettheten, som er nødvendig til å konvert referansestrømmen fra masse til volum, er enten beregnet ved rotoren (se ISO/DIS-9951) eller målt nedstrøm av måleren (se AGA-7). Denne undersøkelsen fokuserer på hvor viktig tetthetsmålingen er og hvordan den påvirker nøyaktigheten av beregnet massestrøm.

Lokaliseringen av trykktappingspunkter, strømningsforholdene og installasjons-betingelsene blir også diskutert.

Statoil er operatøren av Kårstø Måle og Teknologi Laboratorium [K-Lab] som er en «joint-venture» mellom Statoil (2/3) og TOTAL (1/3).

RÉSULTATS D'ÉTUDES COMPARANT QUELQUES UNES DES RECOMMANDATIONS DE ISO-9951 ET DE AGA-7 POUR DES COMPTEURS À TURBINE

RÉSUMÉ

Cette publication étudie les recommandations de la nouvelle ébauche de norme internationale ISO/DIS-9951 sur les compteurs à turbine, en ce qui concerne la mesure de la densité, la localisation des prises de pression, et les conditions d'étalonnage et d'installation, là où elles diffèrent de façon notable du rapport AGA-7.

Les débits volumiques mesurés par plusieurs compteur à turbine ont été comparés en gaz naturel aux débits massiques mesurés par des tuyères soniques qui sont les compteurs de référence à K-Lab. La masse volumique, nécessaire pour transformer le débit de massique de référence en débit volumique, est soit calculée au niveau du rotor (confer ISO/DIS-9951) soit mesurée en aval du compteur (confer AGA-7). Cette étude souligne l'importance de la détermination de la masse volumique et son influence sur la précision des débits massiques correspondants.

Ce papier fait également le point sur la localisation des prises de pression, et sur les conditions d'installation et d'étalonnage.

Statoil est opérateur de K-Lab [Kårstø Metering and Technology Laboratory], une joint-venture entre STATOIL (2/3) et TOTAL (1/3).

1. INTRODUCTION

Although gas turbine meters are widely used in low pressure distribution networks, new international directives (drafted in «ISO/DIS-9951», see reference n°2) are necessary in order to allow turbine meters in being fully accepted for fiscal service, especially in the North Sea, where operating conditions are far away from usual calibration conditions. The requirements prevailing today are those reported in the Transmission Measurement Committee Report N°7 («AGA-7» in short, see ref. n°1).

This laboratory investigation compares the recommendations circulated in 1990 by the International Standardization Organization for gas turbine metering (ISO/DIS-9951) to those issued in 1985 by the American Gas Association (AGA-7).

Kårstø Metering and Technology Laboratory [K-Lab, a metering laboratory located at Kårstø, Norway] operates a test loop which normally runs on natural gas at pressure ranging from 20 to 156 bar at approximately 37°C. The reference meters for the test loop are a bank of toroidal throat sonic nozzles (see section «reference flowmeters and statement of uncertainty»).

Tests on 6 different types of turbine meters were performed during the period October 90 -August 92.

2. DESCRIPTION OF THE TESTS

2.1 General installation conditions

The turbine meters were installed at K-Lab in a 6" test-section, with an internal diameter of 0.1397 m.

The schematic of the K-Lab test loop is shown on layout 1.

The different test-section installations are detailed in the sections describing the various tests undertaken. The common point of all meter installations is that they comply with both AGA-7 and ISO/DIS-9951.

The flow-straightening vanes used are built according to the AGA-7 requirements. Velocity and swirl profiles have been checked and comply with AGA-7 (see ref. 5 and 7 from the same authors).

2.2 Reference flowmeters and statement of uncertainty

The reference flowmeters are K-Lab's bank of toroidal throat sonic nozzles, designed according to ISO-9300 and individually primary calibrated in K-Lab's gravimetric calibration rig using natural gas.

The reference mass flowrates measured using the sonic nozzles are evaluated to have an uncertainty of 0.3%, calculated with two standard deviations.

2.3 Other instrumentation used during the tests

The two gas density transducers used during testing (a low density transducer from 0 to 60 kg/m³, and a high density transducer from 0 to 400 kg/m³) provide a continuous measurement of gas density. The transducer sensing element consists of a thin metal cylinder which is activated so that it vibrates in a hoop mode at its natural frequency.

The mass of gas, passing over the inner and outer surfaces of the cylinder and vibrating with the cylinder, decreases the natural frequency of vibration. Frequency and gas density are related.

The densitometers were installed and operated according to manufacturer requirements and to normal operating procedures used in metering service (see ref. n°3 and n°4).

The meters sized for 6" pipes were normal, industrial type, gas meters having dual output transmitters fitted for increased accuracy.

They were tested from 20 bar (2 MPa) to 100 bar (10 MPa) and the flowrates ranged from 50 acmh (actual cubic meter per hour) to the maximum (1000 or 1600 acmh) allowable for each turbine meter.

2.4 Calibration procedure

After the check of instrumentation, the control of pressure drop, and the measurement of velocity profiles and swirl angles, the turbine meters were calibrated to check for any hysteresis effect; their linearity and repeatability were checked as well (see ref. 5 and 7). The turbine meters are identified as A, B, C, D, E, F, which is consistent with the notation used in references 5 and 7.

The turbine meter signal recorded was its output pulse frequency. The reference mass flowrates from the sonic nozzles were converted to volume flowrates by the density in the test section. Density measurements were taken at the location of the turbine meter body.

The measurements were then conducted at 37 °C, from 20 to 100 bar. The range of volumetric flowrates corresponded to Q_{min} , 10%, 25%, 40% and 70% of Q_{max} of each meter.

An integration time of 3 minutes has been used.

At each flow rate, 3 separate runs were performed.

During all these tests, no abnormalities were observed.

2.5 Calculations

The flow measurements by turbine meters reported in this paper are expressed in terms of % deviation from the reference flowrates of sonic nozzles and are computed as follows :

$$100 \times [(\text{Turbine Meter flow}) - (\text{Reference flow})] / [\text{ref. flow}]$$

3. DENSITY MEASUREMENTS

The main requirements in fiscal metering stations which will be discussed in this paper within the framework of the two standards are the measurement of gas density at operating condition in order to obtain the mass flowrate, the pressure tapping location, the calibration and the installation conditions of the turbine meter.

Concerning the 2 main first issues, possible differences in both temperature and pressure between the measuring chamber of the densitometer and the pressure tapping were investigated because the mass flowrate calculation provides that the measured density is the true density at the metering pressure tapping.

As turbine meters are volumetric flowmeters, density has to be determined in order to get the mass flowing through these meters. This determination is of paramount importance when a turbine meter is calibrated in facilities which are using mass flowmeters (sonic nozzles for instance) as reference to measure the true mass flowrate through the test section.

Even in laboratory conditions, it is difficult to measure the density accurately. Particularly, densitometers are very sensitive to the temperature of the gas sample circulating through the densitometers.

3.1 Standards requirements

ISO requires in section A.8.3 that :

«The conditions of the gas in the density meter should represent the conditions in the turbine wheel over the operating flowrates of the meter».

AGA specifies in section 3.8.3 that :

«In the use of densitometers, while it is desirable to sample the gas as close as possible to the rotor conditions, care must be exercised not to disturb the meter inlet flow or to create an unmetered by-pass».

In practice (reflected here by the AGA-7 report), a length of 5 pipe diameters (5D) downstream of the meter body, is often considered to be as close as possible, without perturbing the flow profile significantly.

3.2 Laboratory tests

Figure n°2 shows a typical insulated configuration of densitometer for turbine metering. It is a by-pass installation where the sample gas flows through the probe and is then sent to flare through a needle valve.

Even if there is a risk that the measured density in such a by-pass loop does not represent the density at conditions required, this arrangement is often preferred in metering service because maintenance, checks and verifications (such as vacuum test) are more easy to perform. Further, protection of the measuring element is more easy to design and control than with inserted densitometers (see ref. 4). This very configuration is used in K-Lab's test section to get the mass flow rate evaluation when using turbine meters.

The densitometers were installed in a 6" test section, within 5D (5 pipe diameters) downstream of turbine meter A. turbine meter A was installed 15 internal diameters of straight pipe (15D) downstream of 2 twisted bends. A flow conditioner specially designed by K-Lab was installed upstream of the meter. The meter proved during several tests to give very repeatable and reproducible results, which is important for the present tests.

The tests were done in February with a gas temperature of 38°C in the test section, which is about 30°C above the average ambient temperature during the year. The sample gas flow has an initial temperature which is approximately the line temperature. By exchanging heat with the environment the gas temperature of the sample will change. A difference between the temperature inside the densitometer compared to the line temperature might occur, even if the densitometer is installed into a pocket protruding in the pipe. Therefore a cold ambient temperature cools the sample gas, which should ideally be maintained at the same temperature level than the flow.

As the same gas is continuously circulating around the calibration loop, the gas composition could be measured accurately with an in line gas chromatograph and the density, calculated with the AGA-8 equation (1985 version) could be used as reference in this test.

A densitometer was installed in a specially manufactured pipe spool. Both the densitometer and the inlet tubing were well insulated within a box mounted around the instrument. The length of pipe between sample take off and densitometer was minimized and kept as close as possible to the surface of the meter run pipe. There was no heater in the box.

All these precautions were taken because the temperature difference between sample gas flow inside the densitometer and main gas flow depends on the type of insulation, heating or cooling, piping geometry, and sample flowrate as well as on the difference between ambient and run temperature.

As previously said, the piping geometry and the insulation were optimized for these tests. No supplementary heating or cooling was provided in the test section because a temperature equilibrium is difficult to achieve, due to ambient temperature variations and various exposure to sunlight.

When it comes to the standards, two requirements have to be compared : The installation which impact on the temperature used for densitometer correction and the sample flowrate which impact directly on density measurement.

The two following set of tests relate to these two requirements :

3.2.a Densitometer correction related to temperature variation

In these tests, the sample flowrate was fixed to approximately 25% of the maximum sample flowrate available in the first set of testing. This value of 25% represents rotameter reading and was arbitrary chosen within the range recommended by the manufacturer.

The study depends on the location of measuring the true inside temperature. Since densitometers with internal temperature element were not available till now, external temperature element must be installed. Up to now, it is possible to measure the temperature in the metallic wall (T_{wall}) or the temperature upstream of the meter (T_{upstream}); see figure 2.

Laboratory tests proved that the density finish to be adequated with the true density whatever the sample flowrate when the density is stabilized sufficiently long time. By using proper procedure and sample flowrate, the waiting time can be reduced to some minutes. However, during this first set of tests, the sample gas flowrate and the waiting time were deliberately fixed, so that the density was broadly stabilized.

The tests were carried out at 100 bars and 20 bars. At each flowrate 3 test-points were obtained with the measured density. The computed density was then calculated from the mean pressure at the rotor location, mean line temperature and gas composition. The difference between the two is calculated and plotted.

Both results at 100 and 20 bar are summarised in figure n° 3. On this figure, the plotted results referred to wall temperature, used for densitometer correction, because it is assumed to fit better the true density.

3.2.b Density measurements related to sample flowrate variation

The previous calculation documents as well why a laboratory procedure is so useful: Even if precautions concerning density stabilisation, and usual corrections for deviation from an ideal situation can reduce temperature effect in laboratory conditions as explained, one will always have to cope with this problem in field metering.

In that case, adjusting properly the sample gas flowrate will be the solution. This has been investigated further by performing the following tests, which intended to check, and try to improve the procedure K-Lab uses for density measurements by densitometers, using the AGA-8 equation (1985 version) as reference.

Another 6" turbine meter of the same type was installed (see installation sketch n°4). The tests consisted to vary the sample gas flow through the densitometers by closing more or less the needle valve (see figure n°2), from 10% to 100% of the maximum sample flowrate.

Testing was performed at 35 bar and 37 °C. The measured density was obtained with two positions of the temperature sensors used for temperature correction (T_{wall} , and T_{upstream} ; see figure n°2).

Only the results obtained with T_{wall} will be reported here. (However, the same procedure could be done with T_{upstream}).

The temperature of the insulated box was maintained at 28 °C. The tests were runned at 30% and 70% of the maximum flowrate of the turbine meter.

As said before, generally, the density finish to be adequated with the calculated density, whatever the flowrate, when the density is stabilized sufficiently long time. After start up of a cold meter run, it would take hours before the density was stabilized without the proper sample flowrate (with it some minutes were sufficient). During these tests, we always waited for density stabilization.

3.3 Discussion of the results

3.3.a Densitometer correction (see figure 3)

At 100 bar the results show a difference between measured and computed density of 0.5% at 966 acmh (actual cubic meter per hour) and 0.9% at 45 acmh.

This deviation is more than expected and is larger at the lower flowrates. It shows again how difficult it is to measure density without a proper procedure. Moreover, it is especially difficult at low flowrates were the gas cools down faster. For turbine metering, it means that this is not a proper method of measuring the volume reference flow.

At 20 bar the results were expected to be worse than at 100 bar because the gas transports less gas and heat than at 100 bar. Nevertheless the difference between measured and computed density was between 0 and 0.2%, which is within the uncertainty bands of both the densitometer and the AGA-8 equation.

At this pressure, a low-density densitometer was used, but it seems difficult to impute the improved results to it because both high-density and low-density densitometer were of the same type.

The most likely explanation is that the flowrate through the inlet tubing of the densitometer is higher at low pressure. Indeed, if the flowrate has a higher value through the densitometer, the gas has no time to cool down so much, and the densitometer should provide a more accurate density.

The recommended procedure for the densitometers used was to control the sample volumetric flowrate through its rotameter (see pocket installation drawing n°2) to 25% of the maximum sample gas flow at all main flowrates and pressures.

The volume flowrate of sample gas flowing through the rotameter and the densitometer is dependent on the density of the gas; lower density provides higher volume flowrates through the densitometers : The density value at 100 bar is about 86 kg/m³ and the value at 20 bar is about 15 kg/m³. Then, if the sample volume flowrate through the rotameter is 25% of the maximum volume sample flow at both 100 bar and 20 bar, the volume flowrate at 20 bar is several folds the one at 100 bar :

$$\sqrt{(\rho_{100}/\rho_{20})} = 2.4$$

where ρ_{100} is the gas density at 100 bars and ρ_{20} at 20 bar.

The calculation use the general equation given for the rotameters.

Therefore, at lower pressure, the actual sample flowrate through the rotameter and the densitometer becomes higher (even if the level in % is the same); this results in a decrease of transportation time between tapping and densitometer; hence the risk of temperature decrease is minimized.

Such densitometer-correction effect is not taken care of in the AGA-7 reports, but is implicit in the ISO recommendation because it refers clearly to the flow conditions in the turbine wheel.

3.3.b Sample flowrate (see figure 5)

For both pressures tested, the minimum sample gas flowrate (10%) is to be selected in all cases, when using the temperature sensor associated to the densitometer (in the wall).

Such sample-flowrate effect is not taken care of in both standards.

3.4 Conclusions

In AGA-7, the practical procedure recommended for density measurement should be improved by taking care of densitometer correction and of sample flowrate. Replacing measurement by calculation would be another solution, which is implicitly allowed by the new ISO/DIS-9951 requirements.

4. METERING PRESSURE TAPPINGS

4.1 Standards requirements

In section 6.6.1, ISO requires that :

«At least one metering pressure tapping shall be provided on the meter, to enable measurement of the static pressure that equals the static pressure at the turbine wheel of the meter at metering conditions».

AGA recommends in section 3.8.2 that :

«A pressure tap as provided by the manufacturer on the meter body should be used as the point of pressure sensing for recording or integrating instruments».

Some turbine meter have no pressure tapping on the meter body.

Therefore, an alternative has been evaluated :

In the following tests, we have investigated the effect of measuring the pressure far downstream (100D) of the meter.

4.2 Laboratory tests

In these experiments calculated density from the AGA-8 equation (1985) was used to convert mass to volume in the test section.

Testing was conducted at 145 bar and 37°C, of gas turbine meter B (see configuration n°6).

Testing was performed for 25% and 40% of the maximum flowrate of the meter. At these selected flowrates, the measured densities fitted the computed ones within 0.2%. Table 1 show the results.

Average pressure in the meter body and average density computed from pressure measurement at the rotor are compared respectively to average pressure measured at 100D downstream of the meter, and average density computed at the same position.

TABLE 1 : DIFFERENCES IN AVERAGE PRESSURE AND AVERAGE DENSITY FROM TWO DIFFERENT LOCATION OF PRESSURE TAPPINGS

% OF MAX FLOW-RATE	P_{rotor} bar	P_{100D} bar	DIFF %	ρ_{rotor} kg/m ³	ρ_{100D} kg/m ³	DIFF %
25	145.5	145.8	+0.21	130.5	130.8	+0.23
40	146.0	146.2	+0.14	131.0	131.2	+0.15

4.3 Discussion of the results

A raise of about 0.2% could be measured in both pressure and density. This .2% difference would then occur, in mass flowrate through the turbine as well, by using either the rotor pressure tapping, or the one located at 100D.

In spite of the pressure-loss normally occurring in the pipe, the pressure at the rotor is less than the downstream pressure; this could easily be explained by the fact that the first pressure is measured upstream of the rotor :

There, the dynamic pressure tends to increase and the static pressure tends to decrease because of the increasing flow velocity of the gas through the inlet stator of the turbine meter.

4.4 Conclusions

Both requirements will lead to install pressure tappings at the right location, namely at the turbine wheel of the meter.

But the ISO requirements are more precise than the AGA ones, by saying clearly : «at the turbine wheel of the meter». This is important as these tests have pointed out.

5. CALIBRATION CONDITIONS

5.1 Standards requirements

ISO claims in section 8.2.2 that :

«The preferred calibration is one which is carried out at conditions as close as possible to the conditions under which the meter is to operate».

AGA specifies in section 5.6.1 that :

«In the flow measurement of natural gas, the accuracy of a gas turbine meter as indicated by the meter output is generally specified as within $\pm 1.0\%$ of the true volume over a certain specified range and pressure range using air as the calibration flow medium. For accuracy better than $\pm 1.0\%$... meters should be calibrated under conditions near the meter's intended operating condition».

This last specification means that calibration under operating flow conditions should only be necessary when the required accuracy should be better than within the error band, generally specified as within $\pm 1\%$ of the true volume.

5.2 Laboratory tests

A comparison campaign recently conducted at K-Lab or at other laboratories, and reported in reference n°7, investigated the effect of high pressure calibration and of the type of medium used. Testing was performed on 6 turbine meters, including the turbine meters A and B, used in the present paper.

5.3 Discussion of the results

The investigation has documented through experiments that the K-Factor is generally decreasing when pressure is increasing. It reports as well a detectable difference between operating in natural gas and operating in air.

5.4 Conclusions

Calibrations carried out under operating flow conditions are then deemed more appropriate. On this point, the new ISO/DIS-9951 will result in better measurements than AGA-7.

6. INSTALLATION CONDITIONS AT CALIBRATION

6.1 Standards requirements

ISO recommends in section 8.2.4 that :

«The performance of the meter shall not be influenced by the installation conditions of the test facility»,

and in section 8.6 that :

«The conditions for the installation of the meter shall be specified in order that the relative meter error does not differ by more than 1/3 of the maximum permissible error ... from the meter error obtained with an undisturbed upstream flow condition».

Then, and even if the ISO recommendations are somewhat vague by not specifying precise installation requirements, it fix a maximum meter error of 4/3 % for a perturbation to be generally acceptable.

AGA specifies in section 3.2.1 that :

«The recommended installation requires a length of 10 nominal pipe diameters upstream with the straightening vane outlet located at five nominal pipe diameters from meter inlet... A length of five nominal pipe diameters is recommended downstream of the meter».

The AGA requirement gives more precise and less stringent metering-frame, which should be more appealing for practical calibration purposes.

Nevertheless, this last requirement might not be stringent enough. This issue will be discussed in the following.

6.2 Laboratory tests

A recent investigation conducted at K-Lab (reported in ref. n°6), evaluated several installation effects on the accuracy of turbine meters, with natural gas in the high pressure range. Testing was performed for 6 basic upstream configurations and on 4 turbine meters, including turbine meter A used in the present paper.

6.3 Discussion of the results

The investigation has documented notably, through experiments, that the straightening vane recommended in AGA-7 does not produce a proper velocity profile within 10 pipe length diameters, when the perturbation upstream of the meter consists of 5° swirling flow produced by 2 perpendicular bends out of plane and close together.

The general ISO-recommendation, reported above, is then deemed more appropriate, considering the different types of upstream perturbation which can be created by different types of upstream configuration, and which may need different types of installation condition.

Unfortunately, the ISO/DIS-9951 contains an informative annex E, which gives other informations concerning perturbations effect, that we shall question through the following statements :

Namely section E.4.2 determines piping configurations, with two elbows not in the same plane and 5 pipe diameters downstream, as representative for «Low Level Perturbations». The paper ref. n°6 establishes for several turbine meters a swirling flow up to 5° with such configurations and an average overmetering of nearly 1% in natural gas at high pressure. This cannot be deemed as «low level perturbations».

Section E.4.2.2 recommends that «the flow conditioner (preferably of the types mentioned in ISO-5167) should be installed in pipe of (nominal) diameter DN and the end of the flow conditioner will be at least 2 DN from the meter inlet».

Taking into account the deviation error of about 1% reported for instance in the same paper ref. n°6 (with tube bundles within 15 DN and at 5 DN from the meter inlet), it looks doubtful that such conditioners could straighten the flow within 2 DN from the meter inlet.

Finally ISO-sections E.4.3.1 and E.4.3.3 of ISO speaks of «High Level Perturbations ... with a half pipe area plate installed between the two elbows». A general comment will be that these effects should be considered apart one from each other because the influence of asymmetry created by half pipe area plate is generally considered as negligible. this has been also documented in the paper ref. n° 6.

6.4 Conclusions

This review shows again that one has to be very careful when generally speaking about installation effects.

The ISO/DIS-9951 recommendations are deemed more appropriate on this matter, apart from the informative sections in appendix which might be discussed.

Nevertheless, the AGA-7 requirements are more spread and certainly fits better metering needs for practical requirements.

7. CONCLUSIONS

An investigation, evaluating the main requirements covered by two turbine meter standards, has been conducted at K-Lab.

The overall conclusions to be drawn from the tests and the analysis can be summarized as follows :

TABLE 2 : REQUIREMENTS COMPARISON BETWEEN ISO/DIS-9951 AND AGA-7

REQUIREMENTS	AGA-7		ISO/DIS-9951	
	CONCEPT	PRACTICE	CONCEPT	PRACTICE
DENSITY MEASUREMENTS	+	+	++	+
PRESSURE TAPPINGS	++	+	++	++
CALIBRATION CONDIT.	++	+	+++	++
INSTALLATION CONDIT.	-	++	++	-
OVERALL COMPARISON	++++	+++++	+++++	++++

Legend : +++ means very good
 ++ means good
 + means acceptable
 - means questionable

None of the specifications seems to be badly covered, according to this study. Although the new ISO/DIS-9951 requirements should provide metering specialists with good concepts for measurements of gas, their practicality might be improved, at least to the level of those from a well-spread standard, such as the AGA-7 report. It would allow the use of turbine meters with increased confidence.

The comparison, together with other investigations, may contribute towards the improvement and the better understanding of standard requirements for turbine meters; namely on density measurements, pressure tappings location, calibration and installation conditions. All these metering issues should be considered with great care.

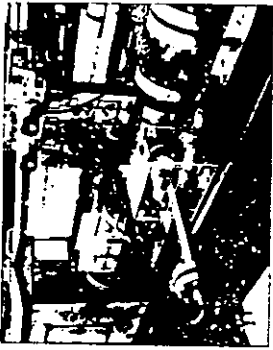
8. ACKNOWLEDGEMENT

This study on turbine metering requirements has been possible thanks to the cooperation of the following manufacturers : Instromet, Faure Herman, Equimeter, Daniel, Elster and Hydril.

The assistance of our colleagues from K-Lab, all along the tests and in their analysis is gratefully recognized.

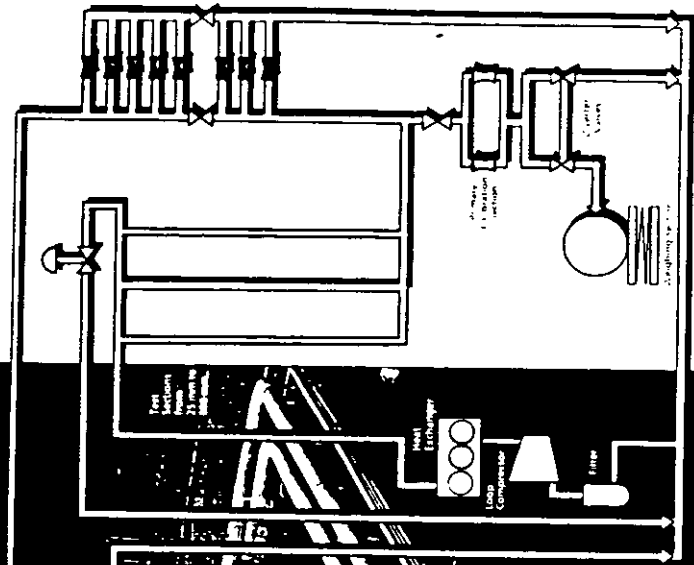
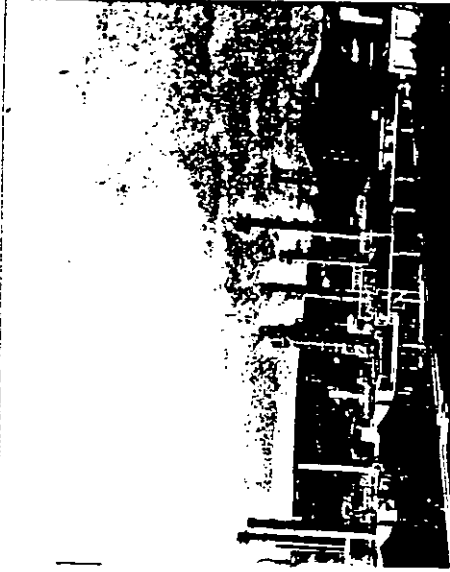
9. REFERENCES

1. « Measurements of Gas by Turbine Meters », " AGA-7 " Turbine Meter Task Group, American Gas Association Transmission Measurement Committee Report N°7 (1985)
2. « Measurement of Gas Flow in Closed Conduits - Turbine Meters » Draft International Standard " ISO/DIS-9951 " International Organization For Standardization (1990)
3. « Petroleum Measurement Manual -Part VII- Density - Section 2 » The Institute of Petroleum, London (1983)
4. « Installation Details For Gas Densitometers » Reidar Sakariassen North Sea Flow Measurement Workshop, Bergen, Norway (Oct. 1991)
5. « Comparison of Repeatability, Reproducibility and linearity for Turbine, Coriolis and Ultrasonic Meters Tested at 100 bars on Natural Gas » Asbjørn Erdal and Jean-François Cabrol North Sea Flow Measurement Workshop, Bergen, Norway (Oct. 1991)
6. « Installation effects on 6" Gas Turbine Meters at 100 Bars » Jean F. Cabrol, Asbjørn Erdal, Jan Bosio, André Chesnoy The 1992 AIChE Spring National Meeting, New Orleans Louisiana Natural Gas Gathering and Transposition (April 1992)
7. « Calibration Results in Natural Gas at 2.0, 5.5 and 10 MPa of 6 Turbine Meters » Asbjørn Erdal, Jean F. Cabrol, and Jan Bosio The 1992 International Gas Research Conference (IGRC 92) To be presented at Orlando, Florida U.S.A (16/19 Nov. 1992)



Flow characterization

A specially designed probe which has been built for high pressure operation (136 bar) measures local flow characteristics across the pipe diameter (150mm). The probe is mainly used for measuring velocity profiles and angles generated by upstream bends and fittings. The probe is also used to assess the efficiency of flow conditioning devices.



Layout 1

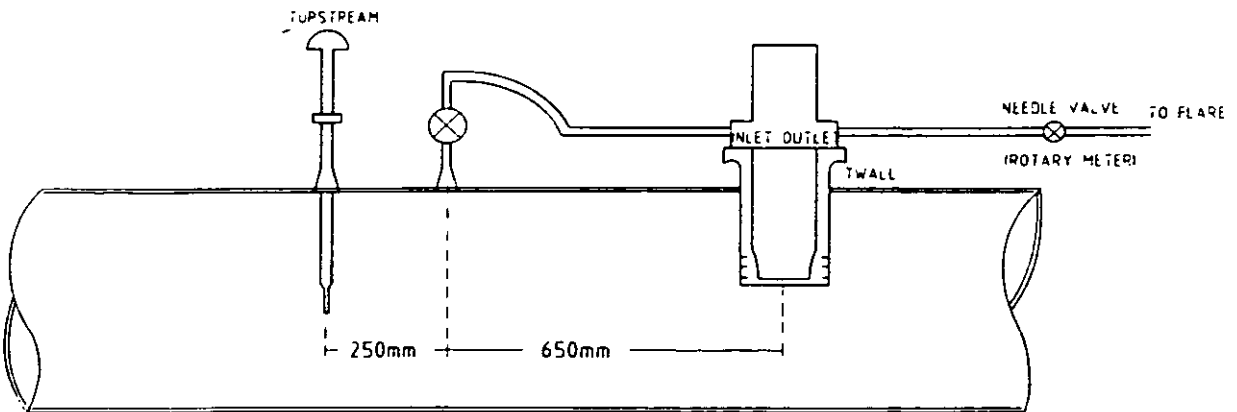
K-Lab loop

The test facilities comprise a main control room, a centrifugal compressor with a 150W electrical flow, an air cooler, a test section area and buildings for the reference flow meters and the primary conditioning system. It is fed from an accommodation wall pipe.

TEGMING OPPDATERT, 14.09.92

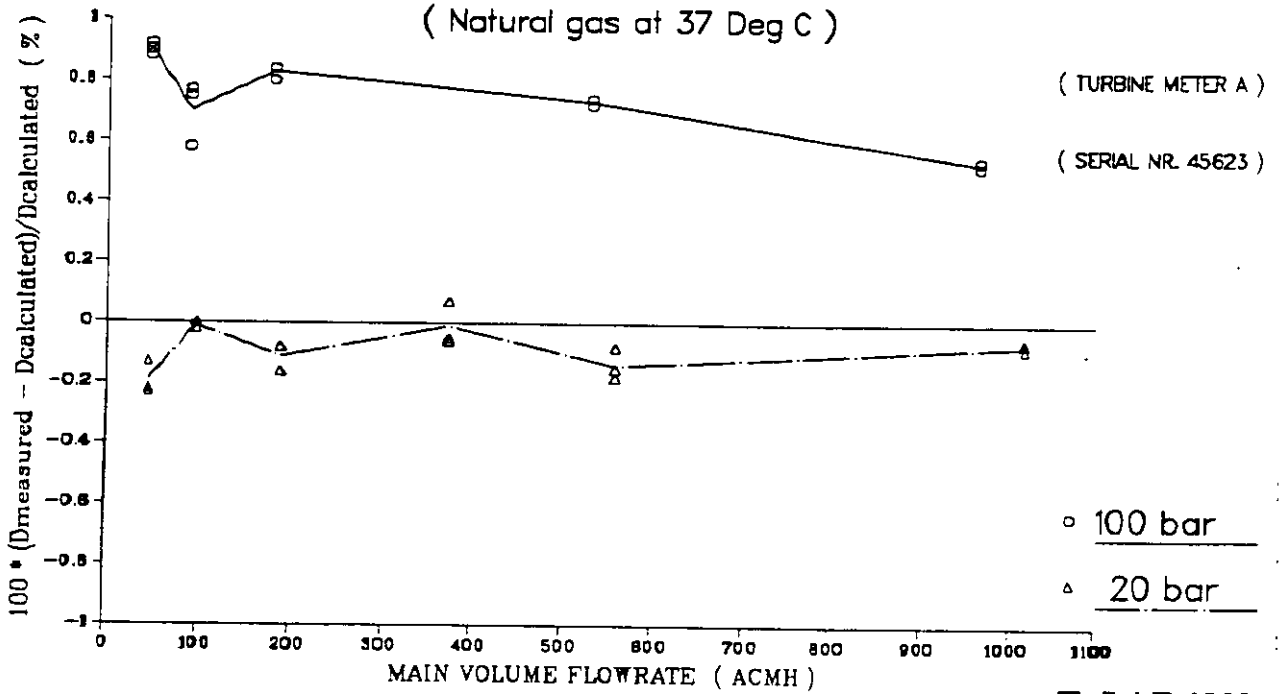
FIG. 2 POCKET INSTALLATION DRAWING

FLOW DIRECTION



DENSITOMETER CORRECTION

Fig. 3 : DIFFERENCE BETWEEN MEASURED AND CALCULATED DENSITY AT DIFFERENT MAIN FLOWRATES FOR GAS TURBINE METER A

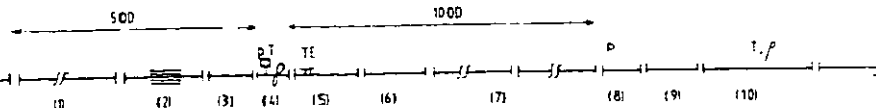


K-LAB 1992

6 HIGH PRESSURE CALIBRATION OF TURBINE METER B

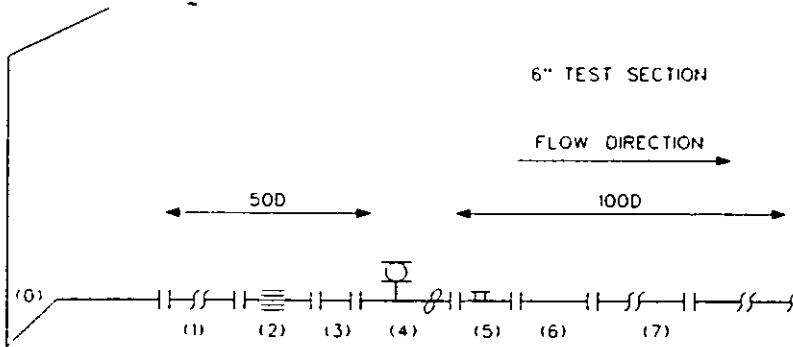
6" TEST SECTION

FLOW DIRECTION →



- (10) 2 90° BENDS WITH 100 IN BETWEEN
- (11) 6m LONG SPOOL PIECE (6", 1500° FLANGED, RTJ)
- (12) 1300mm LONG SPOOL PIECE (6"ND, 1500° FLANGED, RTJ) WITH 19 INTERNAL STRAIGHTENING VANES LOCATED AT 210mm FROM THE OUTLET FLANGE
- (13) 540mm LONG SPOOL PIECE (6", 1500° , RTJ)
- (14) 450mm LONG 6" FAURE-HERMAN TURBINE METER WITH 1500° RTJ FLANGES AND THE HONEYWELL SMART STATIC PRESSURE TRANSMITTER LOCATED AT THE ROTOR
- (15) 1100mm LONG SPOOL PIECE (6", 1500° , RTJ) WITH K-LAB'S SPECIAL THERMOWELL WELDOLET LOCATED AT 500mm FROM THE INLET FLANGE
- (16) 1000mm LONG SPOOL PIECE (6", 1500° , RTJ) [WITH DENSITY SOLARTRON POCKET IN OPTION]
- (17) 2x6m LONG SPOOL PIECE (6", 1500° , RTJ)
- (18) 670mm LONG SPOOL PIECE [WITH PRESSURE OUTPUTS] (6", 1500° , RTJ)
- (19) 800mm LONG SPOOL (6", 1500° , RTJ) THE SMALL RED ONE!
- (110) 160mm LONG INSTRUMENT SPOOL (6", 1500° , RTJ) WITH ONE TEMPERATURE SENSOR AND DENSITOMETER INSTALLED

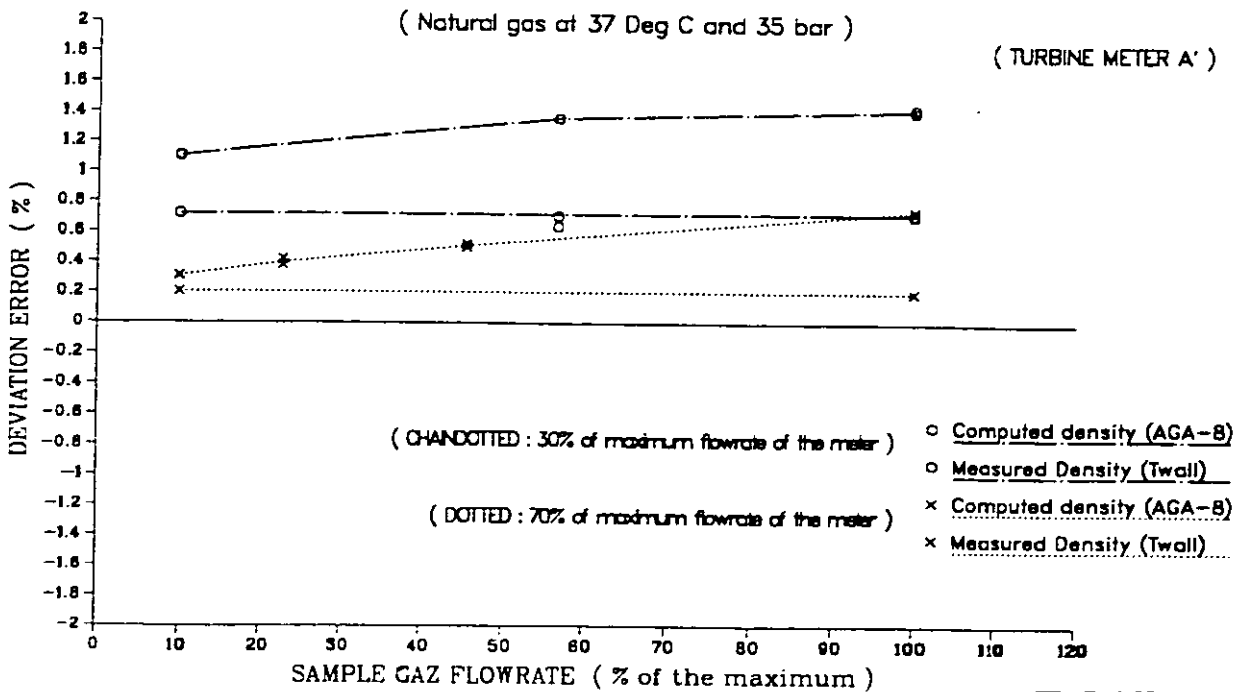
4) HIGH PRESSURE CALIBRATION OF TURBINE METER A



- (0) 2 90° BENDS CLOSE TOGETHER
- (1) 6m LONG SPOOL PIECE (6", 1500° FLANGED, RTJ)
- (2) 1300mm LONG SPOOL PIECE (6", 1500° FLANGED, RTJ) WITH 19 INTERNAL STRAIGHTENING VANES LOCATED AT 210mm FROM THE OUTLET FLANGE.
- (3) 540mm LONG SPOOL PIECE (6", 1500° RTJ UPSTREAM, 600° FLANGED DOWNSTREAM, RTJ)
- (4) 450mm LONG 6" METER A WITH 600° RTJ FLANGES AND THE HONEYWELL SMART STATIC PRESSURE TRANSMITTER LOCATED AT THE ROTOR.
- (5) 1100mm LONG SPOOL PIECE (6" 1500°, RTJ DOWNSTREAM, 600° RTJ UPSTREAM) WITH K-LAB'S SPECIAL THERMOWELL WELDOLET LOCATED AT 500mm FROM THE INLET FLANGE.
- (6) 1000mm LONG SPOOL PIECE (6", 1500°, RTJ) (WITH DENSITY SOLARTRON POCKET IN OPTION)
- (7) 1.6m LONG SPOOL PIECE (6", 1500°, RTJ)

DENSITY EFFECT ON TURBINE METER CALIBRATION RESULTS

Fig. 5 : EFFECT OF SAMPLE FLOW VARIATION ON DENSITY MEASUREMENT



THE AGA TRANSMISSION MEASUREMENT COMMITTEE AND THE REVISION OF
AGA REPORT No 8 COMPRESSIBILITY FACTORS OF NATURAL GAS

by

J Stuart, Pacific Gas and Electric, J Savidge, Gas Research Institute and
S Beyerlein and E Lemmon, University of Idaho

Paper 4.2

NORTH SEA FLOW MEASUREMENT WORKSHOP
26-29 October 1992

NEL, East Kilbride, Glasgow

The A.G.A. Transmission Measurement Committee and the Revision of A.G.A. Report No. 8 on Compressibility Factors of Natural Gas

John Stuart
Chairman, Transmission Measurement Committee
Pacific Gas and Electric

Jeff Savidge
Gas Research Institute

Steven Beyerlein and Eric Lemmon
University of Idaho

SUMMARY

In the United States and Canada, there are several organizations that are directly involved in improving the understanding and practice of natural gas measurement. One of these organizations, the A.G.A. Transmission Measurement Committee, is described in this paper. This paper also discusses the results of a recently completed project of that committee, the 1992 revision to A.G.A. Report No. 8 on Compressibility Factors of Natural Gas. As part of this discussion, two new compressibility calculation methods will be compared to each other and to the NX-19 method for a reference Ekofisk Gas as well as two gas compositions found in the North Sea.

1. FLOW MEASUREMENT ORGANIZATIONS IN THE U.S.

The following is a list of the major U.S. organizations directly involved with the research, testing, technical recommendations, standards, and regulatory matters of natural gas measurement.

A.G.A. / TMC / DMC	American Gas Association / Transmission Measurement Committee / Distribution Measurement Committee
API / COPM / COGM	American Petroleum Institute / Committee on Petroleum Measurement / Committee on Gas Measurement
ASME / MFC	American Society of Mechanical Engineers / Committee on Measurement of Fluid Flow in Closed Conduits
ASTM	American Society for Testing and Materials
GPA	Gas Processors Association
GRI	Gas Research Institute

2. THE AMERICAN GAS ASSOCIATION

The American Gas Association (A.G.A.) is a national trade association with a membership from 250 natural gas distribution and transmission companies located throughout the United States and Canada, as well as overseas.

The A.G.A. staff consists of approximately 180 people located in Arlington, Virginia, just across the Potomac River from Washington, D.C. Another 180 people work in the A.G.A. Laboratories, Cleveland, Ohio, testing and certifying gas appliances. A.G.A.'s annual budget is approximately \$50 million, supported by member dues, testing fees, conference registrations, publication sales and other sources.

The A.G.A. committees are organized into four sections:

1. Legal Section
2. Marketing Section
3. Financial and Administrative Section
4. Operating and Engineering Section

Each section has several committees made up of member company experts. These committees typically meet two or three times a year to discuss mutual problems, share solutions, produce recommended practices and/or standards, and formulate gas industry policies. A.G.A.'s government relations and communications staff then strive to effectively communicate these policies, etc. to legislators, regulators, and industry. For example, A.G.A. spends about \$15 million per year on national advertising, describing the benefits and advantages of natural gas to our customers.

The A.G.A. Operating and Engineering Section consists of about 700 technical experts representing their individual companies, on 17 different committees.

<u>Committee</u>	<u>Members</u>
Automation and Control	38
Compressor	28
Corrosion Control	29
Customer Service and Utilization	40
Distribution, Construction and Maintenance	63
Distribution Engineering	40
Distribution Measurement	35
Environmental Matters	46
Fleet Management	44
Gas Control	35
Materials Management	30
Pipeline	31
Plastic Materials	68
Safety and Occupational Health	37
Supplemental Gas	37
Transmission Measurement	49
Underground Storage	40
TOTAL =	690

Committee activities and projects are aimed at addressing a set of key industry issues: safety, regulations/standards, environmental, communication, Gas Engineering and Operating Practices Series of books, technology, third party damage, quality and productivity improvement, and research identification.

3. THE A.G.A. TRANSMISSION MEASUREMENT COMMITTEE (TMC)

The TMC consists of 20 members from transmission and distribution companies, and 26 associated members from manufacturing, research, and educational institutions.

The scope of projects covered by the TMC include the procedures and practices for installing, operating, testing and maintaining metering and associated equipment, including volume and pressure control equipment which is used in the production, gathering and transmission of natural and substitute gas from the source to the outlet of a transmission line gate station. Also included in the scope of TMC activities are the scientific principles, applications and usage of all types of volumetric, weight, and energy measurement devices associated with the metering equipment specified above.

The current three year plan for the TMC includes the following projects:

1. Revise A.G.A. Report No. 8 on the Compressibility Factors of Natural Gas.
2. Revise A.G.A. Report No. 7 on the Measurement of Gas by Turbine Meters.
3. Revise A.G.A. Report No. 4A on Natural Gas Contract Measurement and Quality Clauses.
4. Develop a small Field Guide for the new revision of A.G.A. Report No. 3 on Orifice Metering.
5. Continue to provide direction to the research community to ensure results have value to members.
6. Provide technical support to other organizations revising measurement standards, e.g. API, GPA, etc.

4. THE REVISION OF A.G.A. REPORT NO. 8

As an example of a recent TMC project, the remainder of this paper will describe a major project just completed, the revision of A.G.A. Report No. 8, Compressibility Factors of Natural Gas and Other Related Hydrocarbon Gases. This report is in the final stages of review and will be available to users in the gas industry in December 1992. This report is based on a large amount of supporting research conducted in North America under the sponsorship of the Gas Research Institute and in Europe under the sponsorship of the Groupe Europeen de Recherches Gazieres (GERG), Gasunie, Ruhrgas, Gaz de France, and British Gas. The report will be accompanied by a diskette of FORTRAN subprograms as well as a utility program for calculating compression factors based on a variety of inputs.

4.1 Background

During the period 1981-1984, the A.G.A. through its Transmission Measurement Committee and the GRI sponsored development of an equation of state to provide the gas industry with state-of-the-art predictions of compressibility factors for natural gas metering applications. Initial work used data ranging in pressure up to approximately 6 MPa obtained from the literature and provided by the GERG. However the GERG data bank was extended considerably in the period 1985-1990. The new data showed that the original equation developed in the period 1981-1984 needed improvement. In addition, velocity of sound data obtained under GRI sponsorship during 1985-1989 showed calculations for rich gases were not sufficiently accurate for critical flow applications. These data were included in a new thermodynamic property correlation for natural gas mixtures. The resulting equation of state is referred to as the Detail Characterization Method and is documented in A.G.A. Report No. 8.

4.2 Natural Gas Characterization Methods

Two highly accurate models for computing compressibility factors in gas measurement applications are presented in A.G.A. Report No. 8. One model applies a detailed knowledge of natural gas composition to compute the compressibility factor (i.e. using standard composition information from a chromatographic analysis). This is the Detail Characterization Method and can be applied over a wide temperature, pressure, and composition regime. A second model applies an aggregate or gross knowledge of natural gas composition to compute the compressibility factor. This model is the Gross Characterization Method which was developed under sponsorship from the Groupe Europeen de Recherches Gazieres (GERG). The method can be applied within the custody transfer region which extends from 265 to 335 K at pressures less than 12 MPa. Neither model is recommended in the liquid phase or within 5K and 0.2 MPa of the critical point.

The Gross Characterization Method was developed by GERG and modified for implementation in the U.S. These modifications have to do with the specification of reference conditions for metering and for determination of heating value. The Detail Characterization Method was developed using a three step procedure using compressibility factor data obtained from the literature and provided by GERG.

- (1) First, an equation of state for key pure components was developed using compressibility factor data for methane, ethane, nitrogen, hydrogen, and carbon dioxide along with velocity of sound data for methane. The equation of state terms were chosen using a procedure which minimizes the number of terms required for a given accuracy.
- (2) Second, compressibility factor data for key binary mixtures were used to determine binary interaction parameters for key binary component pairs.
- (3) Third, the GERG compressibility factor data for 84 natural gas mixtures were used to evaluate the accuracy of the equation of state for natural gas compressibility factors. In addition, velocity of sound data measured by NIST for four natural gas mixtures were used to evaluate the equation of state for velocity of sound predictions.

The Detail Characterization Method and the Gross Characterization Method have been incorporated into efficient computer programs for computing the

compressibility factor, Z , the mass density, ρ , and the supercompressibility factor, F_{pv} . The programs have been designed for the following purposes: (1) efficient implementation on flow computers, (2) as a guide for the development of application programs in the gas industry, (3) for computational verification; and (4) for utility purposes such as tabulating Z , ρ , or F_{pv} for particular gas mixture compositions.

4.3 Reference Data for Natural Gas Mixtures

During the last two years the Gas Research Institute in coordination with Gasunie, Ruhrgas, and Gaz de France have sponsored highly accurate measurements of natural gas mixtures at the National Institute for Standards and Technology (NIST), Texas A&M, Van der Waals Laboratory, and Ruhrgas. PVT data for the five natural gas mixtures shown in Figure 1 were obtained in this research. All mixtures were gravimetrically prepared and chromatographically verified by NIST and then sent to each of the participating laboratories. Density measurements were taken over temperatures from 225 to 350K and at pressures up to 70 MPa. These "reference data" represent the state-of-the-art in PVT measurements for natural gas mixtures. Intercomparison of the data shows an average agreement between the experimental measurements from the four laboratories of 0.035%. These PVT reference data were acquired after finalization of the Detail Characterization Method and the Gross Characterization Method. As such, these data provide an independent verification of both characterization methods.

Figure 2 compares PVT reference data for Ekofisk gas with density predictions from the Detail Characterization Method as well as the Gross Characterization Method at 275K and 300K. Density deviations are calculated as,

$$(\rho_{\text{data}} - \rho_{\text{calc}}) / \rho_{\text{data}} * 100. \quad (1)$$

Figure 3 compares density predictions from the Gross Characterization Method against those from the Detail Characterization Method for Ekofisk Gas. Density deviations are calculated as,

$$(\rho_{\text{gross}} - \rho_{\text{detail}}) / \rho_{\text{detail}} * 100. \quad (2)$$

Despite the agreement in predicted densities, these methods give significantly different derived properties such as velocity of sound and heat capacity. Figure 4 compares density predictions from the NX-19 Method against the Detail Characterization Method for Ekofisk Gas. Density deviations are calculated as,

$$(\rho_{\text{NX-19}} - \rho_{\text{detail}}) / \rho_{\text{detail}} * 100. \quad (3)$$

Both the Detail and Gross Characterization Methods represent the density Ekofisk Gas within 0.05% at pressures less than 12 MPa, while the NX-19 Method is in error as much as 2%. As the concentration of heavier hydrocarbons increases, the differences in predicted density between all three methods becomes more pronounced. Molar composition of natural gas from two North Sea fields is given in Figure 5. Figure 6 compares density predictions from the Gross Characterization Method against the Detail Characterization Method for the Statfjord Gas. Figure 7 compares density predictions from the NX-19 Method against the Detail Characterization Method for Statfjord Gas. Figure 8 compares density predictions from the Gross Characterization Method against the Detail Characterization Method for Veslefrikk Gas. And Figure 9 compares density predictions from the

NX-19 Method against the Detail Characterization Method for Veslefrikk Gas. Figures 6-9 illustrate that the Detail Characterization Model should be favored in predicting compressibility factors for rich gas mixtures such as those found in the North Sea. Unfortunately, little reference quality experimental data are available for evaluating the accuracy of compressibility factor predictions for rich gas mixtures.

4.4 Recommendation to Gas Industry Users

In the United States the Gross Characterization Method will be implemented primarily for transmission/distribution system applications. This method will only be used for compressibility factor calculations. All derived physical properties will be calculated with the Detail Characterization Method. The Detail Characterization Method is applicable to transmission/distribution conditions and is expected to be applicable to a broad range of production/processing conditions. Research is underway to investigate the data and modeling needs for heavier gas constituents.

REFERENCES

STARLING, K.E. and SAVIDGE, J.L., "Compressibility Factors of Natural Gas and Other Related Hydrocarbon Gases", A.G.A. Transmission Measurement Committee Report No. 8, 1992.

STARLING, K.E., FITZ, C.W., CHEN, Y.C., and RONDON, E., University of Oklahoma, and JACOBSEN, R.T, BEYERLEIN, S.W., CLARKE, W.P. and LEMMON, E., University of Idaho, "GRI High Accuracy Natural Gas Equation of State", ISO TC193/SC1/WG7 Report, 1991.

JAESCHKE, M., Ruhrgas A.G., and HUMPHREYS, A.E., British Gas plc., GERG Technical Monograph 5, 1991.

SCHOUTEN, J., MICHELS, J.P., and JAESCHKE, M., "Calculation of the Compressibility Factor of Natural Gases Based on the Calorific Value and its Specific Gravity", International Journal of Thermophysics, Vol 11, No 1, 145-156, 1990.

- Figure 1. Percent Molar Composition of PVT Reference Data for Natural Gas Mixtures**
- Figure 2. Percent Deviation between Experimental PVT Data and Densities Predicted from the Detail Characterization Method and the Gross Characterization Method.**
- Figure 3. Deviation in Predicted Density between the Gross Characterization Method and the Detail Characterization Method for Ekofisk Gas.**
- Figure 4. Deviation in Predicted Density Between the NX-19 Model and the Detail Characterization Method for Ekofisk Gas.**
- Figure 5. Percent Molar Composition of Natural Gas from the Statfjord and Veslefrikk Fields.**
- Figure 6. Deviation in Predicted Density between the Gross Characterization Method and the Detail Characterization Method for Statfjord Gas.**
- Figure 7. Deviation in Predicted Density between the NX-19 Model and the Detail Characterization Method for Statfjord Gas.**
- Figure 8. Deviation in Predicted Density between the Gross Characterization Method and the Detail Characterization Method for Veslefrikk Gas.**
- Figure 9. Deviation in Predicted Density between the NX-19 Model and the Detail Characterization Method for Veslefrikk Gas.**

		GULF (NIST1)	AMARILLO (NIST2)	EKOFISK (RG2)	High N₂ (GU1)	High CO₂ (GU2)
CH ₄	Methane	96.6	90.7	85.9	81.3	81.2
N ₂	Nitrogen	0.3	3.1	1.0	13.6	5.7
CO ₂	Carbon Dioxide	0.6	0.5	1.5	1.0	7.6
C ₂ H ₆	Ethane	1.8	4.5	8.5	3.3	4.3
C ₃ H ₈	Propane	0.4	0.8	2.3	0.6	0.9
C ₄ H ₁₀	Butane	0.2	0.3	0.7	0.2	0.3
C ₅ H ₁₂	Pentane	0.1	0.1	0.1	-	-

Figure 1. Percent molar composition of PVT Reference data for Natural Gas Mixtures.

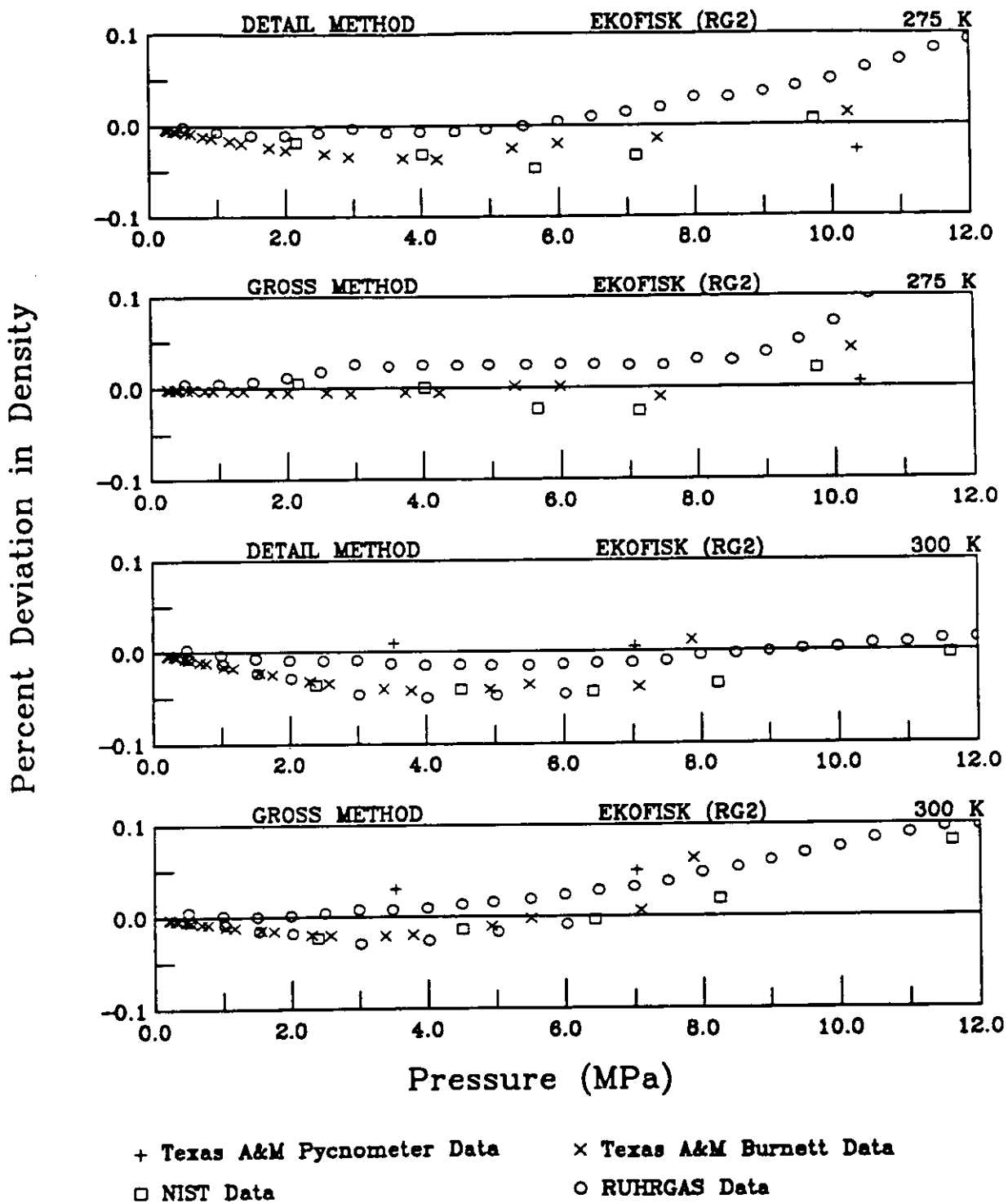


Figure 2. Percent Deviation between Experimental PVT Data and Densities Predicted from the Detail Characterization Method and the Gross Characterization Method.

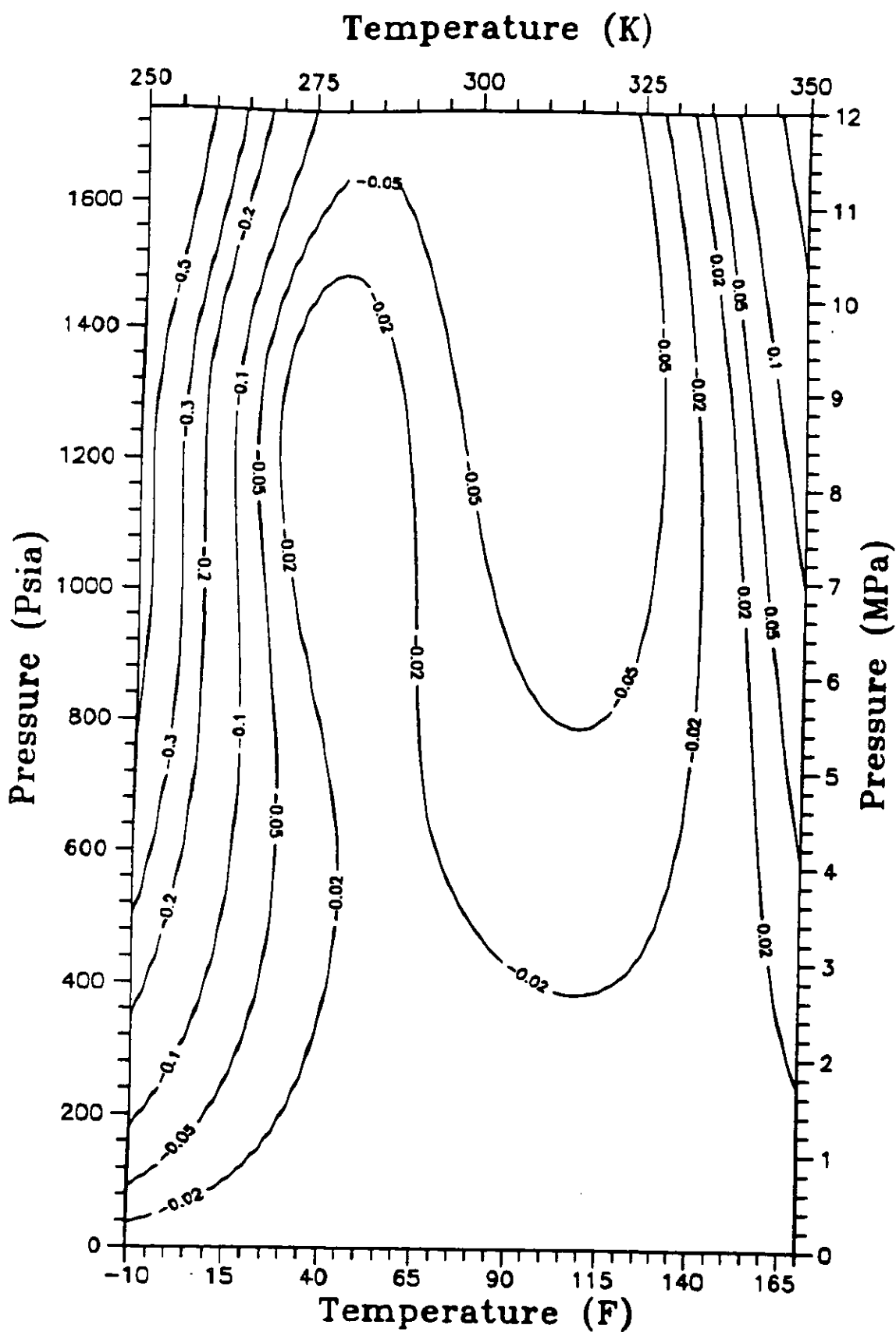


Figure 3. Deviation in Predicted Density between the Gross Characterization Method and the Detail Characterization Method for Ekofisk Gas.

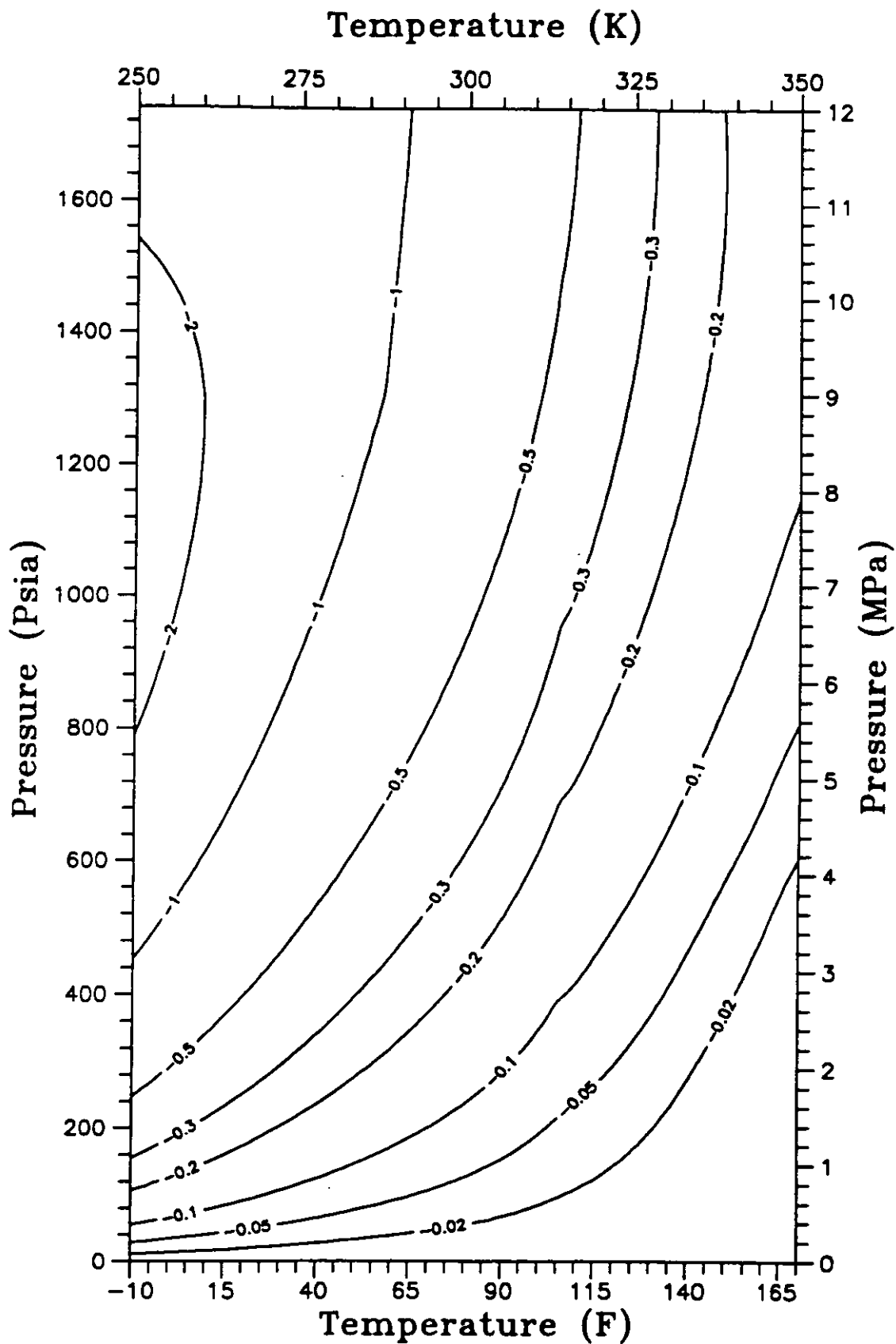


Figure 4. Deviation in Predicted Density Between the NX-19 Model and the Detail Characterization Method for Ekofisk Gas.

		STATFJORD FIELD	VESLEFRIKK FIELD
CH ₄	Methane	73.21	66.5
N ₂	Nitrogen	0.65	1.22
CO ₂	Carbon Dioxide	0.90	3.5
C ₂ H ₆	Ethane	11.97	12.45
C ₃ H ₈	Propane	8.55	11.66
C ₄ H ₁₀	Butane	3.19	3.94
C ₅ H ₁₂	Pentane	0.83	0.57
	heavier Hydrocarbons	0.70	0.09

Figure 5. Percent molar composition of Natural Gas from the Statfjord and Veslefrikk Fields.

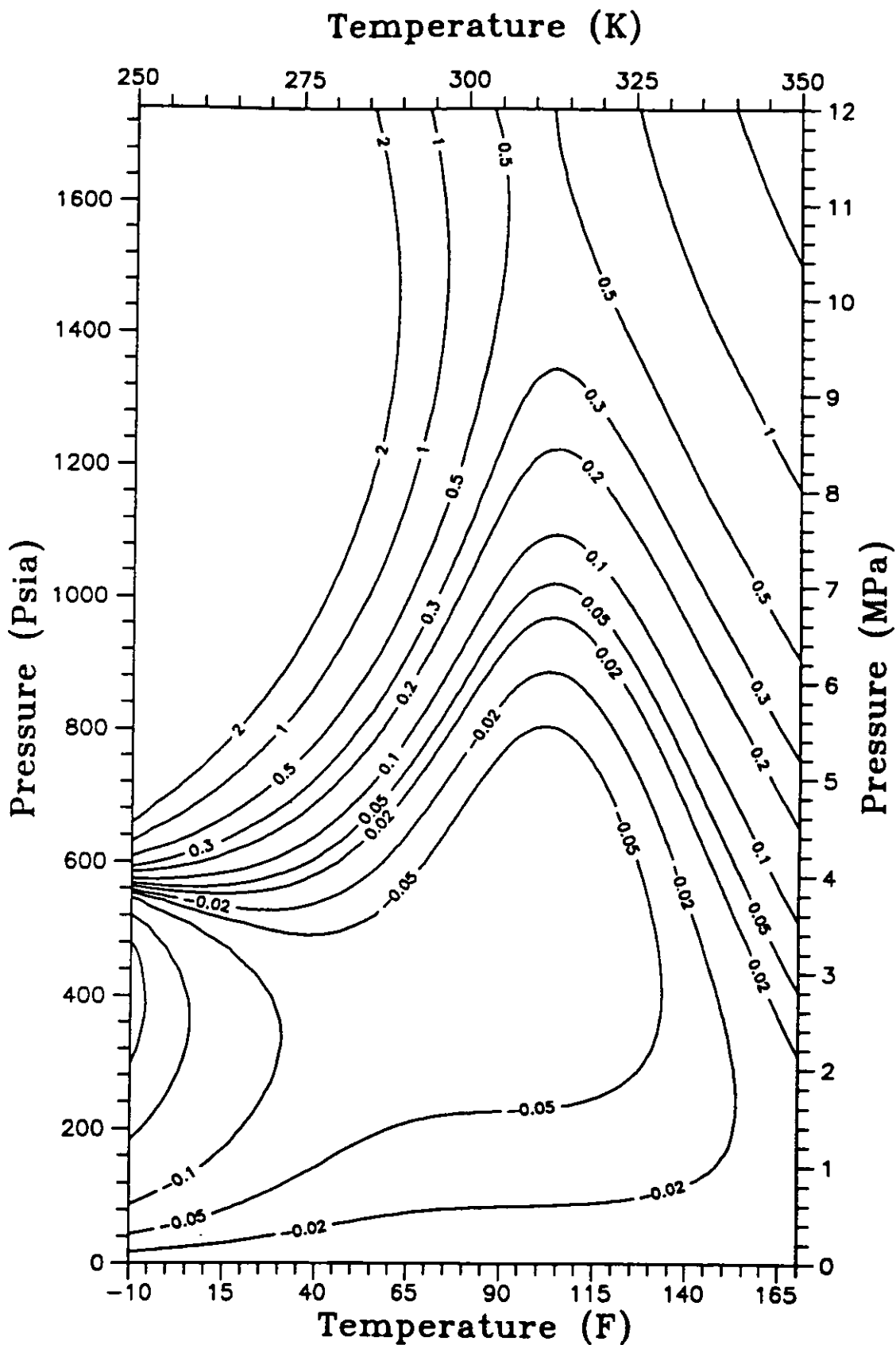


Figure 6. Deviation in Predicted Density between the Gross Characterization Method and the Detail Characterization Method for Statfjord Gas.

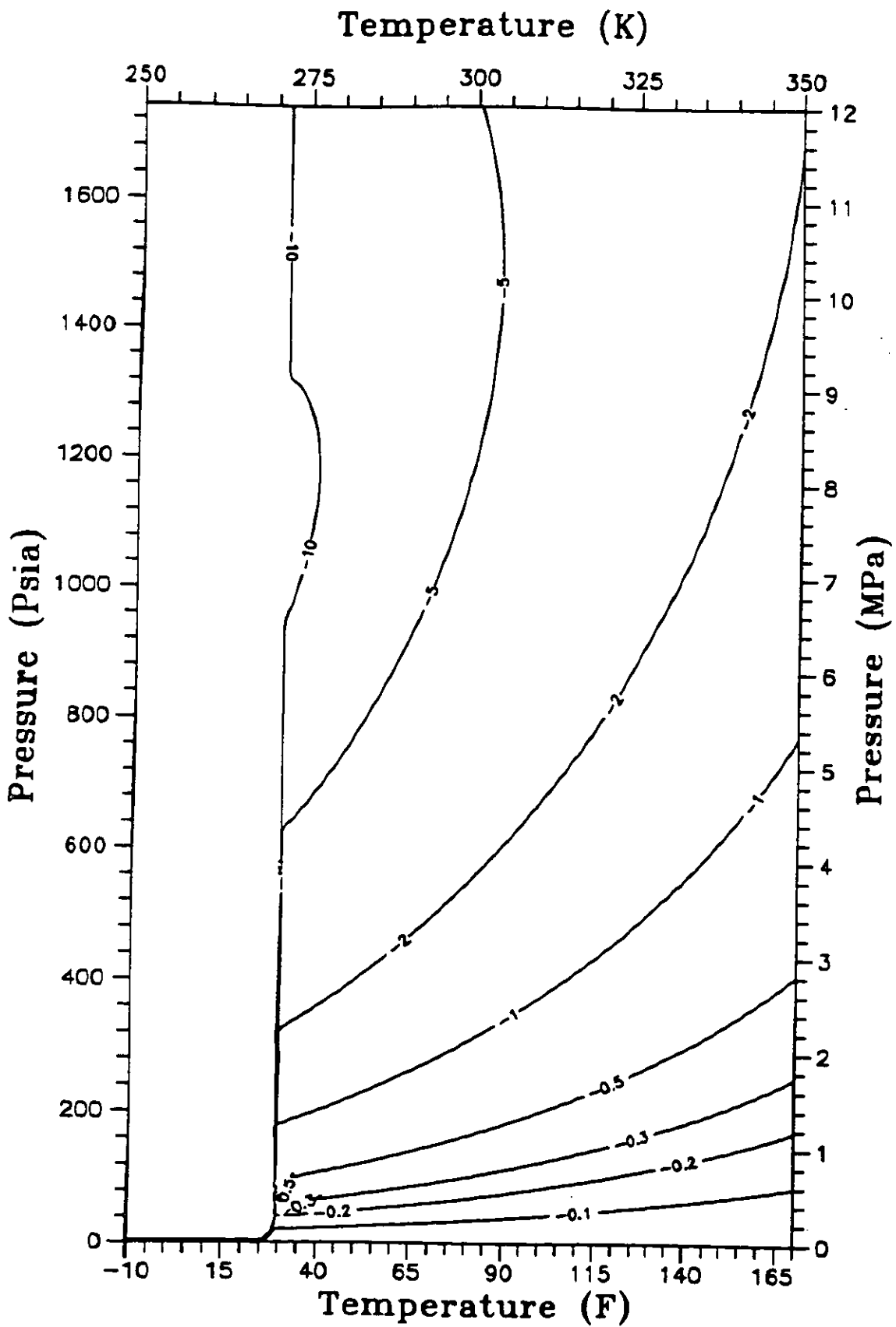


Figure 7. Deviation in Predicted Density between the NX-19 Model and the Detail Characterization Method for Statfjord Gas.

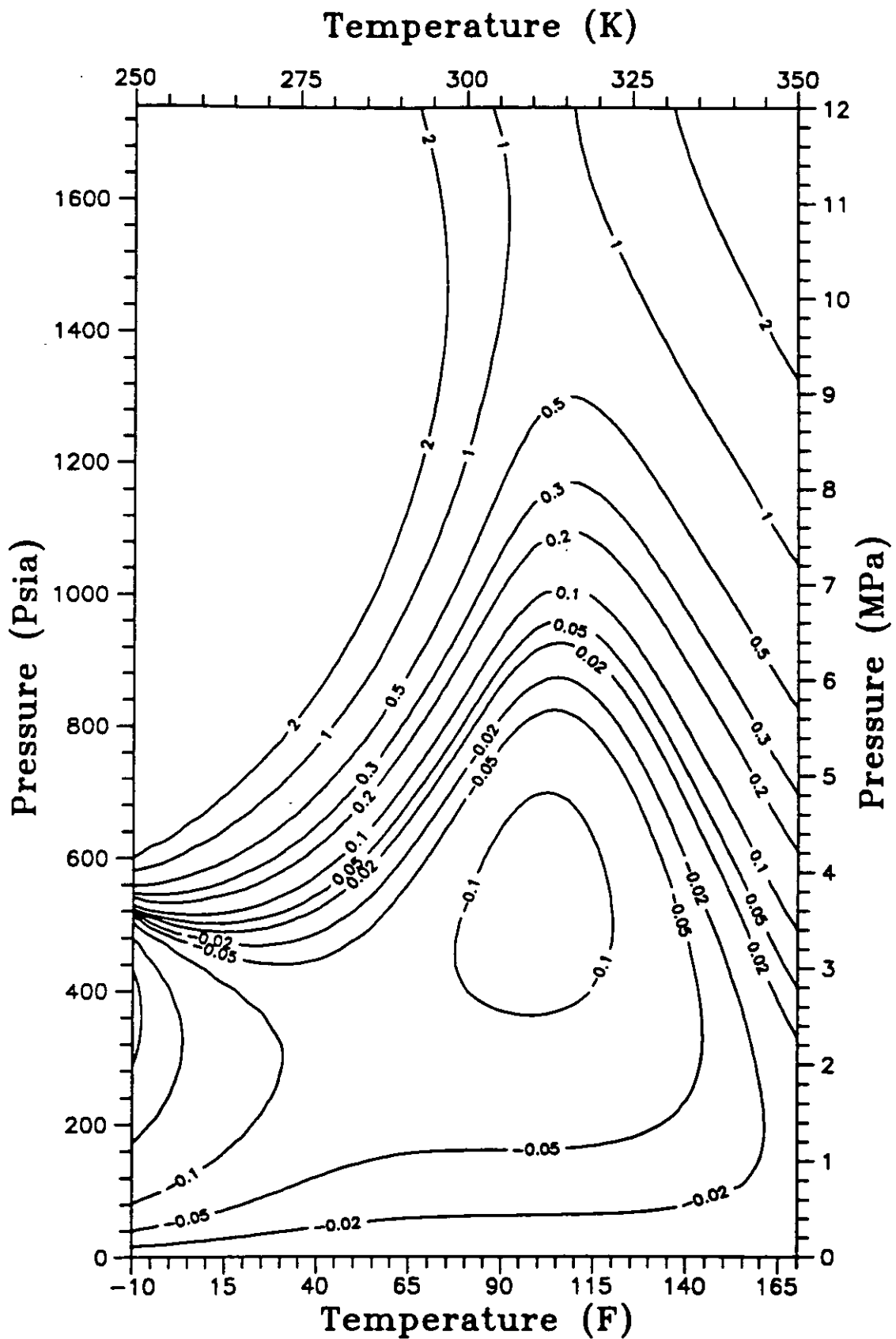


Figure 8. Deviation in Predicted Density between the Gross Characterization Method and the Detail Characterization Method for Veslefrikk Gas.

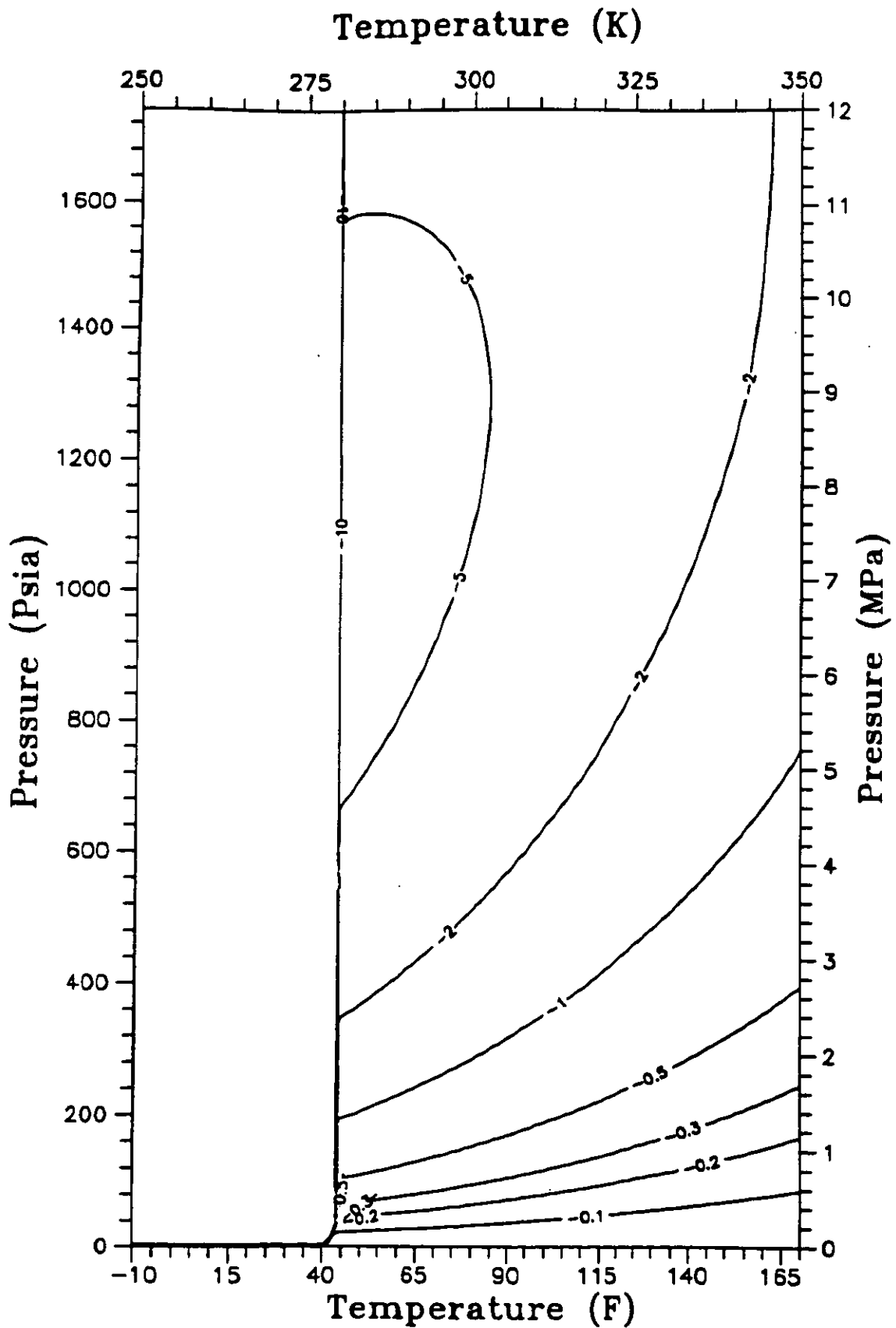


Figure 9. Deviation in Predicted Density between the NX-19 Model and the Detail Characterization Method for Veslefrikk Gas.

DENSITY METERING INSTALLATION METHODS

by

J Gray
Peak Measurement Limited, Sarasota

Paper 4.3

NORTH SEA FLOW MEASUREMENT WORKSHOP
26-29 October 1992

NEL, East Kilbride, Glasgow

DENSITY METERING INSTALLATION METHODS

Jim Gray

Peek Measurement Limited - Sarasota, Kingsworthy, Winchester

SUMMARY

The paper concentrates on density meters which utilize the well established technique of a vibrating element to continuously determine the density of a fluid. A review of 2 primary types of element and 3 methods of installation are used to highlight the benefits of each type and method together with some of the problem areas. The intention of the paper is to help alleviate problems in new metering systems and provide guidelines on trouble shooting existing measurement difficulties.

1.1 THE VIBRATING ELEMENT

This technique is widely accepted as being the most accurate method of continuous density measurement for fiscal duties.

There are two common types of element which are used. The first is a short thin-walled magnetic stainless alloy cylinder often called a spool (or tines). **FIGURE 1** shows a spool mounted in the density meter body which is shown cut away for clarity. The spool is secured so that one end is fixed and the other free and is totally surrounded by the process liquid. The wall thickness varies depending on the required measurement range between 50 microns and 250 microns.

An impulse is supplied by the drive coil from the amplifier which is mounted by a stem on to the density meter body. This causes the spool to vibrate and this movement is detected by the pick up coil and the resulting signal is amplified and supplied back to the drive coil. The spool is therefore maintained in oscillation by this feedback circuit.

The spool vibrates in a hoop mode and this is shown in this section through the spool. Obviously this is very much magnified for clarity and the actual movement is very small indeed. This vibration is of the same type that you get if you rub your finger around the rim of a wine glass. If the wine glass is full it will give a different note from that it gives when empty. This differing frequency of vibration also occurs in the density meter and the spool vibrational frequency varies with the density of the fluid surrounding it.

As can be seen from FIGURE 2, the advantage of this approach is the fluid is present on both sides of the vibrating element (which is called the spool). This means that there is no differential pressure across the thin wall of the spool and therefore the spool is not stressed by increasing pressure. The body of the instrument is merely a pressure vessel in which the spool is mounted and this makes the instrument suitable for operation at high pressures. As mentioned previously, the mode of vibration of a spool is circumferential hoop mode. This is shown diagrammatically on the left hand side of FIGURE 3. The vibration is always mechanically balanced so that there is no reaction on the point where the spool is attached to the body assembly.

If we look at a different mode of vibration as illustrated on the right of FIGURE 3, we can see the second type of vibrating element. Here we have a longer tube that is clamped rigidly at each end. The tube is caused to vibrate in a transverse mode, i.e. the centre of the tube is deflected from side to side. This causes minimal shearing of the fluid and an instrument based on this principle is thus unaffected by the viscosity of the fluid passing through the tube. All the fluid in the tube is forced to take part in the vibration and the measurement is then one of the bulk or average density of the instantaneous sample. This means that non-homogeneous fluids such as slurries can be measured with this technique. By sealing the outside of the tube from the process we can magnetically drive the tube without worrying about the corrosion resistance of the magnetic materials as they need not be in contact with the process fluid. Thus we can use a 316 stainless steel tube with magnetic armatures fixed to the outside of the vibrating tube to give us a magnetically driven density meter with the corrosion resistance of 316 stainless steel. One disadvantage of using this method is that the vibration is no longer dynamically balanced; there is a net reaction on the clamps at each end as the tube is deflected from its rest position.

To look at the practical implications of a density meter using a tube in transverse vibration, as we have just discussed, we must firstly provide a massive clamp at each end of the vibrating tube section to define these points as nodus points of vibration. This limits the energy transfer from the vibrating tube to the holding structure by ensuring there is no movement at the coupling points. This is shown diagrammatically in the top illustration of FIGURE 4, where we have a stiff frame welded on to the tube.

One disadvantage with this meter is with the central tube held rigidly when the temperature of the fluid passing through the vibrating tube varies a stress will be generated in the vibrating tube as the clamping structure remains at ambient temperature.

A method of compensating for this effect is to make the frame a part of the fluid path through the instrument. This is shown here where the fluid flows through the instrument in one continuous path. The top and bottom tubes are made with a thicker wall than the central vibrating element, forming a stiff structure together with the manifolds. As the fluid now passes through the structure as well as the vibrating tube, the whole measuring section reaches fluid temperature. The thermal induced stress on the central tube is then much reduced because the connecting structure can expand and contract with temperature.

1.2 A NEW DESIGN

The design brief for the new transducer was to make a HIGH ACCURACY WITH LONG TERM STABILITY meter. We explored the performance of a whole range of possible ways of making a Ni Span C vibrating tube device, of both theoretically using a mathematical model and building a series of models to measure performance.

We found that the best overall performance was provided by a twin tube device.

The reason for this is in the basic transducer theory. An accurate sensor design only reacts to the required measurement and all other effects (stiffness of tube and mounts, mass of tube) should ideally be constants.

As previously mentioned the tube must be fixed at its ends to define its vibrating length, preferably to an infinitely big mass. In a 3 tube design, this is achieved by 2 thicker outer tubes bracing the ends together. Single tube designs without this bracing can lack the precise definition of vibrating element length and loose out on accuracy and especially long term stability.

Ruling out infinitely large end masses as less than practical, we found by using 2 close spaced tubes and modest end mass the end nodes could be well defined. In using 2 tubes vibrating anti-phase we have perfect dynamic balance with all the shear forces and bending moments nulling out in the end masses.

The twin tube design is not new, it was probably one of the first and best vibrating tube designs. However, we so believe that this implementation is markedly superior to any other liquid density meter.

Before we look at the selection of vibrating element for a type of fluid, we should consider the installation methods. The selection of transducer and element type is often influenced by installation options and the overall design.

1.3 INSTALLATION METHODS

The 3 basic installation options of density measurement currently used worldwide today are:- 'IN-LINE' 'OFF-LINE' and 'ON-LINE' as shown in FIGURE 5. The 3 titles are taken from the IP Petroleum Measurement Manual Part VII Density section 2 Continuous Density Measurement and broadly defined as follows:-

- Density Meter, **IN-LINE** - A density meter in which the transducer is located directly within the main line or vessel and measures continuously. No sampling system is required.
- Density Meter, **OFF-LINE** - A density meter separate from the main line or vessel. This requires a discrete sample to be drawn from the line/vessel for analysis.
- Density Meter, **ON-LINE** - A density meter operating on a sample of the fluid withdrawn continuously from a main line or vessel via a sampling system.

Having defined the methods we can now consider the key aspects and examples of each method. All three methods are used on gas applications, generally only **IN-LINE** and **OFF-LINE** are used for liquid applications.

1.4 GAS APPLICATIONS

IN-LINE GAS measurement should always be used when the highest accuracy of measurement is the prime factor. The Direct Insertion Density Meter is still probably the most accurate gas density measurement installation available today as it measures true In-Line density with a high degree of immunity to gas borne dirt and moisture and no potential of pressure or temperature gradients; factors which are often overlooked when the user is making an assessment of an installation's desired accuracy. Good examples of this are to be found in the rapidly expanding number of installations in chemical plants for the density measurement of ethylene, propylene, propane and butane. Here the temperature and pressure coefficients are so large that any alternative method of installation will potentially produce errors in the order of 3 times the Density Meter accuracy. This is due to variations in the pressure and temperature gradient relative to flow rate between the main line and the point of density measurement.

OFF LINE GAS measurement is normally used for 2 prime reasons:

- 1 To allow the product to be conditioned to ensure the removal of excessive dirt or moisture or elevate the temperature of the density meter and product above the product's dew point. A typical example is a By-pass Density Meter installed in a custom built gas filtering system to measure the density of aggressive dirty and variable composition flare gas; an application where a great deal of expertise and experience in both on-shore and off-shore installation, is needed to ensure reliable measurement.
- 2 To measure density at a defined pressure and or temperature irrespective of the main line conditions for determination of product quality composition or calorific value. A typical example is a By-Pass Density Meter, used within a relative density (SG) system. The line pressure is reduced to just above atmospheric conditions and absolute pressure of the system is measured using a 0.1% accuracy integral transmitter this combined with a high sensitivity PT100 temperature element determines the relative density (SG) of the gas at near reference conditions. At these conditions compressibility effects can be considered to be negligible for all gases. This method is thus ideal on fuel gas applications where line pressure, temperature, density and most important of all product composition vary therefore, making it almost impossible to accurately correct the compressibility of the gas due to un-identifiable and continual change in product composition.

ON-LINE GAS measurement is a useful combination from both In-Line and Off-Line methods, whilst the insertion Density Meter will always be the ultimate in overall accuracy terms. The Pocket Density Meter has the same transducer calibration accuracy capability. On applications where the temperature changes of the product in the main line are relatively small and fluctuations do not occur instantaneously, then this accuracy can be reflected in the overall installation performance. An ideal application for this method would be a natural gas pipeline where the change in temperature of the gas is only influenced by ambient temperature.

FIGURE 6 is an overview of the most common configurations of installations used for gas applications.

If we now look at each in turn we can identify some of the aspects which are sometimes overlooked.

"G1" (FIGURE 7) is a typical OFF-LINE fuel gas. We have started with one of the most difficult system applications. This is used where the gas composition can be anything from Hydrogen to C6 plus heavy ends. In the "REAL WORLD" it will often be dirty, corrosive (sour) and "wet". Gas applications normally use the short cylinder (spool) type element. Selection of material is important as Ni-Span C is not suited to sour gas with H₂S present.

To a first order, this type of element does not work on "wet gas". However, "wet gas" should be better defined as gas with liquid droplets. A vibrating cylinder element on gas service will not work if liquid droplets are present on the element. This is recognisable in the field as a very erratic output caused by the liquid droplet rolling up and down the element.

Two methods have been used to reduce this problem. A combination of cyclone and coalescing filters together with a heat tracing technique, usually in the form of an electrical self regulating system as steam tracing is often not available.

It is very difficult to achieve a totally successful design on this type of application from "best estimate composition data often from a design process engineer for a platform yet to be built. However, many successful systems have been custom designed and used mainly where the measurement engineer has been able to obtain real composition data on an established platform or plant. Heat tracing, where the product is maintained at a temperature above the lowest dew point value is the most successful of the two methods. Some systems built by analyzer Companies, with limited experience on density measurement, appear to work satisfactory due to the removal of the heavy ends as well as the dirt and water. The result is a non-representative clean dry light ends only sample.

Accurate quick response, low thermal mass, temperature thermowells are a critical component for this type of application to correct to reference or line conditions. In many cases, we have to design and build our own, due to the low volume throughput dictated by the conditioning system. Attention to any pressure reduction is also needed as this can create more liquid formation. Short well lagged impulse pipe work increases the potential performance of this measurement as well.

The combined cooperation and experience of the user and the supplier is the key to this application.

"G2" (FIGURE 8) is a typical IN-LINE density meter with a retractor mechanism for removal under line conditions. As mentioned previously this is the most accurate method of measurement of gas density. The basic design has been available for many years, however. A number of developments have occurred more recently. In the "REAL WORLD" it could be said that there is no such thing as a totally clean fluid on a platform or in a pipeline, therefore any direct insertion density meter must have some protection from dirt and liquid droplets on gas applications.

FIGURE 9 shows a successful development in this area.

Ideally a filter should have a large surface area to reduce the potential of undesirable differential pressure due to contaminate. However, by having the inlet on the back face of the transducer and a round profile body very little dirt or liquid droplets ever reach the filter. As both of these contaminates are a heavier mass than the gas the increase in velocity generated by the round profile means they will tend not to be drawn in to the inlet.

The retractor mechanism has often two vent valves. One is normally used to vent the small volume of pressure in the chamber after the main ball valve has been closed. An important point for all gas transducers is to always depressurize the instrument slowly otherwise liquid drop-out can be created from hydrocarbon gases. The second vent valve can be used for purging and installation of a test gas. Oxygen free nitrogen is not only a good test gas, easy to obtain pure grade (99.99% pure), safe, and good data available, but it also is very good at absorption of hydrocarbon liquid drop out. This sometimes saves the requirement for demounting the system for cleaning.

Some of our clients prefer to take test point values using pure gases. However, we have never seen a density transducer successfully checked on a simple vacuum test fail on line in terms of accuracy. Therefore we recommend an insitu frequency reading with a vacuum of better than 1mm mercury is both a practicable and accurate, on site check. For safety reasons an air driven vacuum pump should be used in hazardous areas. Also we recommend the pump is not left pulling vacuum for more than half an hour as oil within the pump can back stream into the density meter.

The paper, "Experimental Evaluation Of Densitometers In The Presence Of Condensation Or "Wet Gas"" by Dr S Kostic, Dr T M Svartas and G Staurland from the Rogaland Research Institute presented at the 8th North Sea Flow Measurement Workshop in 1990, identified that the direct insertion density meter recovered significantly faster than the pocket density meter after an injection of "wet gas". In general, most gas density meters are subjected to occasional liquid carry over. If the gas is continuously wet then only "G1" should be considered.

Direct insertion density meters with their unique inherent accuracy can be used, particularly as most modern fiscal metering stations now use two transducers with back up PTZ calculation to qualify the transducer's status.

Lube oil mist down-stream of a compressor on Natural gas pipelines can cause problems which are difficult to identify without PTZ back up calculation.

Unlike other liquid carry over which is easily identified by erratic performance, lube oil mist can form a very fine deposit on the element not visible to the eye. Dual density meters have been seen to be more than 2% off specification but still within 0.2% agreement. Where ever possible on new metering installations, it is best to avoid locations immediately down-stream of compressors. Hopefully in the future there will be a filter which can totally remove this. A dimension of how far down-stream this type of mist becomes relatively harmless droplets should be identified.

When used with a retractor mechanism another option is available to the user to improve performance should there be an excessive frequency and volume of liquid carry over. As we have already mentioned, the latest sampling technique is similar to what occurs in the chimney when wind passes over the tip. This draws the sample from the base of the probe. The instrument therefore suffers no loss of response time if the inlet is positioned in the pipe stub away from the contamination. Furthermore, in extreme cases, heat tracing can be applied to the pipe stub to ensure the carry over stays in the vapour phase.

The final comment for this type of installation is applicable to all installations of density meter. When it humanly possible, ensure the density meter is kept off-line or isolated until 24 hours after start up. Flow computers etc can be given "fall back" values to get the system running. More damage is caused to density transducers in this time frame than the rest of the instrument's life time.

"G3" (FIGURE 10) is another installation of an IN LINE density meter. The density meter is 8D down-stream of the orifice plate and is mounted on a welded flange. This is a cost effective method which is often used on multiple meter tubes where removal from the line whilst not on line is practical. Because the meter is at the point of full recovery, no theoretical correction for the orifice downstream pressure wake is required. The only additional area of caution required is to ensure the metering engineer liaises with the piping engineer for the correct dimensions and orientation of the pipe stub, (normally 80mm (3") diameter.)

"G4" (FIGURE 11) IN-LINE installation is 5D downstream of the gas turbine. Gas turbines are becoming increasingly popular especially onshore. Unlike the orifice plate the turbine meter has a small differential pressure drop often preventing the use of the recovery method. However, this does not present a problem when using the direct insertion method. The mounting flange on this installation shows the alternative compression fitting method which permits initial field orientation of the meter.

"G5" (FIGURE 12) is the last variance of installation of an IN-LINE meter shown. There are an increasing number of small diameter pipe metering installations where the benefits of IN-LINE density meters are required. For line sizes greater than 150mm (6") the dimensions of the instrument, ie, blockage factor is not normally a problem.

When the line size is below 100mm (4") we recommend the use of 100mm (4") equal tee with eccentric reducers to suit the actual line size. Problems have occurred with turbines etc when concentric reducers are used due to the pipe work "trough" collecting dirt/liquid and eventually causing slug flow, when there is a significant change in flow rate. From our experience accurate results are achieved as long as the area of the pipe excluding the area of the density transducer body is greater than or equal to the area of the incoming pipe work.

"G6" (FIGURE 13) The ON-LINE pocket density meter is designed for use on gas applications. The process gas is extracted from the main line via, typically, 6mm Diameter pipe, through an isolation valve and transported to the density meter in a thermal pocket welded into the main line. After measurement it is normally returned back to the main line again although, it can be fed to a vent where the differential pressure is small, as often experienced on gas turbine systems.

A differential pressure technique is the most common method used to generated through-flow. Two different d.p. hook-ups are used, which based upon established methods recommended by the Institute of Petroleum.

The preferred method employs a take-off close to the pocket density meter normally 8 diameters down stream of the orifice plate with sample flow return to the low pressure area at the downstream tapping of the orifice plate. This method avoids 'unregistered flow' as all product flows through the orifice plate. The other method is to simply connect the inlet and outlet pipe work across the DP of the orifice plate.

In either method it is essential that the sample lines/valves are fully lagged together with insulation on the pocket density meter to reduce errors due to temperature differences between the sample and main pipeline.

A range of wall thickness on the pockets selectable on the basis of maximum design/operating pressure, ensures thermal mass of the pocket is kept to a minimum, enabling the quickest possible response to a change in the main pipeline temperature.

When using a class 900 lb pocket, a 5 degree centigrade change in temperature could typically take approximately 20 minutes before equilibrium between the mainline and the measuring element is restored. This aspect was more extensively covered by Mr Reidar Sakariassen from Statoil in his paper Installation Details For Gas Densitometers at the 9th North Sea Flow Measurement Workshop.

Finally on the construction The most important feature of any Pocket Density Meter is an integral PT100. Based on years of experience in IN-LINE and OFF-LINE density and flow measurement we have proven that a custom built integral PT100 unit is a mandatory requirement for any accurate form of density meter installation. It ensures that there is no temperature gradient error between the precise point of density and temperature measurement within the transducer.

Furthermore, on installations operating at extreme temperatures, it allows the user to monitor, correct and/or alarm on any potential temperature differentials between the point of density measurement and the main line. Often where the user is using the density meter as a component of a mass flow metering system, errors due to temperature differential can cause significant offset in the overall system accuracy.

We recommend and always include an external two microns filter to protect the measurement cell. This filter has a large surface area and will therefore, require a far lower frequency of maintenance than an alternative small area integral filter with potentially difficult access. Ideally two filters should be installed in parallel to allow changeout without having to shutdown the stream and depressurise the sample system. For extreme applications coalescing filters can also be used.

A suitably rated variable area flow meter fitted between the filter and the transducer has proved to be a valuable maintenance tool. With experience this can be used to verify filter status. Prevention of errors due to very stable density values the impulse pipe work being blocked with hydrocarbon liquid or as we have seen several times in Scandinavia frozen moisture! Two other points will assist in the prevention of the problem. First avoid impulse pipe work configurations which can become liquid traps, a side tapping rather than the common top tapping can often assist in achieving this. Secondly, the return pipe work should ideally be 12 or 15mm diameter pipe work with no restrictions and a full bore automatic valve included in the

valve logic of the shut off valves. Many problems with liquid dropout occur during start up of a meter tube and also rapid depressurization.

Another strange effect we have seen several times in the last few years is dual installations where a density offset is maintained to an installation even when the transducers have been changed over to the other installation. On one occasion manufacturers were also changed and the exact same offset was still present. After changing the lengths and diameters of impulse pipe work the problem was found to be due to use of a common tapping for the return from the density meter and the low pressure side of the DP cell.

To further prove the point, impulse pipe work lengths were changed after providing an individual tapping and all the density meters still maintained their agreement.

"G7" (FIGURE 14) As previously mentioned the recovery method can not easily be used with gas turbines. A common technique is to vent the outlet but care should be taken to ensure the turbine hub pressure is maintained within the transducer.

"G8, G9, G10, (FIGURE 15) shows OFF-LINE and small diameter IN LINE types of installations of density meter. The points previously mentioned apply also to this configuration of installation. Additional points of merit are to always flow vertically downwards to improve the exit of any undesirable contaminants and also to ensure some degree of downstream back pressure to maintain take off pressure, prevent liquid dropout and high velocity noise due to excessive velocity.

All of the above examples of gas installation are based on the totally immersed vibrating element. Whilst there are many complex design aspects, the main reasons for the use of this type of element is the sensitivity required for accurate gas density measurement which restricts the wall thickness of the element. This in turn means that the alternative element with fluid on just the inside could not withstand typical gas application pipeline pressures.

1.5 LIQUID APPLICATIONS

FIGURE 16 As mentioned previously, generally, only 2 of the 3 methods of installation are used on liquid service. Unlike the gas applications, liquid applications utilize both types of vibrating element.

IN-LINE liquid measurement should be used when the liquid has a large thermal expansion coefficient.

Table 1 taken from IP Petroleum Measurement Manual, Part VII Density, Section 2, Continuous Density Measurement, shows 4 good product examples.

TABLE 1. Differences in pressure and temperature that will each cause a change in liquid density of 0.03 per cent.

STABILIZED CRUDE OIL	
Density	0.850g/ml
Temperature coefficient	0.0007g/ml°C
Pressure coefficient	0.00007g/ml/bar
Therefore	
Maximum temperature difference	0.4°C
Maximum pressure difference	4 bar
*LIQUID BUTANE AT 0°C	
Density	0.580g/ml
Temperature coefficient	0.0011g/ml°C
Pressure coefficient	0.00025g/ml/bar
Therefore	
Maximum Temperature difference	0.16°C
Maximum Pressure difference	1.2 bar
*LIQUID PROPANE AT 0°C	
Density	0.520g/ml
Temperature coefficient	0.0015g/ml°C
Pressure coefficient	0.0003g/ml/bar
Therefore	
Maximum Temperature difference	0.10°C
Maximum Pressure difference	1.0 bar
GASOLINE	
Density	0.660g/ml
Temperature coefficient	0.00075g/ml°C
Pressure coefficient	0.00019g/ml/bar
Therefore	
Maximum Temperature difference	0.26°C
Maximum Pressure difference	1.58 bar

*** NOTE:** The above values are specific to the conditions quoted and change dramatically around the critical region.

From this table it can be seen that a 1 degree C difference in temperature between the point of flow measurement will generate 0.3% of reading error on propane and almost 0.2% of reading error on butane, making an **IN-LINE** density meter essential for these 2 liquids if 0.1% of reading is to be realistically achieved.

The installation position can be upstream or downstream. Upstream disturbances have more effect on the flow meter performance. Upstream distances without any intrusive objects are usually greater than downstream therefore downstream is normally preferable. However, if the flow meter itself causes a significant pressure loss which in itself causes a temperature change then upstream installation is the more obvious choice.

OFF-LINE measurement is the most common method for liquid density measurement, especially for viscous and dirty fluids.

The differential pressure required to induce a suitable flow rate through an **OFF-LINE** density meter can sometimes be provided by such means as a pitot-tube scoop arrangement, or a main stream pipeline restriction device like a part closed valve or orifice plate, or bend in main stream pipeline etc. However, in order to provide a reliable flow rate and any additional pressure for proving, a pumped system is often necessary. We will consider this aspect in more detail as we review the common configuration of liquid installations as seen in **FIGURE 17**.

"L1" **FIGURE 18** is a basic pumped **OFF-LINE** system. This provides a rapid system response time irrespective of flow rate. Some density meter manufacturers design and supply custom built packages based on knowledge and experience of this type of measurement but many are also built by metering companies and end users. Whilst every application has some unique constraints and requirements the following general guidelines can be considered.

- A) Inlet pipe work length should be kept to a minimum and thermally lagged to ensure temperature equilibrium.
- B) When using a pump a minimum of 180 degrees, ideally 270 degrees, of bends in the pipe work should be placed between the pump outlet and the density meter inlet. Good quality density meters are designed with good immunity to external mechanical vibration even when transmitted via the connecting pipe work. However, the small, pressure pulsation outputted from a typical centrifugal pump can be transmitted via the fluid to the density meter. The frequency range of this

pulsation can be the same as the operating frequency or a harmonic resonance of the vibrating element. This can cause an unstable output and under extreme conditions an offset in the performance. 180 degrees of pipe bends will normally eradicate this.

With dual density meters on a typical fiscal metering station the same effect can occur between the 2 density meters if they are operated close together in series. This is not normally a problem as the conventional installation method is to operate them in parallel on identical pipe work configurations to avoid different thermal gradients and maintain operation if one unit is removed.

- C) On a few occasions the parallel installations can show a small bias. The installation of a small volume header appears to resolve this effect.
- D) When selecting a pump always ensure it will not cause the liquid to cavitate or generate bubbles from dissolved gases. Incorrect sizing of the pump can also significantly elevate the liquid temperature. Different manufacturers and their various models have different recommended flow rates. In general most operate efficiently at around 50 litres per minute. This should be reduced to 20 litres per minute if the liquid has abrasive solid particles, to reduce the effect of erosion. The normal minimum flow rate of 4 to 5 litres per minute should ensure the fluid velocity overcomes the surface tension of bubbles on the measurement element and prevent the deposit of solids.
- E) Correct orientation of this type of **OFF-LINE** density meter will enhance the reliability of measurement. 3 tube and some 2 tube types which do not have a straight through flow path should be mounted horizontally to prevent any build up of vapour or particles at low flow velocities. Twin and single tube types with a straight through flow path are best mounted vertically with upwards flow. On dirty applications with significant solid particles the flow should be downwards.

If headroom or pipe work constraints prevent vertical installation other orientations can be used if the previous flow rates can be maintained. Irrespective of orientation on straight through flow path density meters, a minimum of 10 diameters of straight pipe should be used on the upstream pipe work to alleviate effects of flow profile bias on the measurement tube. 90 degree elbows immediately upstream of the density meter have shown to offset the density meter performance under certain conditions which are difficult to predefine.

- F) For fiscal measurement using these **OFF-LINE** density meters, especially when they are installed on the common header of a multi tube metering system, pressure and particularly temperature in the density meter should be measured.

These readings should not only be used for correction of any systematic errors due to pressure and temperature coefficients of the density meter. The establishment of powerful flow computers permits continuous comparison, correction and or alarms to be performed relative to the values of pressure and temperature at the point of volume flow measurement.

- G) One of the major application problems of density measurement on off shore crude oil is the deposition of high melting point wax on the measurement tube especially when the flow is stopped and the density meter cools down. Anti-waxing agents and sophisticated hot kerosine flushing systems have been previously used to overcome this problem. A new approach has been developed, originating from the even more demanding application of density measurement of Bitumen. Many of these type of **OFF-LINE** density meters are designed and perform like a thermos flask mainly to eliminate the effect of ambient conditions. The adverse effect of this is the density meter is difficult to heat trace. With the fitting of integral heat tracing this design aspect becomes advantageous. Furthermore, the integral PT100 element can be used for precise regulation of heat required by way of a user selected "wax pour point". It can be said that an elevated operating temperature of the density meter could increase the overall uncertainty of measurement but in the "**REAL WORLD**" a wax free density meter, on an annual basis, will provide a more accurate performance.

- H) Whilst the liquid should ideally be at a pressure well above its vapour pressure, if you experience an erratic output due to the presence of undissolved gas, often a small amount of back pressure on the downstream side of the bypass pipe work will remove the problem. Like most conventional flow meters, density meters can measure "two phase" flow, but only one phase at a time!

"L2" is mechanically identical to the "G2" direct insertion **IN-LINE** density meter with a retractor mechanism. As previously mentioned, **IN-LINE** should be used when the liquid has a large thermal expansion coefficient. Due to the type of vibrating element this method should not be used when the viscosity of the liquid exceeds 20 centipoise or the location of the measurement is in a pigged line.

"L3" FIGURE 19 shows the pitot tube scoop method. The response time and thermal and pressure gradient will change with flow rate and condition of product. Therefore this method is only suitable when the span of the flow rate is known to generate sufficient differential pressure. Each application will require specific design based on product composition, line size and flow rate. Under low flow conditions, stratification of density and "vapour locks" can occur in the by-pass pipe work.

"L4" FIGURE 20 shows the use of a main pipeline restriction to generate a flow around the by-pass pipe work. The operating characteristics are similar to the pitot tube scoop method. Additional care is needed to ensure the potential downstream gas bubbles do not adversely effect any other measurement devices. An advantage of this method can be the ability to fine tune the system on site by use of a partially closed valve as the restriction in the main pipeline. Downstream flow rate reduction must also be reviewed when installing this method of installation onto an existing process plant or pipe line.

"L8" FIGURE 21 is a pipe work configuration which has been successfully used on 50 to 100mm (2" to 4") diameter lines. Dependant on the flow rate and product condition etc the ratio of pipe diameters of the two lines can be varied. With the 3 valves shown, flow rate, back pressure and isolation for maintenance can be achieved. Using the "pipe splitter" shown, this installation has been particularly successful on applications where the 3 previous OFF-LINE installations can have problems in achieving a representative by-pass sample of a non homogeneous liquid.

"L5" FIGURE 22 is the most cost effective method of liquid density measurement. The selection and operating criteria are the same as "L6", "G3", "G4" and "G5". Caution is required with other liquid density meters where the vibrating element is directly in the main stream flow path. These types of devices are often flow rate sensitive and susceptible to a higher degree of contamination.

"L9" FIGURE 23 is another cost effective compact method of OFF-LINE density meter installation. The differential pressure required to flow the product around the by-pass pipe work is achieved by the inlet being positioned at the external radius, high velocity, high pressure point of a pipe work bend. The outlet is positioned at an angle suited to the lower velocity and pressure internal radius position of the same or downstream bend. This method should only be considered when measuring low viscosity fully homogeneous clean liquids. The centrifugal forces at ~~the~~ can cause separation where the heavier components move towards the external radius of the bend.

Now we have completed our review of the installation methods, I would like to suggest a simple rule which a metering engineer unfamiliar with density measurement may find helpful.

MASS FLOW SYSTEM ACCURACY WITH DENSITY MEASUREMENT IS DEPENDENT ON YOUR ABILITY TO DEFINE THE TEMPERATURE EXACTLY AT THE POINT OF FLOW AND DENSITY MEASUREMENT.

In most cases the above is a large potential component to the overall uncertainty of accurate mass flow measurement.

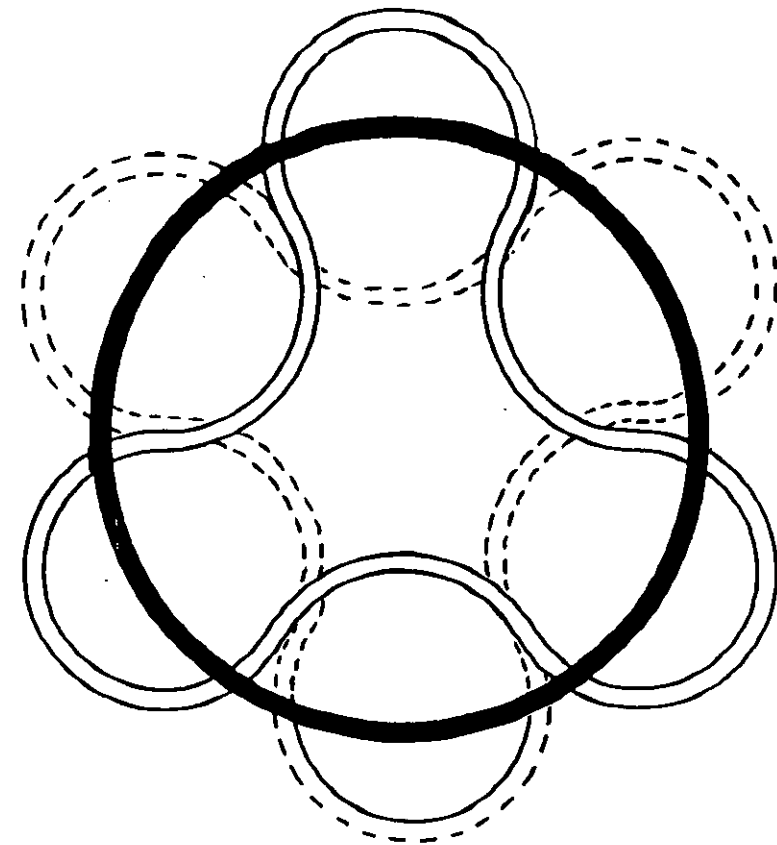
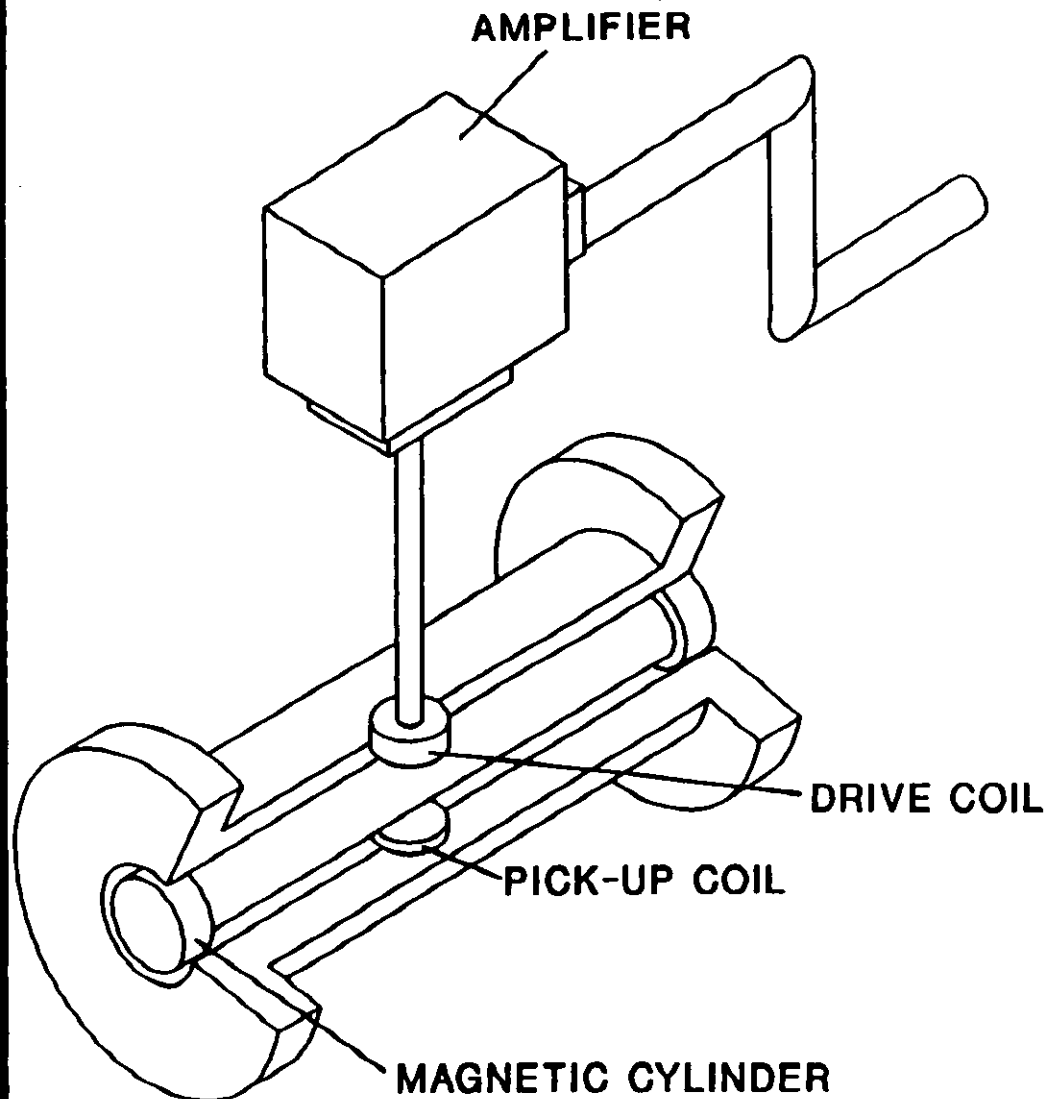
SUMMARY

In an attempt to provide guidelines for density measurement there will always be a minority of exceptions. The intent of this paper to improve the performance of density meters by the awareness of problems. From user awareness and supplier knowledge the best solutions and performance of density meters will evolve.

REFERENCES

1. The IP Petroleum Measurement Manual, Part VII, Density Section, 2 Continuous Density Measurement.
2. Experimental Evaluation of Densitometers In The Presence Of Condensation Or Wet Gas, By Dr S Kostic, Dr T M Svartas and G Staurland from the Rogaland Research Institute presented at the 8th North Sea Flow Measurement Workshop in 1990.
3. Installation Details For Gas Densitometers at the 9th North Sea Flow Measurement Workshop, by Mr Reidar Sakariassen from Statoil.
4. "REAL WORLD" at many previous workshops by Mr Brian Henderson from Amoco.

PRINCIPLE OF OPERATION



HOOP MODE
VIBRATION

Figure 1

FD700

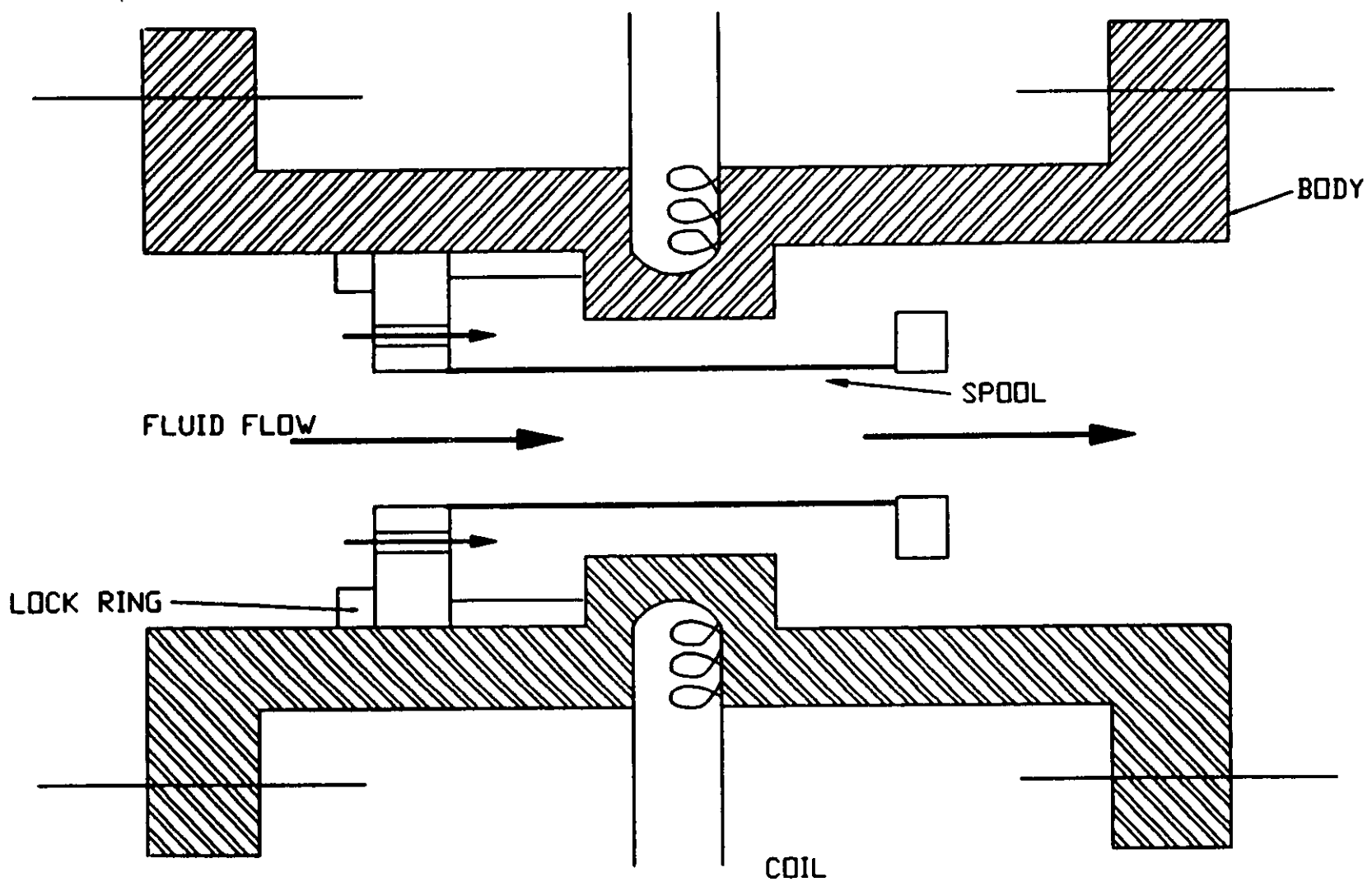
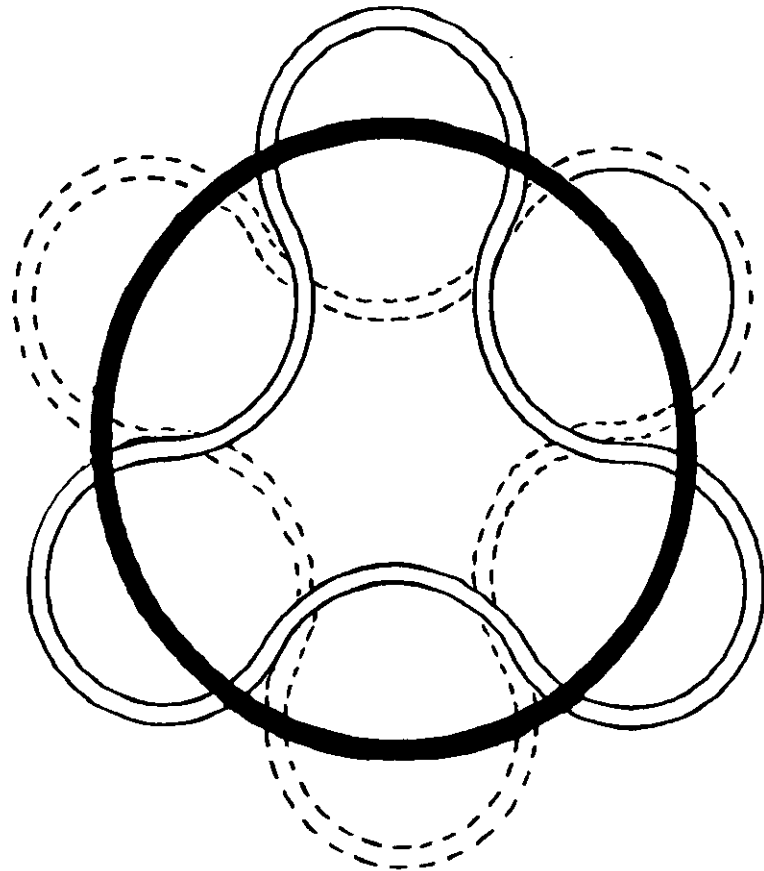
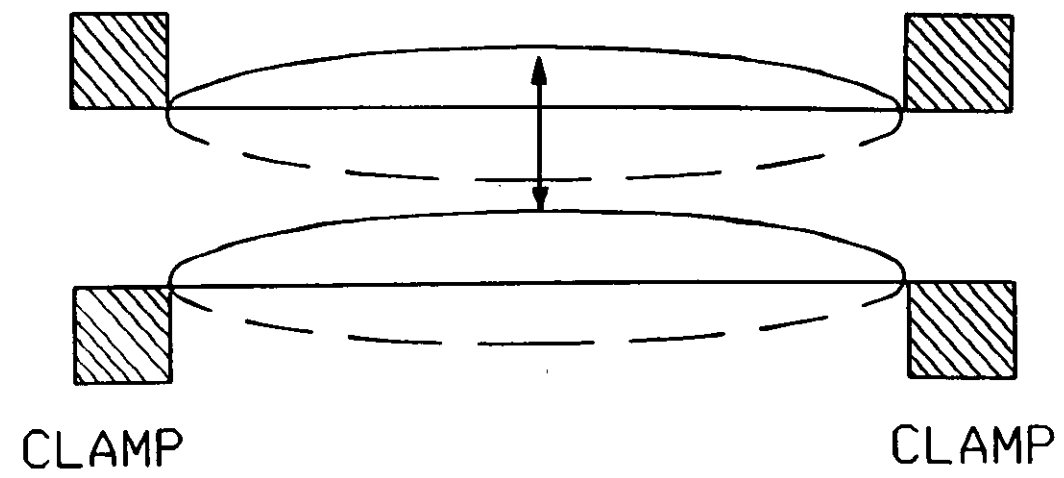


Figure 2

PRIME VIBRATION PRINCIPLES



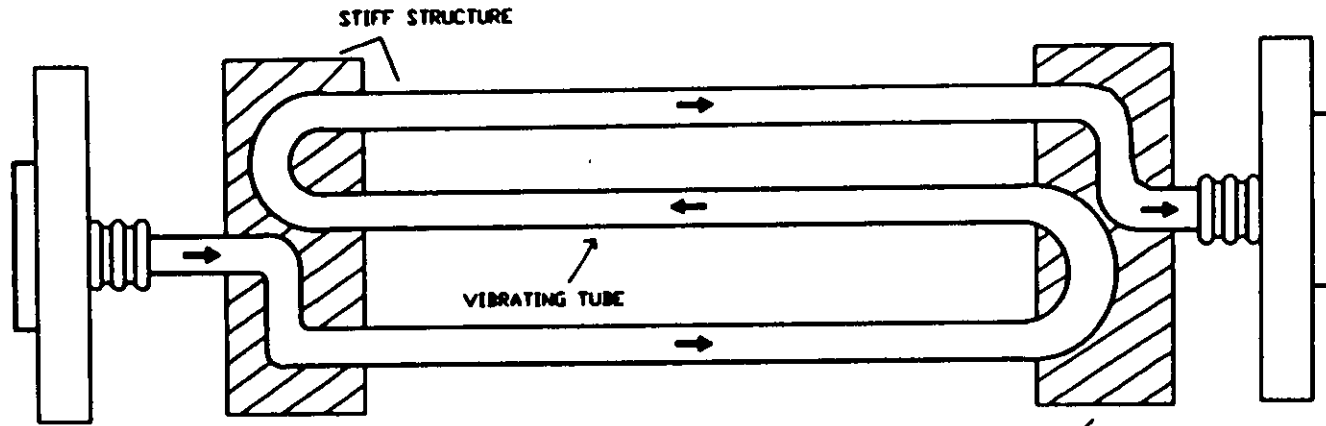
*HOOP MODE
VIBRATION*



*TRANSVERSE MODE
OF VIBRATION*

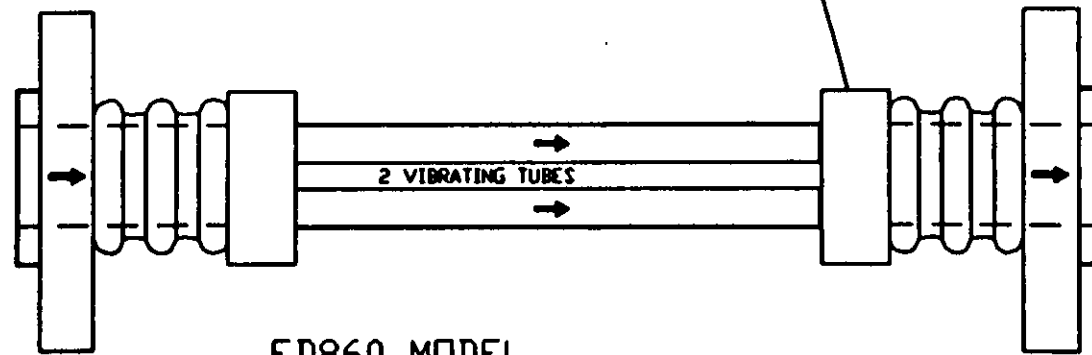
Figure 3

FD800 SERIES



FD810 - 850 MODELS

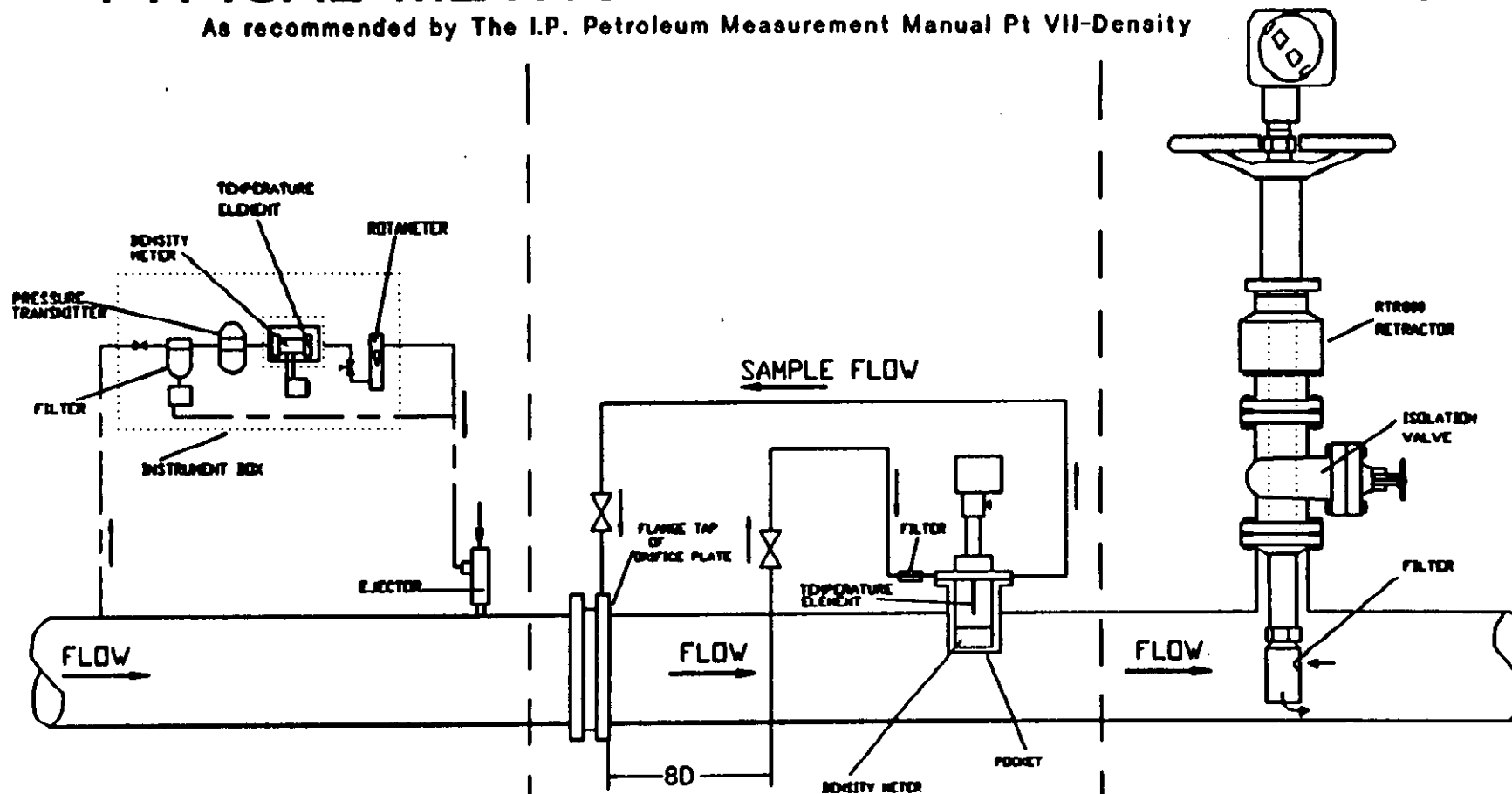
MANIFOLD



FD860 MODEL

TYPICAL METHODS OF GAS INSTALLATION

As recommended by The I.P. Petroleum Measurement Manual Pt VII-Density

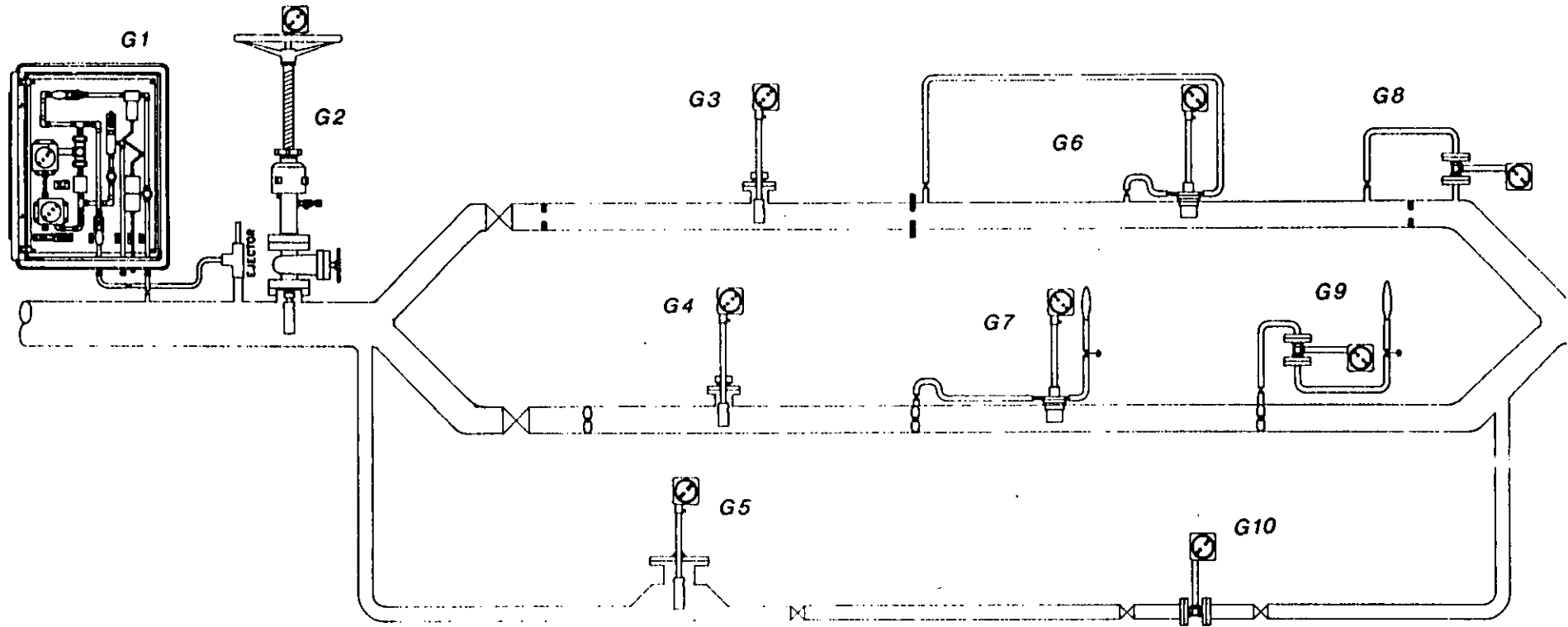


SG800 SPECIFIC
GRAVITY SYSTEM
'OFF-LINE'

PD700 POCKET DENSITY METER
'ON-LINE'

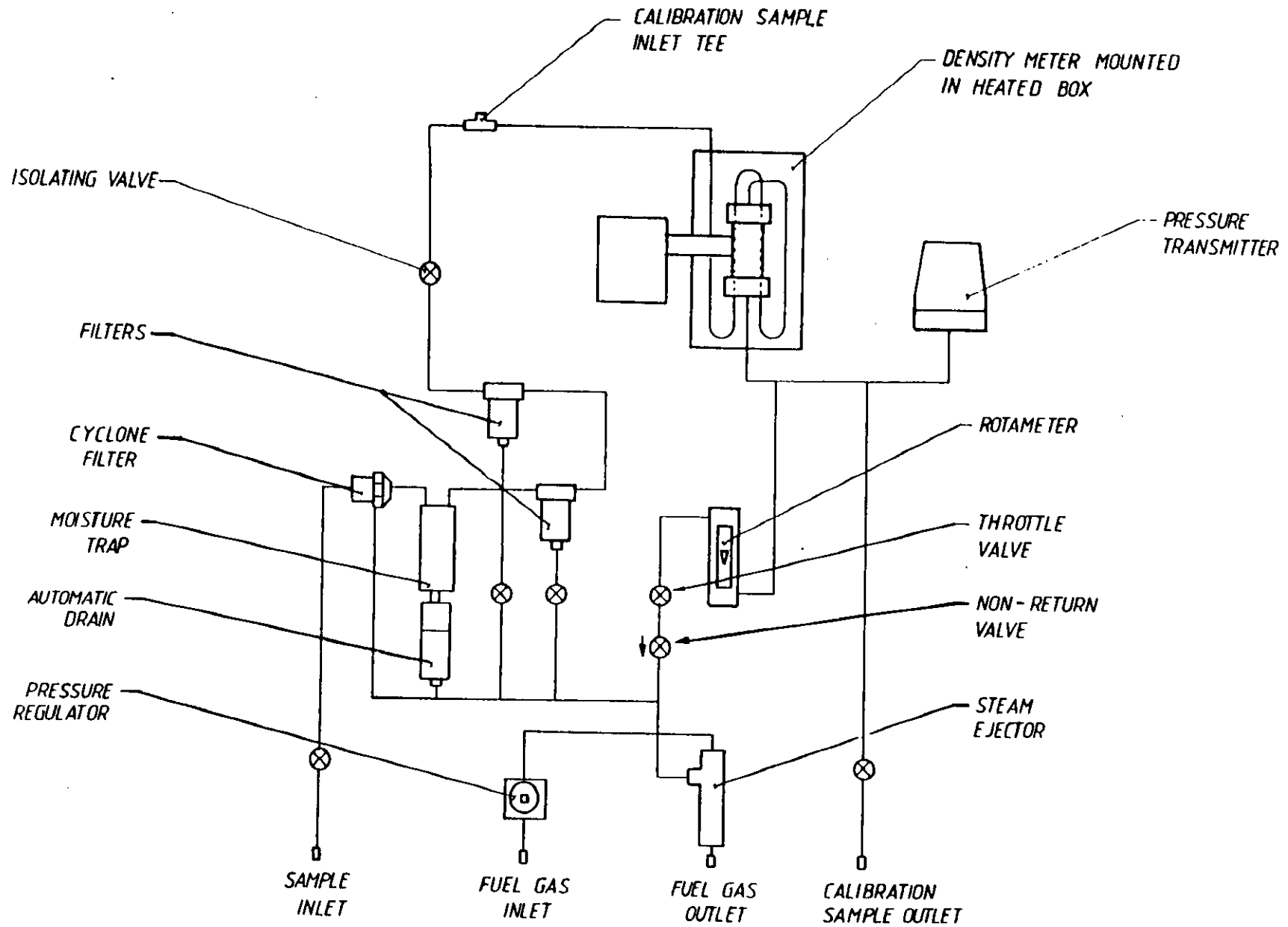
ID700 DIRECT INSERTION
DENSITY METER
'IN-LINE'

Figure 6



Typical GAS Installation Configurations

Figure 7



OFF-LINE Gas Filter System

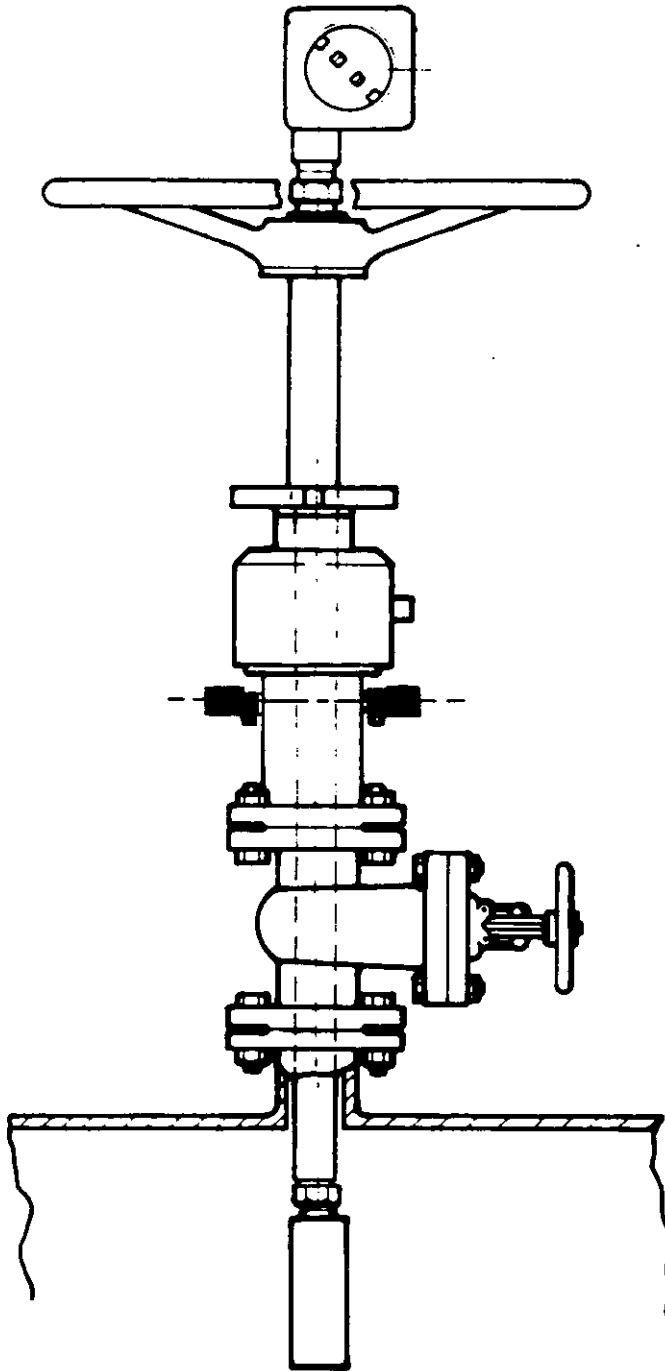
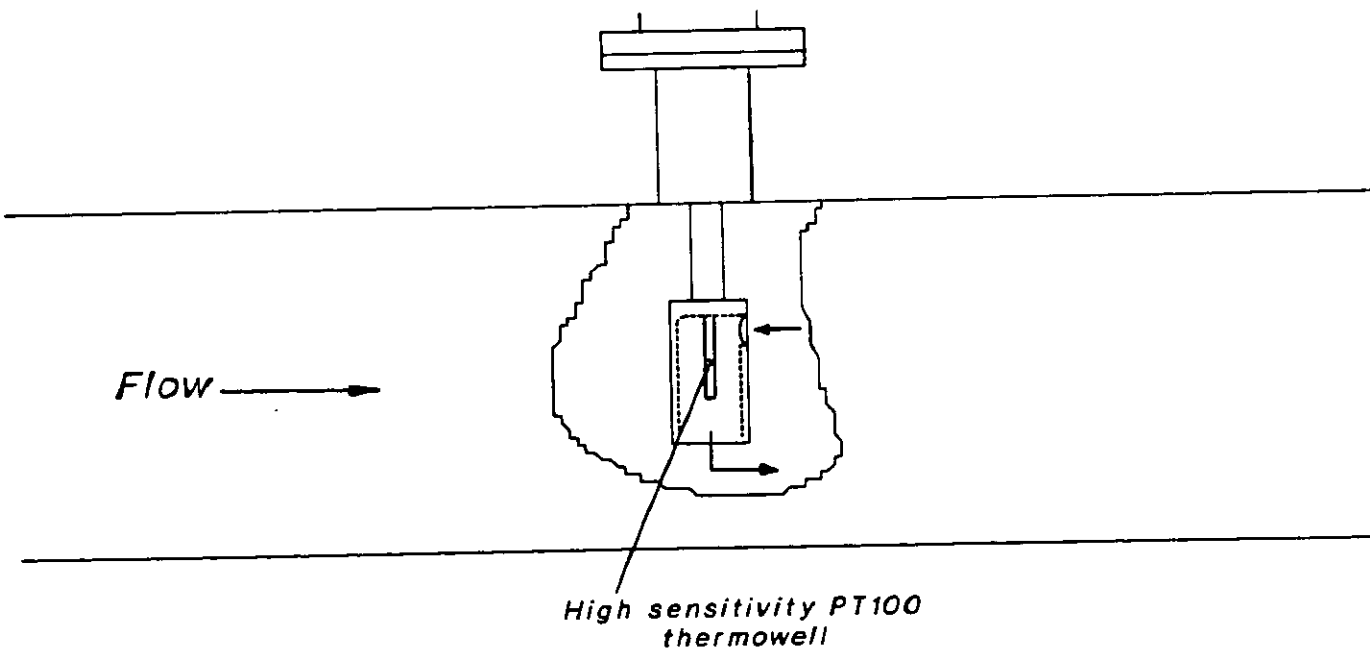
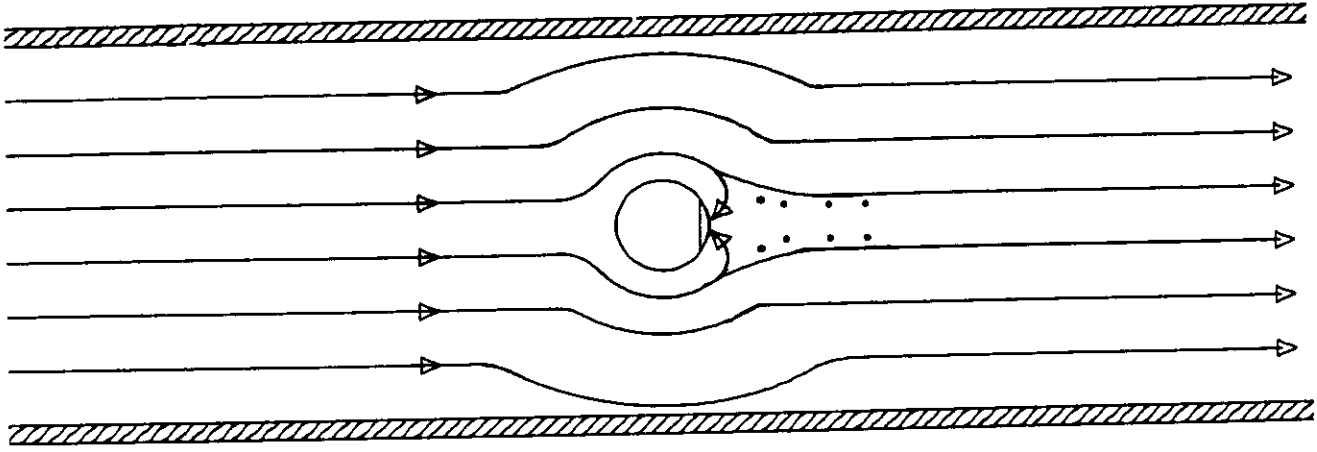


Figure 8

*IN-LINE Direct Insertion Density Meter
With High Pressure Retractor
& Calibration Connections*

Figure 9



*Flow Path Performance of an
IN-LINE Direct Insertion
Density Meter*

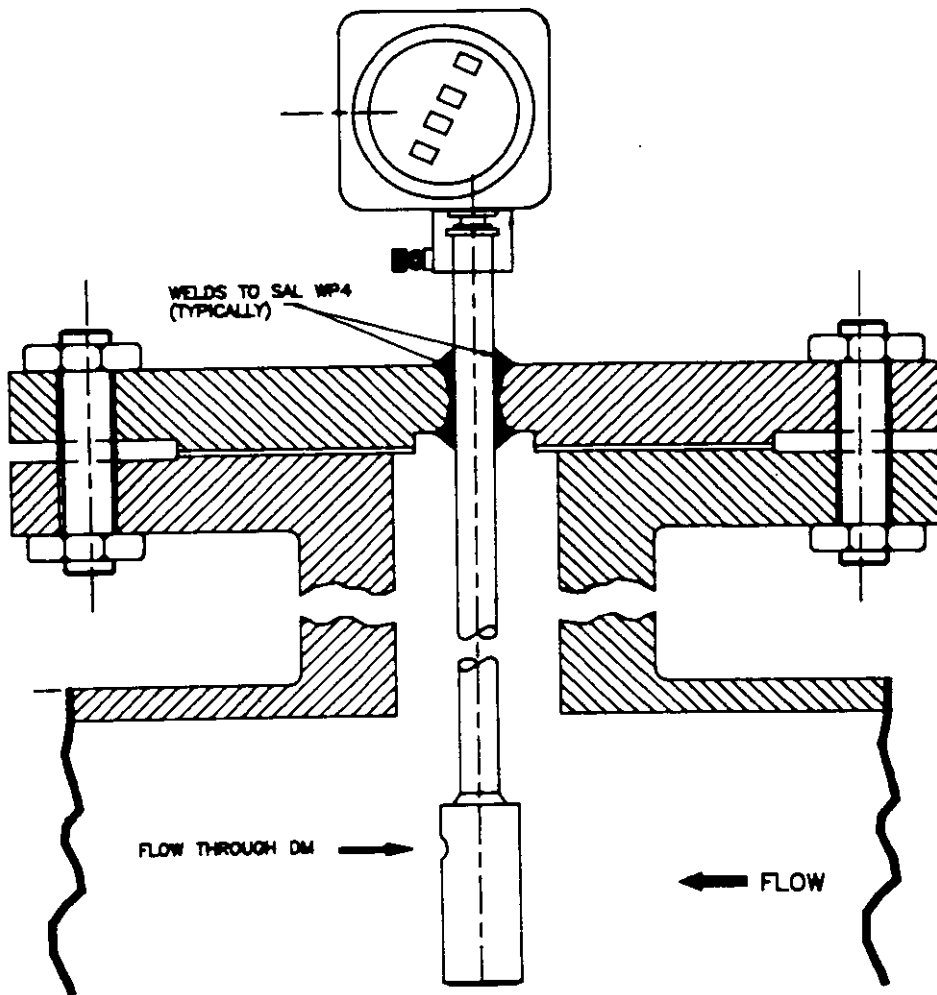


Figure 10

*IN-LINE Direct Insertion Gas Density Meter
With Welded Flange*

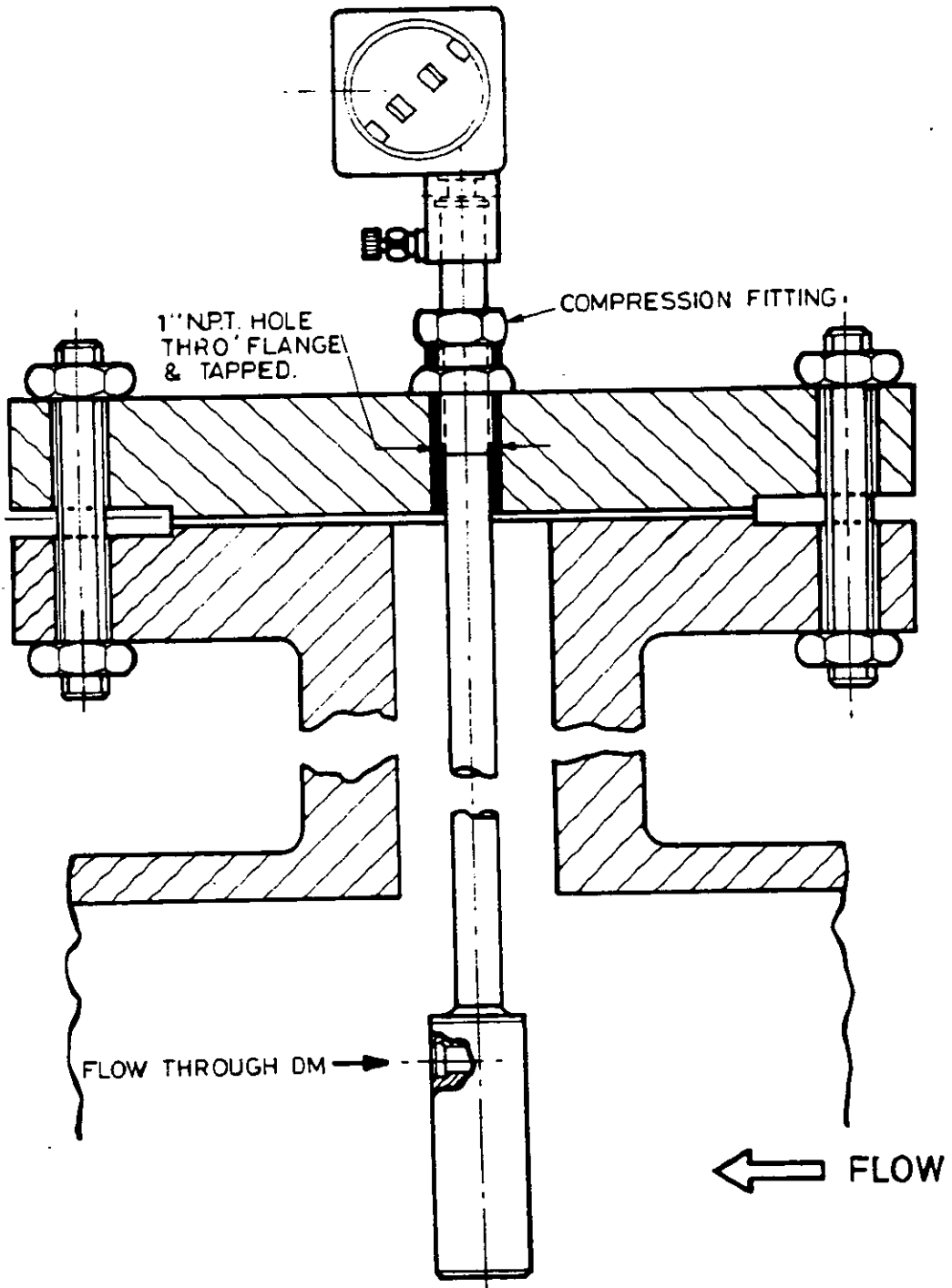


Figure 11

*IN-LINE Direct Insertion Density Meter
With Compression Fitting-Type Flange*

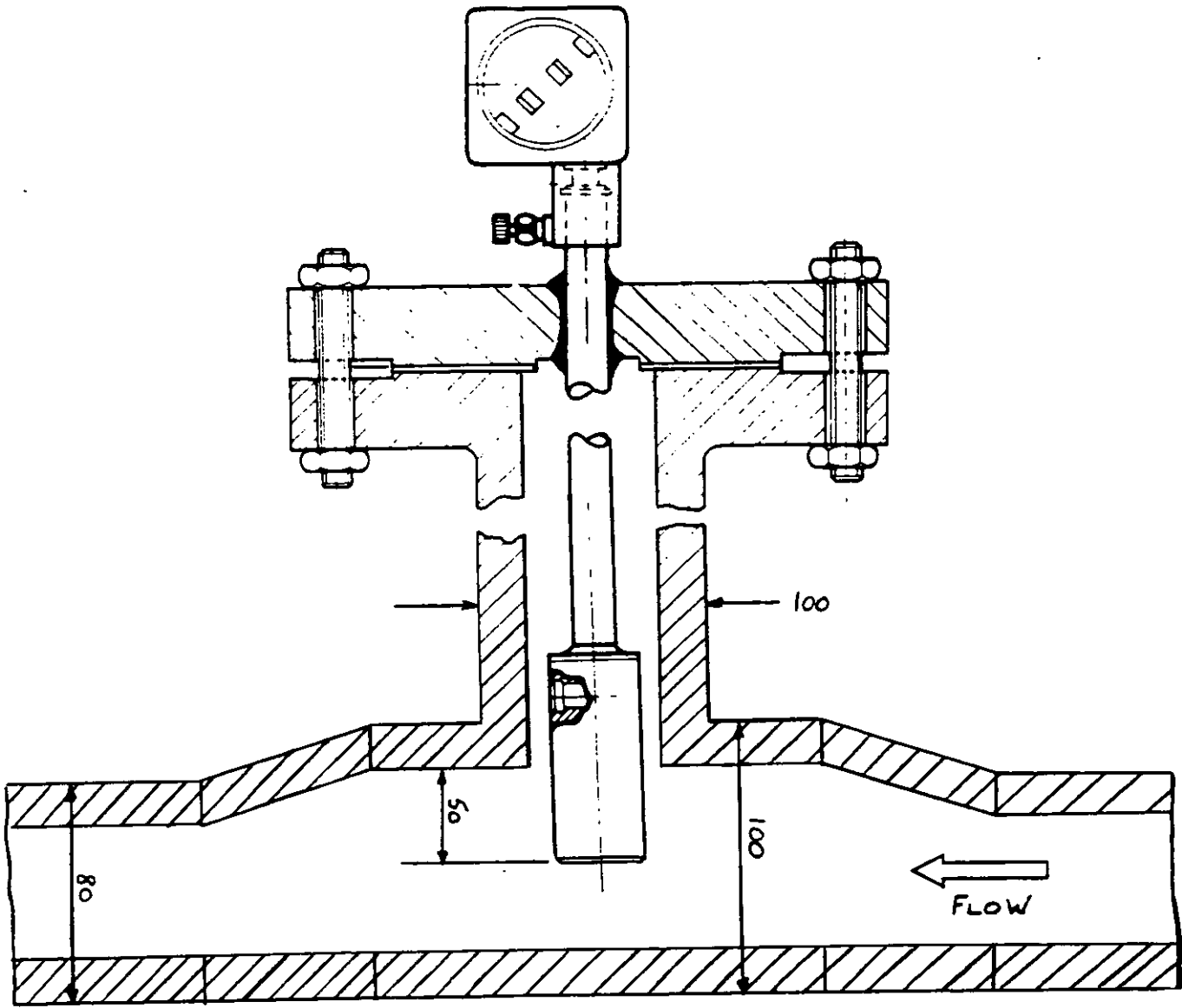
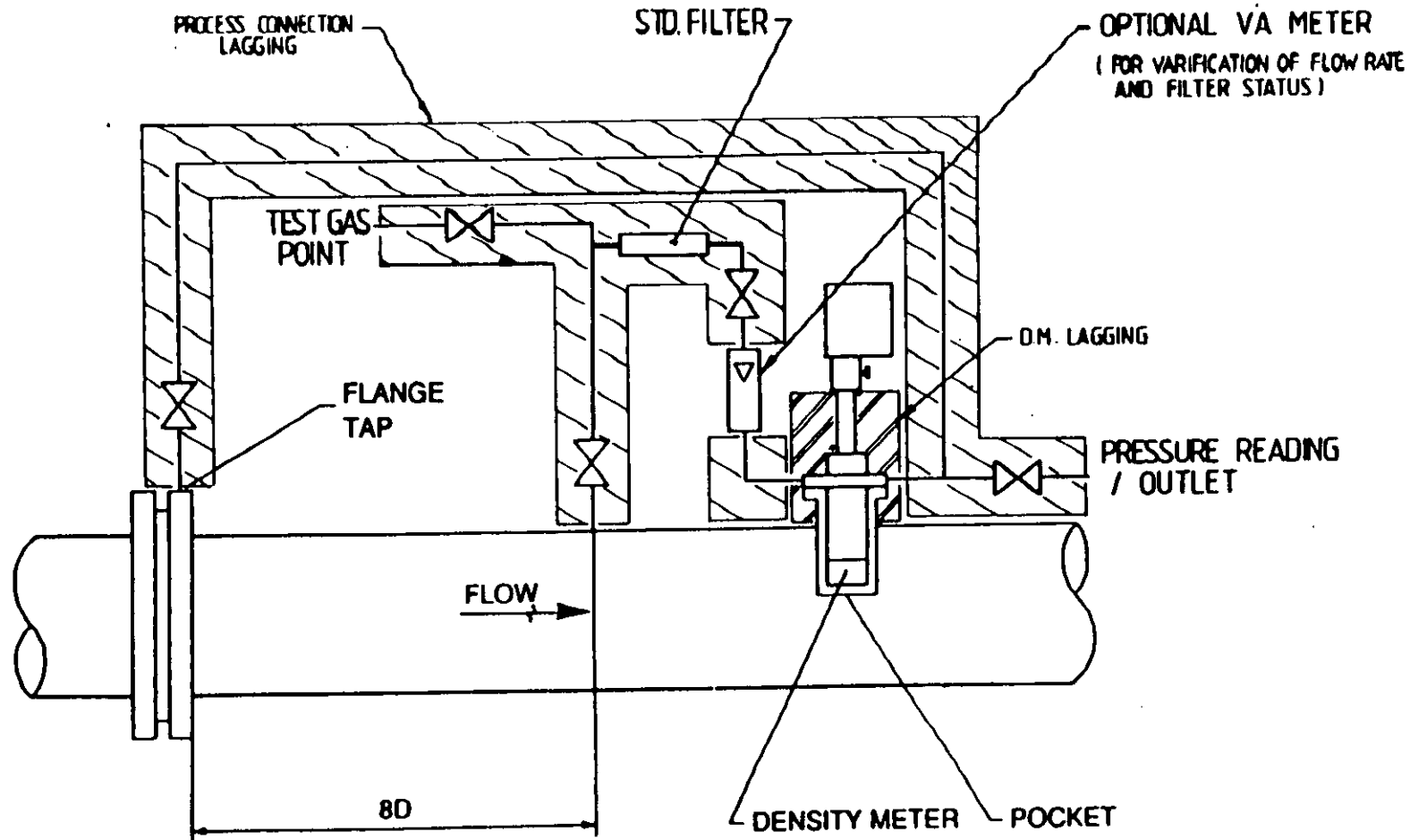


Figure 12

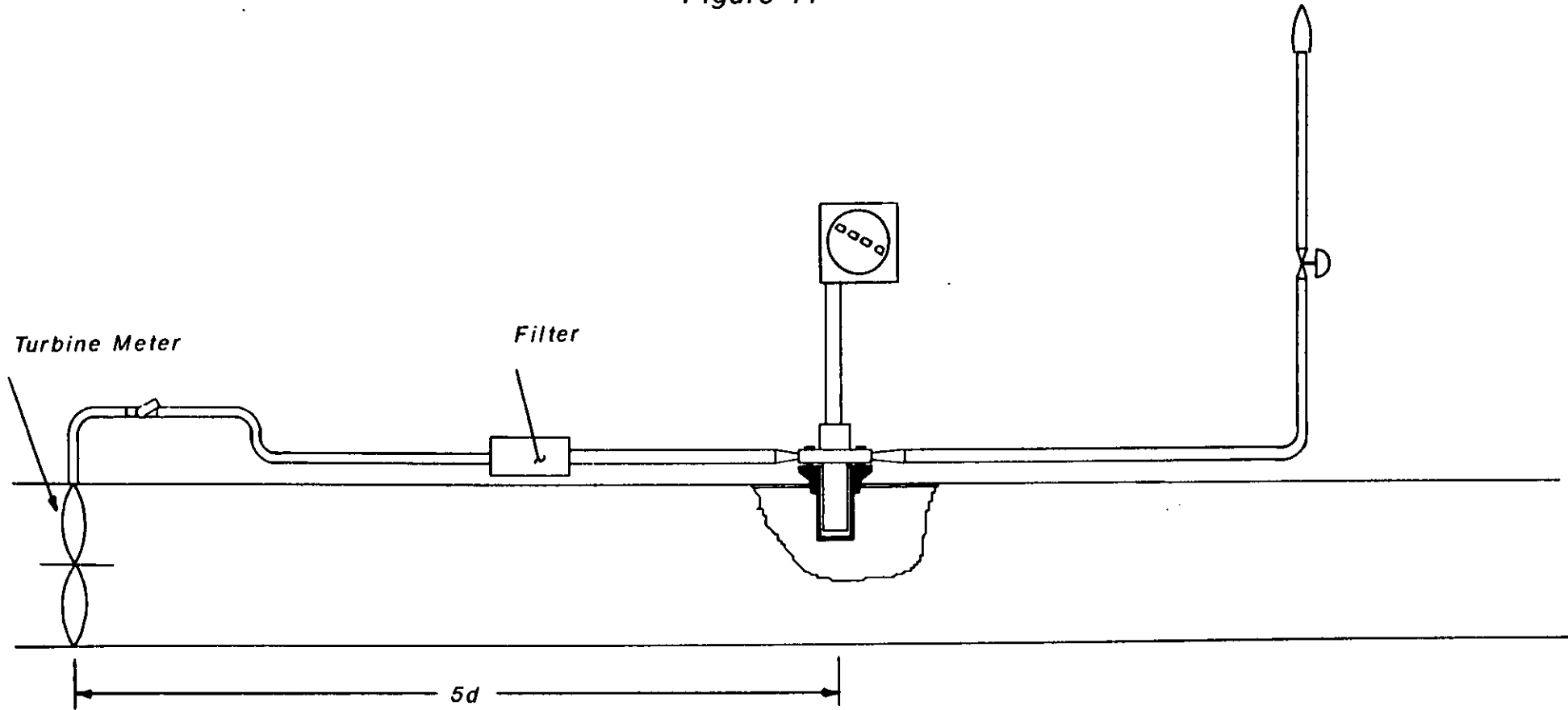
*IN-LINE Direct Insertion Density Meter
For Pipes of <100mm Diameter*

Figure 13



INSTALLATION OF GAS DENSITY METER ON AN ORIFICE PLATE SYSTEM USING THE PRESSURE RECOVERY METHOD TO AVOID UNREGISTERED FLOW

Figure 14



Typical "ON-LINE" Pocket Density Meter
installation with a gas turbine meter

CONNECTIONS	
1	10 - 20V GAS
2	OUTPUT
3	0V (EARTH)
Z	PLATINUM RESISANCE THERMOMETER (IF FITTED)
X	
Y	
W	

CABLE ENTRY 1/2" NPT
HOLE (FOR CABLE GLAND
OR CONDUIT CONNECTION)

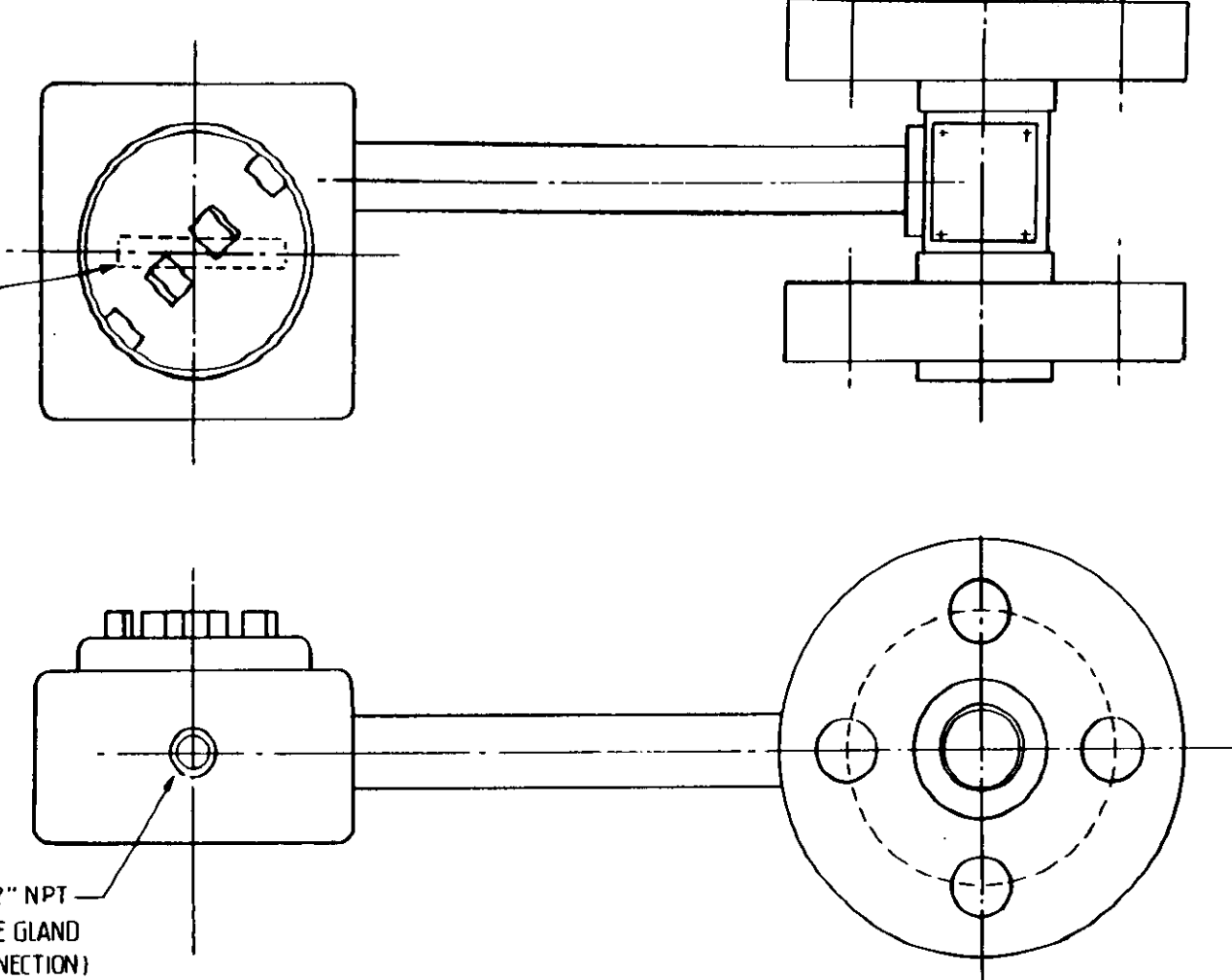


Figure 15

OFF-LINE Flanged By-pass Gas Density Meter

TYPICAL METHODS OF LIQUID INSTALLATION

As recommended by the I.P. Petroleum Measurement Manual Part VII - Density

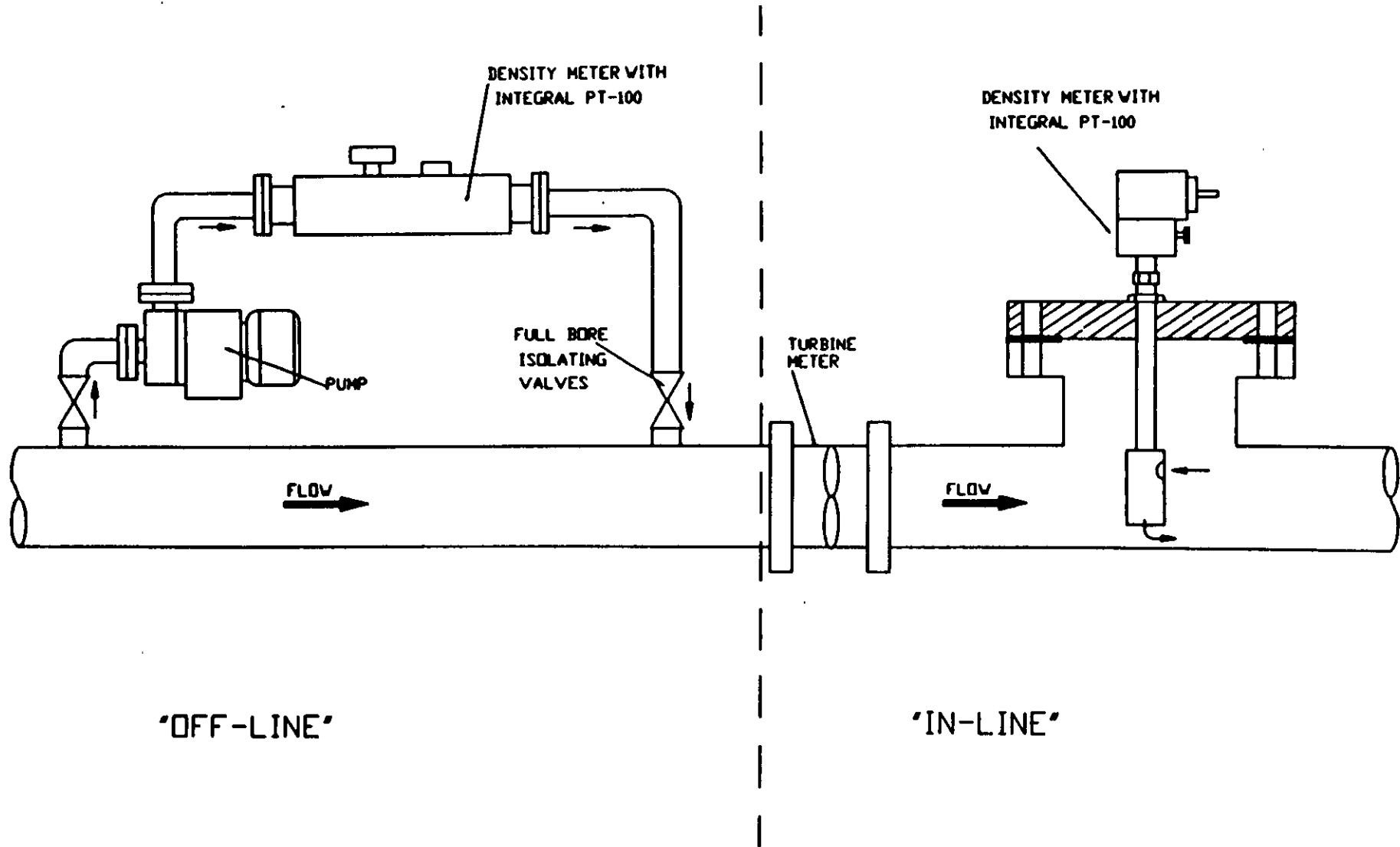
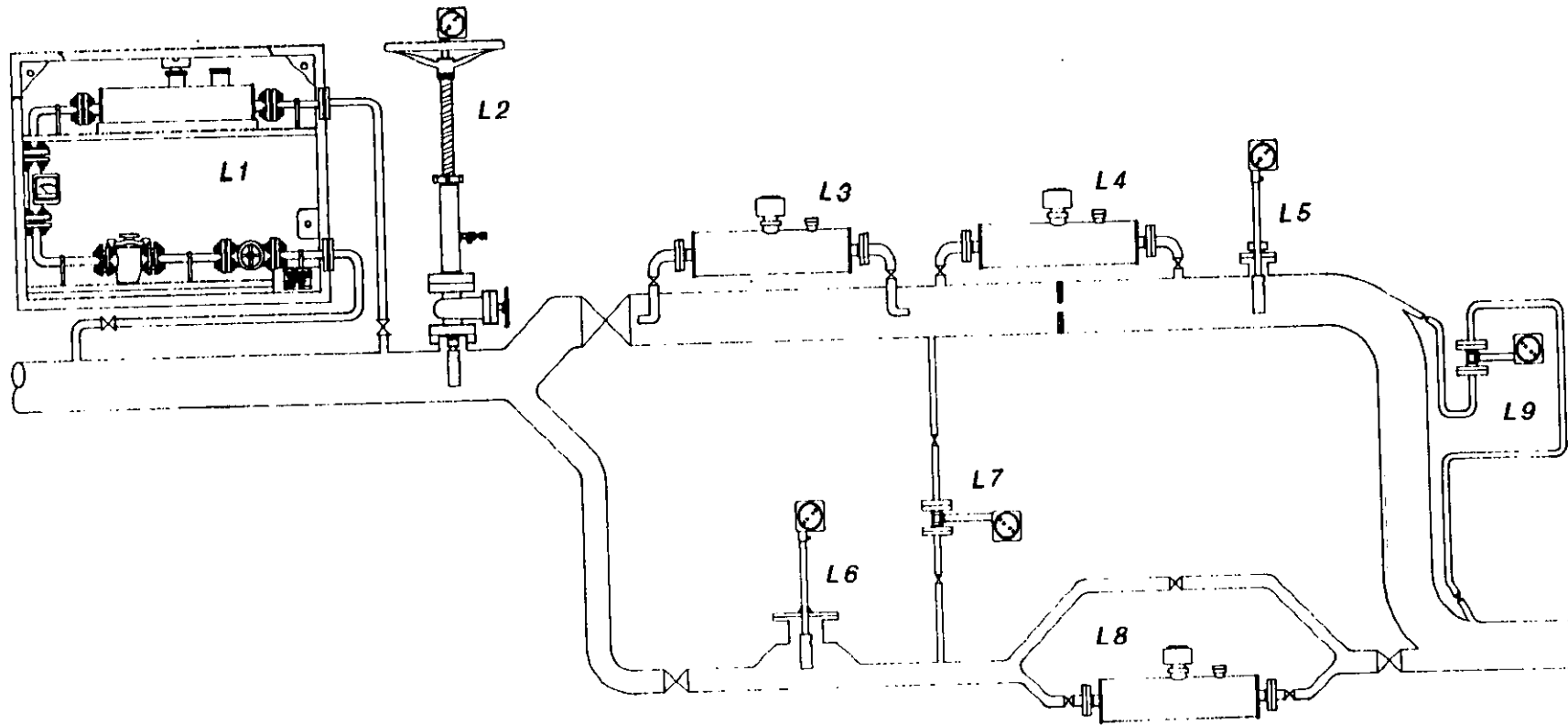
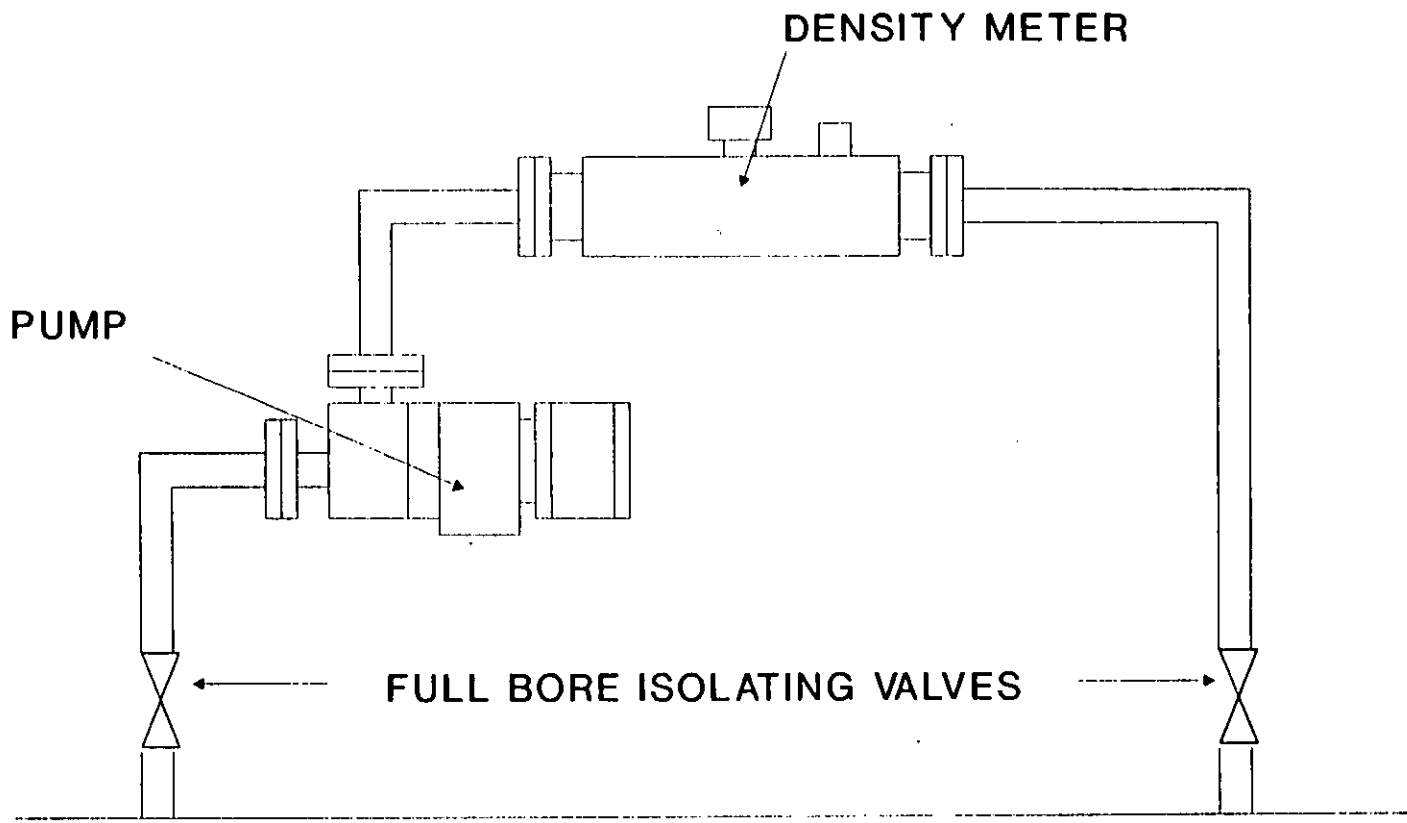


Figure 17



Typical LIQUID Installation Configurations



DENSITY METER

PUMP

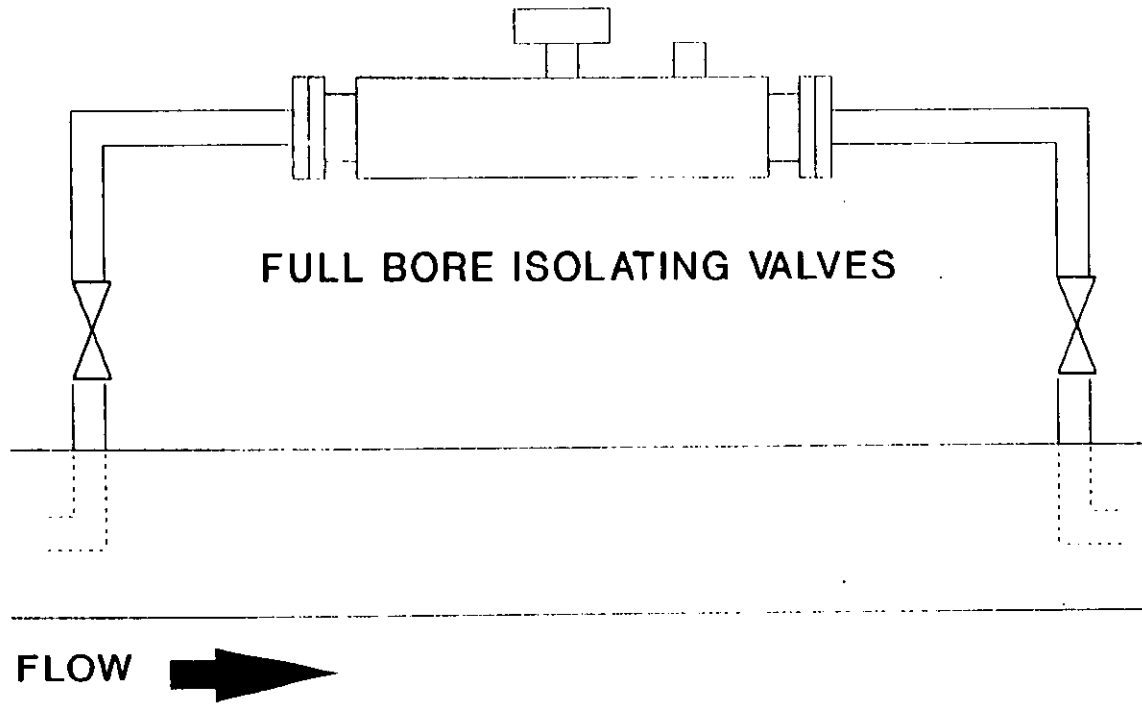
FULL BORE ISOLATING VALVES

FLOW 

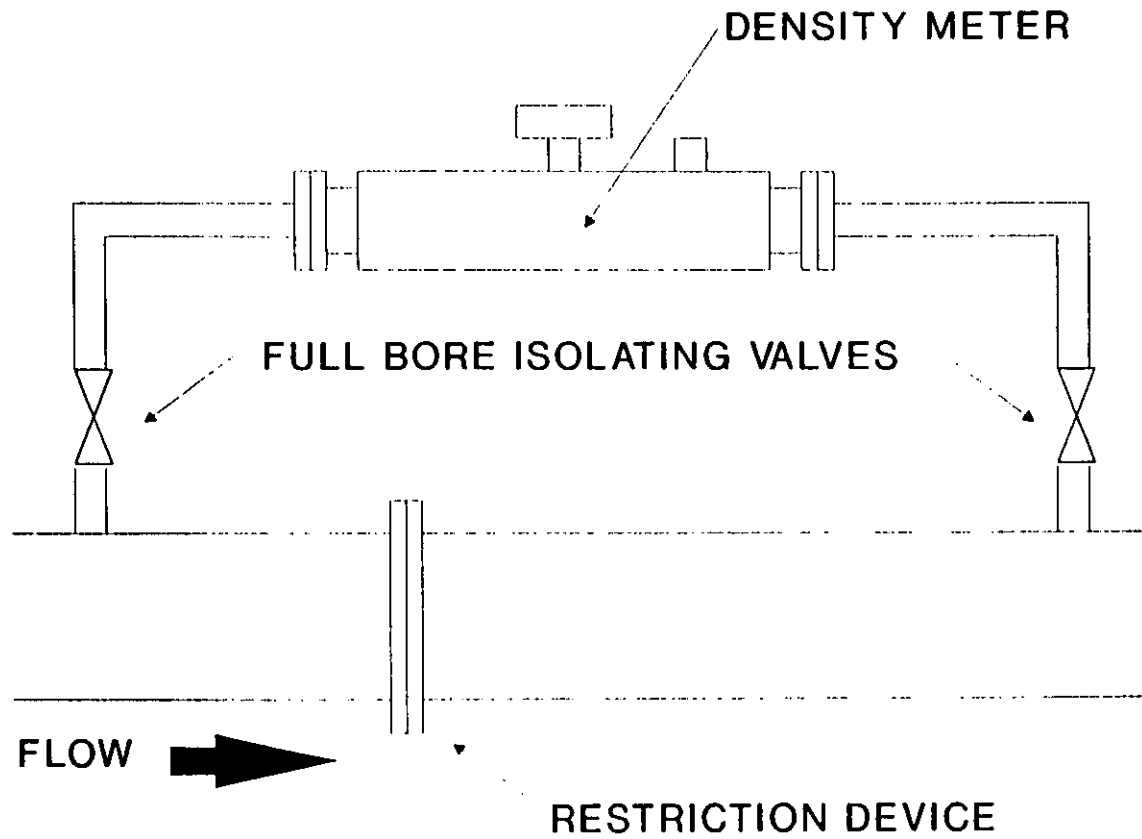
INSTALLATION WITH PUMP

Figure 19

DENSITY METER

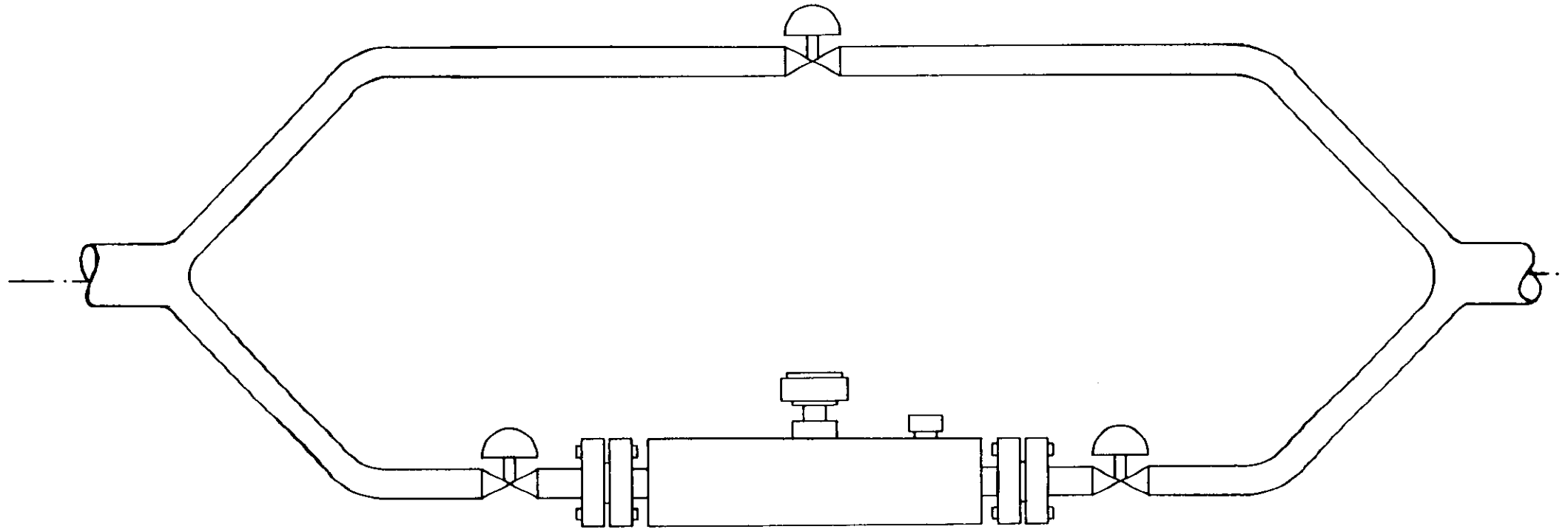


INSTALLATION WITH PITOT TUBE SCOOPS



A RESTRICTION DEVICE TO CREATE A PRESSURE DIFFERENTIAL

Figure 21



*BY-PASS Configuration for
use with 50 to 100mm Diameter Lines*

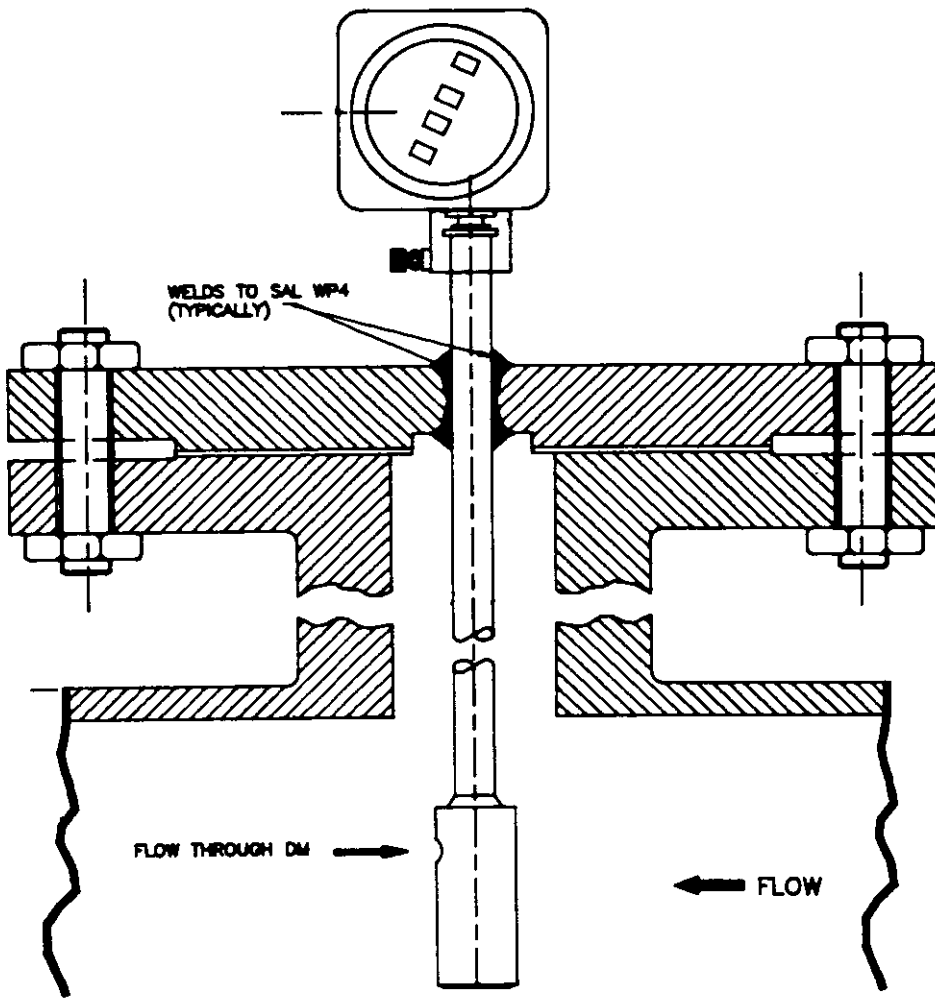
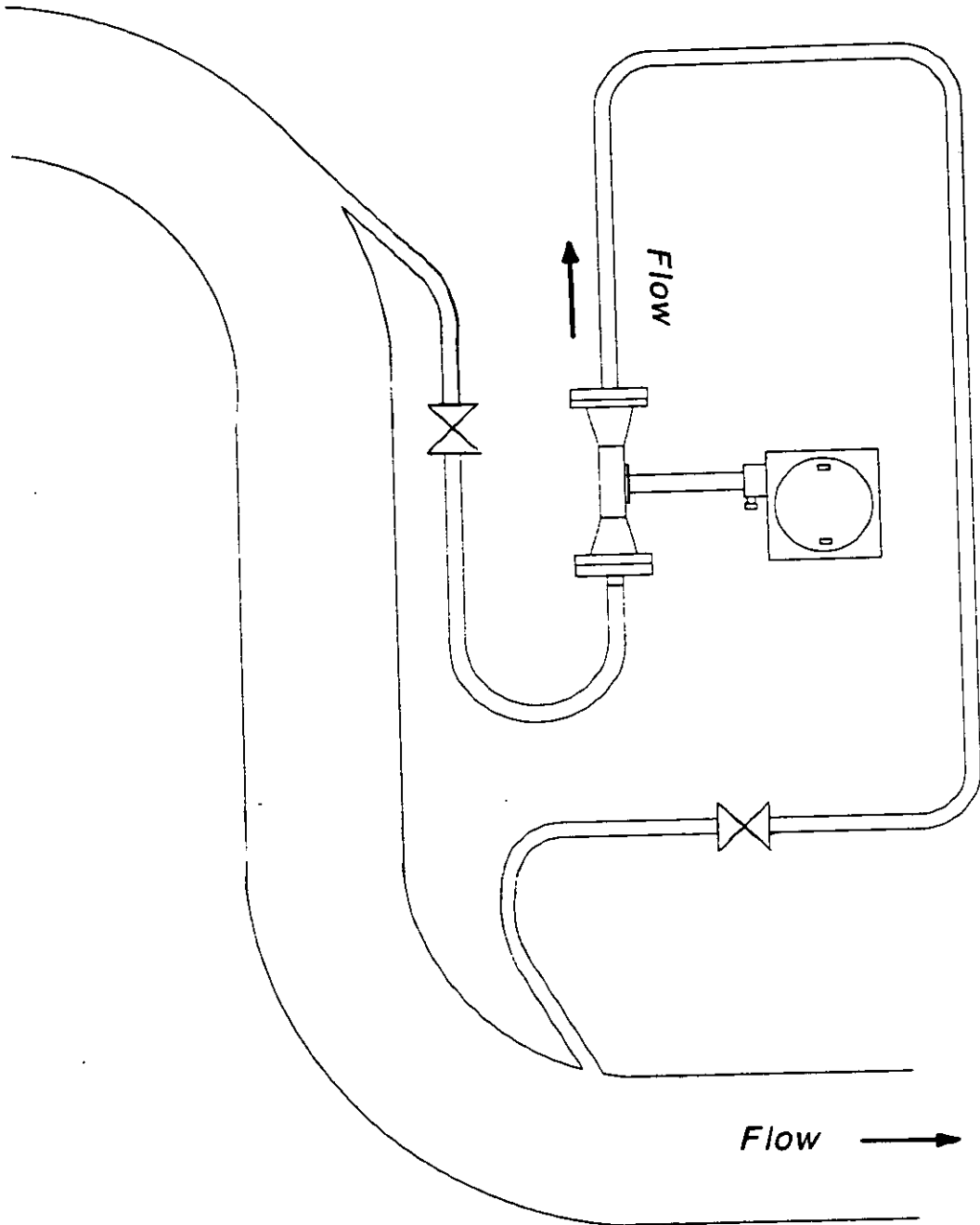


Figure 22

*IN-LINE Direct Insertion Liquid Density Meter
With Welded Flange*

Figure 23



*OFF-LINE density meter
utilising the differential pressure
of main-stream bends*

A NEW MULTI-BEAM ULTRASONIC FLOWMETER FOR GAS

by

A Lygre, CMI, R Sakariassen, Statoil
and D Aldal, Fluenta

Paper No 5.1

NORTH SEA FLOW MEASUREMENT WORKSHOP
26-29 October 1992

NEL, East Kilbride, Glasgow

CONTENTS		Page
1	INTRODUCTION	1
2	MEASUREMENT PRINCIPLE	2
3	SYSTEM DESCRIPTION	4
4	FLOW METER PERFORMANCE	6
	4.1 Calibration tests	6
	4.2 Flow analysis	9
5	SPECIAL FEATURES	14
6	PROVING	15
	6.1 Zero calibration	15
	6.2 Flow calibration	16
	6.3 Self diagnostics	16
	6.4 On-site zero calibration	18
7.	CONCLUSIONS	18
8.	ACKNOWLEDGEMENTS	19
	REFERENCES	

**A new
multi-path ultrasonic flow meter
for gas**

**Asle Lygre, Trond Folkestad, Christian Michelsen Research AS
Reidar Sakariassen, Statoil AS
Dag Aldal, Fluenta AS
Norway**

ABSTRACT

Offshore metering stations based on orifice plates are bulky and require much space. Accordingly, the platform costs are considerable, and can be significantly lowered if the size of the metering station is reduced.

Ultrasonic transit time multi-path meters will allow compact metering stations to be constructed due to increased flow meter capacity and reduced installation lengths. In addition these meters offer improved flow meter performance and potential for simpler maintenance procedures.

A new multi-path flow meter for gas has been developed by Christian Michelsen Research in Norway. The flow meter has undergone testing on natural gas at K-Lab, Norway. The flow meter (FMU 700) will be manufactured by Fluenta AS.

The FMU 700 features new technical solutions such as titanium housed ultrasonic transducers, automatic gain control, on-line measurement of transit time delay in cables and electronics, and software pulse detection.

The deviations between the K-lab sonic-nozzle reference mass metering system and the FMU 700 are less than 0.8% at gas velocities between 1 and 8 m/s. These results were achieved with 10D straight inlet pipe downstream of a 90° bend. Tests were also performed with the FMU 700 installed only 5D downstream a 90° bend. At gas velocities between 2 and 8 m/s the measurement uncertainty is not changed despite the reduction in upstream straight pipe length from 10D to 5D. The observed deviations were independent of the test pressure varying from 55 to 100 bar. The test results show that it is quite feasible to build a very compact and light metering station compared to conventional solutions and at the same time comply with the requirements set to fiscal metering stations.

The following procedure is suggested for proving of a multi-path meter in a fiscal metering station :

- Zero calibration of flow meter when delivered from manufacturer.
- Flow calibration prior to installation in the metering station.
- Use of the flow meter's self diagnostic properties to indicate if and when zero calibration should be repeated.
- On-site zero calibration of individual transducer pairs which are removed from the pipe line and installed in a zero calibration cell.

1 INTRODUCTION

Offshore metering of natural gas has been, and still is, based on the orifice plate. This technology is proven and well known both to the operators and the authorities. However, metering stations based on orifice plates are bulky and require much space. Accordingly, the platform costs are considerable, and can be significantly lowered if the size of the metering station is reduced [1,2].

Statoil, as a major gas producer, has been concerned with reducing the costs of offshore metering of gas [1]. Based on the general development within electronics and sensor technology during the 80's, it became clear that multi-path ultrasonic flow meters represented a realistic alternative to orifice plates. Specifically, multi-path meters would allow compact metering stations to be constructed due to increased flow meter capacity and reduced installation lengths. In addition these meters offered the advantages of :

- low uncertainty,
- no moving parts,
- no pressure loss,
- rapid response,
- potential for omitting flow calibration,
- self-checking possibilities,
- reduced maintenance.

Thus, it was recognized that introduction of ultrasonic meters would both reduce costs and improve flow meter performance. In a study carried out by Statoil, savings of 100-150 mill.NOK were estimated if offshore metering stations were based on ultrasonic rather than orifice meters [1].

On this basis Statoil and Christian Michelsen Research (CMR) launched a project in 1988 with the objective of developing a 12" multi-path meter. The project was funded by Statoil. The design phase was successfully concluded by the end of 1990 and it was decided to build and test a 12" prototype fiscal metering system (FMU 700). The prototype and testing phase of the development was funded by Statoil and Fluenta, a subsidiary of CMR. The FMU-project was carried out jointly by Statoil, CMR, Fluenta and Kongsberg Offshore (KOS).

CMR has been active within ultrasonic flow meter technology for more than a decade [3,4], and proposed as early as in 1981 to develop a multi-path gas flow meter.

These projects served as a technology basis for the FMU-project where CMR developed the ultrasonic transducers, the geometrical arrangement of the sensors on the spool piece, the hazardous and safe area electronics, the flow computer solution and software as well as the signal processing technique.

The project was coordinated by Fluenta which also will manufacture the FMU 700 flow meter.

KOS developed design solutions for metering stations based on multi-path meters and provided the secondary spool piece carrying temperature, pressure and density sensors.

The meter was tested on natural gas from mid November 91 to early February 92 at K-Lab which is a high-pressure flow calibration facility located at Kårstø, Norway. K-Lab is a joint venture between Total and Statoil and is operated by Statoil.

In this paper we describe the results of the FMU-project focusing on the flow meter concept, a discussion of some of the test results and finally a presentation of procedures for proving of multi-path ultrasonic gas flow meters.

2 MEASUREMENT PRINCIPLE

Transit time principle

The FMU 700 is based on the well established acoustic transit time principle. The measurement principle utilize the fact that the direction and propagation velocity of an ultrasonic pulse will be modified by the flowing medium. An ultrasonic pulse propagating with the flow will experience an increase in velocity while an ultrasonic pulse propagating against the flow will experience a decrease in velocity.

Basic formulas

In Figure 1 a single-path ultrasonic flow meter is illustrated with two ultrasonic transducers facing each other at an oblique angle to the pipe axis. The individual upstream (t_{21}) and downstream (t_{12}) transit times are given by [6]

$$t_{12} = L / [(c^2 - v^2 \sin^2 \theta)^{1/2} + v \cos \theta] , \quad (1a)$$

$$t_{21} = L / [(c^2 - v^2 \sin^2 \theta)^{1/2} - v \cos \theta] . \quad (1b)$$

It is readily shown that combining Eq.(1a) and Eq.(1b) yield

$$v = L(t_{21} - t_{12}) / (t_{12} t_{21} 2 \cos \theta) , \quad (2)$$

and

$$c = L [(t_{12} + t_{21})^2 \cos^2 \theta + (t_{21} - t_{12})^2 \sin^2 \theta]^{1/2} / (t_{12} t_{21} 2 \cos \theta) \quad (3)$$

where

- v = Axial flow velocity averaged along a chord D which is the projection of L in a plane perpendicular to the pipe axis, see Fig. 1,
- c = Speed of sound in the fluid averaged along the chord D ,
- L = The portion of the intertransducer center line lying in the flowing fluid,
- θ = Angle between the intertransducer center line and a line parallel to the pipe axis,
- t_{12} = Downstream transit time, from transducer 1 to 2,
- t_{21} = Upstream transit time, from transducer 2 to 1.

We observe that both the flow velocity v and the speed of sound c in the fluid are measured. Thus, the transit time flow meter also provides information on a physical property of the fluid.

In practice the transducers are often set back, i.e. the actual distance between the transducers is larger than L as e.g. shown in Fig. 1. Accordingly the measured transit times also incorporate the transit time in the cavity in front of the transducers. However, it is easy to implement a procedure in the flow computer which allows the measured transit time to be corrected for the unwanted time delay in the transducer cavity. For low Mach number flows this practical problem can also be solved as described in [7].

Volume flow measurement

By measuring along five different acoustic paths across the pipe, the gas volume flow can be measured accurately even when the flow profile is distorted. Figure 2 illustrates the positioning of the ten ultrasonic transducers in the FMU 700 ultrasonic gas-flow meter. The measured velocities v represent averages along the parallel chords shown in Fig. 2, i.e. the acoustic transit time technique in facts integrates the velocity profile along the parallel chords. The volume flow is given by

$$q = \int_{-r}^r D(y)v(y)dy \tag{4}$$

where

- y = The axis across the pipe perpendicular to the chords,
- D(y) = The length of a chord perpendicular to the y-axis,
- v(y) = Axial flow velocity averaged along a chord D(y),
- r = The radius of the pipe.

The multi-path meter measures v along a limited number of chords and the integral in Eq.(4) can be approximated by

$$q = \sum w_i v_i \tag{5}$$

where

w_i = Weight factors depending on the numerical integration technique applied in Eq. (5).

The geometrical configuration of the ultrasonic transducers, or the position of the parallel chords in Fig. 2, therefore depends on the numerical integration technique which is applied.

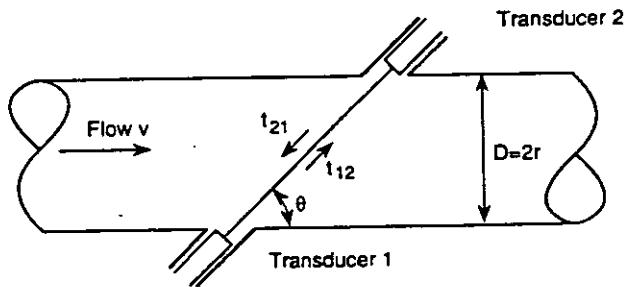


Figure 1 Illustration of the principle of a single-path ultrasonic transit time flow meter.

TRANSDUCER POSITIONING

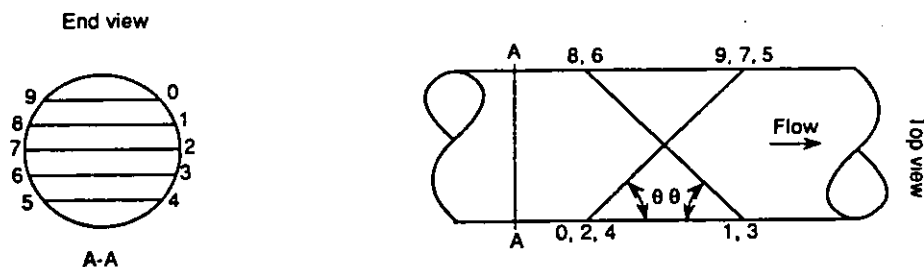


Figure 2 Transducer positioning in the five-path FMU 700 ultrasonic gas-flow meter.

3 SYSTEM DESCRIPTION

General description

The flow meter measures volume flow, flow velocities and speed of sound averaged along parallel chords, see Figs.1-2. Mass flow can be computed provided the density is made available to the flow computer.

The FMU 700 five-path ultrasonic gas flow meter consists of, see Fig. 3 :

- A cabinet containing a computer and an electronics unit,
- Two signal cables and one optical cable,
- Intrinsically safe electronics,
- 10 titanium-housed ultrasonic transducers,
- A flanged spool piece.

A secondary spool carrying temperature, pressure and density sensors, can be installed downstream of the flow meter. If required, the signals from the secondary sensors can be received and converted to physical values by the flow computer.

The flow computer can store all measured data and diagnostic parameters and transfer the information on digital format to an external computer via a series communication link (RS232).

Specifications

The following design specifications apply :

Diameter range	: $\geq 6''$
Operational temperature range	: -10 to +70 °C,
Pressure range	: 50 to 200 bar,
Velocity range	: 0.4 to 20 m/s,
Velocity resolution (12")	: < 1.4mm/s,
Volume flow sampling frequency	: appr. 10 Hz.

The design temperature range for the pipe work, e.g. -46 to +105 °C, will normally exceed the operational temperature range. However the flow meter spool will comply with the requirements set for the pipe work. But as yet, the flow meter is not designed to operate over the entire pipe work design temperature range.

At K-Lab the flow meter was tested down to 20 bar and no change of the flow meter performance were observed. This indicates that the pressure range can be extended below 50 bar.

Installation requirements

The flow meter was designed to operate with 10D of straight pipe upstream of the meter spool and 3D straight pipe downstream of the meter spool. The total installation length amounts to appr. 16D. The total installation length does not change if the 3D downstream spool is equipped with a thermowell or an intrusive densitometer, i.e. if the downstream spool acts as a secondary spool.

For a bi-directional installation, the total installation length will be 23D without a secondary spool and 26D with a secondary spool.

The tests at K-Lab indicate that downstream of a 90° bend, the upstream length may be reduced to 5D. In this case the installation lengths reduce to 11D for an installation with a fixed flow direction. For a bi-directional installation the total installation lengths may reduce to 13D(no secondary spool) and 16D(including secondary spool).

Flow computer

The flow computer is based on an industrial PC with keyboard and color graphics screen. The computer controls the entire measurement process in real time according to a pre-set measurement procedure stored in file during the configuration of the meter. Instructions to the hazardous area electronics from the flow computer is transmitted via an optical cable to ensure fast and reliable transmission of the control parameters. The sensor signals are transmitted via two cables between the control room and the flow meter.

The operator can only get access to the flow computer by specifying the correct password, and the flow computer program can only be halted by specifying the correct password. In a practical measurement situation the keyboard can be removed or locked to increase the security. Further, the flow computer operation will be made independent of the hard disk by storing all programs in ROM. If the hard disk fails this will not influence the meter performance.

The computer initiates the transmission of ultrasonic pulses and then reads a representation of the received pulse into the computer's memory in real time. In a measurement cycle each of the 10 transducers act once as a transmitter and once as a receiver and 10 pulse representations are recorded during the cycle. Based on the 10 recorded pulses, 10 transit times are computed representing a single sample of the volume flow. When volume flow samples have been acquired over a user specified time interval, 10 mean times-of-flight are computed in software from the individual transit times recorded during the interval.

From the 10 calculated times-of-flight the flow velocities and speed of sound along each of the five acoustic paths are calculated. The volume flow is calculated by integrating the flow velocities across the pipe profile. The mean flow velocity in the pipe, mass flow, total volume and mass are then calculated along with statistical data. Readings are displayed on the computer screen and are sent in digital format to e.g. the computer in the fiscal measurement station.

There is no additional microprocessor in the system except for the standard processor installed in the PC.

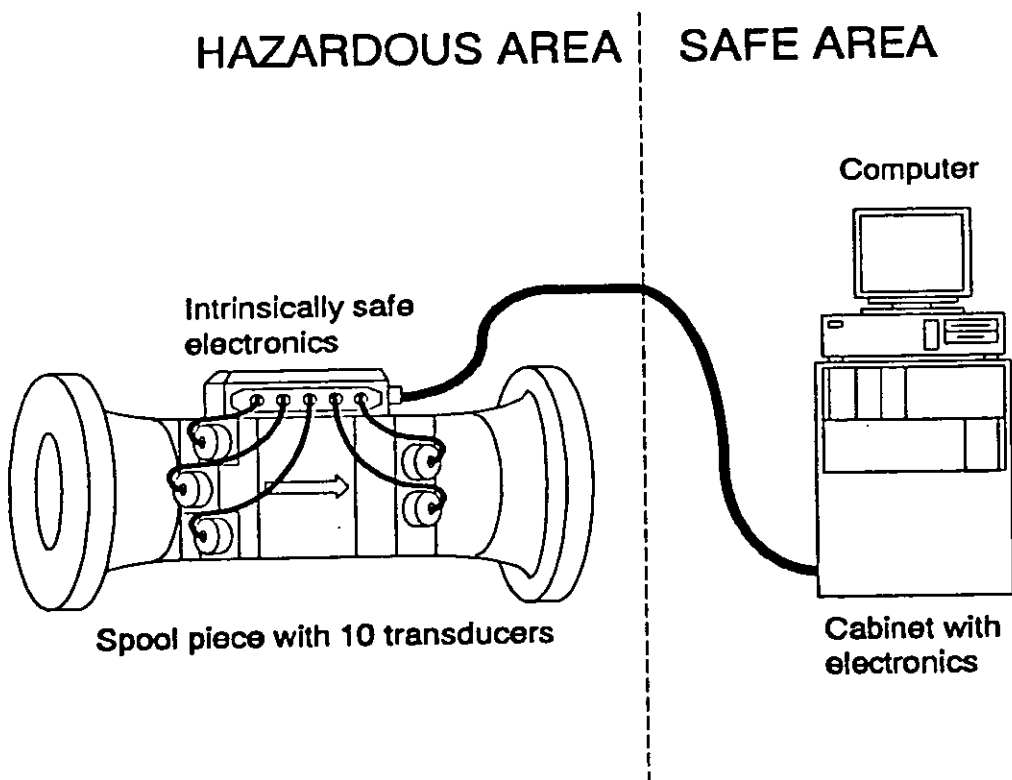


Figure 3 The FMU 700 ultrasonic gas-flow meter.

4 FLOW METER PERFORMANCE

4.1 Calibration tests

Test procedure

During the tests, the gas density in the test section was calculated based on measured pressure, temperature and gas composition (AGA 8). The mass flow was computed from the FMU-metered volume flow and the calculated density. The FMU 700 was configured to average the volume flow, flow velocities and the speed of sound for each path over a period of 10sec. The number of samples in a 10sec period is approximately 110. The flow meter readings were continuously transmitted to the K-Lab computer on digital format.

The reference mass flow rate for a single comparison test was defined as a 300sec average reading of the nozzles, and the FMU 10sec-readings were averaged over the same time interval. During each run the flow conditions were kept as stable as possible.

At each velocity, at a given pressure, 5 or usually 3 consecutive runs were made.

The temperature during the tests reported here varied between 36.7 and 37.9 °C. The velocity range was 0.4 to 8 m/s which is the maximum value in a 12" pipe at K-Lab, and the pressure was set to 55, 70 or 100 bar. The flow meter was tested 10D and 5D downstream of a 90° bend. The 3D long secondary spool was installed downstream of the meter spool "flange to flange", carrying a pressure sensor and a thermowell.

The uncertainty of the K-lab reference mass metering system is estimated by K-lab to be 0.3%.

Comparisons with sonic nozzles

The deviations between the K-lab sonic-nozzle reference mass metering system and the FMU 700 are less than 0.8% at gas velocities between 1 and 8 m/s, see Figure 4. These results were achieved with 10D straight inlet pipe downstream of a 90° bend. Tests were also performed with the FMU 700 installed only 5D downstream a 90° bend. At gas velocities between 2 and 8 m/s the measurement uncertainty is not changed despite the reduction in upstream straight pipe length from 10D to 5D. From Figure 4 we can also see that the measurement uncertainty is independent of pressure changes. In Fig. 5 the individual 300sec readings are plotted to give an impression of the repeatability (2σ -uncertainty) of the meter under test. As can be observed, the repeatability is satisfactory, see below.

The sonic nozzle readings were also converted to volume flow and compared with the volume flow measured by the FMU meter. The observed variability of the FMU and nozzle readings were quite similar.

It should be noted that the test results referred to above, were achieved without using any calibration or meter factor in the FMU 700 meter. The FMU 700 flow meter was zero-calibrated independently of the K-lab reference system and then installed at K-lab, see Section 6.

2- σ uncertainty

The 2- σ uncertainty is defined here as $2\sigma/(\text{average reading})$ where σ is the sample standard deviation of N flow meter readings recorded in a given time interval where the flow rate is constant.

An important property of the FMU 700 flow meter is the stability of the flow meter, see Figure 5. During the tests at K-lab it was demonstrated that the observed repeatability is comparable to a good turbine meter, which is recognized as a very stable and repeatable flow meter.

Table 1 displays 3 different estimates for the 2σ -uncertainty of the FMU 700 during the tests at K-lab during a period when the flow rate was particularly stable. It is important to be aware of that the ultrasonic flow meter measures the turbulent fluctuations of the flow and turbulence will contribute to the 2σ -uncertainty together with the contribution from the finite resolution of the transit time measurement. The 2σ -uncertainty will decrease when

the time averaging interval increases because the average reading gets closer and closer to the true mean, and this is also observed from Table 1¹. In Figure 6 some of the data in Table 1 are plotted.

Table 1 2 σ -uncertainty for the FMU 700 based on 150 consecutive flow meter readings. The 150 readings represent either 10sec averages, 100sec moving average of 10sec readings or 300sec moving average of 10sec readings. During the 1500sec time interval the flow conditions were kept as stable as possible.

Measurement series: (1500sec time slices used)	Mean flow velocity [m/s]	Average 10sec 2 σ uncertainty	Moving average 100sec 2 σ uncertainty	Moving average 300sec 2 σ uncertainty
10D, 100 BarG, 2.5% Sonic nozzles.	0.394	0.560%	0.177%	0.102%
10D, 100 BarG, 6.25% Sonic nozzles.	0.986	0.512%	0.123%	0.046%
10D, 100 BarG, 13.75% Sonic nozzles.	2.168	0.281%	0.074%	0.041%
10D, 100 BarG, 27.5% Sonic nozzles.	4.321	0.237%	0.062%	0.034%
10D, 100 BarG, 50% Sonic nozzles.	7.736	0.204%	0.061%	0.023%
10D, 70 BarG, 2.5% Sonic nozzles.	0.394	0.695%	0.178%	0.091%
10D, 70 BarG, 6.25% Sonic nozzles.	0.997	0.447%	0.132%	0.071%
10D, 70 BarG, 13.75% Sonic nozzles.	2.192	0.301%	0.096%	0.048%
10D, 70 BarG, 27.5% Sonic nozzles.	4.355	0.212%	0.068%	0.020%
10D, 70 BarG, 50% Sonic nozzles.	7.811	0.206%	0.070%	0.027%
10D, 55 BarG, 2.5% Sonic nozzles.	0.398	0.571%	0.212%	0.106%
10D, 55 BarG, 6.25% Sonic nozzles.	1.009	0.458%	0.207%	0.074%
10D, 55 BarG, 13.75% Sonic nozzles.	2.216	0.335%	0.107%	0.061%
10D, 55 BarG, 27.5% Sonic nozzles.	4.400	0.218%	0.065%	0.026%
10D, 55 BarG, 50% Sonic nozzles.	7.890	0.186%	0.051%	0.016%
5D, 100 BarG, 2.5% Sonic nozzles.	0.384	0.773%	0.206%	0.102%
5D, 100 BarG, 6.25% Sonic nozzles.	0.981	0.762%	0.234%	0.132%
5D, 100 BarG, 13.75% Sonic nozzles.	2.168	0.597%	0.172%	0.083%
5D, 100 BarG, 27.5% Sonic nozzles.	4.313	0.487%	0.093%	0.043%
5D, 100 BarG, 50% Sonic nozzles.	7.723	0.445%	0.152%	0.101%

¹ Accordingly, a comparison of the 2 σ -uncertainty between various flow meters is only meaningful if the averaging intervals are similar for the various meters.

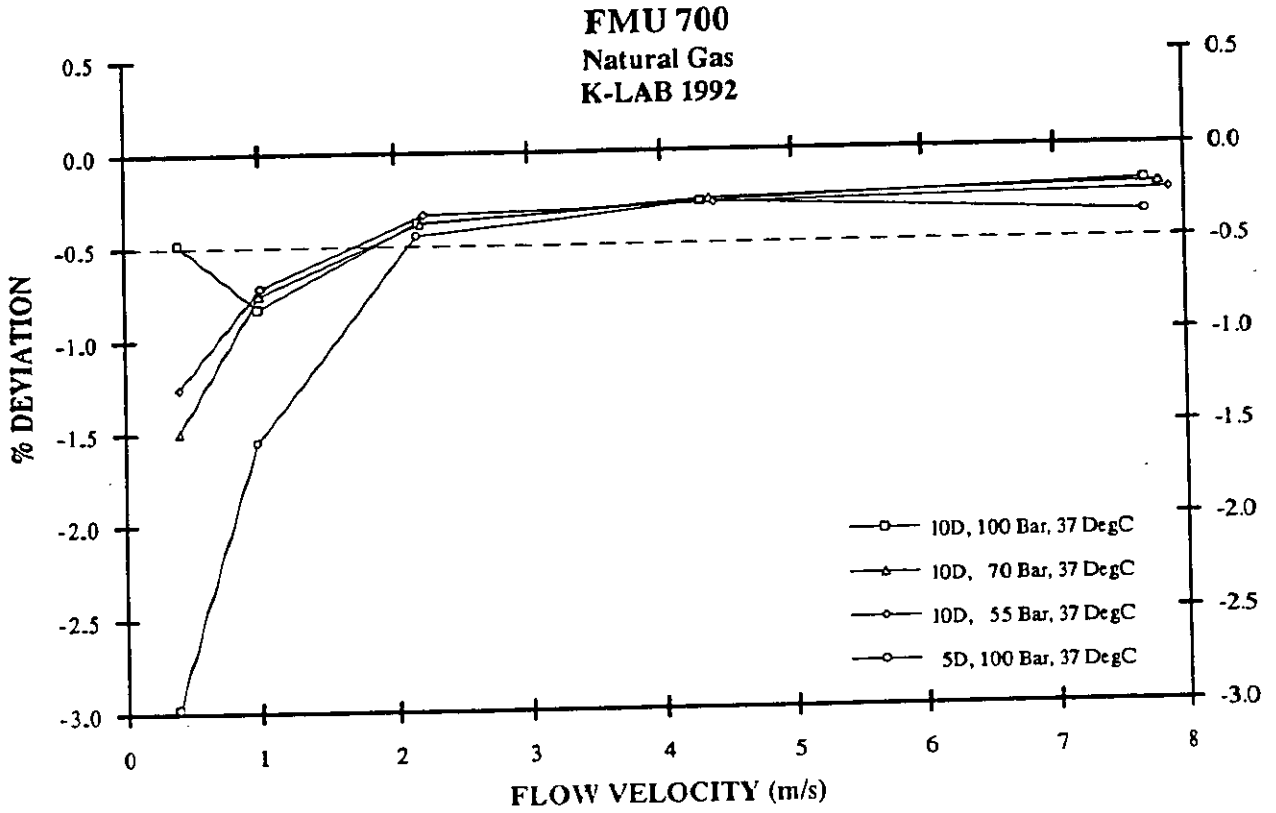


Figure 4 Calibration test results at K-lab for FMU 700. 10D and 5D measurements.

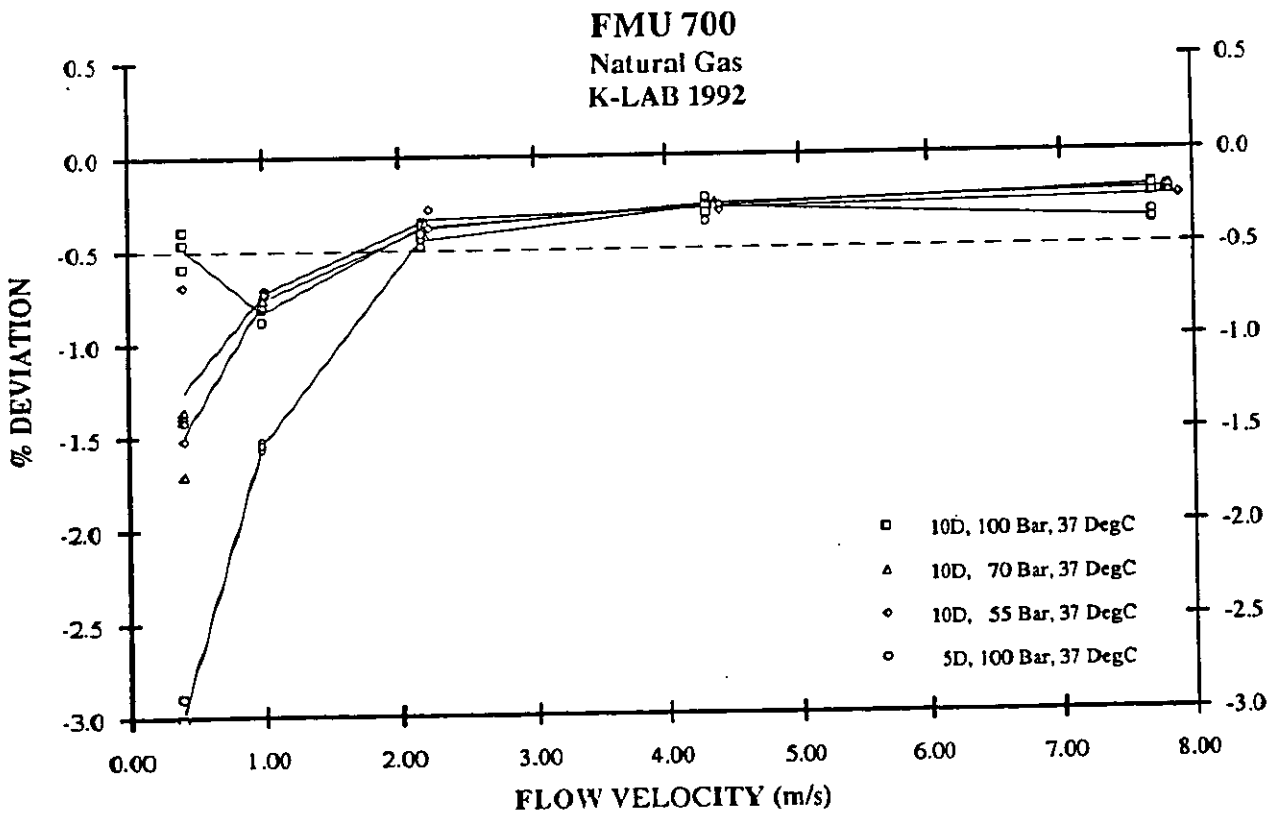


Figure 5 Calibration test results at K-lab for FMU 700. 10D and 5D measurements which indicate the good repeatability of the meter.

FMU 700, 37 DegrC, 300 sec. moving average
Natural Gas
K-LAB 1992

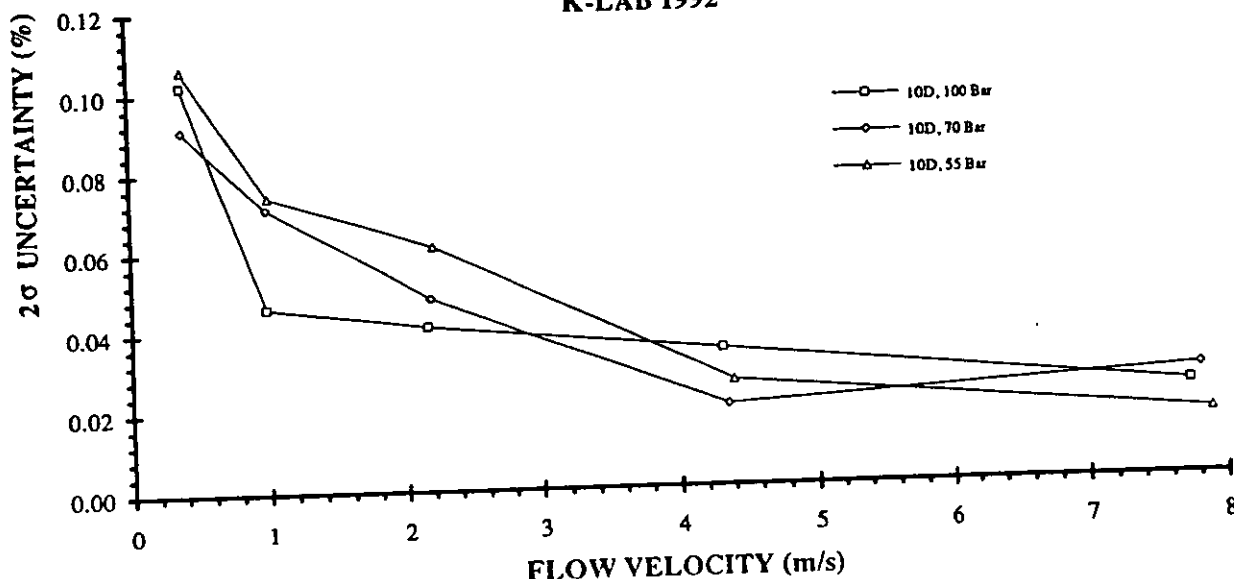


Figure 6 Estimates of the 2σ -uncertainty of the FMU 700 during the tests at K-lab. The 2σ -uncertainty displayed here is based on a 300sec moving average of the 10sec average flow meter readings. At K-Lab each comparison between the FMU 700 and the reference nozzles was based on an average reading over 300sec.

Conclusion, K-Lab test

The results show that it is quite feasible to build a very compact and light metering station compared to conventional solutions and at the same time comply with the requirements set to fiscal metering stations.

4.2 Flow analysis

The flexibility of the flow meter may be utilized by e.g. calibration laboratories to monitor the flow conditions as shown in the following. In view of the good repeatability of the flow meter, it should also be fully possible to use it as a reference flow meter in calibration loops.

During continuous metering, measured data can be stored in a file by giving an appropriate command. Similarly, the system can be set to measure only a single path, for test, trouble shooting or calibration purposes. Stored data can be used to examine earlier series of measurements by fetching data from file and displaying them on the screen. This enables the operator to scan rapidly through the data to interesting areas of the measurement series.

Figure 7 is an example of such a stored time series from the tests at K-lab, where an interesting part has been plotted showing mean flow velocity and velocities along each of the five acoustic paths around an abrupt change of the flow velocity. In Figure 8 the same incident is shown for the speed of sound along each of the five acoustic paths. The mean flow velocity and the speed of sound along one of the acoustic paths are plotted on top of one another in Figure 9 to show the simultaneous change in both measured values. This event also illustrates the flow meter response the ability to resolve rapid changes of the flow rate.

In Figure 10 another part of the time series is plotted showing the turbulent fluctuation in mean flow velocity and velocities along each of the five acoustic paths at a constant flow rate. Notice how the flow velocities along the acoustic paths closest to the pipe wall, 0-9 and 4-5, display the highest turbulent fluctuation and how the fluctuations appear to inversely correlate. The same is the case for the mid-paths, 1-8 and 3-6, but with less turbulent fluctuation. The center path is less influenced by turbulence while the calculated mean flow velocity is almost constant. Another

interesting observation is that the turbulent fluctuation along two paths on the same side of the center path, f. ex. 0-9 and 1-8, also inversely correlate while the turbulent fluctuation along two asymmetric paths on different sides of the center path, e.g. paths 0-9 and 3-6, correlate. This correlation and inverse correlation effect between the turbulent fluctuations along different acoustic paths is easier seen in Figure 11. It shows an extract of the time series from Figure 10, with the flow velocity along the five paths plotted as a profile, with time as parameter.

In Figure 12 the same part of the time series as in Figure 10 is plotted showing the fluctuation of the speed of sound along each of the five acoustic paths. No rapid fluctuations of the speed of sound are observed. The slow overall fluctuation of the speed of sound is probably due to the regulation system on the centrifugal compressor circulating the gas around the loop at K-lab.

During test metering, the received ultrasonic pulse representations can be stored in file. Due to the large amount of data that a single ultrasonic pulse represents, only short time series can be stored. The stored ultrasonic pulses can be examined later by a separate program which e.g. can produce various plots of single pulses as shown in Fig. 13 and time series of computed times-of-flight as shown in Fig. 14. Individual pulses and transit times can also be valuable tools for analyzing various flow phenomena.

Analyses as described above can provide information on the meter performance and the flow conditions.

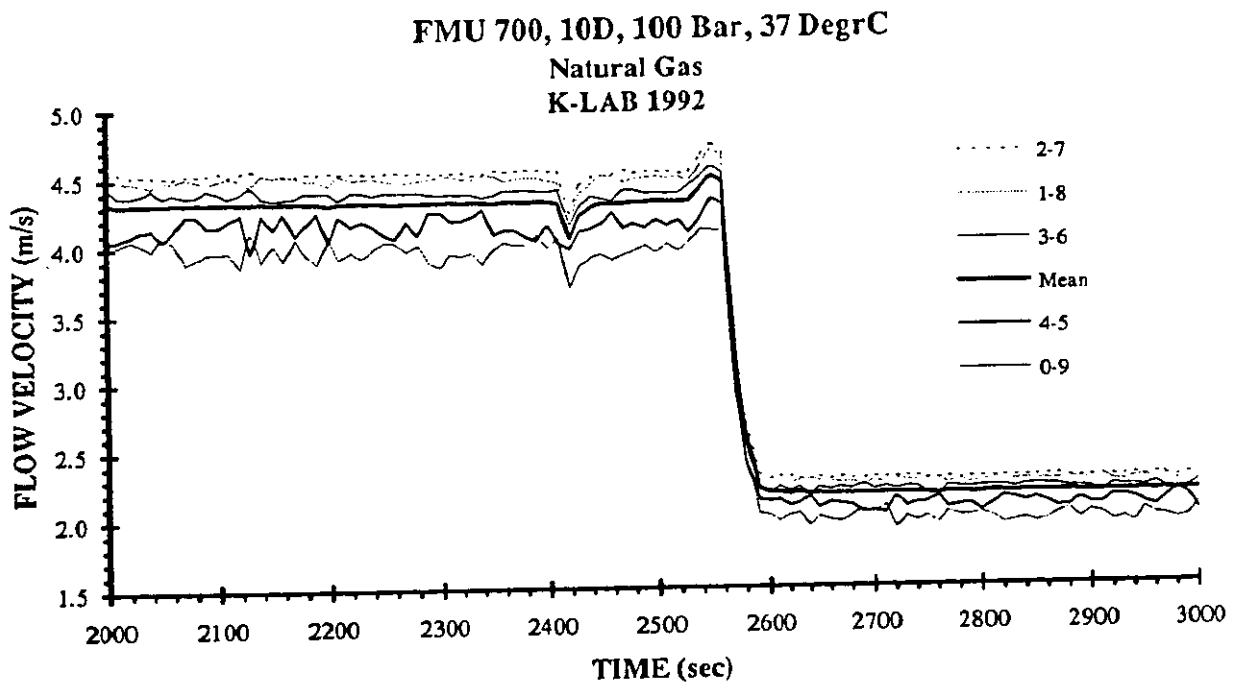


Figure 7 Tests at K-lab. Showing mean flow velocity and velocities along each of the five acoustic paths around an abrupt change in flow velocity.

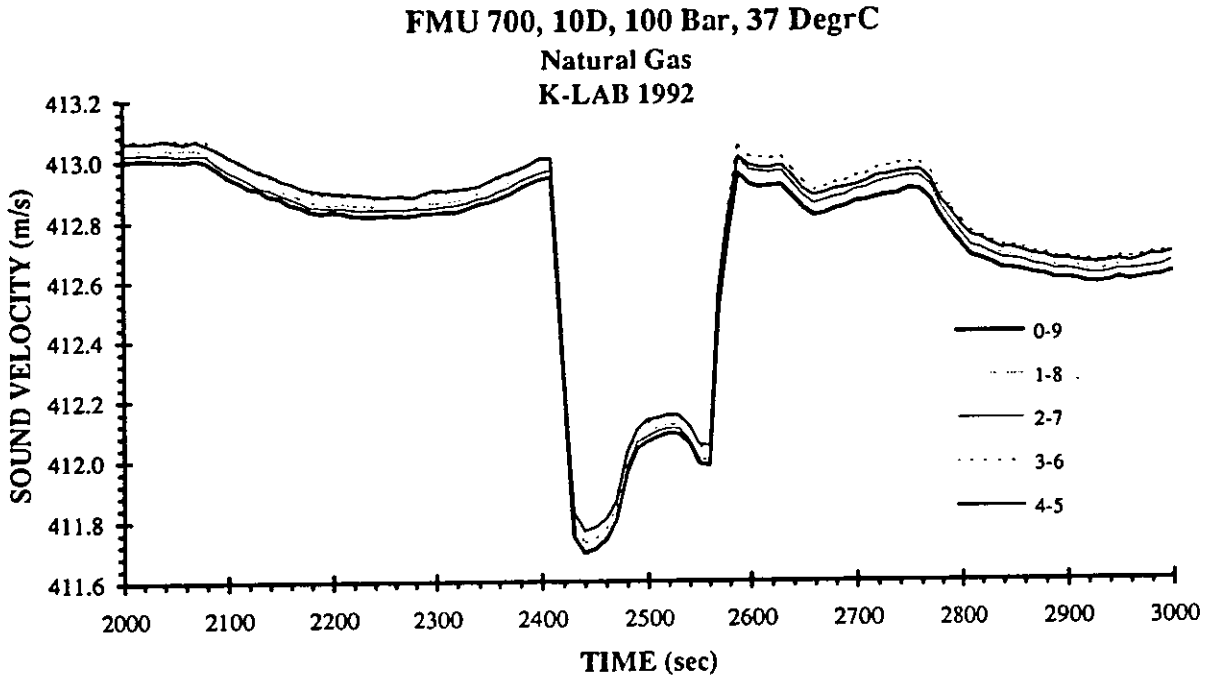


Figure 8 Tests at K-lab. Showing speed of sound along each of the five acoustic paths around the abrupt change of the flow velocity displayed in Fig.7.

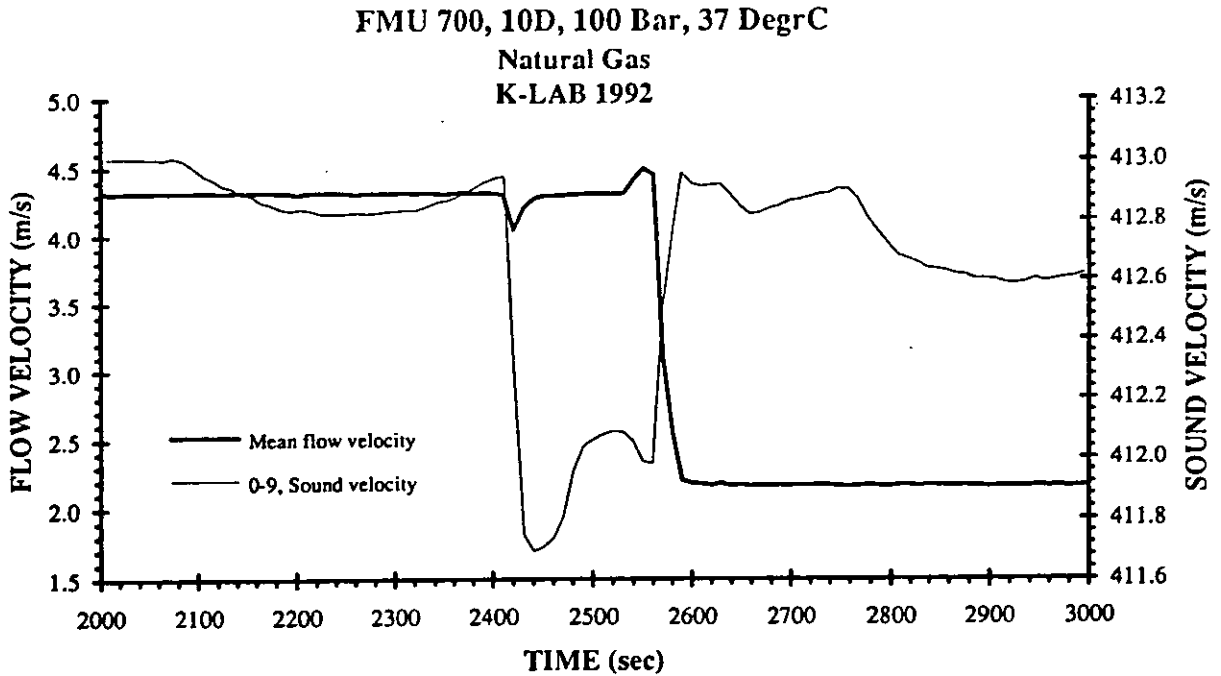


Figure 9 Tests at K-lab. The mean flow velocity and the speed of sound along one of the acoustic paths are plotted on top of one another to show the simultaneous change of both measured values.

FMU 700, 10D, 100 Bar, 37 DegrC
Natural Gas
K-LAB 1992

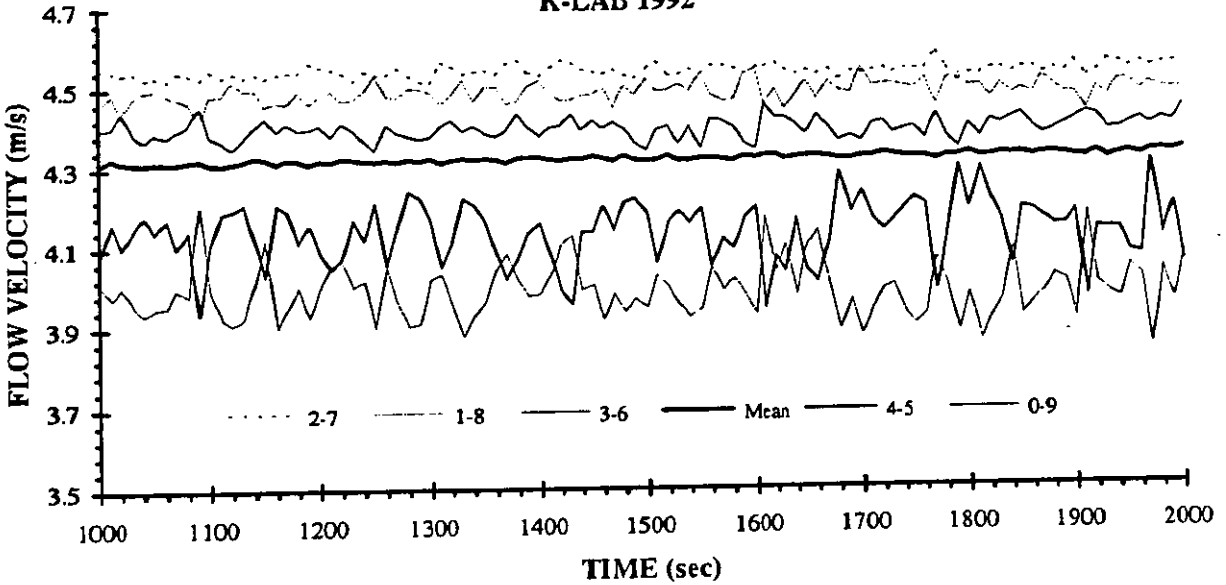


Figure 10 Tests at K-lab. Showing the turbulent fluctuation in mean flow velocity and velocities along each of the five acoustic paths at a constant flow rate. Notice the correlation and inverse correlation effect between the turbulent fluctuations along different acoustic paths.

FMU 700, 10D, 100 Bar, 37 DegrC
Natural Gas
K-LAB 1992

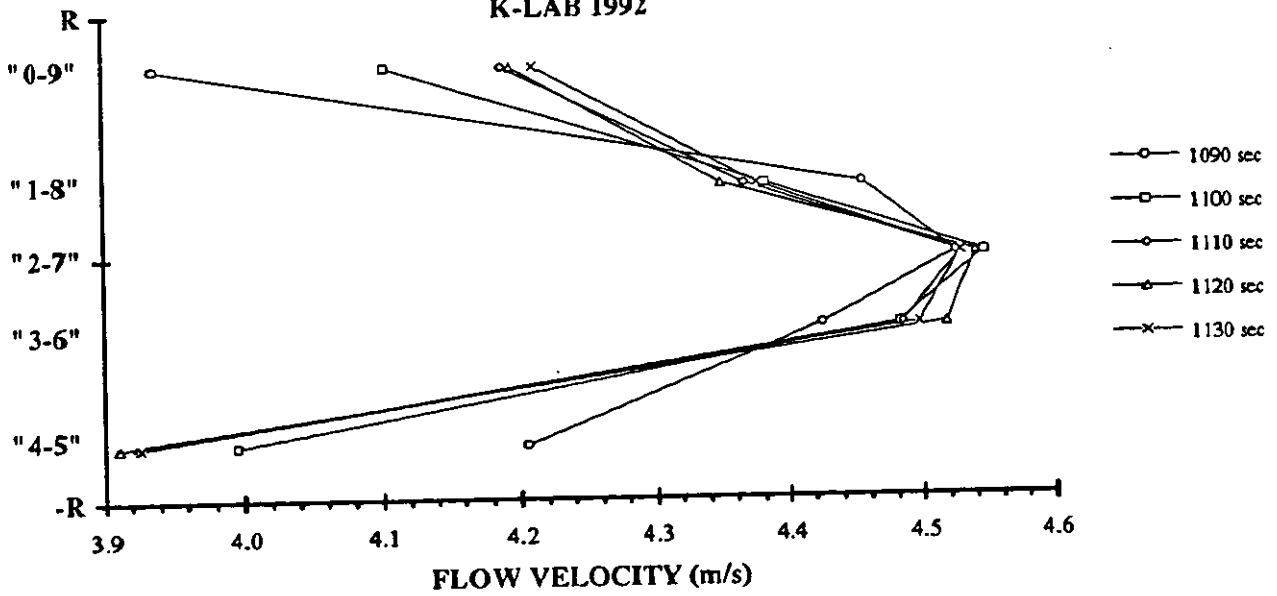


Figure 11 Tests at K-lab. Showing an extract of the time series from Figure 10, with the flow velocity along the five paths plotted as a profile, with time as parameter. Notice the correlation and inverse correlation effect between the turbulent fluctuations along different acoustic paths.

FMU 700, 10D, 100 Bar, 37 DegrC
 Natural Gas
 K-LAB 1992

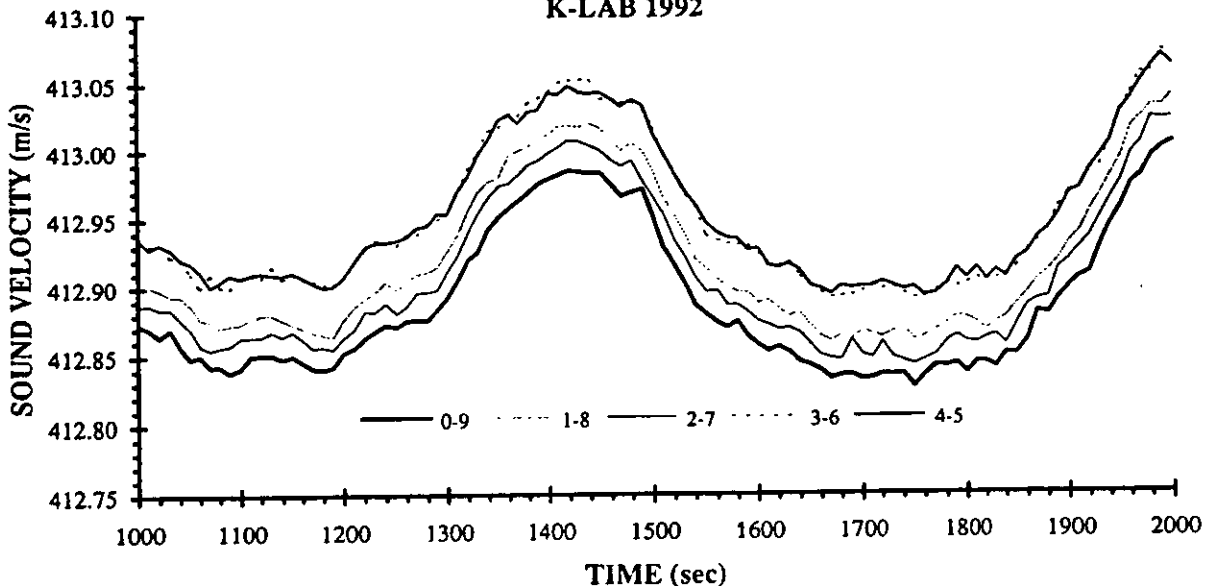


Figure 12 Tests at K-lab. Showing the fluctuations of the speed of sound along each of the five acoustic paths.

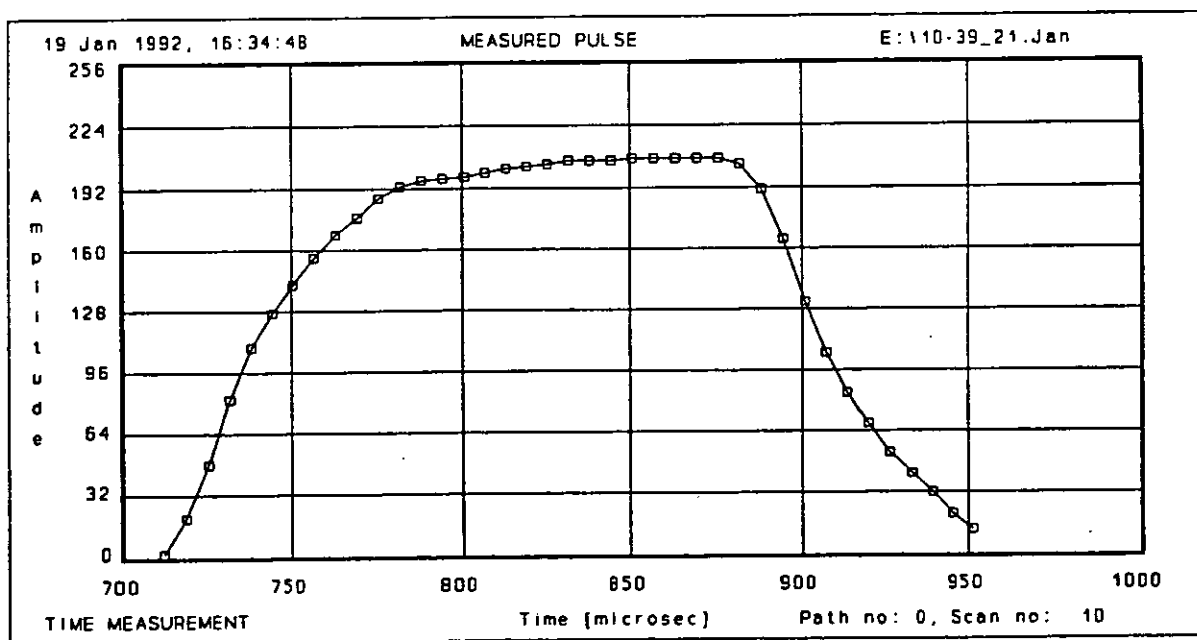


Figure 13 Tests at K-lab. Received ultrasonic pulse representation showing peak amplitude and negative going zero-crossing time for each period of the received pulse.

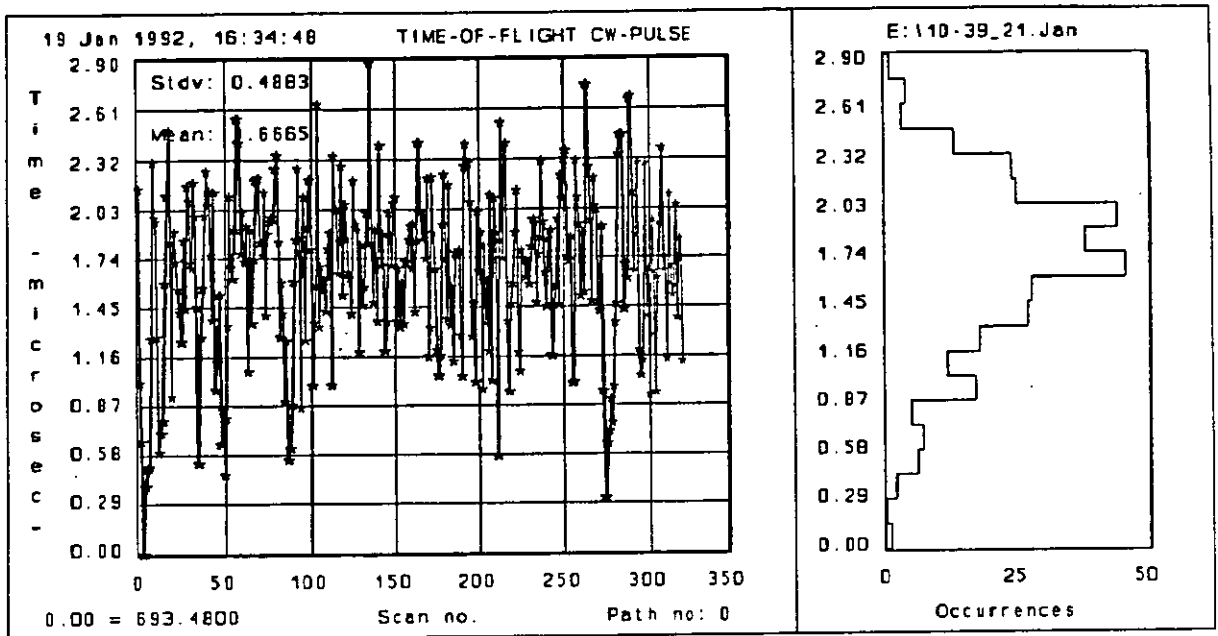


Figure 14 Tests at K-lab. Time series and distribution of computed times-of-flight for a single path at 8 m/s.

5 SPECIAL FEATURES

In the following we will highlight some of the technical achievements which are of particular importance to the users. Particularly the FMU 700 features :

Titanium housed ultrasonic transducers which eliminates the risk of gas penetration into the transducer and subsequent transducer failure.

Automatic gain control keeping the amplitude of the received ultrasonic pulses at a constant level. This makes it possible for the flow meter to operate over a wide temperature, pressure and flow velocity range without any manual adjustment of the electronics. If automatic gain control is lacking, the flow meter will cease to operate if e.g. the pressure changes.

On-line measurement of transit time delay in cables and electronics is implemented and accounted for in the transit time measurement. In most ultrasonic flow meters fixed values for these time delays must be implemented in the flow computer and drift in the transit time delay will not be accounted for.

Software pulse detection eliminating electronics for pulse detection and making it possible to implement a signal processing technique which is able to recognize pulses modulated by turbulence effects, pressure and temperature changes. Accordingly the flow meter reliability is improved.

The geometrical arrangement of the ultrasonic transducers and the corresponding integration technique, see Eq. (5), was developed as result of extensive numerical simulations where various methods were investigated. Based on set of 34 flow profiles an adaptive and robust integration method was developed particularly designed to integrate asymmetric flow profiles.

The flow computer concept, based on an industrial PC, has several advantages since this solution results in :

A less complex flow meter electronics,
Easy access to flow meter raw data which makes service and testing simple,
Simple procedures for upgrading flow computer software, e.g. diagnostic software,
Use of standard equipment which is under continuous technological improvement,
A computer environment most operators are familiar with.

The technical solutions implemented in the FMU 700 flow meter, thus represent a general improvement of the ultrasonic flow meter technology and will help to improve the flow meter reliability.

6 PROVING

An important aspect of the introduction of multi-path ultrasonic flow meters for fiscal or allocation measurement of gas, is the proving procedure for the meter. In the following we will discuss some possibilities and propose a practical solution as to how proving can be carried out.

The following procedure is suggested for proving of a multi-path meter in a fiscal metering station :

1. Zero calibration of flow meter when delivered from manufacturer.
2. Flow calibration prior to installation in the metering station.
3. Use of the flow meter's self diagnostic properties to indicate if and when zero calibration should be repeated.
4. On-site zero calibration of individual transducer pairs which are removed from the pipe line and installed in a zero calibration cell.

In addition to the above items it is fully possible to increase the redundancy by installing two meters in series. Since the flow meters are non intrusive they can be installed close to each other, potentially "flange to flange".

In the following we will describe the proposed procedure with reference to the experimental experience gained during the testing of the FMU 700.

6.1 Zero calibration

The basic measured parameter is the acoustic transit time in the flowing gas, see Eq.(2). However, the measured transit times also contain the transit times in the acoustic transducers and the accompanying electronics. Thus, the measured transit time must be corrected for these time delays. It is of particular importance to ensure that the flow meter reading is zero when the gas is at rest, i.e. the transit times in the gas in each direction along the same path must be identical at zero flow. It is easy to measure the transit time difference accurately. But, the absolute time delay is more difficult to measure. Accordingly the transit time difference at zero flow is measured precisely and the less accurate measurement of the absolute time delays are adjusted to secure zero measured flow in a gas at rest.

When the time delays and the transit time differences have been measured they are stored in the flow computer. During flow meter operation, the measured transit times are corrected prior to calculation of the flow velocity by Eq.(2).

The FMU 700 was zero calibrated by pressurizing the spool piece using nitrogen. Before pressurizing the spool piece, the distances between the acoustic transducers were measured with an uncertainty of 0.04mm. To ensure stable conditions, i.e. no thermal flows, the pressurized spool piece was kept in a temperature bath during calibration. The transit times were then measured over the pressure and temperature range in question. Based on the transit times, the transit time difference corrections were calculated. Using the measured transducer distances, corrected for thermal expansion, the time delays and the speed of sound in the gas were calculated. For control purposes the measured speed of sound was compared to calculated values using the IUPAC-tables[5]. The deviations between the measured and the calculated values were less than 0.5 m/s, i.e. 0.15%. The measured "zero calibration times" were subsequently stored in the configuration file of the flow computer.

At present we are working on a new method for zero calibration which may represent a significant improvement and simplification of the above procedure. The new method will soon to be tested at CMR.

6.2 Flow calibration

The zero calibration ensures that the inherent offset in the measured transit times can be accounted for when calculating the velocity using Eq.(2). This offset is independent of the flow velocity. Due to the simple relationship between the flow velocity and the transit times given by Eq.(2), where calibration constants are not required, it should not be necessary to carry out a flow calibration. When the transit times are measured correctly, Eq.(2) will provide the flow velocity without the use of additional calibration constants.

As described above the FMU 700 was zero calibrated on nitrogen prior to transportation and installation at K-Lab. The acoustic transducers were not removed from the spool piece after zero calibration. The meter was zero calibrated at 37 °C (normal operating temperature at K-Lab) and then transported to K-Lab. During the transportation the meter was exposed to temperatures around 0 °C and then installed at K-Lab and warmed up to 37 °C again. During the test period the meter was exposed to temperature cycling between normal operating temperature and ambient temperature (0 °C) on several occasions. The observed deviations shown in Fig. 4 were obtained without any adjustment of the flow meter after zero calibration at CMR. The meter was simply installed and the tests begun. It is of considerable practical importance to notice that the zero calibration was carried out without the long signal cables (approx. 130m) which were used at K-Lab. This is possible because the FMU 700 features on-line measurement of the transit time delay in signal cables, safe area electronics and parts of the intrinsically safe electronics.

During the test period we did not observe any detectable drift in the zero calibration. This verifies that it is not necessary to carry out a flow calibration if the meter is properly zero calibrated.

However, for fiscal purposes it is likely to assume that a flow calibration will be required.

6.3 Self diagnostics

Ultrasonic flow meters offer the possibility to monitor the flow meter performance to a certain extent. This can be utilized both as an indicator of when proving is necessary and to reduce the work load connected to inspection and maintenance. If an abnormal situation occurs a message will be written to the system log in the flow computer and/or a warning can be given to the operator depending on the nature of the detected error.

In the FMU 700 meter the following meter performance parameters can be monitored continuously :

- Comparisons of the measured speed of sound along the five acoustic paths,
- Transducer failure,
- Transit time error,
- Frequency modulation of pulse,
- Failure to recognize received pulse,
- Measured versus calculated speed of sound,
- Standard deviation of the speed of sound measurements,
- Standard deviation of the flow measurement.

Based on the above diagnostic parameters ultrasonic flow meters can detect meter malfunctioning and give the operator a warning in contrast to e.g. an orifice meter where it is nearly impossible to detect a change in the meter performance.

Comparisons of sound speeds

If the properties of the acoustic transducers or the electronics change with time this may lead to a drift in the zero calibration, and the flow meter uncertainty is likely to increase. It is particularly important to avoid drift in the measured transit time difference in Eq.(2). Drift in the absolute transit times is far less important.

In a multi-path meter the speed of sound in the gas is measured for each path. If the pipeline is properly insulated, the temperature difference between the area close to the pipe wall and the central portion of the pipe will be very small (if any). Consequently the speed of sound will be constant across the pipe section and the measured speed of

sound along the paths should be equal. For very low flow velocities and large temperature difference between the gas and the surroundings, a small temperature gradient may be present. This was in fact observed at K-Lab.

During the K-Lab tests, the difference between the maximum and the minimum values of the measured speed of sounds were typically less than 0.07 m/s, (0.01%), even during abrupt changes of the flow velocity, see Figs. 8 and 12. This difference is due to the measurement uncertainty of the transit times (not the transit time differences) or inhomogeneities in the flow.

If this difference exceeds 0.1m/s, i.e. a change of 0.04m/s, this may represent a drift in the transit time difference measurement of 100ns. At 5m/s a 100ns drift corresponds to a shift in the calibration of the meter of around 1%. Thus, there is a potential for detecting a change in the calibration of the meter by continuously monitoring the difference of the measured sound speeds.

However, the speed of sound is proportional to the sum of the transit times and not the transit time difference. Accordingly, changes in the measured speed of sound can also occur even if the transit time difference is unaffected. At CMR more work will be undertaken to establish a procedure for using the speed of sound difference as a diagnostic parameter.

Measured speed of sound versus calculated

Based on measured temperature and pressure and a specified gas composition, the speed of sound can be calculated. Comparing the measured and calculated speed of sound, can be used as a rough, but independent, check of the transit time measurements.

Transducer failure

If one of the acoustic transducers fail and is unable to emit or receive an acoustic pulse, this will be detected immediately and a proper warning will be given. If a transducer pair drops out, the flow meter is still able to measure the flow by using the transducer pairs in operation to estimate the velocity along the path which has dropped out.

Nonphysical transit times

Nonphysical transit times, i.e. transit times which cannot occur based on the known distance between the acoustic transducers and known upper and lower limits for the speed of sound, will never be measured due to the time gating system incorporated in the flow meter.

Pulse recognition

The percentage of pulses recognized by the flow computer is monitored continuously and will be stored in the system log. Normally 100 % of the pulses are recognized by the flow computer. During transducer malfunctioning, heavy turbulence, electric or acoustic noise, the percentage of pulses accepted may be low and a warning will be given.

Pulse frequency check

Every accepted pulse is checked for "period error", i.e. if for some reason a pulse period is missing. If a "period error" is found the pulse is rejected.

The frequency content of every recognized pulse is checked and strict limits are set for the allowed variation of the pulse frequency around the known frequency of the emitted pulse in order to ensure a high-quality transit time measurement. If these limits are violated the pulse is rejected and the number of rejected pulses is monitored and will be stored in the system log. If the number of rejected pulses is high, a proper warning will be given.

Filtering

When the transit times have been computed a filtering algorithm checks the measured set of transit times for outliers. This filtering is based on the measured transit time distributions. Transit times lying outside the allowed spreading are discarded from the data set which is used when calculating the flow velocity.

Standard deviation

The standard deviation of the measured flow velocity and the measured speed of sound are calculated for each path, see Figure 6. The standard deviation can be used as a meter performance parameter as well as an indicator of the stability of the flow.

6.4 On-site zero calibration

Ideally, it should be possible to carry out zero-calibration of the flow meter on-line, i.e. when the meter is installed in the pipe line. This implies that the flow must be bypassed and it must be possible to keep the gas in the spool piece at absolute rest at a constant temperature. In a practical measurement situation this is not easily obtained. However, "in-line" zero calibration may be a future possibility.

On-site zero calibration can e.g. be carried by:

By removing the meter from the pipe line and installing the spool in a zero calibration facility. This requires the flow to be bypassed in addition to the mechanical work needed to remove the meter spool.

By removing a single transducer pair and the corresponding electronics and carry out zero calibration of only one transducer pair at a time in a special zero calibration facility. In this case it is not necessary to bypass the flow and the meter will be able to operate at a slightly reduced uncertainty.

The latter method is by far the best method from an operational point of view. The acoustic transducers can be removed from the pressurized pipe line either by installing permanent ball valves at each transducer port or by using an extractor tool which can be moved from one transducer port to another. Both techniques are being considered for the FMU 700.

The zero calibration facility will be a pressure cell which should be immersed in a temperature bath and pressurized with nitrogen. Ideally the cell should resemble the meter spool as much as possible. This is important in order to ensure that the sound diffraction effects in the flow meter and in the calibration cell are as similar as possible. This may be of importance for the measurement of the transit time delay. After zero calibration the transducers and the electronics are reinstalled, and the transit time delays in the flow computer are changed if necessary.

In order for such a procedure to work it is important that the distance between the transducers is unaffected by the dismantling and reinstallation of the transducers. At CMR the distance between the transducers was measured before the sensors were removed and after they had been reinstalled. The distance did not change more than 0.03mm, and this is well below the acceptable limit, i.e. 0.1mm.

Since the FMU 700 measures transit time delay in signal cables, safe area electronics and the intrinsically safe electronics on-line, this zero calibration method is particularly attractive for this meter.

7 CONCLUSIONS

A new multi-path ultrasonic flow meter for gas has been developed and tested on natural gas.

The development has contributed to major technical achievements within the ultrasonic gas flow meter technology such as titanium housed ultrasonic transducers, automatic gain control, software pulse detection and on-line measurement of transit time delay in electronics and signal cables. These achievements represent a significant improvement of the flow meter reliability.

The test results show that it is quite feasible to build a very compact and light metering station compared to conventional solutions and at the same time comply with the requirements set to fiscal metering stations.

8 ACKNOWLEDGEMENTS

The authors would like to express their thanks to Statoil and Fluenta for the opportunity to publish the project results and for making the FMU-project feasible by providing the necessary financial support.

The authors acknowledge the high-quality work carried out by the rest of the CMR-project team consisting of Reidar Bø, Per Lunde, Atle Johannessen, Magne Vestheim, Gunnar Wedvich, Hans Ingebrigtsen, Stig Heggstad and Roald Toftevaag.

Further we would like to thank Framo Services and Framo Engineering for doing an excellent job on both design and fabrication of the spool piece and Kongsberg Offshore for providing the secondary instrumentation.

Finally we appreciated the service and the enthusiasm shown by the K-Lab staff during the test period.

REFERENCES

- [1] Sakariassen R. : "Development of a new gas metering system". Paper presented at "Gas Transport Symposium", Haugesund-Norway, January 30-31, 1989. Norwegian Petroleum Society.
- [2] Hannisdal : "Metering study to reduce topside space and weight". Paper presented at the "9th North Sea Flow Measurement Workshop, 1991" in Bergen, Norway, October 22-24, 1991. Norwegian Society of Chartered Engineers.
- [3] Mylvaganam K.S. : "Ultrasonic flowmeters measure flare gas in the North Sea". Oil&Gas Journal, 17 October, 1988.
- [4] Folkestad T. and Mylvaganam K.S. : "Acoustic measurements detect sand in the North Sea flow lines". Oil&Gas Journal, 27 August, 1990.
- [5] IUPAC : "Nitrogen International Thermodynamic Tables of the Fluid State - 6". International Union of Pure and Applied Chemistry, Chemical data series no. 20. Pergamon Press, 1979.
- [6] McCartney M.L., Courtney P.M. and Livengood R.D. : "A corrected ray theory for acoustic velocimetry". Journal of Acoustical Society of America, Vol. 65, No. 1, January 1979.
- [7] Daniel Industries : "Multipath ultrasonic flowmeter for gas custody transfer". Sales brochure, Daniel Industries, Scotland.

EXPERIENCE WITH COMPARATIVE TESTING AND CALIBRATION OF CORIOLIS
AND TURBINE METER OFFSHORE AND IN THE LABORATORY

by

L Mandrup-Jensen
Force Institute

Paper 5.2

NORTH SEA FLOW MEASUREMENT WORKSHOP
26-29 October 1992

NEL, East Kilbride, Glasgow

"Experience with comparative testing and calibration of Coriolis and turbine meter off-shore and in the laboratory"

By Lars Mandrup-Jensen, Mech.Eng. M.Sc. , Denmark
Force Institutes, Metrology Division, Liquid flow section

Table of contents :

	page
1. Introduction.....	2
2. Set-up off-shore on Tyra West.....	3
2.1 Testseparator configuration.....	3
2.2 Condensate measurement system.....	4
2.2.1 Turbinemeter.....	5
2.2.2 Coriolis mass flowmeter.....	6
3. Test / calibration on Tyra West.....	7
3.1 Method.....	9
3.2 Results.....	11
4. Calibration in laboratory.....	11
4.1 Method.....	11
4.2 Results.....	12
5. Conclusion.....	13

1. Introduction

On request from the Danish company "Mærsk Olie og Gas", Dantest has performed comparative testing and calibration of a Coriolis mass flowmeter and turbine meter. The calibrations were first performed off-shore and then in Dantest's laboratory onshore.

The meters were installed in series on the outlet of a test separator, measuring the condensate, on a platform off-shore in the North Sea. Comparative tests have been performed during the platform staff's ordinary 6 hours determination of the gas / condensate / water from the individual wells.

After the off-shore tests, the meters were dismantled and shipped on-shore. In the laboratory the Coriolis mass flowmeter was calibrated on a gravimetric test rig under controlled conditions. This was to determine the meter's accuracy and offset, as well as to determine and evaluate possible installation effects.

2. Set-up off-shore on Tyra West

In the following the set-up of the turbine meter and the mass flowmeter off shore on Tyra West will be described.

2.1 Test separator

The test separator is used in connection with testing and determining the production of gas and condensate from each well. In the test separator the mixture from the well is separated into three parts: condensate, water and gas, see the diagram in figure 2.1.1. Each well is tested during 6 hours, in which mean hour values of condensate, water and gas is registered.

Turbine meters are used to measure the amount of condensate and water. The two meters are connected in parallel (tk1, tk2 and tv1, tv2, see the figure) and each cover a different flow range. An orifice meter (or) is used to measure the gas.

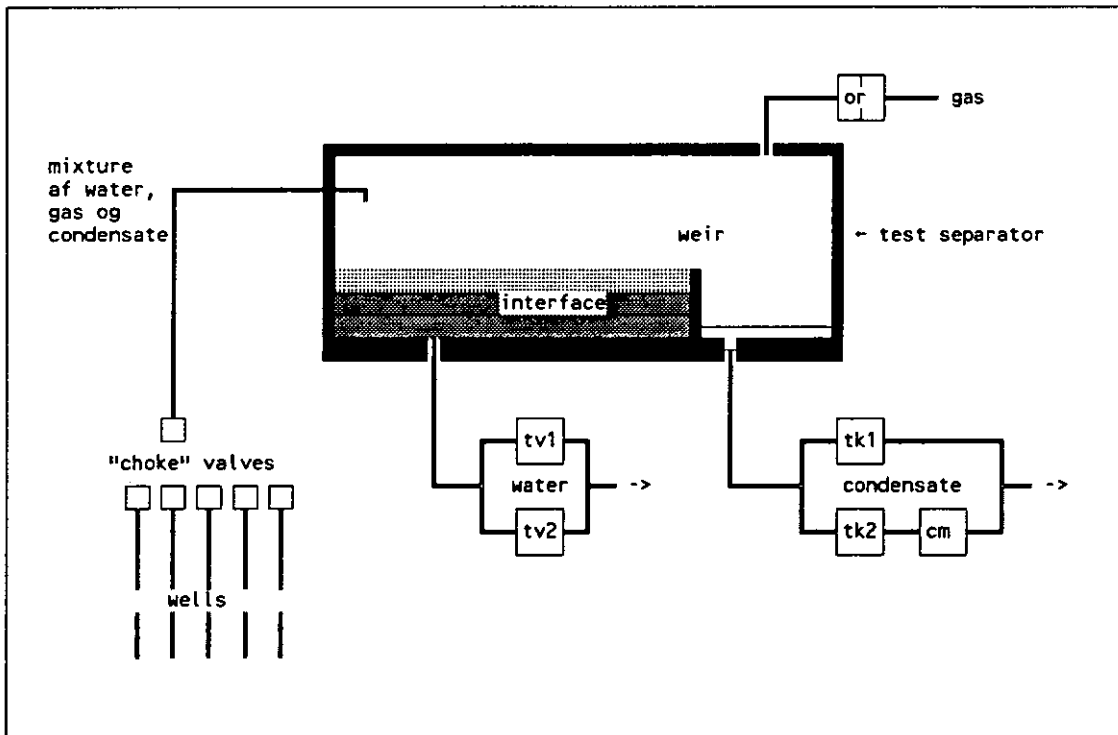


Figure 2.1.1 : Schematic diagram of the test separator on Tyra West

2.2 Condensate measurement system

The condensate measurement system is comprised of two turbine meters (tk1 & tk2) connected in parallel (see figure 2.1.1); each meter with a different flowrange. A mass flowmeter is installed in series downstream the small turbine meter, see the photo in figure 2.2.1 :

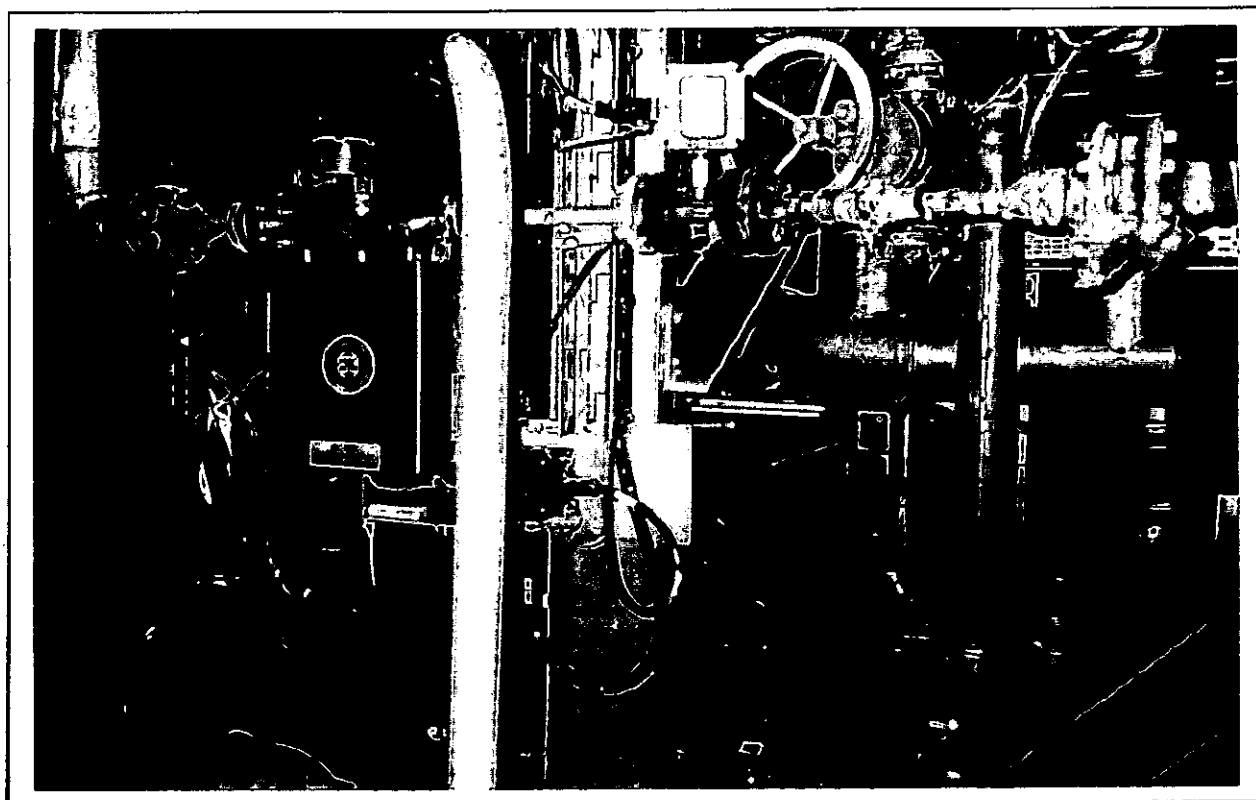


Figure 2.2.1 : Photo of the condensate measurement system the small turbine meter in series with the Coriolis mass flowmeter, Tyra West.

The turbine meter and the mass flowmeter will be described in more detail in the next two sections.

2.2.1 Turbine meter

The signal from the turbine meter is transmitted via cables to the "Auxiliary Metering System" display in the control room. Besides the data from the condensate turbine meters the display also monitors the signals from the water- and gas metering system and the flare gas metering system. Some selected data for the turbine meter is:

Manufacturer: Hydril, AOT Flow Systems
 Model, s/n : Model F/0.75"/ 30 , S/N : 50242
 Size : 3/4 ", 0.8 - 8 m³/hour
 Accuracy : Linearity , spec. ± 0.25 %
 Repeatability , spec. ± 0.02 to ± 0.05 %

The turbine meter has last been calibrated (with water) 22.11.88 by Hydril, with following calibration results : Average K-factor : K = 433.24 pulses/litre & linearity ≈ ± 0.29 %

On the control room display (WA-23401) the following parameters for the turbine meter can be read :

1) GROSS VOL. :	$Q_{t,g}$	[m ³ /h]	$V_{t,g}$	[m ³]
2) NET. VOL. :	$Q_{t,n}$	[m ³ /h]	$V_{t,n}$	[m ³]
2) MASS :	$Q_{t,m}$	[kg/h]	$M_{t,m}$	[kg]

Re.1) Gross vol. is the total volume: volume flow ($Q_{t,g}$) and accumulated volume ($V_{t,g}$), which are calculated as :

$$Q_{t,g} = 3.6 \cdot (f / K) \quad ; \quad V_{t,g} = \Sigma Q_{t,g} \cdot d\tau$$

where f = pulses per. second from the turbine meter
 $K = 433.24$ pulses/liter, $d\tau$ = integr./summ. time

Re.2) Net vol. is the net volume : volume flow ($Q_{t,n}$) and accumulated net volume ($V_{t,n}$), calculated as :

$$Q_{t,n} = Q_{t,g} \cdot C_{t1} \cdot C_{pe} \quad ; \quad V_{t,n} = \Sigma Q_{t,n} \cdot d\tau$$

where C_{t1}/C_{pe} = temperature/pressure correction factor
 $d\tau$ = integration/summation time

Re.3) Mass is the total mass: flow rate ($Q_{t,m}$) and the accumulated mass ($M_{t,m}$), the parameters are calculated as follows:

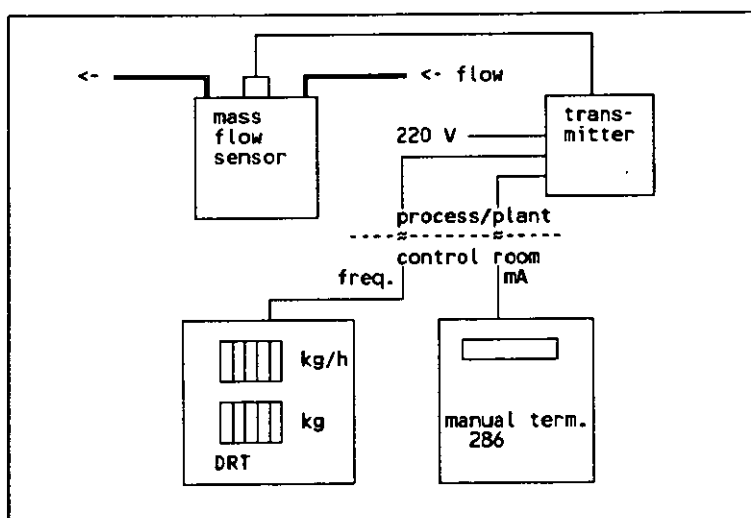
$$Q_{t,m} = Q_{t,g} \cdot \text{density} \quad ; \quad M_{t,m} = \Sigma Q_{t,g} \cdot 640 \cdot d\tau$$

Note that the density is fixed at a constant value : 640 kg/m³ !

2.2.2 Coriolis mass flowmeter

The signal from the sensor of the mass flowmeter is send via cabel to the transmitter, from which the frequency (and milliampere-) signal is transmitted to the Digital Rate Totalizer, DRT (and manual terminal, 268) in the control room.

A shematic diagram of the connections can be seen in figure 2.2.2.1.



Figur 2.2.2.1 : Electrical connections of the mass flowmeter

Some selected data for the mass flowmeter is:

Manufacturer: Micro Motion
 Sensor : Model DS065 S , s/n : 136894
 Size : DN 15 mm , Qmax = 136 kg/minute(8160 kg/hour)
 Transmitter : in EX box in proces/plant
 DRT : Model FMS-3
 Model, s/n : Model F/0.75"/ 30 , S/N : 50242
 Size : 3/4 " , 0.8 - 8 m³/hour
 Accuracy : Spec. ± 0.2 % of rate \pm zero stability
 where zero stability = 0.84 kg/hour

The mass flowmeter is latest calibrated 91-11-16 (with water) by Rosemount, with following results :

Flow calibration factor = 20.5205.13
 Density calibration factor = 12550142754.44

3. Test / calibration on Tyra West

The calibrations on Tyra West in the periode 25th of January to the 28th of January 1992 were performed by Lars Mandrup-Jensen (Force Institutes) with the help of Simon Hockenhuil.

3.1 Method

The Coriolis mass flowmeter is tested / calibrated against the turbine meter both mounted on the condensate pipe downstream the test separator on Tyra West. The zero point of the Coriolis meter has been adjusted before the calibration, by performing a Zero Calibration with the valves before and after the meter closed (no flow condition).

The method applied in the calibrations is flying start/flying stop. The accumulated mass shown on the turbine meter ($M_{t,m}$) is noted simultaneously with the accumulated mass shown by the mass flowmeter (M_c), and these two values are compared using following equation :

$$F_{c-t} = \frac{M_c - M_{t,m} \cdot (Dc/640)}{M_{t,m} \cdot (Dc/640)} \cdot 100 (\%) \quad [3.1.1]$$

where: F_{c-t} = Deviation in percent between the coriolis meter and the turbine meter.

M_c = the mass flowmeter's display of total mass in kg.

$M_{t,k}$ = the turbine meter's display of total mass.

Dc = density (kg/ltr), measured by the mass flowmeter

Other relevant parameters have also been noted, e.g. the process temperature and the process pressure. Also the temperature and density displayed by the coriolis meter.

Calculating the uncertainty of F_{c-t} :

The uncertainty of the determination of F_{c-t} can be estimated by applying the law of propagation of uncertainties as seen in equation [3.1.2].

$$u^2 (F_{c-t}) \approx [(\delta F_{c-t} / \delta M_c) \cdot u(M_c)]^2 + [(\delta F_{c-t} / \delta M_t) \cdot u(M_t)]^2 + [(\delta F_{c-t} / \delta D_c) \cdot u(D_c)]^2 \quad [3.1.2]$$

By rewriting equation [3.1.2] and applying the approximations $M_t \approx M_c$ and $F_{c-t} \ll 100$ equation [3.1.3] can be written.

$$u(F_{c-t}) \approx 100 \cdot [(u^2(M_c) + u^2(M_t)) / M_c^2 + u^2(D_c) / D_c^2]^{1/2} \quad [3.1.3]$$

The uncertainties of M_c , M_t og D_c is estimated in the following:

The display of the mass flowmeter (M_c) is "triggered" (manually read) at the same time as the shift in the display of the turbine meter (M_t), which is updated with every 4 kg. The display of the mass flowmeter is updated with every 1 kg. On this basis the uncertainty of M_c og M_t , on a 95 % confidence level, is estimated to be:

$$u(M_c) \approx (0.5^2 + 0.5^2)^{1/2} \approx 0.7 \text{ kg} \quad [3.1.4]$$

$$u(M_t) \approx (1^2 + 1^2)^{1/2} \approx 1.4 \text{ kg} \quad [3.1.5]$$

The density (D_c) determined by the coriolis meter, which is necessary for the calculation of F_{c-t} , is calculated as the mean value over the duration of the measurement. On this the uncertainty of D_c is estimated to be :

$$u(D_c) \approx 0.5 \text{ kg/m}^3 \quad [3.1.6]$$

By inserting equation [3.1.4], [3.1.5] og [3.1.6] in equation [3.1.3], the uncertainty of F_{c-t} can be calculated as :

$$u(F_{c-t}) \approx 100 \cdot [2.45 / M_c^2 + 0.25 / D_c^2]^{1/2} \quad [3.1.7]$$

As the value of D_c is approximately 650 kg/m^3 following values for the uncertainty of F_{c-t} as a function of M_c can be given:

M_c [kg]	100	500	1000	2000	∞
$u(F_{c-t})$ [%]	1.6	0.3	0.2	0.1	0.08

The values of F_{c-t} determined by equation [3.1.1] should therefore be regarded in the light of and with respect to the estimates for the uncertainty as given in the table above. It should although be noted that besides the above mentioned contributors to the uncertainty there is of course contributions from the non-stability of the two meters due to variations in the process parameters (flow, temperature and pressure) as well as from the accuracy /repeatability of the coriolis meter regarding the determination of the density.

3.2 Results

The test / calibrations of the coriolis meter versus the turbine meter has been performed simultaneously with the platforms normal "6 hours test" on the following wells : TW B08, TW B12 og TW C02. The table given in Figure 3.2.1 gives an extraction of the results.

date (m/d/y)	well I.d.	flow (kg/h)	Dev. (%)	density (kg/m ³)	X _m , s, n % %	Q _{min} - Q _{max} (kg/h)	Mc [kg] u(Fc-t) (%)
1/26/92	TW B12	288.0	8.98	666.8	X _m = 9.49 s = ± 0.50 (n = 4)	288 - 320	≈ 100 - 200 ≈ 1.6 - 0.8
1/26/92	TW B12	300.0	9.95	667.0			
1/26/92	TW B12	302.0	9.89	666.5			
1/26/92	TW B12	302.1	9.13	666.9			
1/26/92	TW B12	970.9	1.75	665.9	X _m = 1.39 s = ± 0.25 (n = 4)	971 - 1083	≈ 300 -1000 ≈ 0.5 - 0.2
1/26/92	TW B12	1,012.5	1.37	665.8			
1/26/92	TW B12	1,062.0	1.27	665.9			
1/26/92	TW B12	1,082.9	1.18	665.9			
1/25/92	TW B8	1,584.0	.73	665.3	X _m = 0.88 s = ± 0.18 (n = 22)	1584 - 2180	≈ 1000-1500 ≈ 0.2 - 0.1
1/25/92	TW B8	1,664.5	1.10	663.5			
1/25/92	TW B8	1,783.6	.82	665.3			
1/25/92	TW B8	1,815.0	.81	664.0			
1/25/92	TW B8	1,835.6	.84	665.0			
1/25/92	TW B8	1,842.9	.90	665.6			
1/25/92	TW B8	1,854.9	.90	664.8			
1/25/92	TW B8	1,864.4	.89	665.3			
1/25/92	TW B8	1,876.9	.93	664.0			
1/26/92	TW B12	1,877.0	.83	665.7			
1/25/92	TW B8	1,886.9	.88	663.5			
1/25/92	TW B8	1,929.4	.80	663.9			
1/26/92	TW B12	1,938.2	1.23	666.2			
1/26/92	TW B12	1,940.0	.77	668.3			
1/26/92	TW B12	1,947.9	1.09	665.9			
1/26/92	TW B12	1,979.0	.96	665.7			
1/26/92	TW B12	2,000.0	.67	666.0			
1/26/92	TW B12	2,032.0	.88	665.8			
1/26/92	TW B12	2,038.7	.69	665.8			
1/25/92	TW B8	2,042.0	.73	664.3			
1/26/92	TW B12	2,042.1	1.31	666.1			
1/26/92	TW B12	2,180.0	.55	665.9			
1/27/92	TW C02	3,050.8	.59	645.0	X _m = 0.53 s = ± 0.12 (n = 11)	3051 - 3369	≈ 1500-3000 ≈ 0.1 - 0.1
1/27/92	TW C02	3,054.2	.48	644.8			
1/27/92	TW C02	3,099.3	.39	645.4			
1/27/92	TW C02	3,105.0	.41	645.5			
1/27/92	TW C02	3,108.0	.69	644.1			
1/27/92	TW C02	3,143.6	.55	645.6			
1/27/92	TW C02	3,154.3	.76	643.8			
1/27/92	TW C02	3,246.8	.54	644.7			
1/27/92	TW C02	3,290.0	.58	645.0			
1/27/92	TW C02	3,322.5	.35	646.1			
1/27/92	TW C02	3,369.2	.54	645.2			

Figure 3.2.1 : Extraction of the results from the cal. on Tyra West.

Explanation to Figure 3.2.1 :

- flow : Mean flow, mass divided by measured time
- Dev. : Deviation between the Coriolis- and the turbine meter (F_{c-t})
- density : density measured by the coriolis meter
- X_m : mean value of the deviation for measurements within a flow range
- s : standard deviation for n measurements
- Q_{min}/Q_{max}: min. and max. values of flow for n measurements
- Mc : nominal amount measured for one test.
- u(Fc-t) : Uncertainty on Fc-t

The values listed in Figure 3.2.1 are shown grafically in Figure 3.2.2 which represents an "error curve".

CALIBRATION Coriolis (C) versus Turbinemeter (T)
TYRA WEST, 25th - 28th. january 1992

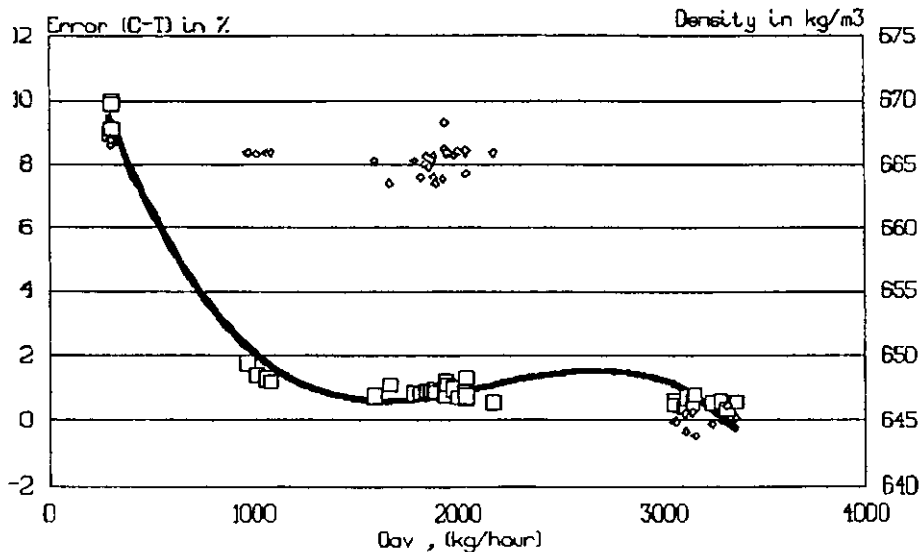


Figure 3.2.2 : "Error curve" , Dev./density versus flow

Figure 3.2.2 shows the deviation between the coriolis meter and the turbine meter (F_{c-t}) as a function of the flow. The measurement points (shown with large rectangles) are joined by a 3rd degree regression curve determined by the "least square method".

The density has been plotted (with small "diamond" symbols) with the y-scale on the right-hand side. It can be seen that the value for the density at the flow range around 3000 kg/hour is somewhat lower than for the other flows. This is due to the lower density of the condensate from TW C02 well.

The deviation can be seen to be very constant in the range of 1000 kg/hour to approximately 3300 kg/hour the mean value of the deviation being around $0.9\% \pm 0.4\%$. This is a good result when the calibration uncertainties are taken into account.

In the range from approximately 1000 kg/hour down to 300 kg/hour the deviation grows to around 9%. The question that immediately arises is which meter is not measuring correctly: the coriolis meter or the turbine meter. This question will be reflected upon on the next section: Calibration in the laboratory.

4. Calibration in laboratory

The calibrations in the Dantest Liquid Flow Laboratory were performed by Lars Mandrup-Jensen (Force Institutes) with the help of Simon Hockenhull.

4.1 Method

The plan was that the metering section consisting of the turbine meter and the mass flowmeter, was to be calibrated against a weighing system.

But as the turbine meter was damaged when it arrived to the laboratory (probably during the transportation off-shore to the laboratory), calibration of this meter was not possible in the laboratory.

The mass flowmeter was calibrated against the weighing system using mineral turpentine (\approx kerosine) with a density of appr. 770 kg/m^3 at $20 \text{ }^\circ\text{C}$. The principle applied is standing start and standing stop and an amount corresponding to minimum 30 seconds calibration periode has been measured.

The error for the mass flowmeter (F_{c-v}) is determined as:

$$F_{c-v} = \frac{M_c - M_v \cdot BCF}{M_v \cdot BCF} \cdot 100 (\%) \quad [4.1.1]$$

where: F_{c-v} = Error in percent for the mass flowmeter
 M_c = Total mass of the mass flowmeter in kg
 M_v = Display of the weight in kg
 BCF = bouyancy correction factor, nom. = 1.0014

The uncertainty of F_{c-v} is estimated to be better than $\pm 0.2 \%$.

4.2 Results

The results from the calibration of the mass flowmeter against the weighing system is shown in the table below. \bar{x}_m is the mean value and s is the standard deviation.

Cal. Nr.	Flow [kg/h]	Fc-v [%]	\bar{x}_m [%]	s [%]
1	223	-0.33		
2	303	-0.25		
3	310	-0.38	-0.29	0.06
4	312	-0.19		
5	315	-0.32		
6	316	-0.25		
7	1284	-0.48		
8	1292	-0.44		
9	1295	-0.46		
10	1306	-0.45	-0.46	0.02
11	1307	-0.42		
12	1307	-0.42		
13	1309	-0.49		
14	1313	-0.48		
15	2527	-0.51		
16	2537	-0.51		
17	2557	-0.49	-0.52	0.02
18	2561	-0.54		
19	2588	-0.54		

Figure 4.2.1 : results from the calibration of the mass flowmeter against weighing system.

The mean value of the error in the flow range of 223 to appr. 2600 kg/hour is -0.42% with an unlinearity of $\pm 0.11\%$, which at least regarding the unlinearity is within the specifications.

Comparing these results with the off-shore calibration results (see figure 3.2.1 and figure 3.2.2) it can be seen that it was the turbine meter that was in error in the low flow range. This is in accordance with theory and practise of the calibration curve of a "normal" turbine meter.

Besides the above calibrations the mass flowmeter has been calibrated using pulsating flow. The flow was turned up and down every 10 seconds a total of ten times during a calibration. 5 repeat measurements have been performed, in which the mean value of the error was measured to be -0.48% with a standard deviation of 0.02% . Therefore no significant difference from the calibration with non-pulsating flow.

5. Conclusion

The Coriolis meter has been tested off-shore against a turbine meter, and acceptable results were obtained. The turbine meter and the Coriolis meter compare well down to 1000 kg/hour. In the flow range under 1000 kg/hour the deviation between the meters grow as the error of the turbine meter grows. This is to be expected from a normal turbine meter.

In the laboratory the Coriolis meter has been calibrated against a weighing system and there the meter has shown good repeatability but an off-set of approximately -0.42% . The Coriolis meter was found not to be significantly sensitive to pulsations.

In the following will be given some benefits and non-benefits in using Coriolis meters off-shore, which have been deduced from the calibrations performed in this project off-shore and in the laboratory :

Benefits:

- Good measurement uncertainties in a large measuring range.
- Small sensitivity towards pulsations
- Measures the density and temperature of the fluid continuously
- Will not be damaged by particles in contrast to turbine meter

Non-benefits:

- Safety risk in the case of fatigue fracture, as the fluid then will flow uncontrolled (in contrast to turbine meter)
- Sensitive to air in the fluid
- Possible sensitivity to vibrations in the fundament

On the basis of the results from the performed calibrations the Coriolis mass flowmeters are evaluated to be possible alternatives to conventionally applied metering systems off-shore.

The performed calibrations have although not tested the Coriolis meters under every possible condition and therefore this project is intended to be followed by a more complete investigation. Such an investigation could besides uncovering all benefits, also involve several manufacturers of meters, long term tests especially to test the possibility of fatigue fracture, variation in the content of particles and air in the fluid and possible vibrations of the fundament.

COMPACT LARGE BORE DIRECT MASS FLOWMETERS

by

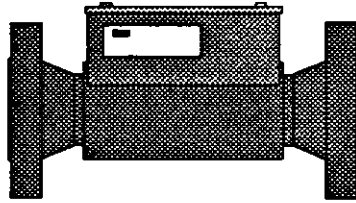
A J Matthews and C L Ayling
Schlumberger Industries

Paper 5.3

NORTH SEA FLOW MEASUREMENT WORKSHOP
26-29 October 1992

NEL, East Kilbride, Glasgow

COMPACT LARGE BORE DIRECT MASS FLOW METERS



A. J. Matthews and C. L. Ayling

Schlumberger Industries, Industrial Transducer Division,
Farnborough, England.

SUMMARY

Although suitable for the measurement of hydrocarbons, few large bore direct mass flow meters are available, and these are generally limited in their application by their large size.

This paper presents a compact direct mass flow meter that uses a novel concept to sense the flow. A resonating tuning fork is used which enables the size to be kept similar to that of a turbine meter for bore sizes of 4 inch and above. The meter provides outputs of mass flow, density and temperature. Its naturally rugged design offers very high pressure containment.

The research has been performed by Schlumberger Industries in collaboration with Statoil. Tests results from Norsk Hydro, Porsgrunn are presented showing repeatability of $\pm 0.05\%$ and linearity of $\pm 0.25\%$ for a 4 inch bore meter at flow rates up to 350 tonnes/hr.

CONTENTS

1.0 Introduction

2.0 Meter Design

2.1 Theory of operation

2.2 Pick-up and drive mechanism

2.3 Mechanical configuration

3.0 Meter Performance

3.1 Effects on meter performance (theory)

3.2 Test results

3.3 Secondary outputs

4.0 Conclusions

1.0 INTRODUCTION

Direct mass flow meters are rapidly being accepted as a good method of measuring mass flow rate to custody transfer standards. Meter sizes are available from a variety of manufacturers in sizes from 3 mm bore up to 6 inch. All of these meters work on the principle of passing the fluid to be measured through the inside of one or two resonating tubes. These tubes can be configured in straight or bent configuration dependent on the manufacturer. Only one meter is currently available in 6 inch bore and this has a shipping weight of 636 Kg and is 1m x 0.3m x 2m in size. This generic physical size, which creates difficulties both for the manufacturer and the user, seems to be the major limitation on these meters.

For the Schlumberger Industries single straight tube design the problem was even more severe. In order to achieve the required pressure ratings combined with suitable mass flow sensitivity, a 4 inch meter would be 3 meters in length and weigh 300 Kg and a 6 inch meter would be 4.5 meters in length and weigh 1100 Kg. This was believed to be impractical and so an alternative solution was required.

2.0 METER DESIGN

In order to overcome the pressure and mass flow sensitivity limitations connected with passing the fluid through a resonating tube, this meter turns the problem inside out and inserts the resonating sensor into the flow. This means that the pressure rating is not limited by the sensor itself and the mass flow sensitivity can be adjusted as desired.

The meter takes the form of a stretched tuning fork either cast or wire eroded from a solid billet of stainless steel. The configuration is shown in fig 2.0.1.

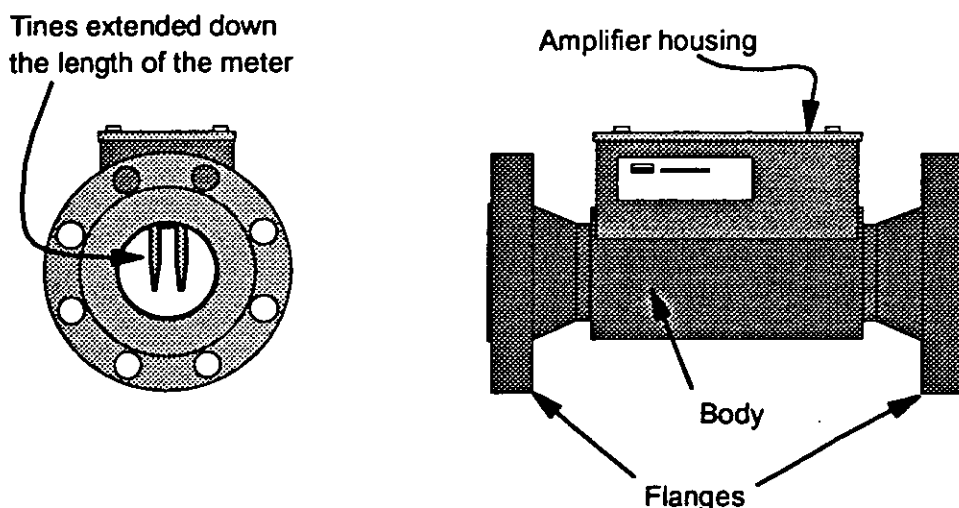
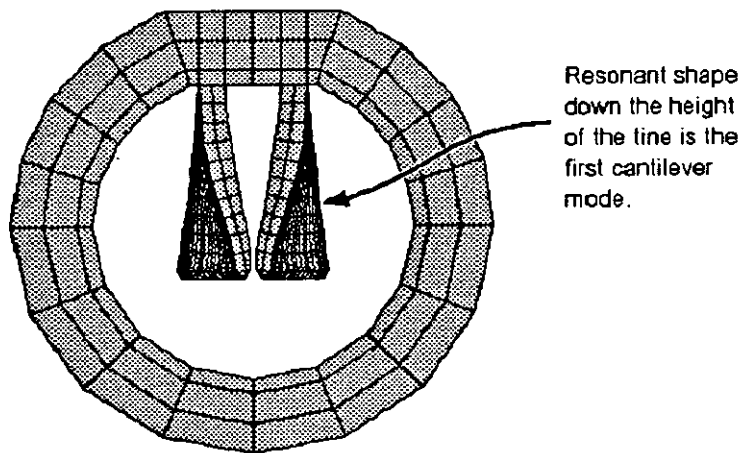


Fig 2.0.1 Mass Meter Tine Configuration

2.1 THEORY OF OPERATION

The operation of this meter is similar in theory to that of the tube type Coriolis meters, although the mathematics is a little more complicated. The tube wall defines a volume of fluid that acts on the resonant tines. The resonant frequency of the tines is dependent on the combined resonant mass of the tines and the fluid surrounding them. Thus the resonant frequency is dependant on the fluid density, which enables an accurate density output ($\pm 0.5 \text{ Kg/m}^3$) to be computed. As fluid flow occurs Coriolis forces are generated which distort the tines' resonant mode shape. The magnitude of this distortion is proportional to the mass flow rate of the fluid flowing past the tines. This distortion can be detected as a phase shift in detectors mounted at each end of the tines.

It should be remembered that the tine movement is only micrometers in amplitude, and hence cannot be seen. All diagrams of the tine mode shapes are grossly magnified.



View down the bore of the meter.
The tines are showing their resonant shape (grossly exaggerated) in mode (1,3).

Fig 2.1.1 End View of Tine Resonance.

One significant advantage of this design is that the magnitude of the phase shift can be designed to be as high as required by controlling the relative positions of the operating mode and the associated twisting modes. In practice, operating phase shifts above 15 degrees create practical problems with linearity and density effects on the meter factor. This phase compares to tube meters which have a full flow phase shift of about 4 degrees.

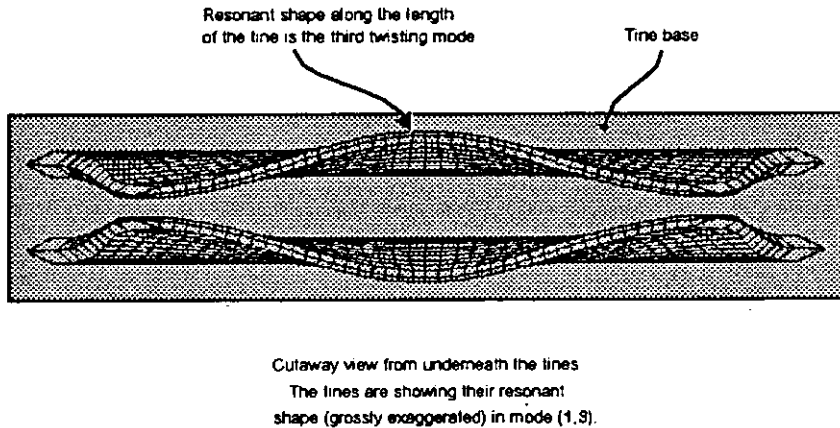


Fig 2.1.2 View of Resonance from Underneath Tines.

The resonant mode chosen is a combination of the first tuning fork mode shape with the third longitudinal mode shape. This can be denoted as mode (1,3) and was found to be the most suitable mode due to a combination of physical characteristics. The discussion of such effects is beyond the scope of this paper.

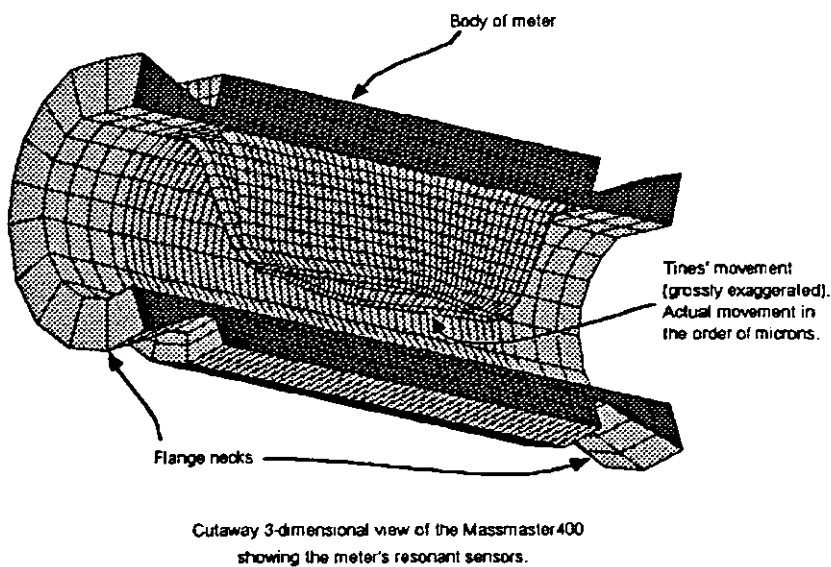


Fig 2.1.3 Three-Dimensional View of Tine Resonance.

2.2 PICK-UP AND DRIVE MECHANISM

The mechanism for maintaining the tuning fork in resonance is similar to other Coriolis meters in principle: a single drive transducer translates electrical energy into tine movement, and two pick-up transducers detect the movement, developing electrical signals which are fed back into the drive circuit.

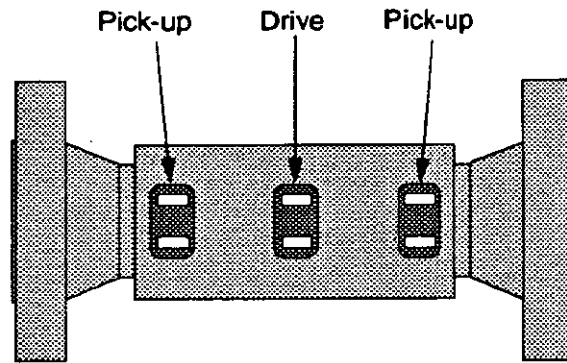


Fig 2.2.1 Pick-up and Drive Arrangement

Since the pick-ups are displaced up- and down-stream of each other, a phase difference is detected between the two signals during flow. This is the prime measurement for the mass flow calculation.

2.3 MECHANICAL CONFIGURATION

The meter has an extremely high pressure containment ability as can be seen from the wall thickness in figure 2.1.1. The one inch thick wall is thinned only over very small areas, visible in figures 2.2.1 and 2.2.2. The wall thickness in the base of each area is still 5mm.

TINE SHAPE

The shape of the resonating tines has been chosen with a view to optimising Coriolis performance whilst avoiding cavitation, minimising erosion and preventing the build up of fibrous particles. The taper and profile of the tines are shown.

The existing design has been designed for oil/condensate applications although some generality of application can be assumed. For other specific applications such as gas mass flow a different tine profile may be used to optimise performance.



Fig 2.3.1 Tine X-section

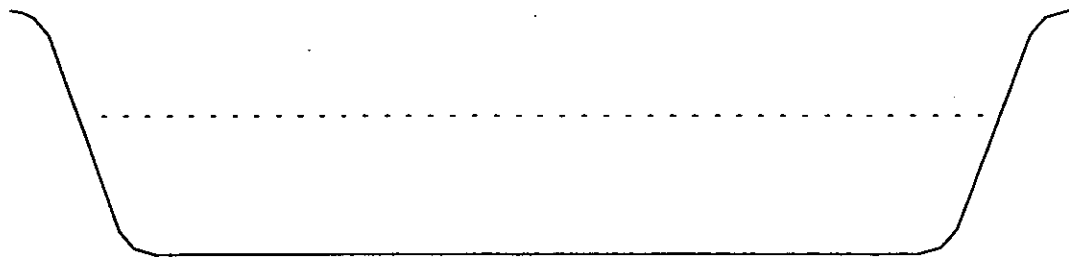


Fig 2.3.2 Tine Side View

3.0 METER PERFORMANCE

The meter produces outputs of phase shift, resonant frequency and line temperature in identical fashion to most other Coriolis mass flow meters. Also the factors that affect the meter's performance are very similar to those that affect traditional tube type Coriolis meters.

Accordingly the output can be compensated for all the characterised systematic effects using a flow computer.

3.1 EFFECTS ON METER PERFORMANCE (THEORY)

EFFECT OF TEMPERATURE

Changes in temperature affect the meter output primarily due to changes in the material modulus and to a lesser extent due to dimensional changes. The magnitude of these effects are;

Effect on mass flow sensitivity	+0.04% / deg C (for 316 st. steel)
Effect on density output	+0.6 Kg/m ³ / deg C (for 316)

It is easy to compensate for these effects, which are characteristic of the material composition. They are of the same magnitude as for tube type meters.

EFFECT OF PRESSURE

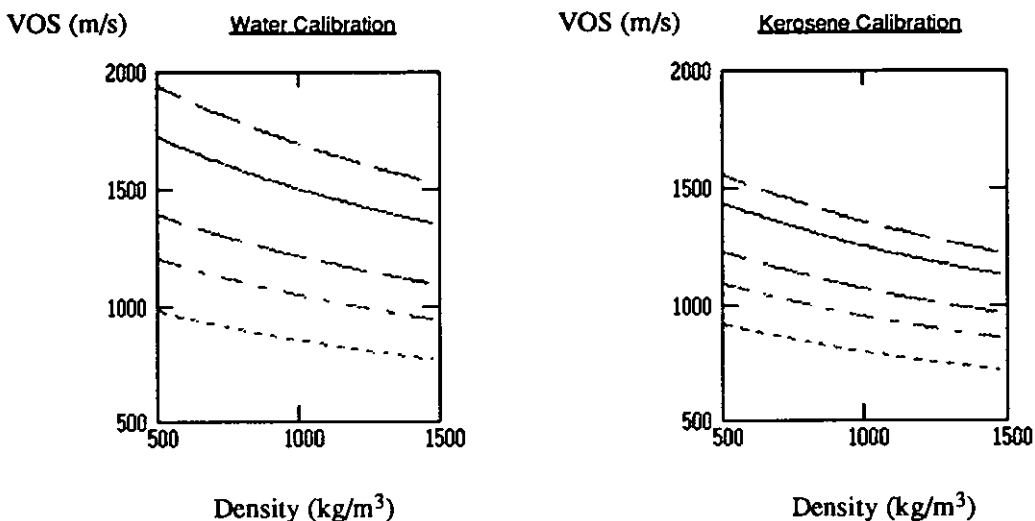
Because the tines are completely surrounded by fluid and no stress or dimensional changes occur in the tines, there is NO PRESSURE EFFECT on this type of meter on either density or massflow measurement.

EFFECT OF VISCOSITY

Homogeneous viscous fluids should have little effect on meter accuracy. High viscosity will damp the tine movement and the effective viscous range of the meter will depend upon the power setting of the drive. The present drive levels have been chosen to comply with intrinsic safety approval limits, but the useful viscous range has yet to be determined on these prototypes.

EFFECT OF FLUID VELOCITY OF SOUND (VOS)

The VOS of a fluid causes the resonant weight to be heavier than the static mass of a volume of fluid. Hence Coriolis meters always 'overread'. However since all meters are calibrated on real fluids the effect is automatically compensated for the calibration fluid. Subsequent use on a different fluid produces VOS errors.



Offsets -0.2%; 0; +0.5%; +1%; +2% respectively (top to bottom)

Fig. 3.1.1 Graphs of constant Massflow VOS offset.

EFFECT OF FLOW PROFILE

The meter could conceivably be sensitive to some types of flow profile within the pipeline. However no such effect has yet been identified and the sensitivity could be negligible. Through symmetry, swirl is not expected to create any systematic offset. Initial installations could use the same flow conditioning that is used for turbine meters, although tests may oneday prove that this level of conditioning is unnecessary.

3.2 TEST RESULTS

In collaboration with Statoil, a development program of tests has been planned and started. The results displayed herein are from the initial prototype, tested at Norsk Hydro, Porsgrunn, Norway on 3-4 October 1991.

NOTE ON FIG. 3.2.1

On the first day of testing, an attempt was made to find the flow range of the meter. Linearity was lost above 350 t/h due to the onset of cavitation. At low flow a zero error caused the percentage error to veer positive.

Developments both in streamlining to minimise cavitation and optimising zero stability are continuing at Schlumberger.

NOTE ON FIG. 3.2.2

On the second day of testing, the repeatability was assessed at three flow rates. The results at 170t/h and 300t/h were within the $\pm 0.05\%$ specification of the volumetric flow rig at Norsk Hydro.

NOTE ON FIG. 3.2.3

Loose wiring was identified as the source of the zero instability causing the 50t/h repeatability to appear worse than that at higher flows. After refitting the results in Fig. 3.2.3 were taken, showing 50t/h repeatability now under $\pm 0.05\%$ as well.

Naturally, repeatability is the first quality required of mass flow meter prototypes, but eventually tests on different fluids and flow conditions are intended. Testing on full simulated North Sea conditions is planned as soon as possible and off-shore experience anticipated soon after.



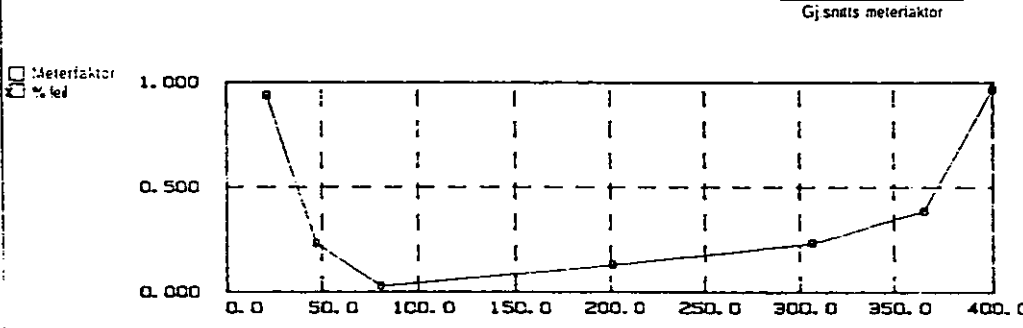
Porsgrunn
Automatiseringsavdelingen

Kalibreringsbevis for
gjennomstrømningsmålere

Bevis nr. F-2046

Dokumentnummer: FMAS									
Måletype: Massflow			Produsent: Schlumberger			Dimensjon: 4"			
Typebetegnelse: Prototype			Seriener: 001			Måleområdet: 40-400 m³/h			
Nominelle verdier					Måletilkobling				
Væskestrømningsvolum	Fluksvolum	Normal	Temperatur	Korrigert volum	Væskestrømsindik	Indikeret volum	Pulser	Meterfaktor	Føl
<input type="checkbox"/> m ³ /h	<input type="checkbox"/> m ³ /h	<input type="checkbox"/>	<input type="checkbox"/> °C	<input type="checkbox"/>	<input type="checkbox"/> Hz	<input type="checkbox"/> Teileverk	<input type="checkbox"/> Pulser	<input type="checkbox"/> m ³	<input type="checkbox"/>
<input type="checkbox"/> m ³ /h	<input type="checkbox"/> m ³ /h	<input type="checkbox"/>	<input type="checkbox"/> °C	<input type="checkbox"/>	<input type="checkbox"/> mA	<input type="checkbox"/> Ut. integ.	<input type="checkbox"/>	<input type="checkbox"/> pl	<input type="checkbox"/>
<input type="checkbox"/>	<input type="checkbox"/>	<input type="checkbox"/>	<input type="checkbox"/>	<input type="checkbox"/>	<input type="checkbox"/>	<input type="checkbox"/>	<input type="checkbox"/>	<input type="checkbox"/>	<input type="checkbox"/>
400.00	12092.00	H	22.2	12077.80		12194.80			0.97
365.00	12074.00	H	22.5	12059.26		12106.00			0.39
306.00	12098.00	H	22.5	12090.20		12118.60			0.23
201.00	12041.00	H	22.8	12025.50		12041.20			0.13
80.00	5928.00	H	22.0	5921.30		5923.10			0.03
47.00	6004.00	H	23.0	5996.19		6009.98			0.23
21.00	2012.00	H	23.0	2009.34		2028.20			0.94

* R: Hulmålnormal; Nøyaktighet: ± 0.05%; Temperaturkorreksjonsfaktor: 1-0.00005 · T; °C;
 * R: Referansemåler; Nøyaktighet volum: ± %; Nøyaktighet væskestrøm: ± %
 Korrigert etter kalibrering mot hulmålnormal.



Væskestrøm: l/min m³/h % av FS ms
 Kalibreringspunkt: Løst For: DN DN 100 DN mm Rett rørstrekk foran: DN

Bemerkninger: **OMGJORT VOLUMETRISK TIL MASSE.**

2/26 5.54 100 10/1/2008

Forordningen: **9/10 9/1** Utgitt av: **Hans Drage** Ansvarshavende: **Børge M. Leff**

Fig.3.2.1 Test Results: Day 1.



Porsgrunn
Automatiseringsavdelingen

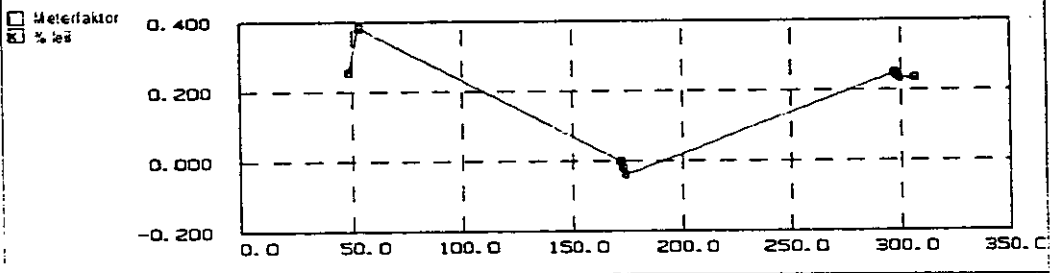
Kalibreringsbevis for
gjennomstrømningsmålere

Serial nr
E-2047

Egenskaper					
FIMAS.					
Måletype	Massflow		Proseser	Schlumberger	
Dimensjon	4"				
Typemåletype	Prototype		Serialnr	001	
Måleområde	40-400 m ³ /h				
Måletype			Måletype		
Væsketype	Arbeitsvolum	Temperatur	Korrigert volum	Væskestrømningsmåler	Proseser
<input type="checkbox"/> H ₂ O	<input type="checkbox"/> m ³	<input type="checkbox"/> °C	<input type="checkbox"/> m ³	<input type="checkbox"/> Hz <input type="checkbox"/> mA	<input type="checkbox"/> Fasterelek <input type="checkbox"/> NH ₄ steg <input type="checkbox"/> Kg
					<input type="checkbox"/> Pulser
					Meterfaktor <input type="checkbox"/> m ³ <input type="checkbox"/> l
					Feil %
306.00	12098.00	H 22.5	12090.20	12118.60	0.23
297.00	12085.00	H 22.2	12070.80	12100.90	0.25
298.00	12079.00	H 22.5	12064.20	12093.20	0.24
299.00	12094.00	H 22.5	12079.20	12107.40	0.23
172.00	12052.00	H 22.7	12036.80	12036.60	-0.00
173.00	12039.00	H 22.9	12023.40	12021.00	-0.02
174.00	12027.00	H 23.0	12011.10	12006.40	-0.04
48.00	6009.80	H 23.0	6001.88	6017.19	0.26
53.00	6040.20	H 23.6	6031.55	6054.59	0.38

* R: Hulmålnormal. Nøyaktighet: ± 0.05%. Temperaturkorreksjonsfaktor: 1-0.00005 · T (°C).
 * R: Referansemåler. Nøyaktighet volum: ± 0.05%. Nøyaktighet væskestrom: ± 0.05%.
 Korrigert etter kalibrering mot hulmålnormal.

Gjennomsnittlig meterfaktor



Væsketype: l/min m³/h % av FS ms
 Måleområde: 100 mm

OMGJORT VOLUMETRISK TIL MASSE.

Porsgrunn 7/10 71 | utført av *Hans E. Dings* | Ansvarshavende *St. M. Dahl*

Fig.3.2.2 Test Results: Day 2.

3.3 SECONDARY OUTPUTS

The meter can be calibrated to compute **density** from the resonant time period, in a similar fashion to other Schlumberger 'Solartron' densitometers. A 3 liquid calibration with temperature calibration should achieve accuracies of $\pm 0.5\text{kg/m}^3$. Knowledge of the generic characteristics of VOS, flow and viscous effects will then permit accurate density measurement of the full 4" flow stream. As previously mentioned, there is no pressure effect on this meter. Knowing the mass rate and line density enables the **volume** rate to be derived.

A PT100 embedded into a tine gives an accurate measurement of **Temperature** for density referral calculations. Hence **referred density, standard volume, and nett mass** can easily be computed.

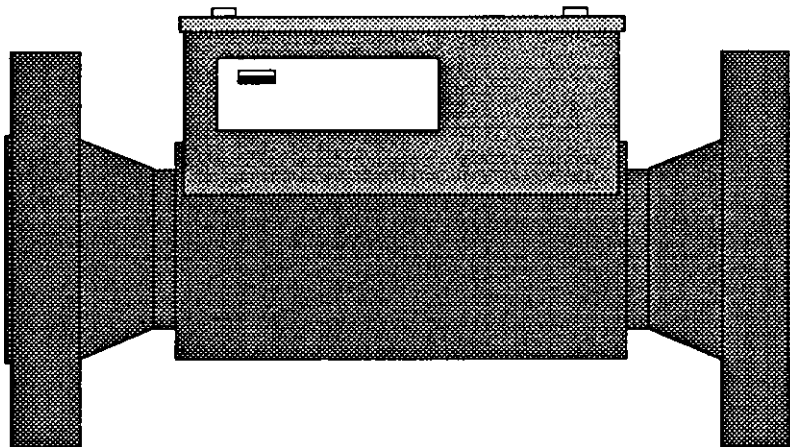
Despite the radical mechanical differences between this new meter and the standard Coriolis meter, the information output is identical. Hence the meter interfaces directly to a Schlumberger flow computer in which secondary calculations can be performed.

4.0 CONCLUSIONS

This meter places the sensing resonator within the fluid, instead of surrounding the fluid with a resonating tube. Thus it overcomes the problems of scale by turning the problem inside out. Large bore coriolis meters of only 3 diameters length will soon be commercially available.

Initial test results show that this design of meter can achieve similar performance to that of existing mass meters, yet have the advantages of compact size, rugged design and high pressure capabilities.

Work is planned to continue in optimising the design of a 4 inch meter and to produce 6 and 8 inch versions during 1993. Initial applications are expected to be on refined single phase products, LPGs and gases.



PIPE ELBOW EFFECTS ON THE V-CONE FLOWMETER

by

S A Ifft and E D Mikkelsen
Ketema Inc

Paper 5.4

NORTH SEA FLOW MEASUREMENT WORKSHOP
26-29 October 1992

NEL, East Kilbride, Glasgow

PIPE ELBOW EFFECTS ON THE V-CONE FLOWMETER

Stephen A. Ifft and Eric D. Mikkelsen

Ketema Inc. / McCrometer Division, Hemet, California

SUMMARY

The paper discusses the performance of the McCrometer "V-Cone" differential pressure meter in installations after single 90° elbows and double 90° elbows out-of-plane.

The National Institute of Standards and Technology (N.I.S.T.) in Gaithersburg, Maryland is studying installation effects on several flowmeter technologies, including a typical orifice plate flowmeter. McCrometer, along with an independent test facility, has conducted tests on the V-Cone using similar configurations. All tests on the orifice plate and the V-Cone use water as the test fluid in 50 mm stainless steel pipe.

In matching configurations and Reynolds number ranges, the V-Cone is less susceptible to elbows upstream than a typical orifice plate flowmeter.

NOTATION

Cd	Meter coefficient of discharge	--
D	Nominal pipe diameter	mm
D _i	Inside pipe diameter	ft
d	Outside cone diameter	ft
G _c	Gravitational constant	$\frac{ft}{sec^2}$
K	Meter factor	$\frac{ft^{2.5}}{sec}$
k	Isentropic exponent	--
P _s	Static line pressure	psfa
Q	Volumetric flowrate	ACFS
Y	Adiabatic expansion factor	--

β	Beta ratio	--
ΔP	Differential pressure	psf
ρ	Fluid density	$\frac{ft^3}{lb}$

1. INTRODUCTION

1.1 Background

Recently, much interest has been focused on the effect of different installations on flowmeter accuracy. More people are becoming aware that a flowmeter primary element is only part of the entire flow measurement system. The accuracy of the measurement system depends as much on the primary element of the flowmeter as the secondary instrumentation and the upstream and downstream pipe runs adjacent to the flowmeter.

Each flowmeter technology requires a certain distance of straight, undisturbed pipe before and after the primary element. Depending on the flowmeter requirements, these distances are often difficult or impossible to achieve. For instance, a flowmeter may require more piping than is available in an existing system where flow measurement was not necessary before. A new application may have limited area, such as on oil platforms or vehicles. Perhaps the distance is available but the cost of providing straight pipe before and after the primary element is limiting. In systems with 25 mm line sizes, installation requirements may only require a meter or two. This cost may not be significant. However, in systems where line sizes reach over 700 mm, the cost of providing 35 D of straight run before a meter may be prohibitive.

The design engineer can usually compromise in some way to accommodate the limitations of the flowmeter. However accuracy or permanent pressure loss sacrifices. Accuracy decreases if the piping requirements are ignored. Permanent pressure loss increases if a flow conditioner is employed upstream of the meter. Either solution is less than ideal.

With these problems in mind, the National Institute of Standards and Technology (N.I.S.T.) in Gaithersburg, Maryland, decided to form a consortium consisting of sponsor members from industry and other government programs, both domestic and foreign. N.I.S.T. thus began the "Industry-Government Consortium Research Program on Flowmeter Installation Effects." The goal of this group was to study the flow patterns of water after common installation problems such as single elbows, double elbows out-of-plane, tees, and reducers. N.I.S.T. then installed flowmeters after these disturbances. Industry members donated two flowmeters to represent a typical differential pressure orifice plate flowmeter and a typical turbine flowmeter. Characteristic curves were plotted to show the flowmeter's variance at different positions relative to the elbows or other disturbances. This might allow end users of orifice plates or turbine meters to characterize their meter's performance according to the installation.

One hope of the consortium was that industry members with proprietary meters would run tests parallel to the tests run at N.I.S.T. Ketema/McCrometer Division, a flowmeter manufacturer

and consortium member, in Hemet, California decided to run installation effects tests on the V-Cone differential pressure flowmeter. This is a patented design, differential pressure producing device using the same basic principles of flow measurement as the orifice plate. The overall goal of these tests was to define installation requirements for the V-Cone downstream of common disturbances. McCrometer converted an existing test lab to emulate N.I.S.T. test conditions. Configurations tested to date have been the single 90° elbow and the double 90° elbows out-of-plane .

1.2 The V-Cone differential pressure flowmeter

McCrometer introduced the V-Cone flowmeter in 1986 as an alternative to traditional differential pressure flowmeters. The goal in the development of this device was to create a meter that emphasized the advantages, but overcame the limitations, associated with traditional differential pressure flowmeters.

The geometry of the V-Cone suggests a radically different approach to differential pressure flowmetering, see Figure 1. As with other differential pressure devices, the flow constricts to create high and low velocity areas, which creates a differential pressure signal. However, the V-Cone's constriction is not a concentric opening through the center of the pipe. The V-Cone creates an annular opening, forcing the fluid to flow around a cone suspended in the center of the pipe.

Equations for the V-Cone are slightly different from an orifice plate or venturi. The Beta ratio, β , is the ratio between the square root of the open area in the pipe and the square root of the open area at the meter's constriction. The V-Cone's Beta ratio is:

$$\beta = \frac{\sqrt{D_i^2 - d^2}}{D_i} \quad (1)$$

The standard equation for differential pressure flowmeters is:

$$Q = KY\sqrt{\frac{\Delta P}{\rho}} \quad (2)$$

The k factor for the V-Cone is:

$$K = \frac{\pi}{4}\sqrt{2G_c} \frac{D_i^2\beta^2}{\sqrt{1-\beta^4}} C_d \quad (3)$$

For compressible flow, McCrometer applies the standard equation for the adiabatic expansion factor, Y :

$$Y = \left\{ \frac{[1 - \beta^4] \left[\frac{k}{k-1} \right] \left[1 - \frac{\Delta p}{p_s} \right]^{\frac{2}{k}} \left[1 - \left(1 - \frac{\Delta p}{p_s} \right)^{\frac{k-1}{k}} \right]}{\left[1 - \beta^4 \left(1 - \frac{\Delta p}{p_s} \right)^{\frac{2}{k}} \right] \left[1 - \left(1 - \frac{\Delta p}{p_s} \right) \right]} \right\}^{\frac{1}{2}} \quad (4)$$

Note: The adiabatic expansion factor applied only if $Y > 0.96$. Otherwise a characteristic expansion factor must be derived for the meter based on calibration data in a compressible fluid.

2. TEST PARAMETERS

The test parameters for the V-Cone tests were set to follow the test parameters established by N.I.S.T. tests on the orifice plate.

The McCrometer static gravimetric flow calibration stand can test 12 mm to 100 mm nominal diameter flowmeters. Figure 2 shows a schematic diagram of the testing apparatus. Figure 3 shows a scaled diagram of the test section.

The closed system recirculates water constantly from a 2200 liter storage tank. An electric pump draws the flow from the tank through a 100 mm PVC pipe. From the pump, the water enters an upstream header. The 250 mm by 1200 mm chamber incorporates straightening vanes and a dampening screen to lessen pulsations from the pump. A recirculating by-pass line of 50 mm PVC pipe also helps to reduce pulsations. The water leaves the header horizontally through a 50 mm PVC ball valve, used to ease startup vibrations.

The water passes through 50 D of straight 50 mm PVC pipe before entering the single elbow or the double elbows out-of-plane. The elbows are all 90° long radius (centerline curvature=1.5 D.) Flow then passes through the 200 D of horizontal test section. Test section piping is schedule 40, stainless steel with an approximate wall roughness of 3 μm . After passing the test section, the water turns vertical, passing a PVC ball valve. This valve is used for flow regulation purposes. The diverter section follows.

A pneumatic system diverts the water to either a receiving tank, open directly to the storage tank, or to a collection tank. The collection tank weighs the collected water over a measured time. An optical sensor on the diverter triggers a timer to measure the precise time of the collection period. A mercury thermometer measures the fluid temperature.

In the test section, the meter was leveled prior to testing. Differential pressure taps on the meter face the "inside" of the elbows. A "smart" differential pressure transmitter measured the differential pressure created by the meter. The 4 to 20 mA signal from the transmitter was measured with a multimeter. A computer collected 200 data points over the test period through an IEEE-488 bus.

Prior to testing, the transmitter was calibrated using a pneumatic dead weight tester. The "smart" capability of the transmitter allowed the full scale differential pressure of the transmitter to be scaled to the full scale created by each meter at the desired maximum flowrate.

3. TEST RESULTS -- INSTALLATION EFFECTS OF ELBOWS UPSTREAM

3.1 McCrometer results with the V-Cone

The objective of the first set of McCrometer tests was to detect the effect of upstream elbows, both a single 90° elbow and double 90° elbows out-of-plane, on a V-Cone meter. The double elbows were close coupled.

Accuracy for the V-Cone primary element is $\pm 0.5\%$. During the evaluation, a deviation outside of $\pm 0.5\%$ was considered to be an effect of the elbow configuration.

The McCrometer tests included three 50 mm V-Cone flowmeters with Beta ratios of 0.363, 0.650, and 0.750. Beta ratios for V-Cones represent the same area ratio that standard orifice plate Beta ratios represent. These meters represent the typical range of Beta ratios for V-Cone applications. End connections were standard ANSI flanges (150 pound, raised face, slip-on.) The test fluid was water at approximately 20°C.

Test conditions were to include the following flowrates:

V-Cone meter	Flowrate range (GPM)	Reynolds number range
Beta= 0.363	6 to 37	11,000 to 65,000
Beta= 0.650	8 to 31	14,000 to 51,000
Beta= 0.750	15 to 65	25,000 to 110,000

The meter was first placed a maximum distance from the elbows. The data taken at this point was the baseline data for the particular meter. In this position the meter was 190 D away from the elbows. Each meter was then moved in intervals closer to the elbows. Six different positions relative to the elbows were tested. The positions were approximately 190, 23, 9, 2, and 0 D away from the elbows.

At each position, each meter was tested at five flowrates covering the range stated above. At each flowrate a repeat point was taken for verification. Thus for each position, a total of ten test points were taken. These ten points were then averaged and plotted on figures 4 and 5.

Figure 4 shows the change in the meter's coefficient of discharge, Cd, versus the distance of the meter from the single elbow in nominal pipe diameters. The change in the meter's Cd represents the percentage deviation from the baseline data taken at 190 D. These points represent an average Cd of the Reynolds number range.

Two dashed error bars show the stated accuracy of the meter. These bars are at $\pm 0.5\%$. Points outside these bars are considered results of the elbow upstream. On Figure 4, the V-Cone with $\beta = 0.750$ showed a deviation at 0 D of $+0.622\%$ from the baseline data. All other points fell within the $\pm 0.5\%$ of the meter. The maximum effect of the single 90° elbow on the three V-Cones during the McCrometer testing was 0.122% . This was the largest deviation from baseline data with the V-Cone.

Figure 5 uses slightly different X and Y scales to show the effect of double elbows out-of-plane on the V-Cone. Only one point falls outside the accuracy bars. This point is at 100 D with the V-Cone at $\beta = 0.650$. The deviation was $+0.504\%$. The maximum effect of the double 90° elbows out-of-plane on the three V-Cones during the McCrometer testing was 0.004% .

3.2 Independent test results with the V-Cone

SIREP in England performed an evaluation of installation effects on the V-Cone. SIREP is an international instrument users' association. The international industry members of SIREP approached McCrometer with the offer to evaluate the V-Cone according to the specifications of the meter. SIRA is the instrument testing branch of SIREP and was responsible for the evaluation process. Installation effects tests were among the variety of tests SIRA was to perform.

SIRA tested both the single 90° elbows and double 90° elbows out-of-plane before the V-Cone. The double elbows were close coupled. SIRA was to test the single elbow in two configurations, once with the taps in the same plane as the elbow, another with the taps perpendicular to the plane of the elbow.

McCrometer provided a standard 50 mm V-Cone for the tests. End connections were standard ANSI flanges (150 pound, raised face, slip-on.) The test fluid was kerosene at 30°C (density = 801.4 kg/m^3 , viscosity = 1.73 cSt.)

The flow criteria for these tests were to be as follows:

V-Cone meter	Flowrate range (GPM)	Reynolds number range
Beta= 0.600	57 to 540	13,000 to 125,000

The meter was placed at two positions relative to the elbow configurations, at 2 and 10 D downstream. Baseline data was taken from a straight line test with no elbows. At each position, the meter was tested at five flowrates. Three points were taken at each point.

SIRA results concur with McCrometer results on both the single and double elbow tests. On request, McCrometer will provide a copy of the SIREP evaluation report E 1705 S 92.

3.3 NIST results with a typical orifice plate flowmeter

Dr. George Mattingly and Dr. T.T. Yeh of the Fluid Flow group of the N.I.S.T. in Gaithersburg, Maryland performed installation effects on a typical orifice plate flowmeter. This was part of a government-industry consortium to study such effects.

Both a single 90° elbow and double 90° elbows out-of-plane were tested. The double elbows were close coupled.

The N.I.S.T. tests included three orifice plates in a 50 mm line. The stated accuracy of the meters was taken to be $\pm 0.5\%$. The Beta ratios tested were 0.363, 0.500, and 0.750. Flange connections were weld-neck ANSI flanges. The test fluid was water. Flow criteria for these tests were the same as the McCrometer tests.

The positions of the orifice plate to the elbows were similar to the McCrometer tests.

Figure 6 shows the effects of the single elbow on a typical orifice plate. The scales for the X and Y axis match those of figure 4, single elbow effects on the V-Cone. The orifice plate showed significant effects from the single elbow. The maximum effect of the elbow (at 3 D with $\beta = 0.750$) was approximately -4.5% .

Figure 7 shows double elbow effects on the orifice plate. Again, the scales of Figure 9 match those of figure 5, double elbow effects on the V-Cone. The orifice plate showed slightly less effect from the double elbows than the single elbow. The maximum effect of the elbows (at 3 D with $\beta = 0.363$) was approximately $+2.6\%$.

4. CONCLUSIONS

In matching piping configurations and Reynolds number ranges, the V-Cone demonstrated less susceptibility to elbows upstream than a typical orifice plate flowmeter.

V-Cones showed some effect from the elbows, up to 0.122% in one test. Orifice plates, however, showed extreme effects. This was not unexpected according to existing international orifice metering standards, both ISO-5167 and ANSI/API-2530. With a Beta ratio = 0.750 orifice plate, ISO-5167 recommends 70 D upstream for double elbows out-of-plane. ANSI/API-2530 recommends 35 D for the same installation.

McCrometer's goal was to identify installation requirements for the V-Cone. These first tests were not conclusive for those purposes. These tests do quantify the effects of elbows upstream of the V-Cone. For any V-Cone with a Beta ratio between 0.363 and 0.750, the maximum effect of either a single elbow or double elbows out-of-plane would be approximately 0.12%.

More research is necessary to describe the V-Cone's total performance. The geometry of the meter does not easily lend itself to comparison with other meters. Past studies have noted the flow pattern through a V-Cone primary element. Fluid traveling in the center of the pipe is forced by the cone to the wall of the pipe and through the annular constriction. This mixing of

the low and high velocity areas of the flow creates a pronounced "flattening" of the flow profile directly upstream of the meter. This characteristic of the V-Cone is the most probable cause of the V-Cone's consistent performance in less than ideal flow situations.

REFERENCES

1. MILLER, R. W. - Flow Measurement Engineering Handbook, Second Edition, McGraw Hill, New York, 1989.
2. MATTINGLY, G. E. and YEH, T. T. - Effects of pipe elbows and tube bundles on selected types of flowmeters. *Flow Measurement and Instrumentation*, Vol. 2, Number 1, p. 4, 1991.
3. MATTINGLY, G. E. and YEH, T. T. - Summary Report of NIST's Industry-Government Consortium Research Program on Flowmeter Installation Effects with Emphasis on the Research Period November 1988 to May 1989. U.S. Department of Commerce, NISTIR 4310, 1989.
4. MATTINGLY, G. E. and YEH, T. T. - Summary Report of NIST's Industry-Government Consortium Research Program on Flowmeter Installation Effects with Emphasis on the Research Period May 1989 to February 1990: Tube Bundle Effects. U.S. Department of Commerce, NISTIR 4751, 1990.
5. BAGGE, D. J. - Evaluation of Keterna, V-Cone Flowmeters. Test Report E 1705 S 92, SIREP, 1992.

The $\sqrt{\text{CONE}}^{\text{®}}$ Differential Pressure Flowmeter

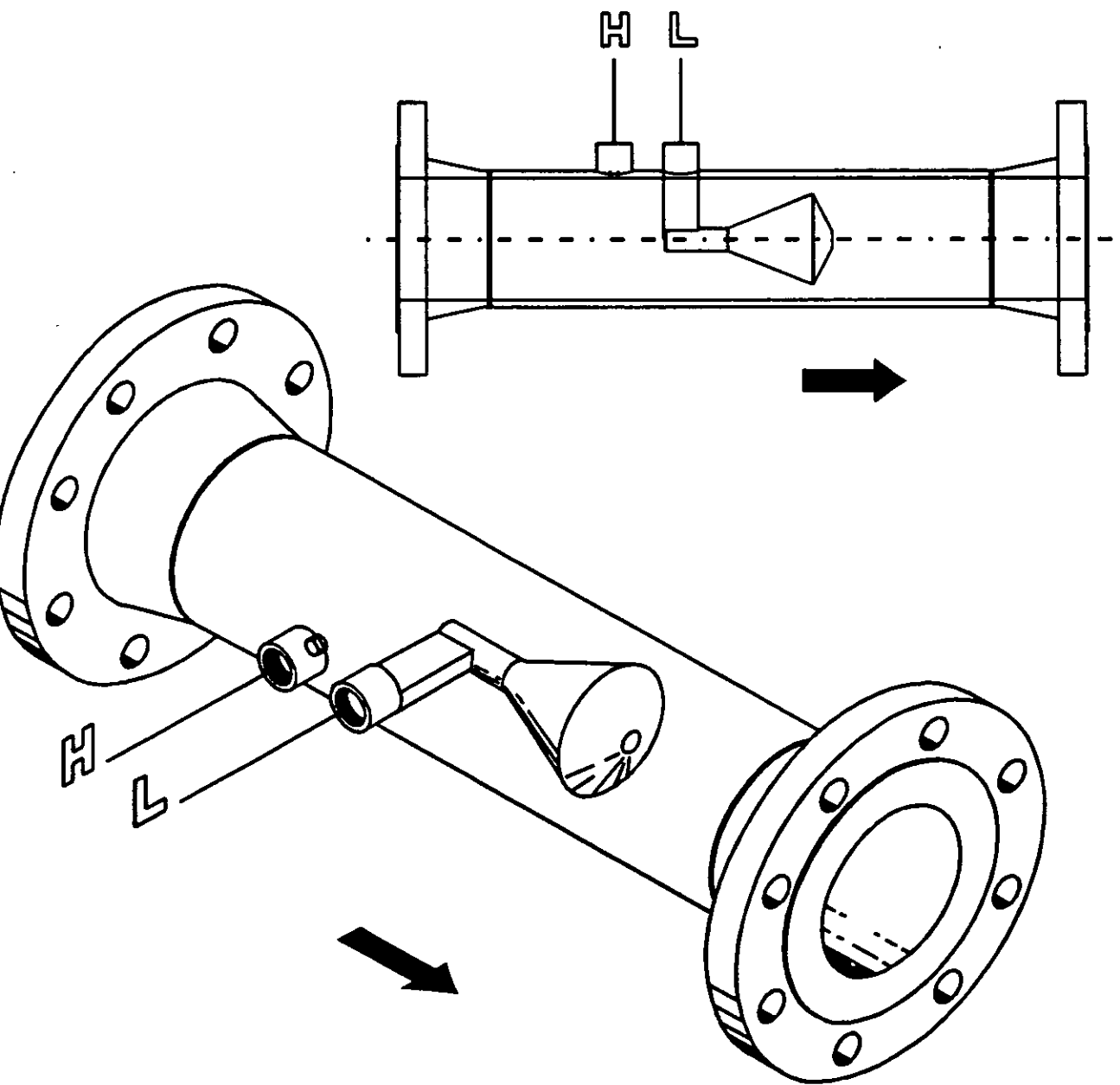


Figure 1

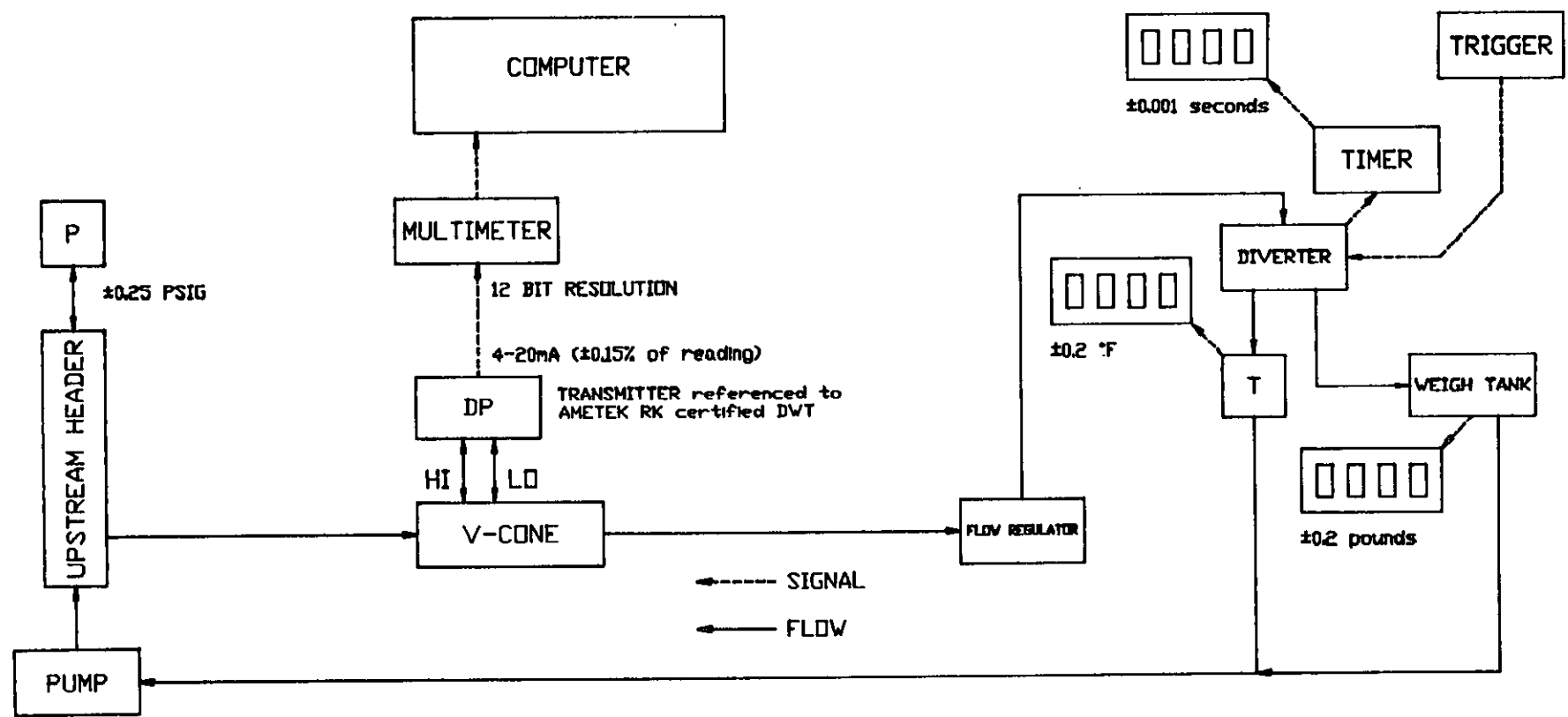
NUMBER
Figure 2



TITLE
SMALL STAND OPERATIONAL SCHEMATIC

S.A.I. _____ DATE 08-27-92

REV DATE & BY: _____ FILE NAME _____ DRAWN _____ CHECKED _____ APPROVED _____ DATE _____



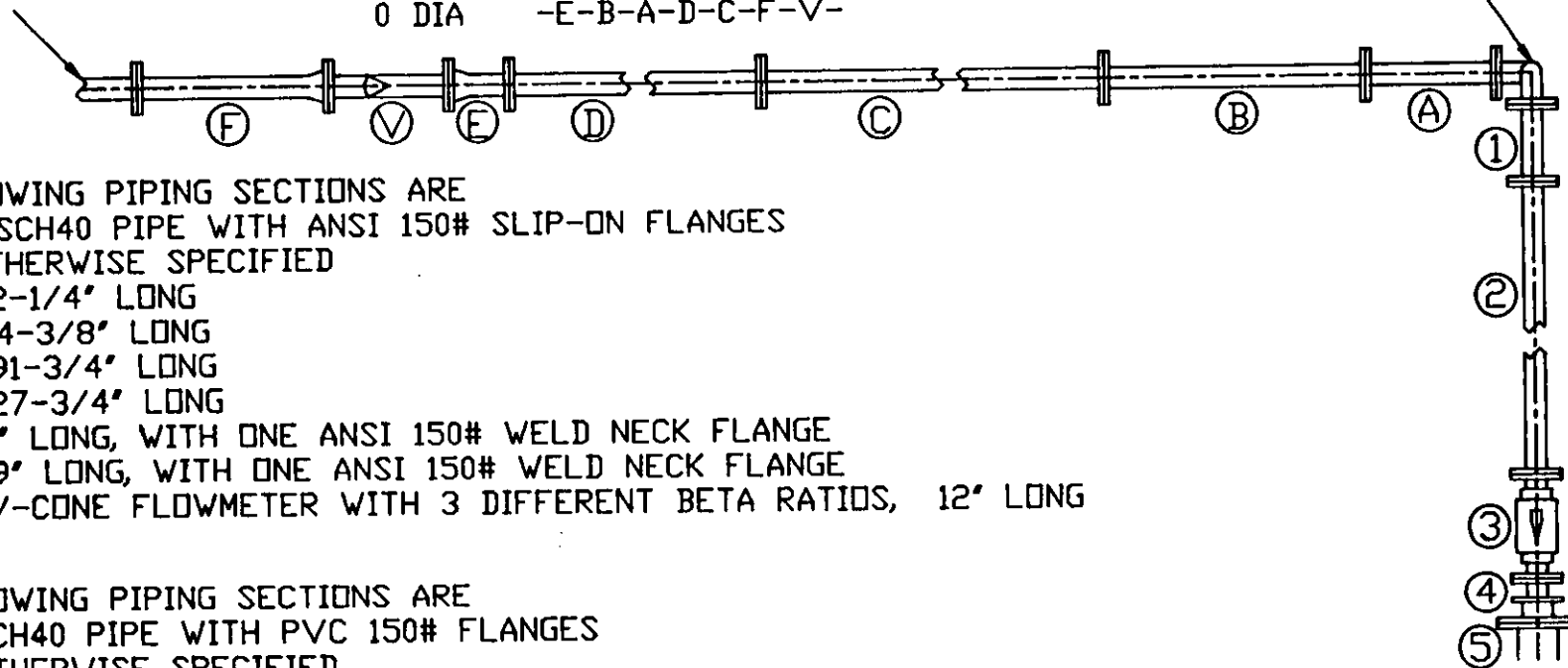
PIPING CONFIGURATIONS FOR V-CONE TO NIST INSTALLATION EFFECTS COMPARISON TESTING

TEST PIPING CONFIGURATIONS

190 DIA	-F-V-E-D-C-B-A-
100 DIA	-B-A-D-F-V-E-C-
20.3 DIA	-D-C-F-V-E-B-A-
8.7 DIA	-B-D-C-F-V-E-A-
2.9 DIA	-B-A-D-C-F-V-E-
0 DIA	-E-B-A-D-C-F-V-

TWO ELBOWS OUT OF PLANE
304SS 2" SCH40 LONG RADIUS ELBOWS
ANSI 150# WELD NECK FLANGES
CLOSE COUPLED

CONNECTED TO 2" PVC PIPE
LEADING TO DIVERTER



THE FOLLOWING PIPING SECTIONS ARE
304SS 2" SCH40 PIPE WITH ANSI 150# SLIP-ON FLANGES
UNLESS OTHERWISE SPECIFIED

- A 12-1/4" LONG
- B 24-3/8" LONG
- C 191-3/4" LONG
- D 127-3/4" LONG
- E 6" LONG, WITH ONE ANSI 150# WELD NECK FLANGE
- F 19" LONG, WITH ONE ANSI 150# WELD NECK FLANGE
- V V-CONE FLOWMETER WITH 3 DIFFERENT BETA RATIOS, 12" LONG

THE FOLLOWING PIPING SECTIONS ARE
PVC 2" SCH40 PIPE WITH PVC 150# FLANGES
UNLESS OTHERWISE SPECIFIED

- 1 7" LONG
- 2 97-1/2" LONG
- 3 2" REGULATING BALL VALVE
- 4 4x2 REDUCER SECTION
- 5 304SS 4" SCH40 PIPE CONNECTED IMMEDIATELY TO UPSTREAM HEADER

SINGLE ELBOW EFFECTS ON V-CONE
tested at Ketema/ McCrometer Div.

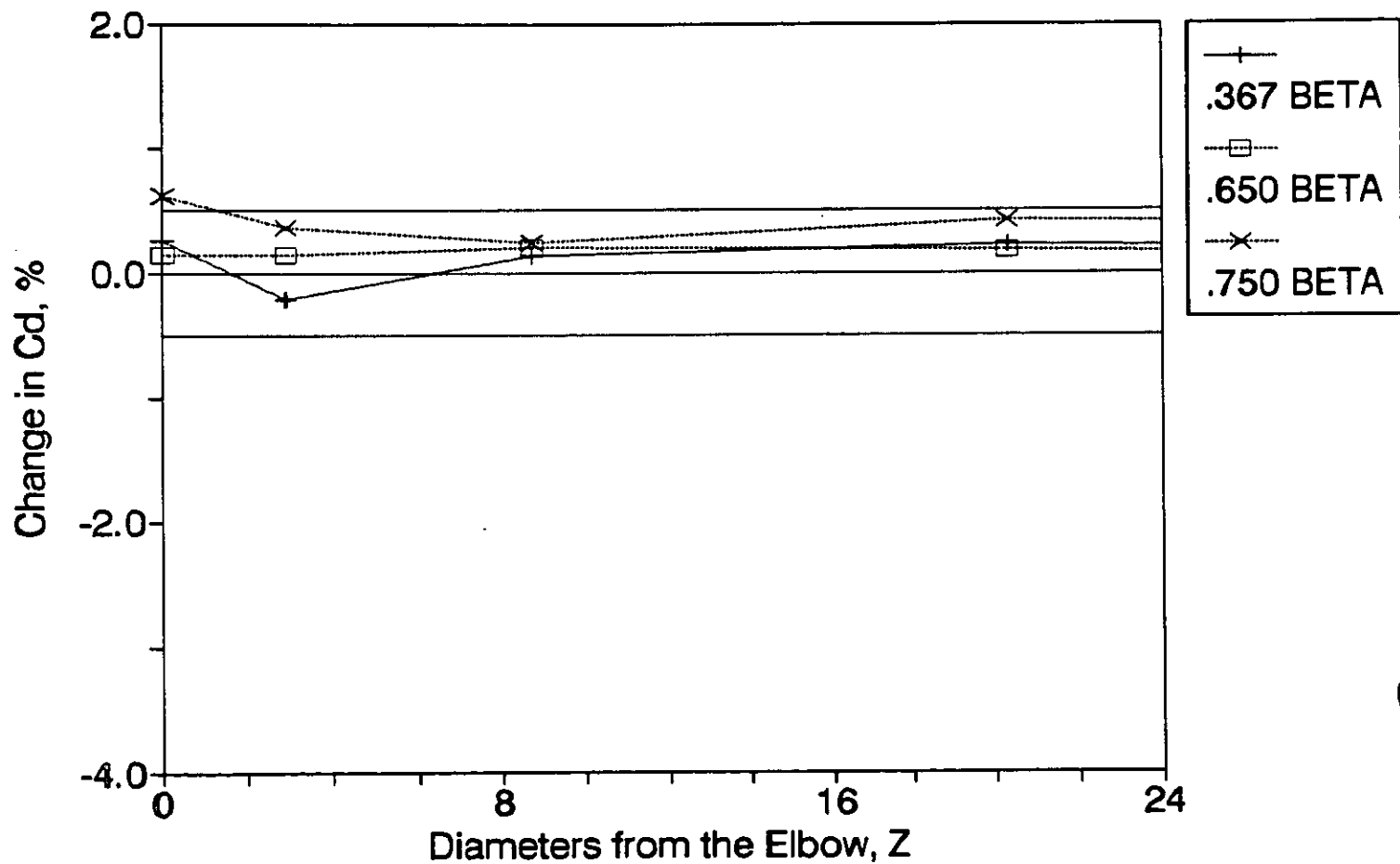


Figure 4

DOUBLE ELBOW EFFECTS ON V-CONE
tested at Ketema/ McCrometer Div.

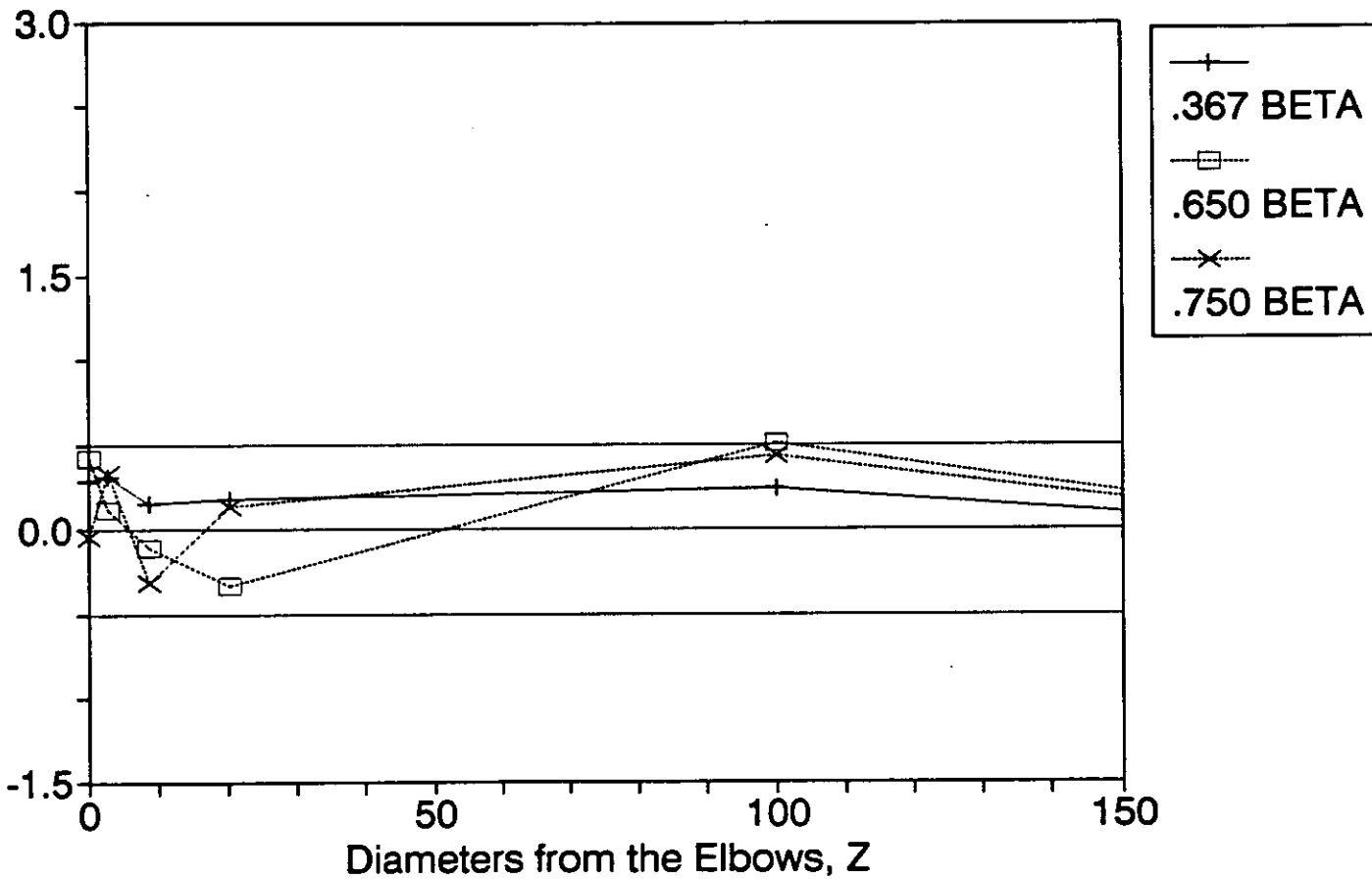


Figure 5

SINGLE ELBOW EFFECTS ON ORIFICE PLATE tested at NIST

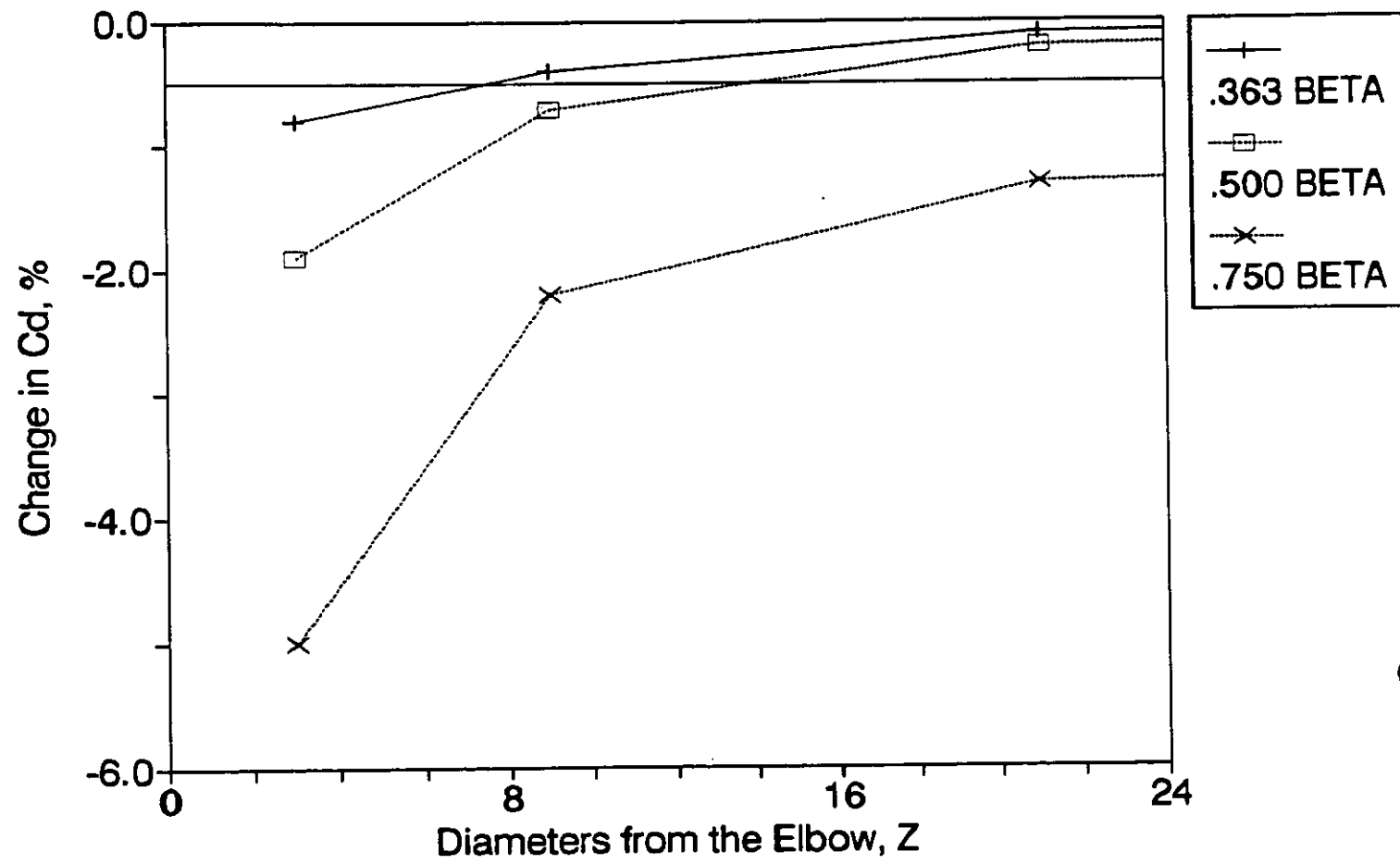


Figure 6

DOUBLE ELBOW EFFECTS ON ORIFICE PLATE tested at NIST

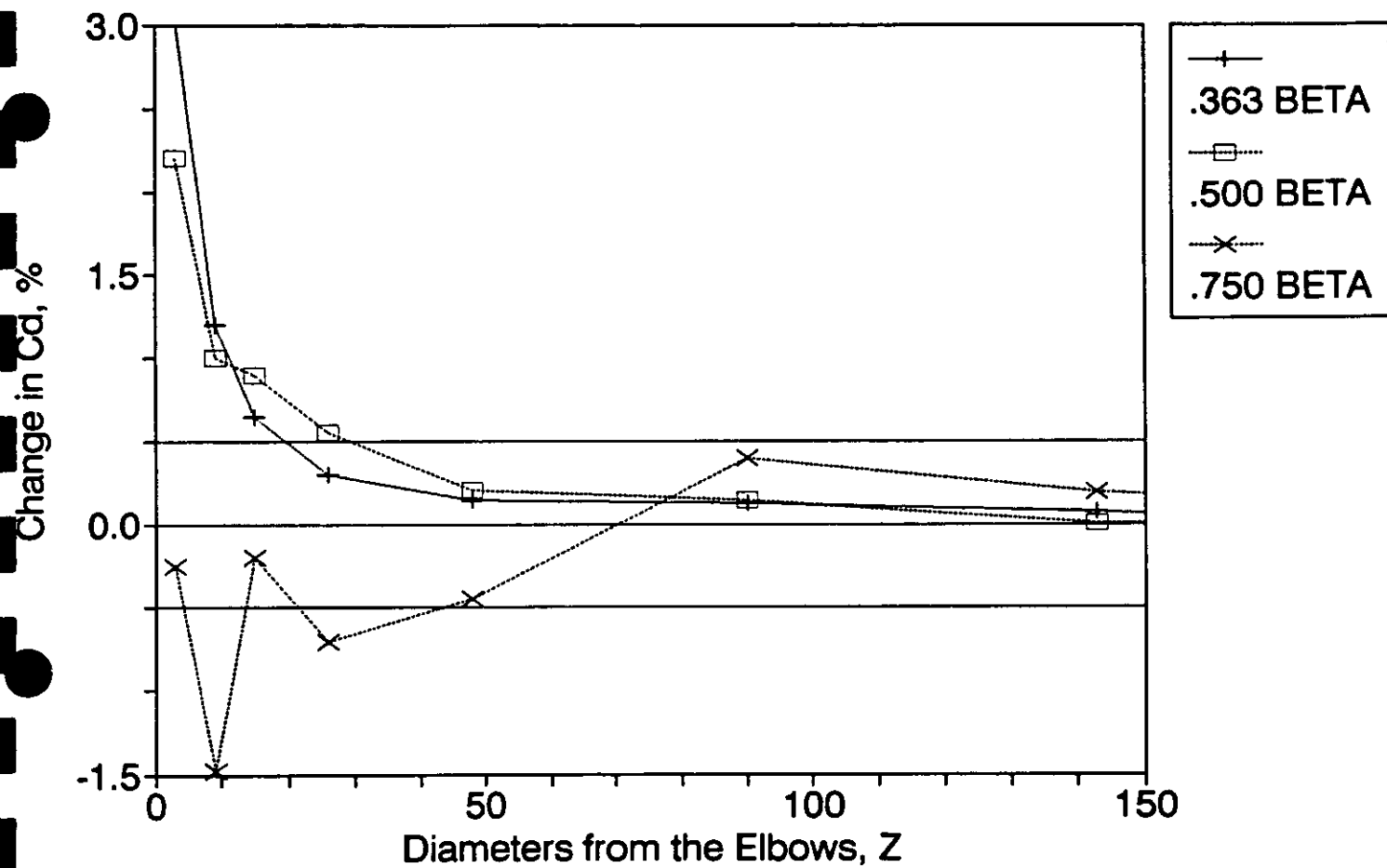


Figure 7

60

FLOW MEASUREMENT - THE NEXT TEN YEARS**J. E. Gallagher, P.E. - Shell, USA****"To Accomplish Great Things, We Must Not Only Act But Also Dream,
Not Only Plan But Also Believe." - Anatole France****1. GLOBAL OUTLOOK**

The global economy, the political events in the Middle East, Eastern Europe, the European Community's (EC) unification, the Commonwealth of Independent States (CIS) and the USA's regulatory atmosphere continues to drive the energy industry. Until the global recession ends the demand growth in most industrialized nations will remain flat.

As a result, this decade will be the most challenging for the petroleum and natural gas industry. Though oil and gas remains among the world's biggest businesses, consolidations, restructuring, "rightsizing" and layoffs permeates the global community. The global recession has accelerated these changes, particularly in the upstream sector.

The requirements for success are challenging - a clear vision complemented by strategy, corporate structure and required systems (Figure 1). For mature industries, functional excellence and competitive cost leadership are goals required for survival.

Today even the best-managed companies are transforming their cost structures, and companies that fail to do likewise probably won't survive as independent companies. More consolidations can be expected in this decade for companies that do not adapt to the economic realities of a mature business.

For example, the effort to overcome the political, technical, and commercial obstacles for adequate energy supply to Eastern Europe and the CIS may pose one of the biggest entrepreneurial challenges of this century. Going or not going into these markets is a decision that could make or break global integrated companies.

The cultural differences, the lack of a free market infrastructure, the legal system and the political risks are significant issues. Protection of investment, free profit distribution in hard currency, operating management and other issues frequently call for joint ventures to minimize risk associated with a single project. Expansion of these markets will occur only when experience meets expectations over time.

Progress will emerge slowly. Patience is needed as much as capital, if not more. The culture shock of moving to a free market system is enormous for both sides of the equation.

At today's oil prices, the investments required over the next decade is a formidable challenge. The sums needed are not likely to be met out of cash flows alone. Also, increasing production in the regions mentioned above will involve leading edge western technology combined with excellent management skills for increasingly complex projects.

East Asia is also a major player on the energy scene. Its decisions and choices affect the global community. Obviously, the presence of Japan within the region is the primary factor in this development.

As energy consumers, the USA and Western Europe remain at the heart of the world energy drama. While they continue to exert great influence, many of the levers of power are now found in the Middle East, South America, Northern Africa, East Asia and, in the next century, the CIS.

Competition among the sources of energy will grow as a result of environmental legislation, market forces and capital investments (Figure 2). The future energy situation can be stated simply - Energy demand will continue to grow steadily with the economies of the world. Alternative energy sources will be developed as a result of economics and the environment.

Concerns about the environmental impacts of the energy industry - on the daily life of neighboring communities or, on a grand scale, in global climatic effects - is no passing fashion. The necessity of choosing between competing fuels based on their environmental credentials is with us to stay. Taking these views means, among other things, that the science underlying these environmental beliefs needs to be sound and

comprehensive.

Due to these global pressures, the future for flow measurement and quality assurance is bright.

2 UPSTREAM SECTOR

With declining prospectivity, companies are reducing and retargeting exploration budgets, consolidating E&P operations, shifting their efforts towards the CIS, South America and Asia, and taking an increasingly stern view of E&P performance. The cash flow demands for most CIS projects are matched by their profitability - big and bigger. The peculiarity of the CIS crude oil reserves is their concentration in gigantic and large fields. In the EC and North America, it takes at least five years after exploration efforts are initiated to bring new production online.

The production facilities of the future will be cleaner, sophisticated, and more capital-intensive. Emissions to the air and water will be significantly reduced, and efforts will be made to eliminate solid wastes.

Sophisticated computer control systems will be used to instantly and continuously monitor wells and protect the environment. Information will be stored on several different systems (relational data bases) linked via networks. Support software will be task oriented with a user-friendly front end to perform low level systems work. All data and operating manuals will be accessible via computer (laptop, personal, workstation).

E&P personnel will be highly trained, reflecting the increasingly complex nature of their jobs. Regional training centers will be an integral part of international companies.

Crude Oil

Basins for conventional exploration of crude oil are well drilled in the United States (USA) and Canada. An accelerated decrease in the USA domestic production will occur due to the maturity of the producing fields and environmental pressures. The USA currently imports 57% of their crude oil needs.

The North Sea will experience significant growth through 1995. After this period, the prodigious North Sea

activity will level off and gradually migrate to a mature region.

In the crude oil supply picture there exists an interesting dichotomy. Greater than anticipated growth in key national economies - USA, Japan, and Germany - will boost petroleum demand and cause a supplier driven pricing scenario. The International Energy Agency (IEA) estimates a lack of spare production capacity in the global oil market in the near term. As a result, crude oil prices will rise sharply with the economic growth of these key national economies.

Natural Gas

The international gas industry has undergone an extremely dynamic evolution over the two decades. This evolution was spawned by energy policies oriented towards supply diversification, crude oil substitution, environmental concerns, and in the USA - regulatory restructuring of the transmission segment.

The worldwide demand for natural gas is projected grow rigorously over the next decade. Conversion of power generation plants, home heating systems, mass transportation vehicles and fleet vehicles are projected as a result of environmental regulations and alternative energy pricing structures.

Natural gas is believed to be more environmentally friendly than crude oil. Whether or not the science behind this belief is sound, there seems little doubt that gas as a source of energy will become increasingly acceptable and, where economics permit, preferable to other fuels.

2. DOWNSTREAM SECTOR

In recent years, refining capacity for the key industrialized nations has remained at a constant level. Since 1984, USA refining capacity has declined slightly due to environmental legislation - the Clean Air Act (CAA), and the Clean Water Act (CWA), and the global decline of sweet crude oil. As product demand increases and additional refineries permanently close their doors, capacity utilization rates, now at 87%, will increase to 90-95%.

Refiners can't or won't add capacity, due to the capital

investments and the resulting cash flow crunch associated with compliance to the CAA and CWA. Capital investments required by the CAA alone is currently estimated to be approximately 40-50 billion USD by 1995. This cash flow drain will not increase capacity and will consume most if not all short term profits. Joint ventures, toll processing and a migration by some refineries to niche markets will be necessary to survive in the North American market.

As a result, the USA will have to import additional volumes of finished product to keep up with demand. These imports will be required to comply with the CAA Reid Vapor Pressure (RVP) gasoline requirements, benzene limits, gasoline oxygenate requirements, and by 1995 the reformulated gasoline specifications. In addition, new regulations will require low sulfur diesel fuel for all "on-road" vehicles.

Refineries of the future will be cleaner, sophisticated, and more capital-intensive. Emissions to the air and water will be significantly reduced, and efforts will be made to eliminate solid wastes. These complexes will be enormous in size to offset the environmental investments associated with the waste heat recovery systems, waste water treatment systems, vapor recovery systems, air emissions' scrubbing system, CAA gasoline specifications, and so forth.

Instant and continuous monitoring via sophisticated computers will ensure optimization of yields and protection of the environment. Hydrocarbon management systems will emerge to maximize the raw materials needed to meet short term market demands for finished products.

Crude oil quality is emerging as a key to efficient and effective refinery operations. The refiner must receive a consistent crude slate to optimize yields, conform to product specifications, meet the market demands, and comply with the environmental limitations. All crude oil is not created equal in the eyes of the refiner.

Refinery personnel will be highly trained, reflecting the increasingly complex nature of their jobs. In-house training centers will be an integral part of refining complexes.

3. TRANSPORTATION SECTOR

The transportation industry will undergo significant expansion, contraction and regulatory changes over the next ten years.

Current and future customers still want the same things that yesterday's customers wanted, namely, a quality transportation sector which provides reliability and security of supply. But they may have uncomfortable perceptions regarding supply reliability, and/or pipeline capacity reliability.

The transportation business will be accelerating towards computerized transfers of commodities, pipeline movements, tariff billings, pipeline scheduling and supply contracts/agreements. One analogy is that of the international banking industry and its dependence on computerization to conduct daily business.

In highly populated nations, the need for high discrimination line integrity systems will be fierce. Densely populated regions should not be subjected to the uncertainty of eighty year old systems not being monitored for dynamic leak detection. Regulations requiring internal inspection and possibly hydrotesting on a set time interval are probable if the leak detection technology has not met the needs of the general public.

The industry has only scratched the technology surface that can provide the kinds of service customers will pay for. Technology is the key that starts the economic engine. Willingness to work together globally is the engine. The resources that we apply to the task is the fuel that runs the engine and makes all things work.

One thing is for sure, the oil, natural gas, refined products and chemical industry isn't going anywhere without pipelines. But even more than that, the industry must demonstrate to the customers that we can get the commodity to the right place at the right time and the least cost. Dr. Edward Deming would probably agree that the challenge awaits those who wish to pursue progress and viability.

Oil Systems

The oil transportation sector will undergo the most significant pains (Figure 3). As domestic production in the USA continues to accelerate its decline, the grid demographics will be redefined towards imported crude movements. Older onshore domestic crude oil pipeline

grids will be eliminated and replaced with independent operators or truck gathering alternatives. Offshore pipelines will grow only when the pricing structure meets the capital investments required for deep water operations. New batched crude oil pipeline systems and modifications to existing domestic pipelines will be justified to satisfy the appetite for imported crude oils.

The refiners' sensitivity to crude oil quality assurance (QA) will be amplified due to refinery design, environmental regulations, market demands, product specifications and economics. The transportation industry will need to address these customer concerns with clear vision, a creative atmosphere and mutual agreement on acceptable performance levels.

Natural Gas

Overall, the natural gas transportation systems will be expanding in all industrialized nations (Figure 4). In the USA, Canada, North Sea, Western Europe, the CIS, the Middle East and the Mediterranean significant pipeline projects are currently planned and/or underway to satisfy the growing demand for natural gas. The environmentally friendly fuel is anticipated to replace petroleum based products in power plants, heating systems, government and/or commercial fleet vehicles, and mass transportation systems (buses).

Recent regulatory revisions by USA's Federal Energy Regulatory Commission (FERC) will focus the transportation companies to invest in basic infrastructure, cost control, and operating issues.

Natural gas quality will become a significant issue in Europe. To a lesser extent, gas quality will be sensitized in North America. The difference is the age of the grids and the customers' requirements. In North America, the customers have not required stringent gas quality specifications.

Refined Products' Systems

With the uncertainty associated with refined products markets, existing pipeline systems will support the application of drag reducing agents (DRAs) and localized capital expansions (Figure 5). The auto mileage improvements required by the CAA should offset the economy's demand growth. To add to this complexity, the

market will be regionalized with respect to economic growth.

By 1995, North America will have transported RVP limited gasolines, benzene limited gasolines, oxygenated gasolines and reformulated gasolines through almost every products pipeline without a significant increase in capital facilities. A formal RVP assurance program is now regulated during the control period. QA programs will be required to ensure that no "off-spec" product enters the pipeline or is received unknowingly by the customer.

Chemical Systems

With the cycles associated with sophisticated chemicals, existing pipeline systems will grow at a rate directly with the global economy (Figure 6). Again, the market will be regionalized with respect to economic growth.

Online analyzers will be required to ensure that no "off-spec" product enters the pipeline or is received unknowingly by the customer. The move towards ISO 9000 certification will occur over the next five years for chemical transportation systems.

4. QUALITY ASSURANCE & IT'S IMPORTANCE

Quality assurance is a requirement for any viable company. Zero defects to outside customers is a prerequisite in a competitive environment. The aspect of crude oil, natural gas, refined product, and chemical online QA analyzers brings fear and heart palpitations to all senior pipeline management personnel (Figure 6). The issues of increased capital investment, operating and maintenance costs, training costs, additional personnel and ISO 9000 certification are real concerns in today's business climate.

However, QA will also reap benefits. By applying statistical quality control (SQC) to equipment performance, the maintenance costs and risks will be minimized. By investing in equipment which has a record of quality performance, minimum operating and maintenance costs will be achieved. This plateau does not occur at the lowest capital investment level. Other returns are the minimization of store stock inventory for equipment which hardly ever breaks, standardization of equipment, and training costs.

5. FLOW MEASUREMENT TECHNOLOGY

Instrumentation is selected based on its technical and commercial specifications. Usually the selection process considers only the instrument's capital cost and not the full cost of ownership over the its lifetime.

The full cost of ownership consists of the initial capital, commissioning, training, spare parts, maintenance and calibration costs for the lifetime of the equipment. The full cost is several times the initial capital investment and should be the deciding factor in equipment selection.

The technical selection - accuracy, repeatability, drift, ease of calibration as well as reliability indirectly affects the cost of ownership.

Proper installation and application of flowmeters are two of the most significant parameters in the measurement chain. These parameters influence the factors mentioned above and are neglected in most assessments. The misapplication of any device brings the wrath of field personnel on the operating company's engineering staff -- as it should! More effort is required by the user community to match their expectations with reality. The selection, installation, operation and maintenance of quality equipment, if properly performed, is almost never discussed by operating personnel.

Modularization of discrete instrumentation is a key to success in the future (Figure 7). While some users have proposed the combination of all measurement instrumentation into a single control, computing, totalization, and communications device, this is obviously incorrect. Discrete functions will persist in order to satisfy performance, security, auditability and technology requirements.

6. PRIMARY FLOW DEVICES

The future vision of primary flow devices is clear and defined. The vision consists of "smart" flowmeters, new flowmeters, and in situ calibration or central calibration technology for both incompressible and compressible fluids (Figure 8).

Installation Effects

The problems associated with installation effects of flowmeters have been with us a long time. Pragmatic solutions have evaded our industry due to our limited insights into the "real" flow field.

Experiments over the last ten years has shed light on increasing our insights. In the USA, Canada and EC, scientists have recently conducted installation effects research on turbine, orifice and ultrasonic flowmeters. This data measured the meter's performance as a result of interaction with the near term flow field. With this insight, postulates have been proposed and are planned to be validated or revised within the year.

With the application of microchip technology into smart transmitters, sophisticated flow computers, personal computers, Computational Fluid Dynamics (CFD), thermal anemometry (TA) probes (i.e., hot wire, hot film, x-wire), Laser Doppler Velocimetry or Anemometry (LDV/LDA), characterization of flow meters in real time, high pressure gas piston provers, ultrasonic flowmeters, coriolis flowmeters, videoimagescopes, etcetera, large steps toward lowering the flow measurement uncertainty is possible. These "new" tools are providing significant advances in the refinement of existing metering equipment as well as the birth of new technology.

The advent of LDV/LDA technology has provided a tool to perform three dimensional flow field measurements. This technology is capable of measuring three non-orthogonal velocity components simultaneously, resolving from those three independent orthogonal velocity components, and then computing the mean velocity vector, the time averaged Reynolds stress tensor, and other items associated with those values. In this manner, variations in the flow field (upstream and downstream of flow conditioners, flow meters, fittings, etc.) can be documented. The next step involves comparing these measurements to Computational Fluid Dynamics (CFD) predictive models such as Create's FLUENT code. Through these comparisons the optimum turbulence model can be identified. The final results should have a predictive model which approximates the decay of distorted flow fields through flow conditioners and flow meters.

A fundamental understanding of the effects of upstream flow conditioning on flowmetering is essential for significant improvements. Recent LDV/LDA and TA probe

research is attempting to provide a thorough understanding of the complex flow field. The LDV/LDA, or TA probe are tools which provide us with the needed insight to the microscopic flow field. Studies at NIST Gaithersburg (Mattingly and Yeh), Texas A&M (Morrison et. al.), NIST Boulder (Brennan, et. al.), SwRI (Morrow, Park et. al.), NOVA Husky (Karnik, et. al.), CERT (Gajan et. al.), NEL (Reader-Harris, et. al.), Gasunie, K-Lab (Wilcox et. al.) and others have recently measured mean velocity profiles and turbulence structure associated with upstream flow conditioning effects.

The optimum turbulence model does not currently exist for CFD installation effects' applications. Hopefully, existing and planned turbulence structure measurements and installation effects research will provide future scientists with the needed insight for this development. Irrespective of this limitation, CFD technology will still be utilized to maximize the experimental pattern efficiency and to provide sensitivity analyses.

The goal of current orifice research programs is to focus on the effects of various installation conditions for natural gas applications. Since significant deviations from the Law of Similarity cause measurement errors, the main goal is to identify and quantify the error associated with these flow disturbances.

Present industry standards provide installation specifications for pipe length requirements and flow conditioner location upstream of flowmeters. Current upstream effects research has focused on assembling experimental data for evaluation of straight length requirements stated in the respective standards.

Flow Conditioners

All flowmeters are subject to the effects of velocity profile, swirl and turbulence structure approaching the meter. The meter calibration factors or empirical coefficients calculated from the discharge coefficient equations are valid only if similarity exists between the metering installation and the experimental data base. These parameters should not be significantly different from those at the time of meter calibration, or from those which existed in the empirical coefficients of discharge data base. Technically this is termed the Law of Similarity.

Many piping configurations and fittings generate

disturbances with unknown characteristics. Even a simple elbow can generate very different flow conditions from "ideal" or "fully developed" flow. In reality, multiple piping configurations are assembled in series generating complex problems for standard writing organizations and flow metering engineers. The problem is to minimize the difference between "real" and "fully developed" flow conditions on the selected metering device thus maintaining the low uncertainty required for fiscal applications. For clarity, we will refer to this as "pseudo-fully developed" flow.

A method to circumvent the influence of the fluid dynamics (swirl, profile and turbulence) on the meter's performance is to install a flow conditioner in combination with straight lengths of pipe to "isolate" the meter from upstream piping disturbances. Of course, this isolation is never perfect. After all, the conditioner's objective is to produce a "pseudo-fully developed" flow.

In general, upstream piping elements may be grouped into the following categories -

- * those that distort the mean velocity profile but produce little swirl
- * those that both distort and generate bulk swirl

Flow conditioners may be grouped into three general classes based on their ability to correct the mean velocity profile, bulk swirl and turbulence structure (Figure 9).

The first class of conditioners is designed to primarily counteract swirl by splitting up the flow into a number of parallel conduits. This class of conditioners includes A.G.A. radial tube bundles, A.G.A. hexagonal tube bundles, ISO 5167 tube bundles, AMCA's honeycomb and the Etoile.

The second class of conditioners is designed to generate an axisymmetric velocity profile distribution by subjecting the flow to a single or a series of perforated grids or plates. The profile is redistributed by use of the blockage factor or porosity of the flow conditioner. This class of conditioners includes the Sprengle, Zanker and Mitsubishi designs.

The third class of conditioners are designed to generate a "pseudo-fully developed" velocity profile distribution through porosity of the conditioner and the generation of a turbulence structure. The turbulence structure is generated by varying the radial porosity distribution. This class of conditioners includes the Sens and Teule, Bosch and Hebrard, K-Lab and Laws designs

In the next two years, additional research into the third class of flow conditioners should result in a significant decrease in the uncertainty associated with installation effects and velocity profiles for "real" field installations. The adoption of existing conditioner designs, or the refinement of these devices, or the creation of a new design will occur at the termination of this research.

Smart Flowmeters

With the application of microchip technology, large steps towards lowering flow metering uncertainties are possible due to the advent of sophisticated flow computers, personal computers, characterization of flow meters in real time, etcetera. These "new" tools are providing significant advances in the refinement of existing metering equipment as well as the birth of new technology.

The application of Statistical Quality Control (SQC) techniques is viable today. By using serial meters of differing technology, it is possible to monitor the performance of each flowmeter separately as well as the ratio (or difference) of the two meters. The user should be able to discern when one of the devices is in need of repair. Additionally, each meter should be equipped with predictive performance software as a function of Reynolds number or other appropriate correlating parameters. The objective is to discern systematic bias shifts between the devices at a level that is acceptable to the economic value of the commodity transferred between the parties.

Ultrasonic Flowmeters

For incompressible fluids, the ultrasonic flowmeter is fast approaching the performance levels of custody transfer flowmeters (CTMs). Tests are currently being conducted in the USA on the application of a new platform of ultrasonic flowmeters for line integrity purposes. For liquid systems, preliminary results indicate +/- 0.3% agreement with CTMs without the installation of flow

conditioners.

If additional tests confirm this performance, the installation of flow conditioners upstream of ultrasonic flowmeters should lower the uncertainty by minimizing the installation effects on its' performance. In other words, it is better to have a flat, repeatable velocity profile, for ultrasonic flowmeters rather than a fully developed one.

For compressible fluids, tests conducted by Gasunie and Daniel Industries indicate the viability of this technology to natural gas applications. To date, additional development effort is needed in the electronic packages associated with these devices. The future looks promising.

Coriolis Flowmeters

One of the most unique flowmeters introduced in the last decade is the coriolis meter. This device measures the total mass as a function of the rotational forces exerted on a specially configured tube.

Mixed results have been reported to date. However, it appears that this device will be viable in sizes up to 100mm. Velocity profile, velocity of sound, mechanical installation, and vibration are known to adversely affect the meter's performance.

There is evidence that the coriolis meter may prove to be the future custody transfer meter for direct mass measurement of LPG and similar viscosity fluids. However, the problem of providing a dynamic mass prover for calibration under operating conditions presents a stumbling block. Currently, tests are being conducted by an API Working Group to determine the feasibility of a SVP and density meter combination as a suitable transfer package.

In Situ Calibration

In situ calibration of incompressible fluids has been performed successfully since the 60s. The challenge of the measurement community is the calibration of compressible fluids such as natural gas.

Verifying the accuracy of flowmeters in specific compressible fluid applications has been one of the desires of the user community. Shop tests of orifice

meters and turbine meters with various upstream configurations have been conducted for several years to aid in the design of high volume metering facilities. The question posed by the user community is - "Can the operator ensure the parties involved in the fiscal transfer that the measurement station is adequately described by the tested design?".

In response to the North American community's request, the Gas Research Institute (GRI) has initiated funding for assessment of in situ calibration devices - sonic nozzles, master meters and piston provers. These tests, planned for 1993, will be conducted at GRI's MRF facility.

In situ calibration of flowmeters now appears feasible with the advent of the gas piston prover. In the last decade, high pressure gas piston provers were introduced to the natural gas community. The application of this device was inspired by the chemical industry's development for highly compressible polymer grade ethylene systems in Europe and North America. At this same time, the liquid small volume prover (SVP) demonstrated the acceptability of double chronometry interpolation techniques for turbine meters. Through the pioneering efforts of Gasunie, Shell, Amoco, DSM, Ruhrgas and Ogasco, a modified SVP approach was developed for chemical, CO₂ and natural gas applications.

The piston prover has been used as a primary standard to prove a turbine meter or a master turbine meter installed in series with an orifice meter. This arrangement ensures calibration under normal operating conditions - velocity profile, instrumentation, etcetera. Additionally, wet gas will not alter the performance of the piston prover as long as the flowing conditions are not lower than the hydrocarbon dew point. Small amounts of fine solids will have no effect unless the bore of the calibrated section or the piston seals are damaged.

At this time, the high pressure gas piston prover is being successfully applied by Gasunie, Shell USA, Amoco USA and Ruhrgas for fiscal applications and/or laboratory flow standards. Gasunie has replaced their "bootstrapping" method with the piston prover. Shell USA has applied this technology to chemical and CO₂ systems since 1984 to identify out of tolerance metering facilities. Amoco USA has operated an Ogasco design for the calibration of small turbine meters in a coal degasification project since 1990.

Potentially, the piston prover offers the best opportunity for successful field calibration of flowmeters on multiple component natural gas streams. However, the measurement community needs; additional research, an established gas piston prover design, and certification standard. The additional research needs will be assessed with the GRI activities for 1993. In answer to the need for standards, the API Committee on Gas Measurement (COGM) has recently established a Working Group to address the global community input and concerns.

7. SECONDARY DEVICES

Secondary devices consist of instrumentation which is not a part of the primary flow device such as smart transmitters, chromatographs, viscometers, moisture analyzers, densitometers, etcetera (Figure 10).

The future vision of secondary devices is also clear. This vision consists of advancement in "smart" transmitters, field calibration standards, online viscometers and QA analyzers, portable analyzers and density meters for both incompressible and compressible fluids.

Smart Transmitters

Smart transmitter experience has proven the adoption of these devices is justified due to lower the full cost of ownership. There are few improvements to be made in the type and application of smart transmitter technology except for the digital transmission issue.

Smart transmitters have exhibited twice the mean time between failures than previous analog transmitters. The actual failures proved to be dependent on installation conditions rather than on manufacturers' construction. The devices should be positioned to minimize vibration, rapid temperature changes, blockage and corrosive/erosive conditions.

Digital means of communications are available but not standardized at this time. The short term performance level for smart transmitters using analog outputs is $\pm 0.10\%$ of full span. Internal tests have indicated digital output techniques would provide a short term performance of $\pm 0.05\%$ of reading. This is a significant improvement!

Field Calibration Standards

With the advent of smart transmitters, field calibration standards have been required to improve. Using SQC and corrective software, field standards will improve in the next five years due to market forces. After all, if the transmitter is good for 0.05% of reading, why can't the field standard be at least twice as good?

Other Instrumentation

Other secondary instrumentation will be required for efficient and effective operations.

Improvements in viscometers have occurred to address moderately viscous fluids. When used in combination with a densitometer, the calculation of real time Reynolds numbers are possible. This leads to the possibility of meter factor footprinting as a function of Reynolds number for flowmeters. Other viscometer applications include pipeline interfacial mixing, batch cutting and power optimization.

Online and portable QA analyzers are emerging at a fast pace. Graebner RVP offline analyzers were required to comply with the CAA gasoline requirements. Additional analyzers are being evaluated for oxygenate analysis. Other QA measurement applications will arise as the industry adopts a proactive approach to quality in operations.

8. OPERATIONAL ENHANCEMENTS

Several operational enhancements are attainable in the next ten years. The objective is increased performance through intelligent capital investment which is offset by lower operating and maintenance costs (Figure 11).

Flowmeter Applications

Flowmeters will be selected not only on short term performance but also long term performance, training costs, SQC software, frequency of calibration and calibration technology.

The increasing use of liquid ultrasonic meters will occur in refineries and chemical plants. The uncertainty and performance is approaching CTMs. The current performance combined with its non-intrusive design will be difficult

to match with other devices. It will be possible to calibrate and inspect flowmetering devices on process units prior to plant turnarounds.

The life of the orifice meter has been extended as a direct result of "smart" transmitter technology and new flow conditioner designs. This meter will continue to be preferred on certain fluids because of its lower sensitivity to density determination errors.

Extended Calibration Intervals

Operational enhancements are needed in extending the calibration intervals of the associated primary and secondary equipment (flowmeters, flow computers, smart transmitters, chromatographs, etc.), required physical inspection intervals (i.e., videoimagescopes, etc.), required certification of field standards on specified intervals, and statistical footprinting of field devices and standards.

Line Integrity Systems

The detection of leaks in pipelines presents a number of technically challenging problems. Compounding the technical difficulty of leak detection is the environmental and safety concerns. The leak detection response rate must be sufficiently fast and of a high resolution.

As a practical matter, pipelines cannot afford to install CTMs every 200 kilometers. Therefore, the number of monitoring points should be minimized by the resolution and response of the device.

Changes in temperature between monitoring points can result in significant changes in fluid and pipe volumes. Also, operating conditions such as batched operations, elevation differences, and dynamic transients pose unique problems.

Leadership

To succeed, Measurement Teams will need to establish and maintain free and open communication. The Team will need to achieve seamless communications across all organizations and through all necessary levels of those organizations (hourly field personnel to senior management). The objective of the effort and the important steps necessary to achieve that objective will be communicated clearly along with the

requirements. Leadership should be perceived as competent, credible, and sharing a unified direction toward a stated purpose by all customers.

Technology transfer and optimization of individual skills should be an ongoing effort by all members of the Team.

Loss Control Targeting

The following targets for annual loss control performance has been established by Shell Pipe Line Corporation's (SPLC) Measurement Team -

- * 0.03% major crude pipelines
- * 0.02% refined products systems
- * 0.10% crude gathering systems
- * 0.10% LPG pipelines
- * 0.10% chemical & CO2 pipelines

The Team should aggressively promote the following measurement philosophies -

- * Manage the business by being proactive towards loss prevention
- * Conformance to the requirements (tariff & contractual obligations, federal & state regulations, measurement standards, and customer established requirements)
- * Document measurement problems or nonconformances (troubleslip system)
- * Maintain 5 year evergreen plan covering performance levels, personnel training, and capital investments
- * Establish a daily loss control on large tank farms & key transportation systems

Innovation and Creativity

An important part of SPLC's strategy is the establishment of the Targeted Loss Unit (TLU) Program. SPLC operated systems are divided into over one hundred separate loss units (or measurement systems) to monitor their performance. The majority of loss units operate within acceptable Statistical Quality Control limits and require no attention. The TLU Program maximizes the effectiveness of our efforts by focusing our fiscal and manpower resources. Working as a team, HO Measurement and field personnel select ten loss units -

commonly referred to as the "Ten Most Wanted". Manpower and fiscal resources are then directed towards identifying the "root cause" for their performance. The list is "rolling" in nature. When a targeted loss unit's problems are defined and corrected, it is removed from the list and replaced by the next loss unit in line.

The SPLC's Team is challenged by the breadth of operations which covers crude oils, refined products, LPGs, chemicals and CO2 measurement applications. Measurement is a technically demanding, complex, state of the art field with significant impact on the profitability of any transportation system. Technology, research and testing of hardware, instrumentation and flow standards are ongoing efforts due to this state of the art field. Innovation, creativity and realistic assessment capabilities are required traits of any quality measurement organization to adapt new technology with an acceptable level of risk. This blend was the key to establishing new levels of performance in SPLC while maintaining low operating costs.

Measurement Information Systems

As an example, innovation and creativity in the field of measurement is being applied through the use of laptop computers for measurement ticketing, proving reports and analysis techniques (Figure 12).

A goal of any large transportation system is to minimize monthly losses (Figure 13). A program to monitor the daily loss performance for tank farms and key transportation systems is critical to attain loss prevention. Expansion of this concept is currently underway. SPLC has established a corporate goal - accurate daily loss performance for all large transportation systems and storage facilities within the next five years.

Innovation and creativity by the SPLC Team resulted in computerized automation of monthly loss control reports thereby eliminating redundant effort throughout the organization. The report package is layered to provide management with overview information, and measurement specialists with two levels of detailed information. This approach places the required information in the necessary format for the appropriate individual.

Certification of Technicians

With the complexity of future technology, the need will occur for certification of measurement and laboratory technicians.

Eventually the ISO 9000 philosophy will provide market distinction and enhanced profitability for companies with visions.

Application of Quality Concepts

Measurement personnel has always applied quality concepts. This approach is natural in problem solving dynamic systems. The following discussion presents SPLC's application of quality concepts to its measurement mission.

Customer Focus. SPLC operates transportation systems for a multitude of owners and focus on our customers' requirements has always been a high priority. A summary of our measurement performance is presented annually to the various owners who provide feedback on our performance and mutual agreement on the requirements.

Prevention. As mentioned above, the Team identified the need for daily loss control on large tank farms and key transportation systems. Most systems identified are now monitored daily resulting in early detection and prevention of significant losses.

Problem Solving. Measurement is a technical field and requires problem solving skills by all participants. The Team exhibited this process individually and jointly in areas of limited knowledge/experience (cross training). Innovative problem solving is shared by all Team members through quarterly newsletters, technical awareness bulletins and annual Team meetings.

Continuous Improvement. The Team is by nature on a continuous improvement path. Constant assessment of competitors, technology, culture, loss performance, training requirements and staffing needs are a part of the Team's culture. A positive competitive atmosphere within the Team members promotes continuous improvement.

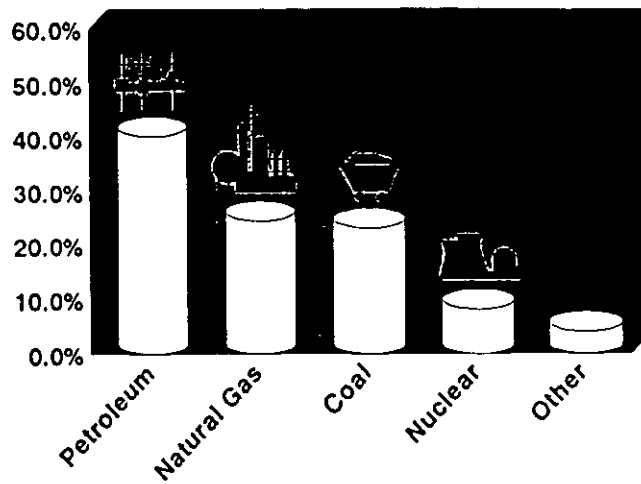
Measurement. As previously mentioned, SPLC operations are divided into over one hundred separate loss units (or measurement systems) to measure their performance. Statistical data bases are archived for each loss units monthly performance from 1985 to the current month's business. Individual charting of data, meter factor analysis, measurement ticket analysis are all done on a monthly basis to assure proper statistical control (Figure 14). In addition, daily loss performance is computerized (with manual entry) to provide preventive measurement.

9. SUMMARY

We have attempted to provide a vision of the measurement community's direction for the next ten years. The technological advances will be fast and fierce. Companies should be positioned to take advantage of these opportunities through a strategy, structure, systems and people. The elements to success in the next ten years will be flexibility, proper corporate cultures, innovation and creativity, maximization of current capital investments, and prudent capital investments.



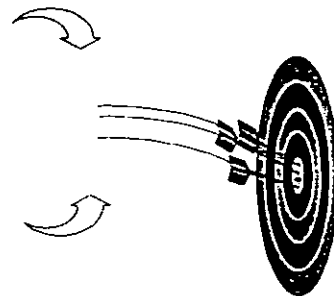
USA Sources of Energy



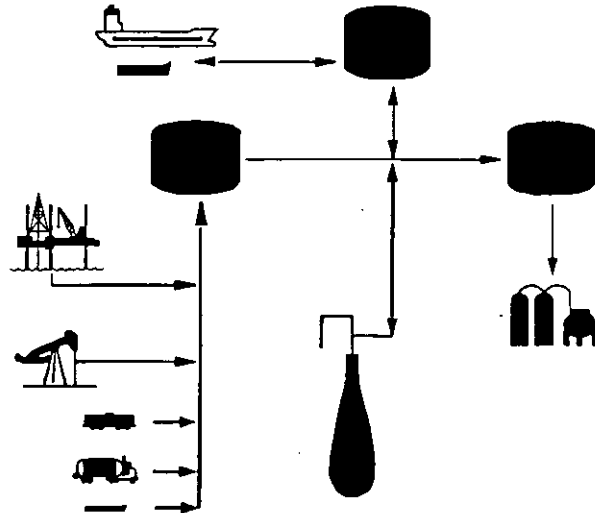
Requirements for Success

Clear Vision

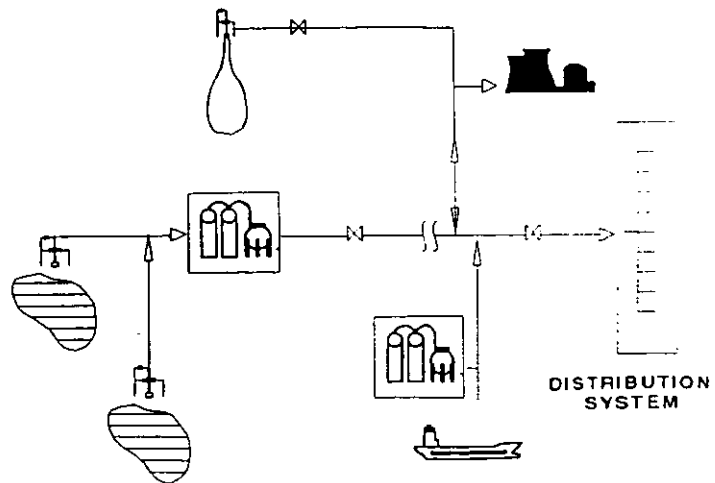
People
Strategy
Structure
Systems



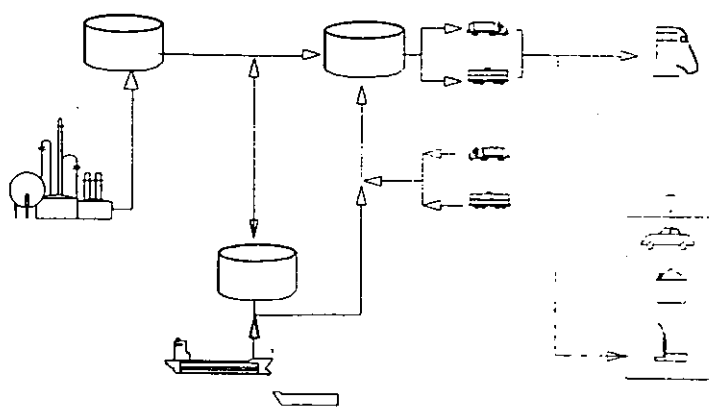
CRUDE OIL SYSTEM



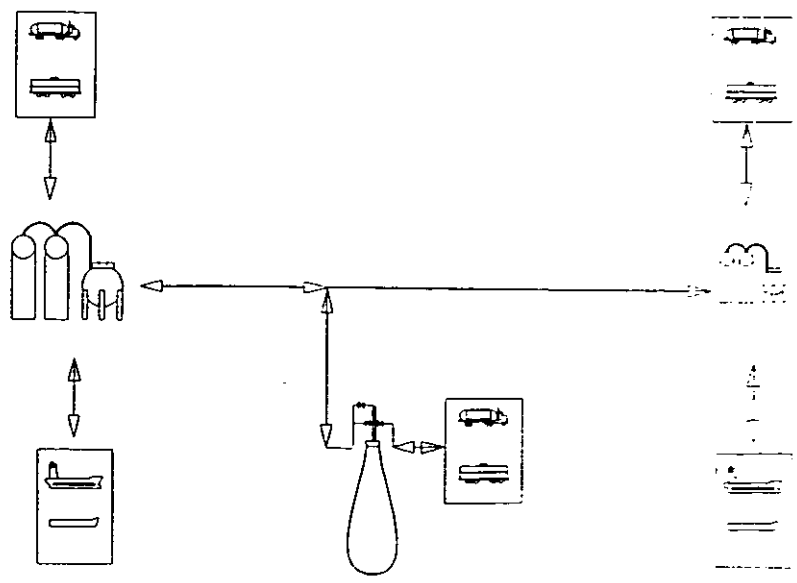
NATURAL GAS SYSTEM



REFINED PRODUCTS' SYSTEM



CHEMICAL SYSTEM





Classification of Flow Conditioners

Type	Class	Head Ratio	Cost
Tube Bundles			
Radial	I	1	Lo
Hexagonal	I	1	Lo
Etoile	I	1	Med
AMCA Honeycomb	I	1	Med
Mitsubishi	II	2	Lo
Zanker	II	6	Hi
Sprenkle	II	15	Hi
Laws	III	2	Med
K-Lab	III	3	Med
Sens & Teule	III	5	VHi
Bosch & Hebrard	III	5	VHi

SECONDARY DEVICES Future Direction

- ▶ Smart Transmitters
- ▶ Field Calibration Standards (dP, P & T)
- ▶ Online Viscometers
- ▶ Online QA Analyzers
- ▶ Portable QA Analyzers
- ▶ Portable Densitometers

OPERATIONAL ENHANCEMENTS

Future Direction

- Flowmeter Applications
- Extended Calibration Intervals
- In Situ Calibration
- Line Integrity Systems
- Loss Control Targeting
- Measurement Information Systems
- Certification of Technicians
- Allocation Metering

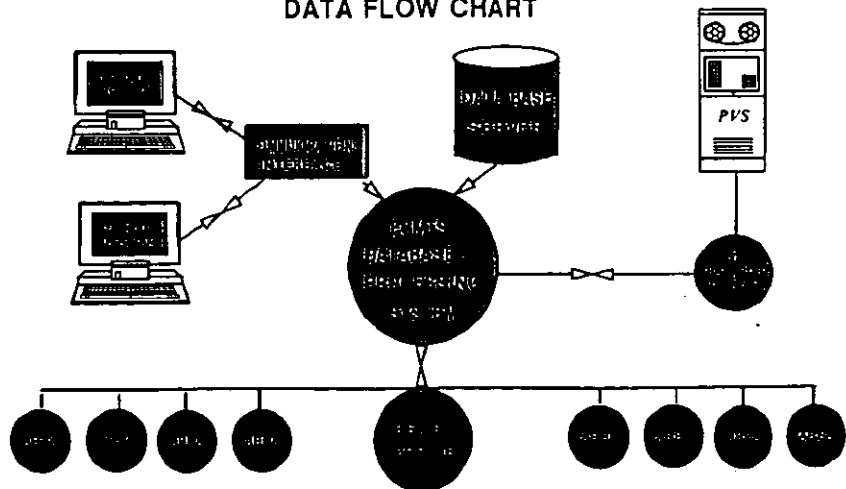


1992 North Sea Workshop



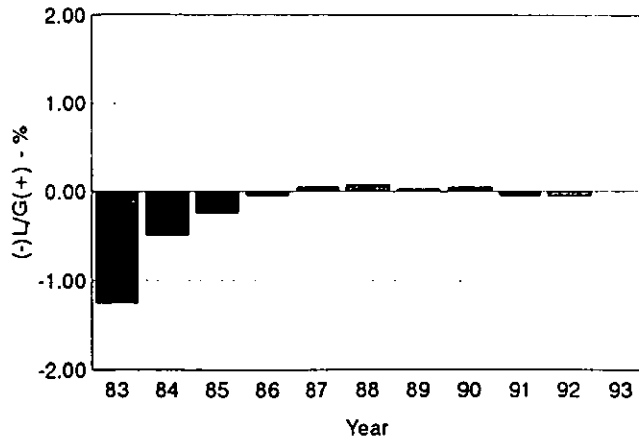
ECMTS PROJECT

DATA FLOW CHART





Ethylene Pipeline Annual Loss Control Performance



METER FACTOR CONTROL CHART

LACT METER - Noncompensated : Meter 002

